Minnesota Department of Transportation

RESEARCH SERVICES

Office of Policy Analysis, Research & Innovation

Recycled Unbound Materials

Tuncer B. Edil, Principal Investigator
Department of Civil and Environmental Engineering
Geological Engineering Program
University of Wisconsin – Madison

November 2012

Research Project
Final Report 2012-35

Your Destination...Our Priority

To request this document in an alternative format, please contact the Affirmative Action Office at 651-366-4723 or 1-800-657-3774 (Greater Minnesota); 711 or 1-800-627-3529 (Minnesota Relay). You may also send an e-mail to ADArequest.dot@state.mn.us.

(Please request at least one week in advance).

Technical Report Documentation Page

1. Report No.	2.	3. Recipients Accession No.	
MN/RC 2012-35			
4. Title and Subtitle Recycled Unbound Materials		5. Report Date November 2012	
		6.	
7. Author(s) Tuncer B. Edil, James M. Tinjum, and Craig H. Benson		8. Performing Organization Report No.	
9. Performing Organization Name and Address Department of Civil and Environmental Engineering Geological Engineering Program University of Wisconsin – Madison 1415 Engineering Drive Madison, WI 53706		10. Project/Task/Work Unit No.	
		11. Contract (C) or Grant (G) No. (C) 89264 (WO) 2	
12. Sponsoring Organization Name and Address Minnesota Department of Transportation Research Services 395 John Ireland Blvd., MS 330 St. Paul, MN 55155		13. Type of Report and Period Covered Final Report	
		14. Sponsoring Agency Code	
15. Supplementary Notes http://www.lrrb.org/pdf/201235.pdf			

16. Abstract (Limit: 250 words)

The objective of this project was to characterize the properties of crushed recycled concrete (RCA) and asphalt pavement (RAP) as unbound base without being stabilized, to assess how RCA and RAP behave in the field and to determine how pavements can be designed using RCA and RAP. Issues to be considered include variability in material properties, purity of material, climatic effects, how to identify and control material quality, and leaching characteristics. This project included laboratory specimen and large-scale model tests and evaluation of field data from MnROAD test sections constructed using recycled materials. To identify the characteristics of RAP and RCA typically available in different parts of the country, samples were obtained from eight states: California, Colorado, Michigan, Minnesota, New Jersey, Ohio, Texas, and Wisconsin covering a geographically diverse area. A conventional base course was used as a control material. The extensive investigation undertaken on RCA and RAP indicate that these materials are generally suitable for unbound base course applications and they show equal or superior performance characteristics compared to natural aggregates in terms of stiffness, freeze-thaw and wet-dry durability, and toughness. Their typical compositional and mechanical properties and their variability are defined in this study providing a basis for design considerations. Their relative differences from natural aggregate such as temperature sensitivity, plastic deformations, and water absorption and retention characteristics are also well established. It is noted that some RAP may be sensitive to temperature change that may lead to rutting. This aspect needs to be considered in design.

17. Document Analysis/Descriptors	18. Availability Statement		
Recycled materials, Concrete aggregates, Freeze thaw tests, Wetting and drying tests, Modulus of resilience, Plastic deformation, Compaction, Thermal stresses, Impurities, Brick, Durability, Experiments, Reflectometers, Hydraulic properties, Water retention, Leaching	No restrictions. Document available from: National Technical Information Services, Alexandria, Virginia 22312		
19. Security Class (this report) Unclassified	20. Security Class (this page) Unclassified	21. No. of Pages 340	22. Price

Recycled Unbound Materials

Final Report

Prepared by:

Tuncer B. Edil
James M. Tinjum
Craig H. Benson

Department of Civil and Environmental Engineering
Geological Engineering Program
University of Wisconsin – Madison

November 2012

Published by:

Minnesota Department of Transportation
Research Services Section
395 John Ireland Boulevard, Mail Stop 330
St. Paul, Minnesota 55155

Acknowledgments

Financial support for this study was provided by Pool Fund TPF-5 (129) entitled Recycled Unbound Materials partnered by the California, Michigan, Minnesota, Ohio, Texas and Wisconsin Departments of Transportation. The lead agency was the Minnesota Department of Transportation. The conclusions and recommendations in this report are solely those of the authors and do not reflect the opinions or policies of the supporting agencies. Appreciation is expressed to Mr. John Siekmeier, the Lead Agency Contact and Messrs. Ben Worel, Tim Clyne, and Andrew Eller for supporting the field activities. The representatives of the partnering transportation agencies are acknowledged for their invaluable input to the research and providing large quantities of samples for testing. Drs. Young-Hwan Son and Ali Soleimanbeigi contributed to the analysis and project reports. Mr. Xiaodong Wang constructed the field lysimeters and assisted with programming of the test software. Graduate students Ryan F. Shedivy, Ozlem Bozyurt, Gregory J. Schaertl, Kongrat Nokkaew and Jiannan Chen undertook different parts of the laboratory and field research and contributed to the task reports. Numerous undergraduate assistants participated in laboratory investigations and field leachate sampling.

Table of Contents

List of Tables

List of Figures

Executive Summary

This document is the final report that presents the findings of research on unbound recycled materials, specifically recycled asphalt pavement (RAP) and recycled concrete aggregate (RCA), as road base course. The literature review conducted focused on evaluating the previous research conducted on RCA and RAP when used as an unbound base course. RAP and RCA are the two most common recycled construction materials used as base course. The literature implied that RAP and RCA have higher resilient moduli than natural aggregate; however, a lack of in-depth studies on characterizing RAP and RCA compositionally and mechanically was found.

A survey was conducted to better define the current state of practices involving the use, storage, and testing of materials used as granular base course in roadway applications (i.e. RAP and RCA). RCA was the most commonly used material, followed by RAP and recycled pavement material, RPM (defined to include HMA and base course and possibly some subgrade like in full-depth reclamation). However, when RAP and RPM combined account for a higher frequency and quantity of use than RCA. RAP and RCA are more commonly stockpiled before use while RPM is more commonly used immediately. The most common test used for specification with recycled materials is Grain Size Analysis using a dry sieve. To evaluate aggregate quality, the most common tests were: the California Bearing Ratio test to evaluate aggregate strength, LA Abrasion for toughness, and the Sulfate Soundness test for durability. From the survey, it was apparent that there is limited data for structural properties of RAP and RCA (i.e. no resilient modulus tests are performed).

To identify the characteristics of RAP and RCA typically available in different parts of the country, samples were obtained from eight states: California, Colorado, Michigan, Minnesota, New Jersey, Ohio, Texas, and Wisconsin covering a geographically diverse area. A conventional base course meeting the Class 5 gradation standard of the Minnesota Department of Transportation was used as a control material as well as a 50/50 RCA/Class 5 blend. These materials were characterized with respect to grain size distribution, fines content, asphalt content (RAPs), mortar content (RCAs), specific gravity, absorption, and impurities. The materials, although obtained form 8 different states, had reasonably consistent properties. Fines content was 3-4% for RCAs except two samples and lower for RAPs, i.e., 1-2%. The mortar content was about 50% with small variation for the RCA samples and the asphalt content was about 5% with small variations for the RAP samples. The most distinguishing physical characteristics were the grain size with some samples coarser and others finer. Most samples had grain size distributions within the bounds for RCA and RAP given in the literature.

The amount of deleterious materials present in RCA and RAP varied amongst the source of the materials. The most predominant impurities for RCA were asphalt aggregate, aggregate with plastic fibers, brick, and wood chips. Geotextiles and pavement markings were the predominant type of impurity in RAP. The average impurity content was 1% for RCA and 0.2% for RAP, indicating that recycling industry has developed sufficient controls. The effect of brick content on the resilient modulus and compaction of RCA was investigated at 0, 10, 20, and 30% brick by mass. No apparent trends were observed between SRM and brick content of RCA, but a decrease in plastic strain was observed with increased brick content. An increase in optimum

moisture content and decrease in dry unit weight was observed in RCA mixed with brick at 30% compared to 0% brick. This was attributed to brick having higher absorption and lower specific gravity and density than RCA.

The compaction characteristics were also determined using the modified Proctor test. Maximum dry unit weight (MDU) varies within a narrow range of 19.4 to 21.5 kN/m^3 for RAP at optimum moisture contents (OMC) of 5.2 to 8.8% and 19.4 to 20.8 5 kN/m^3 for RCA at OMC of 8.7 to 11.8%. The OMC of RAP was lower than RCA since asphalt coatings reduce the amount of water required to achieve MDU by preventing the water from reaching the individual particles of the material. RCA has high absorption capacity due to the porous nature of the cement paste portion. Therefore, the amount of water required to achieve the MDU for RCA is higher than for natural aggregate and RAP. Stepwise regression was performed by using multiple linear regressions to develop correlations (models) to predict the compaction characteristics (OMC and MDU) of RCA and RAP based on their gradation characteristics. OMC correlates significantly with the uniformity coefficient and percent moisture absorption and MDU correlates with OMC for both RAP and RCA.

Resilient modulus of the samples was measured on specimens at OMC and 95% modified Proctor MDU. Both simple exponential function with 2 parameters and the MEPDG model with 5 parameters were fitted to the test data. They both give a reasonable representation of the data. A summary resilient modulus (SMR) was calculated from the fitted equations at a stress level representative of the base course layer. A comparison of SRM indicated that RAP/RPM has the highest SRM of the recycled materials evaluated. RCA has slightly lower SRM in comparison to RAP/RPM, while Class 5 aggregate has the lowest SRM. Stepwise regression was performed by using multiple linear regressions to develop correlations (models) to predict SRM of RCA and RAP based on their physical and moisture content. SRM is significantly correlated with D_{30} and moisture content, i.e., OMC for RCA. The correlation for RAP involved other variables such as grain size characteristics (percent fines, D_{60}), asphalt content, specific gravity and percent absorption. Blending recycled materials with natural aggregate result in intermediate modulus between the moduli of the two materials.

The effect of compaction was evaluated by varying the effort of compaction and running resilient modulus tests on the specimens to compare compaction effort on stiffness. A decrease in compaction effort resulted in lower SRM for all materials, but the decrease was greater in the recycled materials than in natural aggregate. The resilient modulus decreased with an increase in moisture content for RAP and RCA. The effect of compaction moisture content on resilient modulus was greater for RCA than RAP. The rate of decrease in SRM for RAP is lower than RCA.

Large-Scale Model Experiment (LSME), a large prototype-scale test developed for simulating the performance of pavement sections in a laboratory setting was conducted on the RAP, RCA, Class 5 aggregate, and RCA-Class 5 blend samples, all from the MNROAD field test sections. The pavement sections, or parts of them, are loaded cyclically to simulate field traffic loads and the resilient modulus is back calculated from the recorded response. The moduli obtained from the LSME testing were compared to the resilient moduli determined using bench-scale laboratory resilient modulus tests in accordance with NCHRP 1-28a and the moduli from the field-scale methods using falling weight deflectometer (FWD). The scalability of the laboratory results to

field conditions was addressed by adjusting the resilient modulus to reflect a comparable stress-state and strain level. The plastic deformation of materials tested in the LSME was also assessed. The plastic deformation of RAP was much greater than that experienced by Class 5, whereas the plastic deformation of RCA was smaller than the plastic deformation experienced by the Class 5. SRM of RCA and RAP from the LSME was greater than that of Class 5. The recycled granular material tested in the LSME is sensitive to layer thickness, indicating that the resilient modulus of the material is sensitive to varying strain levels. After applying corrections for stress-state and strain level, the resulting low-strain moduli for FWD, LSME and bench-scale tests were determined and found to be of the same magnitude within a reasonable amount of variance thus indicating the scalability of laboratory modulus to operating field modulus although the directly obtained moduli from the three have different values.

The mechanical properties of RAP and RCA were also evaluated under different climatic conditions. The effects of freeze-thaw cycling on resilient modulus, wet/dry cycling on particle degradation, and the effects of temperature on resilient modulus were all evaluated. For the freeze-thaw cycles, a decrease in stiffness was observed in RAP after five cycles and further decrease was observed at 10 and 20 cycles. Class 5 aggregate (the control) saw a decrease in stiffness with increased freeze-thaw cycles, but overall a lower percentage of decrease than RAP. The RCA specimens saw a decrease in stiffness after the first five freeze-thaw cycles, but then an increase in stiffness after 10 and 20 freeze-thaw cycles. Overall, both RAP and RCA had higher stiffness than Class 5 regardless of the number of freeze-thaw cycles. To evaluate the effects of temperature on resilient modulus of RAP and RCA, specimens were tested using NCHRP 1-28a protocols at 7, 23, 35, and 50 °C. Essentially no decrease in SRM was observed in the RCA and natural aggregate specimens tested, but a decrease of approximately 30% was observed in two of the three RAPs tested between the 23 and 35 °C temperatures. An increase in strain rate with temperature was also observed in all RAPs, but was not present in the natural aggregates or RCA specimens. Micro-Deval and particle size distribution tests were conducted on RAP, RCA, and natural aggregate after 5, 10, and 30 wet/dry cycles and no apparent trend was found between particle degradation and wet/dry cycling of the material.

The hydraulic properties of RAP and RCA were investigated by determining their unsaturated hydraulic conductivities and also generating their soil-water characteristic curves (SWCCs) fitted with the van Genuchten and Mualem-van Genuchten models. All materials had high drainage capacities. RAP had the best drainage capacity due to the hydrophobic nature of the asphalt coating while RCAs tended to have the best ability to retain water because of its hydrophilic cement mortar. It was found that increasing the gravel content decreased the air entry pressure in recycled and natural aggregates while increasing the fines content increased the air entry pressure.

Samples of RCA were tested in the laboratory to determine their pH and leaching characteristics. Additionally, lysimeters were placed under the RCA base course and leachate samples were collected periodically to track the effluent pH and released metals during the base course service life in the field. Although the MNROAD site showed a consistently neutral pH (6.6 to 8.0), the leaching trend was different than that observed in the laboratory column leaching tests using the same RCA material and a Madison field site. The reasons are not known for this observation. As, Cr, Pb, and Se exceeded the maximum contaminant levels (MCLs) for the USEPA drinking water standard both at the Madison field site and in the laboratory column leaching tests.

However, although the MNROAD site concentrations of As, Pb, and Se for RCA were observed to exceed the corresponding MCL only once or twice and the leaching behaviors were similar to that of Class 5. For RAP, concentrations of As, Se and Sb were slightly higher than the corresponding USEPA groundwater maximum contaiminant level (MCL).

Falling Weight Deflectometer (FWD) tests were conducted at the MnRoad facility on pavement with base course material of RAP, RCA, and a 50/50 blend of RCA/Class 5, and Class 5 to determine deflection and resilient modulus from 2009 to 2012. Class 5 test cells had the most deflection, followed by blended RCA/Class 5, RAP, and RCA, respectively. An increase in air temperature decreased the stiffness of the overlying HMA layers and allowed a greater amount of deflection to occur over the entire pavement system. The stiffness of the HMA layer decreased during warm weather and increased during cold weather, but all other pavement layers (i.e. base, subbase, and subgrade) retained a relatively constant stiffness regardless of temperature. The resilient modulus was greater at the mid-lane compared to the outer wheel path because of the greater overall loading in these areas. Resilient modulus has not indicated any deterioration over the last 4 years.

The extensive investigation undertaken on RCA and RAP indicate that these materials are suitable for unbound base course applications. They show equal or superior performance characteristics compared to natural aggregates in terms of stiffness, freeze-thaw and wet-dry durability, and toughness. Their typical compositional and mechanical properties and their variability are defined in this study providing a basis for design considerations. Their relative differences from natural aggregate such as temperature sensitivity, plastic deformations, and water absorption and retention characteristics are also well established. It is noted that some RAP may be sensitive to temperature change that may lead to rutting. This aspect needs to be considered in design.

1. Literature Search Report on Recycled Asphalt Pavement and Recycled Concrete Aggregate

1.1 Introduction

The production of demolition and construction waste has been increasing at a gradual rate in recent years (Poon et al. 2006). The amount of landfill available to contain this material has been decreasing, and the need to find appropriate disposal locations has been of increasing concern (Kuo et al. 2002). Recycling programs offer a viable solution. The use of these materials as recycled base course in new roadway construction has become more common in the last twenty years, with some municipalities reporting as much as 400,000 tons of recycled materials used in this manner (Bennert et al. 2000, Nataatmadja and Tan 2001).

Recycled roadway materials are typically generated and reused at the same construction site, providing increased savings in both money and time (Bennert et al. 2000). It has been speculated that in some municipalities recycled materials cost less to use than conventional crushed-stone base material by as much as 30% (Blankenagel and Guthrie 2006). Despite the increased acceptance of recycled base materials, research concerning the mechanical properties and durability of such materials has been lacking (Bennert et al. 2000, Guthrie et al. 2007).

The most widely used recycled materials are recycled asphalt pavement (RAP) and recycled concrete aggregate (RCA). RAP is produced by removing and reprocessing existing asphalt pavement (Guthrie et al. 2007, FHWA 2008), and RCA is the product of the demolition of concrete structures such as buildings, roads and runways (Kuo et al. 2002). The production of RAP and RCA results in an aggregate that is well graded and of high quality (FHWA 2008). The aggregates in RAP are coated with asphalt cement that reduces the water absorption qualities of the material (Guthrie et al. 2007). In contrast, the aggregates in RCA are coated with a cementitious paste that increases the water absorption qualities of the material (Poon et al. 2006).

1.2 Production

There is some ambiguity regarding the nomenclature involved in the production of RAP. Based on the experience of the Geo Engineering Program at the University of Wisconsin-Madison, the following classification is recommended to remove ambiguity in nomenclature: RAP refers to the removal and reuse of the hot mix asphalt (HMA) layer of an existing roadway (FHWA 2008); full depth reclamation (FDR) refers to the removal and reuse of the HMA and the entire base course layer; and recycled pavement material (RPM) refers to the removal and reuse of either the HMA and part of the base course layer or the HMA, the entire base course layer and part of the underlying subgrade implying a mixture of pavement layer materials (Guthrie et al. 2007). Unless specified, these three distinct recycled asphalt materials will be collectively referred to as RAP.

RAP is typically produced through milling operations, which involves the grinding and collection of the existing HMA, and FDR and RPM are typically excavated using full-size

reclaimers or portable asphalt recycling machines (FHWA 2008, Guthrie et al. 2007). RAP can be stockpiled, but is most frequently reused immediately after processing at the site. Typical aggregate gradations of RAP are achieved through pulverization of the material, which is typically performed with a rubber-tired grinder (Bejarano et al. 2003).

The production of RCA involves crushing the material to a gradation comparable to that of typical roadway base aggregate. Fresh RCA typically contains a high amount of debris and reinforcing steel, and the RCA must be processed to remove this debris prior to placement. The material is first crushed in a jaw crusher that breaks the steel from the material and provides an initial crushing of the concrete (FHWA 2008). The material is sent down a picking belt where the steel is removed from the material (Kuo et al. 2002). The remaining concrete material is further crushed and screened to a predetermined gradation (FHWA 2008).

1.3 Material Properties

The gradation of RAP can be compared to that of a crushed natural aggregate, although with a higher content of fines. The high fine content is the result of degradation of the material during milling and crushing operations. In RPM the inclusion of subgrade materials in the recycled material also contributes to a higher instance of fines. Finer gradations of RAP are produced through milling operations compared to crushing operations (FHWA 2008). Table 1.1 provides a breakdown of typical physical and mechanical properties of RAP.

RCA is processed exclusively through crushing operations, and is very angular in shape (FHWA 2008). Depending on the crushing methods, the particle size distribution of an RCA can have a wide variability; with a lower particle density and greater angularity than would normally be found in more traditional virgin base course aggregates. Residual mortar and cement paste are typically found on the surface of the RCA, as well as contaminants associated with construction and demolition debris (Kuo et al. 2002). The presence of this mortar contributes to a rougher surface texture, lower specific gravity, and higher water absorption than typical aggregates (FHWA 2008).

The self-cementing capabilities of RCA are an interesting secondary property. The crushed material exposes un-hydrated concrete that can react with water, potentially increasing the materials strength and durability when used as unbound base course for new roadway construction. It follows that service life could also be extended as a result of these properties. Although widely acknowledged, not much actual documentation has been published regarding this secondary hydration (Blankenagel et al. 2006). Although the cause of self-cementing properties has been studied, the actual effect of such parameters as age, grade, and mix-proportions of the RCA on the overall cementitious effect has yet to be determined (Poon et al. 2006). This effect is outside the scope of this literature review.

provides a breakdown of typical physical and mechanical properties of RCA.

1.4 Objective

The purpose of this literature review is to summarize the current state of knowledge regarding the mechanical behavior of RCA, RAP and blends of these recycled materials with traditional

aggregate material. Laboratory and field investigations were considered in the scope of this review, and long-term performance issues were noted. Of particular interest was the effect the recycled material had on resilient modulus values, stress state sensitivity, and overall material degradation.

1.5 Methods For Specification

When considering a recycled material for use as an unbound base course, the two most commonly used specifications are the gradation and the moisture-density relationship of the material. The gradation of a material can provide an indication of what the permeability, frost susceptibility, and shear strength of the material might be, and is determined through the use of material screening tests (Saeed 2008). Screening tests are typically conducted through sieve analysis according to ASTM Standards C 117 and C 136, and AASHTO Standards T-27 and T-11. Some highway agencies and DOTs utilize their own screening test methods, such as Florida DOT FM1 T-027. Classification of soils is performed using the Unified Soil and AASHTO methods according to ASTM D 2487 and AASHTO M 145, respectively.

The determination of moisture-density relationships can help define the ideal density conditions that a material can achieve through compaction. Moisture-density relationships are established through compaction tests conducted according to the following standards: AASHTO T 99 Method C, AASHTO T-180 or ASTM D698, ASTM D 1557. Depending on the compaction effort to be used in the field, compaction tests can be performed in standard or modified variations. The information is used to determine the optimum moisture content (OMC) and the maximum dry density (MDD) of a material. Material properties such as strength, stiffness and moisture susceptibility can be determined through testing of specimens prepared based on this data, (Guthrie et al. 2007).

Other aggregate classification methods involve the determination of the specific gravity, absorption and Atterberg limits of the soils. The specific gravity and absorption characteristics of a given recycled aggregate are determined using ASTM D 854, and Atterberg limits of recycled aggregates are assessed using ASTM D 4318, AASHTO T 89 and T 90 (Blankenagel et al. 2006, Guthrie et al. 2007).

1.6 Summary of Material Degradation

Table 1.3 through Table 1.5 represent the available estimated gradations of the RAP, RCA and RPM encountered in this literature review. These three tables show that the coefficient of variance of gradation for the RAP, RPM and RCA remains approximately 40% or lower for materials retained on the #8 sieve and larger. This trend continues for the RPM and RCA retained in the remaining finer sieves. However, it can be seen that for RAP aggregates finer than the #8 sieve, the coefficient of variance for the data noticeably increases. This is more than likely due to the large gradation values found in the sample Guthrie R1 (Guthrie et al. 2007).

If the data for this sample is removed, the resulting variances fall within the same variance. The sample Guthrie R1 was a composite taken at different locations with different equipment, and therefore the actual source for the erratic gradation of the material could not be determined (Guthrie et al. 2007). Gradation requirements for recycled materials vary from agency to agency.

Unless indicated, the recycled materials referenced in this report passed the gradation requirements specified by the respective agencies.

Blankenagel et al. (2006) performed gradations on material taken from demolition sources as well as from relatively new materials sampled from batch-plant overruns and haul-back material sources. Batch plant overruns refer to excess concrete produced at a batch plant but never delivered to a job site, and haul-back material refers to excess concrete delivered to a job site but returned to the batch plant. The haul-back material was found to have more medium and fine materials than the demolition material. Although Blankenagel recognizes the source of the gradation differences could be due to crushing operations, the most likely reason is probably related to the mechanical breakdown tendencies of the materials. The haul-back material would have a higher porosity and lower strength due to being more properly consolidated and cured, resulting in a greater degree of pulverization regardless of crushing techniques.

In the study conducted by Kuo et al. (2002), gradations of the RCA met Florida DOT specifications. However, for specifications regarding average gradation for each sieve, the standard deviations of the 3/4", 3/8", #4 and #10 sieves were all excessively high and each fell out of specification. The test would indicate that for recycled materials, these sieves might be considered more critical than the others.

1.7 Summary of Moisture-Density Characteristics

Table 1.6 and Table 1.7 represent the available moisture-density relationships for the RAP, RPM and RCA encountered in this literature review. For various blends of RAP with pure aggregate, some trends were noted regarding the effect of RAP content on the MDD and OMC of a material. Guthrie et al. (2007) found that an increase in RAP content led to a decrease in MDD and OMC values (Guthrie et al. 2007). The aggregates particles in the RAP were partially encased in asphalt, which decreased the specific gravity. It was further assumed that the partial asphalt coating reduced the aggregate water absorption potential and inter-particle friction, leading to a reduction in the required water to achieve MDD.

For various blends of RAP with pure aggregate, some trends were noted regarding the effect of RAP content on the MDD and OMC of a material. Guthrie et al. (2007) found that an increase in RAP content led to a decrease in MDD and OMC values. The aggregates particles in the RAP were partially encased in asphalt, which decreased the specific gravity. It was further assumed that the partial asphalt coating reduced the aggregate water absorption potential and inter-particle friction, leading to a reduction in the required water to achieve MDD.

An interesting variation in the study by Kim et al. (2007) was the use of a gyratory compaction test (GCT) instead of a proctor compaction test (PCT) to prepare RAP specimens. Comparisons with field density measurements indicated that MDD and OMC calculations determined from GCT methods were a better correlation than those determined by PCT testing. When compared to PCT results, GCT results showed a large change in MDD values and a small change in OMC values. Kim noted the effect of RAP content on the MDD and OMC of aggregate/RAP blends. As the RAP content of the material increased, the OMC of the material decreased for both the GCT and PCT prepared specimens. As with the study by Guthrie, the increase in asphalt content most likely reduced the absorption of the material, leading to the decrease in OMC. As the RAP

content of the material increased, the MDD decreased for the PCT-prepared specimens and remained the same for GCT-prepared specimens.

Bennert et al. (2000) investigated the effect of recycled content on the MDD and OMC of samples containing both RAP and RCA. The study found that as the RAP and RCA content of a material increased, the MDD of the material decreased. As was found in the Guthrie et al. (2007) and Kim et al. (2007) studies, the OMC of the material decreased with increasing RAP content. However, as the RCA content of the material increased, the OMC also increased.

In the study conducted by Saeed et al. (2008), it was found that in general virgin aggregates had a higher MDD than pure (100%) RAP and RCA samples. In agreement with the study by Kim et al. (2007), the MDD of the material decreased as the RAP and RCA content of recycled material/aggregate mixtures increased.

Blankenagel et al. (2006) noted the effect of material source on the MDD and OMC of RCA. The demolition material used in his study had an OMC of 9.7% and a MDD of 1830 kg/m^3, whereas the haul-back material had an OMC of 10.6% and a MDD of 2,020 kg/m^3. The haul-back material had a higher fines content, which resulted in higher MDD and OMC values than those found in the demolition material. The increased fines, resulting in a tighter aggregate matrix, more readily fill pore spaces.

Investigations on two RPM at the University of Wisconsin-Madison indicated an OMC of 6.5 to 7.5% and a MDD of 2162 kg/m^3 (Carmargo et al. 2009, Wen et al. 2007).

1.8 Methods for Design and Performance Tests

The two most common tests used to determine strength parameters for unbound recycled materials are the Static Triaxial Test and the California Bearing Ratio test. The Static Triaxial Test is typically performed in accordance with ASTM D 2850 and AASHTO T 296, although some state DOTs have been known to use their own standards such as CalTRAN (Bejarano et al. 2003). The California Bearing Ratio test is typically performed in accordance with ASTM D 1883 or AASHTO T 193. Kuo et al. (2002) uses the Limerock Bearing Ratio test, which is indigenous to the Florida DOT, and is documented as standard FM5-515 T.

The two most common tests used to determine the stiffness for unbound recycled materials are the resilient modulus test and the free-free resonant column test. The resilient modulus test is typically performed in accordance with AASHTO TP46-94, Strategic Highway Research Program Test Protocol P-46 (SHRP P-46), or National Cooperative Highway Research Program Protocol 1-28A (NCHRP 1-28A). The free-free resonant column test is typically performed according to ASTM D 4015. Permanent deflection is typically performed by use of a cyclic triaxial test. Moisture susceptibility is typically determined by use of the Tube Suction Test. There is no current standard for the use of the test; however Guthrie and Blankenagel use methods as outlined by Scullion and Saarenketo in 1997 (Blankenagel et al. 2006, Guthrie et al. 2007, Scullion and Saarenekto 1997).

Two typical tests used to assess the durability of a material are the LA abrasion test and the freeze-thaw cycling test. The LA abrasion test is typically performed in accordance with ASTM

C 131, although other methods are sometimes used by different agencies, such as Australian test method AS 1141.23. The freeze-thaw cycling test is typically performed in accordance with ASTM D 560.

A method that follows ASTM D 6035 for specimen conditioning is used at the University of Wisconsin-Madison for frost susceptibility (Carmargo et al. 2009, Wen et al. 2007). ASTM D 6035 describes a method to determine the freeze-thaw effects on hydraulic conductivity; in the UW procedure, resilient modulus tests are performed to determine the freeze-thaw effects instead of hydraulic conductivity. Test specimens are compacted in molds at the specified moisture content and density. Preliminary testing on specimens instrumented with a thermocouple showed that complete freezing occurred within 1 day at -19°C. Thus, all specimens are retained in their mold and wrapped with plastic sheet in the freezer for at least 1 day. After freezing, the height and weight are measured and the specimen is allowed to thaw at room temperature. This process is repeated as many freeze-thaw cycles as desired but typically 5 cycles is used. After the last cycle, specimens are extruded frozen and thawed inside the resilient modulus cell prior to resilient modulus testing.

1.9 Summary of Strength and Stiffness Tests

Bejarano et al. (2003) conducted static triaxial tests on one RAP and two different aggregate materials. Individual RAP and aggregate specimens were compacted at OMC and 95% and 100% of maximum wet density (MWD) according to CalTRANS specification CTM 216. Static triaxial tests were conducted at confining pressures of 0, 35, 70 and 105 kPa. After comparing the shear strengths of the RAP and aggregate, it was determined that the shear strength calculated for the RAP was comparable in magnitude to shear strengths calculated for the representative aggregate materials. This shear strength correlation was valid at both 95% and 100% MWD and each of the four confining pressures. Bejarano et al. (2003) also conducted stiffness tests for the three materials according to SHRP test protocol P-46. Of the three tested materials, the RAP had a higher resilient modulus than the two aggregate materials tested at 95% and 100% MWD. When the compaction level was increased from 95% to 100%, the resilient modulus of the RAP and one of the aggregate materials increased. This change in compaction level had no effect on the resilient modulus of the second aggregate material. Lime stabilized RAP specimens cured for 7 days had a higher resilient modulus than the non-stabilized material in all cases.

Bennert et al. (2000) conducted a similar test in which the shear strength of pure (100%) RAP and RCA were evaluated against the shear strength of a dense graded aggregate base course (DGABC) typical of the area the recycled materials would be used. Static triaxial test results for the pure samples indicate that the aggregate alone had higher shear strength than either RAP or RCA alone. Stiffness tests were also conducted on blends of the materials used in the study. Specimens were prepared combining the aggregate with RAP and RCA percentages of 100%, 75%, 50%, 25% and 0% (100% aggregate). Contrary to the strength behavior, it was found that as the amount of recycled material in the blend increased, the resilient modulus of the blended material also increased. Pure (100%) specimens of RAP and RCA had higher resilient modulus values than pure specimens of the virgin aggregate.

Guthrie et al. (2007) evaluated the effects of RAP content on the shear strength of base course materials using the California Bearing Ratio test. Two RAP and two aggregate materials (one

recycled and one virgin) were acquired for the test. Specimens were prepared at RAP percentages of 100%, 75%, 50%, 25% and 0% (100% aggregate) for each of the permutations of RAP and aggregate samples. The tests found that the shear strength decreased with an increase in RAP content supporting Bennert et al.'s results.

Blankenagel et al. (2006) conducted a study documenting the difference between RCA samples obtained from demolition projects with relatively new RCA samples obtained through batch-plant overruns and haul-backs. The strength of the material was determined immediately after compaction using the California Bearing Ratio test. The demolition RCA and the haul-back RCA had CBR test results of 22% and 55% respectively. Unconfined compressive strength tests conducted on the material were used to determine strength gain over time due to the residual hydration in the RCA. The strength of the demolition material increased 130% and 180% at 3 and 7 days after compaction, respectively. The strength of the haul back material increased 150% to 190% at 3 and 7 days after compaction, respectively. Higher strength gain in the haul back material is most likely due to a greater amount of unreacted cement in the material as well as a finer material gradation. The average 7-day strengths for the demolition and haul-back material were 1260 kPa and 1820 kPa, respectively.

Kuo et al. (2002) incorporated the use of the Limerock Bearing Ratio (LBR) in Florida to determine the strength of RCA to be used as potential base course. The overall LBR values for the materials tested were 182%, which is higher than the required minimum value of 100%.

Kim et al. (2002) studied the effect of RAP content on the resilient modulus of blended aggregate base course. An in-situ blend of FDR was taken during the reconstruction of an existing road along with pure samples of RAP and aggregate materials. The FDR and several blends of the pure RAP and aggregate base material were tested for material stiffness using the resilient modulus in accordance with NCHRP 1-28A protocol. Blended mixtures of the pure materials were prepared at RAP to aggregate ratios (%/%) of 0/100, 25/75, 50/50 and 75/25. The study found that for an increase in RAP content, the resilient modulus of the blended material increased (Li et al. 2007). The effects of increased RAP content were more defined when the blends were exposed to higher confining pressures; however specimens also experienced higher permanent deformation at higher confining pressures. Specimens tested at 65% optimum moisture content had higher resilient modulus values when compared to specimens prepared at 100% OMC. This trend was consistent for all confining pressures. At low confining pressures (~20kPa), specimens with RAP to aggregate ratios of 50% to 50% and specimens consisting of 100% aggregate had resilient modulus values that were approximately equivalent. As the confining pressures increased, the 50/50 and pure RAP blends became stiffer. The 50/50, 100% RAP and in-situ material tested at the corresponding site had similar resilient modulus values.

Nataatmadja et al. (2001) evaluated the resilient modulus of four RCAs. One commercial and three laboratory-produced RCAs were used in the study. The commercial RCA had an estimated original concrete compressive strength of 15 MPa, and the three laboratory manufactured RCAs had original concrete compressive strengths of 18.5, 49, and 75 MPa. The materials were tested individually and were not blended with any other material, although each material was prepared and mixed as to produce a particle size distribution comparable to typical road aggregate blends. The study found that the resilient modulus of each of the RCAs tested was comparable or better (higher) than the typical aggregates used for roadway base course; the resilient modulus seemed

to increase with an increase in the compressive strength of the material. An increase in elongated particles also led to a decrease in resilient modulus, as these particles were more prone to degradation after extensive loading. Nataatmadja suggests that RCA with very high compressive strengths are more prone to break into elongated particles during crushing, resulting in a lower resilient modulus than would otherwise be expected. One exception in the test is that the specimen with a high flakiness index produced a lower strength value than would be expected.

Guthrie et al. (2007) used the free-free resonant column test to determine the stiffness of RAP and aggregate blends. At OMC, the stiffness of the material decreased with the addition of 25% RAP, and then increased with the addition of 50%, 75%, and 100% RAP. When the material was dried for 72 hours, the trend reversed: the stiffness of the material increased with the addition of 25% RAP and then decreased with the addition of 50%, 75% and 100% RAP. This decrease in stiffness can be attributed to the softening of the asphalt in the RAP during the drying process. Each specimen was then soaked for 24 hours prior to being tested for stiffness a third time. As with the oven-dried specimens, the soaked specimens displayed an increase in stiffness with the addition of 25% RAP followed by a decrease with increased RAP content. However, the soaked materials displayed a 40% to 90% decrease in stiffness when compared to the oven-dried materials.

Blankenagel et al. (2006) also used the resonant column test on RCA samples procured from demolition and haul-back sources. During the first 12 hours in 100% relative humidity, the modulus increased 390% for the demolition material and 940% for the haul-back material. Again, a greater amount of unreacted cement in the haul-back material accounts for the larger stiffness. Average 7-days stiffness measurements for the demolition and haul-back materials were 100 MPa and 150 MPa, respectively.

The tests performed at the University of Wisconsin-Madison on two RPMs indicated results in general support of the investigations summarized above (Carmargo et al. 2009, Wen et al. 2007, Wen et al. 2008). The unsoaked CBR values of RPM varied from 9 to 38 and, as an indicator of strength, were lower than the CBR of aggregates with similar gradation. However, higher resilient moduli (257-309 MPa) were measured consistently for RPM compared to different crushed aggregates qualified as base course material (Carmargo et al. 2009).

Addition of fly ash increased the modulus of RPM (at least a factor of 6, which is less than for a similarly stabilized natural aggregate), and the modulus increased as the fly ash content was increased (Carmargo et al. 2009). Modulus also increased with curing time, with the rate of increase being largest between 7 and 28 d of curing. The moduli of RPM stabilized with fly ash were independent of bulk stress and could be described by a constant modulus.

1.10 Summary of Moisture Susceptibility Tests

In the tube suction test, a specimen is oven dried for 72 hours before being allowed to soak in a shallow water bath for 10 days. Over the course of the soaking period, unbound water within the material rises through the aggregate matrix and collects at the surface. The dielectric value at the surface of the material increases with an increase in the amount of unbound water permeating the specimen, and thereby provides an estimate of the materials susceptibility to moisture permeation.

Guthrie et al. (2007) used the tube suction test to determine the effect of RAP content on the moisture susceptibility of RAP/aggregate blends. It was found that the moisture susceptibility of the material increased as RAP was added to the mixture. However, tests were only conducted with the addition of 25% and 50% RAP. Materials with RAP contents above 75% were classified as non-moisture-susceptible and were not tested. Overall, the dry density of the blended material decreased as RAP content increased.

Blankenagel et al. (2006) used the tube suction test on demolition and haul-back RCA to help determine the moisture susceptibility characteristics of the material. The moisture susceptibility of the demolition material was classified as "good", with a dialectic value of 6.4 and a gravimetric water content of 10.6%. The moisture susceptibility of the haul back material was classified as "marginal", with a dialectic value of 15.0 and a gravimetric water content of 2.0%.

1.11 Summary of Durability Tests

Blankenagel et al. (2006) incorporated the LA Abrasion and freeze-thaw cycling test into his study comparing demolition and haul-back materials. Results of the LA Abrasion tests indicated that the demolition and haul-back materials experienced average material losses of 31% and 18%, respectively. The primary cause of the degradation was thought to be the stripping of cement paste from the aggregate. This degradation caused an increase in fines that affected each of the two RCAs differently. The demolition material was initially low in fines content, and an increase in degradation fines would lead to an increase in MDD. The haul-back material was initially high in fines content, and the addition of degradation fines would decrease the structural stability and increase the moisture susceptibility of the material.

Nataatmadja et al. (2001) attempted to use the LA abrasion test to determine the relative hardness of the four RCAs. Commercial RCA had a lower hardness than laboratory manufactured RCAs, even though commercial RCA had the lowest (estimated) compressive strength. The relative hardness between the laboratory- manufactured RCAs could not be differentiated by the LA Abrasion Test method, most likely due to test severity.

Blankenagel et al. (2006) used freeze-thaw cycling to measure the durability of the demolition and haul-back RCMs. Freeze thaw testing was performed after 7 days of curing. Specimens were submerged for 4 hours, frozen (-29 deg C) for 24 hours and thawed (+20 deg C) for 24 hours. Stiffness was measured after each freezing period and after each thawing period. The demolition RCM experienced a 30% stiffness loss within the first two cycles and thereafter stabilized at a stiffness of 70 MPa. The haul-back RCM experience a 90% stiffness loss over the first 9 cycles and thereafter stabilized at a stiffness of 30 MPa. Unconfined compressive strength tests for the materials after freeze-thaw testing indicated strength losses of 52% and 28% for the demolition and haul-back material, respectively.

Freeze-thaw cycling tests performed at the University of Wisconsin-Madison showed that there was a small effect on resilient modulus (less than 15%) for RPM and also for natural aggregate with or without fly ash, with no consistent effect for materials stabilized with fly ash.

1.12 Summary of Permanent Deflection Tests

Bennert et al. (2000) studied the effect of recycled material content on the permanent deflection experienced by base course materials. Specimens were created from blends of aggregate with either RAP or RCA. For cyclic loads of 100,000 cycles, specimens blended with RCA were found to have the lowest amount of permanent deformation, and specimens blended with RAP had the highest amount of permanent deformation.

RPMs tested at the University of Wisconsin-Madison exhibited smaller plastic strains during resilient modulus testing than base course aggregate, i.e., the opposite of the resilient modulus trend (Carmargo et al. 2009). However, other data show that plastic strains for RPM may be higher or lower than those of conventional base aggregates, depending on the type of aggregate used. Plastic strains for RPM stabilized with fly ash were smaller than the plastic strains of the RPM alone.

1.13 Conclusions

Several important findings were noted in the course of this literature review. Kim et al. (2007) compared the compaction properties of specimens prepared by typical proctor methods with specimens prepared with a gyratory compactor and found that the OMC and MDD of the specimens compacted via gyratory compactor were found to more closely correlate with field density measurements. Kim et al. (2007) also found that at low confining pressures, pure aggregate and 50%/50% blends of RAP and aggregate had an equivalent stiffness, but at high confining pressures the 50%/50% blends had a higher stiffness than the pure aggregate. Bennert et al. (2000) found that pure specimens of RAP and RCA had higher resilient moduli than pure virgin aggregate specimens. Bennert also found that specimens of pure aggregate had higher shear strength than pure RAP or RCA specimens. This trend is supported in a study by Guthrie et al. (2007) in which RAP/aggregate blends showed a decrease in shear strength as RAP content increased. In general, RPM seems to show a better response than natural aggregate for similar gradation and compaction in tests that induce relatively smaller strains such as resilient modulus tests than tests that induce large strains such as triaxial compression or CBR tests.

1.14 Tables

Table 1.1 Typical Physical Properties of RAP (FHWA 2008)

Physical Properties	
Unit Weight	1940 - 2300 kg/m^3 (120 - 140 pcf)
Moisture Content	Normal: Up to 5% Maximum: 7 - 8%
Asphalt Content	Normal: 4.5 – 6%
Asphalt Penetration	Normal: 10 – 80% at 25°C (77°F)
Absolute Viscosity or Recovered Asphalt Cement	Normal: 4000 – 25000 poises at 60°C (140°F)
Mechanical Properties	
Compacted Unit Weight	1600 – 2000 kg/m^3 (100 – 125 pcf)
California Bearing Ratio (CBR)	100% RAP: 20 – 25% 40% RAP and 60% Natural Aggregate: 150% or Higher

Table 1.2 Typical Physical Properties of RCA (FHWA 2008)

Physical Properties	
Specific Gravity	2.2 to 2.5 (Coarse Particles) 2.0 to 2.3 (Fine Particles)
Absorption	2 to 6 (Coarse Particles) 4 to 8 (Fine Particles)
Mechanical Properties	
LA Abrasion Loss	20 – 45 (Coarse Particles)
Magnesium Sulfate Soundness Loss	4 or Less (Coarse Particles) Less than 9 (Fine Particles)
California Bearing Ratio (CBR)	94 – 148%

Table 1.3 Gradations of RAP *

Material	% Passing											
	#200	#100	#50	#30	#16	#8	#4	3/8"	1/2"	3/4"	1	1.5
Bejarano et al. (2003) Pulverized	2	3	7	12	20	31	46	68	---	100	---	---
Guthrie et al. (2007) R1	8	11	15	23	35	45	58	82	---	99	---	---
Guthrie et al. (2007) R2	1	3	8	12	21	39	59	82	---	97	---	---
Bennert et al. (2000) RAP	1	2	3	5	10	20	39	68	---	90	---	---
Saeed et al. (2008) RAP-LS-MS	3	5	9	12	19	27	38	62	75	95	95	100
Saeed et al. (2008) RAP-GR-CO	1	2	5	12	18	25	39	63	75	92	97	100
Saeed et al. (2008) RAP-GV-LA	0	2	6	11	17	23	33	61	76	92	98	100
Average Value	2.3	4.0	7.6	12.4	20.0	30.0	44.6	69.4	75.3	95.0	96.7	100
Standard Deviation	2.7	3.3	3.8	5.3	7.5	9.0	10.2	9.0	0.6	3.8	1.5	0.0
Coefficient of Variance	1.2	0.8	0.5	0.4	0.4	0.3	0.2	0.1	0.0	0.0	0.0	0.0

*Gradations estimated from existing gradation curves in literature. Actual percent passing values are within $\pm$1%.

Table 1.4 Gradations of RPM *

Material	% Passing																		
	#200	#100	#60	#50	#40	#30	#20	#16	#10	#8	#4	1/4“	3/8”	1/2"	3/4"	7/8”	1”	1.5”	2”
Li et al. (2007) RPM-1	16	19	24	---	33	---	50	---	66	---	85	---	---	---	---	---	---	---	---
Li et al. (2007) RPM-2	12	15	18	---	24	---	35	---	49	---	66	---	---	---	---	---	---	---	---
Li et al. (2007) RPM-3	3	5	7	---	13	---	26	---	41	---	59	---	---	---	---	---	---	---	---
Li et al. (2007) RPM-4	9	9	13	---	20	---	33	---	50	---	67	---	---	---	---	---	---	---	---
Li et al. (2007) RPM-5	11	12	17	---	25	---	40	---	57	---	76	---	---	---	---	---	---	---	---
Li et al. (2007) RPM-6	6	8	10	---	16	---	27	---	41	---	59	---	---	---	---	---	---	---	---
Li et al. (2007) RPM-7	5	7	9	---	14	---	25	---	38	---	53	---	---	---	---	---	---	---	---
Li et al. (2007) RPM-8	7	9	12	---	20	---	34	---	52	---	70	---	---	---	---	---	---	---	---
Li et al. (2007) RPM-9	9	11	14	---	24	---	39	---	52	---	65	---	---	---	---	---	---	---	---
Li et al. (2007) RPM-10	10	12	16	---	25	---	41	---	55	---	70	---	---	---	---	---	---	---	---
Carmargo et al. (2009)	11	13	18	---	22	---	28	---	38	---	54	61	70	78	93	---	100	---	---
Wen & Edil (2009)	6	6	---	9	---	16	---	26	39	38	60	---	69	77	96	---	99	---	100
Wen et al. (2007)	4	5	---	8	---	14	---	22	31	34	51	---	72	82	---	98	99	100	---
Wen et al. (2007)	3	5	7	---	13	---	22	---	35	---	55	62	74	84	95	97	99	---	100
Average Value	8.0	9.7	13.8	8.5	20.8	15	33.3	43.3	44.8	60.1	63.3	68.0	75.8	86.4	95.8	98.7	99.4	100	100
Standard Deviation	3.8	4.2	5.1	0.7	6.0	1.4	8.2	2.8	9.9	2.8	9.6	0.7	2.2	3.3	1.5	0.7	0.5	0	0
Coefficient of Variance	0.4	0.4	0.4	0.08	0.3	0.1	0.2	0.1	0.2	0.0	0.2	0.0	0.0	0.0	0.0	0.0	0.0	0.0	0.0

*Gradations estimated from existing gradation curves in literature. Actual percent passing values are within $\pm$1%.

Table 1.5 Gradations of RCA *

Material	% Passing												
	#200	#100	#50	#30	#16	#10	#8	#4	3/8"	1/2"	3/4"	1	2"
Bennert et al. (2000) RCA	7	10	15	24	28	---	32	42	56	---	76	---	---
Blankenagel et al. (2006) Demolition	3	6	9	12	15	---	20	31	60	---	---	---	---
Blankenagel et al. (2006) Haul-Back	8	10	13	23	37	---	46	60	72	---	---	---	---
Saeed (2008) RCP-LS-IL	4	8	15	26	36	---	48	60	89	---	99	100	---
Saeed (2008) RCP-GV-LA	8	11	16	26	32	---	48	64	74	---	89	96	---
Saeed (2008) RCP-GR-SC	3	5	9	13	19	---	27	38	62	76	95	98	---
Kuo et al. (2002) District 1	4	---	12	---	---	30	---	45	52	---	76	99	100
Kuo et al. (2002) District 2	5	---	17	---	---	30	---	40	53	---	76	99	100
Kuo et al. (2002) District 4	5	---	11	---	---	28	---	40	56	---	81	99	100
Kuo et al. (2002) District 5	4	---	18	---	---	45	---	56	80	---	100	100	100
Kuo et al. (2002) District 6	5	---	20	---	---	30	---	33	37	---	50	86	99
Kuo et al. (2002) District 7	5	---	20	---	---	40	---	50	63	---	82	99	100
Average Value	5.1	8.3	14.6	20.7	27.8	33.8	36.8	46.6	62.8	76.0	82.4	97.3	99.8
Standard Deviation	1.7	2.4	3.8	6.4	9.1	6.9	12.1	11.2	14.1	---	14.8	4.4	0.4
Coefficient of Variance	0.3	0.3	0.3	0.3	0.3	0.2	0.3	0.2	0.2	---	0.2	0.0	0.0

*Gradations estimated from existing gradation curves in literature. Actual percent passing values are within $\pm$1%.

Table 1.6 Maximum Dry Density and Optimum Moisture Content of RAP and RPM

Material	Proctor Effort	Maximum Dry Density, kg/m3	Optimum Moisture Content, %
Bejarano et al. (2003) Pulverized	Caltrans CTM 216	2332	5.5
Bennert et al. (2000) RAP	Standard	1872	5
Guthrie et al. (2007) R1	Modified	2083	5.6
Guthrie et al. (2007) R2	Modified	1842	5.8
Saeed (2008) RAP-LS-MS	Standard	1988	6.3
Saeed (2008) RAP-GR-CO	Standard	2015	10.3
Saeed (2008) RAP-GV-LA	Standard	1978	5.4
Carmargo et al. (2009) RPM	Standard	2161	7.5
Wen et al. (2007)	Modified	2162	6.5

Table 1.7 Dry Density and Optimum Moisture Content of RCA

Material	Proctor Effort	Maximum Dry Density, kg/m3	Optimum Moisture Content, %
Bennert et al. (2000) RCA	Standard	1984	7.5
Blankenagel et al. (2006) Demolition	Modified	1830	9.7
Blankenagel et al. (2006) Haul Back	Modified	2020	10.6
Saeed (2008) RCP-LS-IL	Standard	1971	11
Saeed (2008) RCP-GV-LA	Standard	1950	9
Saeed (2008) RCP-GR-SC	Standard	1990	9.5
Kuo et al. (2002) UCF	Modified	1823	11.2
Kuo et al. (2002) FDOT	Modified	1839	12.1

2. Results of Survey - The Usage, Storage and Testing of Recycled Materials

2.1 Introduction

The use of recycled material as base course in roadway construction has steadily increased for the past twenty years. Over time the methods associated with these practices continue to evolve, and therefore the data regarding the usage of recycled materials can quickly become outdated (Nataatmadja and Tan 2001). The University of Wisconsin-Madison has conducted a survey to better define the current state of practices involving the use, storage, and testing of materials used as granular base course in roadway applications. The survey focused on three materials: recycled asphalt pavement (RAP), recycled pavement material (RPM), and recycled concrete aggregate (RCA).

2.1.1 *Recycled Asphalt Pavement (RAP)*

The production of RAP material involves the removal and reprocessing of existing asphalt pavement from roadway structures. The top portion of the existing roadway is removed and either crushed on or off-site before being reused as a base course for the new roadway. The process of crushing and milling RAP material typically results in a high content of finer particles present within the recycled material. The aggregates in RAP materials typically display low water absorption properties due to a coating of asphalt cement preventing the water from reaching the individual particles of the material (Guthrie et al. 2007, FHWA 2008).

2.1.2 *Recycled Pavement Material (RPM)*

The production of RPM material is similar to the production of RAP material, except that RPM production involves the pulverization and blending of the part or entire existing roadway rather than only the top HMA portion. The RPM production process may reclaim the existing roadway HMA, base, and part of the existing subgrade to a typical depth of approximately 300 mm. This process of excavating the entire roadway profile is commonly referred to as Full Depth Reclamation (FDR). RPM material typically has a lower strength and stiffness than RAP material due to the larger amount of fines contributed by the subgrade material (Li et al. 2007).

2.1.3 *Recycled Concrete Aggregate (RCA)*

Similar to the production of RAP and RPM materials, the production of RCA involves the removal and reprocessing of existing material. However, whereas the production of RAP involves the recycling of pavement almost exclusively, the production of RCA is expanded to include materials reclaimed from roadways as well as other demolition sources such as old buildings, airport runways, and the like. The RCA is initially crushed to break up the material and to allow any debris and steel reinforcement to be removed. Once the material is free from debris, the material is crushed again to a gradation typical of roadway base aggregate before being used in that capacity. Unlike the asphalt coating that retards water absorption in RAP material, the cementitious paste that coats the aggregate in RCA increases the water absorption

of the material through hydration. In addition, the hydration of residual cementitious paste present in the recycled material contributes to an increase in strength of the material (FHWA 2008, Poon et al. 2006, Kuo et al. 2002).

2.2 Survey Method

The University of Wisconsin-Madison conducted a survey to determine the extent of the use of recycled materials as a granular base course in roadway applications. The survey was conducted in the month of November 2008, and was extended to individuals with a working connection to state and federal transportation agencies involved in roadway planning and construction. Those asked to take the survey were presented with thirteen (13) questions regarding the application, storage, and testing of recycled materials used as roadway base course.

2.3 Survey Results and Discussion

2.3.1 *Material Usage*

Question 1

The first question asked in the survey was "Which of the following recycled materials do you use as a granular base course?" Each of the respondents had the opportunity to select one or more of the following options: Recycled Asphalt Pavement (RAP), Recycled Concrete Aggregate (RCA), and Recycled Pavement Material (RPM). There were 34 unique respondents to this question in the survey. The total responses to each option are represented in Figure 2.1.

Based on the survey information, the most commonly used recycled material type was RCA with 30 responses. RAP and RPM were the second and third most commonly used recycled material types with 18 and 17 responses, respectively. However, the combined RAP and RPM is 35% and slightly more than RCA.

Question 2

The second question presented in the survey was "When are the recycled materials used?" Each of the respondents had the opportunity to select one of the following options for each of the recycled material types: "Stockpiled and Used Later," "Used in Place Immediately" or "Both." There were 36 unique respondents to this question on the survey. The total distribution of responses to each option is represented in Figure 2.2 through Figure 2.4.

Of the three materials considered in this report, RCA is most likely to be exclusively stockpiled for later use, followed by RAP and RPM. RAP is the most common material in situations where stockpiling and in-place use are both utilized, followed by RCA and RPM. With very little exception, RPM is the only material, which is exclusively used-in-place immediately after reclamation. This is most likely a reflection of construction practices associated with FDR techniques and the common use of RPM as aggregate in bituminous mixtures. The data would suggest that the practice of stockpiling materials is far more common than the practice of using the material in place immediately after reclamation.

Question 3

The third question presented in the survey was "In a given year, how much of the recycled material do you use?" Each of the respondents had the opportunity to select one of the following options for each of the recycled material types: "Less than 1,000 Tons," "1,000 to 5,000 Tons," "5,000 to 10,000 Tons," "10,000 to 25,000 Tons," "25,000 to 50,000 Tons," "50,000 to 75,000 Tons," and "More than 75,000 Tons." There were 33 unique respondents to this question on the survey. The distribution of responses to each option is represented in Figure 2.5 through Figure 2.7.

The most common response to the question for all three materials is "more than 75,000 tons" which would indicate that the use of recycled materials is significantly widespread. Of these materials, the use of RAP seems to be the most advanced in terms of quantity, with more than half of the respondents indicating that 75,000 tons of material or more was typically used. RCA is the second most advanced, with more than half the respondents indicating that 25,000 tons of material or more was typically used. RPM seemed to be the least advanced; with more than half of the respondents indicating that 25,000 tons or less was typically used.

The data represented in Figure 2.5 through Figure 2.7 can be further understood if the total tonnage is considered. The total material used in each case was calculated and is represented in Figure 2.8. Three calculations were made for each material corresponding to the maximum, median, and minimum values of tons used for each of the quantity ranges. The maximum value for the "More than 75,000 Tons" option was assumed to be 100,000 tons.

The trends for all three materials represented in the survey can be seen to fall within a clearly visible trend, with RAP material being the most widely used in all three categories. The trend continues with RCA and RPM being the second and third most widely used, respectively. Contrasting this data with the data in Figure 2.1 seems to indicate that although more agencies are currently using RCA as a recycled fill, RAP material is being used in greater amounts. If RAP and RPM are combined, it appears flexible pavement recycling is far greater than RCA, which include rigid pavement recycling as well as building concrete. This is also reflective of the preponderance of flexible pavements compared to rigid pavements.

Question 4

The fourth question presented in the survey was "How long have you been using the recycled materials?" Each of the respondents had the opportunity to select one of the following options for each of the recycled material types: "Less than 1 Year," "1 to 2 Years," "2 to 5 Years," "5 to 10 Years" or "More than 10 Years." There were 34 unique respondents to this question on the survey. The distribution of responses to each option is represented in Figure 2.9 through Figure 2.11.

The overall results indicate that the use of recycled materials has been established for a considerable amount of time. For each of the given materials, more than half of the respondents indicated that the material had been used for more than 10 years. All but one response (for RPM) indicated that each responding agency had used the given material for more than 2 years.

2.3.2 *Aggregate Specification and Quality*

Question 5

The fifth question presented in the survey was "Are any of the following tests used in specifications for the material?" Each of the respondents had the opportunity to select any of the following options for each of the recycled material types: "Grain Size Analysis: Dry Sieve," "Grain Size Analysis: Wet Sieve and Hydrometer," "Liquid Limit," and "Plastic Limit and Plasticity Index." There were 32 unique respondents to this question on the survey. The distribution of responses to each option is represented in Figure 2.12.

It can be seen from Figure 2.12 that the dry sieve method of grain size analysis is by far the most common test used to establish specification compliance for the given material, with plastic limit and plasticity index determinations ranking second by a wide margin. The wet sieve and hydrometer method of grain size analysis and the determination of liquid limit rank third and fourth most common, respectively. From Figure 2.12 it seems that the RCA material is the most rigorously tested of the three materials, with the greatest response totals for all three test methods.

Question 6

The sixth question presented in this survey was "Which of the following aggregate quality tests for shear strength do you perform on the material prior to placement?" Each of the respondents had the opportunity to select any of the following options for each of the recycled material types: "Static Triaxial Test (AASHTO T 296, ASTM D 2850)," "California Bearing Ratio (AASHTO T 193, ASTM D 1883)," "Dynamic Cone Penetrometer (ASTM D 6951)," or "Other." If "Other" was selected, the respondent was requested to indicate the optional test performed. There were 11 unique respondents to this question on the survey. The distribution of responses to each option is represented in Figure 2.13.

Despite the limited amount of response to the question, the California Bearing Ratio test stood out as the most commonly used test to determine shear strength for each of the recycled materials. Four of the respondents chose "other," indicating that their particular agencies used additional tests for shear strength. The collected data indicated that one agency used the Resistance Value test for each of the three materials, and three separate agencies respectively used the following three tests for RCA: "LA Abrasion Test and Sulfate Soundness (Pre-Qualify)," "Sand Equivalency Test," and "Texas Triaxial Test."

Question 7

The seventh question presented in the survey was "Which of the following aggregate quality tests for stiffness do you perform on the material prior to placement?" Each of the respondents had the opportunity to select any of the following options for each of the recycled material types: "Resilient Modulus (AASHTO T 307)," "Resonant Column (ASTM D 4015)," or "Other." If "Other" was selected, the respondent was requested to indicate the optional test performed. There was only one unique respondent to this question on the survey. The distribution of responses to each option is represented in Figure 2.14.

There was only one response to the question, so the data is inconclusive. Neither of the provided options was chosen in response to the question. The sole respondents chose "other" and indicated that their particular agency used the R-Value test as an additional test for stiffness on all three material types. However, based on the data, it appears that the testing of materials for stiffness prior to placement is not common.

Question 8

The eighth question presented in the survey was "Which of the following aggregate quality tests for frost susceptibility do you perform on the material prior to placement?" Each of the respondents had the opportunity to select any of the following options for each of the recycled material types: "Tube Suction Test (Texas Method 144E)," or "Other." If "Other" was selected, the respondent was requested to indicate the optional test performed. There were no respondents to this question on the survey, and therefore it appears that the testing of materials for frost susceptibility prior to placement is not common.

Question 9

The ninth question presented in the survey was "Which of the following aggregate quality tests for permeability do you perform on the material prior to placement?" Each of the respondents had the opportunity to select any of the following options for each of the recycled material types: "Constant Head (AASHTO T 215, ASTM D 2434)," "Falling Head," or "Other." If "Other" was selected, the respondent was requested to indicate the optional test performed. There was only one unique respondent to this question on the survey. The distribution of responses to each option is represented in Figure 2.15.

The only response to the question indicated that the Falling Head test was typically used for permeability determinations. However, the limited response to this question renders the data inconclusive. It appears that the testing of materials for permeability prior to placement is not common.

Question 10

The tenth question presented in the survey was "Which of the following aggregate quality tests for toughness do you perform on the material prior to placement?" Each of the respondents had the opportunity to select any of the following options for each of the recycled material types: "LA Abrasion (AASHTO T 96, ASTM C 131)," "Aggregate Impact Value (BS 812)," "Aggregate Crushing Value (BS 812)," "Aggregate Abrasion Value," "Micro-Deval (AASHTO TP 58 and T 327, ASTM D 6928)," "Durability Mill (Sampson and Netterberg 1989)," "Gyratory Test," or "Other." If "Other" was selected, the respondent was requested to indicate the optional test performed. There were 21 unique respondents to this question on the survey. The distribution of responses to each option is represented in Figure 2.16.

It is clear from Figure 2.16 that the LA Abrasion test is the most commonly used test for the toughness of a material prior to placement and is frequently used for all three material types, but most commonly when RCA material is considered. Despite the minimal data available for the other test methods, the Micro-Deval test for all materials, the Aggregate Abrasion Value test for

RCA and RPM, and the Gyratory Test for RAP were each indicated as being marginally used. None of the respondents indicated that the Aggregate Impact Value, Aggregate Crushing Value or Durability Mill Tests were used.

Two of the respondents chose "other", indicating that their particular agencies used additional tests for toughness. The Sulfate Soundness test and Texas Wet-Mill test were respectively used by two different agencies for toughness testing on RCA material. The Texas Wet-Mill test was described as "similar to the idea of Micro-Deval."

Question 11

The eleventh question presented in the survey was "Which of the following aggregate quality tests for durability do you perform on the material prior to placement?" Each of the respondents had the opportunity to select any of the following options for each of the recycled material types: "Sulfate Soundness (AASHTO T 104, ASTM C 88)," "Canadian Freeze-Thaw (MTO LS-614)," "Aggregate Durability Index (AASHTO T 210 and T 176, ASTM D 3744)," or "Other." If "Other" was selected, the respondent was requested to indicate the optional test performed. There were 12 unique respondents to this question on the survey. The distribution of responses to each option is represented in Figure 2.17.

From Figure 2.17 it can be seen that the Sulfate Soundness test is the most commonly used test for the durability of a material prior to placement, and is frequently used for all three material types. Despite the minimal data available indicating other test methods, the Aggregate Durability Index test for RAP and RCA was indicated as being marginally used. None of the respondents indicated that the Canadian Freeze-Thaw test was used. One of the respondents chose "other," indicating that their particular agency used the Magnesium Sulfate Soundness test as an additional durability test for RCA.

Question 12

The twelfth question presented on the survey was "Which of the following aggregate quality tests for mineralogical composition do you perform on the material prior to placement?" Each of the respondents had the opportunity to select any of the following options for each of the recycled material types: "Petrographic Examination (ASTM C 295)," "X-Ray Diffraction," or "Other." If "Other" was selected, the respondent was requested to indicate the optional test performed. There were four unique respondents to this question on the survey. The distribution of responses to each option is represented in Figure 2.18.

The only response to the question indicated that the Petrographic Examination test method was the only test typically used for the determination of mineralogical composition in recycled materials. However, the limited response would indicate that the data is inconclusive, and therefore it appears that the testing of materials for mineralogical composition prior to placement is not common.

Question 13

The thirteenth and final question presented on the survey was "Which of the following aggregate quality tests for particle geometric properties do you perform on the material prior to placement?" Each of the respondents had the opportunity to select any of the following options for each of the recycled material types: "Particle Shape and Surface Texture Index (ASTM D 3398)," "Flat and Elongated Particles (ASTM D 4791)," "Percentage of Fractured Particles (ASTM 5821)," "Uncompacted Void Content (AASHTO T 326, ASTM C 1252)," "Digital Image Analysis," or "Other." If "Other" was selected, the respondent was requested to indicate the optional test performed. There were four unique respondents to this question on the survey. The distribution of responses to each option is represented in Figure 2.19.

The minimal data available for question thirteen indicates that tests for Particle Geometric Properties are marginally used. The usage of the Percentages of Fractured Particles test was slightly more common than that of the Flat and Elongated Particles test, with the former used for RCA and RPM materials and the latter used for RCA materials only. None of the other three tests were selected for the survey. Based on the results of this survey, it appears that the testing of materials for particle geometric properties prior to placement is not common.

2.4 Conclusions

A survey was conducted by the University of Wisconsin-Madison to determine the extent of use of recycled materials as granular base course in roadway applications. The survey found that of the three recycled materials considered, recycled concrete aggregate (RCA) was the most commonly used material, followed by recycled asphalt pavement (RAP) and recycled pavement material (RPM). However, if RAP and RPM are combined, recycling of flexible pavements is more common both in terms frequency and quantity. Following reclamation operations, it is more common for a recycled material to be stockpiled and used later than to be used immediately after reclamation. However, RPM materials, common to full-depth reclamation efforts, are more likely to be used immediately after reclamation than the other materials considered. In terms of quantity, RAP material represents the greatest total tonnage used, followed by RCA and RPM, respectively. Although RCA is the most common material used, RAP material is used in greater amounts.

The most common test used to determine specification compliance for a recycled material was Grain Size Analysis using dry sieve, followed by Plastic Limit and Liquid Limit determinations and Grain Size Analysis using a wet sieve and hydrometer. The survey indicated that the most common tests for aggregate quality are the California Bearing Ratio test for aggregate shear strength, the LA Abrasion test for aggregate toughness, and the Sulfate Soundness test for aggregate durability. Less common to uncommon tests for aggregate quality were found to be the R-Value test for stiffness, the Falling Head Method test for permeability, the Petrographic Examination test for mineralogical composition, and either the Percent of Fractured Particles test or Flat and Elongated Particles test for particle geometry. The results of the survey gave no indication that frost susceptibility tests were performed for summative quality. It is apparent from the survey that there is limited data for structural properties. For instance, resilient modulus needed for the Mechanistic-Empirical Pavement Design Guide is not performed. Developing a database of such properties for these recycled materials is needed.

2.5 Figures

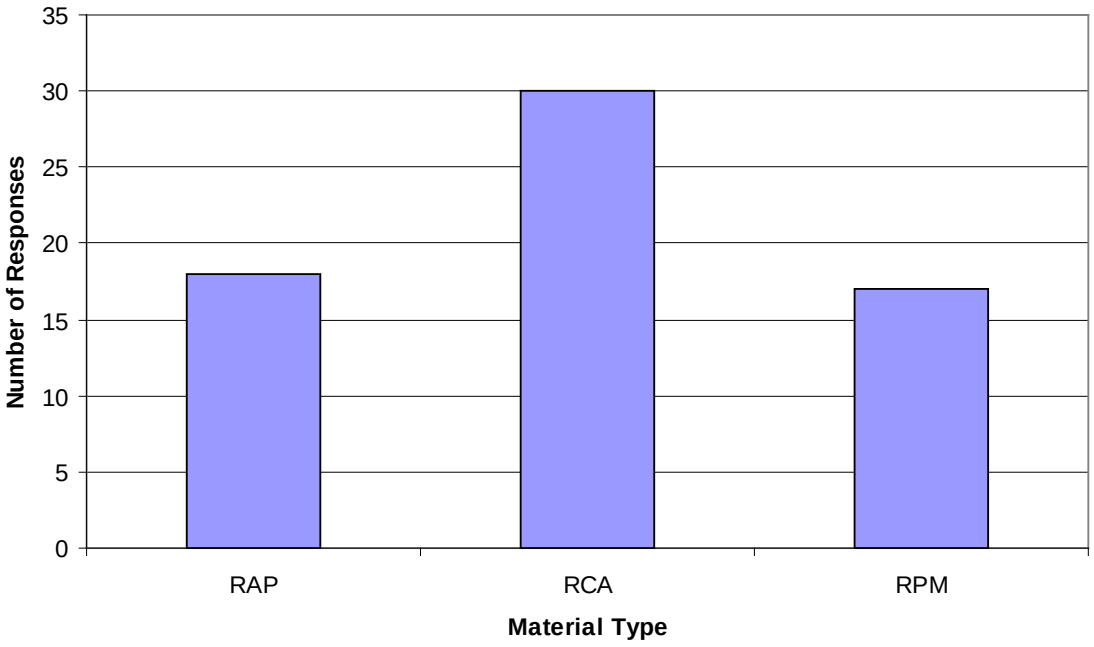

Figure 2.1 Recycled Materials Used as Granular Base Course

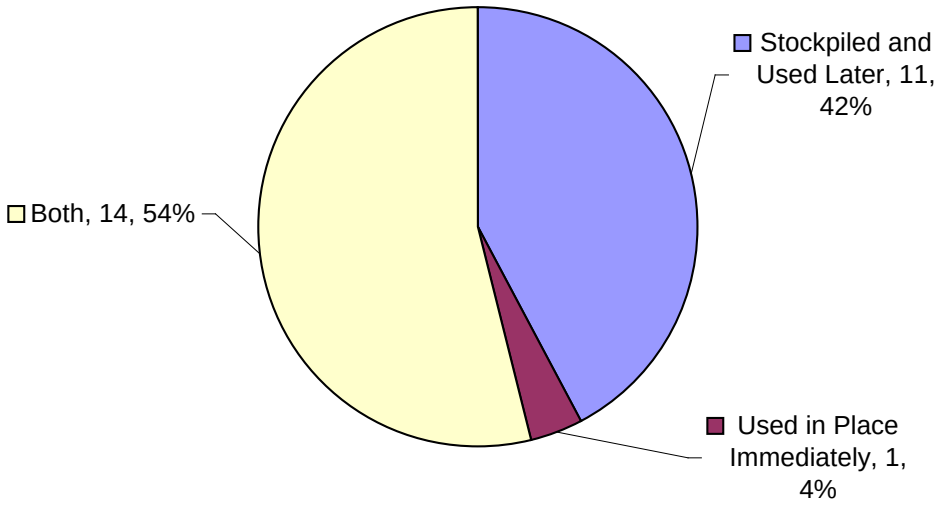

Figure 2.2 RAP Placement Transition Time

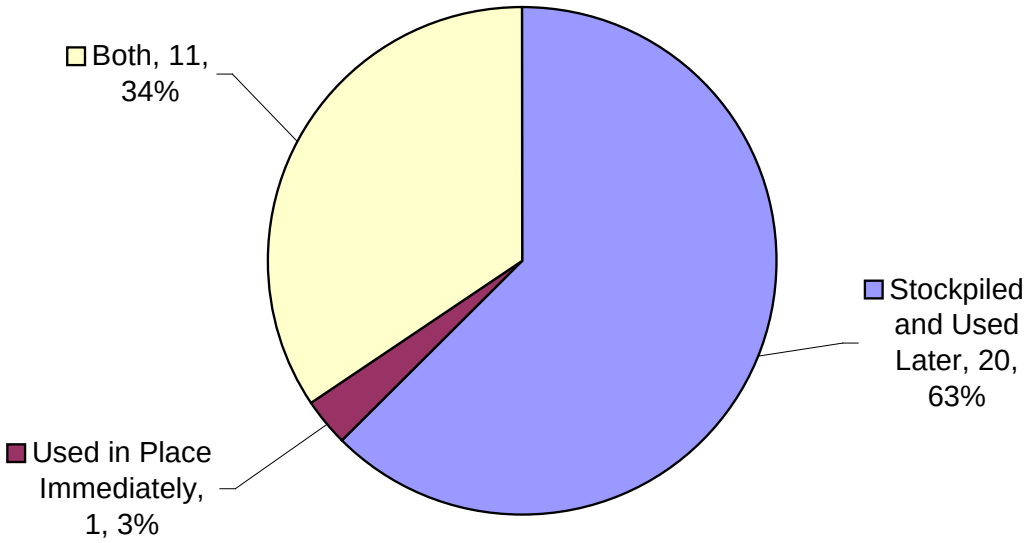

Figure 2.3 RCA Placement Transition Time

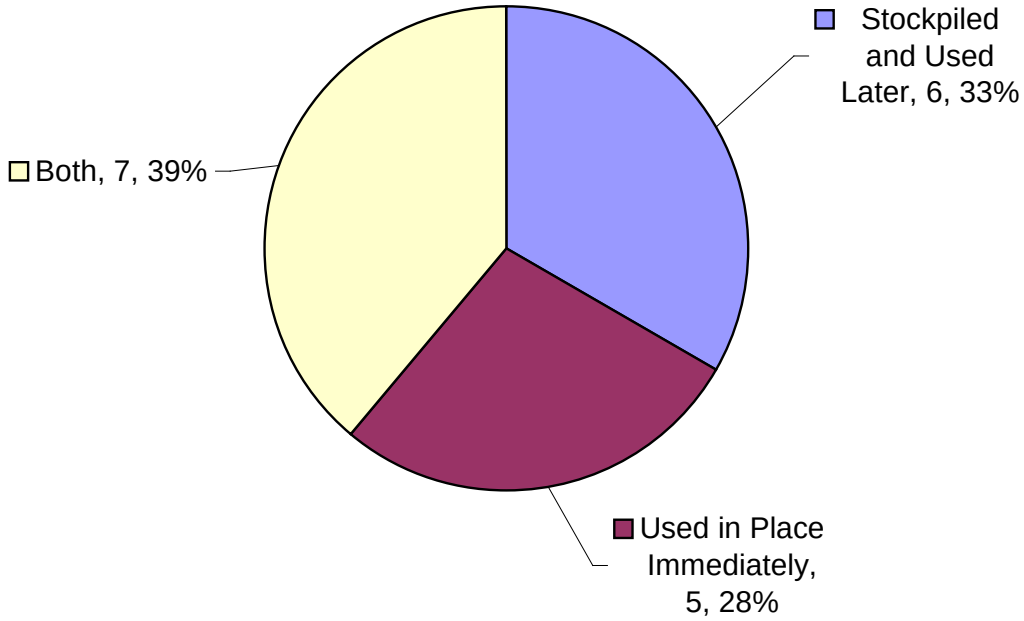

Figure 2.4 RPM Placement Transition Time

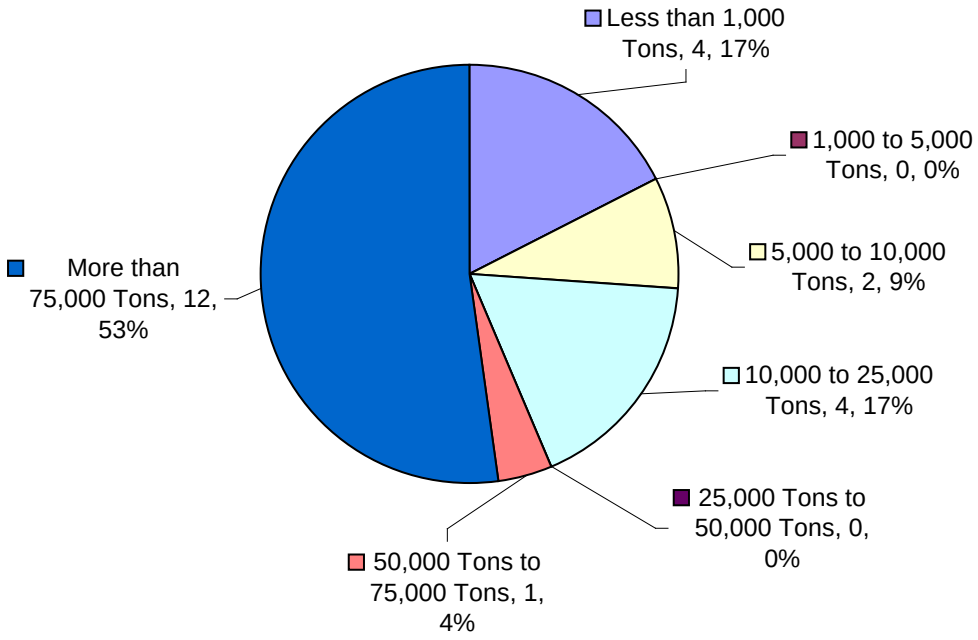

Figure 2.5 Annual Quantity Used: RAP

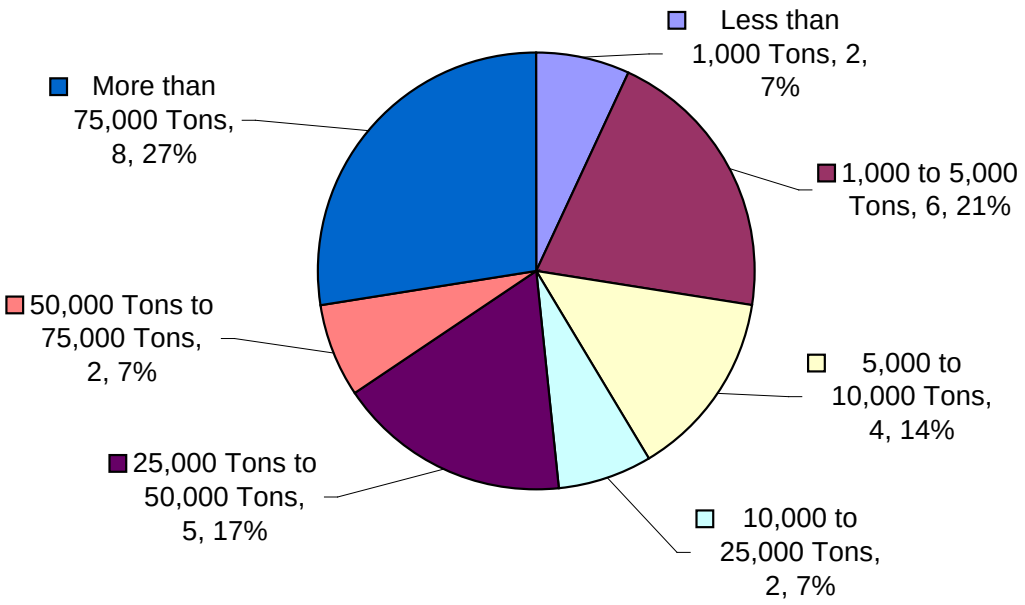

Figure 2.6 Annual Quantity Used: RCA

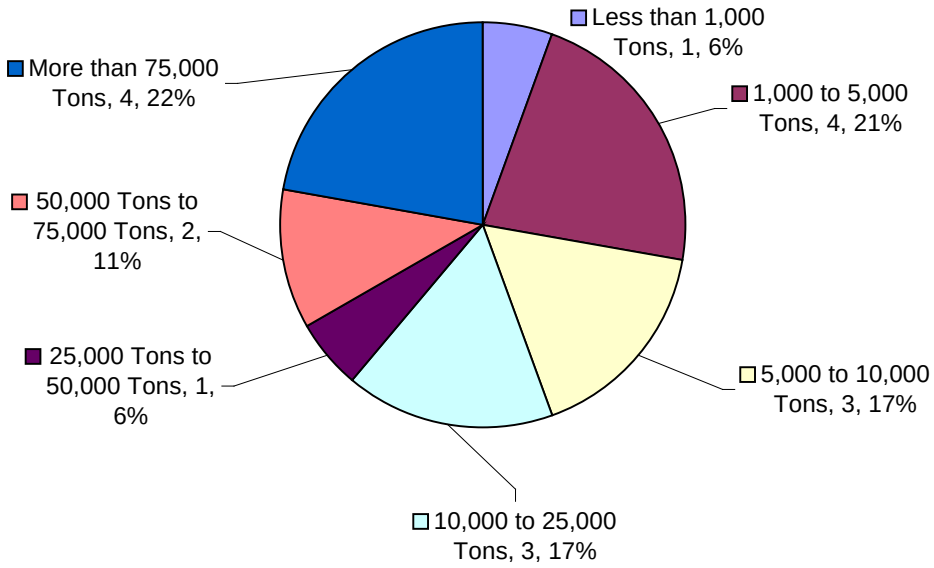

Figure 2.7 Annual Quantity Used: RPM

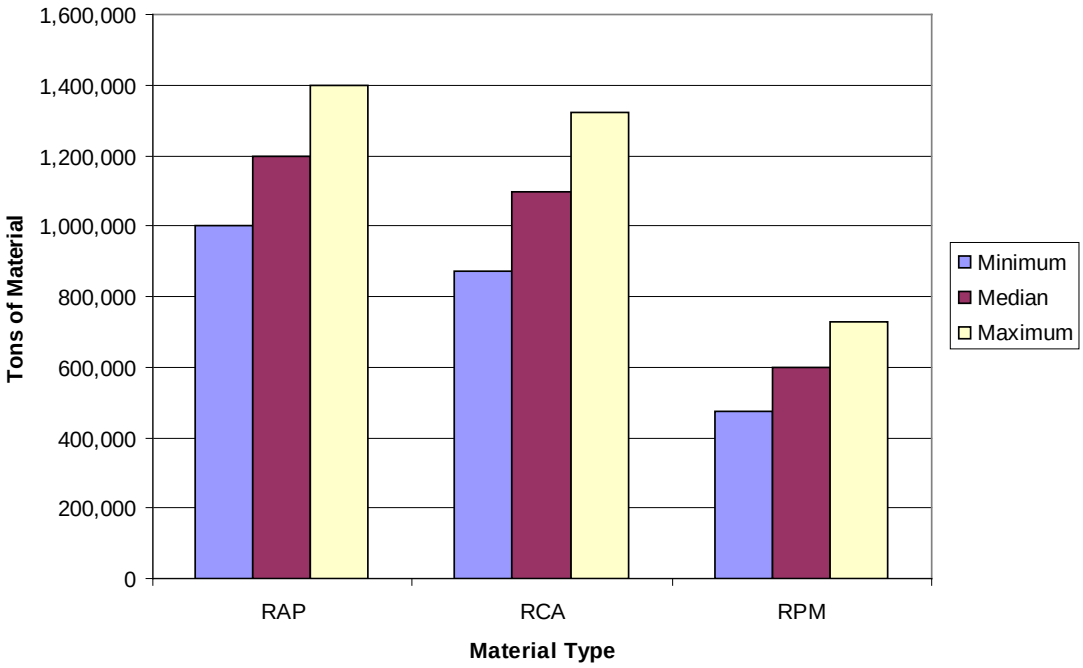

Figure 2.8 Quantity of Each Material Used

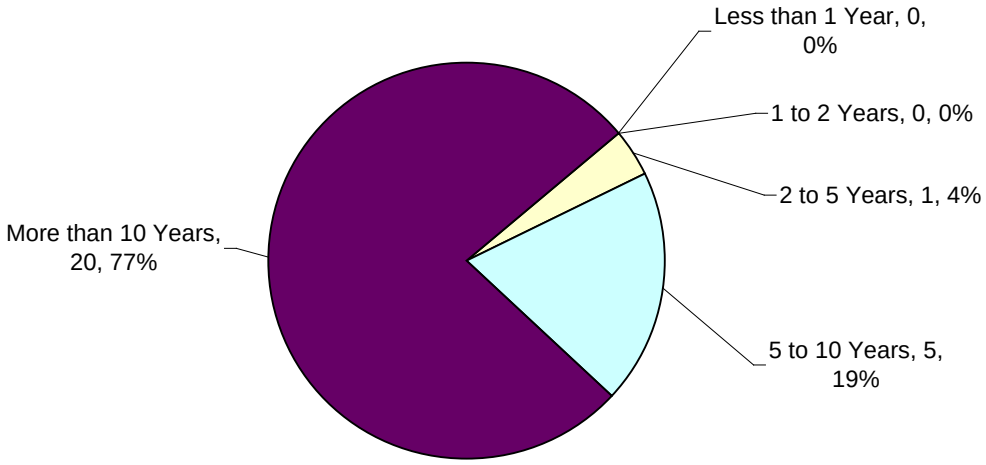

Figure 2.9 Number of Years Used: RAP

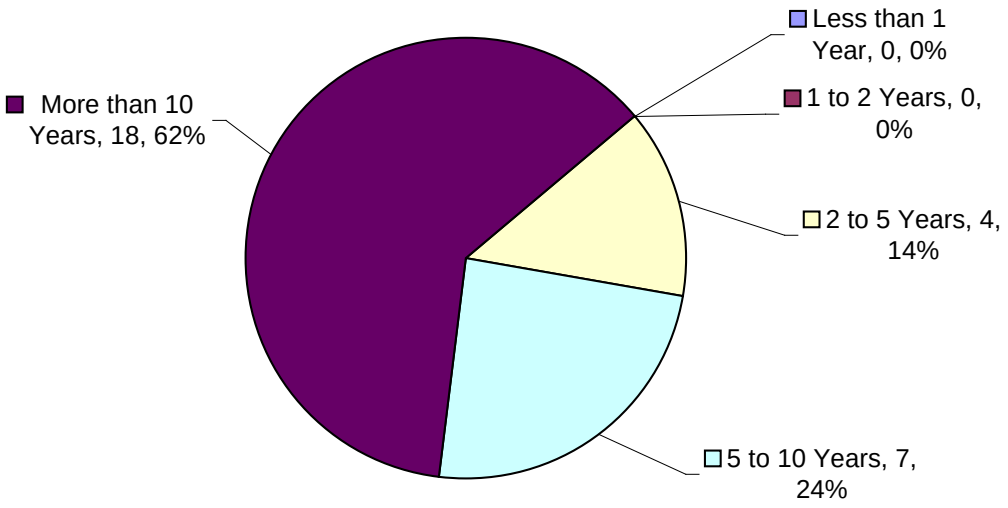

Figure 2.10 Number of Years Used: RCA

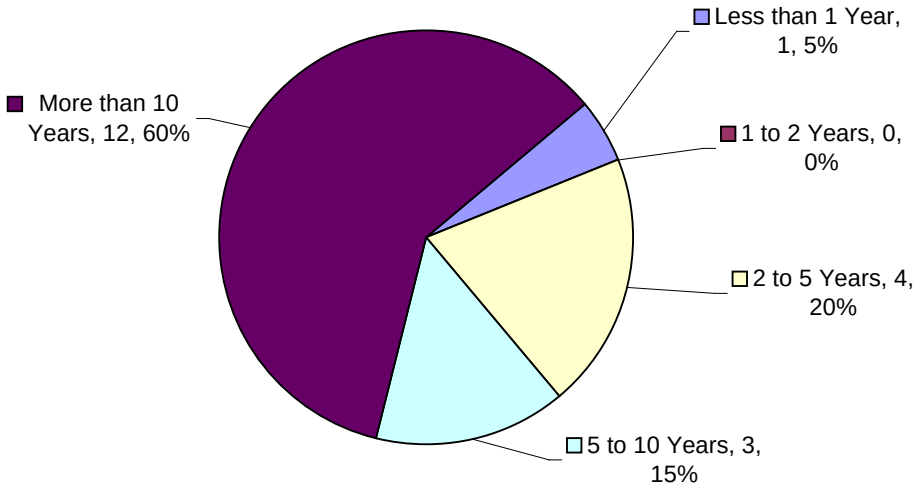

Figure 2.11 Number of Years Used: RPM

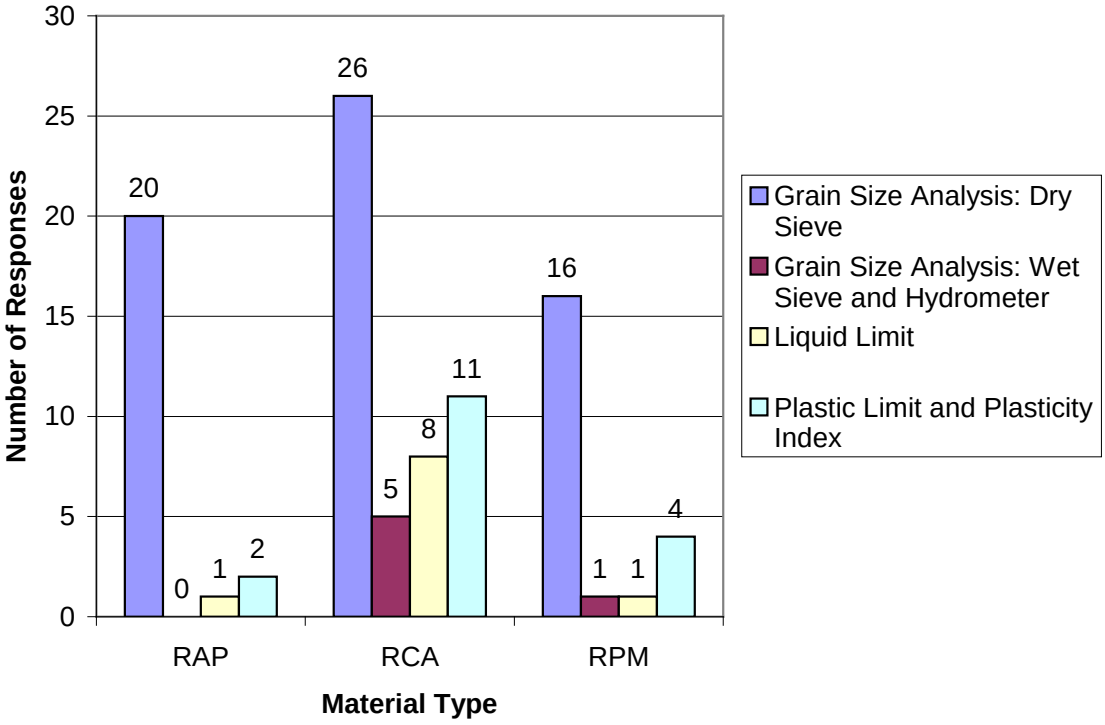

Figure 2.12 Specification Tests Used by Material Type

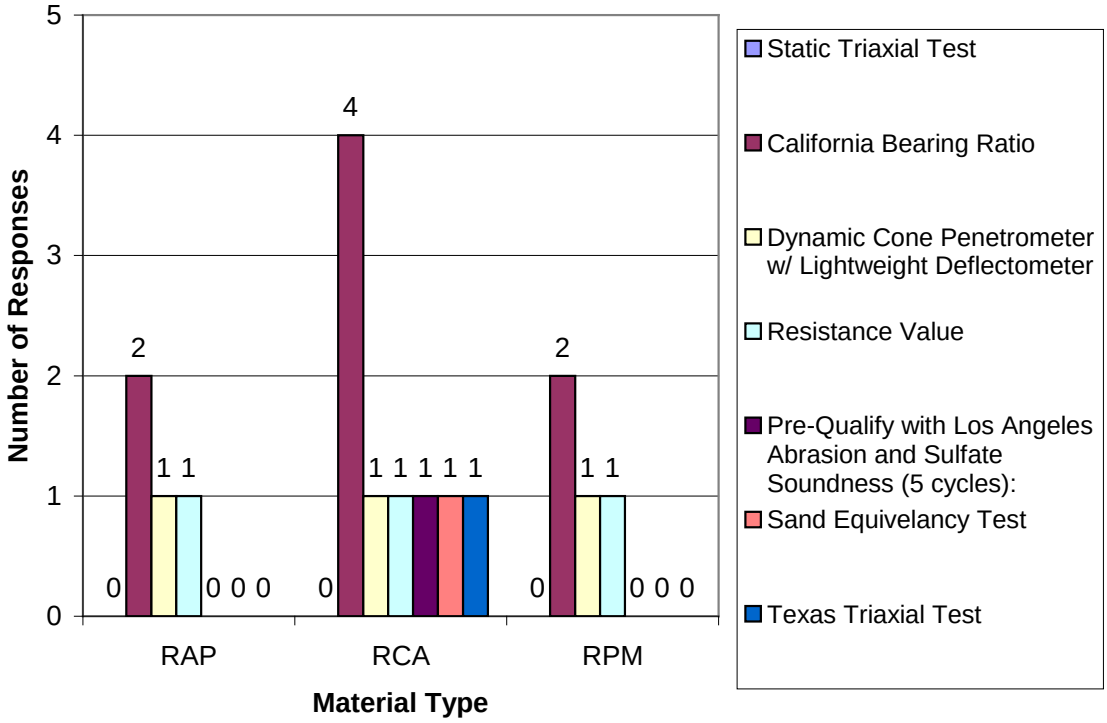

Figure 2.13 Aggregate Quality Tests for Shear Strength

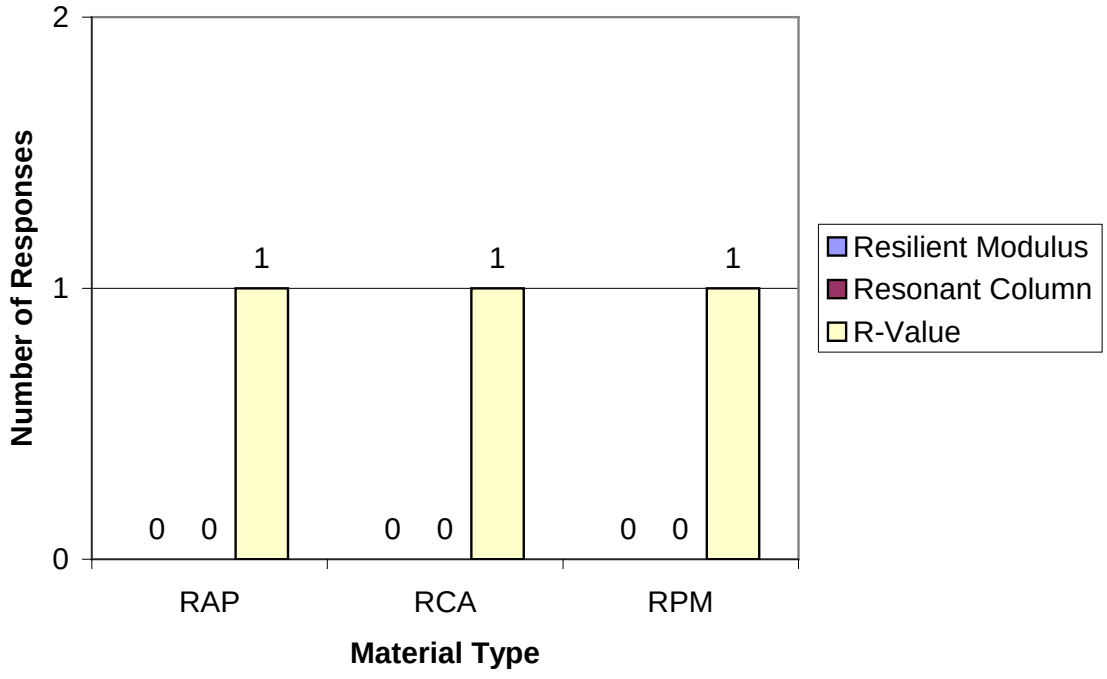

Figure 2.14 Aggregate Quality Tests for Stiffness

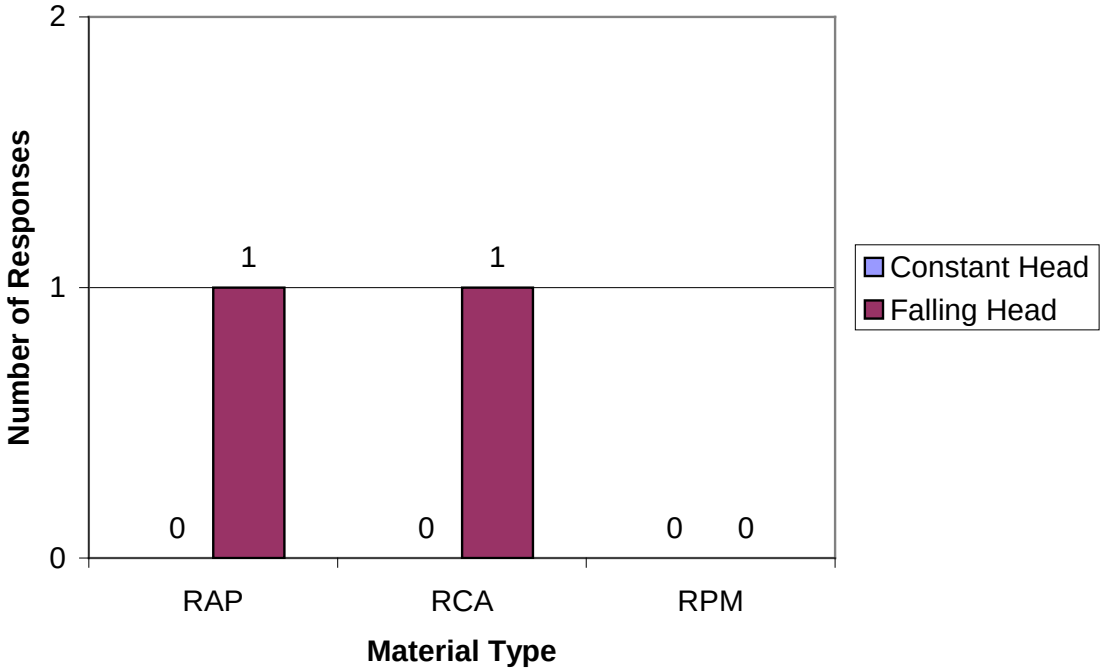

Figure 2.15 Aggregate Quality Tests for Permeability

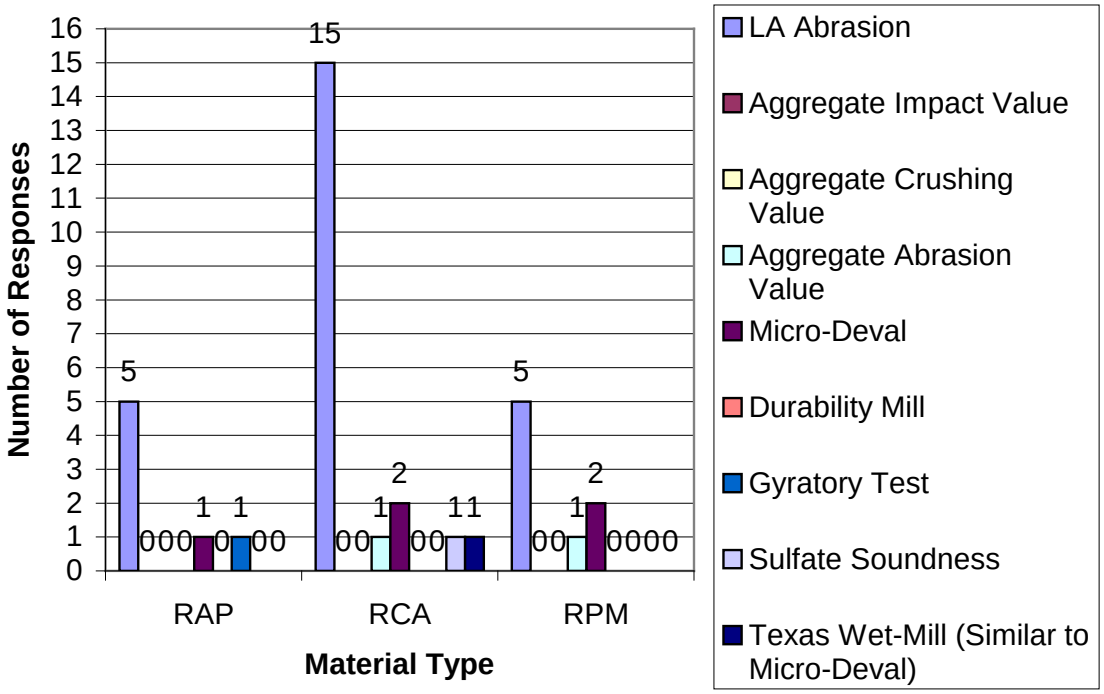

Figure 2.16 Aggregate Quality Tests for Toughness

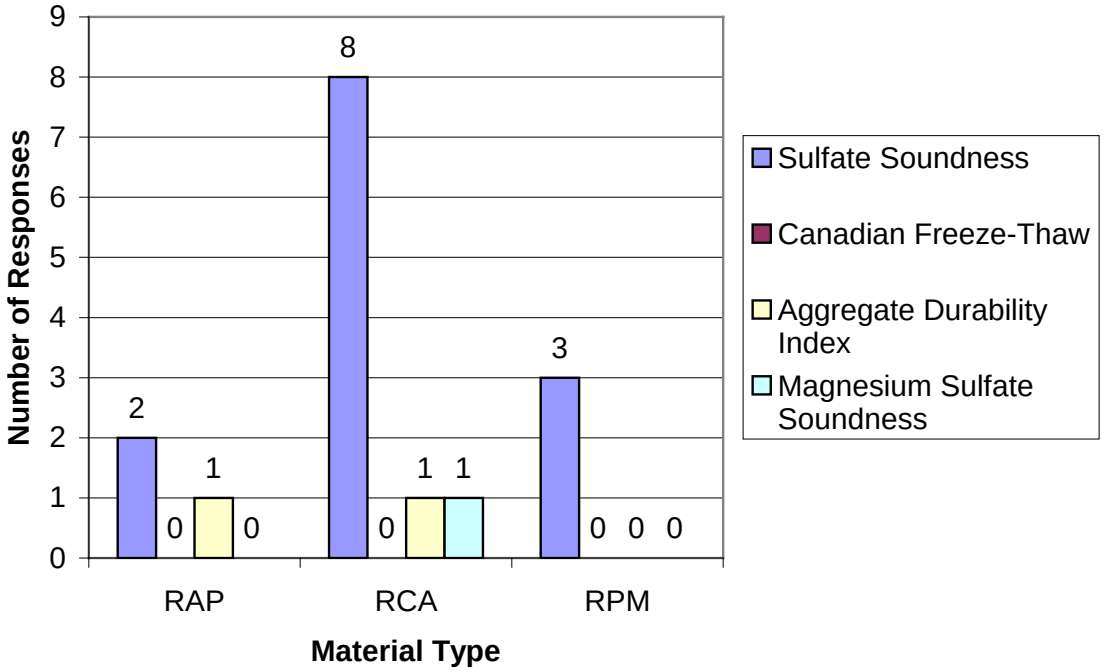

Figure 2.17 Aggregate Quality Tests for Durability

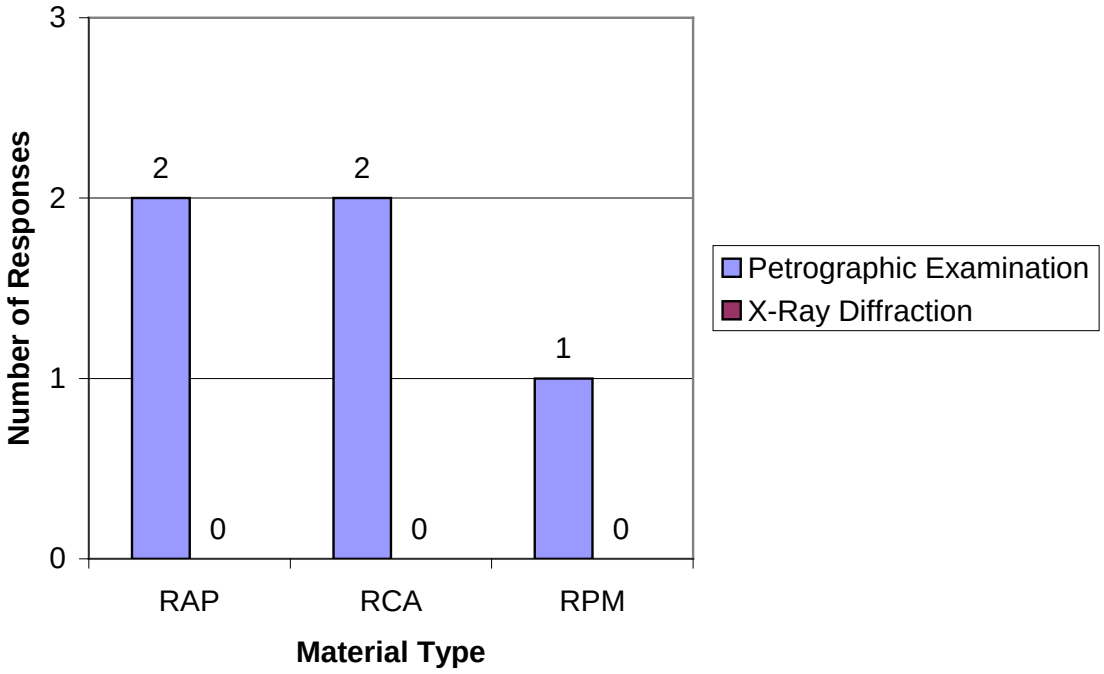

Figure 2.18 Aggregate Quality Tests for Mineralogical Composition

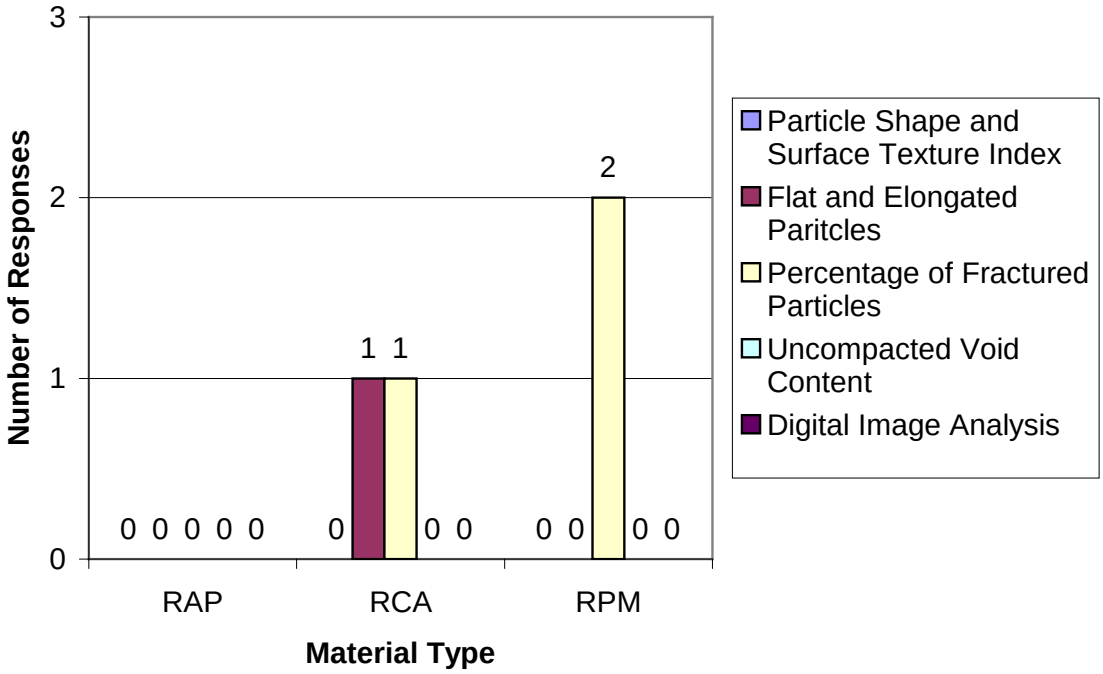

Figure 2.19 Aggregate Quality Tests for Particle Geometric Properties

3. Relationship between Resilient Modulus and Composition of RCA or RAP

3.1 Introduction

The growth in the construction and rehabilitation of the roadway systems in the United States (US) increases the consumption of natural materials and energy (Lee et al. 2010). The United States Geological Survey (USGS 2011) estimated that 508 million tons of crushed stone (natural aggregate) was consumed in the US in 2010, and 82% as construction material. Natural aggregate is largely used for public infrastructure, mostly for highway and road construction and related maintenance (Langer 1988). Road base or road surfacing materials are the major uses of natural aggregate without binder (i.e., unbound aggregate) (USGS 2011). However, rapidly decreasing sources of natural aggregate, along with limits placed upon aggregate production by environmental regulation and land use policies, has caused the price of these materials to increase dramatically (ACPA 2009).

Construction and demolition (C&D) waste makes up 25% to 45% of the waste bound for landfills in the US, thus contributing to reduced landfill life and increased environmental impacts (Leigh and Patterson 2004). The production of C&D waste has increased while the amount of landfill available for disposal has decreased (Chini et al. 2001, Poon et al. 2006). Appropriate means for the final disposition of C&D waste is of increasing concern (Kuo et al. 2002). With increasing generation of C&D waste coupled with landfill space limits, beneficial reuse of C&D waste appears attractive. One accepted way to beneficially reuse these materials is to incorporate them into base/subbase applications in flexible pavement construction.

Using recycled materials in the base and subbase layers can result in reductions in global warming potential by reducing the greenhouse gas emissions, and hazardous waste generation, while extending the service life of the pavement (Lee et al. 2010). The use of recycled material as base and subbase course in new or rehabilitated roadway construction has become common with some municipalities in the US (Bennert et al. 2000). State departments of transportation (DOTs) have participated in the development of markets for recyclables by using recycled materials in highway construction (Pratt 1993). By establishing engineering properties, specifications, and markets for recycled content within infrastructure projects, state DOTs contribute to the demand that sustains the practice of beneficial reuse of recycled material (Pratt 1993).

The most common C&D materials used as unbound base course in pavement construction are recycled concrete aggregate (RCA), recycled asphalt pavement aggregate (RAP) and recycled pavement materials (RPM). RCA is the product of the demolition of concrete structures such as buildings, roads, and runways. RAP is produced by removing and reprocessing existing asphalt pavement (Kuo et al. 2002, Guthrie et al. 2007, FHWA 2008). The material generated from FDR, comprised of existing HMA and underlying base and perhaps some subgrade material, is referred to as RPM (Li et al. 2007, Wen and Edil 2008, Ebrahimi et al. 2010). By beneficially reusing concrete and asphalt, a waste product is converted to a resource for pavement construction (Langer 1988). An increase in the amount of RCA used to replace natural

aggregates in pavement construction has economic and environmental benefits, while extending the supply of traditional construction material (Saeed et al. 2006).

The objective of this study is to evaluate the stiffness of RCA and RAP sources used as unbound base course without treatment and to determine the relationship between the M_r and physical properties (e.g., particle shape, binder type, aggregate mineralogy and contamination) of RCA and RAP through statistical correlations. The M_r of RAP and RCA measured in this study are compared to results from conventional base course.

The effect of varying RAP/RCA content on the stiffness of natural aggregates used as conventional unbound road base/subbase layer was determined. This chapter describes the findings of this study.

3.2 Background

3.2.1 *Resilient Modulus*

RAP and RCA compete with natural aggregates that are currently used in roadway base applications (Guthrie et al. 2007, FHWA 2008). Despite the increased acceptance of recycled base material in construction, research concerning the mechanical properties and durability of such materials is limited (Bennert et al. 2000, Nataatmadja and Tan 2001, Guthrie et al. 2007). Recycled materials should perform well under the intended use in pavement design; therefore, the mechanical properties of recycled materials need to be investigated thoroughly such that appropriate design procedures and specifications can be established.

Schaertl (2010) indicates that RCA and RAP used alone or in blends with natural aggregates can have different resilient modulus (M_r), sensitivity to stress state, and rutting performance compared to natural aggregates. The durability and toughness of recycled materials can also be different than that of natural aggregates (Weyers et al. 2005).

Base and subgrade layers undergo deformation when subjected to repeated loads from moving vehicular traffic. The resilient response of granular material is important for the load-carrying capacity of the pavement and the permanent strain response, which characterizes the long-term performance of the pavement (Lekarp et al. 2000). The M_r is a linear-elastic modulus obtained from dynamic loading, defined as the ratio of the cyclic deviator stress, σ_d, to the resilient (recoverable) strain, ε_r:

$$M_r = \sigma_d / \varepsilon_r \tag{3.1}$$

Design for pavements and rehabilitation of layered pavement systems use M_r as an essential parameter in the design process (Heydinger et al. 2007). Generally, a higher M_r infers a stiffer base course layer, which increases pavement life.

RAP and RCA compete with natural aggregates that are currently used in roadway base applications (Guthrie et al. 2007, FHWA 2008). Recycled materials should perform well under the intended use in pavement design; therefore, the mechanical properties of recycled materials need to be investigated thoroughly such that appropriate design procedures and specifications

can be established. Despite the increased acceptance of recycled material as base course, research concerning the mechanical behavior of such material is lacking (Guthrie et al. 2007).

3.3 Materials

Sixteen recycled materials, one conventional base course, and one blended recycled/conventional material were used in this investigation. Seven of the recycled materials were recycled asphalt pavement (RAP), six were recycled concrete aggregate (RCA), and two were recycled pavement materials (RPM). The recycled materials used in this study were obtained from a wide geographical area, covering eight different states: California, Colorado, Michigan, Minnesota, New Jersey, Ohio, Texas and Wisconsin (Figure 3.1). The materials named according to the origin of the materials. The reference base course was a gravel meeting the Class 5 aggregate specifications for base course in Minnesota per the Minnesota Department of Transportation (MnDOT). Class 5 aggregate is formed by quartz, granite and carbonates (limestone and dolomite). The ratio of quartz/granite to carbonates is 2.1. The percentage of mineral type in Class 5 aggregate is 68 % for Quartz/Granite and 32 % for Carbonates. Percent quartz/granite (aggregate and concrete) and percent carbonate of gravel (aggregate and concrete) of gravel are 43% and 20%, respectively. The blend (MN) was a mix of approximately equal parts (by mass) RCA from MnDOT (50%) and Class 5 aggregate (50%). The Class 5 aggregate was used as the control in this study.

The material from MnDOT was obtained during construction of roadway cells at the MnROAD test facility in Maplewood, Minnesota for investigation of the field behavior. The RAP was milled from the surface of roadway cells that were previously constructed at the MnROAD test facility. The RCA was obtained from a stockpile maintained by the Knife River Corporation at their pit located at 7979 State Highway 25 NE in Monticello, Minnesota.

The RAP from the Ohio Department of Transportation (ODOT) came from an existing asphalt pavement, processed through a portable plant, and stored in approximately 2268 Mg stockpiles. The Ohio RCA is from a 1.2-m-high barrier wall that existed between the north- and south-bound lanes of State Route 315 in downtown Columbus, Ohio. The broken-up concrete was taken from the project to a portable processing plant, crushed, sized, and stockpiled. The material for this project came from stockpiles of approximately 9071 Mg. The RCA samples provided were 100% RCA.

The material received from the Colorado DOT was collected from over 500 demolition sites from curb, gutter, sidewalk, highways, high-rise buildings, and housing foundations. Although the concrete came from varied sources, the aggregates for the production of the concrete originated from rock in Colorado, most from the quarries in Morrison and Golden and some aggregates were sourced from the Platte River.

The material provided by the New Jersey DOT (NJ DOT) is from stockpiles for demolition projects, primarily in New Jersey. The material in the stockpiles is in flux since NJ DOT constantly adds new loads and removes content for different purposes.

The RAP from California DOT is a combination of roadway millings and waste from an HMA plant (discharge from warm up and cleaning processes). The RCA is broken concrete rubble

from the demolition of structures. Stockpiling in California is usually done three times a year. These stockpiles are not added to throughout their life cycle. If stockpiled material is still unavailable during visits from subcontractors, new material is used to create a new stockpile.

The RCA sent by the Texas DOT is from a commercial source; therefore, the individual sources of aggregate or material characteristics included in the RCA are not known. The Texas RAP is from a highway project where the contractor milled the "binder" course after approximately 1.5 years of service. The RAP l from Michigan was provided by the Michigan DOT and is from highway reconstruction projects.

A summary of the grain characteristics and classifications for the seventeen materials is shown in Table 3.1. The materials used in this study are classified as non-plastic per the Unified Soil Classification System (USCS). The Class 5 aggregate is classified as well-graded gravel (GW-GM) per the USCS (ASTM D 2487) and A-1-b per the AASHTO Soil Classification System (ASTM D 3282). The blended RCA/Class 5 is classified as A-1-b according to ASTM D 3282 and as poorly graded sand (SP) according to ASTM D 2487. The samples of RCA range from an SP to a well-graded gravel (GW) classification via USCS and A-1-a or b for AASHTO. The various RAPs and RPMs classify as SP, SW, or GW, whereas their AASHTO classifications are A-1-a or b. All materials are coarse-grained granular materials with fines contents mostly less than 7% except Class 5 aggregate and one RCA sample.

The particle size distribution (PSD) curves were determined according to ASTM D 422. Samples were wet-sieved through a No. 200 (75 μm opening) sieve to separate the fine particles attached to the coarser aggregates. The PSDs for the RCA and the RAP/RPM samples are shown in Figure 3.2 and Figure 3.3 respectively, along with the upper and lower bounds from the literature.

To evaluate the effects of RAP content in blends on M_r, CO RAP and CA RAP were selected. The materials were chosen according to the availability of materials obtained from DOTs for this study. Additionally, RCA (MN)-Class 5 aggregate blend as obtained from the field project was also tested and compared with pure component materials.

3.4 Methods

3.4.1 *Compaction*

The modified Proctor compaction test was performed on each material in accordance with ASTM D 1557, and the optimum moisture content (OMC) and maximum dry unit weight (MDU) were determined. Before running the compaction test, the samples were screened through a 25 mm sieve.

3.4.2 *Resilient Modulus Test*

Resilient modulus tests were performed on compacted specimens according to NCHRP 1-28a Procedure Ia, which applies to base and subbase materials. The materials used in this study classify as Type I material in NCHRP 1-28A, which requires a 152 mm diameter and 305 mm high specimen for resilient modulus testing (NCHRP 2004). Specimens were prepared at OMC

and compacted to 95% of maximum modified Proctor density. Specimens were compacted in six lifts of equal mass within 1% of the target dry unit weight and 0.5% of target moisture content to ensure uniform compaction (NCHRP 2004).

Resilient modulus tests were conducted with internal and external linear variable displacement transducers (LVDT). External LVDTs have an accuracy of ± 0.005 mm, and internal LVDTs have an accuracy of ± 0.0015 mm. Clamps for the internal LVDTs were built in accordance with NCHRP 1-28A specifications. Internal LVDTs were placed at quarter points of the specimen to measure the deformations over the half-length of the specimen, whereas external LVDT measured deformations of the entire specimen length. An MTS Systems Model 244.12 servo-hydraulic machine was used for loading the specimens. Loading sequences, confining pressures and data acquisition were controlled from a computer running LabView 8.5 software.

The loading sequence was applied using a haversine load pulse with a frequency 1Hz. The load was applied for 0.1 second at the beginning of each cycle, and was followed by a 0.9 second rest period. An MTS Systems Model 244.12 servo-hydraulic machine was used for loading the specimens. Loading sequences, confining pressure, and data acquisition were controlled by a PC equipped with Labview 8.5 software. Resilient moduli (M_r) from the last five cycles of each test sequence were averaged to obtain the resilient modulus for each load sequence.

The M_r for each load sequence was obtained by averaging the M_r from the last five cycles of each test sequence. The M_r data were fitted with the power function model proposed by Moosazedh and Witczak (1981)

$$M_R = k_1 \times \theta^{k_2} \tag{3.2}$$

where M_r is resilient modulus, θ is bulk stress and k_1 and k_2 are empirical fitting parameters. The constants k_1 and k_2 are unique to a given material and are independent of one another. k_1 and k_2 are material-dependent parameters. For a given material, k_2 obtained from replicate tests were averaged and fixed for that material (Camargo 2008). Bulk stress is another means of quantifying confining pressure and deviator stress in a single term and is defined as the sum of the three principle stresses. Bulk stress is defined as

$$\theta = \sigma_1 + \sigma_2 + \sigma_3 \tag{3.3}$$

where σ_1, σ_2, and σ_3 are the principal stresses acting on the specimen.

The M_r data were also fitted with the NCHRP model(NCHRP 2004) defined

$$M_r = k_1 . p_a . \left(\frac{\theta - 3k_6}{p_a}\right)^{k_2} . \left(\frac{\tau_{oct}}{p_a} + k_7\right)^{k_3} \tag{3.4}$$

where M_r is resilient modulus, k_1, k_2, k_3, k_6, and k_7 are constants, p_a is atmospheric pressure (101.4 kPa), τ_{oct} is octahedral shear stress, and θ is bulk stress.

For base course, the summary resilient modulus (SRM) corresponds to the M_r at a bulk stress of 208 kPa and octahedral shear stress of 48.6 kPa, as suggested by Section 10.3.3.9 of NCHRP 1-

28a. M_r is used to determine the layer coefficient, which is a required input in the AASHTO pavement design equation (Tian et al. 1998).

3.4.2.1 Blended RAP/RCA Effect on Stiffness of Recycled Materials

To investigate the behavior of RAP or RCA blended with Class 5 aggregate, specimens were prepared by blending RAP or RCA with Class 5 aggregate and tested for M_r along with pure RAP or RCA and pure Class 5 aggregate. The modified Proctor compaction test was performed on the blended materials (50%RAP or RCA-50%Class 5 aggregate) in accordance with ASTM D 1557 to determine the OMC and MDU of the blended materials. Resilient modulus tests were performed on the compacted specimens according to NCHRP 1-28a Procedure Ia.

3.5 Results and Analysis

3.5.1 *Compaction Characteristics*

Optimum moisture content (OMC) and maximum dry unit weight (MDU) for RCA, RAP/RPM, RCA, (MN)-Class 5 aggregate blend and Class 5 aggregate are summarized in Table 3.2 Maximum Dry Unit Weight and Optimum Water Content for Material Used in This Studyand the associated compaction curves are given in Figure 3.4. The respective averages (AVG), standard deviations (SDT), and coefficients of variation (CV) for RCA and RAP/RPM are summarized in Table 3.3. The averages of MDU and OMC for RCA and RAP/RPM as obtained from this study are compared with those from the literature in Table 3.4 (Blankenagel and Guthrie 2006, Bejarano et al. 2003, Saeed et al. 2008, Camargo 2008, Guthrie et al. 2007, Wen et al. 2008, Bennert, et al. 2000, Kuo et al. 2002).

The compaction characteristics (MDU and OMC) of RCA follow a similar trend to the compaction characteristics of RAP/RPM with higher MDU and lower OMC (Figure 3.5). The high coefficient of variation (R^2=0.89 for RAP/RPM and R^2=0.83 for RCA) between the compaction characteristics of RCA and RAP/RPM from different sources indicates that the values are statistically significant. MDU is within a narrow range of 19.4 to 21.5 kN/m^3 for RAP/RPM at lower OMCs (5.2 to 8.8%) and 19.4 to 20.8 5 kN/m^3 for RCA at higher OMCs (8.7 to 11.8%). The OMC of RAP/RPM was lower than RCA since asphalt coatings reduce the amount of water required to achieve MDU by preventing the water from reaching the individual particles of the material (Kim et al. 2007). RCA has high absorption capacity due to the porous nature of the cement paste portion (Arm 2001). Therefore, the amount of water required to achieve the MDU is higher than for natural aggregate and RAP (Juan and Gutierrez 2009).

3.5.2 *Resilient Modulus*

The resilient modulus presented is based on deformation measured with internal and external LVDTs. Variability in determining M_r was assessed by performing triplicate tests. The SRM for Class 5 aggregate, RCA, and RAP/RPM, computed in accordance with Procedure Ia of NCHRP 1-28A, are summarized in Table 3.5, along with parameters (k_1 and k_2) for the power function model (Equation 3.2) and the parameters (k_1, k_2, k_3, k_6, and k_7) for NCHRP model (Eqn.3.3) in Table 3.6. These SRM and parameters correspond to compaction at OMC and 95% modified Proctor MDU.

The estimated SRM by both models were compared with the measured modulus for RCA (Figure 3.6) and RAP/RPM (Figure 3.7). These comparisons are based on internally measured axial deformations. Statistical analysis indicated that results using both models are significant at a 95% confidence level, and both models represent the data reasonably well for RCA (R^2=0.85 from power function model and R^2=0.96 from NCHRP model) and for RAP (R^2=0.91 from power function model and R^2=0.97 from NCHRP model). The NCHRP model has less dispersion of the data than the power function for RCA and RAP. The power function model assumes constant Poisson's ratio and considers only the sum of the principal stresses (the bulk stress) as the effect of stress on M_r (Lekarp et al. 2000). However, the NCHRP model considers the bulk stress and the magnitude of the shear strain influenced mainly by shear or deviator stress (Lekarp et al. 2000).

The relationship between internal SRM and external SRM (from the power function model) for unbound recycled materials, blend, and Class 5 aggregate is shown in Figure 3.8. The SRM based on internal LVDT measurements of deformation were found to be consistently higher than those based on external LVDT measurements of deformation for all specimens. Camargo et al. (2009) reported that deformation measured with internal LVDTs more accurately describe deformation of the specimens for computation of resilient modulus. Since the external LVDT measurements are affected by bedding errors, specimen end effects, and machine compliance, results tend towards larger deformation measurements and, consequently, lower modulus for a given applied cyclic stress (Ping et al. 2003, Bejarano et al. 2002, Camargo 2008). The ratio shown in Figure 3.8, however, should not be considered typical as it is much higher than reported elsewhere in this report as well as other investigators for base course materials. It also can be expected to depend on the equipment and the material being tested.

The measured M_r of the recycled materials is compared to the conventional base course based on deformations measured with the internal and external LVDTs fitted to the power function model (Figure 3.9 and Figure 3.10, respectively). RAP/RPM has the highest SRM of the recycled materials evaluated. RCA has slightly lower SRM in comparison to RAP/RPM, while Class 5 aggregate has the lowest SRM, irrespective of the internal or external deformation measurements.

Previous research has reported that the stiffness of road base or subbase layers containing RCA or RAP has equal or higher M_r in comparison to natural aggregates (Kim et al. 2007, Bejarano et al. 2003, Wen et al. 2008). Wen et al. (2008) evaluated untreated RPM and crushed aggregates used at MnROAD test facility in terms of M_r and found that RPM has higher modulus than crushed aggregate. Bejarano et al. (2003) evaluated the stiffness of RAP compared to typical base course using M_r testing in accordance with Strategic Highway Research program test protocol. The stiffness of RAP was greater than that of the typical base course. Kim et al. (2007) performed M_r tests on an aggregate base blended with varying RAP contents (0 to 75%), with pure aggregate used as base course. All blends of aggregate base and RAP had M_r higher than the aggregate base alone, which explains the high SRM for RAP when compared to materials of similar USCS classification.

3.5.3 *Plastic Strain*

Plastic strains were determined for base materials from M_r testing by using the measured permanent deformations from the internal LVDTs with the power function model (Table 3.5). Plastic strains were calculated as the sum of the plastic strains for each loading sequence during resilient modulus test by excluding the plastic strains in the conditioning phase (Sequence 1). RCA showed average plastic strains of 0.7 %, whereas RAP, RPM and Class 5 showed plastic strain of 1.4 %, 1.5 % and 1.6 %, respectively. These results are different from those in Camargo (2009), but similar to those in Kim et al. (2007), Wen and Edil (2008, 2009), and Schaertl (2010). Camargo (2009) reported that RPM showed a plastic strain of 1.9 %, whereas Class 5 aggregate showed a plastic strain of 3.3 %. However, Kim et al. (2007) indicated that specimens with RAP exhibited higher plastic strains than the typical aggregate base material. Wen and Edil (2009) performed M_r tests on RPM and conventional crushed aggregate (Class 6sp) in accordance with NCHRP 1-28A test protocol. RPM had higher internal modulus (257 MPa) compared to Class 6sp (220 MPa). However, RPM showed higher plastic strains (2.8%) than Class 6sp (0.7%) indicating higher potential for rutting.

Schaertl (2010) determined the plastic deformation of RAP, RCA, Class 5 aggregate and blend (50%RCA and 50%Class 5 aggregate) by using Large-Scale Model Experiments (LSME) for two layer thickness (0.3 m and 0.2 m). The plastic deformation of RAP (211% and 102% in two experiments) was found to be greater than that experienced by Class 5 aggregate and RCA at the end of 10,000 cycles of load. LSME is a prototype pavement experiment and allows many cycles of loading, thus its data are considered to be more representative.

3.5.4 *Correlations*

Stepwise regression was performed by using multiple linear regressions to develop correlations (models) to predict the SRM and compaction characteristics (OMC and MDU) of RCA and RAP based on their gradation characteristics. Regression methods estimate the predictive equation and compute a correlation coefficient to describe how strongly the value of one variable is associated with another. Regression was preferred because of the simplicity to ensure statistical significance of each independent variable and the clarity to evaluate the physical significance between the dependent and independent variables (Bareither et al., 2008).

A multiple regression model was developed between the compaction characteristics (w_{opt} and γ_{dmax}) and index properties (i.e. C_u, C_c, sand%, gravel%, fines%, D_{10}, D_{30}, D_{50}, D_{60}, absorption, asphalt content, specific gravity and deleterious materials) (given in Table 3.3) for RCA and RAP is summarized in Table 3.7. The models of compaction characteristics for RAP have relatively high R^2 values (0.92 for w_{opt} and 0.70 for γ_{dmax}) from the regression analysis in comparison to those for RCA (0.65 for w_{opt} and 0.67 for γ_{dmax}). The variability in the source of RCA materials is more significant than RAP materials.

A multiple linear regression model was developed between external and internal SRM (given in Table 3.9) and index properties (given in Table 3.1) for RCA and RAP. The correlations are summarized in Table 3.8. The model has relatively high R^2 value of the regression analysis for external and internal SRMs for RCA (0.89), and all the independent variables used in the model

have p-values smaller than 0.05. The coefficients of the models have also physical significance. The negative coefficient on D_{30} indicate that SRM decreases with increasing fines content (Tutumluer and Seyhan 1998) and the negative coefficient on w_{opt} (%) indicates that SRM decreases with increasing w_{opt} (%) (Pan et al. 2006, Attia and Abdelrahman 2010). The change in D_{30} may affect the gradation of the materials as the increase in fines is likely to increase the water holding capacity of RCA (Saeed et al. 2008, Alam et al. 2010), which may reduce the resilient modulus (Tutumluer and Seyhan 1998).

The model for external and internal SRM for RAP has an R^2=0.99, and all the independent variables used in the model have p-values smaller than 0.05. The coefficients have also physical significance. The negative coefficient of fines content indicate that external and internal SRM decreases with increasing fines and the negative coefficients on absorption indicate that internal SRM decreases with increasing water holding capacity of the specimen. The positive coefficient on D_{60} or D_{30} and asphalt content (%) indicates that SRM increases with increasing D_{60} or D_{30} and asphalt coating. The increase in asphalt coating may increase the water drainage during compaction while reducing the absorption capacity of the material (Attia and Abdelrahman 2010). The decrease in water content tends to increase the M_r of the materials (Pan et al. 2006). D_{60} and D_{30} reflect the influence of gradation on the materials. This strong relationship between SRM and index properties suggests that the external or internal SRM of RCA and RAP could be estimated from the index properties although the statistical relations are different for each.

The internal SRMs reported in Chapter 3 are not considered accurate and should not be used. The internal LVDTs were different from the LVDTs used later and had a shorter range for recording displacement. This shorter range did not allow the entire M_r test to proceed without resetting the interior LVDTs in the middle of the test, which could have altered the data collected and led to higher SRM values. The external LVDTs were calibrated correctly and SRM calculated from these LVDTs is considered accurate. Furthermore, the ratio of internal to external SMR is too high and does not check with other tests on unbound base course materials. This issue was not known at the time this task was completed. The internal SRMs reported elsewhere in the report are considered accurate.

3.5.5 *Blended RAP/RCA Effect on Stiffness of Recycled Material*

The effect of the amount of RAP blended with natural aggregate on the stiffness was investigated by blending 50% of CO RAP and CA RAP with Class 5 aggregate. Modified Proctor compaction tests were conducted on the blend to obtain the OMC and MDU. Figure 3.11 and Figure 3.12 show the compaction curves of CA RAP and CO RAP blended with Class 5 aggregate, respectively along with the compaction curves of the blending components. Adding RAP to Class 5 aggregate causes a shift in compaction curve. The type of shift depends on the type of the recycled material used (Kim et al. 2007). Increasing RAP content is associated with decreasing OMC and MDU values, since the presence of asphalt coating does reduce the amount of water required to achieve the MDU probably due to reduced water absorption capacity (Alam et al. 2010).

Previous studies showed that the increase in the percentage of RAP in base materials increased the resilient modulus (Bennert et al. 2000, Guthrie et al. 2007). The results of the effect of RAP content on Class 5 aggregate are summarized in Table 3.9. Samples containing 100% RAP has a

higher SRM compared to samples containing 50% RAP, and 0% RAP (Class 5 aggregate) as presented in Figure 3.13 in terms of SRM based on internal LVDTs. The 50% increase in the CO RAP and CA RAP increased the stiffness of the Class 5 aggregate, 11% and 39%, respectively.

The effect of RCA amount on the stiffness of unbound base layer was investigated by using the field blended materials (50% RCA (MN) and 50% Class 5 aggregate) obtained from MnDOT. Modified Proctor compaction test conducted on the 50% RCA (MN) blended with Class 5 aggregate to obtain the OMC and MDU are already given in Figure 3.4. Adding RCA (MN) to Class 5 aggregate causes a shift in compaction curve and that the type of shift. Increasing RCA content is associated with increasing OMC and decreasing MDU due to the high water absorption capacity of RCA (FHWA 2008). The 50% increase in the MN RCA increased the stiffness of the Class 5 aggregate by 20 % (Figure 3.13).

Figure 3.14 shows normalized SRM of the RAP and RCA blends (relative to SRM of Class 5 aggregate) as a function of blending percentage based on internal LVD measurements. Even though the rate of increase in SRM varied with the type of RAP, the trend in the increase in SRM for Class 5 aggregate is similar. Some recent studies also reported that an increase in RAP content improves the stiffness of unbound base course. Kim et al. (2007) investigated the stiffness of base course containing different ratios of RAP and natural aggregate. Resilient modulus tests were conducted on the recycled material in accordance with NCHRP 1-28a. The 50% aggregate-50% RAP specimens developed stiffness equivalent to the 100% aggregate specimens at lower confining pressures (~ 20 kPa); at higher confinement (~ 120 kPa), the RAP specimens were stiffer. Alam et al. (2010) also blended natural aggregates with different percentages of RAP and a significant amount of increase was observed in M_r. Even though the rate of increase in SRM varied with recycled materials, the trend in the increase in SRM for Class 5 aggregate is similar.

3.6 Summary and Conclusions

This laboratory investigation dealt with the characterization of the engineering properties of the recycled materials (recycled asphalt pavement (RAP), recycled pavement material (RPM) and recycled concrete aggregate (RCA), as well as one field blended materials consisting of 50% RCA and 50% conventional base material used as unbound base/subbase layer without treatment. These recycled materials were collected from a wide geographical area, covering eight states in the U.S: California, Colorado, Michigan, Minnesota, New Jersey, Ohio, Texas and Wisconsin. A conventional base material meeting the gradation standard of Minnesota Department of Transportation Class 5 aggregate was used as a reference material. The investigation also dealt with the determination of the influence of compaction effort, compaction moisture content, and freeze-thaw cycling on the engineering properties of unbound recycled materials, and the behavior of RAP or RCA blended to Class 5 aggregate used as unbound base/subbase layer.

The objectives were to investigate the mechanical properties of the recycled materials as unbound base or subbase material without treatment or stabilization under laboratory conditions. The objectives were met by determining the resilient modulus of the recycled materials in

accordance with NCHRP 1-28a protocol measuring deflections both externally and internally on the specimens.

RAP/RPM had higher SRM than Class 5 aggregate and RCA. RAP/RPM exhibited slightly smaller plastic strain than Class 5, whereas RCA (0.7%) showed the lowest plastic strain during the M_r testing. There were quantitative differences in the stiffness of recycled materials from different sources. However, considering the wide geographic area they were obtained from, the differences were not extraordinary. Two commonly used resilient modulus functions (Power Function and NCHRP models) for unbound base aggregates both captured the stress dependency of M_r satisfactorily. The multiple linear regression models were developed to estimate summary resilient modulus (SRM) from compaction parameters and materials parameters that exhibited high coefficient of determination for RAP and for RCA.

Blending recycled materials with natural aggregate result in intermediate modulus between the moduli of the two materials. Recycled materials had higher moduli then natural aggregate in this study.

3.7 Tables

Table 3.1 Index Properties for Recycled Materials and Class 5 aggregate

Material	States	D_{10} (mm)	D_{30} (mm)	D_{50} (mm)	D_{60} (mm)	C_u	C_c	G_s	Absorption (%)	Asphalt Content /Mortar Content (%)	Impurities (%)	Gravel (%)	Sand (%)	Fines (%)	USCS	AASHTO
Class 5 Aggregate	MN	0.1	0.4	1.0	1.7	21	1.4	2.57	_	_	0.25	22.9	67.6	9.5	GW-GM	A-1-b
Blend	MN	0.2	0.6	1.5	2.8	13	0.5	_	_	_	0.36	32.7	63.8	3.4	SP	A-1-b
RCA	MN	0.1	0.4	1.0	1.7	21	1.4	2.39	5.0	55	0.87	31.8	64.9	3.3	SW	A-1-a
	MI	0.4	4.1	9.7	12.3	35	3.9	2.37	5.4	_	0.35	68.5	28.3	3.2	GP	A-1-a
	CO	0.1	0.6	2.8	4.9	66	1.1	2.28	5.8	47	0.26	40.9	46.3	12.8	SC	A-1-b
	CA	0.3	1.7	4.8	6.8	22	1.4	2.32	5.0	37	0.26	50.6	47.1	2.3	GW	A-1-a
	TX	0.4	6.5	13.3	16.3	38	6.0	2.27	5.5	45	0.86	76.3	21.6	2.1	GW	A-1-a
	OH	0.2	1.2	3.4	5.3	34	1.7	2.24	6.5	65	0.16	43.2	49.5	7.3	SW-SM	A-1-a
	NJ	0.2	0.5	2.0	5.1	28	0.3	2.31	5.4	_	1.67	41.2	54.6	4.3	SP	A-1-b
RAP	MN	0.3	0.7	1.6	2.3	7	0.7	2.41	1.8	7.1	0.06	26.3	71.2	2.5	SP	A-1-a
	CO	0.4	0.9	2.2	3.3	9	0.7	2.23	3.0	5.9	0.09	31.7	67.7	0.7	SP	A-1-a
	CA	0.3	1.3	3.0	4.2	13	1.2	2.56	2.0	5.7	0.33	36.8	61.4	1.8	SW	A-1-a
	TX	0.7	2.5	5.4	7.9	11	1.1	2.34	1.3	4.7	0.05	41.0	44.9	1.0	SW	A-1-a
	OH	0.5	1.6	2.9	3.8	7	1.3	2.43	0.6	6.2	0.06	32.1	66.2	1.7	SW	A-1-a
	NJ	1.0	2.8	4.9	5.9	6	1.3	2.37	2.1	5.2	0.48	50.9	48.4	0.7	GW	A-1-a
	WI	0.6	1.4	2.7	3.6	6	0.9	2.37	1.5	6.2	0.08	30.9	68.5	0.5	SP	A-1-b
RPM	NJ	0.5	2.1	5.8	8.7	18	1.0	2.35	2.6	4.3	0.04	55.7	43.6	0.6	GW	A-1-b
	MI	0.4	1.7	4.6	6.5	17	1.1	2.39	1.7	5.3	0.13	49.3	50.4	0.4	SW	A-1-b

Note: Asphalt Content determined for RAP/RPM and Mortar Content determined for available RCA

D_{10} = effective size, D_{30} = particle size for 30% finer, D_{50} = median particle size, D_{60} = particle size for 60% finer, C_u = coefficient of uniformity, C_c = coefficient of curvature, G_s= Specific Gravity, AC= Asphalt Content, Abs=Absorption, Note: Particle size analysis conducted following ASTM D 422, G_s determined by ASTM D 854, Absorption of coarse aggregate were determined by ASTM C127-07, USCS classification determined by ASTM D 2487, AASHTO classification determined by ASTM D 3282, asphalt content determined by ASTM D 6307

Table 3.2 Maximum Dry Unit Weight and Optimum Water Content for Material Used in This Study

Specimens	States	Optimum Water Content W_{opt} (%)	Maximum Dry Unit Weight γ_{dmax} (kN/m^3)
Class 5 Aggregate	MN	8.9	20.1
Blend*	MN	8	21.3
RCA	MN	11.2	19.5
	MI	8.7	20.8
	CO	11.9	18.9
	CA	10.4	19.9
	TX	9.2	19.7
	OH	11.8	19.4
	NJ	9.5	19.8
RAP	MN	6.7	20.8
	CO	5.7	20.7
	CA	6.1	20.7
	TX	8	20.3
	OH	8.8	19.8
	NJ	6.5	20.4
	WI	7.3	20
RPM	MI	5.2	21.5
	NJ	6.3	20.6

Note:*Blend consists of 50% RCA (MN) and 50% Class 5 aggregate obtained at MNROAD field site

Table 3.3 Summary of Maximum Dry Unit Weight and Optimum Water Content of RCA and RAP/RPM

Specimens	Optimum Water Content W_{opt} (%)				Maximum Dry Unit Weight γ_{dmax} (kN/m^3)			
	AVG	STD	CV	Range	AVG	STD	CV	Range
RCA	10.4	1.29	12%	3.2	19.7	0.59	3%	1.9
RAP/RPM	6.7	1.13	17%	3.6	20.5	0.49	3%	1.7

Note: AVG=Average, SDT=Standard deviations, CV=Coefficients of variation

Table 3.4 Compaction Characteristics of Recycled Pavements from the Literature

Specimens		Optimum Water Content W_{opt} (%)	Maximum Dry Unit Weight γ_{dmax} (kN/m^3)
		Average	Average
		(range)	(range)
RCA	UW-Madison	10.4	19.7
		(8.7~11.9)	(18.9~20.8)
	Literature	10.1	18.9
		(7.5~12.1)	(17.9~19.8)
RAP/RPM	UW-Madison	6.7	20.6
		(5.2~8.8)	(19.8~21.5)
	Literature	6.4	20.1
		(5.0~10.3)	(18.1~22.9)

Table 3.5 Summary Resilient Modulus (SRM), Power Function Model Fitting Parameters k1 and k2 (Equation 3.1), and Plastic Strain for Base Materials

Material	States	External			Internal			Plastic Strain (%)	SRM_{INT}/ SRM_{EXT}
		k_1	k_2	SRM (MPa)	k_1	k_2	SRM(MPa)		
Class 5 Aggregate	MN	14.9	0.43	152	43.2	0.47	525	1.60	3.5
Blend*	MN	18.2	0.43	182	50.2	0.49	675	1.05	3.7
RCA	MN	18.5	0.44	189	38.3	0.54	680	0.63	3.6
	MI	14.3	0.46	171	40.7	0.54	715	0.80	4.2
	CO	17.4	0.43	175	41.5	0.49	580	0.73	3.3
	CA	15.2	0.46	178	33.0	0.54	627	0.70	3.5
	TX	9.1	0.54	164	17.6	0.64	549	0.83	3.3
	OH	12.6	0.48	163	27.7	0.56	554	0.57	3.4
	NJ	22.0	0.42	208	49.6	0.50	735	0.55	3.5
RAP	MN	23.0	0.39	180	26.3	0.61	674	1.35	3.7
	CO	25.6	0.37	184	75.0	0.41	673	1.47	3.7
	CA	12.3	0.49	173	36.4	0.53	627	1.16	3.6
	TX	21.6	0.42	198	52.4	0.52	776	1.38	3.9
	OH	15.6	0.48	197	42.7	0.52	699	1.32	3.6
	NJ	23.5	0.41	209	54.6	0.48	715	2.13	3.4
	WI	29.5	0.41	266	65.0	0.51	968	0.89	3.6
RPM	MI	14.7	0.46	168	43.5	0.50	631	1.49	3.8
	NJ	26.3	0.43	264	61.6	0.52	989	1.26	3.8

Note:*Blend consists of 50% RCA (MN) and 50% Class 5 aggregate obtained at MNROAD field site

Table 3.6 Summary Resilient Modulus (SRM), NCHRP Model Fitting Parameters k1, k2, k3, k6 and k7 (Equation 3.3)

Material	States	External						Internal					
		k_1	k_2	k_3	k_6	k_7	SRM (MPa)	k_1	k_2	k_3	k_6	k_7	SRM (MPa)
Class 5 Aggregate	MN	1791	0.7	-0.8	-0.4	2.2	144	4416	1.0	-0.9	-28.9	1.8	484
Blend*	MN	15697	1.5	-2.3	-137.8	6.1	191	48303	1.6	-2.2	-95.9	4.4	683
RCA	MN	4164	1.3	-1.7	-110.6	4.4	190	49316	1.7	-2.2	-114.5	5.1	648
	MI	2122	0.8	-1.0	-0.3	1.8	171	9201	0.8	-0.9	-0.5	2.1	715
	CO	1059	1.1	-1.0	-25.8	1.2	162	5358	1.1	-1.2	-8.9	1.5	520
	CA	2199	0.9	-1.2	-0.3	1.7	166	8023	1.0	-1.4	-0.3	1.7	563
	TX	2044	0.9	-1.2	-0.4	1.8	151	6179	1.5	-1.7	-31.1	2.3	490
	OH	1971	0.7	-0.8	-0.1	2.1	158	6819	0.9	-0.9	-0.5	2.6	522
	NJ	2639	0.8	-1.2	-0.6	1.6	203	7080	1.2	-1.4	-17.5	1.4	683
RAP	MN	2190	0.6	-0.8	-0.4	2.2	174	5444	1.2	-0.4	-97.6	4.5	665
	CO	2093	0.6	-0.9	-0.2	1.5	177	7720	0.7	-1.0	-0.2	1.6	629
	CA	2043	0.8	-1.0	-0.3	1.8	166	7935	1.0	-1.2	-0.3	1.8	589
	TX	1749	0.7	-0.7	-11.9	1.3	188	8451	0.5	-0.2	0.0	13.4	779
	OH	2368	0.8	-1.0	-0.2	1.7	192	8727	0.9	-1.2	-0.3	1.7	674
	NJ	2450	0.6	-0.7	-0.2	1.9	207	8680	0.7	-0.8	-0.4	1.9	715
	WI	3251	0.6	-0.7	-0.3	2.0	274	12594	0.7	-0.9	-0.3	1.9	1013
RPM	MI	2019	0.7	-0.9	-0.3	2.0	161	7843	0.7	-0.8	-0.2	2.1	614
	NJ	3207	0.7	-0.9	-0.1	1.8	264	8719	1.1	-1.1	-24.2	1.5	995

Note:*Blend consists of 50% RCA (MN) and 50% Class 5 aggregate obtained at MNROAD field site

Table 3.7 Relationship between Compaction Characteristics and Soil Properties for Recycled Materials

Materials	Compaction Characteristics	Correlation Equations	R^2
RCA	W_{opt} (%)	-0.064 **Cu* + 0.763 **Absorption(%)* + 7.75	0.65
	γ_{dmax} (kN/m^3)	-0.374 **W_{opt}(%)* + 23.6	0.83
RAP	W_{opt} (%)	-0.0626 **Cu* - 1.349 **Absorption(%)* + 9.84	0.92
	γ_{dmax} (kN/m^3)	-0.289* *W_{opt} (%)* + 22.42	0.83

Table 3.8 Relationship between Resilient Modulus, Compaction Characteristics, and Soil Properties for Recycled Material

Materials	Summary Resilient Modulus (SRM) (Mpa)	Correlation Equations	R^2
RCA	SMR_{EXT}	171.646-(3.482*D_{30}) + (22.378*Impurities %)	0.89
	SMR_{INT}	14683.478 - (36.764*D_{30}) - (72.719*Wopt)	0.89
RAP	SMR_{EXT}	(117.493 * D_{30}) + (19.472 *γ_{dmax} + (27.128 * Asphalt Content(%)) - (18.510 * Absorption(%)) -427.329	0.99
	SMR_{INT}	(-2268.783)-(285.884*Fines %)+(628.742*Asphalt content (%))+ (201.107*D_{60})-(483.158*G_s)-(58.243*Absorption (%))	0.99

AC: asphalt content

Table 3.9 Summary Resilient Modulus (SRM) and Power Model Fitting Parameters k1 and k2 (Equation 3.1) for Base Materials for Blended RAP with Class 5 Aggregate

Specimens	External			Internal			$SRM_{Class\ 5}$/ SRM_{Blend}
	k_1	k_2	SRM (MPa)	k_1	k_2	SRM (MPa)	
Class 5 aggregate	66.2	0.20	191	129.2	0.15	281	1.0
Blend (CO-MN)	94.5	0.18	244	44.3	0.37	313	1.1
RAP (CO)	129.3	0.16	297	122.6	0.20	362	1.3
Class 5 aggregate	66.2	0.20	191	129.2	0.15	281	1.0
Blend (CA-MN)	76.4	0.22	245	209.7	0.12	391	1.4
RAP (CA)	122.5	0.14	256	348.8	0.06	473	1.7
Class 5 aggregate	66.2	0.20	191	129.2	0.15	281	1.0
Blend (MN)	90.7	0.17	230	116.8	0.21	350	1.2
RCA (MN)	122.5	0.14	256	348.8	0.06	473	1.7

3.8 Figures

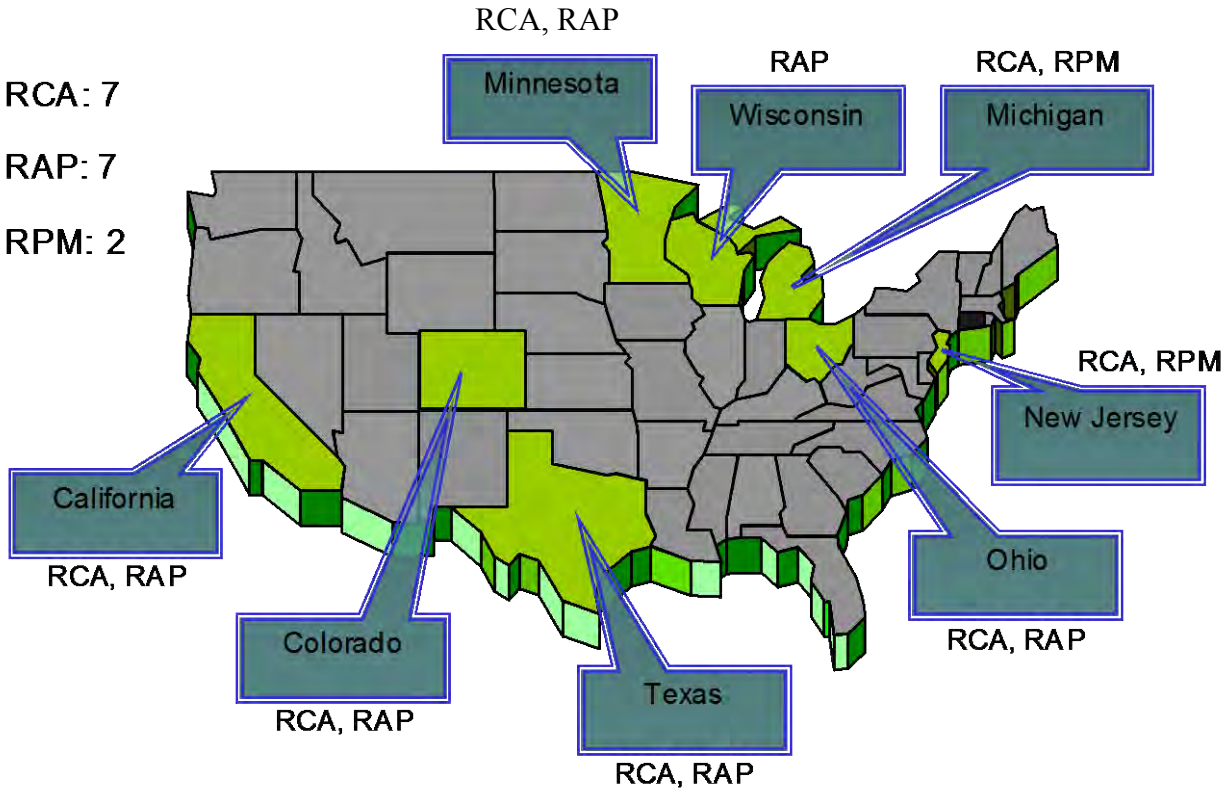

Figure 3.1 Locations of Recycled Material Used in this Study

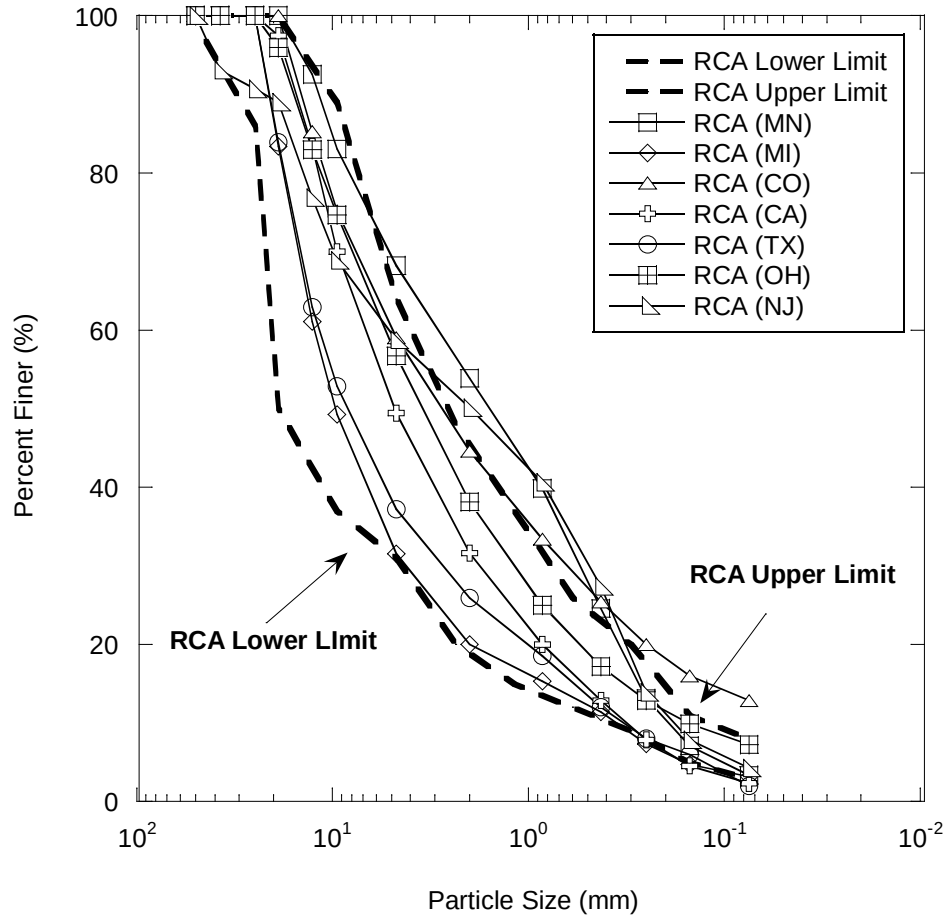

Figure 3.2 Particle Size Distribution for RCA and RCAs Reported Lower and Upper Limits from Literature

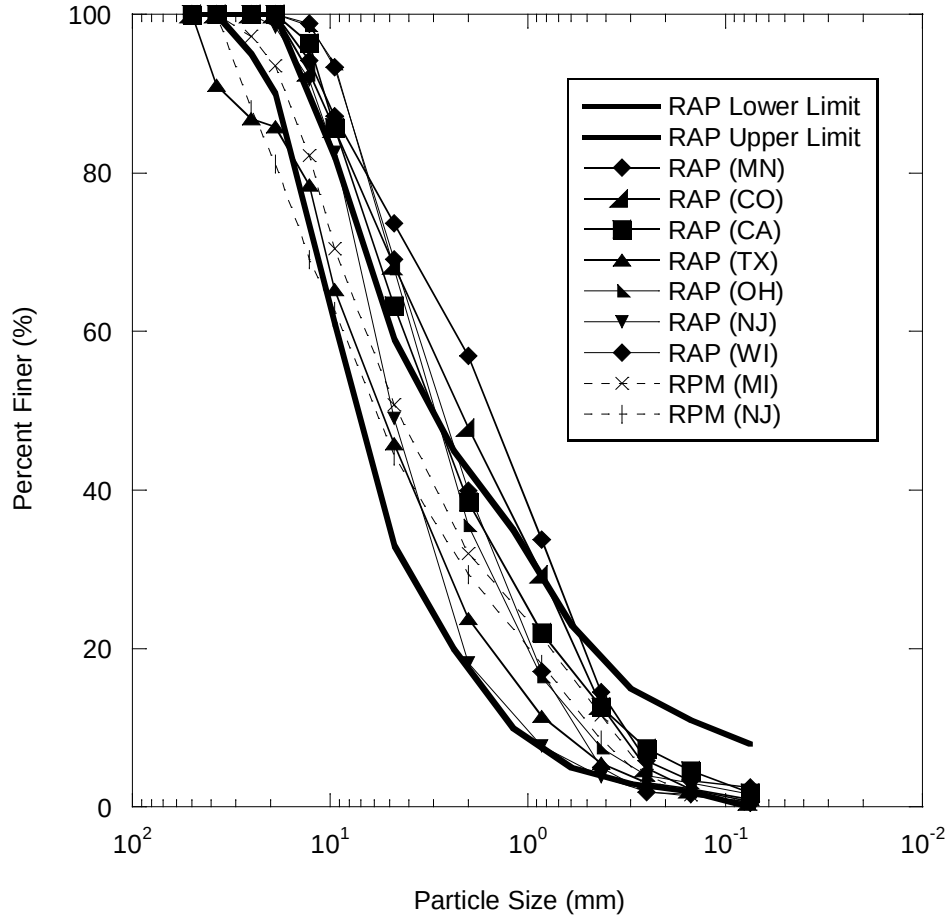

Figure 3.3 Particle Size Distribution for RAP/RPM and RAPs Reported Lower and Upper Limits from Literature

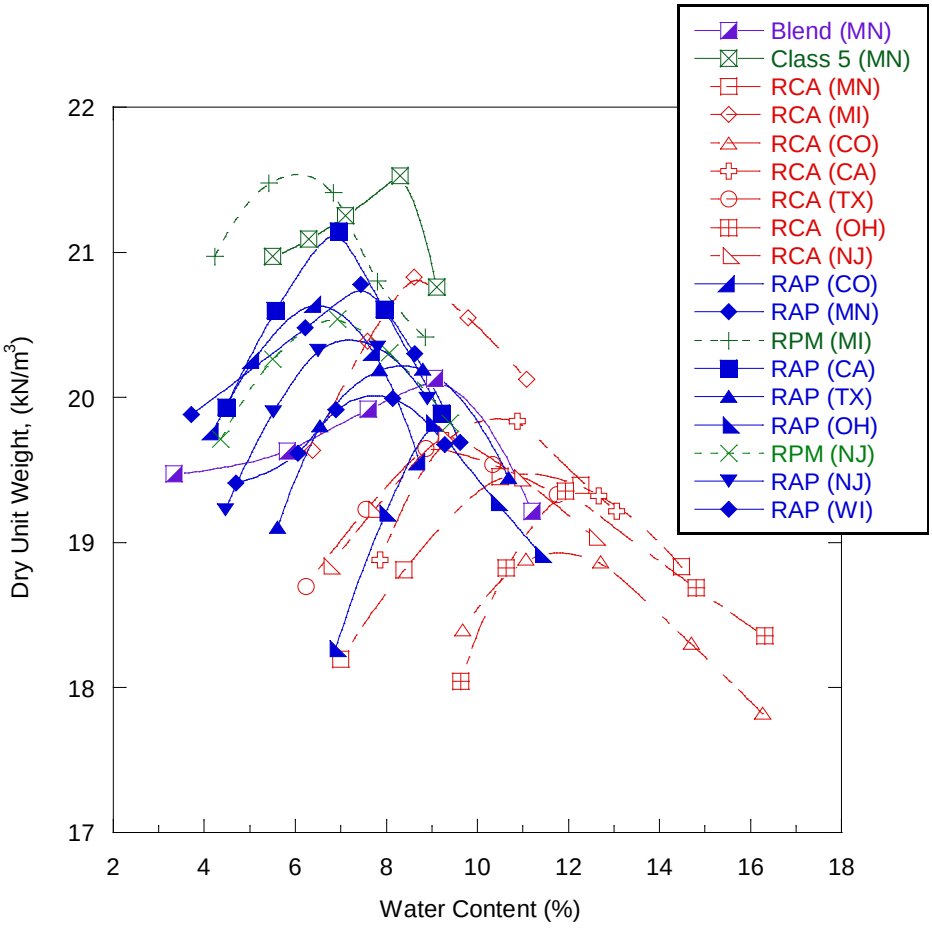

Figure 3.4 Compaction Curves for Recycled Materials and Class 5 Aggregate Used in this Study

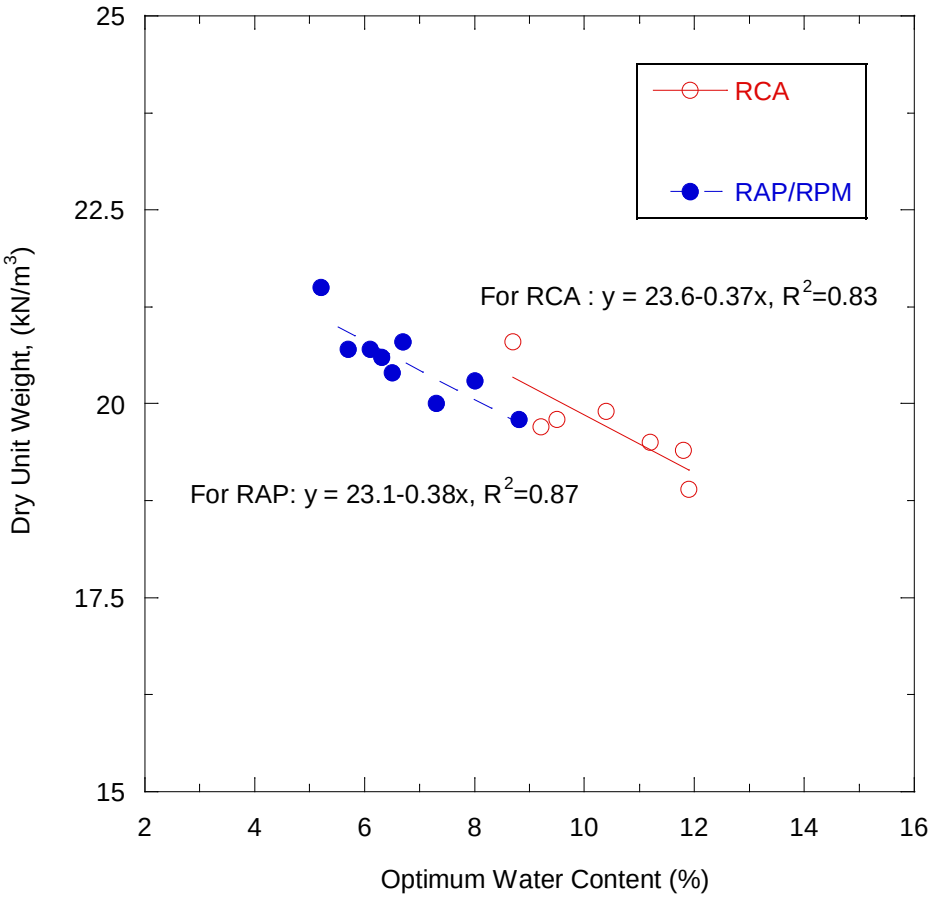

Figure 3.5 Maximum Dry Unit Weight and Optimum Water Content for RCA and RAP

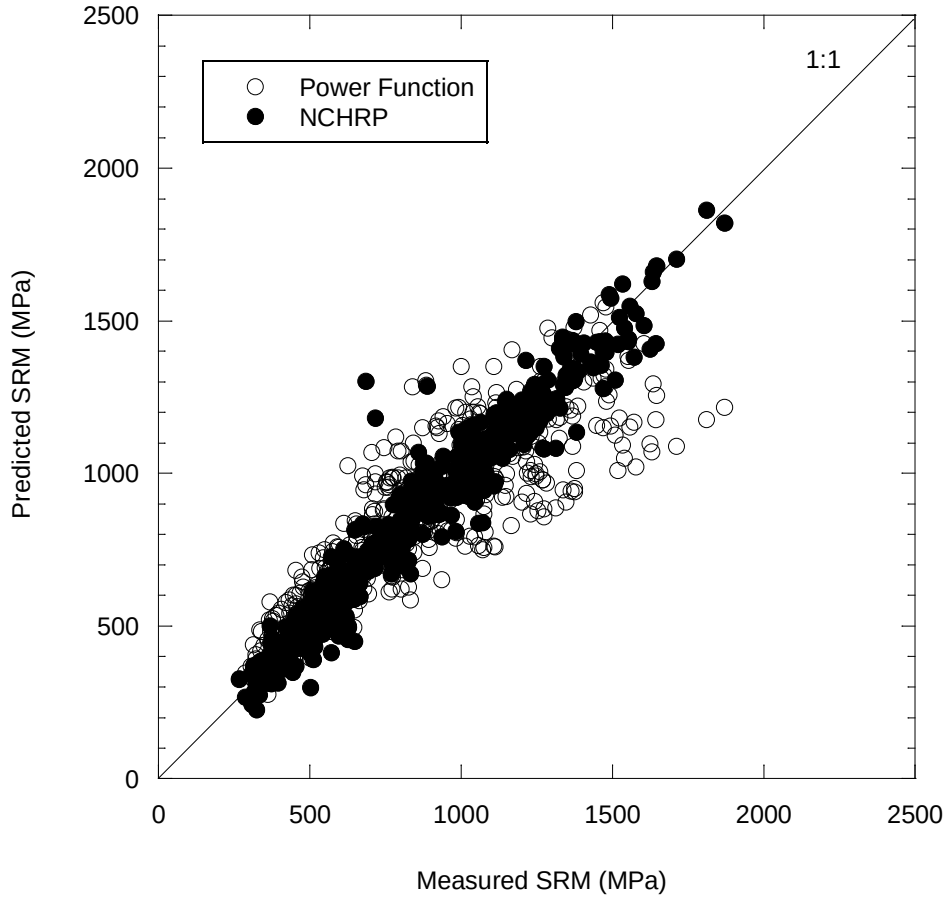

Figure 3.6 Relationship between Measured SRM and Predicted SRM using the Power Function and NCHRP Models for RCA (Internal)

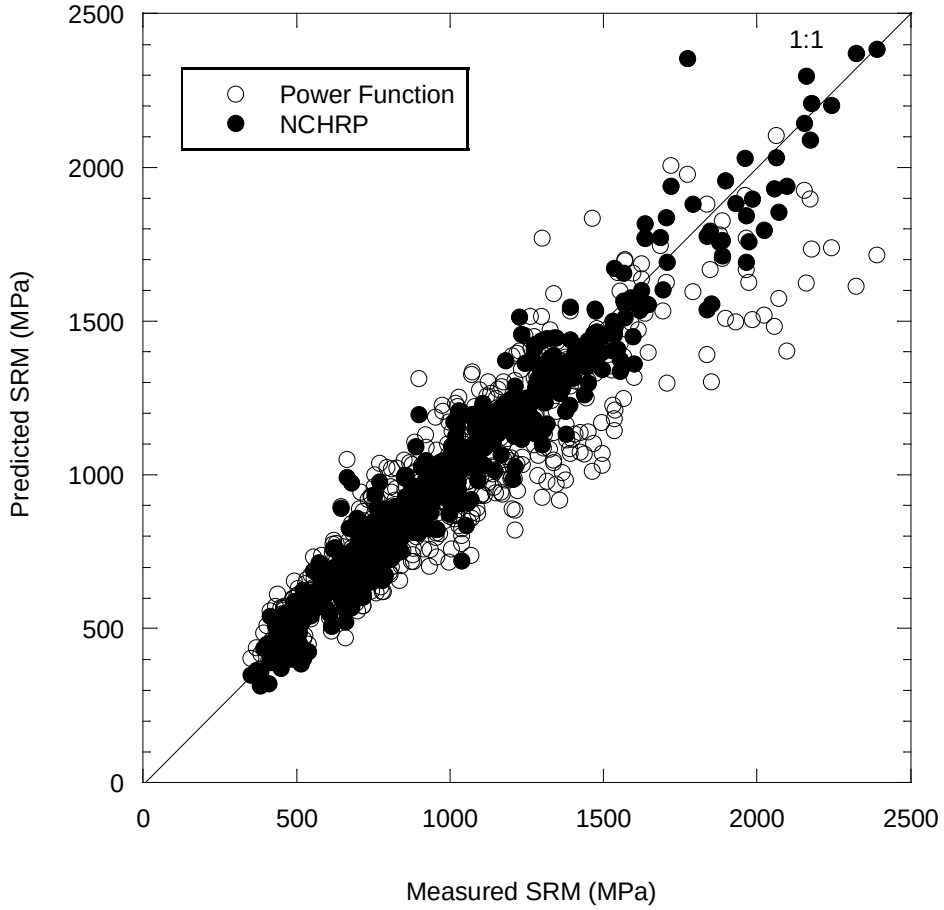

Figure 3.7 Relationship between Measured SRM and Predicted SRM using the Power Function and NCHRP Models for RAP/RPM (Internal)

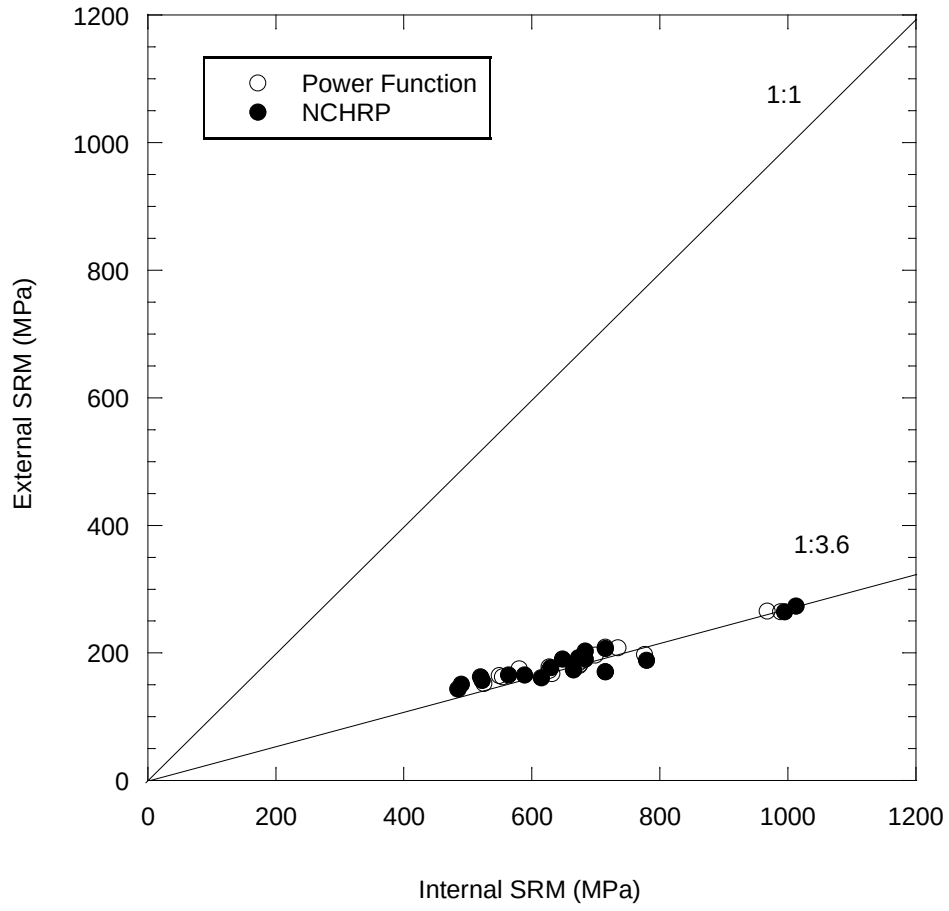

Figure 3.8 Ratio of Internal to External SRM Versus Internal SRM using the Power Function and NCHRP Models for Recycled Materials

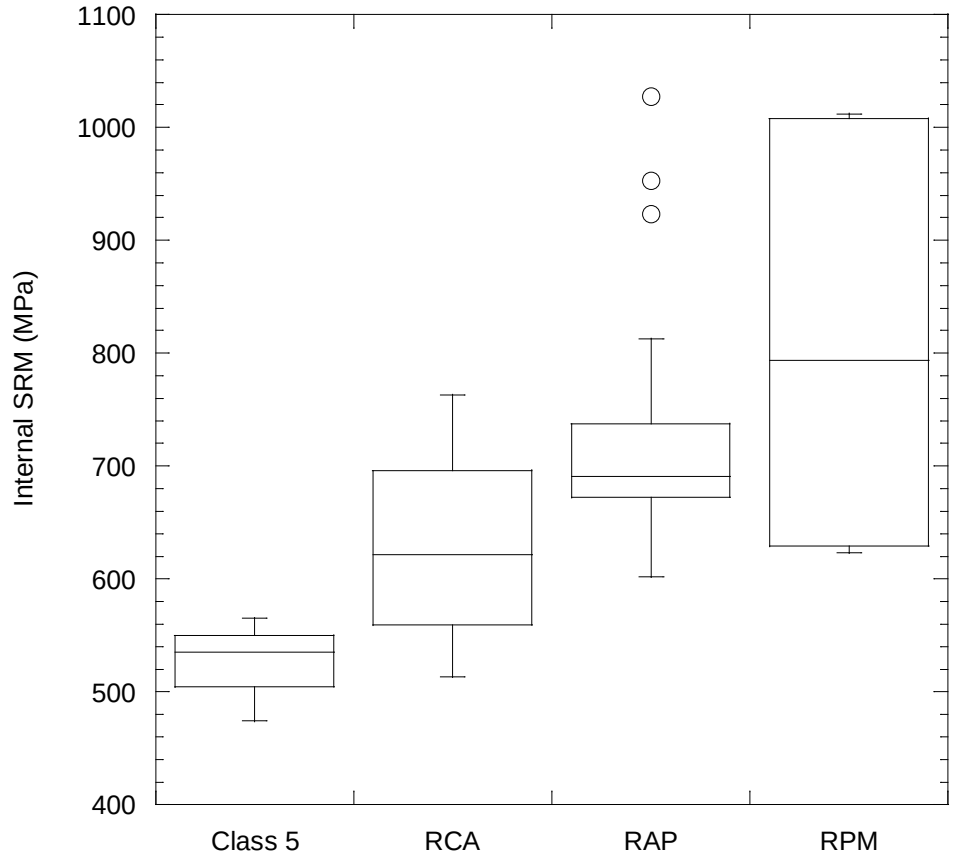

Figure 3.9 Summary Resilient Modulus (SRM) Measured by Internal LVDTs for Class 5 Aggregate, RCA, RAP, and RPM

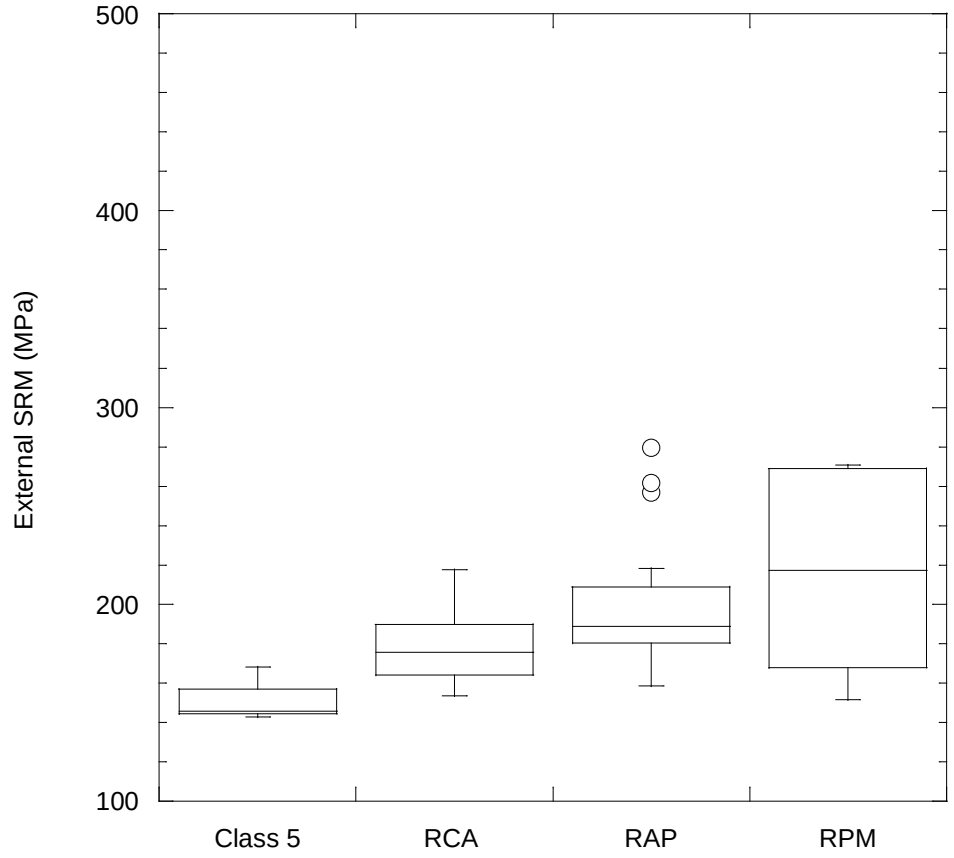

Figure 3.10 Summary Resilient Modulus (SRM) Measured by External LVDTs for Class 5 Aggregate, RCA, RAP, and RPM

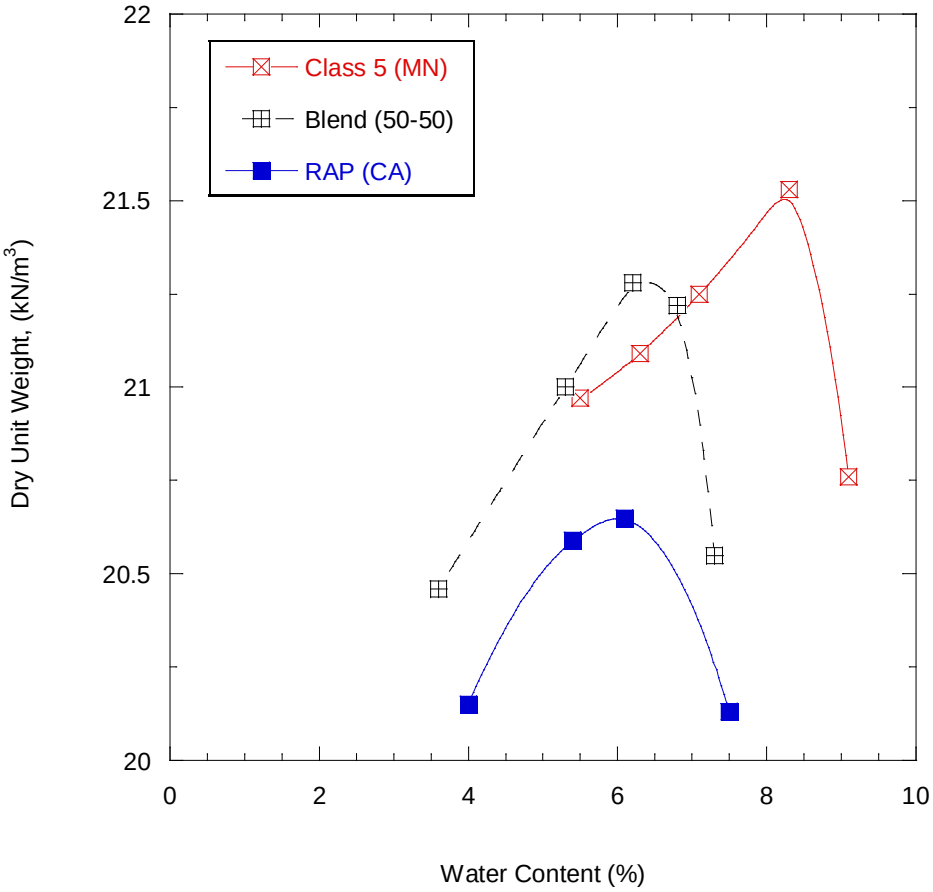

Figure 3.11 Compaction Curves for RAP (CA) and RAP (CA) Blended with 50 % of Class 5 Aggregate

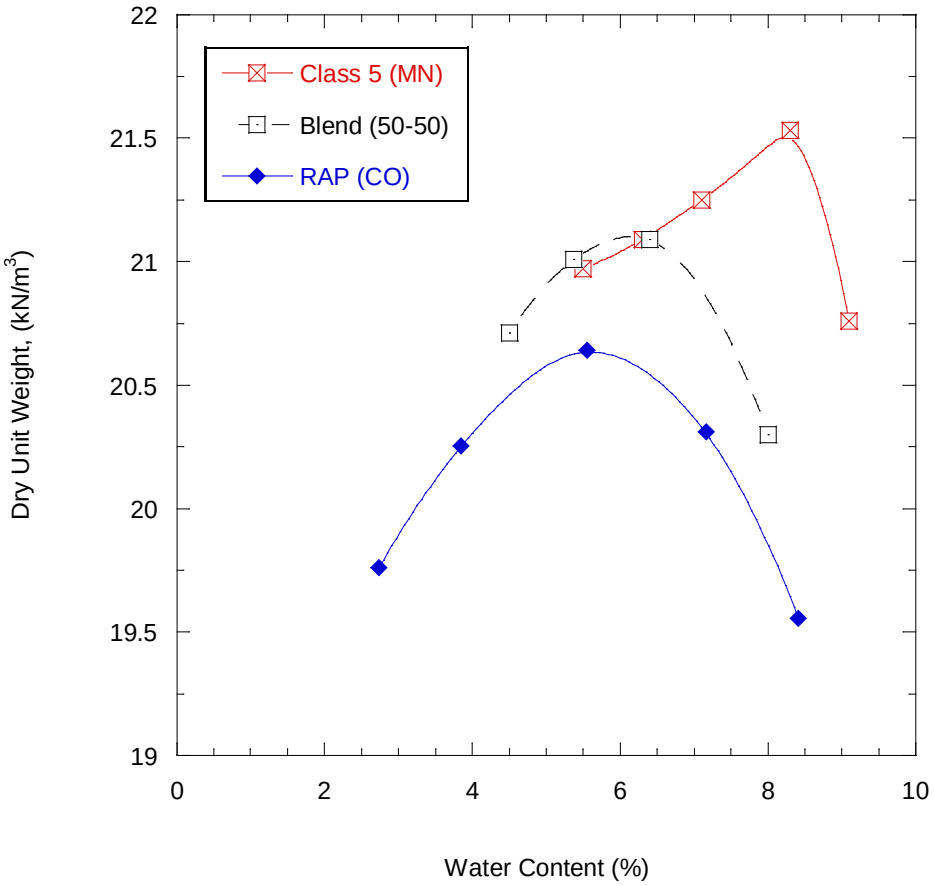

Figure 3.12 Compaction Curves for RAP (CO) and RAP (CO) Blended with 50 % of Class 5 Aggregate

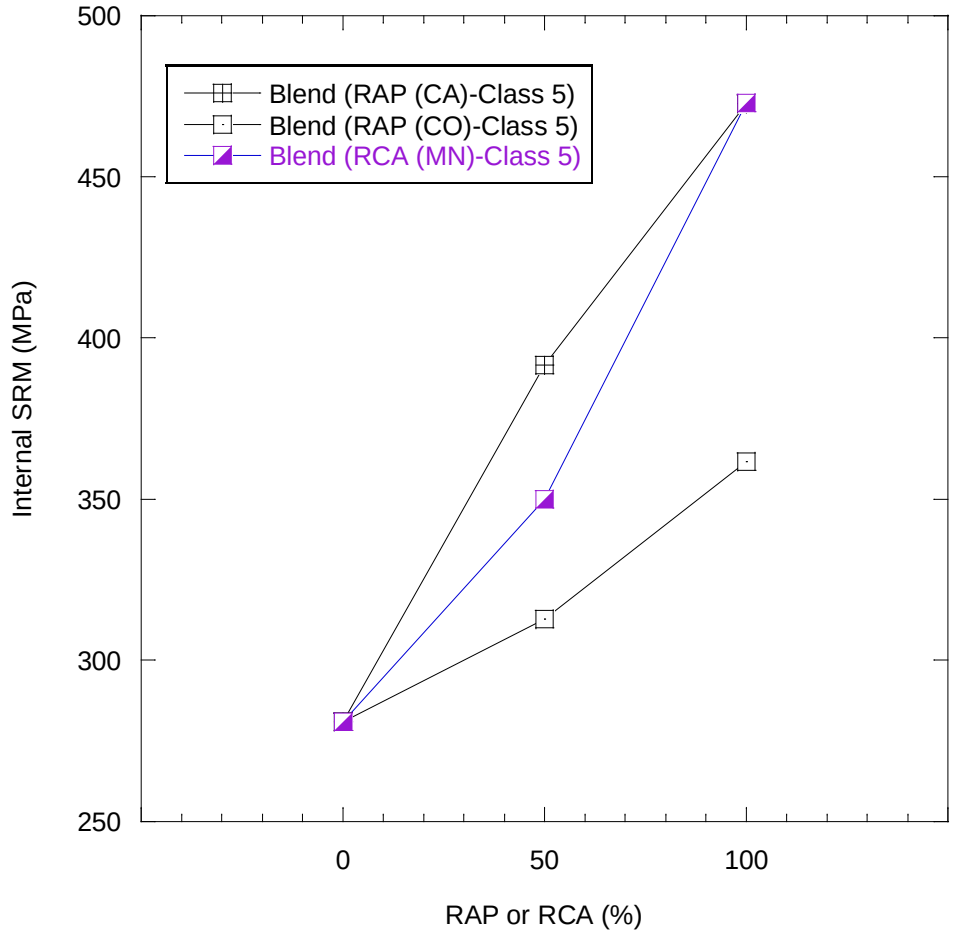

Figure 3.13 Internal Summary Resilient Modulus (SRM) for Class 5 Aggregate Blended with RAP (CO), RAP (CA) and RCA (MN) at Different Percentages (0%, 50%, 100%).

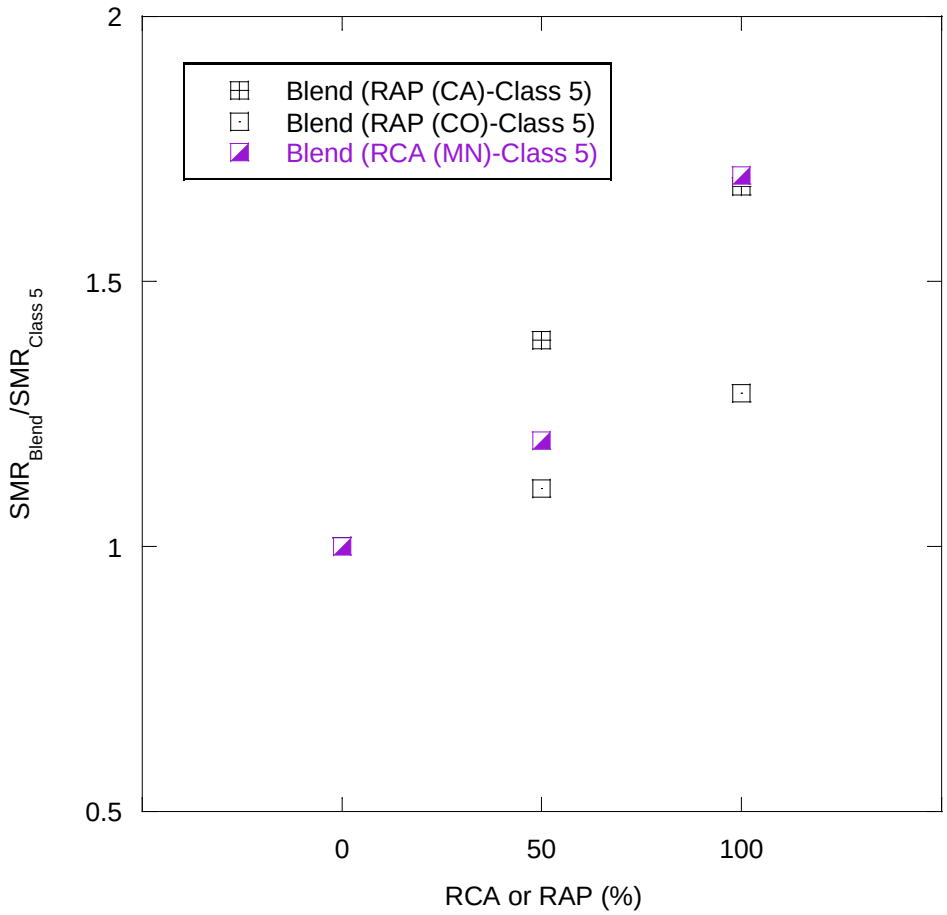

Figure 3.14 Normalized Summary Resilient Modulus (SRM) for Class 5 Aggregate Blended with RAP (CO) and RAP (CA) at Different Percentages

4. Scaling and Equivalency of Bench-Scale Tests to Field-Scale Conditions

4.1 Introduction

The production of crushed stone aggregate in the United States was estimated at 1.2 billion tons in 2010 (USGS 2011), of which the U.S. highway system is estimated to account for over 40 percent of the total demand. However, rapidly decreasing sources of virgin aggregate, along with limits placed upon aggregate production by environmental regulation and land use policies, has caused the price of these materials to increase dramatically (ACPA 2009). Conversely, the production of demolition and construction waste has increased as the amount of landfill available to contain this material has decreased (Poon et al. 2006, Chini et al. 2001). The need to find appropriate disposal locations for this material has been of increasing concern (Kuo et al. 2002). Recycling programs offer a viable solution to both problems.

The use of recycled materials as recycled base course in new or rehabilitated roadway construction has become more common in the last twenty years, with some municipalities reporting as much as 400,000 tons of recycled materials used in this manner (Bennert et al. 2000, Nataatmadja and Tan 2001). Recycled roadway materials are typically generated and used at the same construction site, providing increased savings in both money and time (Bennert et al. 2000). It has been speculated that in some municipalities recycled materials cost less to use than conventional crushed-stone base material by as much as 30% (Blankenagel and Guthrie 2006).

Recycled asphalt pavement (RAP) and recycled concrete aggregate (RCA) are materials commonly used as unbound base course in the construction of roadway pavement. RAP is produced by removing and reprocessing existing asphalt pavement, and RCA is the product of the demolition of concrete structures such as buildings, roads and runways (Kuo et al. 2002, Guthrie et al. 2007, FHWA 2008). The production of RAP and RCA results in an aggregate that is well graded and of high quality, and the costs of recycled materials have been estimated to be 25% to 50% cheaper than traditional aggregates (Guthrie et al. 2007, FHWA 2008). Despite the increased acceptance of recycled base materials in construction, research concerning the mechanical properties and durability of such materials has been lacking (Bennert et al. 2000, Nataatmadja and Tan 2001, Guthrie et al. 2007).

The objectives of this study were to determine the resilient modulus and permanent deformations of RAP and RCA in the laboratory using Large-Scale Model Experiments (LSME) to simulate field conditions, and to determine the effect of varying RCA content and layer thickness on material stiffness. Scaling between LSME, typical bench-scale laboratory, and falling weight deflectometer (FWD) testing in a road section constructed of these materials is also discussed. This chapter describes the findings of the study.

4.2 Background

4.2.1 *Production of Recycled Materials*

Recycled asphalt pavement (RAP) and recycled concrete aggregate (RCA) are two materials commonly used as an alternative to virgin aggregate in roadway construction and rehabilitation. There is some ambiguity regarding the nomenclature involved in the production of RAP. RAP refers to the removal and reuse of the hot mix asphalt (HMA) layer of an existing roadway. Recycled pavement material (RPM) is a term used by some investigators to describe pavement materials reclaimed through a less precise process in which the HMA with either part of the base course layer or the entire base course layer with part of the underlying subgrade is reclaimed for use (Li et al. 2007, Wen and Edil 2009). Unless specified, these two distinct recycled asphalt materials will be collectively referred to as RAP.

RAP is typically produced through milling operations, which involve the grinding and collection of the existing HMA. RPM is typically excavated using full-size reclaimers or portable asphalt recycling machines (Guthrie et al. 2007, FWHA 2008). RAP can be stockpiled, but is most frequently processed immediately and reused on-site. Grading of RAP is typically achieved through pulverization with a rubber tired grinder (Bejarano et al. 2003). Typical RAP gradations resemble a crushed natural aggregate, with a higher content of fines resulting from degradation of the material during milling and crushing operations. The inclusion of subgrade materials in RPM can also contribute to higher fines content. Milling produces a finer gradation of RAP when compared to crushing (FHWA 2008).

RCA production involves crushing to achieve gradations comparable to typical roadway aggregate. Fresh RCA contains a high amount of debris and reinforcing steel that must be removed prior to placement. A jaw crusher breaks any debris from the RCA and provides an initial crushing. Debris is removed along a picking belt, and the remaining concrete is further crushed and screened to a specified gradation (Kuo et al. 2002). RCA is very angular in shape with a lower particle density and greater angularity than would normally be found in traditional virgin base course aggregates. Residual mortar and cement paste found on the surface of RCA contributes to a rougher surface texture, lower specific gravity, and higher water absorption compared to typical roadway aggregates (Kuo et al. 2002, FHWA 2008).

Recycled Materials Used as Unbound Base Course

Several studies have been conducted comparing the mechanical properties of pure RAP and RCA with those of typical roadway base course aggregates. Bejarano et al. (2003) investigated the strength and stiffness of pure RAP compared to typical base course aggregate. Testing was performed on one RAP and two virgin base course aggregates. Individual specimens for each material were compacted at optimum moisture content (OMC) and at 95% and 100% of maximum wet density (MWD) according to CalTRANS specification CTM 216. Static triaxial tests were performed at confining pressures of 0, 35, 70 and 105 kPa. Stiffness tests were conducted according to AASHTO TP-46. Regardless of compaction effort, the shear strength of RAP and virgin aggregate were of comparable magnitude, and the stiffness of RAP was greater

than that of virgin aggregate. An increase in compaction effort increased the stiffness of RAP and one of the aggregate specimens, but had no effect on the second aggregate specimen.

Guthrie et al. (2007) evaluated the effects of RAP content on the shear strength and stiffness of roadway base course aggregate. Two RAPs and two aggregates were chosen for the investigation. Specimens were prepared at RAP percentages of 100%, 75%, 50%, 25% and 0% (100% aggregate) for each of the possible RAP/aggregate permutations using modified compaction effort (ASTM D 1557). Specimen strength was determined by the California Bearing Ratio test (ASTM D 1883). Specimen stiffness was determined by free-free resonant column after compaction, after 72 hours of heating at 60°C to simulate summer conditions, and after an 11-day soaking/submerging period to simulate field saturation.

Specimen strength decreased with an increase in RAP content. The stiffness of specimens tested immediately after compaction decreased with the addition of 25% RAP, and then increased for RAP contents of 50%, 75%, and 100%. This trend reversed after 72 hours of heating: the stiffness of the material increased with the addition of 25% RAP, and then decreased for increased RAP content. Guthrie attributes this decrease in stiffness to the softening of asphalt during the heating process. After 11 days of soaking, the material maintained the same decrease-increase behavior as the heated specimen. However, the soaked materials displayed a 40% to 90% decrease in stiffness when compared to the heated material.

Kim et al. (2007) studied the effect of RAP content on the stiffness of blended aggregate base course. Stiffness tests were performed on pure RAP and aggregate samples and an in-situ blend of full-depth reclamation (FDR) material in accordance with National Highway Research Program testing protocol 1-28a (NCHRP 1-28a). Specimens were prepared at RAP percentages of 75%, 50%, 25% and 0% (i.e., 100% aggregate) and at moisture contents corresponding to 65% and 100% of OMC under standard compaction effort (AASHTO T 99). Stiffness increased for both an increase in RAP content and an increase in confining pressure. At higher confining pressures, the stiffness increased faster for specimens with higher RAP content. Specimens tested at 65% OMC had higher stiffness when compared to specimens prepared at 100% OMC at all confining pressures.

Bennert et al. (2000) investigated the shear strength of pure RAP and RCA compared to typical aggregate, and evaluated the effect of RAP and RCA content on the stiffness of blended aggregate base course. Strength tests were performed on one RAP, one RCA, and one aggregate sample. Specimens were compacted at maximum dry density (MDD) and OMC using standard compaction effort in accordance with methods described in AASHTO TP46-94, and loaded under drained static triaxial conditions at a common confining load of 103.42 kPa. Shear strength was higher for RCA than RAP; however shear strength was higher for pure aggregate than either RAP or RCA.

Stiffness tests were conducted according to AASHTO TP46-94. Specimens were prepared with RAP and RCA percentages of 100%, 75%, 50%, 25% and 0% (100% aggregate). Stiffness was higher for RAP and RCA than pure aggregate, and increased with an increase in RAP or RCA content. RCA experienced lower permanent strain than pure aggregate; however RAP

experienced higher permanent strain than RCA or pure aggregate. Bennert et al. (2000) suggest that the high permanent strains experienced by RAP may be due to either the breakdown of asphalt binder under loading or deficiencies inherent in the testing sequence itself.

Nataatmadja and Tan (2001) evaluated the relationship between the pre-crushing compressive strength and post-crushing stiffness of RCA. Four RCA with pre-crushing compressive strengths of 15, 18.5, 49 and 75 MPA were tested for stiffness according to methods proposed by Nataatmadja (1992). Each material was crushed and mixed to a particle size distribution comparable to typical roadway aggregate. Specimens were compacted at 89% of OMC using modified compaction effort (AS 1289.5.2.1). The stiffness of RCA increased with an increase in compressive strength from 15 MPa to 18.5 MPa, and again from 18.5 MPa to 49 MPa. However an increase in compressive strength from 49 MPa to 75 MPa resulted in a decrease in stiffness. Nataatmadja and Tan suggest that RCA with very high compressive strengths are more prone to break into elongated particles during crushing. Elongated particles were more prone to degradation after extensive loading, resulting in a lower stiffness than would otherwise be expected.

Camargo et al. (2009) compared the strength and stiffness of two recycled materials, RPM and recycled road surface gravel (RSG), to the strength and stiffness of an aggregate graded to the specifications for the Minnesota Department of Transportation (MnDOT) Class 5 base course. Specimen strength was determined by the California Bearing Ratio (CBR) test according to ASTM D 183, and stiffness was determined by NCHRP 1-28a. The RPM and RSG each had a higher CBR than the typical base course aggregate, although all three materials had CBR values that were lower than the typically desired base course CBR value of 50. The RPM and RSG had a higher and lower stiffness, respectively, when compared to the Class 5 aggregate. The plastic strain experienced by the specimens during stiffness testing was lowest for RPM and highest for RSG and Class 5, which shared a plastic strain that was similar in magnitude.

Burrego et al. (2009) tested four RAP materials to quantify the variability of stockpiles in terms of gradation, asphalt content, and sand equivalency. An evident variation in gradation was noted for the RAP taken directly from stockpiles, although the variation was small after the material was subjected to ignition oven testing. The content of gravel, coarse sand, and fine sand were similar for each of the RAP samples. Burrego found that the asphalt content of RAP, which varied from 4.5% to 8.5%, had a significant effect on the gradation of the material. The sand equivalencies of the RAP samples were between 50 and 91.

4.2.2 *Resilient Modulus*

4.2.2.1 Definition of Resilient Modulus

Resilient modulus is a measure of a material's ability to deform elastically under cyclic compressive loading, and relates material stiffness to the mechanistic-empirical design method of pavements (NCHRP 1-37a). The performance of flexible pavement is dependent on the stiffness of the associated base course. Base course layers with higher resilient moduli are stiffer, incur less elastic deformation, and transfer less stress to the overlying asphalt concrete and underlying

subgrade. The reduction in fatigue cracking and rutting associated with this decrease in stress can have a positive effect on pavement life (Bejarano et al. 2003).

Resilient modulus testing involves cyclic loading of a specimen to simulate a moving wheel load. The elastic response of the specimen is recorded for various deviator and confining stresses. Elastic response is initially non-linear and the specimen experiences both plastic and elastic strains. When the applied deviator stress is small compared to the strength of the specimen, the plastic strain gradually dissipates and the remaining strain becomes almost entirely elastic and recoverable (Huang 2004). The linear-elastic modulus based on the recoverable strain is defined as resilient modulus, and is defined mathematically by Eqn. 4.1:

$$M_r = \frac{\sigma_d}{\varepsilon_r} \tag{4.1}$$

in which ε_r is the recoverable elastic strain and σ_d is the applied deviator stress.

4.2.2.2 Factors that affect the Resilient Modulus of Unbound Aggregate

Several factors can influence the resilient behavior of a granular base course material, with stress-state having the greatest overall effect (Lekarp et al. 2000). Resilient modulus increases significantly with an increase in confining stress and decreases with an increase in deviator stress (Monismith et al. 1967, Hicks 1970). The effects of deviator stress are minimal to negligible for purely granular materials, depending on the amount of plastic deformation (Morgan 1966, Hicks and Monismith 1971). Moisture content can affect the stiffness of a granular material, but the extent to which this occurs depends on the degree of saturation. The stiffness of typical granular specimens will stay nearly constant at lower saturation levels, but will decrease significantly as the saturation level rises (Hicks and Monismith 1971, Barksdale and Itani 1989). Lekarp et al. (2000) suggests that excess pore water pressures develop during cyclical loading for high degree of saturation, which decrease the strength and stiffness of the material.

Density, gradation and particle shape have been shown to have a small effect on the resilient modulus of granular material. Increased density contributes to an increased stiffness for granular material; however, increased fines content and increased crushing efforts appear to diminish these effects (Hicks and Monismith, 1971 Kolisojah 1997). Uniformly-graded specimens are stiffer than well-graded materials (Thom and Brown 1988); however the effects of moisture, fines content and particle angularity can increase the stiffness of well-graded aggregate to a degree equal-to or greater-than uniformly-graded aggregate (Plaistow 1994, Van Niekerk et al. 1998). Granular materials with angular to sub-angular particles have been found to have a higher resilient modulus than materials with rounded to sub-rounded particles (Hicks 1970, Thom and Brown 1989).

Research suggests that these influence factors also affect the resilient modulus of recycled aggregates. The resilient modulus of RAP and RCA has been shown to increase under the influence of increasing confining stress (Bennert et al. 2000, Molenaar and Van Niekerk 2002, Bejarano et al. 2003, Kim et al. 2007). Kim further found that increasing deviator stress decreased the resilient modulus of RAP, but had less of an effect than the confining stress.

Tanyu et al. (2003) noted that state of stress and strain amplitude had a significant effect on resilient moduli of various granular materials determined in both small and large-scale tests.

Kim et al. (2007) noted that RAP compacted at moisture contents less than optimum showed an increase in stiffness. Guthrie et al. (2007) found that RAP specimen stiffness decreased after extensive periods of saturation. Molenaar and Van Niekerk (2002) and Bejarano et al. (2003) found that increasing density increased the stiffness of RAP and RCA specimens, respectively. Molenaar and Van Niekerk (2002) also note that the gradation of RCA has limited influence on resilient modulus. Guthrie et al. (2007) found that the strength in RAP increased with particle angularity, although a correlation between angularity and stiffness could not be made.

4.2.2.3 Small-Scale Determination of Resilient Modulus of Unbound Aggregate

The linear-elastic response of unbound aggregate varies with different stress-states, with an increase in confining stress contributing to an increase in resilient modulus. Bench-scale laboratory tests subject a specimen to a sequence of deviator stresses and confining pressures and the resilient modulus of the specimen is determined by the elastic response. These sequences reflect typical field loading situations, and are defined by standards published by AASHTO or NCHRP guides.

One common power-function relating resilient modulus to bulk stress in granular materials is known as the K-θ model, and was proposed by Seed et al. (1967), Brown and Pell (1967), and Hicks (1970). The K- θ model is presented in Eqn. 4.2:

$$M_r = k_1 \left(\frac{\theta}{p_o}\right)^{k_2} \tag{4.2}$$

in which θ is the bulk stress, p_o is a reference stress (1 kPa), and k_1 and k_2 are empirically fitted constants for a given material. The bulk stress is expressed as the sum of the three principle stresses as defined in Eqn. 4.3:

$$\theta = \sigma_1 + \sigma_2 + \sigma_3 \tag{4.3}$$

The reference stress is an atmospheric constant used to eliminate the influence of pressure units on the calculated resilient modulus.

4.2.2.4 Large-Scale Model Experiments for Determination of Resilient Modulus of Unbound Aggregate

The Large-Scale Modeling Experiment (LSME) is a large prototype-scale test developed for simulating the performance of pavement sections in a laboratory setting. The advantage of the LSME testing is that it allows field conditions to be more accurately modeled than typical bench-scale testing methods. The pavement sections, or parts of them, are loaded cyclically to simulate field traffic loads and the resilient modulus is back calculated from the recorded response.

Falling weight deflectometer (FWD) is a non-destructive test used to determine the elastic modulus of pavement sections in the field. A weight of known mass is dropped from a designated height, and the deformation of the pavement at radial distances from the load location is recorded. The elastic modulus is back calculated from these measurements.

Tanyu et al. (2003) used LSME testing to determine the resilient modulus of typical base course material and two granular industrial by-products used as subbase materials. LSME test results were compared to resilient moduli determined from FWD and bench-scale tests. The summary resilient modulus is based on a bulk stress of 208 kPa as suggested for base course materials by NCHRP 1-28a section 10.3.3.9, and calculated according to Equation 4.2. The summary resilient modulus determined from the LSME and FWD tests were found to be similar in magnitude; however the summary resilient modulus determined from the bench-scale tests were found to be lower than those determined from LSME and FWD. Tanyu suggests that the LSME is a good indicator of the resilient modulus of field pavement sections, but that use of laboratory resilient modulus tests should be considered conservative at best. The resilient modulus measured in the LSME was also shown to be sensitive to thickness, with thicker layers having a higher stiffness. The modulus is dependent on strain amplitude: thicker layers contribute to wider stress distributions which lead to lower vertical strains (Seed 1970).

Kootstra et al. (2010) and Ebrahimi et al. (2010) used LSME testing to determine the deformation behavior and resilient modulus of a typical base course material and two recycled road materials, RPM and road surface gravel (RSG), used as base course material. The typical base course material was graded to MnDOT Class 5 aggregate specifications. Plastic strain and resilient modulus for each material were found to increase monotonically with the number of loading cycles. The plastic strain experienced by the Class 5 exhibited plastic shakedown, in which the plastic deformation ceased after an initial deformation period, and the plastic strain experienced by the RPM and RSG experienced creep shakedown, in which the plastic deformation continued constantly during cyclic loading. Kootstra et al. (2010) suggest that the reason for the continuous plastic deformation was respectively due to the viscous deformation of the asphalt in RPM and the amount of plastic fines present in RSG. RPM and RSG were found to have a greater overall susceptibility to plastic deformation than Class 5. Summary resilient moduli determined by LSME testing was compared to bench-scale tests on the same materials conducted by Camargo et al. (2009); however, no clear correlation between the two methods could be made. Ebrahimi (2010) suggests that the difference between the summary resilient moduli determined by these two methods could be due to either a scale effect related to the volume of material involved, or to a difference in the strain amplitude experienced by each specimen.

Bejarano et al. (2003) used FWD testing to investigate the performance of RAP used in roadway rehabilitation. Tests were performed prior to rehabilitation on pavement consisting of asphalt concrete over typical unbound aggregate base course. The asphalt concrete was then pulverized and used as unbound base course for new roadway construction. Additional testing on the rehabilitated roadway indicated that the new pulverized RAP base course had a higher resilient modulus and resistance to shear strength compared to the original base course.

4.3 Materials

Two recycled materials, one conventional base material, and one blended recycled/conventional material were used in this investigation. The two recycled materials were a recycled asphalt pavement (RAP) and a recycled concrete aggregate (RCA). The conventional base material was a gravel meeting the MnDOT Class 5 specifications and the blended material was a mix of approximately equal parts RCA and Class 5. The Class 5 material was used as the control material in this study. These materials are the same materials used in the roadway cells previously constructed at the MnROAD test facility in Maplewood, Minnesota and were obtained during construction. The Class 5 was salvaged from the base course of a previously constructed roadway cell. The RAP was milled from the surface of roadway cells also previously constructed at the MnROAD test facility. The RCA was obtained from a stockpile maintained by the Knife River Corporation at their pit located at 7979 State Highway 25 NE in Monticello, Minnesota. The blended material was mixed on site with the blade of a bulldozer prior to placement in the roadway cell.

A summary of the index properties, compaction test data, soil classifications, and particle gradations for the four recycled materials is presented in Table 4.1 and Table 4.2. The RAP and Class 5 are classified as SP and A-1-b in the Unified Soil Classification System (USCS) (ASTM D 2487) and AASHTO Soil Classification System (AASHTO M 145), respectively. The blended RCA/Class 5 and RCA are classified as A-1-a according to AASHTO, and respectively as SP and GP according to USCS. Each of the materials used in this study are classified as non-plastic. The particle size distribution curves for the four investigated materials as determined according to ASTM D 422 are shown in Figure 4.1, along with the MnDOT specification for Class 5 used as a base course. Compaction tests were performed on each material using the modified compaction effort according to ASTM D 1557. Optimum water contents and maximum dry unit weights are summarized in Table 4.1, with associated compaction curves presented in Figure 4.2.

4.4 Methods

4.4.1 *Small Specimen-Scale Testing*

Small laboratory bench-scale resilient modulus tests were performed on compacted specimens according to NCHRP test protocol 1-28a (NCHRP 1-28a). Cylindrical specimens measuring 152 millimeters in diameter by 305 millimeters in length were prepared from each material. Specimens were prepared at optimum moisture content and compacted to 95% maximum dry density under modified compaction effort. Compaction of specimens was performed in six lifts of equal mass and stiffness to ensure uniform compaction.

Resilient modulus testing was carried out according to NCHRP 1-28a Procedure 1a, which applies to base and subbase materials. Deformations were measured via LVDTs positioned both internally and externally, with each LVDT having an accuracy of $\pm$0.005 mm. The specimens were loaded with an MTS Systems Model 244.12 servo-hydraulic machine. Loading sequences,

confining pressures and data acquisition were controlled from a computer running LabView 8.5 software.

The resilient modulus for each load sequence was obtained by averaging the resilient modulus from the last five cycles of each test sequence. The resilient modulus data were fit to the power function described by Eqn. 4.2. A summary resilient modulus was computed for each test at a bulk stress of 208 kPa, as suggested by Section 10.3.3.9 of NCHRP 1-28a. Further details of the specimen-scale laboratory testing methods are described by Son (2010) who performed the tests for unstabilized recycled materials.

4.4.2 *Large-Scale Model Experiment*

4.4.2.1 Apparatus and Loading Methodology

LSME is a modeling method used to determine the deformation of a pavement structure at prototype scale in a manner that replicates field conditions as closely as practical (Tanyu et al. 2003). A schematic of the LSME is shown in Figure 4.3. Pavement profiles are constructed in a test pit with dimensions 3 m x 3 m x 3 m, and are subjected to 10,000 cycles of simulated traffic loading. The simulated loading is representative of a 4-axle truck applying a tire pressure of 700 kPa to a contact area of 0.05 m^2. Loads are generated by a MTS 280-L/m hydraulic actuator with a 100 kN force rating and 168 mm of stroke. Loads are applied to the pavement surface using a 25 mm thick circular steel plate with a radius of 125 mm. The pulse of the loading varies as a haversine function consisting of a 0.1 second load period followed by a 0.9 second rest period (Benson et al. 2009, Ebrahimi et al. 2010, Kootstra et al. 2010).

The equivalent stress to be applied to the surface of the base course material in the absence of an asphalt layer was determined by non-linear finite-element analysis using the MICHPAVE program to model the performance of the proposed pavement profile (Benson et al. 2009, Kootstra et al. 2009). The base course was assumed to behave as non-linear elastic, and the asphalt surface and subgrade were assumed to behave as linear elastic. Loading and material properties used as inputs into the MICHPAVE program (Harichandran 1989) were determined from typical values (Huang 2004), and are presented in Table 4.3. The vertical stress distribution predicted by MICHPAVE is shown in Figure 4.4. The vertical stress on the surface of the base layer is maximized directly below the center of loading, and decreases with an increase in radial distance. Based on a maximum stress of 133 kPa, a force of 6.7 kN was applied to base layer in the LSME with the loading plate.

Previous LSME testing used the entire 3.0 m x 3.0 m test area to evaluate pavement performance (Tanyu et al. 2003, Benson et al. 2009, Kootstra et al. 2010). However, limited amounts of available base course materials made it necessary to reduce the evaluated test area to 1.0 m x 1.0 m. The remainder of the 3.0 m x 3.0 m test area was made up of recycled pavement material (RPM) to maintain the boundary stress that would otherwise be lost by a reduction in test area. The equivalency of this abbreviated test area and method of preparation are described in Appendix A. Pavement profiles consisted of 0.2 m to 0.3 m thick of base course material over

2.5 m of dense, uniform sand subgrade. The performance of an asphalt layer was not central to the research, and therefore was not included in the LSME analysis.

4.4.2.2 Deformation Measurements

Vertical deformations at the surface of the base course and subgrade were measured during each loading cycle. Linear variable differential transducers (LVDT) were used to measure the deformations to a precision of $\pm$0.005 mm. Deformation of the base course was measured from the top of the loading plate, which was assumed rigid and able to translate the base course deformation. Subgrade deformations were measured by attaching small plates to either end of a thin rod extending through a tube extending through the loading plate and base course. One plate was laid flush with the subgrade surface while the other plate supported the LVDT located above the base course. Deformation of the subgrade was translated by the thin rod and measured by the LVDT. Deformations measured by the LVDTs were recorded using LabView 8.5 software.

4.4.2.3 Data Inversion

The resilient modulus of the base courses tested in the LSME was determined by performing a data inversion approach using MICHPAVE (Harichandran 1989). The elastic deformation of the base course was determined by subtracting the elastic deformation of the subgrade from the total elastic deformation of the profile as measured at the top of the base course. The LSME pavement profile was modeled as a two layer system in MICHPAVE. The elastic behavior of the base course and subgrade layers were modeled as non-linear and linear, respectively. The base course k_2 was determined from small-scale laboratory experiments in accordance with NCHRP 1-28a. The base course k_1 and subgrade elastic modulus were varied until the elastic deformations predicted by MICHPAVE were within $\pm$0.005 of those measured in the LSME. This method assumes that k_2 varies within a narrow range for a given material (Huang 2004) and follows the methods described by Tanyu et al. (2003) and Kootstra et al. (2009).

4.4.2.4 Base Course Compaction

Base course was compacted in lifts of approximately 0.10 m to efficiently and evenly distribute the modified compaction effort. Base course materials were prepared at optimum moisture content, and compacted to 95% of the modified maximum dry unit weight using a jumping-jack style compactor. A nuclear density gauge was employed to measure the in-situ dry unit weight and moisture content of each lift.

4.4.3 *Field-Scale Falling Weight Deflectometer Testing*

Field-scale in situ modulus of the materials was obtained from the Falling Weight Deflectometer (FWD) tests that were performed at the MnROAD testing facility in the roadway cells with the same materials tested in the small laboratory specimen tests and the LSME. Testing was performed using a trailer-mounted Dynatest model 8000 FWD. The FWD was controlled by an on-site computer which also recorded and stored load and deformation data. Three loads of 26.7,

40.0 and 53.4 kN were applied by the FWD to a 300 mm diameter plate in contact with the pavement surface. Surface deformations were measured by nine load transducers located at distances of 0, 0.30, 0.61, 0.91, 1.22, 1.52, and 1.83 meters from the center of the load.

The measured deformations were used to back-calculate the elastic modulus of the pavement layers using the MODULUS program developed at the Texas Transportation Institute. MODULUS uses linear-elastic theory to back-calculate elastic moduli from FWD data. The back-calculation was based on a three-layer model consisting of asphalt concrete, base course, and subgrade layers. Pavement profile and deformation data were provided by the MnDOT. The pavement profiles for the four test cells are presented in Figure 4.5. The asphalt surface and base course layers were assigned a Poisson's ratio of 0.35, and the subgrade layer was assigned a Poisson's ratio of 0.40 (Huang 2004). The depth to the rigid layer was assumed to be at least 6 m and have little effect on the elastic moduli (Bush and Alexander 1985). The range of bulk stresses and vertical strains in the field was estimated using MICHPAVE. Surface loads taken from the FWD data and moduli from the MODULUS back-calculation were used as inputs. Structural layer coefficients were determined from the back-calculated moduli for use in pavement thickness design, as presented in Appendix B.

4.5 Results

4.5.1 *Deformations in LSME*

The total and plastic deformations at the surface of the base course and subgrade in the LSME as a function of loading cycle for RAP, RCA, blended RCA/Class 5, and Class 5 are presented in Figure 4.6 through Figure 4.9. Deformations measured on the surface of the base course with thicknesses of 0.2 m and 0.3 m and subgrade are based on the haversine loading pulse. The total deformation is the peak deformation experienced during the 0.1 second loading pulse, and the plastic deformation of each layer is the unrecovered deformation remaining during the 0.9 second "at-rest" period. The amount of plastic deformation increases monotonically as the test progresses, with the greatest accumulation occurring during the first 50 loading cycles in all cases. The elastic deformation is the difference between the total and plastic deformations for each loading cycle. The net deformation represents the elastic deformation of the given base course layer and is the difference between the total elastic deformation measured at the surface and the elastic deformation of the subgrade. The elastic deformations at the surface and subgrade are presented as a function of loading cycle in Figure 4.10 through Figure 4.13.

The net base elastic deformation for each of the materials slightly decreases as the cyclic loading progresses, which is caused by the gradual compaction of the particles into a denser matrix. The magnitude of the net elastic deformation for RAP and RCA were approximately equal for both layer thicknesses. The magnitude of the net elastic deformation for blended RCA/Class 5 and Class 5 is higher for the 0.2 m layer thickness than for the 0.3 m layer thickness. The thicker layer distributes the stress within the layer more thoroughly, and therefore the amount of strain experienced in the material can be expected to be reduced. The subgrade elastic deformation was nearly constant during the loading of both layer thicknesses for each base course material.

A comparison of the surface and subgrade deformations after 10,000 loading cycles for 0.2 m and 0.3 m thick layers of RAP, RCA, blended RCA/Class 5 and Class 5 is presented in Figure 4.14. The net plastic deformation is the difference between the total plastic deformation measured at the surface and the plastic deformation measured at the subgrade. The sum of the deformations represented in Figure 4.14 is equal to the total deformation measured at the surface of the LSME at the end of loading. RAP and RCA had the largest and smallest amount of both total and net base plastic deformation, respectively, with Class 5 and blended RCA/Class 5 having the second and third largest amounts of both total and net base plastic deformations, respectively. The plastic deformation experienced by the RAP was approximately 211% and 402% greater than that of Class 5 for 0.2 m and 0.3 m layer thicknesses, respectively, whereas the plastic deformation experienced by the RCA was approximately 69% smaller than the plastic deformation experienced by the Class 5 for both layer thicknesses. The blended RCA/Class 5 material experienced plastic deformations that were 39% and 20% smaller than Class 5 for layer thicknesses of 0.2 m and 0.3 m, respectively. The net elastic and plastic deformations for 0.2 m and 0.3 m layer thicknesses of RAP, RCA, blended RCA/Class 5, and Class 5 can be compared in Figure 4.15.

The base plastic deformation of RCA and Class 5 was larger for the 0.2 m layer thickness compared to the 0.3 m layer thickness. Stress is better distributed within a layer of larger thickness, and the corresponding reduction in strain correlates to a reduction in plastic deformation. The plastic deformation of RCA and Class 5 decreased 10% and 13%, respectively, for an increase in layer thickness from 0.2 m to 0.3 m.

The plastic deformation experienced by the 0.3 m layer thickness of blended RCA/Class 5 is 13% larger than the plastic deformation experienced by the 0.2 m layer thickness, which contradicts the deformation that would be expected considering the deformations experienced by RCA and Class 5 alone. The most likely cause for this seemingly contradictory behavior is experimental error. Although LSME compaction was checked with a nuclear density gauge prior to testing, there is a possibility that the material directly under the loading plate was under-compacted. Under-compacted material would experience excess plastic deformation during the 10,000 cycles of loading, which would contribute to the total overall deformation. The effect of this under-compaction would be minimal for elastic deformation, however, as the compaction level required for the material to perform as linear-elastic would remain the same and would be achieved before the termination of loading.

The plastic deformation of RAP is 40% larger for the 0.3 m layer thickness compared to the 0.2 m layer thickness. This is attributed to the viscous nature of the asphalt coating on the RAP particles that contributes to increased amount of deformation of the layer despite the reduction of stress in the larger layer thickness. This could also be because there is greater mass to compact with each load applied before it acts as a monolithic material.

The elastic and plastic net base deformation as a function of RCA content is presented in Figure 4.16 for 0.2 m and 0.3 m layer thicknesses of RCA, blended RCA/Class 5, and Class 5. The elastic deformation decreased slightly with an increase in RCA content, i.e., the 0.2 m and 0.3 m thick layers showed an overall decrease in the elastic deformations, i.e., approximately 0.03 mm

and 0.02 mm, respectively. The plastic deformation also decreased with an increase in RCA content, although at a much higher rate. The 0.2 m and 0.3 m thick layers showed an overall decrease in plastic deformation of approximately 0.17 mm and 0.15 mm, respectively. As the RCA content increases, the elastic and plastic deformations of the different layer thicknesses seem to converge on common values, i.e., the elastic and plastic deformation of 100% RCA is approximately 0.05 mm and 0.07 mm, respectively, for both 0.2 m and 0.3 m layer thicknesses.

The average plastic strain (ε_p) in each base layer can be defined as:

$$\varepsilon_p = \frac{d_p}{t} \times 100 \tag{4.4}$$

where d_p is the plastic deformation within the base layer and t is the layer thickness. The plastic strain of the base course as a function of loading cycle is presented in Figure 4.17 through Figure 4.20 for 0.2 m and 0.3 m layer thicknesses of RAP, RCA, blended RCA/Class 5, and Class 5. The average plastic strain experienced by the 0.3 m thick base layer is greater than that experienced by the 0.2 m thick base layer for each of the tested materials. In addition, each material reaches a steady state condition within 500 cycles for both layer thicknesses.

The steady state condition achieved for RCA, blended RCA/Class 5, and Class 5 maintains a constant plastic strain rate of approximately zero, corresponding to a behavior, which is in accordance with plastic shakedown (Khogali et al. 2004, Yang et al. 2008, Kootstra et al. 2010). The steady state condition achieved for RAP also maintains a constant plastic strain rate; however the strain rate is non-zero and continues to accumulate with increased cyclical loading. The non-zero plastic strain rate in RAP can be attributed to the viscous nature of the asphalt that coats the RAP aggregate, and corresponds to behavior in accordance with creep shakedown (Mohammad et al. 2006, Kootstra et al. 2010).

The strain data from the LSME tests was fitted to the VESYS power function model (FHWA 1978) to estimate rutting potential. The VESYS power function is defined by:

$$\varepsilon_p = aN^b \tag{4.5}$$

where a represents the initial densification after the first pass of traffic, b represents the rate at which permanent strain accumulates, and N is the number of load repetitions. Parameters a and b are dimensionless. The fitting parameters used in Equation 4.5 are summarized in Table 4.4. The cumulative plastic strain in each of the base courses after $3x10^7$ loading cycles (i.e. 4000 daily truck loads over 20 years) was estimated using Equation 4.5. Rutting depths based on the estimated plastic strain are also summarized in Table 4.4.

An acceptable limit to the rutting of flexible pavements has been suggested to be 13 mm (Huang, 2004). Based on LSME data, conventional granular base course (Class 5) can be expected to contribute 4 to 8% of the permissible rut depth. RCA and blended RCA/Class 5 can be expected to contribute 3 to 6% of the permissible rut depth, which is comparable to that of Class 5. Conversely, RAP can be expected to contribute between 30 and 40% of the acceptable rut depth,

which is appreciable compared to that contributed by Class 5. Flexible pavements that incorporate RAP as a base course layer can be expected to encounter some increased rutting, whereas flexible pavements that incorporate RCA and RCA/natural aggregate blends will experience rutting comparable to pavements incorporating conventional base course aggregate.

4.5.2 *Comparison of Large and Small-Scale Resilient Moduli*

The resilient modulus as a function of bulk stress for RAP, RCA, blended RCA/Class 5, and Class 5 are presented in

Figure **4.21** through

Figure **4.24**, respectively. This relationship is presented for both the 0.2 m and 0.3 m thick layers tested in the LSME, as well as for the bench-scale specimen tests performed according to NCHRP 1-28a on the same materials by Son (2010). Bench-scale tests were evaluated for deformations measured externally, relative to the test cell, and internally at the upper and lower quarter points along the specimen length. Fitting parameters k_1 and k_2 determined from the bench-scale tests were used to calculate the resilient modulus as a function of bulk stress as defined by the power function model suggested by Equation 4.2. The parameter k_2 determined from the bench-scale tests was used in the back analysis of the LSME data to determine the parameter k_1 that allowed the matching of the measured deformations in the LSME using the MICHPAVE code with the modulus function according to Equation 4.2. The power- function relationship illustrates the concept that increased bulk stress contributes to an increase in resilient modulus for granular materials. A summary of the k_1 and k_2 obtained in the tests is presented in Table 4.5.

The internal and external bench-scale tests had the highest and lowest resilient modulus, respectively, and the LSME tests for 0.3 m and 0.2 m layer thicknesses had the second and third highest resilient modulus, respectively, for each of the four materials (

Figure **4.21**to

Figure **4.24**). No direct correlation can be made between the resilient moduli measured for bench-scale tests and the resilient modulus back-calculated from the LSME. The magnitudes of the four tests appear to be evenly spaced when referenced between the maximum and minimum values defined by the bench-scale tests. The moduli of both LSME tests seem to trend closer to the internal bench-scale test for the RCA case, and to the external bench-scale test for the blended RCA/Class 5 case; however these trends are slight and should not be considered direct correlations.

A comparison of the summary resilient moduli (SRM) determined for RAP, RCA, blended RCA/Class 5 and Class 5 are presented in Figure 4.25. The SRM is based on a bulk stress of 208 kPa as suggested for base course materials by NCHRP 1-28a sec 10.3.3.9, and calculated according to Equation 4.2 using the k_1 and k_2 presented in Table 4.4. The SRM calculated for each test method is also presented in Table 4.5.

RCA and Class 5 had the highest and lowest SRM, respectively, for each of the four testing methods. The SRMs of the RAP and blended RCA/Class 5 are approximately equal in magnitude for bench-scale testing, with RAP having a marginally higher SRM for both LSME tests. The SRM of RCA was 42% to 77% greater than that of Class 5, while the SRM of RAP was 23% to 33% greater. The SRM of the blended RCA/Class 5 was 18% greater than that of Class 5, which was comparable in magnitude to the SRM of RAP.

The SRM as a function of layer thickness is presented in Figure 4.26 for RAP, RCA, blended RCA/Class 5, and Class 5. The resilient modulus of each material increases with a corresponding increase in layer thickness. The magnitude of this increase, which lies between 130 MPa and 176 MPa, appears relatively consistent for all materials and does not appear to trend differently for any individual material.

The SRM as a function of RCA content is presented in Figure 4.27 for RCA, blended RCA/Class 5, and Class 5. The SRM of the materials increases with an increase in RCA content. The magnitude of the increase seems to increase at the same rate regardless of layer thickness. The blended RCA/Class 5 defines a downward "spike" for both the 0.2 m and 0.3 m layer thicknesses, which interrupts an otherwise linear trend. One possible reason for this spike is that there is some form of particle interaction that is reducing the stiffness of the blended material as a whole. A second, more probable reason for the spike is that the blended material is not a perfect blend of 50% RCA and 50% Class 5. Measuring the mass of materials in the field relies on approximations to a certain extent, and the actual amounts blended together might vary depending on the experience of the field engineer. Also, the material was mixed in the field using the blade of a bulldozer. Such mixing methods are not thorough, and samples taken from such mixtures could vary depending on sample location. Based on these assumptions and the SRM calculated for the blended material, a blend incorporating an RCA content of between 20% and 40% would better fit a linear trend between SRMs calculated for 0% and 100% RCA.

4.5.3 *Scaling Laboratory Results to Field Conditions*

4.5.3.1 Background

The elastic modulus of granular material has been shown to be sensitive to strain amplitude (Seed and Idriss 1970, Hardin and Drnevich 1972, Edil and Luh 1978). Thicker layers distribute stress more efficiently and reduce the amount of strain experienced by the material. The resilient modulus of a material evaluated at a given bulk stress can vary in magnitude depending on which testing method is being used (Figure 4.25). These differences in magnitude are assumed to be due to differences in stress state and strain level (Tanyu et al. 2003, Schuettpelz et al. 2008, Benson et al. 2009). A more accurate comparison between the various testing methods can be established by adjusting the resilient modulus to account for these differences in stress and strain level.

A backbone curve can be used to describe the stress-strain dependency of resilient modulus (Seed and Idriss 1970, Hardin and Drnevich 1972). Backbone curves represent the ratio of shear modulus (G_γ) at a given shear strain to the low-strain shear modulus (G_{max}) as a function of shear

strain amplitude for a given state of stress. The relation between shear modulus and shear strain can be approximated by the following relationship suggested by Hardin and Drnevich:

$$\frac{G_\gamma}{G_{max}} = \frac{M_r}{E_s} = \frac{1}{1+\gamma_h} \tag{4.6}$$

where γ_h is defined as the hyperbolic strain. The hyperbolic strain is the strain normalized with respect to the reference strain (γ_r):

$$\gamma_h = \frac{\gamma}{\gamma_r}\left[1+ae^{-b\left(\frac{\gamma}{\gamma_r}\right)}\right] \tag{4.7}$$

where a and b describe the shape of the backbone curve. The reference strain is defined as the strain at the intersection of maximum shear stress and shear modulus (Hardin and Drnevich 1972). These relationships can be used for resilient modulus dependency on strain amplitude by assuming that the ratio G_γ/G_{max} is equal to the ratio of resilient modulus at a given shear strain to the low-strain Young's modulus (maximum modulus) (M_r/E_s),

4.5.3.2 Measurement of Low-strain Modulus

The low-strain modulus of the materials was determined using the small-scale simple seismic test method suggested by Schuettpelz (2009). The method is based on the propagation of surface waves and is intended to be a much simpler method of data acquisition when compared to methods involving larger testing schemes. Material was compacted to 95% of the maximum dry density under modified compaction effort within a 18.9 liter bucket to a volume of approximately 11 liters. Approximately 0.23 kN of material was used for each test (Figure 4.28). Material was compacted with a tamper in four lifts of equal measure to ensure uniform density. A 150 mm diameter load plate was placed central to the surface of the material, and a small amount of material was removed from opposing sides of the plate. Two accelerometers were placed adjacent to the plate and buried approximately 10 mm below the soil surface. The accelerometers were aligned with one axis parallel to the ground surface, and 500 gram masses were used to seat the accelerometers into the soil and make the first arrivals of elastic waves more distinguishable. The final distance between the accelerometers was recorded for each test. The actuator from the LSME was used to apply varying static loads to the material during testing.

The side of the 18.8 liter bucket was tapped with a rubber mallet and the travel time of the surface wave between the two accelerometers was recorded. The P-wave velocity (V_p) was determined by multiplying the surface velocity (V_r) by a conversion factor based on the Poisson's ratio (ν) (Santamarina et al. 2001, Kramer 1996):

$$V_p = V_r \frac{(1+\nu)\sqrt{\frac{2(1-\nu)}{1-2\nu}}}{0.874+1.117\nu} \tag{4.8}$$

V_p in particulate media is dependent on elastic modulus (E), Poisson's ratio (ν), and density (ρ) (Santamarina et al. 2001, Richart et al. 1970):

$$V_p=\sqrt{\frac{E(1-\nu)}{\rho(1+\nu)(1-2\nu)}} \tag{4.9}$$

The velocity of wave propagation increases with increasing applied load and soil stiffness.

The low-strain elastic modulus can be calculated from the V_p, ρ, and ν of the material by rearranging Eqn. 4.9:

$$E_s=\frac{V_p^2(1+\nu)(1-2\nu)}{(1-\nu)} \tag{4.10}$$

where ν was taken to be 0.35 for the granular material. The low-strain elastic modulus was plotted as a function of the stress applied to the surface of the soil by the loading plate. The low-strain elastic modulus was assumed to increase with the applied stress according to the power function described by Eqn. 4.2. The fitting parameters $k_{1,s}$ and $k_{2,s}$ were varied until a best-fit was found for the plotted data.

The relationship between E_s and the applied stress for the evaluated base course materials is presented in Figure 4.29. The low-strain modulus determined for the RCA and blended material were of approximately the same magnitude, with the Class 5 having a low-strain modulus approximately two-thirds the magnitude of RCA and blended material. The low-strain modulus for the RAP was significantly higher of a magnitude approximately 3.5 to 5 times greater than the other materials. The asphalt coating the RAP is most likely self-adhering, and under small strains and the effects of this adhesion are not as easily overcome as the typical particle friction common in non-bituminous materials. This resistance to strain at the particle level would increase the low-strain modulus of the RAP accordingly.

4.5.3.3 Development of Backbone Curve

The backbone curve was developed from the resilient modulus and shear strain data collected from the bench-scale, LSME and FWD testing. Vertical strains and bulk stresses were determined for the bench-scale tests using NCHRP 1-28a, and for the LSME and FWD tests using MICHPAVE at varying depths within the base course layers. The shear strain was determined from the vertical strain (Kim and Stokoe 1992, Tanyu et al. 2003):

$$\gamma=\varepsilon(1+\nu) \tag{4.11}$$

where γ is the shear strain, ε is the vertical strain, and ν is the Poisson's ratio. The normalized resilient modulus was determined using Eqn. 4.12:

$$\text{Normalized resilient modulus}=\frac{M_r}{E_s} \tag{4.12}$$

where M_r and E_s are the resilient modulus and low-strain Young's modulus for a particular bulk stress, respectively. Parameters a and b in Eqn. 4.7 were adjusted to obtain a best-fit to the calculated points. The bulk stress, resilient modulus, low-strain Young's modulus, and normalized resilient modulus for each test method are presented in Table 4.6.

The backbone curves showing normalized modulus as a function of shear strain are shown in

Figure **4.30** to Figure 4.33 for RAP, RCA, Blended RCA/Class 5 and Class 5. The backbone shape describes the stress-strain behavior of the evaluated base course and is unique for a given material. The bench-scale tests with internally and externally measured deformations produce the lowest and highest strain levels, respectively. The 0.3 m and 0.2 m thick LSME tests produce the second and third lowest strains, respectively, with the FWD producing strains between those produced by the 0.2 m thick LSME and the external bench-scale test. The normalized resilient moduli of the RAP are considerably smaller compared to the normalized resilient modulus of the other tested materials. The bitumen coating the RAP causes the particles to adhere to each other, which leads to an increase in strain resistance at low stresses.

4.5.3.4 Scaling Specimen Tests to Field-Scale Conditions

A comparison of the resilient modulus calculated at field bulk stress is presented in Figure 4.34 for RAP, RCA, blended RCA/Class 5, and Class 5. The field bulk stress is the bulk stress experienced under FWD loading as calculated at the mid-depth of the layer using MICHPAVE. The resilient moduli of the LSME and bench-scale tests were recalculated for the field bulk stress using Equation 4.2. Table 4.7 summarizes the field bulk stress and resilient moduli determined for each loading test.

The low-strain modulus for each material at field bulk stress was calculated by multiplying the resilient modulus by the normalized resilient modulus. The low-strain resilient modulus at field bulk stress for each test method is presented in Figure 4.35 and also summarized in Table 4.7. The variance of the low-strain (maximum) modulus determined for each test method is presented in Table 4.8. The coefficient of variance (CV) for RAP was the highest at 7.6%. The CV for RCA and blended material were approximately equal at 4.1% and 4.4%, respectively. The CV of the Class 5 was the smallest at 2.3%. For all materials, the coefficient of variance was 7.6% or less, indicating a reasonable amount of similarity between the test methods when properly scaled to the same bulk stress and strain level. It is also clear that different strain levels are induced in different tests resulting in varying resilient modulus depending on the test procedure even if at the same bulk stress. Bench-scale resilient modulus tests result in lower moduli based on externally measured deformations and in markedly higher moduli based on internally measured deformations in comparison to FWD or LSME moduli. LSME with 0.3 m thick layer (the same as in the field) resulted in higher moduli than the field moduli obtained from the FWD test. LSME moduli with 0.2 m thick layer were the closest to the field FWD moduli.

4.6 Summary and Conclusions

This laboratory investigation dealt with the determination of the resilient modulus of two recycled materials: recycled asphalt pavement (RAP) and recycled concrete aggregate (RCA). The investigation also dealt with the determination of the resilient modulus of one blended material consisting of approximately 50% RCA and 50% conventional base material (Class 5). The objectives were to assess the stiffness of recycled materials and to determine the scalability of laboratory results to field scale conditions. The objective was met by determining the resilient modulus of the recycled materials using large-scale model experiments (LSME) and comparing to the resilient modulus determined from bench-scale tests in accordance with NCHRP 1-28a and field scale tests using a falling weight deflectometer (FWD). The low-strain modulus of each material was also determined using seismic testing methods, and backbone curves (normalized modulus versus strain) were developed from the resulting stress-strain relationships. A conventional base course meeting the gradation standard of a Minnesota Department of Transportation Class 5 aggregate was used as a reference material in this study.

RAP experienced higher plastic deformations compared to the Class 5, while RCA experienced lower plastic deformations. The plastic deformation of RAP was approximately 211% and 402% greater than that of Class 5 for 0.2 m and 0.3 m layer thicknesses, respectively, and the plastic deformation of RCA was approximately 69% smaller than that of Class 5 for both layer thicknesses. Blended RCA/Class 5 experienced plastic deformations that were 39% and 20% smaller than Class 5 for layer thicknesses of 0.2 m and 0.3 m, respectively. For an increase in layer thickness from 0.2 m to 0.3 m, base plastic deformations of RCA and Class 5 decreased 10% and 13%, respectively. Plastic deformation of RAP is 40% larger for 0.3 m layer thickness compared to 0.2 m layer thickness, which is attributed to the viscous nature of the asphalt coating the RAP particles. Plastic deformation of blended RCA/Class 5 is 13% larger for the same increase in layer thickness, which can most likely be attributed to experimental error. Conventional base course aggregate (Class 5) can be expected to contribute between 4 and 8% to an acceptable rutting depth of 13 mm. RCA and blended RCA/Class 5 can be expected to contribute 3 to 6% to the acceptable depth, and RAP can be expected to contribute 30 to 40%. Flexible pavements that incorporate RAP as a base course layer can be expected to encounter rutting problems. Flexible pavements that incorporate RCA and RCA/natural aggregate blends will experience rutting comparable to pavements that incorporate conventional base course aggregates.

The bench-scale resilient modulus tests with internally and externally measured deformations gave the highest and the lowest resilient moduli, respectively, the LSME tests with the 0.3 m and 0.2-m layer thicknesses having the second and third highest resilient moduli, respectively. The magnitudes of the tests are evenly spaced, and no direct correlation between the four methods can be discerned. The summary resilient modulus (SRM) of RCA was 42% to 77% higher than that of Class 5, whereas the SRM of RAP was 23% to 33% greater. The SRM of blended RCA/Class 5 was 18% greater than that of Class 5, which was comparable in magnitude to RAP. An increase in layer thickness from 0.2 m to 0.3 m had the effect of increasing the SRM of the materials from 130 MPa to 176 MPa. An increase in RCA content increased the SRM at a rate

that was non-linear, suggesting that the blended aggregate sample obtained in the field may have a composition other than the actual 50% RCA/50% Class 5.

Scaling was achieved by normalizing the resilient modulus of a material by the low-strain modulus and plotting the data as a function of the strain level at the corresponding stress state. The resulting plot for all four materials described a backbone curve which illustrates the stress-strain dependency of the given material. However, an uncharacteristically high low-strain modulus value for RAP greatly reduced the normalized resilient modulus and made the construction of a backbone curve difficult. This behavior is attributed to the bitumen coating the RAP particles causing the particles to adhere to each other, which leads to an increase in strain resistance at low stresses. Different test methods induce different strain levels at the same bulk stress, resulting in varying resilient modulus. Internally and externally measured bench-scale tests resulted in higher and lower resilient moduli, respectively, compared to FWD or LSME moduli. The LSME with 0.3 m thick layer (the same as in the field) resulted in higher resilient modulus compared to the field moduli obtained from the FWD test. The LSME with 0.2 m thick layer resulted in resilient moduli which were close to the field FWD moduli. However, when properly scaled for the stress and strain levels, the low-strain modulus estimated from the different test methods are remarkably close to each other indicating the scalability of laboratory modulus to operating field modulus.

4.7 Tables

Table 4.1 Index Properties for RAP, Class 5, RCA, and Blended RCA/Class 5

Sample	D_{50} (mm)	C_u	C_c	w_{opt} (%)	$\gamma_{d\ max}$ (kN/m^3)	Asphalt Content (%)	LL (%)	PL (%)	Gravel Content (%)	Sand Content (%)	Fine Content (%)	USCS Symbol	AASHTO Symbol
RAP	1.51	6.9	0.7	6.7	20.8	4.8	NP	NP	26.3	71.2	2.5	SP	A-1-b
Class-5	1.63	9.9	0.6	8.0	20.7	-	NP	NP	32.8	65.4	1.8	SP	A-1-b
RCA	5.90	20.6	0.9	11.2	19.5	-	NP	NP	54.9	43.5	1.6	GP	A-1-a
Blend	3.35	18.8	0.4	8.9	20.1	-	NP	NP	44.6	53.4	2.0	SP	A-1-a

D_{50} = median particle size, C_u = coefficient of uniformity, C_c = coefficient of curvature, w_{opt} = optimum water content, $\gamma_{d\ max}$ = maximum dry density, LL = liquid limit, PL = plastic limit, NP = nonplastic.

Note: Particle size analysis conducted following ASTM D 422, $\gamma_{d\ max}$ and w_{opt} determined by ASTM D 1557 (AASHTO T-180), USCS classification determined by ASTM D 2487, AASHTO classification determined by AASHTO M 145 (ASTM D 3282), asphalt content determined by ASTM D 6307 (AASHTO TP-53), and Atterberg limits determined by AASHTO T-89 and T-90 (ASTM D 4318).

Table 4.2 Particle Gradations for Materials

	Class 5	**Blend**	**RCA**	**RAP**
Sieve Opening	Percent Finer	Percent Finer	Percent Finer	Percent Finer
(mm)	(%)	(%)	(%)	(%)
50.0	100	100	100.00	100
37.5	100	100	100.00	100
25.0	100	100	100.00	100
19.0	98.28	100.00	100.00	100.00
12.7	90.79	87.35	92.56	94.19
9.5	86.89	77.92	83.05	87.18
4.8	77.10	67.28	68.19	73.67
2.0	63.38	55.02	53.86	56.92
0.9	46.12	40.39	39.86	33.80
0.4	29.11	23.27	24.62	14.49
0.3	18.72	11.82	13.10	5.90
0.2	13.28	6.51	7.08	3.33
0.1	9.49	3.44	3.34	2.50
Pan	0.00	0.00	0.00	0.00

Table 4.3 Inputs Used for MICHPAVE for Determining Stress on Base Layer. (Adapted from Kootstra 2009)

Material Property of Load Condition	Asphalt	Base	Subgrade
Applied Load (kN)	35.0	6.7	NA*
Loading Radius (cm)	12.7	12.7	NA*
Thickness (cm)	12.7	20.3	NA*
Modulus (kPa)	3,300,000	398,000	48,000
k_1, k_2 (Eqn. 2.2)	NA*	27,600 kPa 0.5	NA*
Poisson's Ratio	0.35	0.35	0.45
Unit Weight (kN/m^3)	22.8	20.4	18.8

*NA = non-applicable

Table 4.4 Summary Resilient Modulus (SRM) and Power Model Fitting Parameters k1 and k2 Equation 4.2) for Base Materials

Material	Thickness (m)	Equation 4.x		ε_p (%) due to cyclic load for N=3x10^7	Rutting depth due to plastic strain in base (mm)
		a	b		
RAP	0.2	0.051	0.220	2.25	4.5
	0.3	0.058	0.197	1.72	5.2
RCA	0.2	0.004	0.243	0.26	0.5
	0.3	0.003	0.230	0.16	0.5
Blend	0.2	0.017	0.165	0.29	0.6
	0.3	0.011	0.178	0.24	0.7
Class 5	0.2	0.025	0.173	0.49	1.0
	0.3	0.021	0.134	0.21	0.6

Table 4.5 Summary Resilient Modulus (SRM) and Power Model Fitting Parameters k1 and k2 Equation 4.2) for Base Materials

Material	Test Method	Thickness (m)	Measured Parameters		
			k1	k2	SRM (MPa)
RAP	Bench-Scale – Internal	0.30	26.3	0.61	674
	Bench-Scale – External	0.30	23.0	0.39	180
	LSME	0.20	12.1	0.61	314
		0.30	18.3	0.61	474
Class 5	Bench-Scale – Internal	0.30	43.2	0.47	525
	Bench-Scale – External	0.30	14.9	0.44	152
	LSME	0.20	19.2	0.47	236
		0.30	31.5	0.47	386
Blend	Bench-Scale – Internal	0.30	50.2	0.49	675
	Bench-Scale – External	0.30	18.2	0.43	182
	LSME	0.20	20.4	0.49	278
		0.30	33.2	0.49	454
RCA	Bench-Scale – Internal	0.30	38.3	0.54	680
	Bench-Scale – External	0.30	18.5	0.44	189
	LSME	0.20	23.3	0.54	417
		0.30	30.6	0.54	547

Note: SRM calculated at a bulk stress of 208 kPa.

* Bench-scale SRM reported by Son (2010).

Table 4.6 Bulk Stress, Resilient Modulus, Low-Strain Modulus and Normalized Resilient Modulus for FWD, LSME and Bench-Scale Tests

Test Method	Bulk Stress (kPa)	Resilient Modulus (MPa)	Low-strain Modulus (MPa)	Normalized Resilient Modulus
Recycled Asphalt Pavement				
FWD	112	195	3076	0.06
LSME (0.20 m)	169	276	3969	0.07
LSME (0.30 m)	117	335	3161	0.11
Bench-Scale – External	110 – 858	128 – 345	3,042 – 10,867	0.04*
Bench-Scale – Internal	110 – 858	435 – 2,071	3,042 – 10,867	0.15*
Recycled Concrete Aggregate				
FWD	137	265	977	0.27
LSME (0.20 m)	159	360	1,058	0.34
LSME (0.30 m)	116	398	893	0.45
Bench-Scale – External	113 – 857	141 – 403	882 – 2,582	0.15*
Bench-Scale – Internal	113 – 857	484 – 1,644	882 – 2,582	0.56*
Blended RCA/Class 5				
FWD	117	225	895	0.25
LSME (0.20 m)	166	248	1,047	0.24
LSME (0.30 m)	116	341	893	0.38
Bench-Scale – External	109 – 867	142 – 428	868 – 2,204	0.17*
Bench-Scale – Internal	113 – 867	492 – 1,857	881 – 2,204	0.64*
Class 5				
FWD	127	97	619	0.16
LSME (0.20 m)	170	215	698	0.31
LSME (0.30 m)	118	297	601	0.49
Bench-Scale – External	95 – 839	94 – 326	550 – 1,344	0.20*
Bench-Scale – Internal	95 – 839	309 – 1,291	550 – 1,344	0.71*

* - Average value

Table 4.7 Resilient Modulus and Low-Strain modulus at Field Bulk Stress

Test Method	Resilient Modulus @ Field Bulk Stress (MPa)	Normalized Resilient Modulus	Low-strain Modulus (MPa)
Recycled Asphalt Pavement, Bulk Stress = 112 kPa			
FWD	195	0.06	3076
LSME (0.20 m)	215	0.07	3071
LSME (0.30 m)	325	0.11	2954
Bench-Scale – External	145	0.04	3625
Bench-Scale – Internal	468	0.15	3120
Recycled Concrete Aggregate, Bulk Stress = 137 kPa			
FWD	265	0.27	977
LSME (0.20 m)	332	0.34	976
LSME (0.30 m)	436	0.45	968
Bench-Scale – External	161	0.15	1073
Bench-Scale – Internal	545	0.56	973
Blended RCA/Class 5, Bulk Stress = 117 kPa			
FWD	225	0.25	895
LSME (0.20 m)	210	0.24	875
LSME (0.30 m)	342	0.38	900
Bench-Scale – External	141	0.17	829
Bench-Scale – Internal	518	0.64	809
Class 5, Bulk Stress = 127 kPa			
FWD	97	0.16	619
LSME (0.20 m)	187	0.31	603
LSME (0.30 m)	307	0.49	626
Bench-Scale – External	126	0.20	630
Bench-Scale – Internal	421	0.71	592

Table 4.8 Variance of Low-Strain Elastic Modulus Obtained at Field Bulk Stress

Method	Low-strain Modulus at Field Bulk Stress (MPa)			
	RCA	RAP	Blend	Class 5
FWD	977	3076	895	619
LSME (0.20 m)	976	3071	875	603
LSME (0.30 m)	968	2954	900	626
Bench-Scale – External	1073	3625	829	630
Bench-Scale – Internal	973	3120	809	592
Mean Average	992	3160	863	614
Standard Deviation	40	239	38	14
Coefficient of Variance	4.1%	7.6%	4.4%	2.3%

4.8 Figures

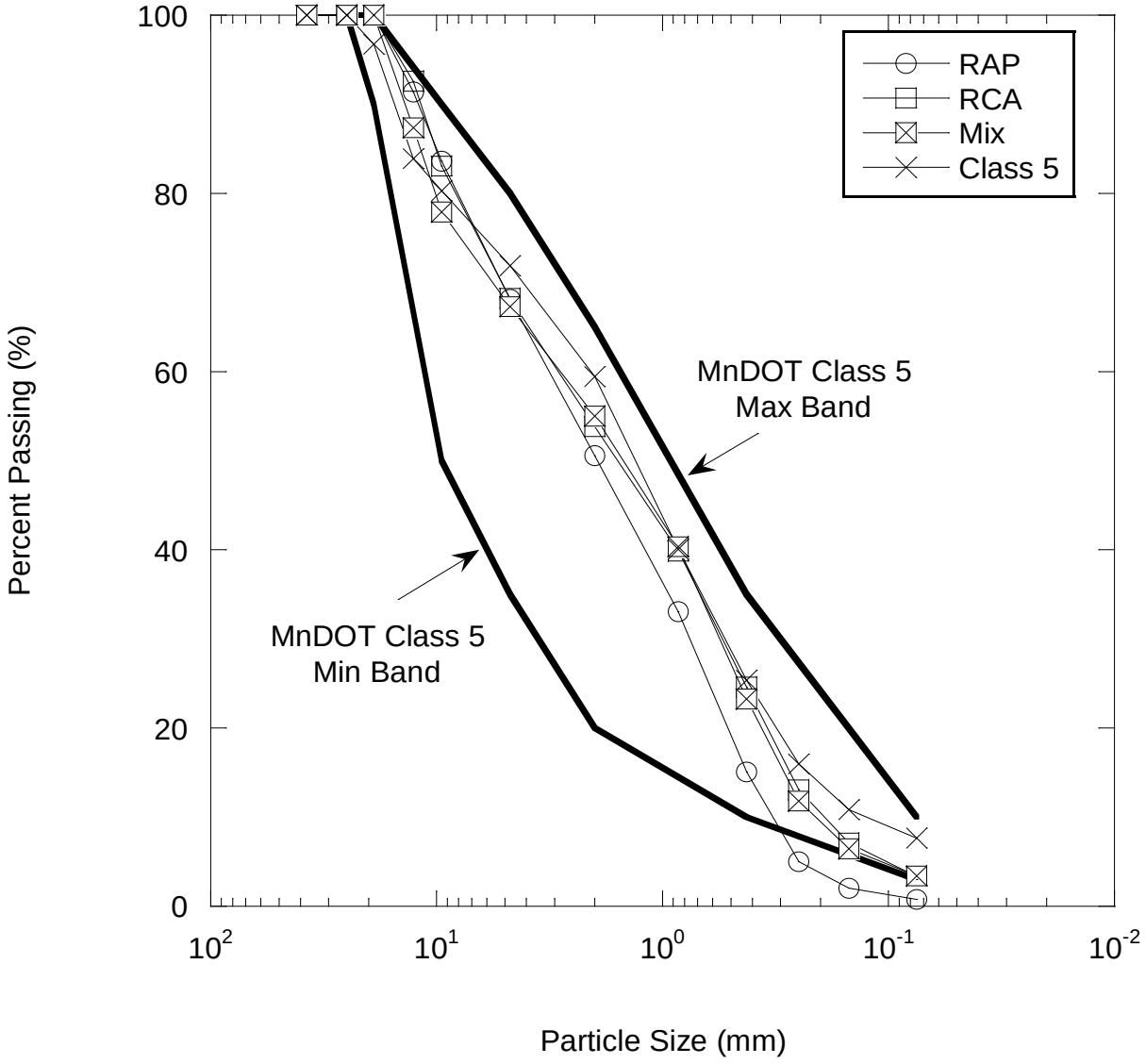

Figure 4.1 Particle Size Distributions for RAP, RCA, Blended RCA/Class 5 and Class 5 with MnDOT Specifications

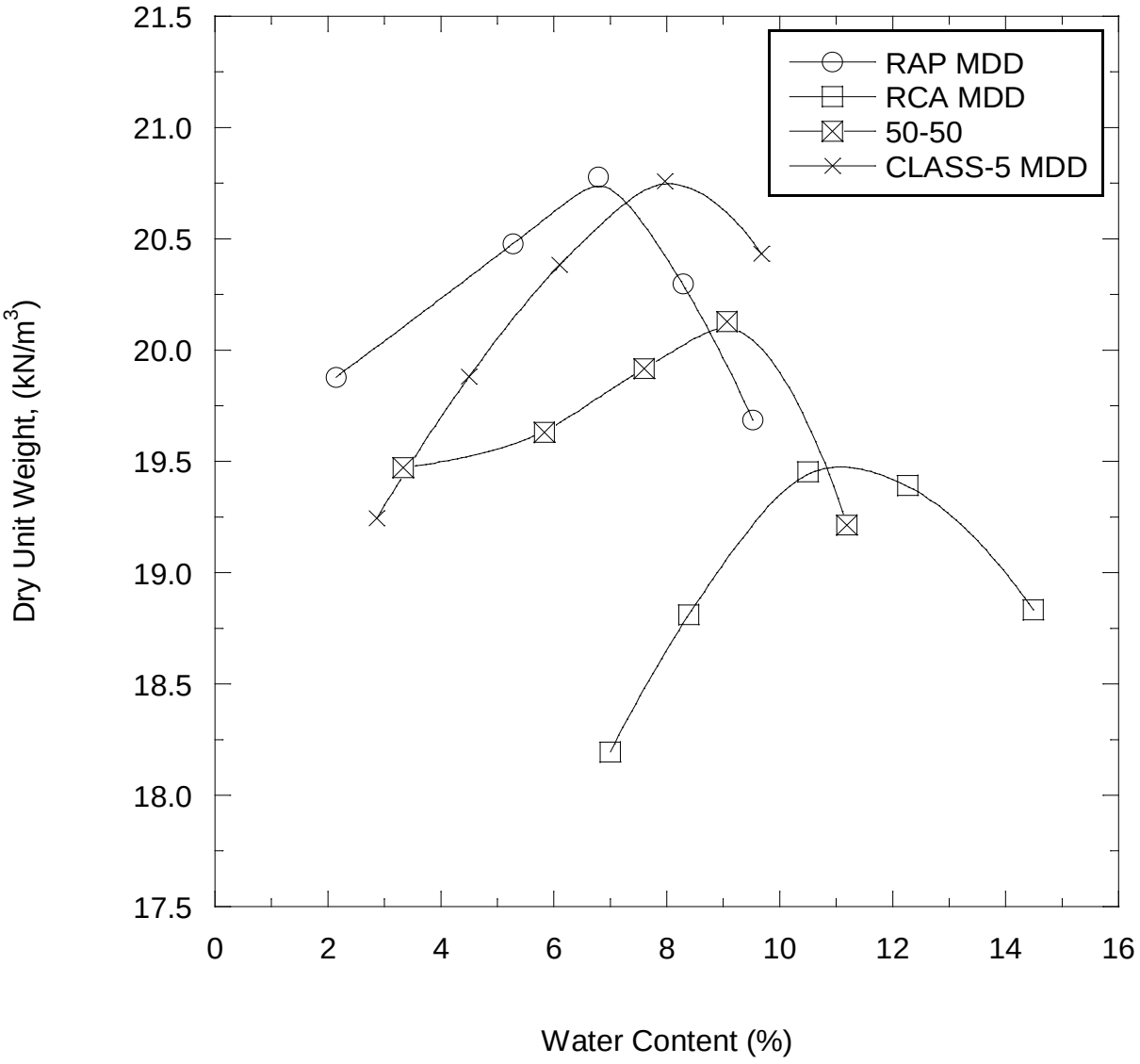

Figure 4.2 Modified Compaction Curves for RAP, RCA, Blended RCA/Class 5 Base, and Class 5

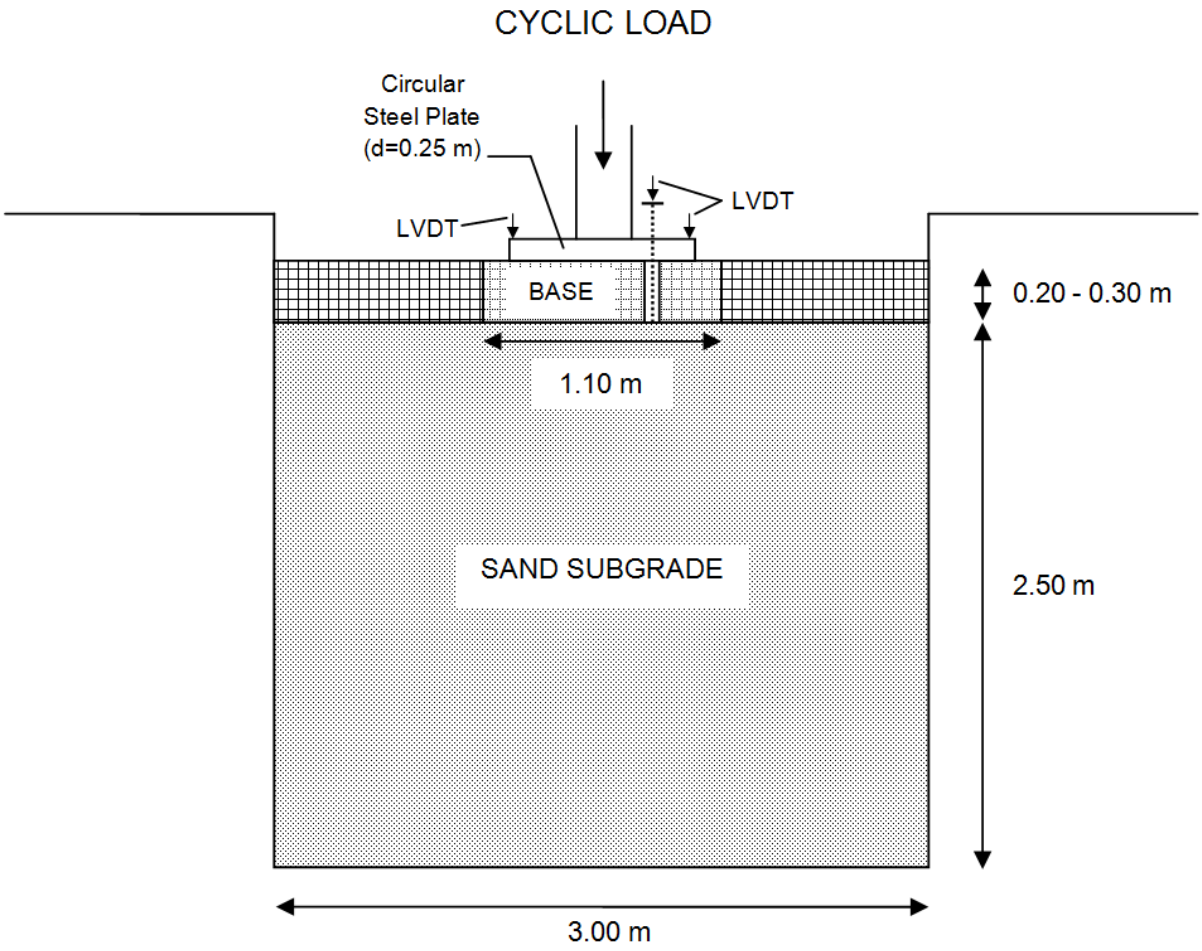

Figure 4.3 Schematic of LSME Testing Setup

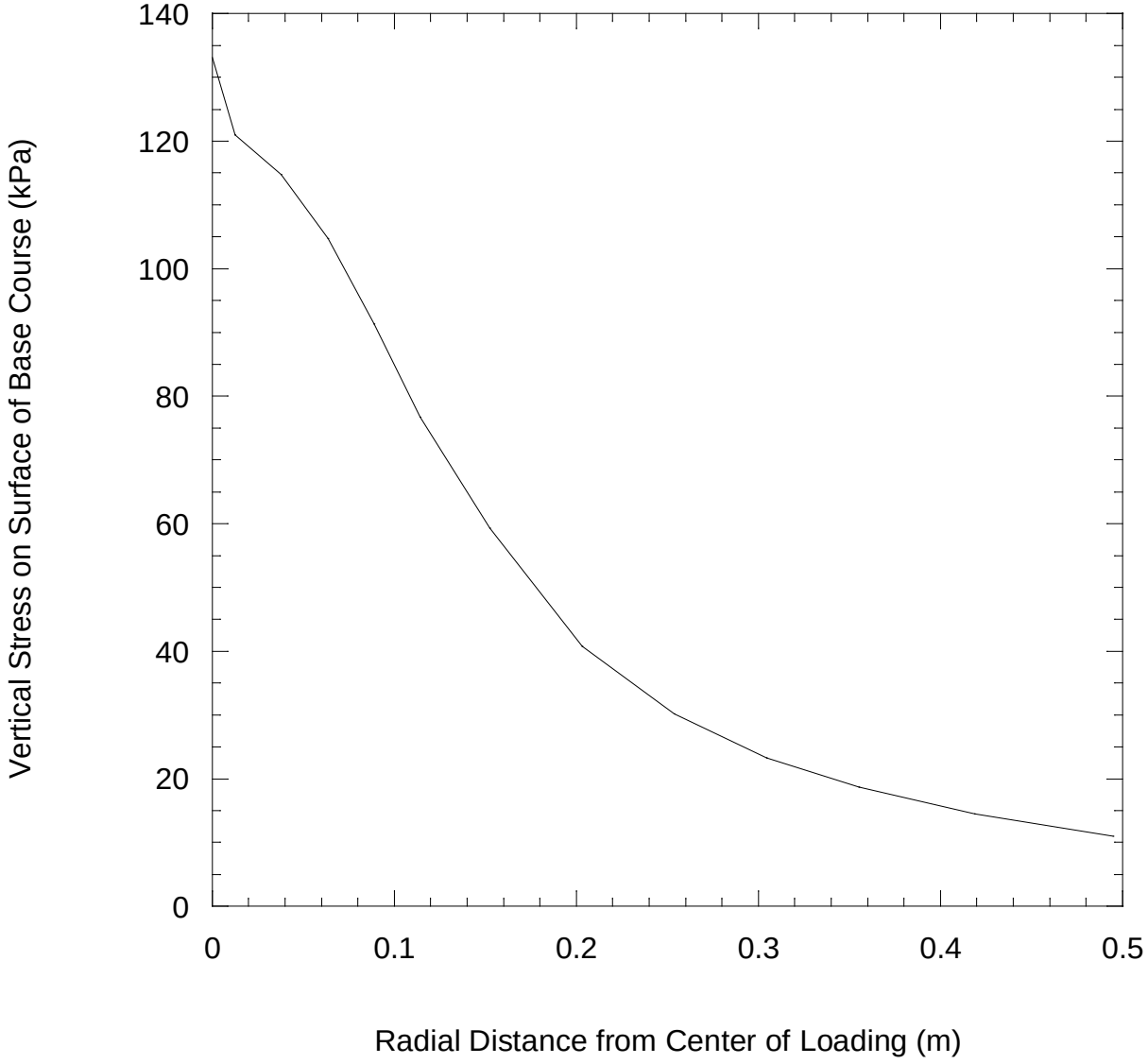

Figure 4.4 Vertical Stress on Surface of Base Course vs. Radial Distance from Center of Traffic Loading Predicted by MICHPAVE

Cell 16: Recycled Concrete Aggregate (RCA)	Cell 17: Blended 50% / 50% RCA/Class 5 (Blend)	Cell 18: Recycled Asphalt Pavement (RAP)	Cell 19: Mn/DOT Class 5 Aggregate (Class 5)
127 mm Asphalt Concrete	127 mm Asphalt Concrete	127 mm Asphalt Concrete	127 mm Asphalt Concrete
305 mm RCA	305 mm Blend	305 mm RAP	305 mm Class 5
305 mm Class 3 Aggregate	305 mm Class 3 Aggregate	305 mm Class 3 Aggregate	305 mm Class 3 Aggregate
178 mm Select Granular Material	178 mm Select Granular Material	178 mm Select Granular Material	178 mm Select Granular Material
Clay	Clay	Clay	Clay

Figure 4.5 Pavement Profiles of Cells Tested Using FWD at MnROAD Testing Facility (Adapted from Johnson et al. 2009)

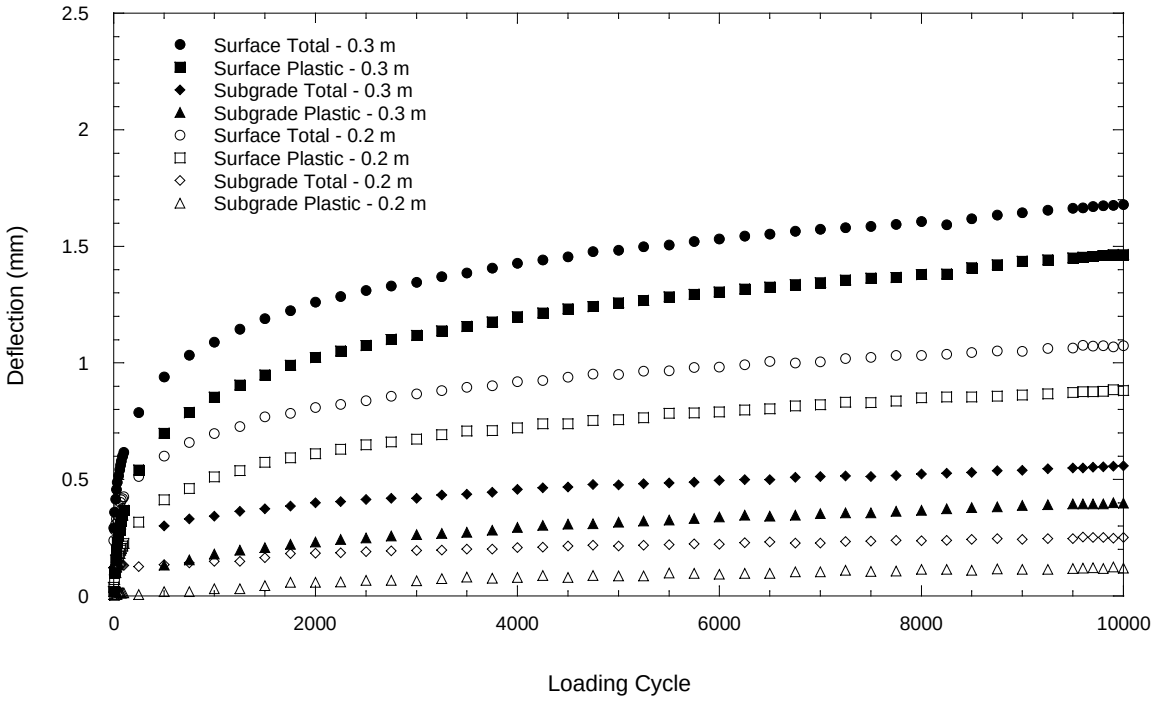

Figure 4.6 Total and Plastic Deformation of Surface and Subgrade Layers versus Number of Loading Cycles for RAP

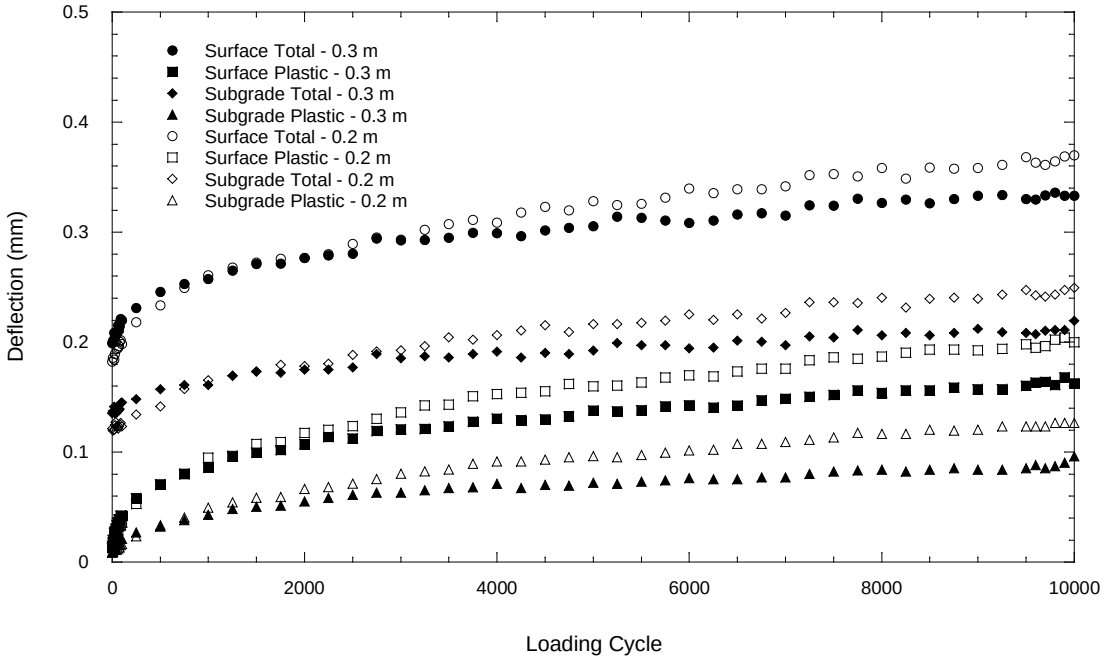

Figure 4.7 Total and Plastic Deformation of Surface and Subgrade Layers versus Number of Loading Cycles for RCA

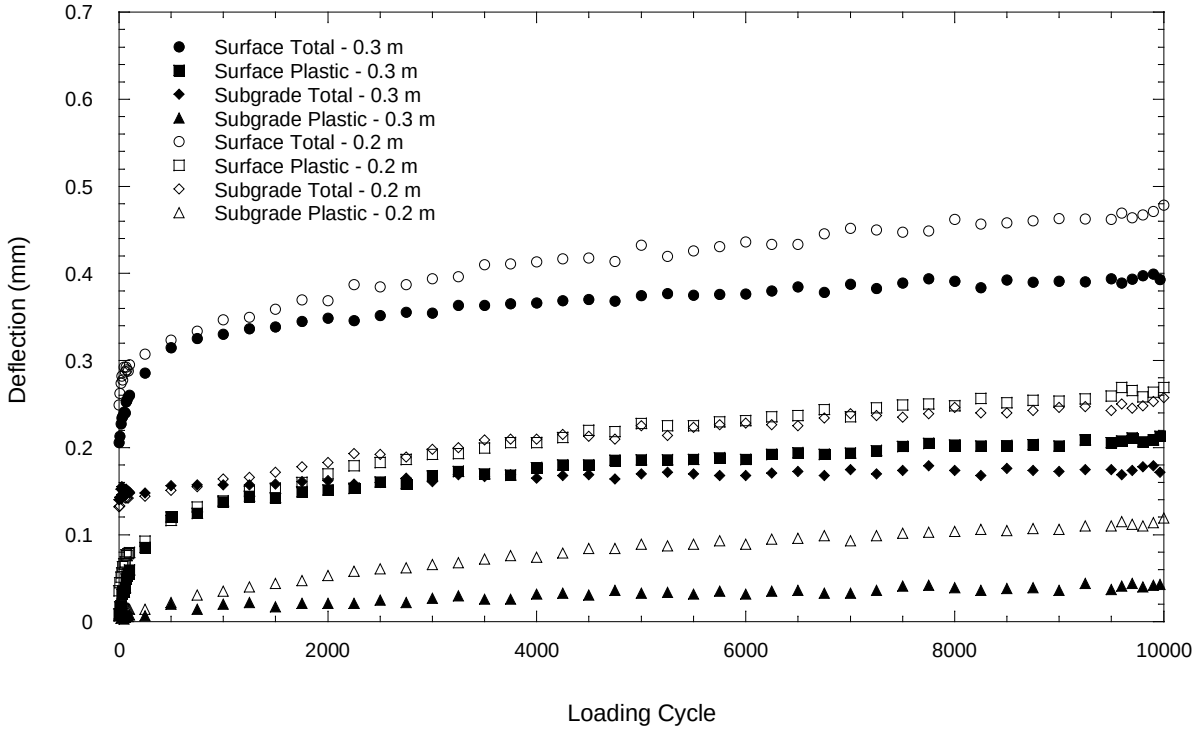

Figure 4.8 Total and Plastic Deformation of Surface and Subgrade Layers versus Number of Loading Cycles for Blended RCA/Class 5

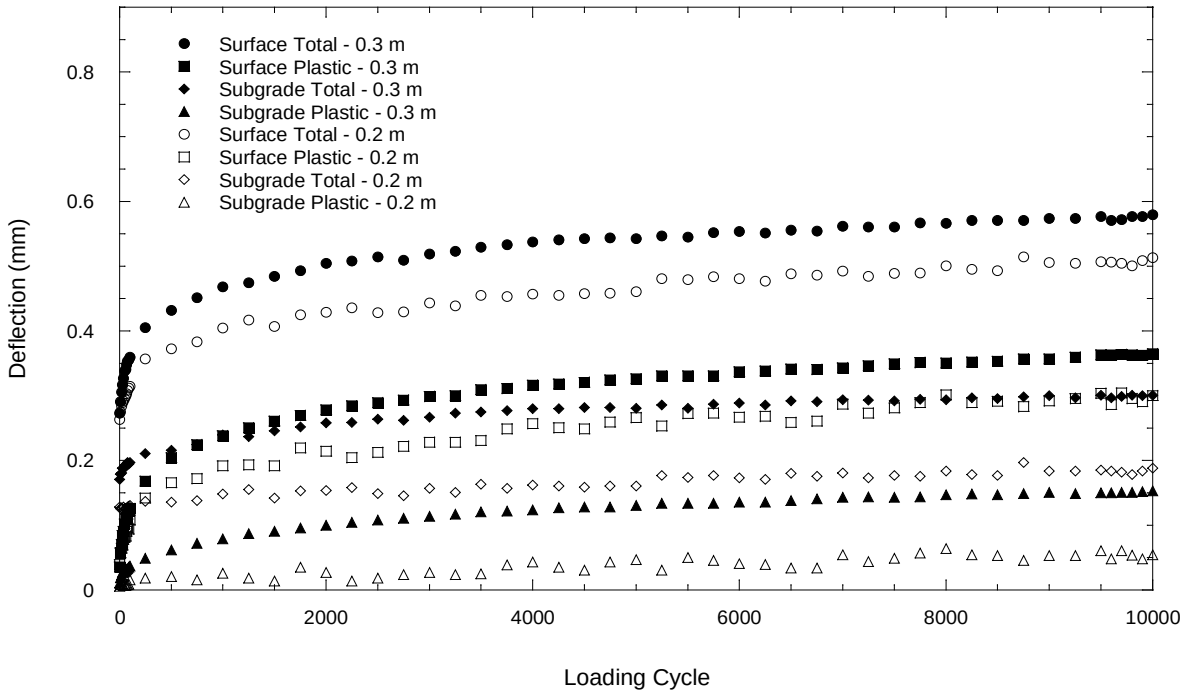

Figure 4.9 Total and Plastic Deformation of Surface and Subgrade Layers versus Number of Loading Cycles for Class 5

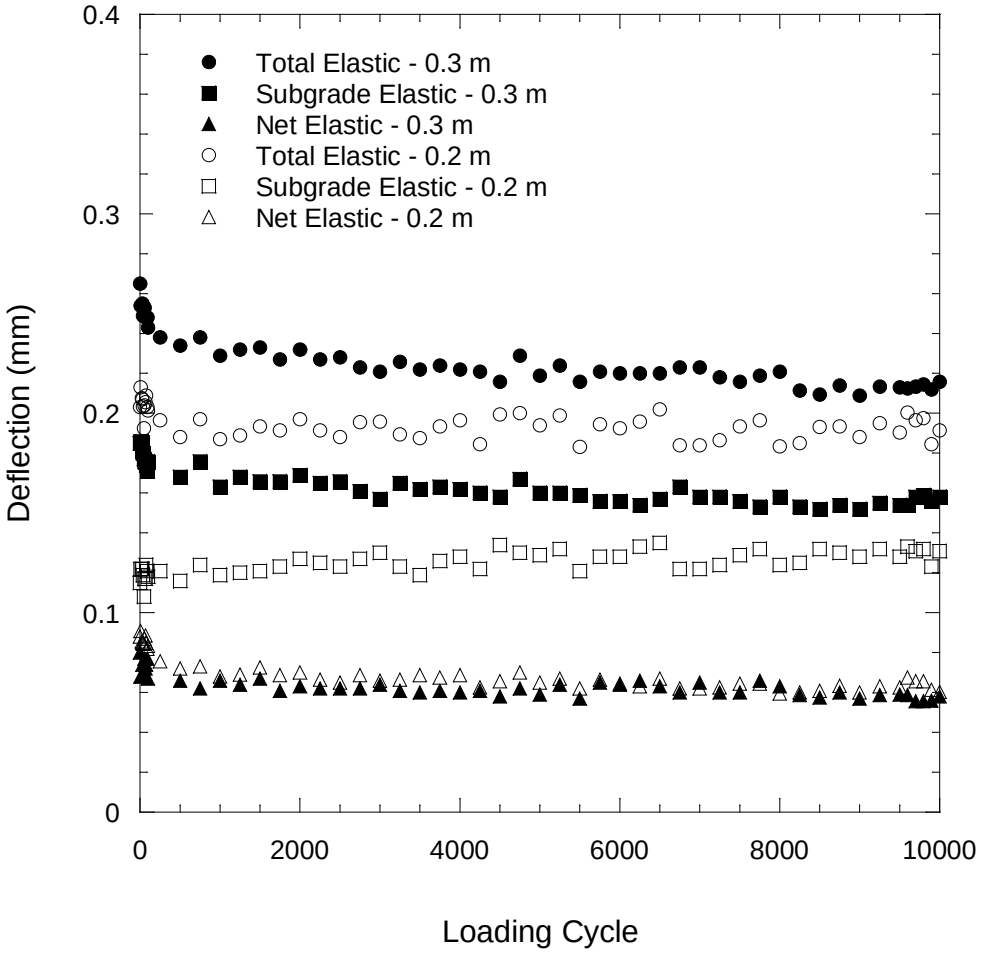

Figure 4.10 Surface (total), Subgrade, and Net Elastic Deformation versus Number of Loading Cycles for RAP

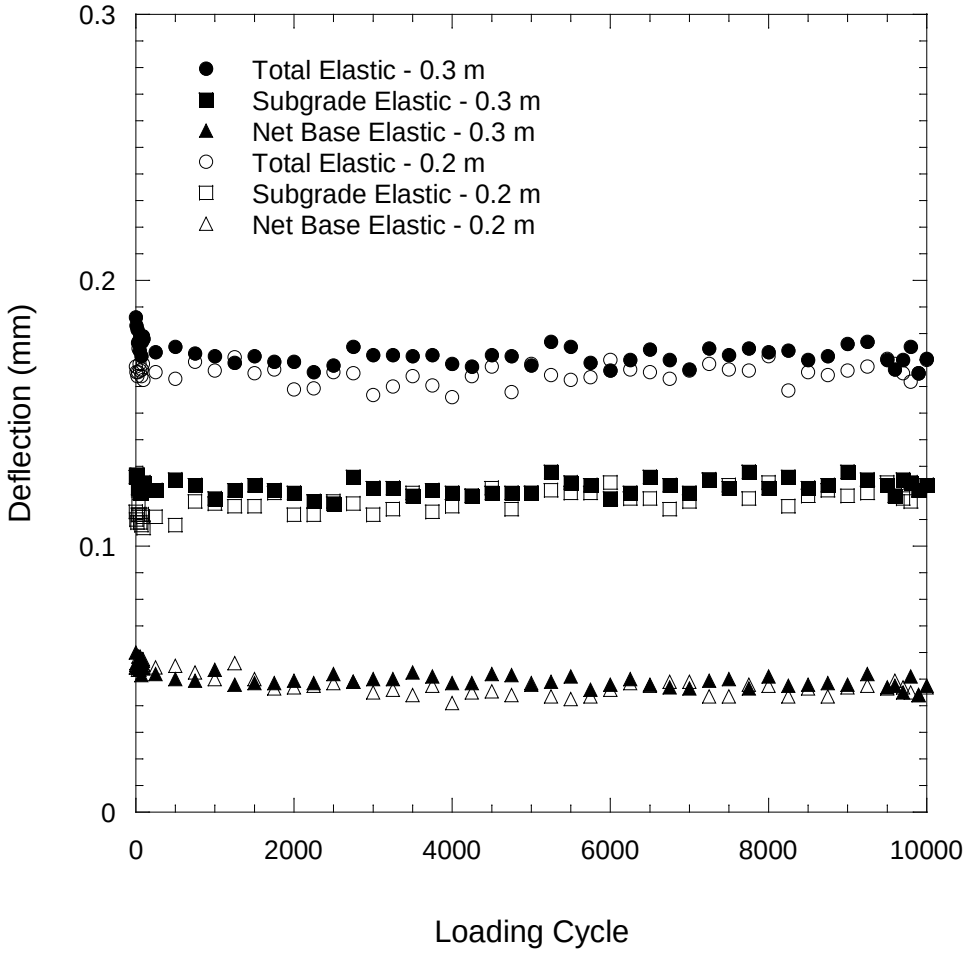

Figure 4.11 Surface (total), Subgrade, and Net Elastic Deformation versus Number of Loading Cycles for RCA

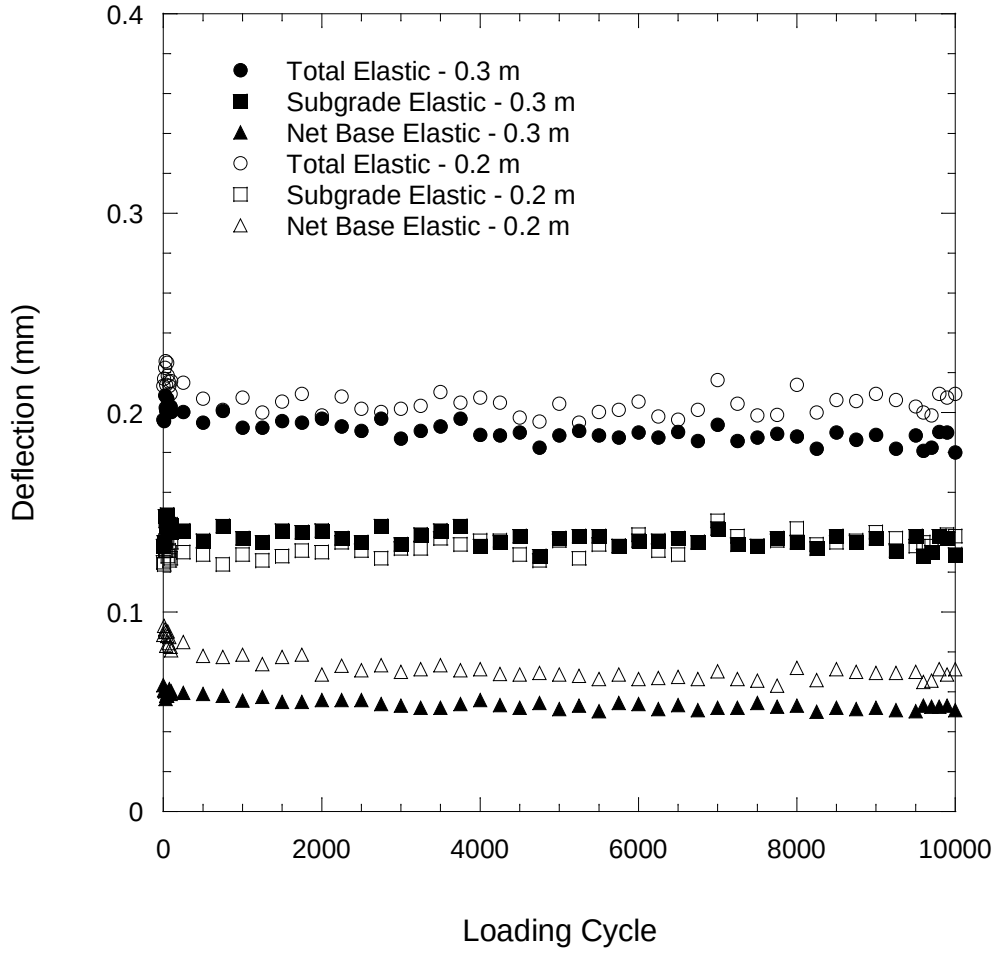

Figure 4.12 Surface (total), Subgrade, and Net Elastic Deformation versus Number of Loading Cycles for Blended RCA/Class 5

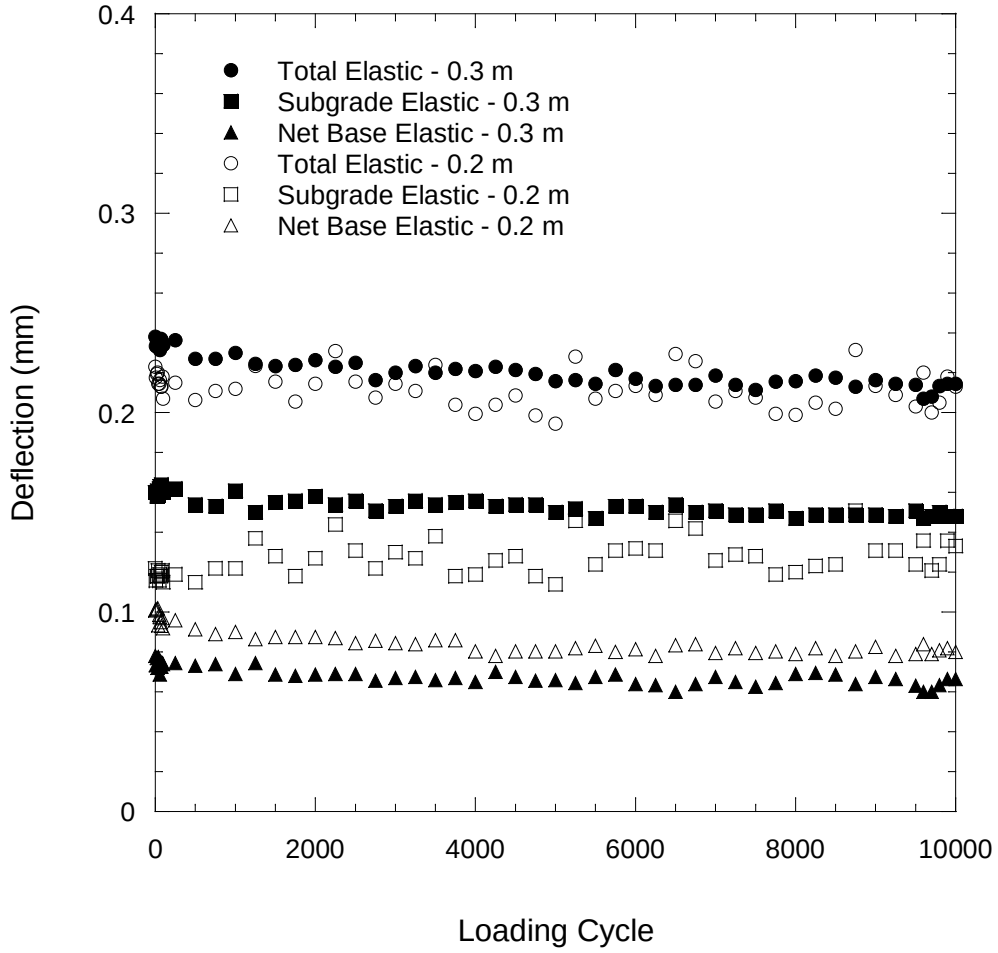

Figure 4.13 Surface (total), Subgrade, and Net Elastic Deformation versus Number of Loading Cycles for Class 5

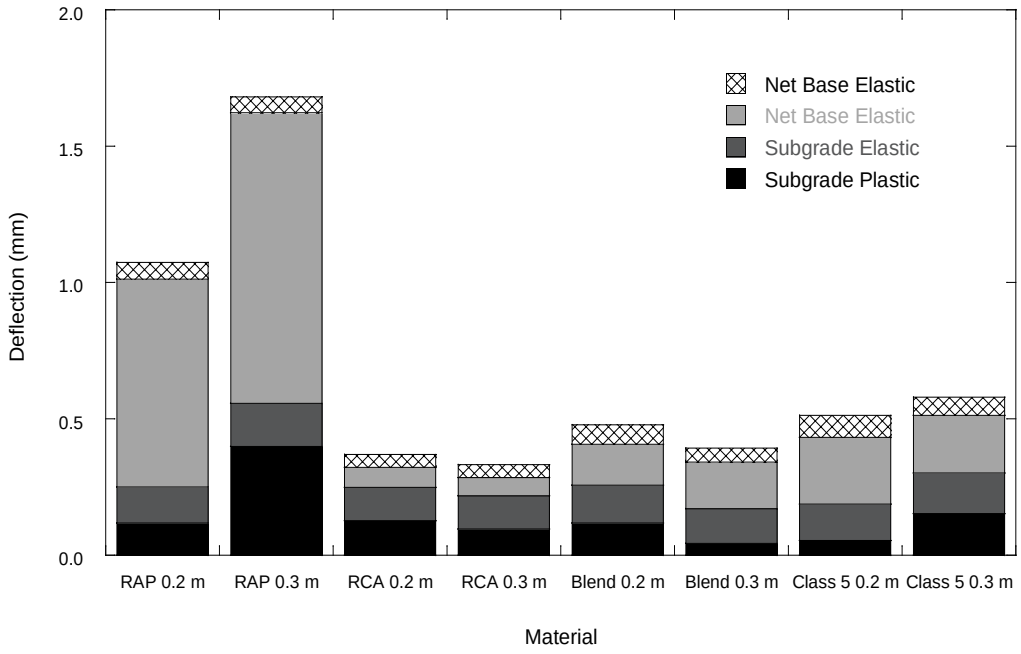

Figure 4.14 Comparison of Surface and Subgrade Deformations for RAP, RCA, Blended RCA/Class 5, and Class 5

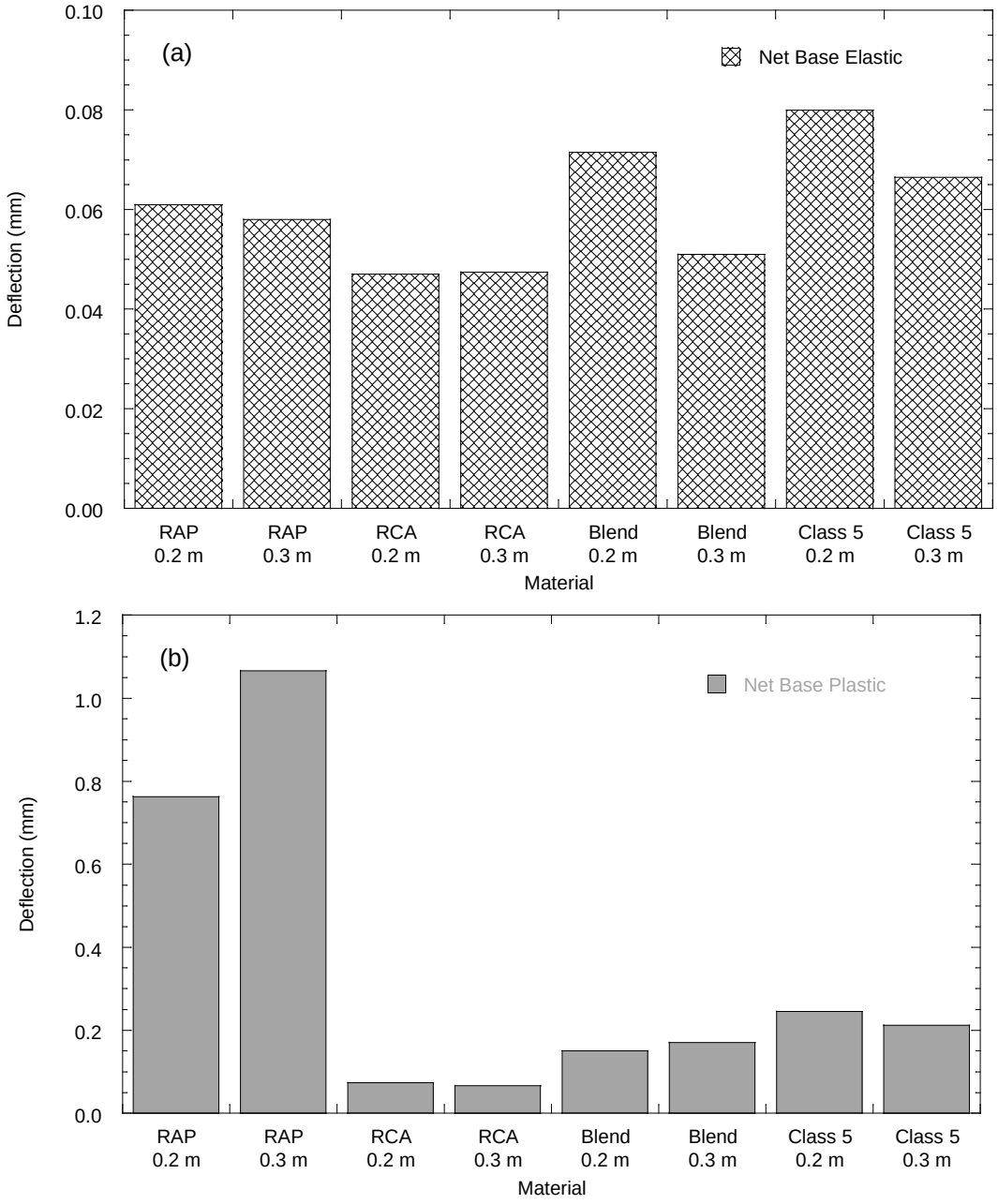

Figure 4.15 Comparison of (a) Net Elastic and (b) Net Plastic Deformations for RAP, RCA, Blended RCA/Class 5, and Class 5

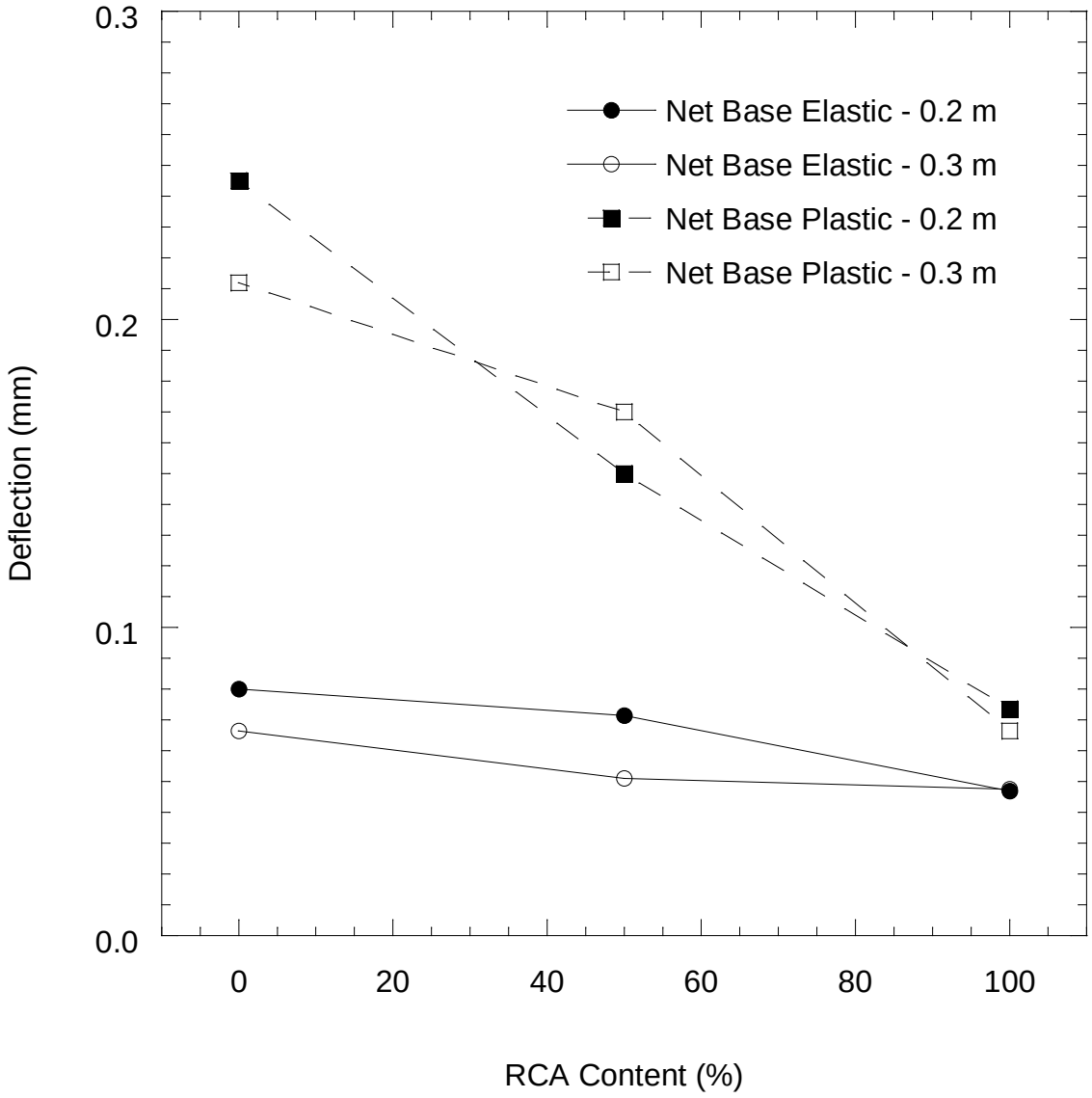

Figure 4.16 Comparison of Net Base Elastic and Net Base Plastic Deformations versus RCA Content for RCA, Blended RCA/Class 5, and Class 5

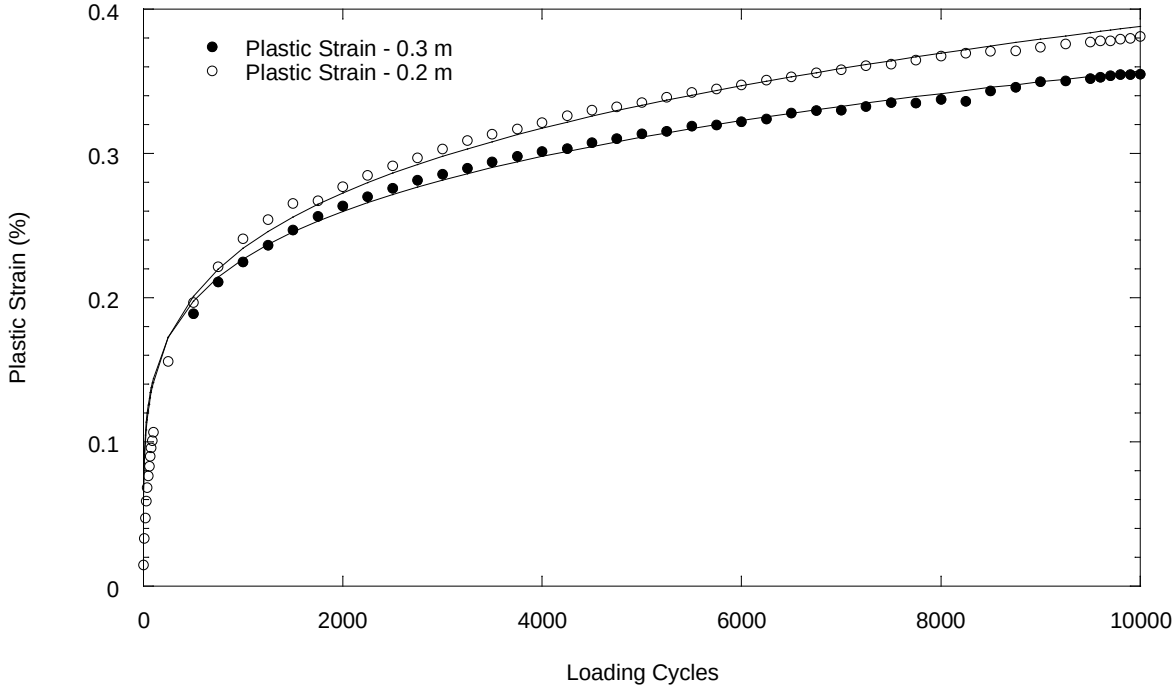

Figure 4.17 Plastic Strain versus Loading Cycle for RAP

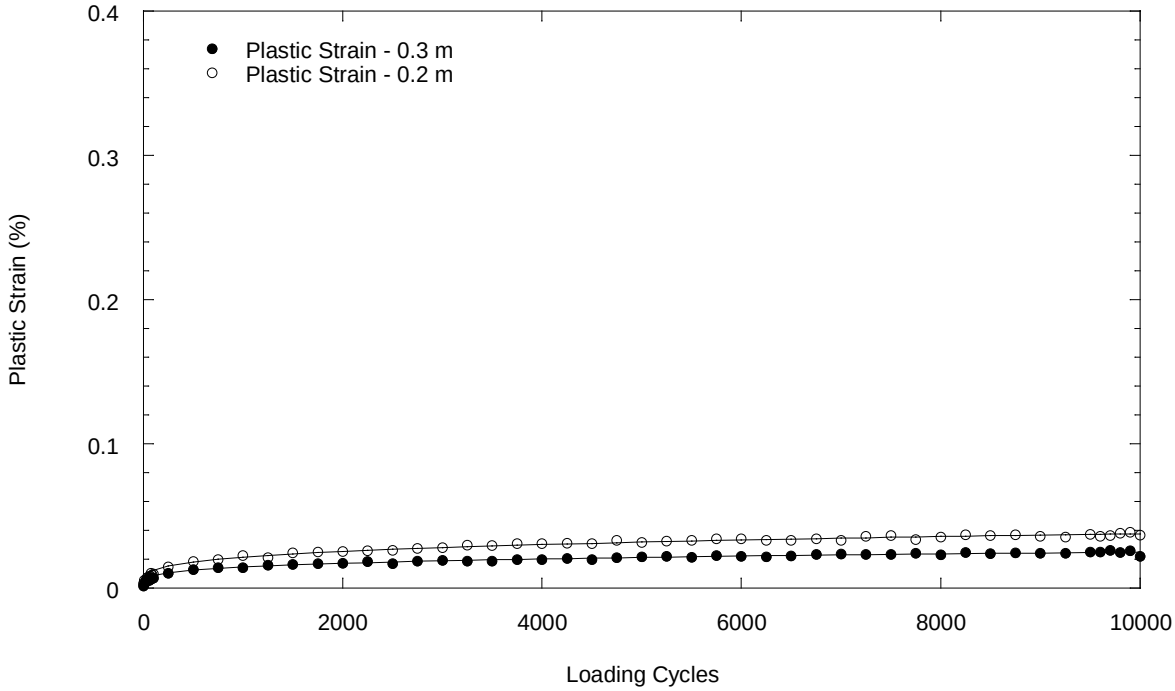

Figure 4.18 Plastic Strain versus Loading Cycle for RCA

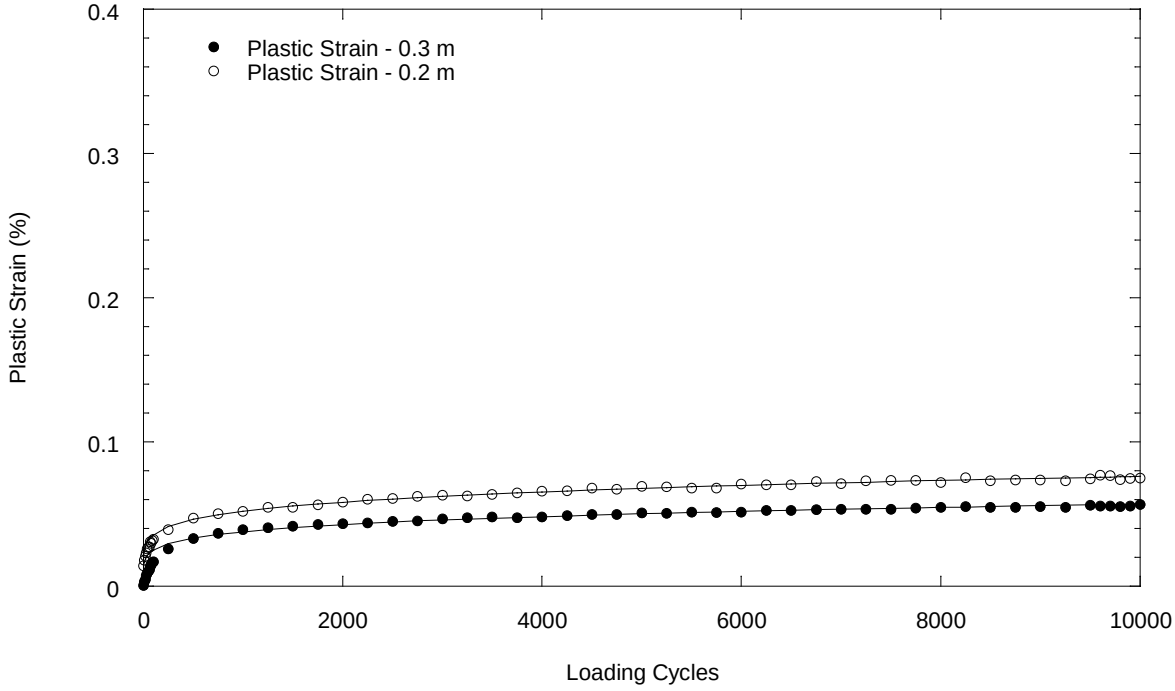

Figure 4.19 Plastic Strain versus Loading Cycle for Blended RCA/Class 5

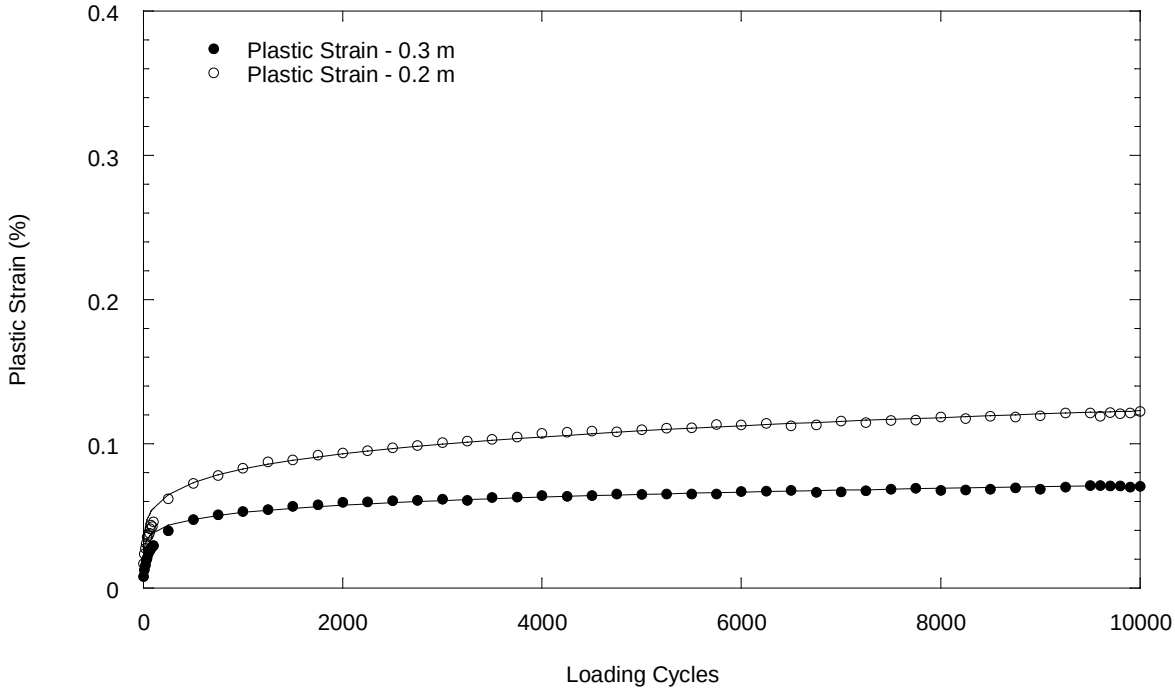

Figure 4.20 Plastic Strain versus Loading Cycle for Class 5

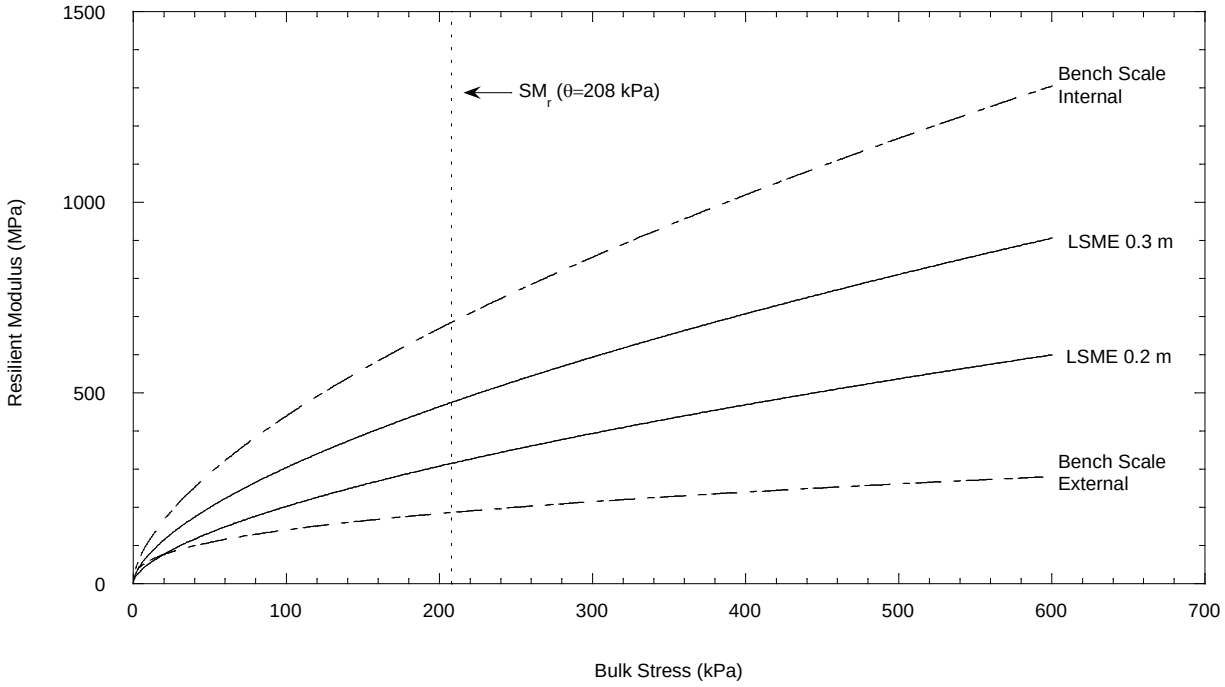

Figure 4.21 Resilient Modulus versus Bulk Stress for Bench-Scale and LSME Test Methods for RAP

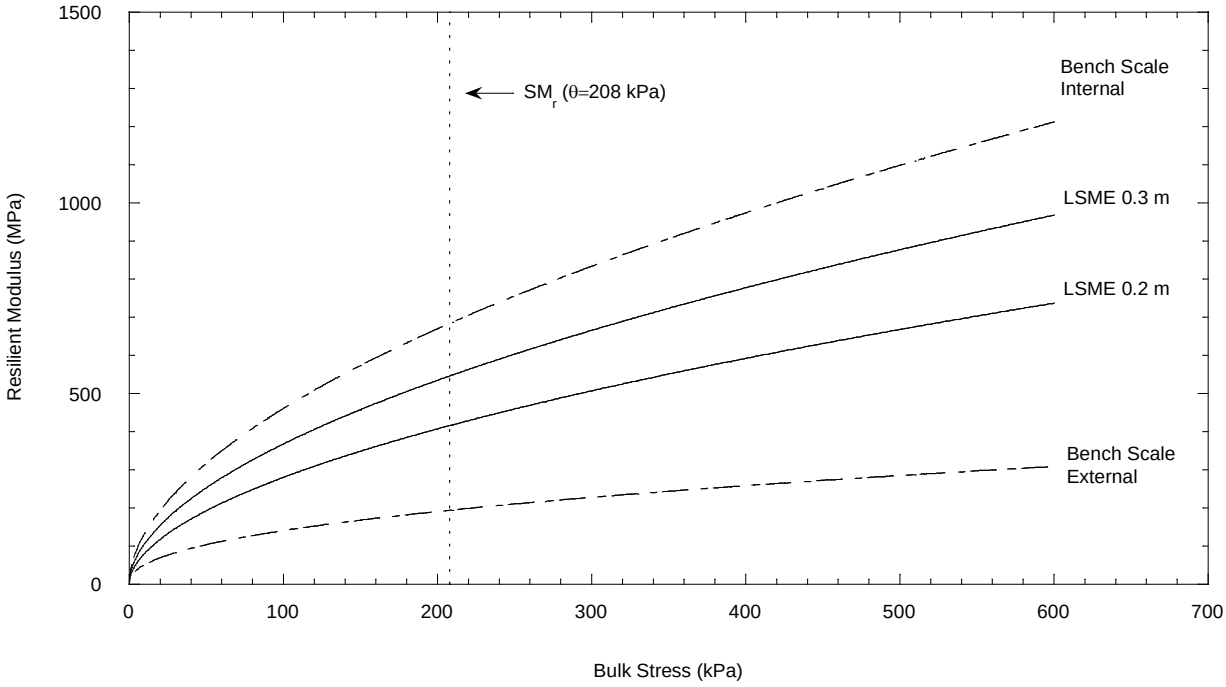

Figure 4.22 Resilient Modulus versus Bulk Stress for Bench-Scale and LSME Test Methods for RCA

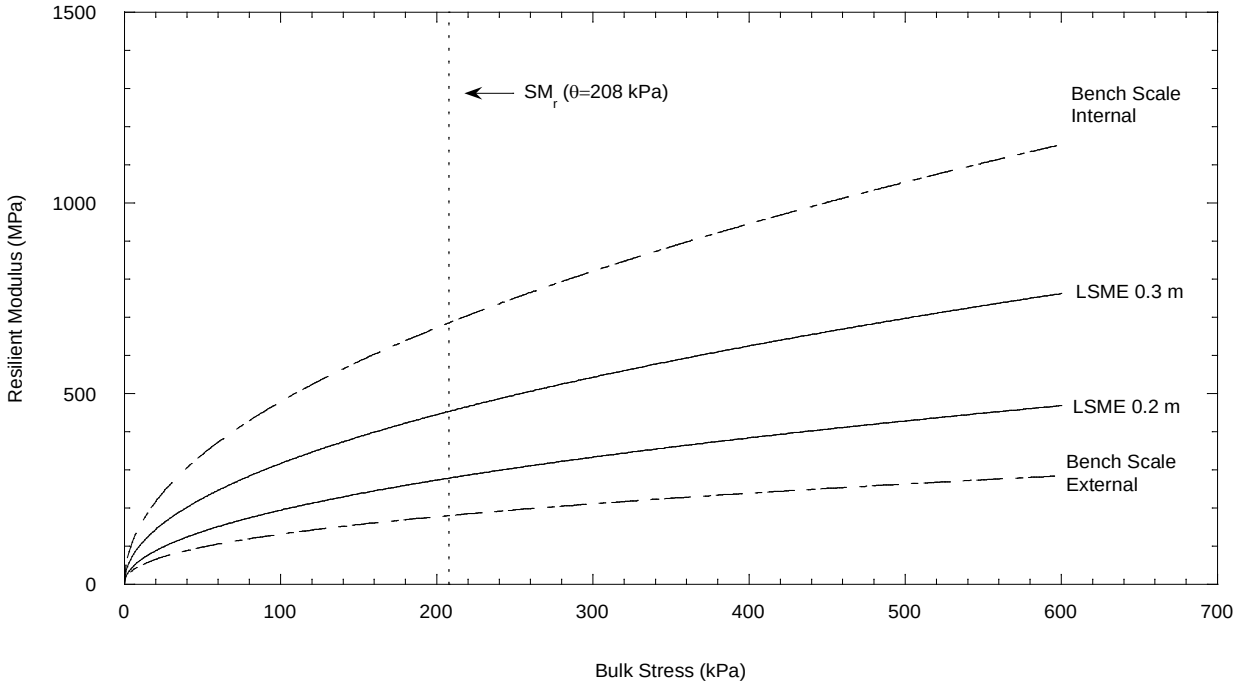

Figure 4.23 Resilient Modulus versus Bulk Stress for Bench-Scale and LSME Test Methods for Blended RCA/Class 5

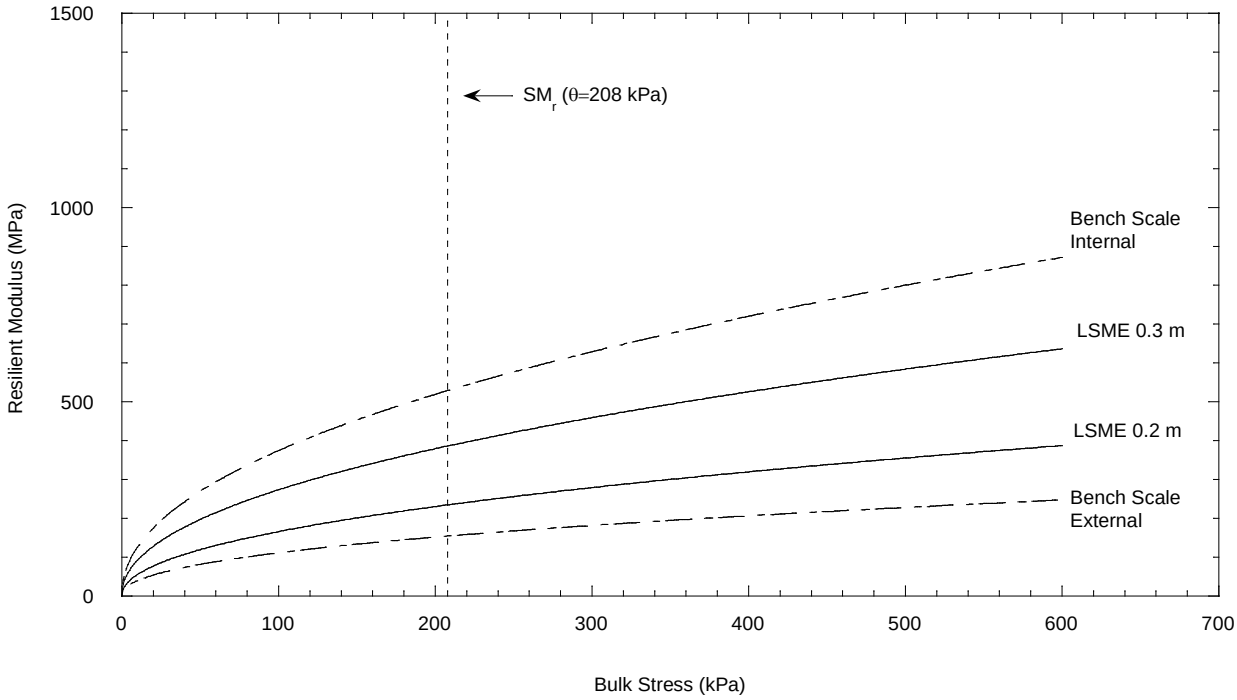

Figure 4.24 Resilient Modulus versus Bulk Stress for Bench-Scale and LSME Test Methods for Class 5

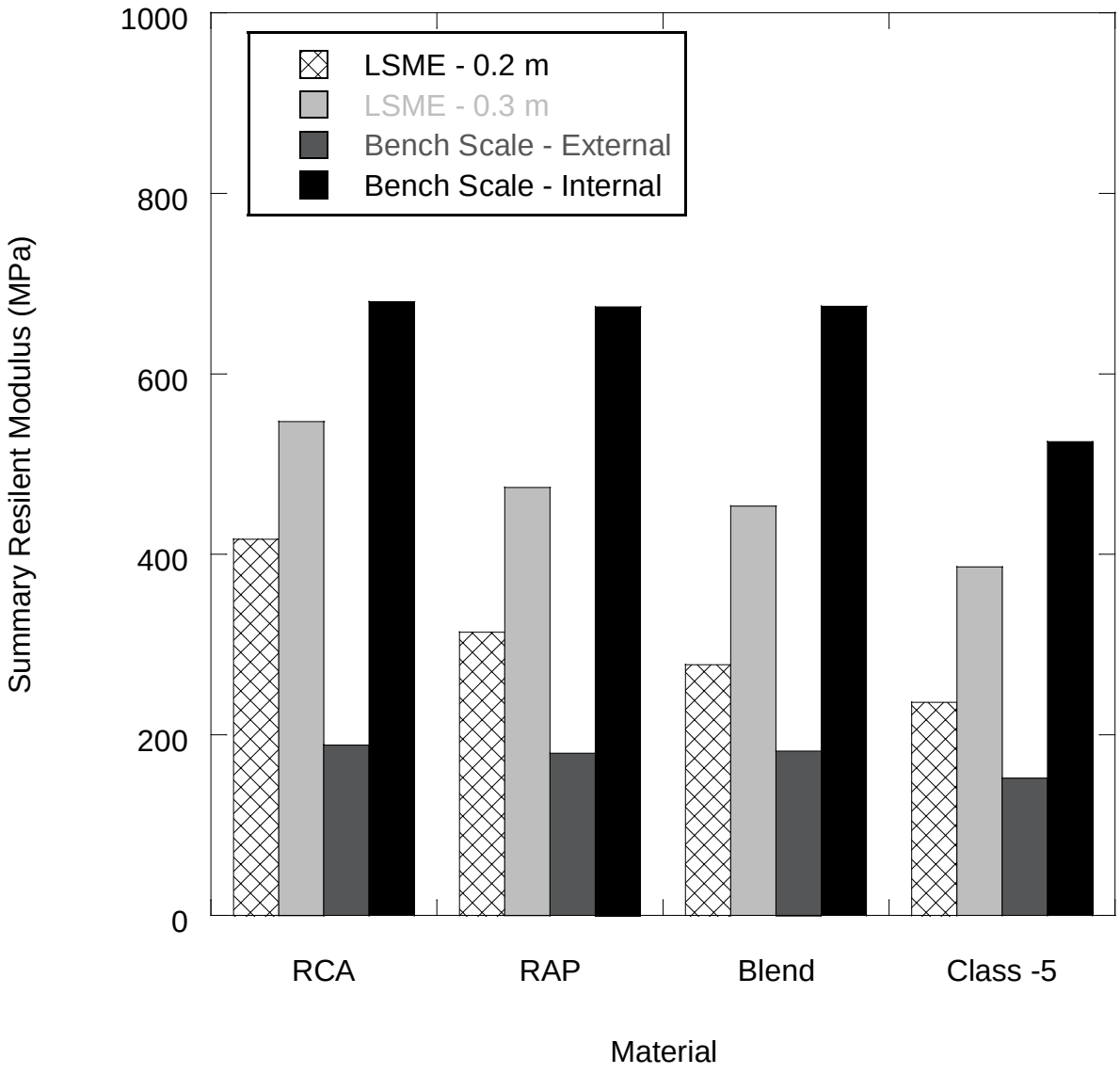

Figure 4.25 Comparison of Summary Resilient Modulus for RAP, RCA, Blended RCA/Class 5, and Class 5

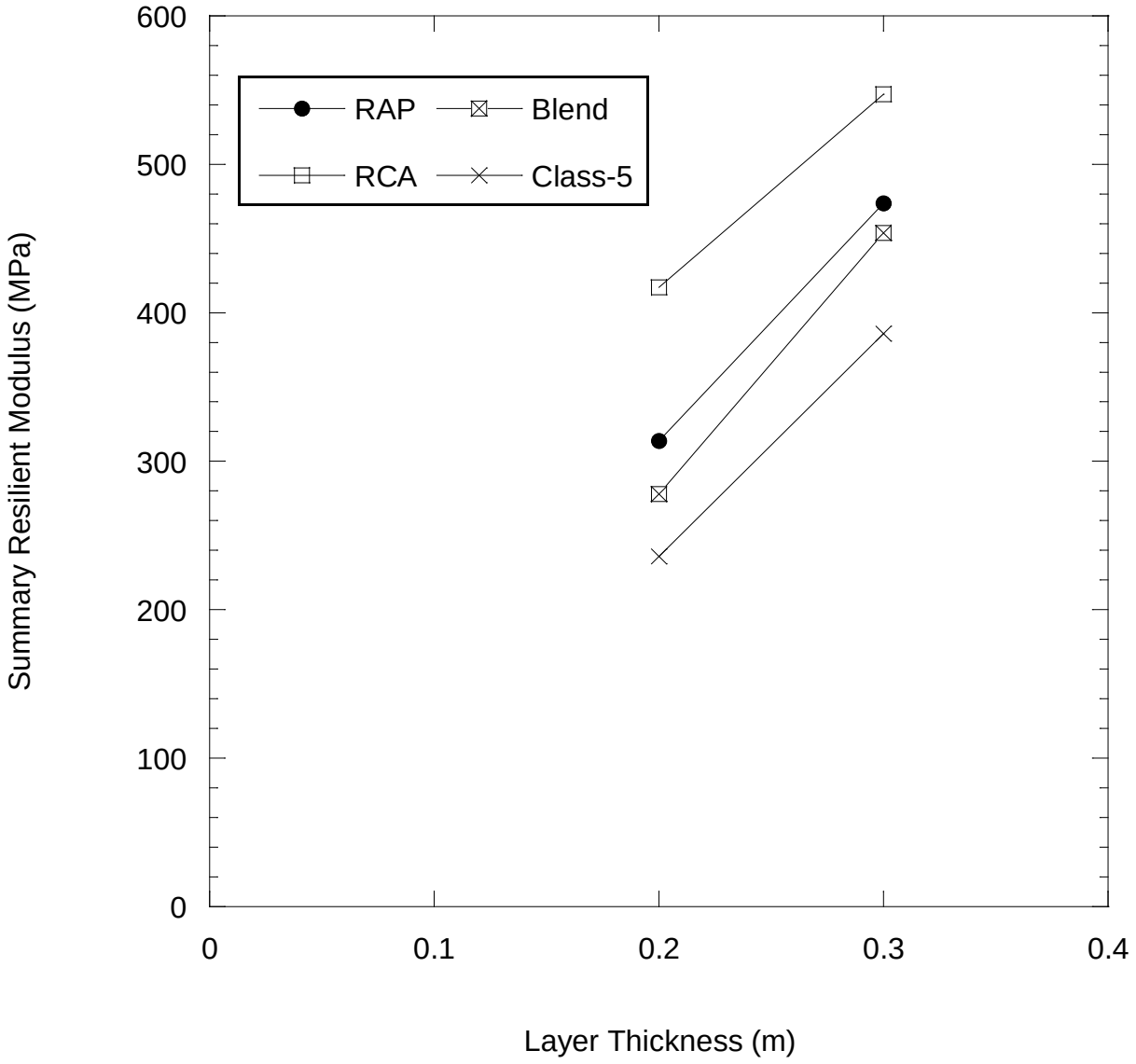

Figure 4.26 Summary Resilient Modulus versus Layer Thickness for RAP, RCA, Blended RCA/Class 5, and Class 5

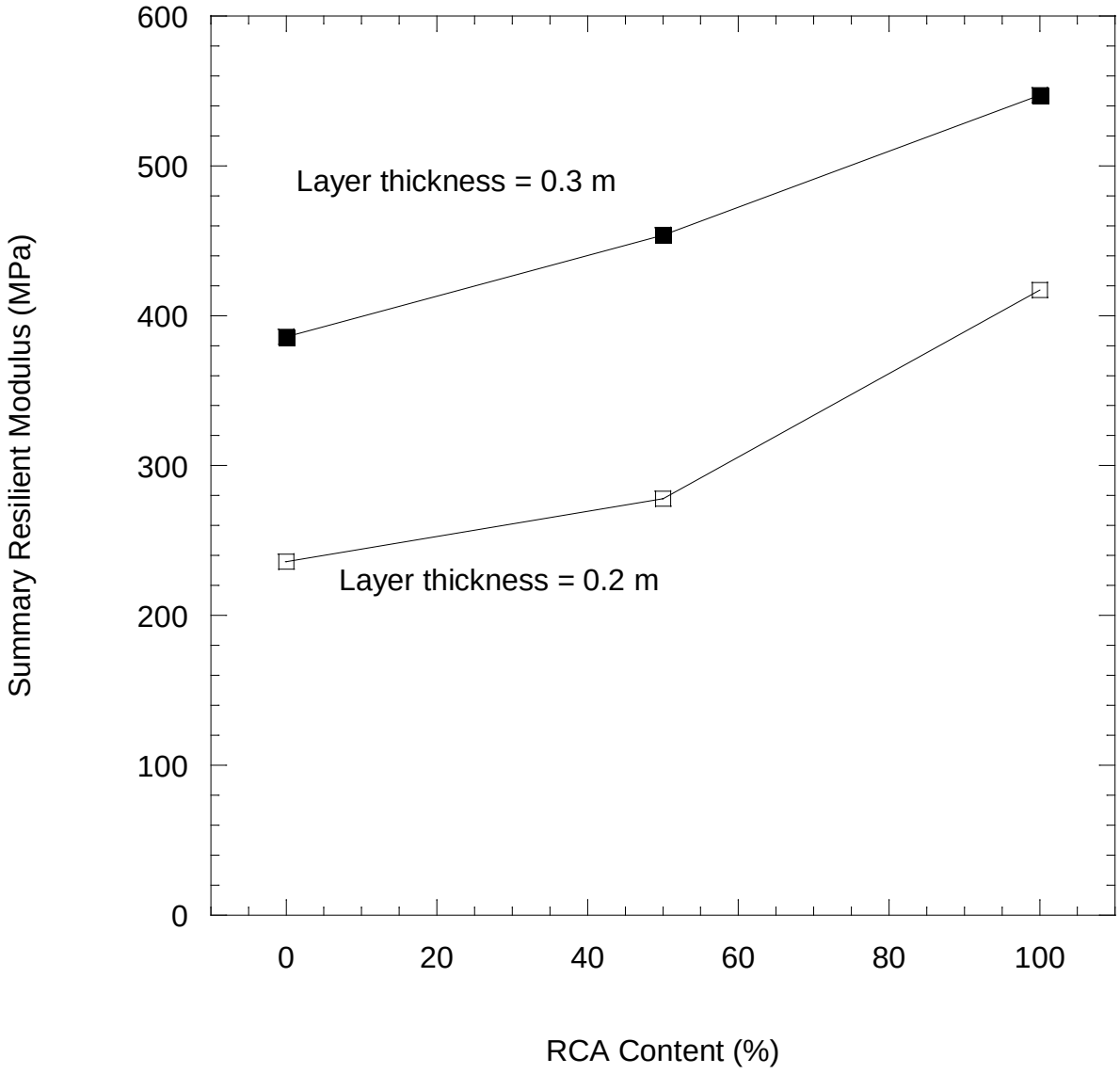

Figure 4.27 Summary Resilient Modulus versus RCA Content for RCA, Blended RCA/Class 5, and Class 5

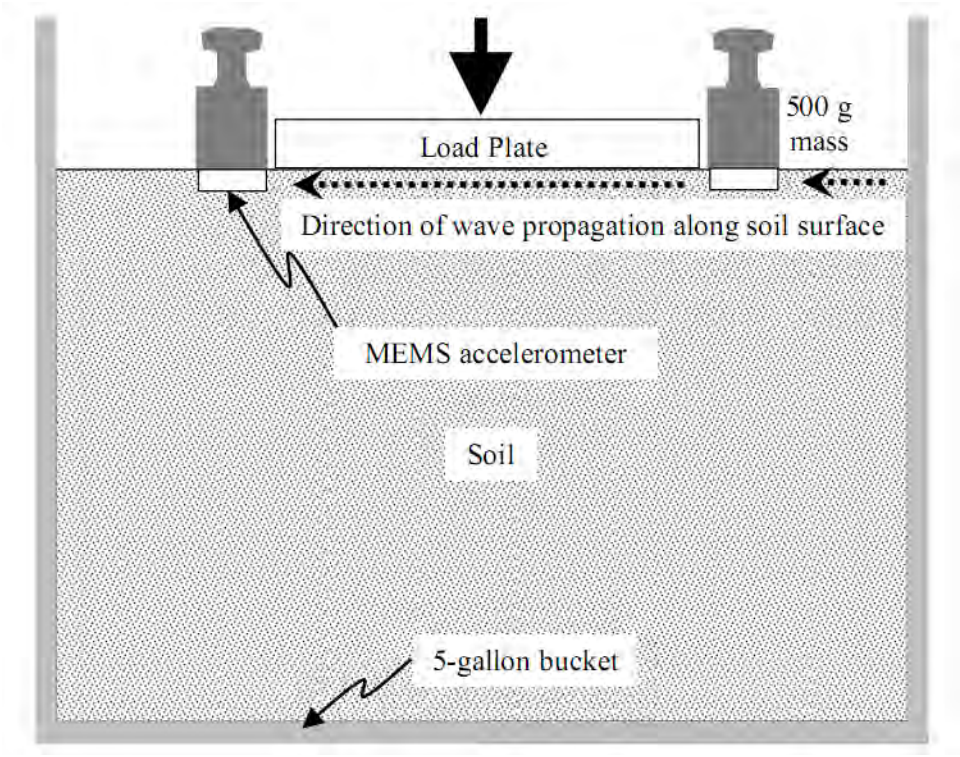

Figure 4.28 Simplified Test Setup to Determine Low-Strain Constraint Modulus with Applied Stress near the Surface (Adapted from Edil and Fratta 2009)

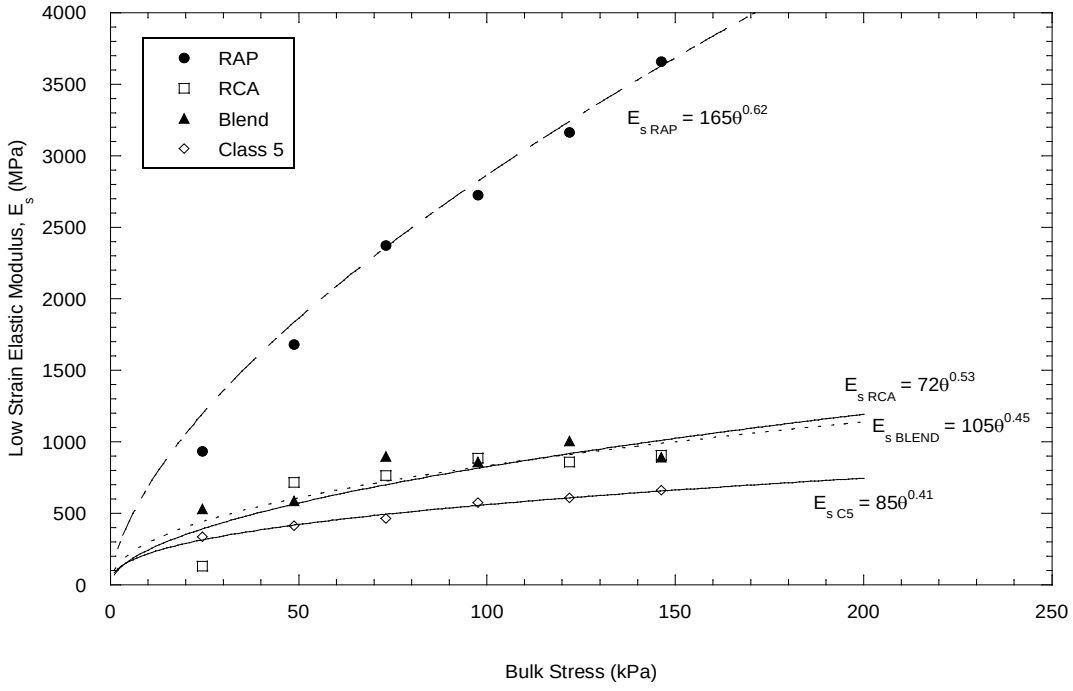

Figure 4.29 Low-Strain Elastic Modulus as a Function of Applied Vertical Stress

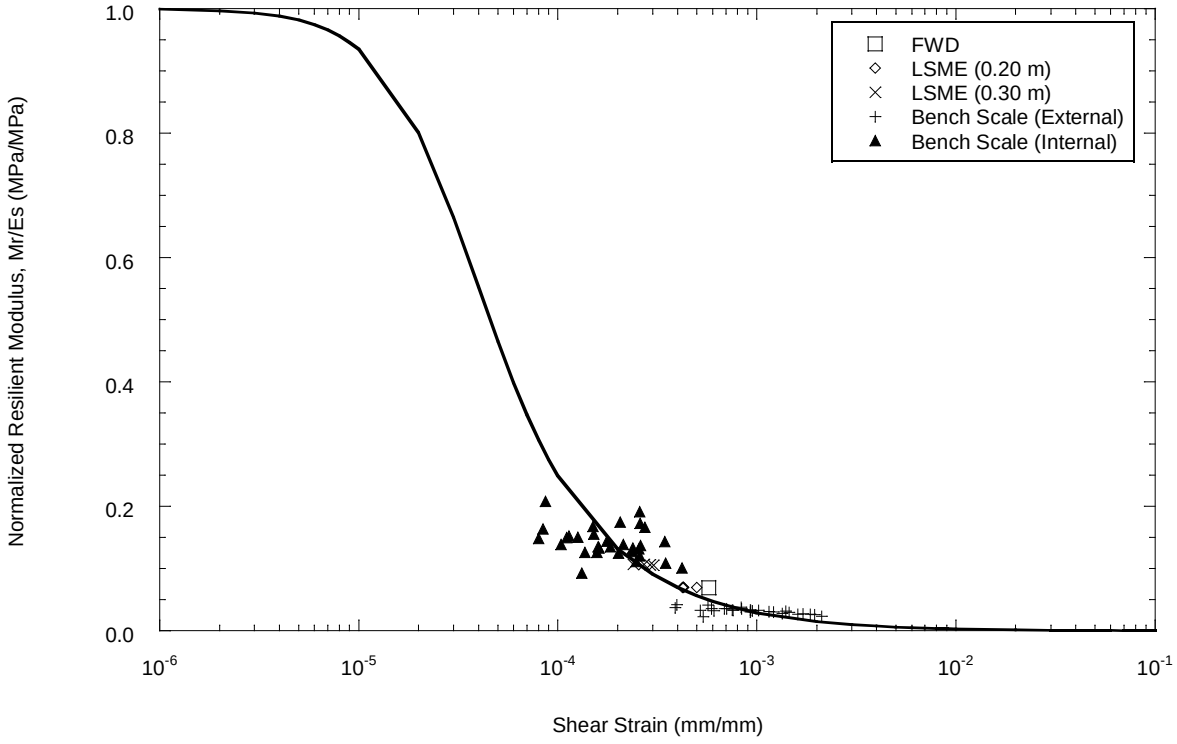

Figure 4.30 Backbone Curve Fit to FWD, LSME and Bench-Scale Data for RAP

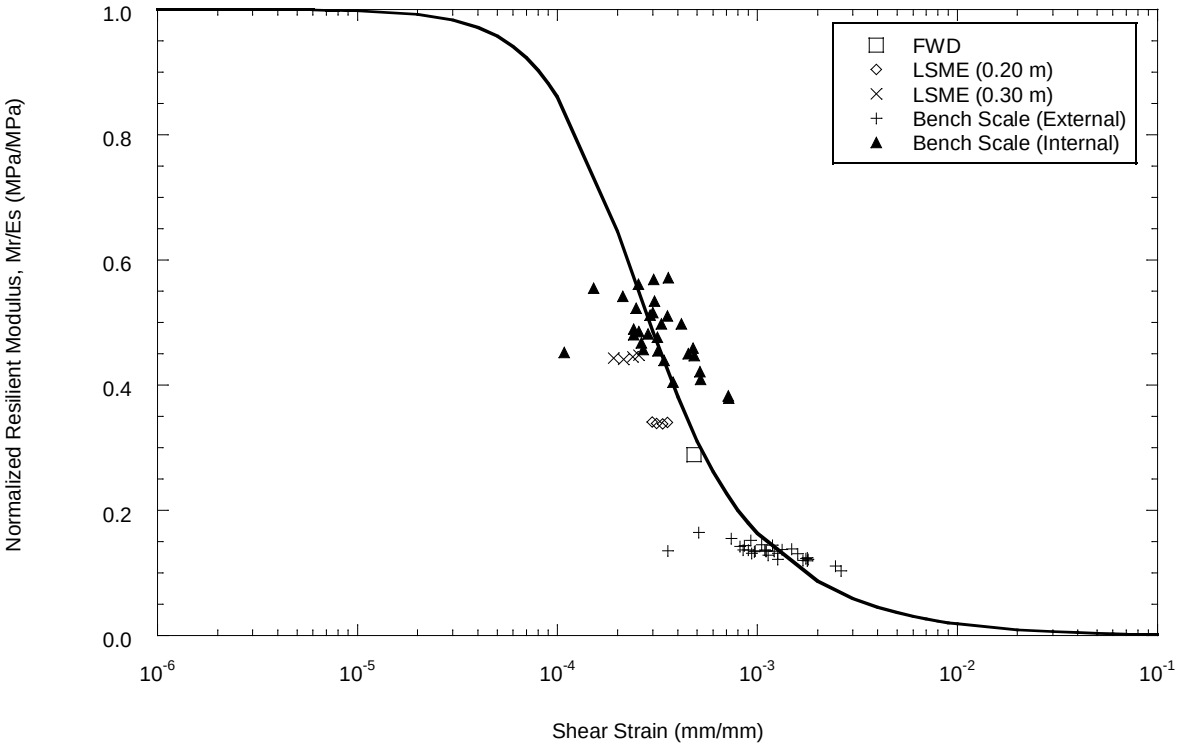

Figure 4.31 Backbone Curve Fit to FWD, LSME and Bench-Scale Data for RCA

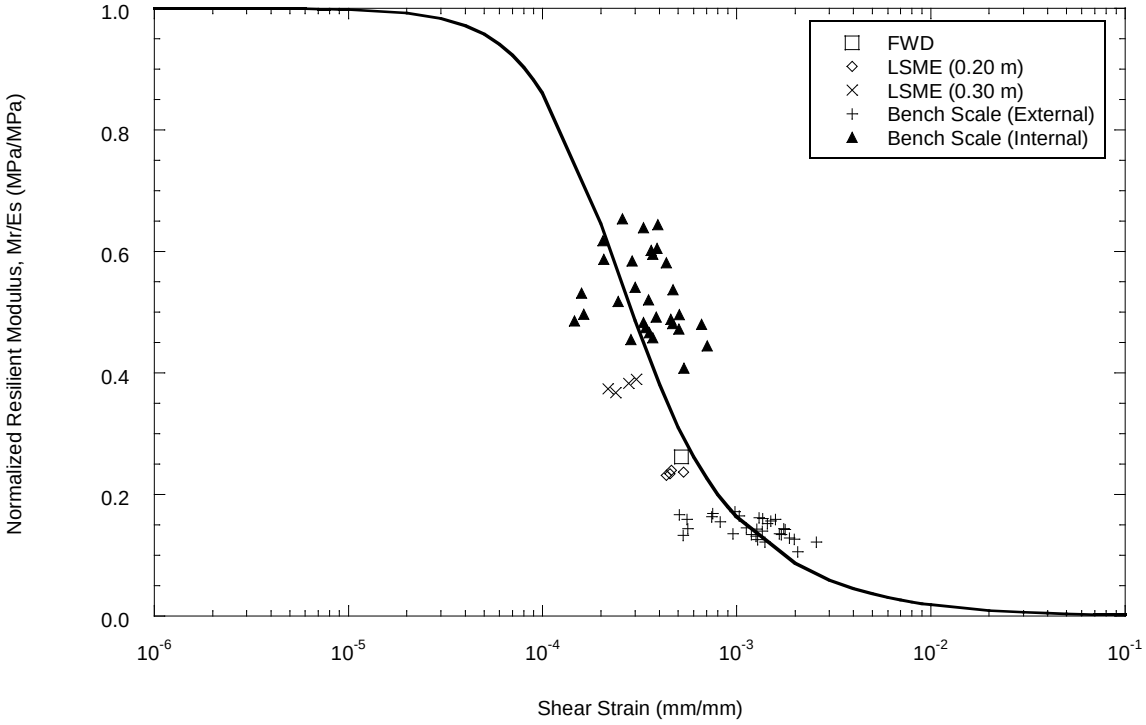

Figure 4.32 Backbone Curve Fit to FWD, LSME and Bench-Scale Data for Blended RCA/Class 5

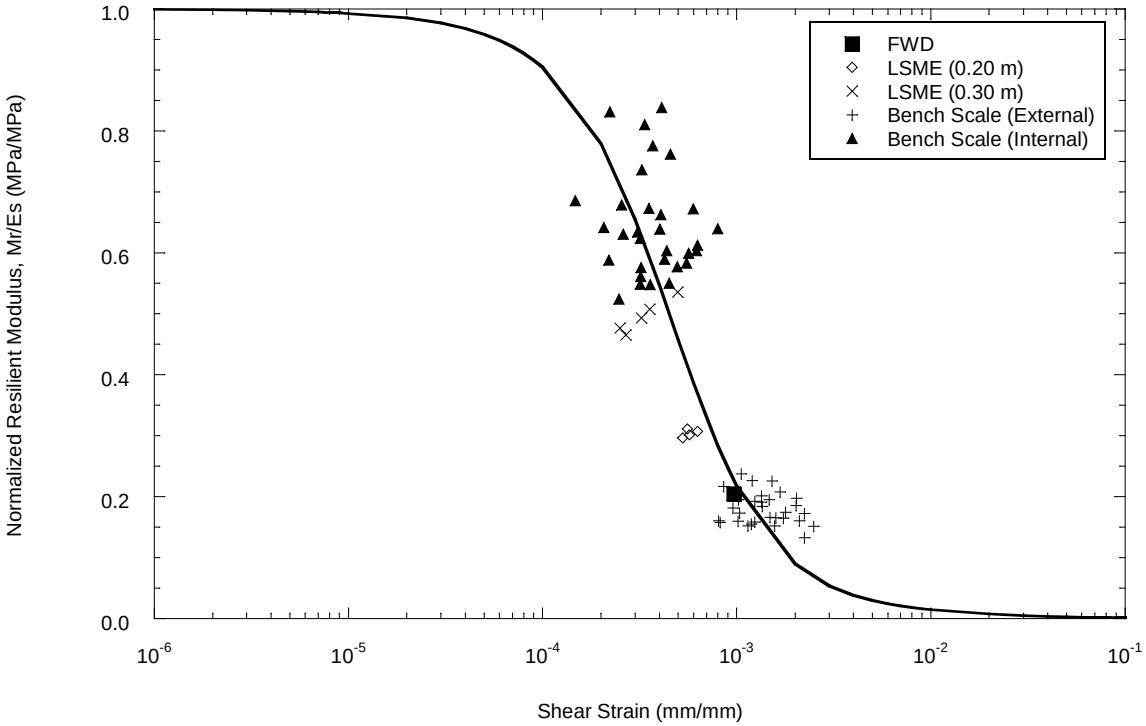

Figure 4.33 Backbone Curve Fit to FWD, LSME and Bench-Scale Data for Class 5

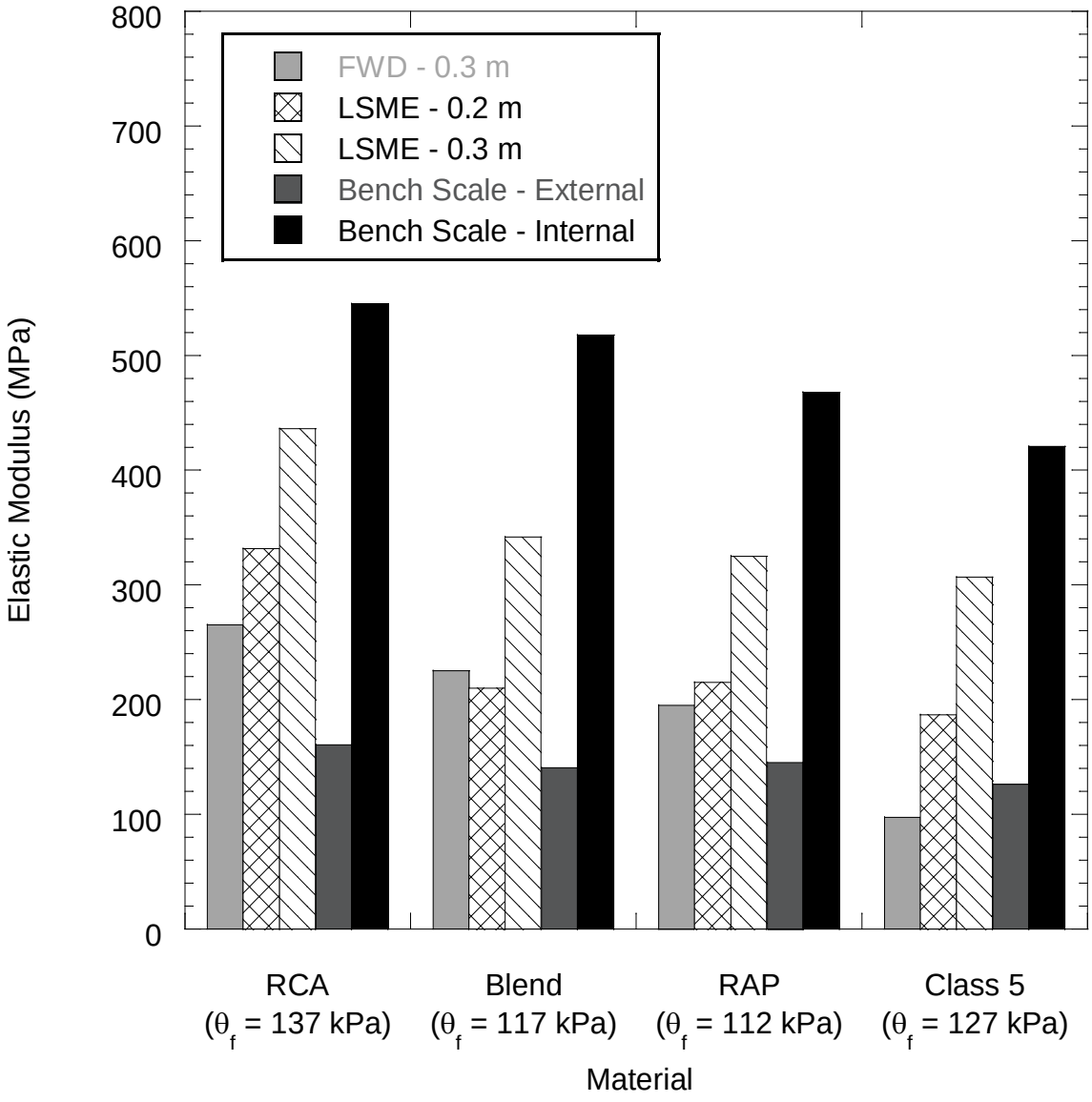

Figure 4.34 Resilient Modulus at Field Bulk Stress (θ_f) for RAP, RCA, Blended RCA/Class 5, and Class 5

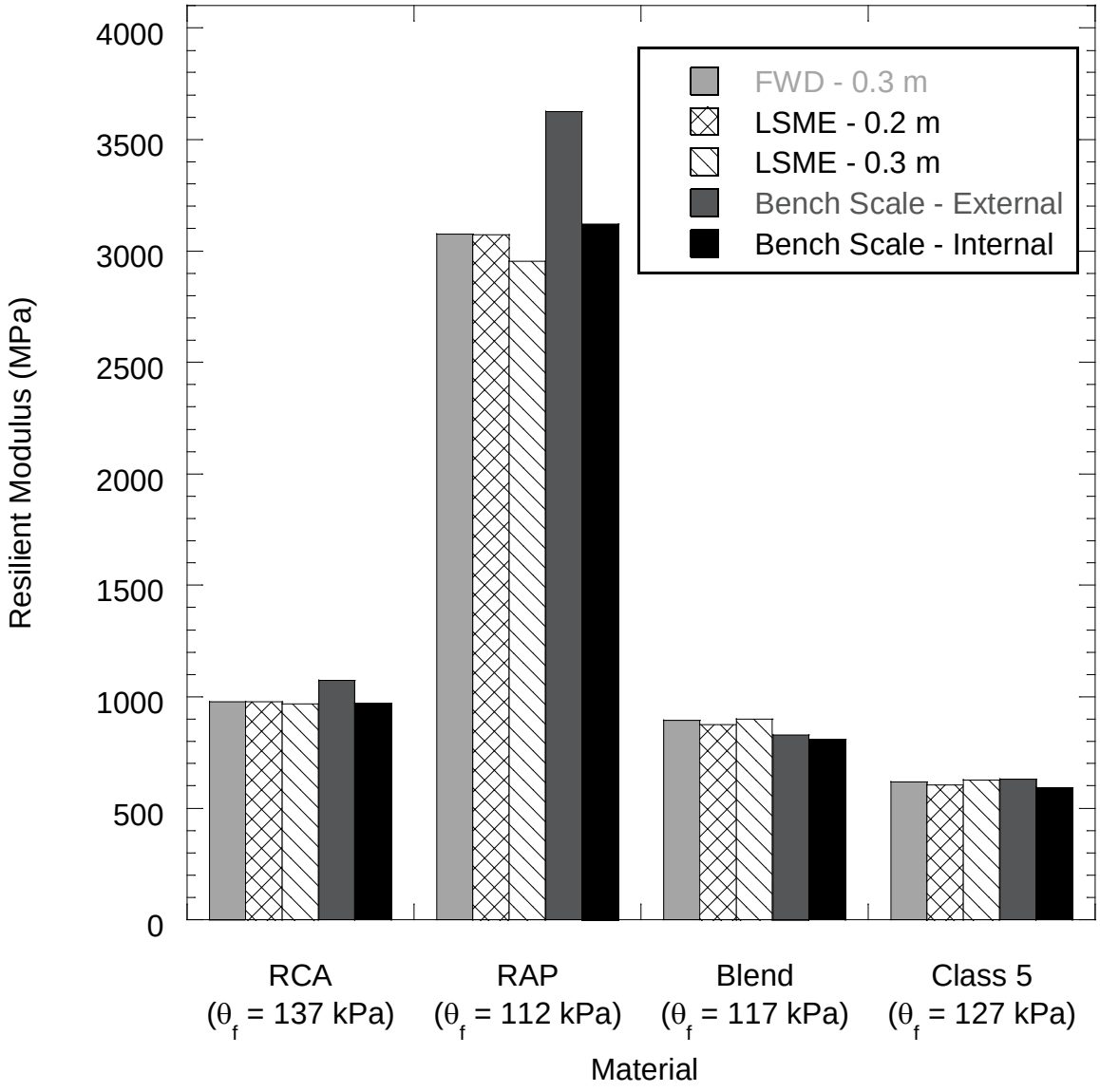

Figure 4.35 Low-Strain Elastic Modulus at Field Bulk Stress (θf) for RAP, RCA, Blended RCA/Class 5, and Class 5 as Estimated from different Test Method

5. Climate Effects

5.1 Introduction

There are over 6.5 million km of roads in the United States (US) (FHWA 2010). The most common raw material used in road construction and reconstruction is natural aggregate, created by crushing rock. Use of natural aggregates has increased from approximately 229 million metric tons in 1950 to 1.15 billion metric tons in 2011, of which 82% was used as construction material, mainly for road construction (USGS 2011). Access to natural aggregates has become more difficult because of reduced "ideal" sites caused by increasing environmental regulations and previous depletion of resources (Carpenter et al. 2007). The price of natural aggregates has increased due to increased demand in conjunction with a decreased supply near building locations (Robinson and Brown 2002). With decreased supply and increased demand, alternatives for natural aggregate have been considered.

Sustainable alternatives to natural aggregate that are increasing in use are recycled asphalt pavement (RAP) and recycled concrete aggregate (RCA). RAP is produced by removing and crushing asphalt pavement, while RCA is a collection of concrete acquired from demolition of buildings, runways, and roadways (Kuo et al. 2002, Guthrie et al. 2007, FHWA 2008). As of 1998, only 80% of all asphalt concrete aggregate debris was recycled, with the remaining 20% landfilled (Wilburn 1998). Concrete is even less recycled. Approximately 50% of concrete debris is recycled.

The use of RAP and RCA as a substitute for natural aggregate can also reduce costs. The majority of costs from using natural aggregate are incurred from transportation of the material from the quarry to the job site (Robinson and Brown 2002). By recycling old roadway material on-site, the transportation costs are reduced significantly. Furthermore, there are no costs associated with mining or tipping fees for the construction and debris (C&D) waste. The only additional costs incurred are associated with crushing, sorting, and handling the material on-site.

In addition to the benefit of cost savings, greenhouse gas emissions can be reduced by using RAP and RCA (Horvath, 2003). Mining emits greenhouse gases through the stripping of vegetation surrounding the mine and using fossil fuels to operate machinery. The use of recycled materials will reduce the need for mining and, in turn, reduce the greenhouse gas emissions produced by mining.

Although RAP and RCA are currently used as an alternative road base material, studies characterizing the mechanical properties of the materials are lacking (Bennert et al. 2000, Nataatmadja and Tan 2001, Guthrie et al. 2007, FHWA 2008). Specifically, the thermo-mechanical behavior, influence of wetting and drying, and the effects of freeze-thaw cycles have not been thoroughly investigated (Bozyurt 2011). RCA and RAP perform well at room temperature, but the climatic effects (i.e., freeze-thaw, temperature, and wet/dry) associated with the use of these materials year-round in varying climates need to be investigated to recommend more accurate design procedures based on location

The effects of temperature on the resilient modulus and plastic deformation of RCA and RAP when used as unbound base course has not been investigated. RAP contains a temperature-sensitive material, asphalt binder, which becomes less viscous as temperature increases (Griffin et al. 1959). RCA also can contain asphalt binder as a deleterious material. To investigate the effects that temperature has on RAP when used as an unbound base course, resilient modulus tests were conducted at varying temperatures. From this test, plastic strain could be calculated for each material at each temperature. Natural aggregates were used as a control material.

Wetting and drying is a typical test conducted on concrete to evaluate the effects of wetting and drying on soil-cement losses, water content changes, and volume changes (ASTM D559). There is no wet/dry standard for testing unbound aggregate. A procedure was developed for wet/dry testing of unbound aggregates to see the effects the process had on particle degradation. RAP, RCA, and natural aggregates were subjected to varying wet/dry cycles and both particle size distributions (PSDs) and Micro-Deval tests were performed before and after the wetting and drying.

Road base aggregates have to withstand constant variation in temperature in temperate climates. During the spring and fall, road bases can undergo multiple cycles of freezing and thawing daily. Freezing and thawing of aggregates can have detrimental effects on the aggregate because of expansion and contraction of the water inside the pore space of the aggregate. When water freezes within the pore space of the compacted aggregate, aggregates can foul and produce excess fines, reducing the competency of the road base. To investigate this climatic effect, material was compacted at optimum moisture content (OMC) and subjected to varying freeze-thaw cycles. Resilient modulus tests were then conducted on the specimens to evaluate the effects of freeze-thaw on stiffness.

5.2 Background

5.2.1 *Recycled Unbound Base Materials*

Researchers have investigated the use of RCA in road base or subbase courses to provide a viable option for the reuse of this C&D waste (Poon and Chan 2005). RCA is used predominantly in pavement construction as replacement for natural aggregates and cement-treated subbase layers (Saeed et al. 2006). Molenaar and Niekerk (2002) investigated the engineering properties of RCA and suggested that good-quality road base or subbase can be built from these materials. The Federal Highway Administration (2008) reported that, when compared to natural aggregates, RCA has lower density, higher water absorption, higher soundness mass loss, and higher content of foreign material. In most cases, however, the properties of RCA are within the specifications for base course or concrete aggregate.

Park (2003) investigated the characteristics and performance of RCA as road base and subbase for concrete pavement by comparing the engineering properties of RCA with those of crushed stone aggregate. The performance characteristics were evaluated based on compatibility, shear resistance, and stability of RCA; and the mechanical properties were evaluated in the field using a falling weight deflectometer to determine deformations. RCA had the same compactibility as crushed stone aggregate and shear resistance equal to or better than crushed stone aggregate.

Park (2003) concluded that the RCA can be used as base and subbase materials in place of crushed stone aggregate for supporting a concrete pavement system.

The National Asphalt Pavement Association (NAPA) (2009) reported that asphalt pavement is the most recycled material in the US. The US highway construction industry annually produces more than 100 million tons of RAP that is recycled into new pavements (NAPA 2009). According to FHWA (2011), RAP is a valuable and high-quality material that may demonstrate good performance as a granular road base and a replacement for more expensive virgin aggregate.

Guthrie et al. (2007) conducted free-free resonant column tests on RAP and natural aggregate blends to evaluate the effects of percentage change of RAP on the stiffness of road base. Blends were prepared according to the following RAP and natural aggregate percentages: 100/0, 75/25, 50/50, 25/75, and 0/100. Stiffness was determined after compaction at OMC, after a 72-h period of heating at 60 ^{0}C to simulate summer conditions; and after a 10-d period of capillary soaking followed by a 24-h period of submersion to simulate conditions of field saturations. At OMC, the stiffness decreased with the addition of 25% RAP, then increased with the addition of 50%, 75%, and 100% RAP. When the material was heated for 72-h, the stiffness increased with the addition of 25% RAP and then decreased with the addition of 50%, 75%, and 100% RAP. According to Guthrie et al. (2007), the decrease in stiffness is related to the softening behavior of asphalt due to heat. In the soaked condition, the stiffness of the material behaved similar to the samples in the dry condition, but with stiffness values between 40% and 90% lower.

Kim et al. (2007) investigated the stiffness of base course containing different ratios of RAP and natural aggregate. Resilient modulus tests were conducted on the recycled material in accordance with National Cooperative Highway Research Program testing protocol 1-28A (NCHRP 1-28a). The 50% aggregate-50% RAP specimens developed stiffness equivalent to the 100% aggregate specimens at lower confining pressures (~ 20 kPa); at higher confinement (~ 120 kPa), the RAP specimens were stiffer.

Bennert et al. (2000) compared the mechanical properties of two types of C&D waste, RCA and RAP, with dense-graded aggregate base course, used in roadway base applications in New Jersey. The RAP and RCA were mixed at varying percentages with the dense-graded aggregate base course. Bennert et al. (2000) found that the pure RAP and RCA samples had higher stiffness than the dense-graded aggregate base course, and the stiffness of the base course increased with an increase in RAP and RCA content. The pure RCA specimens accumulated the least amount of permanent strain. Even though pure RAP was stiffer than the dense-graded aggregate base course, the RAP accumulated the greatest amount of permanent strain. Bennert et al. (2000) reported that the resulting contrast between the pure RAP resilient modulus and its permanent deformation might be due to the breakdown of asphalt binder under loading.

5.2.2 *Resilient Modulus*

The design of roadway pavement relies on proper characterization of the load-deformation response of the pavement layers (Tian et al. 1998). Base and subgrade deform when subjected to repeated loads from vehicular traffic. The M_r defines the nonlinear elastic response of pavement geomaterials, such as unbound aggregate base and subbase, under repeated traffic loads. The

resilient behavior of unbound aggregate layers is affected by the stress state experienced because of wheel loading and the physical properties of aggregate (Pan et al. 2006). The M_r is a linear-elastic modulus obtained from dynamic loading, defined as the ratio of the cyclic deviator stress to the resilient (recoverable) strain, and is defined as:

$$M_r = \left({}^{\sigma_d}/_{\varepsilon_r} \right) \quad (5.1)$$

where ε_r is the recoverable elastic strain and σ_d is the applied deviator stress.

Design of pavements and rehabilitation of layered pavement systems use M_r as an essential parameter in the design process (Heydinger et al. 2007). The M_r is a key input in NCHRP 1-37 (mechanistic-based pavement design approach), which is being evaluated for adoption by numerous state highway agencies (Pan et al. 2006). The performance of pavement is dependent on the stiffness of the pavement structure under specified traffic loads and environmental conditions. Generally, a high M_r for a base course infers a stiffer base course layer, which increases pavement life. The resilient response of granular material is important for the load-carrying ability of the pavement and the permanent strain response, which characterize the long-term performance of the pavement and rutting phenomenon (Lekarp et al. 2000).

5.2.3 *Freeze-Thaw Effect on RAP and RCA*

Seasonal variation in moisture and temperature occurs in most areas of the US. The M_r of road base and subbase tends to change throughout the pavement's life due to these seasonal variations. The freeze –thaw (F-T) cycling of pavement profiles may significantly influence pavement performance. The M_r of an aggregate base/subbase is thought to increase during freezing and drying and decrease during thawing and wetting (Kootstra et al. 2009). Therefore, pavement design in regions where variations in temperature and moisture are appreciable should consider these factors (Zaman and Zhu 1999).

Rosa (2006) reported that when the air temperature at the surface is lower than the temperature of the soil, heat is extracted from the soil and removal of heat from the soil causes its temperature to drop. If the surface temperature is below 0 °C, a freezing front advances into the soil and ice crystals begin to form along the freezing front. When pore water freezes within unbound base/subbase aggregate, the volume of the voids increases. This volume change causes degradation, and ultimately decreases the stiffness of road base layers. A study conducted by Rosa (2006) on the effect of F-T on the engineering properties of one road surface gravel (RSG) and four recycled pavement materials (RPMs) mixed with fly ash found that the M_r decreased with increasing F-T cycling, leveling off after 5 cycles.

Camargo (2008) investigated the effects of F-T on M_r of RPM, RSG, and Class 5 base with and without fly ash stabilization. Specimens without fly ash were compacted at OMC using modified Proctor, and no inflow or outflow was allowed during subjecting specimens to F-T cycles. The resilient modulus test was conducted according to NCHRP 1-28a. RPM had a higher summary resilient modulus (SRM), which is the M_r corresponding to the typical level of 208 kPa bulk stress in the base course layer and also exhibited smaller plastic strain accumulations during M_r testing than Class 5 aggregate (without subjecting to any F-T cycling). A reduction in SRM was observed in Class 5 base and RSG after subjecting materials to 5 F-T cycles. There was no

consistent effect of F-T cycling on materials without fly ash; the SRM of Class 5 base decreased slightly (7%), whereas RPM and RSG increased slightly (14% and 1%). F-T cycling was found to have a small effect on SRM of Class 5 base without any additives. In this study, no net changes in the volume were observed for Class 5 base and RPM, whereas the volume change for RSG, which contained 10-14% fines, ranged from 0.4 to 0.6 %. The small effect of F-T cycling on the SRM is consistent with the small volume changes recorded during freezing and thawing, which indicate little change in soil structure (Simonsen et al. 2002). Camargo (2008) concluded that freezing and thawing results in a looser soil structure, which causes a lower resilient modulus.

5.2.4 *Temperature Effects on Resilient Modulus*

Roads in certain climates can experience a large range and/or fluctuation in temperature. While road surface courses experience this hot and cold weather directly, the road base course is insulated by the surface course and does not experience as great a fluctuation in temperature. Unbound base course typically comes from rock that has been crushed. Rock contains no material that is affected by the temperature change experienced by road base courses, but recycled materials can contain components that could make them susceptible to temperature.

RAP contains bituminous asphalt, a material that exhibits decreased viscosity with increased temperature (Griffin et al. 1959, Roberts et al. 1996, Lee et al. 2008, West et al. 2010). Because bituminous asphalt coats many of the aggregates in RAP, a decrease in viscosity has the potential to impact the particle interlocking of the material during or after compaction. A decrease in asphalt stiffness due to a decrease in viscosity is also observed as a result of increased temperature. Asphalt binder increases in stiffness but becomes brittle in nature at temperatures below freezing (Marasteanu and Anderson 1996). Materials with asphalt binder also observe increased strain at elevated temperature (Soleimanbeigi 2012). Soleimanbeigi (2012) observed an exponential increase in secondary compression index with increased temperature with a recycled asphalt shingles/bottom ash mixture. Kim and Labuz (2007) investigated the effects of various natural aggregate/RAP blends on M_r and cumulative plastic strain and found both cumulative plastic strain and M_r increased with increasing RAP content.

Wen et al. (2011) studied the effects of temperature on M_r for natural aggregate base course mixed at 0%, 20%, 40%, and 60% RAP. The materials were mixed at OMC and compacted to 95% maximum dry unit weight, then subjected to -20 °C, 20 °C, and 60 °C temperatures. The results showed that there was little effect on M_r with increase of temperature from 20 °C to 60 °C on the 0% and 20% RAP. For the 40% and 60% RAP mixes, there was up to 5% and 30% decreases, respectively in M_r with increased temperature from 20 °C to 60 °C. The decrease in M_r with increased temperature in the 40% and 60% RAP mixtures was attributed to the reduction in asphalt stiffness with temperature increase. A decrease in M_r with increased RAP content was observed on the specimens tested at -20 °C. The opposite effect was observed with the RAP mixtures at 20 °C; M_r increased with increasing RAP content, a characteristic also observed at UW-Madison.

5.2.5 *Wet/Dry Cycling*

Unbound base courses experience numerous wetting and drying cycles throughout their lifetime. These wet/dry cycles are mostly caused from influxes in precipitation, but can also stem from other sources such as water table increases and flooding. Aggregates used in road construction should be weather resistant so they do not degrade and breakdown when subjected to wetting and drying (Wu et al. 1998). Bozyurt (2011) investigated the effects of weathering and handling of RAP and RCA using the Micro-Deval test (AASHTO T-327). RAP and RCA had higher Micro-Deval losses than the Class 5 natural aggregate control material, but both recycled materials had lower losses than the recommendation for natural aggregate in design manuals (i.e., DOT specifications).

The wet/dry cyclic test is a standard test used in concrete. This test has been used to evaluate the effects on soil-cement losses and volume changes with increased cycles on concrete (ASTM D559). Previous studies have not been completed to evaluate the effects of wet/dry cycles on unbound aggregates, nor has any standard been developed.

5.3 Materials

The recycled materials used in this study were obtained from various states in the US. Three RAPs and three RCAs were collected and named according to the state of origin. The materials represent coarser, medium, and finer gradations based on their grain size (D_{50}, C_c and C_u). The reference base courses studied and used as the controls in this study were a gravel meeting Class 5 aggregate specifications for base course per the Minnesota Department of Transportation and crushed basalt from Senegal, Africa. The basalt was material studied previously by a visiting scholar at the University of Wisconsin-Madison.

Nine recycled materials and two conventional base courses were used in the first part of this investigation. Five of the recycled materials were recycled asphalt pavement (RAP) and four were recycled concrete aggregate (RCA). The recycled materials used in this study were obtained from a wide geographical area, covering six different states: California, Colorado, Michigan, Minnesota, New Jersey, and Texas. The materials named according to the origin of the materials. The reference base courses were a gravel meeting the Class 5 aggregate specifications for base course in Minnesota per the Minnesota Department of Transportation (MnDOT) and crushed basalt. Class 5 aggregate is formed by quartz, granite and carbonates (limestone and dolomite). The ratio of quartz/granite to carbonates is 2.1. The percentage of mineral type in Class 5 aggregate is 68 % for Quartz/Granite and 32 % for Carbonates. Percent quartz/granite (aggregate and concrete) and percent carbonate of gravel (aggregate and concrete) of gravel are 43% and 20%, respectively. The crushed basalt was 100% basalt crushed in Senegal, Africa and transported to the University of Wisconsin. The basalt was acquired by a visiting Senegalese scholar to mechanically characterize, and the remaining unused material was used for this study.

The RAP from MnDOT was obtained during construction of roadway cells at the MnROAD test facility in Maplewood, Minnesota for investigation of the field behavior. The RAP was milled from the surface of roadway cells that were previously constructed at the MnROAD test facility.

The RAP received from the Colorado DOT was collected from hundreds of reclaimed highways. Although the RAP came from varied sources, the aggregates for the production of the asphalt originated from rock in Colorado, most from the quarries in Morrison and Golden and some aggregates were sourced from the Platte River.

The material provided by the New Jersey DOT (NJ DOT) is from stockpiles for demolition projects, primarily in New Jersey. The material in the stockpiles is in flux since NJ DOT constantly adds new loads and removes content for different purposes.

The RAP from California DOT is a combination of roadway millings and waste from an HMA plant (discharge from warm up and cleaning processes). The RCA is broken concrete rubble from the demolition of structures. Stockpiling in California is usually done three times a year. These stockpiles are not added to throughout their life-cycle. If stockpiled material is still unavailable during visits from subcontractors, new material is used to create a new stockpile.

The RCA sent by the Texas DOT is from a commercial source; therefore, the individual sources of aggregate or material characteristics included in the RCA are not known. The Texas RAP is from a highway project where the contractor milled the "binder" course after approximately 1.5 years of service. The RAP l from Michigan was provided by the Michigan DOT and is from highway reconstruction projects.

A summary of the index properties and soil classifications is shown in Table 5.1. The materials used in this study are classified as non-plastic per ASTM D 2487, the Unified Soil Classification System (USCS). The recycled materials (three RCAs and three RAPs) classified as A-1-a and Class 5 and basalt aggregates classified as A-1-b according to the AASHTO soil classification system (ASTM D 3282). Specific gravity (G_s) and absorption tests were conducted according to AASHTO T 85. Asphalt content was determined by ASTM 6307. The modified Proctor compaction test (ASTM D 1557) was performed to determine the optimum moisture content (w_{opt}) and maximum dry unit weight (γ_{dmax}). The PSD for the investigated materials were determined according to ASTM D 422 and are shown in Figure 5.1 and Figure 5.2, along with upper and lower bounds reported in literature (Bennert et al. 2000, Bejarano et al. 2003, Blankenagel and Guthrie 2006; Guthrie et al. 2007, Saeed 2008, Kuo et al. 2002).

5.4 Methods

5.4.1 *Resilient Modulus*

Resilient modulus tests were performed on compacted specimens according to NCHRP 1-28a Procedure Ia, which applies to base and subbase materials. The materials used in this study classify as Type I material in NCHRP 1-28A, which requires a 152-mm diameter and 305-mm high specimen for resilient modulus testing (NCHRP 2004). Specimens were prepared at OMC and compacted to 95% of maximum modified Proctor density. Specimens were compacted in six lifts of equal mass within 1% of the target dry unit weight and 0.5% of target moisture content to ensure uniform compaction (NCHRP 2004).

Resilient modulus tests were conducted with internal and external linear variable displacement transducers (LVDT). External LVDTs have an accuracy of ± 0.005 mm, and internal LVDTs

have an accuracy of ± 0.0015 mm. Clamps for the internal LVDTs were built in accordance with NCHRP 1-28A specifications. Internal LVDTs were placed at quarter points of the specimen to measure the deformations over the half-length of the specimen, whereas external LVDT measured deformations of the entire specimen length. An MTS Systems Model 244.12 servo-hydraulic machine was used for loading the specimens. Loading sequences, confining pressures and data acquisition were controlled from a computer running LabView 8.5 software.

Various factors influence the M_r including loading conditions (confining and deviatoric stresses), physical properties (water content, void ratio, matric suction), and soil properties (particle size distribution and plasticity). The most important factors are stress conditions. Because of this, multiple models have been proposed to examine the relationship between M_r and stress factors (i.e., deviatoric and confining stresses). The two models used in this study were the Power model proposed by Moosazedh and Witczak (1981) and the NCHRP model. Both are described below. First the M_r for each load sequence was obtained by averaging the M_r from the last 5 cycles of each test sequence. The M_r data were fitted with the Power function model proposed by Moosazedh and Witczak (1981)

$$M_r = k_1 \times (\theta)^{k_2} \tag{5.2}$$

where M_r is resilient modulus, θ is bulk stress, and k_1 and k_2 are empirical fitting parameters. The constant k_1 is unique to a given material and is independent of k_2. k_2 represents the effect of stress on the modulus and varies within narrow limits (0.45 to 0.62 for granular base (Huang 2004)). k_1 and k_2 are material-dependent parameters. The range of k_1 varies greatly and its value is largely controls M_r predicted. Bulk stress is another means of quantifying confining pressure and deviator stress in a single term and is defined as the sum of the three principle stresses. Bulk stress is defined as

$$\theta = \sigma_1 + \sigma_2 + \sigma_3 \tag{5.3}$$

where σ_1, σ_2, and σ_3 are the principal stresses acting on the specimen.

The M_r data were also fitted with the NCHRP model (NCHRP 2004) defined

$$M_r = k_1 . p_a . \left(\frac{\theta - 3k_6}{p_a}\right)^{k_2} . \left(\frac{\tau_{oct}}{p_a} + k_7\right)^{k_3} \tag{5.4}$$

where k_1, k_2, k_3, k_6, and k_7 are constants, p_a is atmospheric pressure (101.4 kPa), τ_{oct} is octahedral shear stress, and θ is bulk stress.

For every specimen tested, it is important that the M_r values calculated at the end of each cycle and used to determine the SRM are accurate. To determine the accuracy of the values calculated, a coefficient of variance was determined for the last five M_r values of each sequence, which are averaged to calculate the M_r of a sequence. M_r values with a coefficient of variation above 8% were not used to calculate the SRM of the specimen.

For base course, the SRM corresponds to the M_r at a bulk stress of 208 kPa, as suggested by Section 10.3.3.9 of NCHRP 1-28a. SRM is used to determine the layer coefficient, which is a

required input in the AASHTO pavement design equation (Tian et al. 1998). The Power function (Equation 5.2) is a simple model that is widely used for granular materials. The estimated SRM per the Power function model was compared to the measured modulus. Statistical analysis indicated that results from the Power function model are significant at a 95% confidence level, and the model represents the data reasonably well for RCA ($R^2 = 0.85$) and for RAP ($R^2 = 0.90$) (Bozyurt 2011).

5.4.2 *Freeze-Thaw Cycling*

The effect of F-T cycling on the engineering properties of the recycled materials was determined by measuring the M_r of specimens subjected to F-T cycles. A method that follows ASTM D 6035 for specimen conditioning was used at the University of Wisconsin-Madison (UW-Madison) for frost susceptibility (Rosa 2006, Camargo 2008). ASTM D 6035 describes a method to determine the F-T effects on hydraulic conductivity. Specimens conditioned in accordance with ASTM D 6035 were subjected to resilient modulus test.

Specimens for F-T testing were prepared in the same manner as for resilient modulus test. Test specimens were compacted in plastic molds at the specified moisture content and maximum dry unit weight. Specimens, instrumented with a thermocouple, were tested to insure that complete freezing occurred within 24 hours at -19 °C.

Accordingly, specimens were retained in their plastic mold, wrapped with plastic sheeting, and placed in a freezer for one day. The plastic molds were sealed carefully to prevent exposure to moisture during F-T cycling. Thus, the bulk water content was kept constant during F-T cycles.

After freezing, the height and weight of the specimens were measured to monitor the volume change during freezing. The specimens were then thawed at room temperature for 24 h. After the designated number of F-T cycle, specimens were extruded frozen and thawed inside the resilient modulus cell. Resilient modulus testing was then conducted, as described previously. In this study, the effect of 5, 10, and 20 F-T cycles was investigated.

5.4.3 *Temperature Effects on Resilient Modulus*

The effect of temperature on the engineering properties of the tested materials was determined by completing M_r tests at varying temperatures. M_r tests were carried out on specimens at four different temperatures: 7 °C, 23 °C, 35 °C, and 50 °C. The lower and upper bounds were selected because of the limits imposed by the equipment used that would allow for the NCHRP 1-28a standard to be followed. Specimens were compacted at OMC and at 95% maximum modified dry unit weight and prepared according to the NCHRP 1-28a standard as outlined in Section 5.4.1.

Due to the hydraulics needed for the M_r test, the equipment could not be moved to a temperature controlled room for the tests to be conducted at varying temperatures. Instead of controlling the temperature around the entire platform of the hydraulic actuator, the temperature control was limited to the acrylic cell containing the specimen. Figure 5.3 and Figure 5.4 show the M_r setup of the temperature-controlled cell with hot water and with cold water, respectively. The NCHRP 1-28a standard specifies that air must be used as the confining fluid during the M_r test. Due to

air being used as the confining fluid, temperature-controlled water was circulated through 15.2-m of 6.35-mm-diameter copper coil wrapped around the inside of the acrylic cylinder to heat or cool the specimen through heating or cooling the confining air. The temperature the specimen could reach was limited due to the confining air insulating the heat transfer from the copper coil to the specimen.

The temperature-controlled water was heated in a 152-mm permeameter using a Watlow FIREROD immersion heater, which operated at 100 °C. A thermocouple was placed inside the water-filled permeameter to determine the temperature of the circulating water. The thermocouple was connected through a data logger, which was controlled by a LabVIEW program that turned the heater on and off to regulate the circulating water temperature. Water was circulated from the permeameter to the copper coil using a 2650 L/h magnetically driven pump that was placed outside of the permeameter. 6.35-mm-diameter Tygon tubing was used to transfer the water from the permeameter to the copper coil and back. A similar setup was used for the 7 °C temperature goal, except a freezer was used to hold a 75-L container of water. The 2650 L/h pump was placed inside the 75-L container and 6.35-mm-diameter tubing was again used to transfer water from the reservoir to the copper coil and back. For tests at 35 °C, and 50 °C, a blanket was wrapped around both the acrylic cell and the water reservoir to limit heat dissipation. For tests conducted at 7 °C, a blanket was wrapped around the acrylic cell and placed over the freezer to reduce cold air dissipation.

To determine the specific temperatures to test the material at, calibration of the equipment was conducted to determine the limiting temperature of the equipment. Class 5 aggregate was used as the calibration material. To determine the temperature of the specimen at a given time while heating or cooling, three thermocouples were compacted into the specimen. The thermocouples were compacted at mid-height of the specimen and placed in the middle, outside, and halfway between the middle and outside. After the first test, only one thermocouple at the center of the specimen was necessary because there was little temperature change from edge to center after equilibration. Using one thermocouple compacted inside the specimen also reduced disturbance to the specimen. Thermocouples were placed within the cell to determine the air temperature and in the water reservoir to measure water temperature.

As seen in Figure 5.5 to Figure 5.7, constant temperature was achieved within 15-h of the temperature of the water being circulated. The maximum water temperature achieved with the Watlow heater was 76 °C, which corresponded to an air temperature of 58 °C and specimen temperature of 50 °C (± 1 °C). Although the likelihood of a base course reaching 50 °C is very minimal once pavement is installed, this temperature is possible to achieve during compaction and before pavement is installed, which insulates the base course. 7 °C (± 1 °C) was the lowest temperature the specimen would reach when circulating 0 °C water, marking the minimum temperature tested. The specimens were also tested at room temperature (23 °C) as a control. The 35 °C temperature was set as a temperature between room (23 °C) and 50 °C to help evaluate any trend and because this temperature is more of a realistic maximum temperature base course will experience after being insulated by pavement. Figure 5.5 to Figure 5.7 show the thermocouple data for the calibration at each temperature except 23 °C.

Quality control compaction tables for each specimen tested are presented in Table 5.2 to Table 5.3. All specimens were compacted within the NCHRP 1-28a standard of ± 0.5% of OMC. The

majority (84%) of the specimens were compacted within ± 1% of the target dry density, in accordance with the NCHRP 1-28a standard. The five specimens (16%) that were compacted outside of the 1% target were the Class 5 specimens and the 7 °C TX RAP specimen. The TX RAP specimens were around 6 to 7% above the target dry density, but were all within 0.6% standard deviation of one another. Because the four TX RAP specimens are within only 0.6% standard deviation of one another, these tests were considered valid because they were all representative of one another. As for the one Class 5 specimen, it was 0.1% above being rounded to 1%. Further testing could not be completed to correct the errors due to lack of material.

5.4.4 *Wet/Dry Cyling of Unbound Recycled Materials*

The procedure for wet/dry cycling of unbound recycled materials was based upon a similar procedure for compacted soil-cement mixtures (ASTM D559). Unlike ASTM D559, the recycled aggregate is unbound, so an apparatus was created to contain the material in its compacted state while still allowing water to flow through the aggregate. Loss of material was not weighed due to the unbound nature of the material. This test was conducted to evaluate the effects of wet/dry cycles on particle degradation of the material, not loss of material.

To replicate the in-field conditions of the recycled materials and natural aggregates tested, aggregates were compacted in the same mold used for M_r testing following the same steps as used in Section 1.4.1. All specimens were compacted at OMC and at 95% maximum modified Proctor dry unit weight. Once compacted, specimens were extruded from the mold and placed into the wet/dry apparatus.

A wet/dry apparatus had to be fabricated to hold the specimens intact throughout the entire wetting and drying of the material. Due to the unbound nature of the aggregate, loss of material existed, but minimizing the loss was important. One sheet of non-woven geotextile was wrapped around the specimens and held in place using ten rubber bands (Figure 5.8). Two 152-mm-diameter pieces of non-woven geotextile were also used on the top and bottom of the cylindrical specimens. The non-woven geotextile used in this test kept the specimens intact while still allowing water to freely move through.

Two 152-mm-square plates were placed on the top and bottom of the specimen and locked into place using four 38-cm threaded rods. Each plate had approximately twenty 6.35-mm holes drilled into it to allow for water to enter and exit the specimen. The plates used for the RAP were made from polyvinyl chloride (PVC) and the plates used to hold the RCA and natural aggregates specimens were made from aluminum. Aluminum was used for RCA and natural aggregate because of the high temperature (100 °C) oven used to dry the material. PVC was used for the RAP because of availability and applicability in the lower temperature (50 °C) oven used to dry RAP. Eight bolts and washers threaded through the 38-cm rods were used to tighten the plates to the specimens.

Calibration of the wetting and drying time of the aggregates was conducted to determine the time for full saturation and drying. Specimens were placed in 114-L drums filled with tap water to achieve saturation. Saturation was achieved quickly (< 30-min) without vacuum as opposed to five hours as dictated by ASTM D559. Saturation was defined as the point when the weight of

the specimen did not change more than ± 0.05 kg after a 30-min increment. To be conservative, all materials were submerged in water for one hour during the wetting cycle.

For drying, RAP and RCA/natural aggregate specimens were placed in ovens at 50 °C and 100 °C. 50 °C drying temperature was selected for RAP to reduce the potential for softening of the asphalt binder because aged asphalt binder found in RAP starts to soften around 60 °C (Read and Whiteoak 2003). 100 °C drying temperature was selected for the RCA and natural aggregates because these materials did not contain any temperature-sensitive material, and the higher temperature decreased drying time for these hydrophilic materials. Calibration tests revealed that the RAPs, RCAs, and natural aggregates were considered dry after 22-h in their respective ovens. Dry was defined as the weight of the material not changing more than +\- 0.05 kg after a 30-min increment. RAP was able to dry after the same amount of time, but at a lower temperature than the RCAs and natural aggregates because it is a hydrophobic material.

Specimens were put through a 1-h wetting and 22-h drying cycle to complete one wet/dry cycle. A new specimen was created for each of the five, ten, and thirty wet/dry cycle procedures. Once the specimen completed its final cycle, pictures were taken for documentation of the intact specimen and then specimens were broken apart from their compacted state and dried for PSD and Micro-Deval tests.

PSDs (ASTM D422) were completed on all coarse-grained materials after the last wet/dry cycle. There were no deviations from the ASTM D422 standard. PSDs were also carried out on each material at 0 wet/dry cycles, but after compaction. Micro-Deval tests were conducted on all material following AASHTO T-327. All specimens were prepared as an oven dried sample of 19.0-mm except Class 5 and NJ RAP because of lack of material at certain particle sizes. All Class 5 wet/dry specimens used only 1000-g of material for each Micro Deval test. 250-g were retained on the 16 mm sieve, 250 g on the 12.7-mm sieve, and 500-g on the 9.7-mm sieve. NJ RAP was not tested at 5 cycles due to lack of material. NJ RAP specimens had 750-g retained on the 6.35-mm sieve and 750-g retained on the 4.76-mm sieve.

5.5 Results and Discussion

5.5.1 *Freeze-Thaw Effects on Recycled Asphalt Pavement*

SRM for recycled materials and Class 5 aggregate are summarized in Table 5.4, along with the parameters k_1 and k_2 for the power function model (Equation 5.2) and the rate of decrease for F-T cycles (0, 5, 10 and 20). The effect of freeze-thaw (F-T) cycling on SRM for the representative RAP and Class 5 aggregate material is shown in Figure 5.9 and Figure 5.10.

F-T cycling has a relatively small effect (7% decrease over five F-T cycles) on the SRM of Class 5 aggregate in comparison to the RAP. Camargo (2008) also observed a 7 % of decrease in SRM for natural aggregate after five F-T cycles. However, the rate of decrease for Class 5 aggregate over 10 and 20 F-T cycles was 14% and 21%, respectively. The SRM of the RAPs showed the most reduction after the first five F-T cycles, with relatively small change thereafter. The differences in the effects of F-T cycles on a material can be attributed to the differences in material gradation, mechanical properties, and mineralogy and origin of aggregate.

For instance, RAP (TX) (coarser) exhibited the smallest rate of decrease (28%) in SRM after 20 (F-T) cycles compared with RAP (CA) (medium) (32%) and RAP (MN) (finer) (32%). The rate of decrease of SRM for RAP ranged from 20 to 66%, which is similar to the range reported by Rosa (2006) for various coarse and fine grained soils. Even though the SRM of RAP decreases over 20 F-T cycles, the SRM of the RAP was still greater than that of Class 5 aggregate as revealed in Figure 5.9.

In this study, the specimens were compacted in a PVC mold, and sealed very carefully to prevent water loss during the conditioning process. Due to the asphalt coating around the fine particles in RAP, water retention capacities are less than natural aggregates; therefore, the lubrication effect of water between RAP particles is higher. Consequently, RAP does not have the same ability to retain moisture during F-T cycling like natural aggregate.

The reduction in the stiffness over time may be related to the volume change of the water retained in the pores, the hydrophobicity of asphalt, and the weakness occurred in asphalt binders over time. Rosa (2006) reported that when pore water freezes within unbound base/subbase aggregates, the volume of the voids increases; and this resulting volume change causes degradation, and ultimately decreases the stiffness of road base layers. Arm (2001) reported that degradation, owing to poor F-T resistance, occurs because the volume of water present in the pores expands upon freezing, thus generating considerable forces that break up the aggregate particles. Therefore, the pavement moduli change during F-T cycles might occur as a result of changes in the phase of the pore water over time (Da-tong et al. 1998).

In this study, relatively low volume changes were observed because specimens underwent F-T cycles in a closed system (i.e., no external source of water), the only water present remained within the pores of the material; therefore, frost action was limited to change in volume of the post-compaction pore water upon freezing. No net volume changes were observed for Class 5 aggregate and RAP

An increase in the stiffness of RAP after F-T cycles has been reported in other studies. For instance, Attia and Abdelrahman (2010) reported that M_r of RAP increased after two F-T cycles for specimens were kept in latex membranes to keep moisture content constant during the test. However, during the conditioning process, a significant amount of water loss may occur, which may be a significant factor for the M_r increase over time. Camargo et al. (2009) found 14 % increase in SRM of RPM after five F-T cycles. This difference in SRM may be attributed to different mechanical properties of RPM as compared to RAP due to different recycling processes and inclusion of base and possibly subgrade materials in RPM.

5.5.2 *Freeze-Thaw Effects on Recycled Concrete Aggregate*

The effect of F-T cycling on the SRM for representative RCA and Class 5 aggregate is presented in Figure 5.11. For RCA, SRM decreased after five F-T cycles, followed by a consistent increase. The rate of decrease during the first five F-T cycles varied according to the material geographical origin. As the source and origin of the RCA differ (i.e., the gradation, compaction characteristics, and mechanical properties differ), these variations affect the rate of change in SRM. This variation affects the rate of change in SRM, however a similar trend observed over time among the RCA material remained as seen in Figure 5.12.

The SRM for RCA (TX) decreased 10% over five F-T cycles followed by an increase over 20 F-T cycles back to 30% above the initial SRM (at zero F-T cycle); RCA (MI) decreased 18 % over five F-T cycles followed by an increase back to 38 % above the initial SRM. The same trend was observed for RCA (CA) with an 11% decrease over five F-T cycles followed by an increase of 5% above the initial SRM over ten F-T cycles.

The self-cementing properties of RCA and fine content generation over time could explain why an increase in stiffness after five F-T cycles occurred. These trends are consistent with other research in which the strength of subbase prepared with RCA has been found to increase with time (Arm 2001). RCA particles typically have a coarser and more angular shape than natural aggregates as a result of material crushing and processing operations (Saeed et al. 2006), leaving a significant amount of mortar adhered to the surface of the particles (Saeed et al. 2006, Juan and Gutierrez 2009, Gokce et al. 2011). Processed RCA has hardened cement paste that holds smaller aggregate particles together (Saeed et al. 2006). The amount of cement paste attached to aggregate in RCA depends on the process used to produce RCA and the properties of the original concrete (Chini et al. 2001).

Poon et al. (2006) stated that unhydrated cement content retained within the adhered mortar was the cause of self-cementing in RCA used for unbound base. Arm (2001) conducted a field investigation over two years on the stiffness of unbound base layers made of crushed concrete from demolished structures. An increase in M_r with time was observed and attributed to the self-cementing properties of RCA. Arm (2001) conducted repeated load triaxial tests on crushed virgin aggregate and concrete specimens after certain storing periods (1, 3, 7, 28 and 90 days). An increase in modulus was observed for crushed concrete specimens, but not for natural base layers, over time. Arm (2001) postulated that the self–cementing properties of crushed concrete were the reason behind the increase of stiffness, with time, in unbound base layers made with crushed demolished concrete.

There was an increase observed in the fines amount of the RCA specimens after 20 freeze-thaw cycles. Recent studies show that the fines percentage increase has an important effect in the stiffness of aggregates. Mishra et al. (2010) investigated the effect of fines on compaction for dolomite samples and they found that the MDU increased as the percentage of fines in the sample increased. Since the addition of fines gradually filled the voids, the aggregate matrix became denser. They also found that as the fines content increased beyond a certain point, all the voids in the uncrushed gravel matrix (rounded aggregate particles, had a lower amount of total voids than crushed samples) were filled, and the coarse particles started to float in the matrix. This resulted in a reduction in the dry density without a corresponding significant decrease in aggregate material matrix strength. This phenomenon was also observed by Ebrahimi et al. (2011) during the investigation of ballast void filling with fouling materials (i.e., fines and water content).

Increased density contributes to an increased stiffness for granular material; however, increased fines content and increased crushing efforts appear to diminish these effects (Hicks and Monismith, 1971). For example, fines content > 12% may significantly decrease the M_r of unbound granular materials (Barksdale and Itani, 1989). The fines percentage in the soil matrix likely improves the M_r of unbound aggregates to a point, after which the matrix starts to be dominated by the fines in which the M_r starts to decrease. The increased in the SRM for RCA

specimens could be also related to the change in the matrix of specimen due to the increase of the fines. The increased fines content probably filled the voids in RCA specimens, and the specimen became stiffer over time.

Relatively low volume changes were observed for Class 5 aggregate and recycled materials, because specimens were freezing and thawing in a closed system (no external sources of water available), the only water present remained within the pores of the material; therefore, frost action was limited to change in volume of the in situ pore water upon freezing (Rosa 2006).

5.5.3 *Temperature Effects on Resilient Modulus*

5.5.3.1 Temperature and Summary Resilient Modulus

The effects of temperature on SRM can be seen in

Table 5.5 for both internal and external LVDT calculated SRMs using both NCHRP and Power fitting models. More detailed NCHRP SRM fitting parameters at varying temperatures for RCA/Basalt/Class 5 and RAP are shown in Table 5.6 and Table 5.7, respectively. Table 5.8 and

Table 5.9 display the Power model fitting parameters at varying temperatures for RCA/Basalt/Class 5 and RAP, respectively. The NCHRP external LVDT SRM values are plotted in Figure 5.13 through Figure 5.16. NCHRP modeled SRM as opposed to the Power modeled SRM was plotted because the coefficient of determination was higher on average than that of the Power modeled SRM. The NCHRP modeled SRM is the SRM used in the Mechanistic Empirical Pavement Design Guide (MEPDG).

Figure 5.17 and Figure 5.18 show a 1:1 comparison of internal SRM to external SRM using the NCHRP model and the Power model, respectively. As observed by many other studies (Bozyurt 2011, Camargo et al. 2012), the calculated internal SRM was higher than the external SRM. The ratio of internal to external SRM in this phase of the study was on average 1.7, similar to findings by Camargo et al.'s (2012) of an average of 1.5 on base course. Table 5.6 and Table 5.7 show the internal to external SRM ratio for the SRMs calculated using the NCHRP model. Table 5.8 and

Table 5.9 show the internal to external SRM ratio for the SRMs calculated using the Power model.

The 1.7 internal to external SRM ratio in this chapter is much lower than previous data collected and reported in Chapter 3, which had ratios closer to 3. Figure 5.19 and Figure 5.20 show the comparison between SRM calculated earlier by Young-Hwan Son at UW-Madison (reported in Chapter 3) and SRM calculated by Shedivy in this chapter at room temperature (23 °C) on the same material. As seen in these figures, Son's 2011 internal SRM values were much higher (270% of the original value) than those calculated by Shedivy. Whereas Son's external SRM values were slightly higher (130% of the original value) than the SRM values by Shedivy, but much closer than the internal SRMs. This difference is attributed to malfunctioning internal LVDTs used by Son. The internal LVDTs used by Son were thought to be calibrated incorrectly, recording incorrect displacements which increased the overall internal SRMs for each material

tested. Son's internal LVDTs were also different from the LVDTs used in this study and had a shorter range for recording displacement. This shorter range did not allow the entire M_r test to proceed without resetting the interior LVDTs in the middle of the test, which could have altered the data collected and led to higher SRM values. Son's external LVDTs were calibrated correctly and SRM calculated from these LVDTs is considered accurate.

The values for Son's internal SRM data are reported in Chapter 3 and as a previous task report (Task IB) submitted to this project. The internal SRMs reported in Chapter 3 are not considered accurate and should not be used. The interior LVDTs used in this chapter and elsewhere in this report are considered calibrated and the SRM values calculated from these LVDTs is considered accurate. Due to this problem with internal LVDTs, comparisons with the previous modulus data given in Chapter 3 should only be done using external SRM values. External SRM values yielded much more consistent values than internal SRM values (Bozyurt 2011).

To evaluate change in SRM with temperature for each material, coefficients of variation in SRM were determined for control specimens to determine the margin of error between each test. Aggregate that did not contain temperature-sensitive material (e.g., asphalt) and did not experience a change in SRM or plastic strain with temperature variation were used as controls. The natural aggregates were not temperature sensitive. After further data analysis, the RCAs were also considered not sensitive to temperature change. Four replicate M_r tests were conducted on each control specimen to calculate the material's coefficient of determination. Each replicate test was completed at a different temperature (i.e., 7 °C, 23 °C, 35 °C, and 50 °C). Table 5.10 shows the coefficients of variation for each control specimen. The highest coefficient of variation for internal SRM calculations was determined to be 13%, while external SRM was 15%. To be conservative, 15% was deemed to be the margin of error in SRM calculations due to equipment, instrumentation, and rounding errors. A SRM value outside of the 15% error was considered to have been affected by temperature.

Table 5.11 displays coefficients of variation for each RAP tested. Both CO RAP and TX RAP have coefficients of variation above the 15% error, indicating both RAP's SRM were altered by temperature. NJ RAP's SRM was within the margin of error, indicating it was not affected by temperature change. This data does not follow the same trend as CO RAP and TX RAP, indicating a possible error in the test or NJ RAP has a different characteristic than CO RAP and TX RAP that makes it not susceptible to temperature change. For this reason, replicate tests could have confirmed this lack of change in SRM, but a limited quantity of material available did not allow for this; therefore, the SRM data collected for NJ RAP was not evaluated any further.

As seen in Figure 5.14, NJ RAP has the least fluctuation in SRM at varying temperatures, but both TX RAP and CO RAP have dramatic (37% and 30%, respectively) differences in SRM between 23 °C and 35 °C, but all SRM values for the RAPs were still approximately the same or higher than the SRM values for the RCAs and natural aggregates tested at 35 °C. Little change (< 13 MPa or 9%) in SRM is observed in any of the RAPs from 7 °C to 23 °C and 35 °C to 50 °C. The coefficient of variation would be much larger for both CO RAP and TX RAP if it were not for the similar values from 7 °C to 23 °C and 35 °C to 50 °C. This trend of a decrease in M_r with increased temperature was also observed by Wen et al. (2011), but between the temperatures of 20 °C and 60 °C and at RAP contents of 60% to natural aggregate. Wen et al. (2011) saw a decrease in M_r of 30% with the increase in temperature.

The 60% decrease in SRM between 23 °C and 35 °C could be attributed to the asphalt in the material reaching its softening point, where the asphalt binder starts to behave less viscously (Read and Whiteoak 2001). This softening point typically occurs between 45 °C and 80 °C, so another explanation may be warranted for this decrease. Wen et al. (2011) claimed the decrease in M_r between the RAP he tested at 20 °C and 60 °C was due to decreased asphalt stiffening with temperature increase, but 60°C is within the softening point range of asphalt, whereas 35 °C is not. With a decrease in viscosity of the material, the asphalt binder coating the aggregates reduces in shear strength, decreasing the stiffness of the material under loading. It is recommended that further M_r tests on RAP at temperature between 23 °C and 35 °C be completed so that a more accurate temperature at which the SRM starts to decrease can be determined. It is also recommended that further M_r tests at these temperatures be done with other RAPs so that this trend can be further evaluated. Table 5.12 shows the ratios of SRM values at 23 °C and SRM values at 35 °C or 50 °C. The average of the external SRM ratios between 23 °C and 35 °C was 1.4. To be conservative, a reduction factor of 1.5 can be considered when evaluating the SRM of a 100% RAP base course to accommodate the effects of temperature on the SRM of RAP. More M_r tests on 100% RAP at different temperature can be performed to further analyze this decreasing trend in SRM with temperature.

5.5.3.2 Temperature and Plastic Strain (as an index)

The noticeable difference in SRM between 23 °C and 35 °C for TX RAP and CO RAP indicates that there is a temperature at which the asphalt starts to behave less viscously when loaded. This temperature range is much lower than the typical softening point of asphalt binder (between 45 °C and 80 °C according to Read and Whiteoak (2003)). This behavior was not observed in NJ RAP through SRM values, but was observed when evaluating the strain rates of each specimen during the first sequence of the M_r test that conditions the specimen. No data is used to calculate M_r during this phase. During the conditioning phase NJ RAP experienced the highest strain rates of any material at 35 °C and 50 °C. CO and TX RAPs did not have as high strain rates during the conditioning phase at these temperatures.

Figure 5.21and Figure 5.22 show this quick increase in strain rate for RAPs during the 100, 500, and 900 cycles of the conditioning phase at different temperatures. From Figure 5.21 and Figure 5.22 it can also be observed that NJ RAP had the fastest strain rate increase among the RAPs, followed by TX and CO RAP. A better comparison can be made between each material's strain rates during the first 100 cycles through the bar graphs displayed in Figure 5.23 at different temperatures. This figure displays the large impact temperature has on strain rate for RAPs, but the little impact it had on materials without asphalt (i.e. RCA and natural aggregate). This trend can be seen throughout the entire conditioning phase in Figure 5.24 to Figure 5.25. NJ RAP had the highest strain rate at each temperature, followed by TX RAP and then CO RAP.

Figure 5.26 and Figure 5.27 show the effects temperature had on cumulative plastic strain of the RAP, RCA, and natural aggregate throughout the M_r test. For RAPs, a trend of increasing plastic strain with increased temperature was observed. This trend supports the theory that strain rate increases with increased temperature in RAP when used as an unbound base course. There was no apparent trend observed for the RCAs and natural aggregates tested except that there is little to no effect and the plastic strains stay relatively constant regardless of temperature.

Further support of the increasing plastic strain with RAP temperature theory is evident in Figure 5.28 and Figure 5.29, which show the effect of temperature on cumulative plastic strain during the conditioning phase and during the remainder of the M_r test. An exponentially increasing cumulative plastic strain trend with increasing temperature was observed during the first sequence of the M_r test for all RAPs. The opposite trend in plastic strain is seen in the remaining 30 sequences with a decreasing trend observed. Figure 5.28 shows that, except for the cumulative plastic strain values at 7 °C, total cumulative plastic strains for RAPs at each temperature are consistent. These observed trends in Figure 5.28 and Figure 5.29 show that increasing temperature in RAPs results in faster accumulation of plastic strain without increasing total cumulative plastic strain. The low total cumulative plastic strain for all RAPs at 7 °C shown in Figure 5.29 was attributed to the rigidity of the asphalt coating the aggregates at near freezing conditions (Griffin et al. 1959). Figure 5.28 shows that NJ RAP had the largest increase in plastic strain with increase in temperature, followed by TX RAP and CO RAP, similar to the findings in strain rate.

Figure 5.30 to Figure 5.33 show the effects of temperature on cumulative plastic strain for the RCAs and natural aggregates tested. Little plastic strain is accumulated during the first sequence in the RCA and natural aggregate specimens. No change in cumulative plastic strain outside of the expected margin of error due to instrumentation and rounding is observed in any of the RCAs or natural aggregates at varying temperatures. All values of cumulative plastic strain can be seen in Table 5.13 to Table 5.15.

RAP exhibited the highest plastic strains for all materials tested, which was a trend also observed by Kim and Labuz (2007) where plastic strains in RAP at room temperature were greater than two times those of natural aggregate. This trend of higher plastic strain with material containing asphalt was also observed in Ebrahimi et al. (2012) where recycled pavement material containing asphalt exhibited higher plastic strains than natural aggregate. This increase in plastic strain was attributed to the viscous creep of the asphalt coating the aggregates in the recycled pavement material and it was suggested that this deformation could lead to rutting in flexible pavements. Although this was the case, Ebrahimi et al. (2012) found that the overall life of the road would be increased using recycled pavement material as opposed to other materials because of the higher M_r of the material. The service life of a pavement constructed with RAP/RPM may be similar to the service life for a pavement with natural crushed aggregate base (using the same base layer thickness), even though RAP/RPM has higher rutting potential compared to crushed aggregate. This is because RAP/RPM has higher resilient modulus than crushed aggregate, which results in different stress distribution and consequently different contributions to rutting from the base course layer. Consequently, rutting may be comparable for RAP/RPM and crushed aggregate base as shown by Ebrahimi et al. (2012).

A problem associated with these high (> 6%) total cumulative plastic strain values in the RAP and Class 5 material is the problem with long-term performance of the pavement. High strain values lead to long-term rutting issues in the pavement, which decreases pavement life (Huang 2004). Because of this increased total cumulative plastic strain and increased strain rate due to temperature, further tests should be conducted on compaction of RAP at higher temperatures. As seen from the increased strain rates at increased temperatures, compaction at increased temperatures could decrease the total cumulative plastic strain accumulated in RAPs. In addition, the temperature effects on hydraulic conductivity of RAP should be evaluated. The

softening of the asphalt binder under loading can decrease pore space, reducing hydraulic conductivity of the material. High hydraulic conductivity in road base is important to allow water to drain away from the pavement system.

The mechanism causing this increased plastic strain at higher temperatures in RAP is hypothesized to be the asphalt coating the aggregates. The asphalt coating decreases roughness of the aggregates; therefore, decreasing contact friction angles. RAP has characteristically lower maximum dry unit weights when compacted than RCA and natural aggregate, which is attributed to the poor compaction ability of asphalt-coated aggregates (Bozyurt 2011). The asphalt coating also becomes more viscous at higher temperatures, which could allow for the specimens to consolidate due to decreased friction angles.

5.5.4 *Wet and Dry Cycling*

Particle degradation due to wet/dry cycling was evaluated through PSDs and Micro-Deval tests conducted after compaction, but before wetting and drying (0 cycles), and after 5, 10, and 30 cycles of wetting and drying. Figure 5.34 to Figure 5.39 show the PSDs for all four cycles. Figure 5.39 does not include wet/dry cycle five because of the lack of NJ RAP available during this test. For the natural aggregates, no change in PSD is observed outside of the expected error from the sample collected. For CA and TX RCA, no trends are observed; but for CA RCA, both 0 and 5 cycle are shown having finer material than the 10 and 30 cycle material. This is also observed for the 0 cycle TX RCA material. This observation is assumed to be due to the error in sampling the specimen for PSD material and not because of the wet/dry process. This assumption is made because the PSD of the material changes throughout the barrel the material is stored in. Outside of this measurement error, there is no observable change in PSD with the change in number of wet/dry cycles. A similar result can be observed for the TX and NJ RAP (Figure 5.38 and Figure 5.39, respectively).

During the wetting and drying processes, the loss of fines was documented. Fines migrated to the bottom of the cylinders during drying and were lost during wetting. The amount of fines lost was negligible (< 20 g) in relation to the size of the specimen, but a noticeable trend of increasing fines content with increased wet/dry cycles was observed in the PSDs. Figure 5.40 shows this trend observed in the natural aggregate and RCA specimens. No trend was observed for the RAP material. Figure 5.41 to Figure 5.46 show pictures of each specimen after 5, 10, and 30 cycles. From these figures it can be observed that both RAPs tested were able to stay much more intact than the RCAs and natural aggregates through the wetting and drying. This does not show that RAP will behave better through wetting and drying *in situ*, but does show that RAP when compacted, has higher cohesive properties than both RCA and natural aggregate. This increased cohesion could be due to the drying temperature of the material being 50 °C, which may have altered the asphalt binder within the RAP, bonding particles together.

Micro-Deval testing was completed on the materials to evaluate the effects of wet/dry cycles on abrasion resistance. Samples were collected for Micro-Deval analysis from the tested specimens. The Micro-Deval tests results can be observed as percent loss in Figure 5.47. No trend was observed in any of the materials because all percent losses were within the single operator coefficient of variation 3.4%. All losses were similar (within 3.4% COV) to previous Micro-

Deval studies conducted at 0 wet/dry cycles (Bozyurt 2011). Table 5.16 shows the exact values of the Micro-Deval losses for each material tested at each wet/dry cycle.

5.6 Conclusions

Freeze/thaw cycling was found to influence the stiffness properties of unbound recycled pavement and recycled concrete aggregates used for base course. Resilient modulus was used to investigate the effect of freeze-thaw (F-T) cycles on unbound road base/subbase layers consisting of natural aggregate, RAP, and RCA. The stiffness of RAP decreased over the first 5 F-T cycles, with smaller decrease recorded thereafter. This decrease in stiffness of RAP subjected to F-T cycles may be attributed to particle degradation and progressive asphalt-binder weakening. For RCA, the exposure to F-T cycles led first to a decrease in stiffness, followed by an increase, which may be attributed to progressive generation of fines and hydration of cement paste. The seismic modulus method confirmed the trends of changing stiffness of RCA during F-T cycling. Among the recycled materials evaluated in this study, quantitative differences in F-T response was observed, which was reflective of material grading and source. Exposure of the natural aggregate control (Class 5 base) to F-T cycles resulted in relatively small decreases in stiffness; however, the stiffness of the recycled materials was always greater than the natural aggregate, even after F-T induced decreases. Overall, RAP and RCA do not display a particular sensitivity to freeze-thaw than natural aggregates.

Temperature effects were investigated by resilient modulus tests at four different temperatures: 7, 23, 35, and 50 °C on three RAPs, three RCAs, and two natural aggregates. Increased temperature decreased the SRM of TX and CO RAP, but no change in SRM for NJ RAP was observed. Temperature did not affect the SRMs of any natural aggregate or RCA specimens tested. All RAP specimens were affected to some degree by increased temperature because of the asphalt content. There was a step drop in SRM of greater than 30% between the specimens tested at 23 °C and 35 °C for both TX and CO RAP; however, this trend did not continue between 35 °C and 50 °C. This trend was not observed in NJ RAP. This decrease in SRM implies that there may be a critical temperature between 23 °C and 35 °C that, when reached, starts to alter the physical characteristics of the asphalt binder coating the aggregates. Further studies are recommended to confirm this observation.

Cumulative plastic strain was calculated as an index using the M_r test data. Increased temperature caused the cumulative plastic strain and the strain rate to increase in all RAPs. No such effect was observed in the RCAs and natural aggregates with increasing temperature. NJ RAP had the highest strain rate, followed by TX RAP and then CO RAP. The majority of the increases in strain rate for RAP with temperature occurred within the first 1,000 cycles (conditioning phase) of the M_r test. Total cumulative plastic strains were overall high (> 7%) for RAPs at room temperature compared to other materials as was shown in previous studies, but increased temperature increased the rate at which the total plastic strain was achieved. Because of this trend, RAP compacted during the warmest time of the year could reduce total plastic strain after pavement is laid down. Further studies are recommended to evaluate if compacting RAP at elevated temperatures reduces subsequent total cumulative plastic strain. Plastic strain tests with higher cycles of loading at a constant deviatoric and confining stress would need to be completed to further evaluate this theory. The potential effects of temperature on hydraulic

conductivity of RAP should also be evaluated because, when heated, void space in the RAP may decrease due to softening of the asphalt at elevated temperatures.

A procedure for evaluating the effect of wetting and drying of unbound aggregates was developed. 5, 10, and 30 wet/dry cycles were conducted on two RAPs, two RCAs, and two natural aggregates to evaluate the effects wetting and drying have on particle degradation. To evaluate particle degradation, Micro-Deval and particle size distribution tests were completed on each specimen after the specified wet/dry cycle. No significant change that was outside of the coefficient of variation indicated by the standard in Micro-Deval loss was observed due to wet/dry cycles of any of the materials tested. Also, no significant change in particle size distribution was observed. However, increases in percent fines was observed with increasing wet/dry cycles for the two RCAs and two natural aggregates, but not change in fines content was seen for the two RAPs. Overall, RCA and RAP appear insensitive to wetting and drying.

5.7 Tables

Table 5.1 Index Properties of Recycled Materials and Class 5 Aggregate

Material	States	D10 (mm)	D_{50} (mm)	C_u	C_c	G_s	AB (%)	AC (%)	w_{opt} (%)	γ_{dmax} (kN/m^3)	Gravel (%)	Fines (%)	USCS
Class 5 Aggregate	MN	0.08	1.0	21	1.4	2.6	-	-	8.9	20.1	22.9	9.5	GW-GM
Basalt	Senegal	0.10	7.0	125	6.6	2.9	0.5	-	4.2	22.0	58.0	7.8	GP
RCA	CA	0.31	4.8	22	1.4	2.3	5.0	-	10.4	19.9	50.6	2.3	GW
	TX	0.43	13.3	38	6.0	2.3	5.5	-	9.2	19.7	76.3	2.1	GW
	NJ	0.18	2.0	28	0.3	2.3	5.4	-	9.5	19.8	41.2	4.3	SP
RAP	TX	0.72	5.4	11	1.1	2.3	1.3	4.7	8.1	20.3	54.2	1.0	GW
	NJ	1.00	4.9	6	1.3	2.4	2.1	5.2	6.5	20.4	50.9	0.7	GW
	CO	0.35	2.2	9	0.7	2.2	3.0	5.9	5.7	20.7	31.7	0.7	SP

Note: AC=Asphalt Content, AB=Absorption, MN=Minnesota, CA=California, NJ=New Jersey, CO=Colorado, TX=Texas

Table 5.2 Quality Control of Class 5, Basalt, and RCA Specimen Preparation for Mr Test

	Temperature of Resilient Modulus Test	ω_{opt}	$\omega_{compacted}$	Percent ω Difference	ω Standard Deviation	Mass after Compaction Goal (kg)	Mass after Compaction (kg)	Percent Mass Difference	Mass after Compaction Standard Deviation	*95% g_{dmax} (kN/m^3)*	Dry Unit Weight of Compacted Material (kN/m^3)	Dry Unit Weight Difference	Standard Deviation
Class 5	7° C	8.90%	9.00%	0.10%	0.17%	11.79	12.65	7.29%	0.55%	19.1	20.47	7.17%	0.56%
	23° C	8.90%	8.90%	0.00%		11.79	12.6	6.87%		19.1	20.41	6.85%	
	35° C	8.90%	9.30%	0.40%		11.79	12.55	6.45%		19.1	20.25	6.03%	
	50° C	8.90%	8.80%	0.10%		11.79	12.5	6.02%		19.1	20.26	6.09%	
Basalt	7° C	4.20%	4.40%	0.20%	0.13%	13.59	13.65	0.44%	0.35%	23	23.06	0.27%	0.27%
	23° C	4.20%	4.60%	0.40%		13.59	13.7	0.81%		23	23.10	0.44%	
	35° C	4.20%	4.40%	0.20%		13.59	13.6	0.07%		23	22.98	0.10%	
	50° C	4.20%	4.30%	0.10%		13.59	13.7	0.81%		23	23.17	0.73%	
CA RCA	7° C	10.40%	10.84%	0.44%	0.19%	11.82	11.85	0.25%	0.38%	18.88	18.86	0.12%	0.27%
	23° C	10.40%	10.60%	0.20%		11.82	11.8	0.17%		18.88	18.82	0.33%	
	35° C	10.40%	10.10%	0.30%		11.82	11.7	1.02%		18.88	18.74	0.72%	
	50° C	10.40%	10.40%	0.00%		11.82	11.75	0.59%		18.88	18.77	0.57%	
TX RCA	7° C	9.20%	9.10%	0.10%	0.21%	11.56	11.6	0.35%	0.15%	18.68	18.75	0.39%	0.23%
	23° C	9.20%	9.60%	0.40%		11.56	11.55	0.09%		18.68	18.59	0.50%	
	35° C	9.20%	9.20%	0.00%		11.56	11.55	0.09%		18.68	18.66	0.13%	
	50° C	9.20%	8.80%	0.40%		11.56	11.6	0.35%		18.68	18.81	0.67%	
NJ RCA	7° C	9.50%	9.80%	0.30%	0.13%	11.65	11.6	0.43%	0.21%	18.76	18.63	0.67%	0.18%
	23° C	9.50%	9.80%	0.30%		11.65	11.6	0.43%		18.76	18.63	0.67%	
	35° C	9.50%	9.10%	0.40%		11.65	11.55	0.86%		18.76	18.67	0.47%	
	50° C	9.50%	9.40%	0.10%		11.65	11.6	0.43%		18.76	18.70	0.31%	

Table 5.3 Quality Control of RAP Specimen Preparation for M_r Test

	Temperature of Resilient Modulus Test	ω_{opt}	$\omega_{compacted}$	Percent ω Difference	ω Standard Deviation	Mass after Compaction Goal (kg)	Mass after Compaction (kg)	Percent Mass Difference	Mass after Compaction Standard Deviation	*95% g_{dmax} (kN/m^3)*	Dry Unit Weight of Compacted Material (kN/m^3)	Dry Unit Weight Difference	Standard Deviation
CO RAP	7° C	5.70%	5.90%	0.20%	0.05%	11.76	11.8	0.34%	0.15%	19.62	19.65	0.17%	0.12%
	23° C	5.70%	5.60%	0.10%		11.76	11.75	0.09%		19.62	19.63	0.03%	
	35° C	5.70%	5.60%	0.10%		11.76	11.75	0.09%		19.62	19.63	0.03%	
	50° C	5.70%	5.80%	0.10%		11.76	11.8	0.34%		19.62	19.67	0.26%	
NJ RAP	7° C	6.50%	6.30%	0.20%	0.10%	11.7	11.6	0.85%	0.41%	19.37	19.25	0.63%	0.34%
	23° C	6.50%	6.20%	0.30%		11.7	11.5	1.71%		19.37	19.10	1.40%	
	35° C	6.50%	6.10%	0.40%		11.7	11.55	1.28%		19.37	19.20	0.88%	
	50° C	6.50%	6.90%	0.40%		11.7	11.6	0.85%		19.37	19.14	1.19%	
TX RAP	7° C	8.00%	8.40%	0.40%	0.15%	11.8	11.65	1.27%	0.41%	19.27	18.96	1.63%	0.55%
	23° C	8.00%	7.80%	0.20%		11.8	11.65	1.27%		19.27	19.06	1.08%	
	35° C	8.00%	8.10%	0.10%		11.8	11.75	0.42%		19.27	19.17	0.51%	
	50° C	8.00%	7.60%	0.40%		11.8	11.7	0.85%		19.27	19.18	0.47%	

Note: ω_{opt} = Optimum moisture content; $\omega_{compacted}$ = Compacted moisture content;

ω Standard Deviation = Variability in percent moisture content difference; Std. Dev. = Standard Deviation

Table 5.4 SRM and Power Model Fitting Parameters k1 and k2 for Base Materials after 0, 5, 10 and 20 F-T Cycles

Material	States	Freeze-Thaw Cycles	External			Internal			SRM_0/ SRM_N
			k_1	k_2	SRM (MPa)	k_1	k_2	SRM (MPa)	
Class 5 Aggregate	MN	0	66.2	0.20	191	129.2	0.15	281	1.0
		5	59.1	0.21	186	59.1	0.28	261	0.9
		10	35.5	0.30	177	34.7	0.36	240	0.9
		20	24.8	0.34	153	24.7	0.41	223	0.8
RCA	CA	0	119.4	0.15	262	273.6	0.13	550	1.0
		5	74.8	0.21	227	113.4	0.27	489	0.9
		10	99.1	0.20	282	185.7	0.21	578	1.1
	MI	0	32.7	0.34	199	107.2	0.25	400	1.0
		5	22.8	0.39	191	55.3	0.35	361	0.9
		10	47.8	0.32	257	177.5	0.18	472	1.2
		20	83.6	0.22	268	388.7	0.07	553	1.4
	TX	0	74.6	0.23	258	236.1	0.13	464	1.0
		5	43.6	0.30	211	76.8	0.32	419	0.9
		10	44.6	0.31	236	120.8	0.26	471	1.0
		20	81.1	0.24	289	150.2	0.28	601	1.3
RAP	CA	0	122.5	0.14	256	348.8	0.06	473	1.0
		5	122.5	0.13	249	147.9	0.20	436	0.9
		10	76.6	0.20	223	136.2	0.19	379	0.8
		20	66.0	0.21	203	122.8	0.18	323	0.7
	MN	0	93.9	0.174	238	236.1	0.127	464	1.0
		5	57.6	0.25	220	85.8	0.27	361	0.8
		10	54.0	0.25	200	80.2	0.27	344	0.7
		20	31.2	0.33	180	57.3	0.32	314	0.7
	TX	0	156.6	0.14	334	358.7	0.12	686	1.0
		5	155.2	0.12	287	344.1	0.10	585	0.9
		10	88.6	0.21	272	259.1	0.15	566	0.8
		20	63.6	0.26	254	103.2	0.29	497	0.7

Table 5.5 Summary Resilient Modulus (SRM) at Varying Temperatures Calculated using both NCHRP and Power Models

		SMR (Mpa)							
		CA RCA	**TX RCA**	**NJ RCA**	**CO RAP**	**NJ RAP**	**TX RAP**	**Class 5**	**Basalt**
7 °C	Int NCHRP	199	211	169	200	261	459	123	157
	Int M & W	226	248	200	230	254	398	147	182
	Ext NCHRP	150	138	115	133	150	203	87	117
	Ext M & W	170	153	130	145	162	206	96	134
23 °C	Int NCHRP	245	188	163	228	290	369	123	180
	Int M & W	278	231	181	245	294	348	142	210
	Ext NCHRP	140	99	84	151	166	200	91	130
	Ext M & W	152	108	93	162	174	213	107	151
35 °C	Int NCHRP	215	180	154	208	234	371	141	168
	Int M & W	252	220	192	224	241	356	153	199
	Ext NCHRP	123	102	99	105	153	126	108	121
	Ext M & W	136	112	110	127	159	122	103	140
50 °C	Int NCHRP	197	193	188	177	NA	341	145	174
	Int M & W	207	233	223	202	NA	290	137	192
	Ext NCHRP	115	108	104	109	154	109	112	114
	Ext M & W	125	113	111	122	162	107	108	123

Note: Int = Internal LVDT recorded; Ext = External LVDT recorded

Table 5.6 SRM NCHRP Fitting Parameters for Natural Aggregate and RCA at Varying Temperatures

Material	Temperature	Internal						External						SRM_{int}/SRM_{ext}
		k_1	k_2	k_3	k_6	k_7	SRM (MPA)	k_1	k_2	k_3	k_6	k_7	SRM (MPA)	
Class 5	7 °C	21.0	3.6	-2.8	-206.9	3.0	123	0.4	5.2	-3.6	-450.1	5.8	87	1.41
	23 °C	0.7	4.2	-2.3	-291.8	2.6	123	6.8	3.9	-2.8	-251.5	3.5	91	1.35
	35 °C	0.003	5.14	-1.8	-405.3	1.0	141	1.3	2.4	0	-473.5	1.0	108	1.31
	50 °C	0.008	4.52	-0.7	-450.0	1.0	145	1.7	2.3	0	-473.5	1.0	112	1.29
Basalt	7 °C	23.2	2.9	-1.5	-168.8	2.1	157	101.5	2.1	-1.3	-109.6	2.0	117	1.34
	23 °C	0.003	6.6	-3.4	-515.1	4.5	180	8.7	4.0	-2.9	-273.9	4.1	130	1.38
	35 °C	1,031	1.1	-0.8	0.0	1.0	168	13.5	3.0	-1.7	-182.5	2.1	121	1.39
	50 °C	3.6	4.0	-2.5	-319.8	4.1	174	46.9	2.2	-1.0	-143.2	2.0	114	1.53
CA RCA	7 °C	6.5	3.5	-2.1	-248.1	2.2	199	12.5	4.1	-3.3	-368.7	5.3	150	1.33
	23 °C	0.7	5.4	-4.0	-406.2	4.4	245	1.2	4.4	-2.9	-471.2	5.8	140	1.75
	35 °C	6.0	3.6	-2.2	-202.9	1.7	215	24.9	2.9	-1.9	-220.2	3.0	123	1.75
	50 °C	0.006	4.7	-1.3	-478.4	1.1	197	111.7	1.7	-0.8	-101.4	1.2	115	1.71
TX RCA	7 °C	0.9	5.3	-3.8	-397.1	4.5	211	0.2	5.9	-4.3	-578.5	7.1	138	1.53
	23 °C	3.6	3.9	-2.4	-223.1	2.0	188	0.20	4.9	-3.0	-480.3	5.8	99	1.90
	35 °C	9.4	3.7	-2.6	-224.5	2.5	180	6.5	3.8	-2.6	-326.7	4.7	102	1.76
	50 °C	5.0	5.1	-4.1	-392.7	5.5	193	0.1	6.2	-4.4	-686.7	10.1	108	1.79
NJ RCA	7 °C	0.2	6.2	-4.6	-480.8	5.2	169	12.5	3.5	-2.5	-298.8	4.1	115	1.47
	23 °C	0.0002	5.9	-1.5	-480.1	1.0	163	15.0	2.8	-1.6	-212.5	2.9	84	1.94
	35 °C	74.6	2.9	-2.3	-148.9	2.5	154	0.9	4.3	-2.7	-412.9	4.8	99	1.56
	50 °C	0.1	6.5	-5.0	-481.2	5.2	188	9.6	5.1	-4.3	-586.6	11.1	104	1.81

Table 5.7 SRM NCHRP Fitting Parameter for RAP at Varying Temperatures

Material	Temperature	Internal						External						SRM_{int}/SRM_{ext}
		k_1	k_2	k_3	k_6	k_7	SRM (MPA)	k_1	k_2	k_3	k_6	k_7	SRM (MPA)	
CO RAP	7 °C	7.8	3.6	-2.4	-242.5	2.4	200	0.4	4.6	-2.8	-517.0	5.8	133	1.50
	23 °C	0.01	4.6	-1.1	-476.0	1.0	228	12.6	3.1	-2.0	-326.2	3.8	151	1.51
	35 °C	3.5	2.9	-1.0	-267.1	1.0	208	2.0	2.7	-0.6	-349.7	2.4	105	1.98
	50 °C	13.5	2.7	-1.4	-225.6	1.7	177	0.01	4.4	-0.7	-479.3	1.0	114	1.55
NJ RAP	7 °C	11.1	3.3	-2.1	-271.9	2.3	261	1.9	4.1	-2.6	-441.9	5.1	150	1.74
	23 °C	4.8	3.5	-1.9	-255.5	1.8	290	9.2	3.0	-1.6	-369.1	4.5	166	1.75
	35 °C	0.4	3.1	0.0	-460.8	1.0	234	1,125.8	0.7	-0.4	0	1.1	153	1.53
	50 °C	NA	NA	NA	NA	NA	NA	0.10	3.7	0	-473.5	1.0	154	NA
TX RAP	7 °C	1.8	4.0	-2.3	-397.9	2.6	459	4.7	3.5	-2.1	-393.0	4.0	203	2.26
	23 °C	7.5	3.8	-2.7	-361.6	3.4	369	4.9	4.1	-2.9	-415.8	5.2	200	1.85
	35 °C	0.01	5.5	-0.8	-819.1	1.0	371	3.4	2.8	-0.7	-456.3	18.2	126	2.94
	50 °C	0.02	3.9	-0.9	-707.5	1.1	341	7.7	2.0	0.0	-322.3	1.0	109	2.53

Table 5.8 SRM Power Model Fitting Parameters for Class 5, Basalt, and RCA at Varying Temperatures

Material	Temperature	Internal			External			SRM_{int}/SRM_{ext}
		k_1	k_2	SRM (MPa)	k_1	k_2	SRM (MPa)	
Class 5	7 °C	6,803	0.58	147	3,784	0.61	96	1.53
	23 °C	4,020	0.67	142	3,821	0.62	107	1.33
	35 °C	3,496	0.71	153	3,879	0.61	103	1.49
	50 °C	1,656	0.83	137	4,553	0.59	108	1.27
Basalt	7 °C	5,695	0.65	182	5,318	0.6	134	1.36
	23 °C	4,012	0.74	210	6,149	0.6	151	1.39
	35 °C	11,128	0.54	199	5,642	0.6	140	1.42
	50 °C	7,212	0.62	193	3,670	0.66	123	1.57
CA RCA	7 °C	21,074	0.44	226	16,574	0.44	170	1.33
	23 °C	21,074	0.48	278	11,827	0.48	152	1.83
	35 °C	20,000	0.47	252	8,849	0.51	136	1.85
	50 °C	18,160	0.46	207	8,645	0.5	125	1.66
TX RCA	7 °C	20,000	0.47	248	11,927	0.48	153	1.62
	23 °C	20,000	0.46	231	5,350	0.56	108	2.14
	35 °C	20,000	0.45	220	6,015	0.55	112	1.96
	50 °C	17,628	0.48	233	5,214	0.58	113	2.06
NJ RCA	7 °C	19,828	0.43	200	11,122	0.46	130	1.54
	23 °C	11,755	0.51	181	4,429	0.57	93	1.95
	35 °C	12,943	0.50	192	8,182	0.49	110	1.75
	50 °C	20,000	0.45	223	6,300	0.54	111	2.01

Table 5.9 SRM Power Model Fitting Parameters for RAP at Varying Temperatures

Material	Temperature	Internal			External			SRM_{int}/SRM_{ext}
		k_1	k_2	SRM (MPa)	k_1	k_2	SRM (MPa)	
CO RAP	7 °C	21,074	0.45	230	12,118	0.46	145	1.59
	23 °C	21,074	0.46	245	17,138	0.42	162	1.51
	35 °C	21,074	0.44	224	5,245	0.56	107	2.09
	50 °C	17,195	0.46	202	5,077	0.60	122	1.66
NJ RAP	7 °C	22,148	0.46	254	14,528	0.45	162	1.57
	23 °C	23,221	0.48	294	14,475	0.47	174	1.69
	35 °C	8,467	0.63	241	11,071	0.50	159	1.52
	50 °C	NA	NA	NA	5,656	0.63	162	NA
TX RAP	7 °C	22,148	0.54	398	18,212	0.45	206	1.93
	23 °C	23221	0.51	348	17,138	0.47	213	1.63
	35 °C	24,168	0.50	356	3,687	0.66	122	2.92
	50 °C	25369	0.46	290	4290	0.60	107	2.71

Table 5.10 SRM Calculation Error Results using Temperature Independent Control Material

		Int	Ext
Basalt	Average SRM	170	118.75
	Std. Dev.	12.19	5.91
	Coef. Var.	7%	5%
Class 5	Average SRM	122	100
	Std. Dev.	11.75	11.92
	Coef. Var.	10%	12%
CA RCA	Average SRM	209.75	130.75
	Std. Dev.	27.33	15
	Coef. Var.	13%	11%
TX RCA	Average SRM	192.25	108.5
	Std. Dev.	12.04	16.54
	Coef. Var.	6%	15%
NJ RCA	Average SRM	168.75	99
	Std. Dev.	14.06	12.73
	Coef. Var.	8%	13%

Note:

Std. Dev. = standard deviation of SRM results on 4 replicates of each material
Coef. Var. = coefficient of variation

Table 5.11 SRM Calculation Error Results for RAP

		Int.	Ext.
NJ RAP	Average	263	154.25
	Std. Dev.	29.05	7.41
	Coef. Var.	11%	5%
CO RAP	Average	204.75	125.25
	Std. Dev.	19.14	20.71
	Coef. Var.	9%	17%
TX RAP	Average	369.5	155.75
	Std. Dev.	78.8	48.46
	Coef. Var.	21%	31%

Note:

Std. Dev = standard deviation of SRM results on 4 replicates of each material

Coef. Var. = coefficient of variation

Table 5.12 Ratio of $SRM_{23\,°C}$ to $SRM_{35\,°C}$ or $SRM_{50\,°C}$

		CO RAP	**NJ RAP**	**TX RAP**	**Average**
23 °C-35 °C	Int	1.09	1.25	0.99	1.11
	Ext	1.45	1.07	1.64	1.39
23 °C-50 °C	Int	1.25	NA	1.35	1.30
	Ext	1.32	1.06	1.82	1.40

Table 5.13 1st Sequence (Conditioning Phase) Plastic Deformation and Plastic Strain at Varying Temperatures

		CA RCA	TX RCA	NJ RCA	CO RAP	NJ RAP	TX RAP	Class 5	Basalt
7° C	Int Deformation (mm)	0.3	0.2	0.3	0.6	0.9	0.4	0.99	0.6
	Int Plastic Strain (%)	0.20%	0.10%	0.20%	0.40%	0.60%	0.20%	0.70%	0.40%
	Ext Deformation (mm)	0.7	0.8	1.1	2.5	2.5	1.6	2.5	1.8
	Ext Plastic Strain (%)	0.20%	0.30%	0.40%	0.80%	0.80%	0.50%	0.80%	0.60%
23° C	Int Deformation (mm)	0.3	0.2	0.3	1.2	2.6	1.6	2.7	0.2
	Int Plastic Strain (%)	0.20%	0.10%	0.20%	0.80%	1.70%	1.10%	1.80%	0.10%
	Ext Deformation (mm)	1	0.9	1.2	3.4	5.9	4	5.8	1.4
	Ext Plastic Strain (%)	0.30%	0.30%	0.40%	1.10%	1.90%	1.30%	1.90%	0.50%
35° C	Int Deformation (mm)	0.3	0.3	0.4	2.2	6.8	3.8	1.8	0.4
	Int Plastic Strain (%)	0.20%	0.20%	0.30%	1.40%	4.50%	2.50%	1.20%	0.30%
	Ext Deformation (mm)	1.3	1.1	1.3	6.5	13.6	9	3.7	1.3
	Ext Plastic Strain (%)	0.40%	0.40%	0.40%	2.10%	4.50%	3.00%	1.20%	0.40%
50° C	Int Deformation (mm)	0.5	0.1	0.2	4.4	6.9	5.3	1.2	0.4
	Int Plastic Strain (%)	0.30%	0.10%	0.20%	2.90%	4.50%	3.50%	0.80%	0.30%
	Ext Deformation (mm)	1.2	0.4	0.9	10.4	21.7	11.1	2.9	1.3
	Ext Plastic Strain (%)	0.40%	0.10%	0.30%	3.40%	7.10%	3.60%	1.00%	0.40%

Note: Int = Internal LVDT recorded
Ext = External LVDT recorded

Table 5.14 2nd-31st Sequence Plastic Deformation and Plastic Stain at Varying Temperatures

		CA RCA	TX RCA	NJ RCA	CO RAP	NJ RAP	TX RAP	Class 5	Basalt
7° C	Int Deformation (mm)	3.2	3.2	5.8	4.5	7.6	2.7	9.3	3.9
	Int Plastic Strain (%)	2.10%	2.10%	3.80%	3%	5%	1.80%	6.10 %	2.50 %
	Ext Deformation (mm)	5.7	6.8	12.2	10.6	14.7	6.5	21.1	8.5
	Ext Plastic Strain (%)	1.90%	2.20%	4.00%	3.50%	4.80%	2.10%	6.90 %	2.80 %
23° C	Int Deformation (mm)	3	4.8	8.8	8.9	7.9	7.6	7.2	3.4
	Int Plastic Strain (%)	2%	3.20%	5.80%	5.80%	5.20%	5%	4.70 %	2.20 %
	Ext Deformation (mm)	5.8	9.4	16.8	18.9	16.7	13.8	18.1	8.2
	Ext Plastic Strain (%)	1.90%	3.10%	5.50%	6.20%	5.60%	4.50%	5.90 %	2.70 %
35° C	Int Deformation (mm)	3.6	4.9	8.5	8.2	2.6	5.6	8.4	4.2
	Int Plastic Strain (%)	2.40%	3.20%	5.60%	5.40%	1.70%	4.60%	5.50 %	2.70 %
	Ext Deformation (mm)	7.9	9.6	16.5	16.5	9.6	14	20.8	8.7
	Ext Plastic Strain (%)	2.60%	3.10%	5.40%	5.40%	3.10%	4.60%	6.80 %	2.90 %
50° C	Int Deformation (mm)	5.2	3.5	5.6	5.8	0	3.6	8.9	3.3
	Int Plastic Strain (%)	3.40%	2.30%	3.70%	3.80%	0.00%	2.40%	5.80 %	2.20 %
	Ext Deformation (mm)	9.3	7.6	10.2	12.3	0.7	6.6	21.7	8
	Ext Plastic Strain (%)	3.10%	2.50%	3.30%	4.00%	0.20%	2.20%	7.10 %	2.60 %

Note: Int = Internal LVDT recorded
Ext = External LVDT recorded

Table 5.15 Total Plastic Deformation and Plastic Stain at Varying Temperatures

		CA RCA	TX RCA	NJ RCA	CO RAP	NJ RAP	TX RAP	Class 5	Basalt
7° C	Int Deformation (mm)	3.5	3.4	6.1	5.1	8.5	3.1	10.29	4.5
	Int Plastic Strain (%)	2.3%	2.2%	4.0%	3.4%	5.6%	2.0%	6.8%	2.9%
	Ext Deformation (mm)	6.4	7.6	13.3	13.1	17.2	8.1	23.6	10.3
	Ext Plastic Strain (%)	2.1%	2.5%	4.4%	4.3%	5.6%	2.6%	7.7%	3.4%
23° C	Int Deformation (mm)	3.3	5	9.1	10.1	10.5	9.2	9.9	3.6
	Int Plastic Strain (%)	2.2%	3.3%	6.0%	6.6%	6.9%	6.1%	6.5%	2.3%
	Ext Deformation (mm)	6.8	10.3	18	22.3	22.6	17.8	23.9	9.6
	Ext Plastic Strain (%)	2.2%	3.4%	5.9%	7.3%	7.5%	5.8%	7.8%	3.2%
35° C	Int Deformation (mm)	3.9	5.2	8.9	10.4	9.4	9.4	10.2	4.6
	Int Plastic Strain (%)	2.6%	3.4%	5.9%	6.8%	6.2%	7.1%	6.7%	3.0%
	Ext Deformation (mm)	9.2	10.7	17.8	23	23.2	23	24.5	10
	Ext Plastic Strain (%)	3.0%	3.5%	5.8%	7.5%	7.6%	7.6%	8.0%	3.3%
50° C	Int Deformation (mm)	5.7	3.6	5.8	10.2	6.9	8.9	10.1	3.7
	Int Plastic Strain (%)	3.7%	2.4%	3.9%	6.7%	4.5%	5.9%	6.6%	2.5%
	Ext Deformation (mm)	10.5	8	11.1	22.7	22.4	17.7	24.6	9.3
	Ext Plastic Strain (%)	3.5%	2.6%	3.6%	7.4%	7.3%	5.8%	8.1%	3.0%

Note: Int = Internal LVDT recorded
Ext = External LVDT recorded

Table 5.16 Micro-Deval Results at Varying Wet/Dry Cycles

Material	30 Cycle	10 Cycle	5 Cycle
CA RCA	16%	16%	16%
TX RCA	21%	19%	17%
TX RAP	21%	21%	20%
NJ RAP	24%	22%	-
Basalt	8%	6%	7%
Class 5	11%	12%	12%

Note: NJ RAP 5 wet/dry cycle tests were not run due to lack of material

5.8 Figures

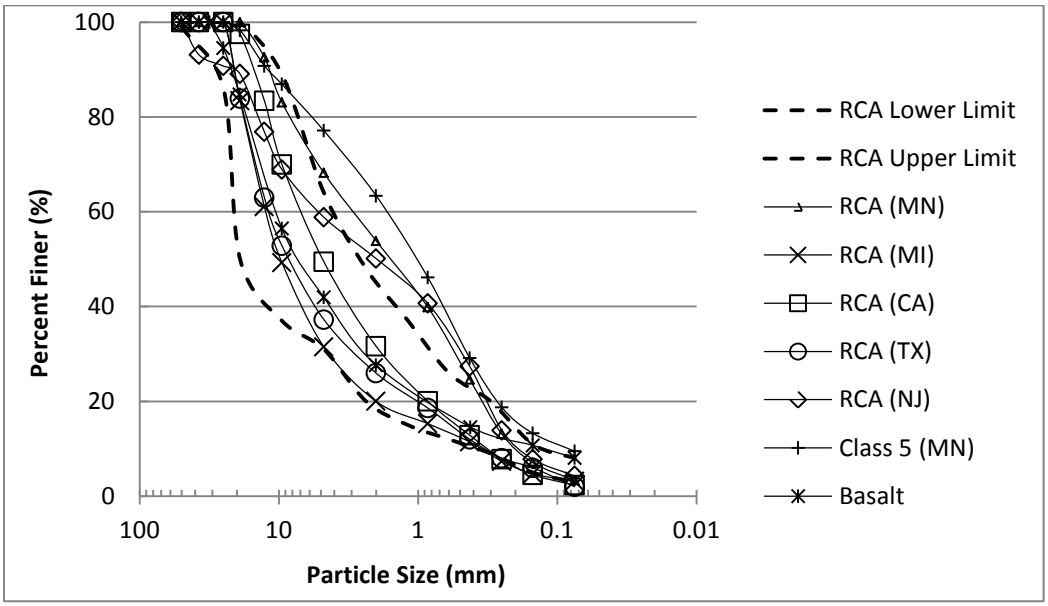

Figure 5.1 Particle Size Distribution for RCA, Basalt, and Class 5 Aggregate with lower and upper Limits of RCA from Literature

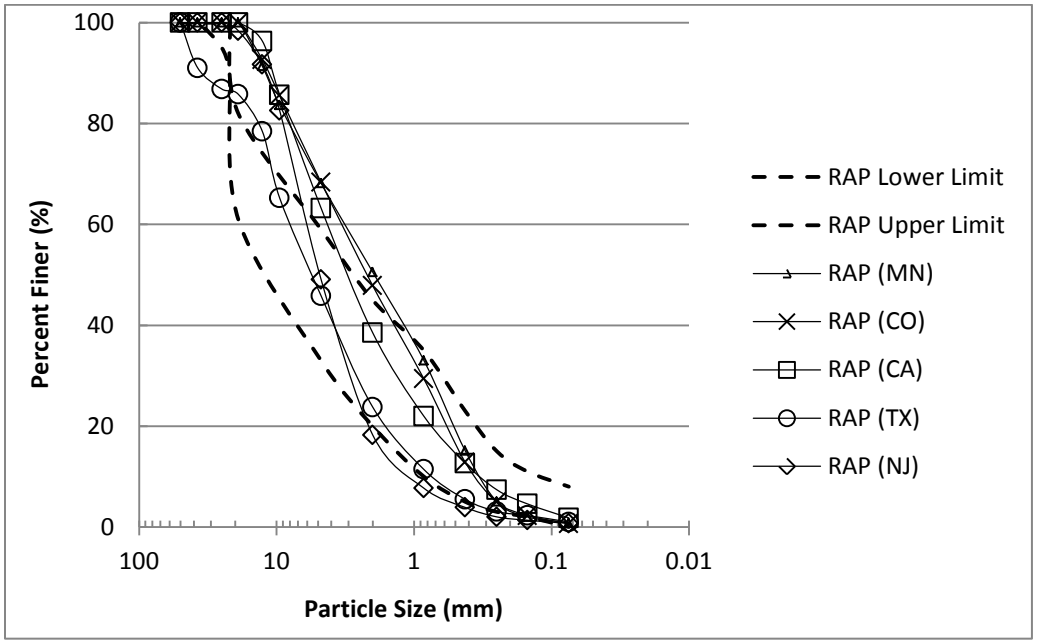

Figure 5.2 Particle Size Distribution for RAP with lower and upper Limits of RAP from Literature

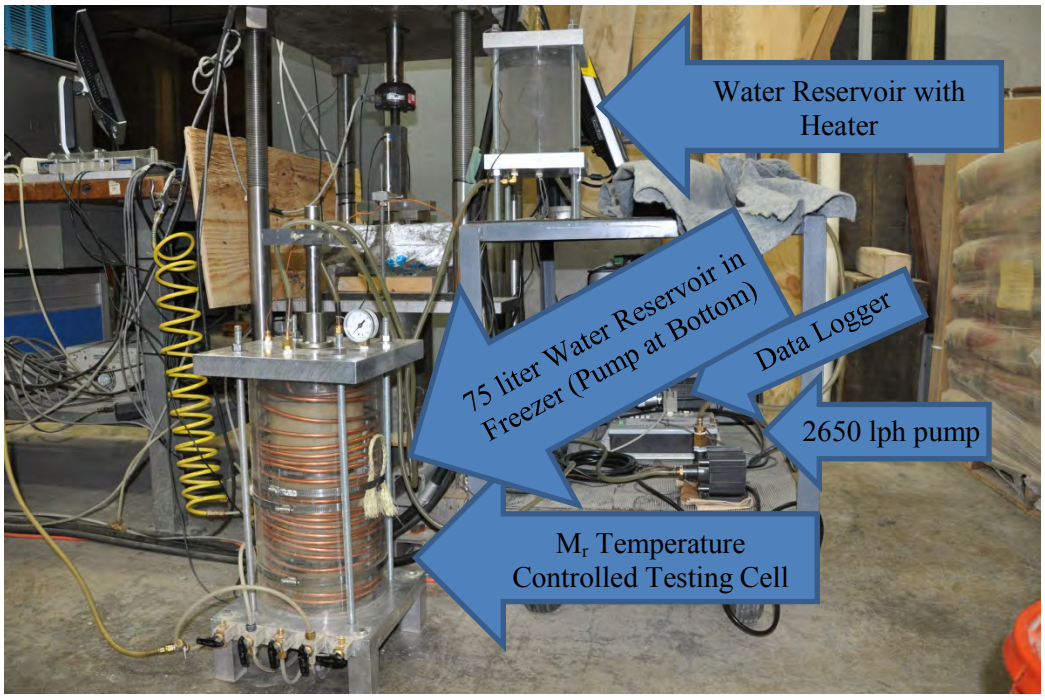

Figure 5.3 Resilient Modulus Testing Equipment with Heated Water

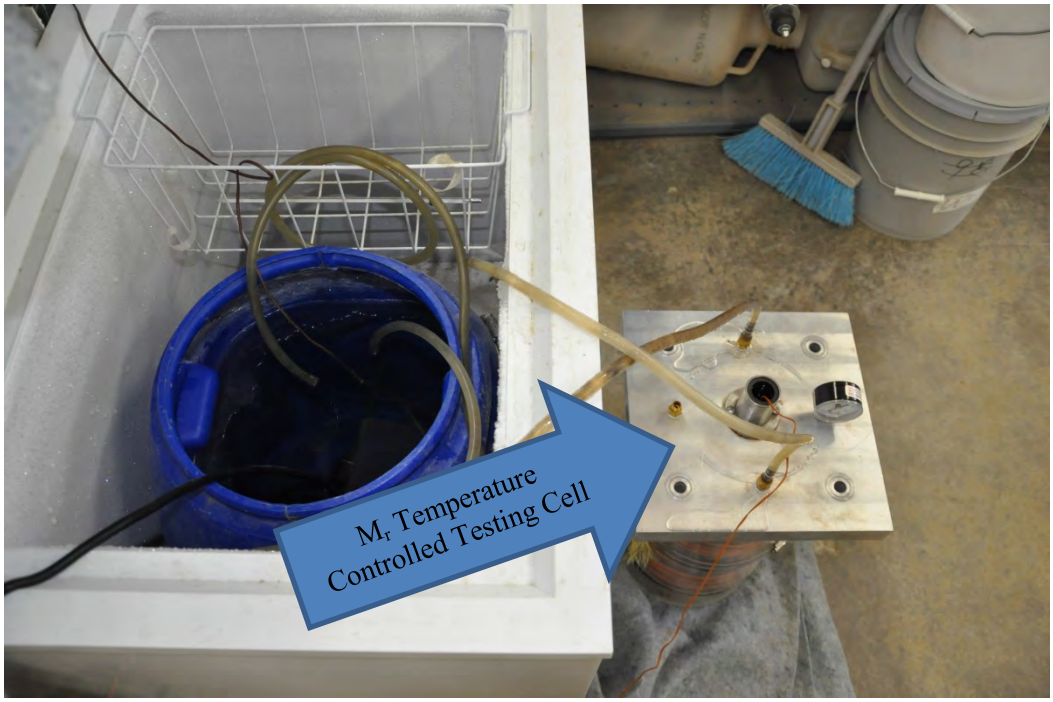

Figure 5.4 Resilient Modulus Testing Equipment with Chilled Water

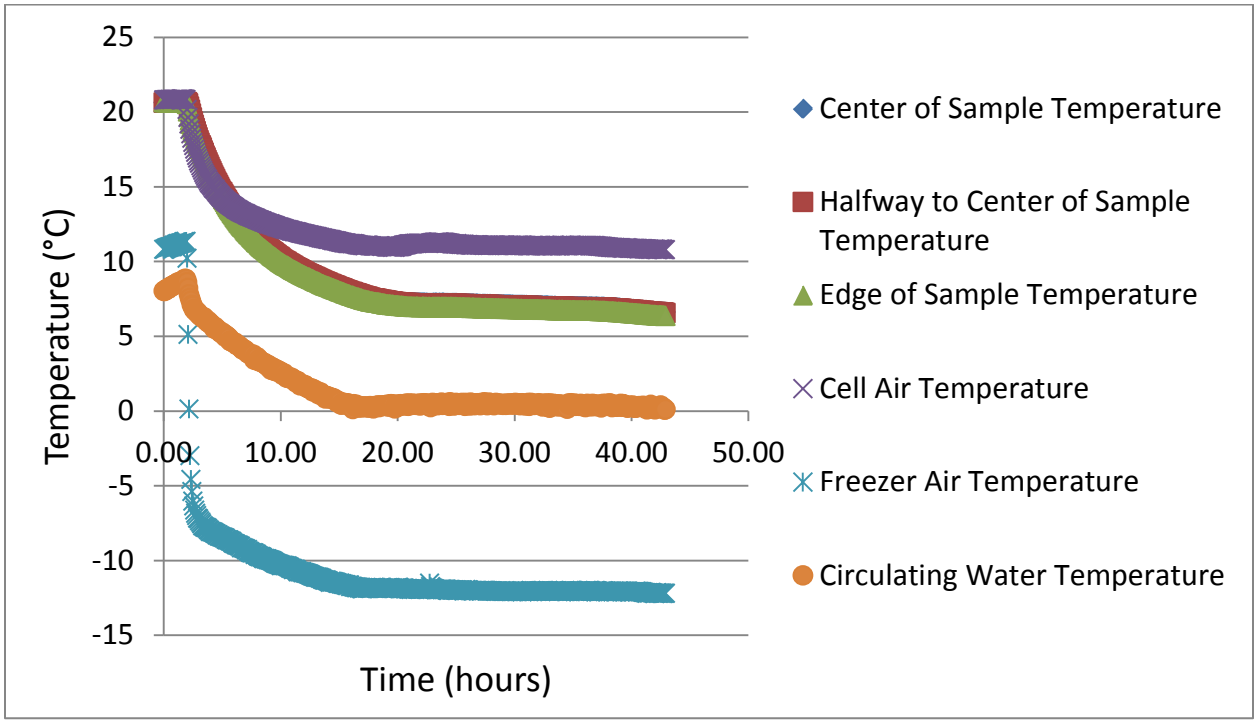

Figure 5.5 7 °C Class 5 Temperature Calibration

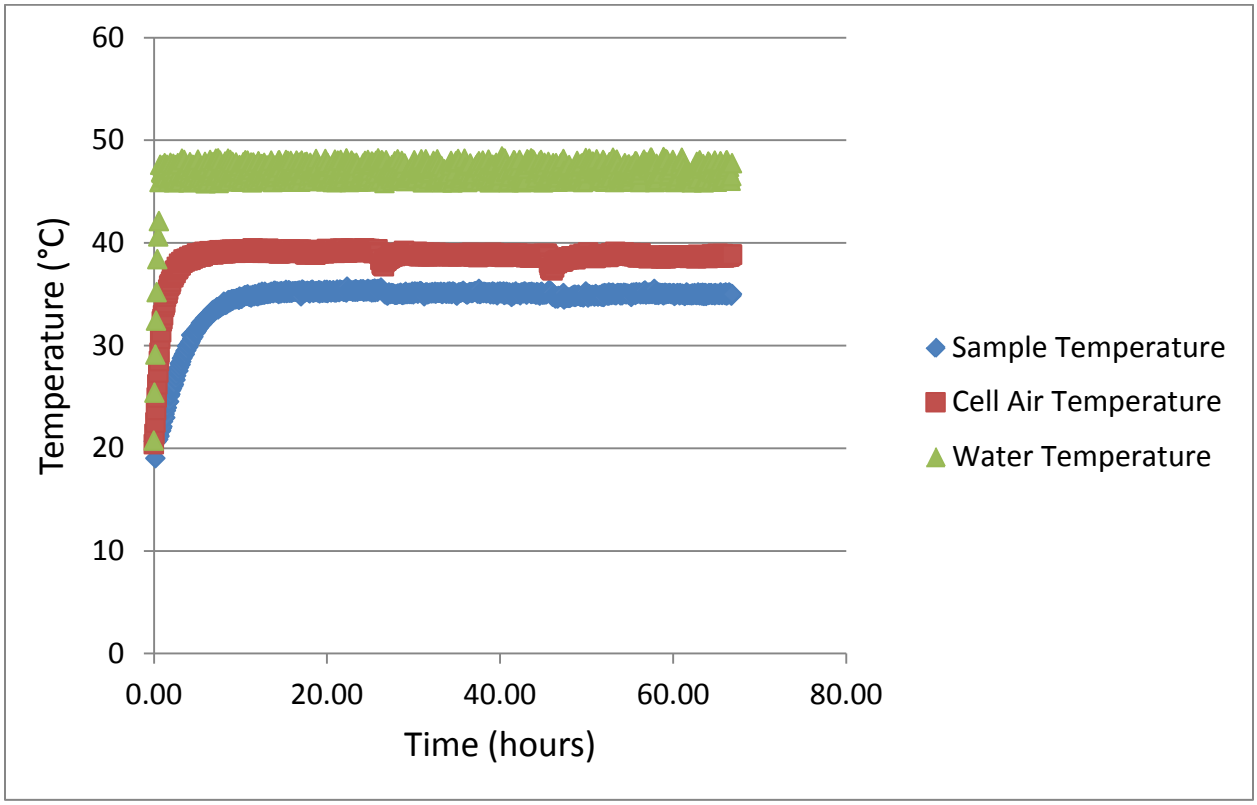

Figure 5.6 35 °C Class 5 Temperature Calibration

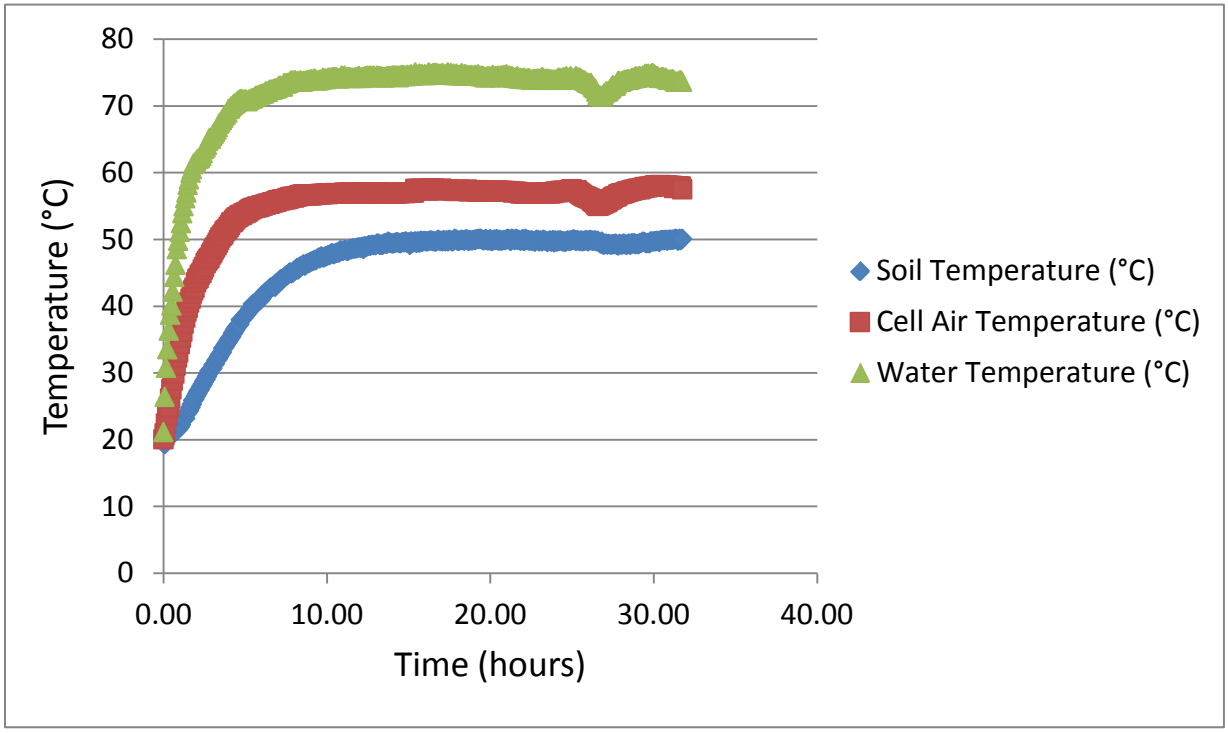

Figure 5.7 50 °C Class 5 Temperature Calibration

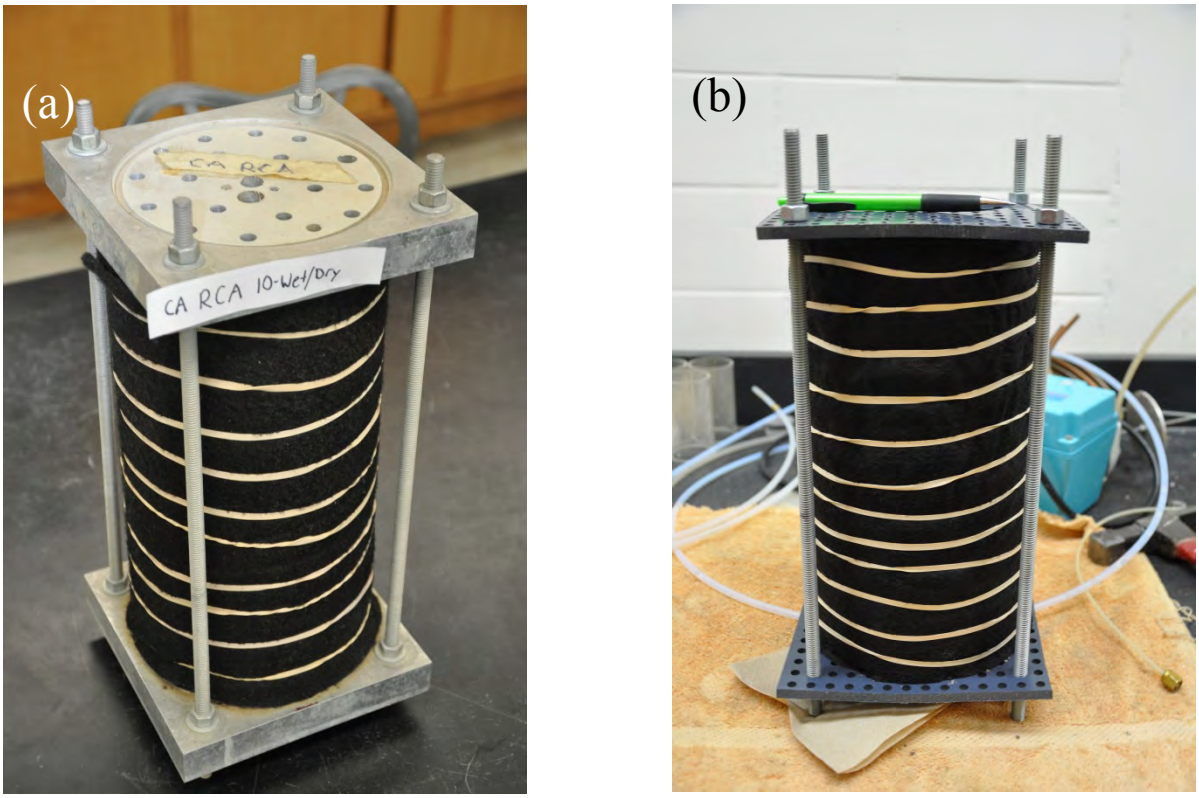

Figure 5.8 (a) Aluminum Wet/Dry Apparatus for RCA, Class 5, and Basalt Specimens; (b) PVC Wet/Dry Apparatus for RAP

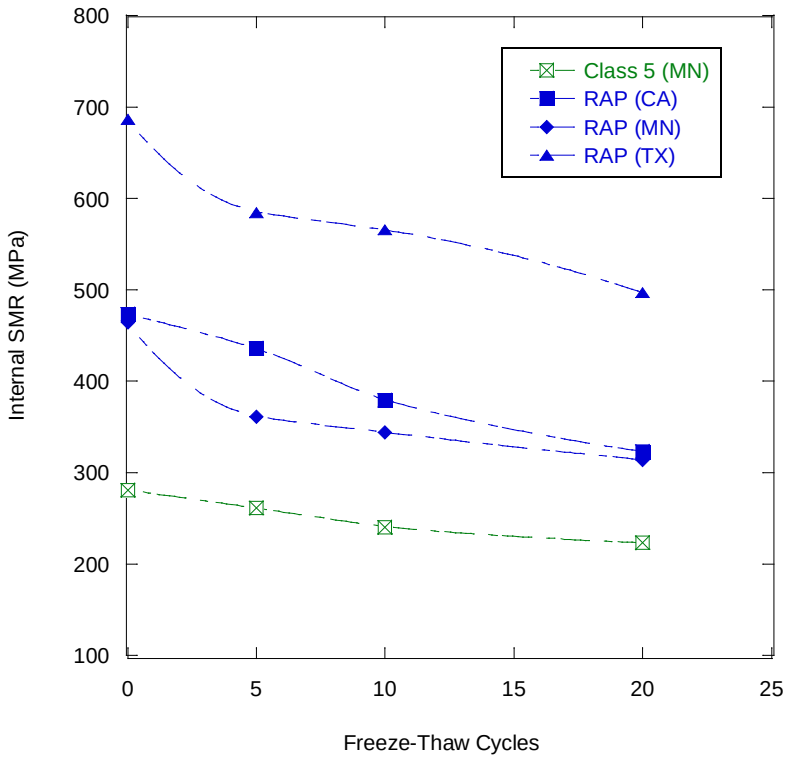

Figure 5.9 Summary Resilient Modulus (SRM) of RAP and Class 5 Aggregate after 0, 5, 10 and 20 Freeze-Thaw Cycles

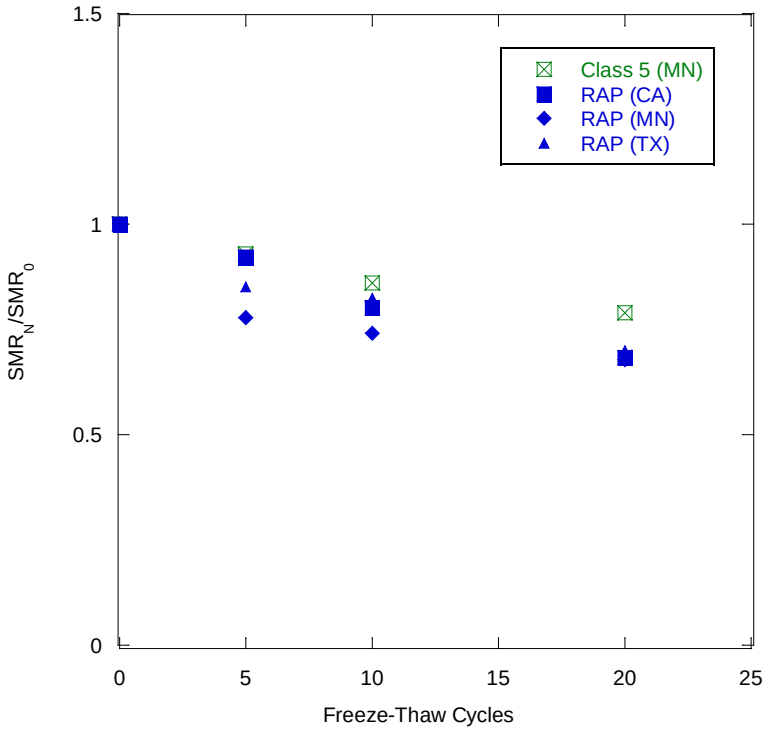

Figure 5.10 Normalized Summary Resilient Modulus (SRM) of RAP and Class 5 Aggregate after 0, 5, 10 and 20 Freeze-Thaw Cycles

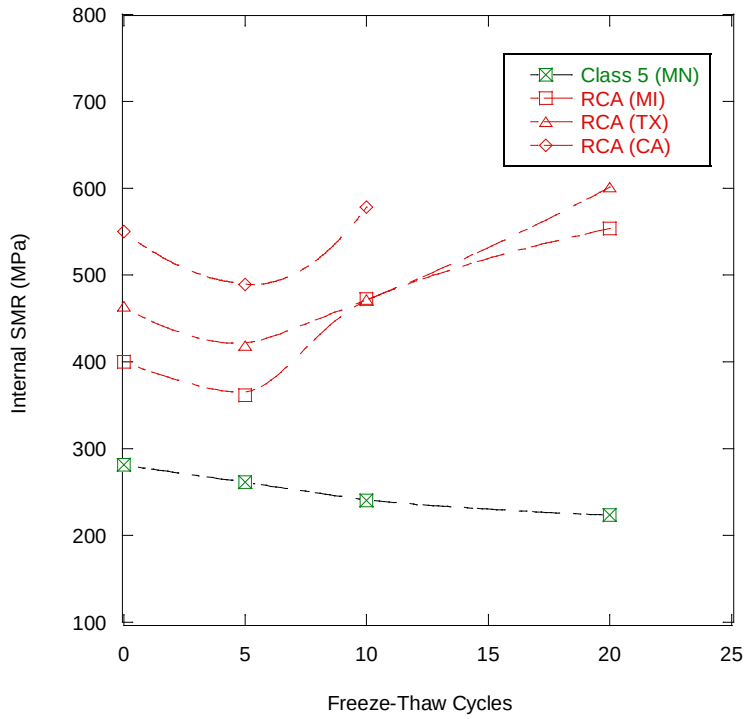

Figure 5.11 Normalized Summary Resilient Modulus (SRM) of RCA and Class 5 Aggregate after 0, 5, 10 and 20 Freeze-Thaw Cycles

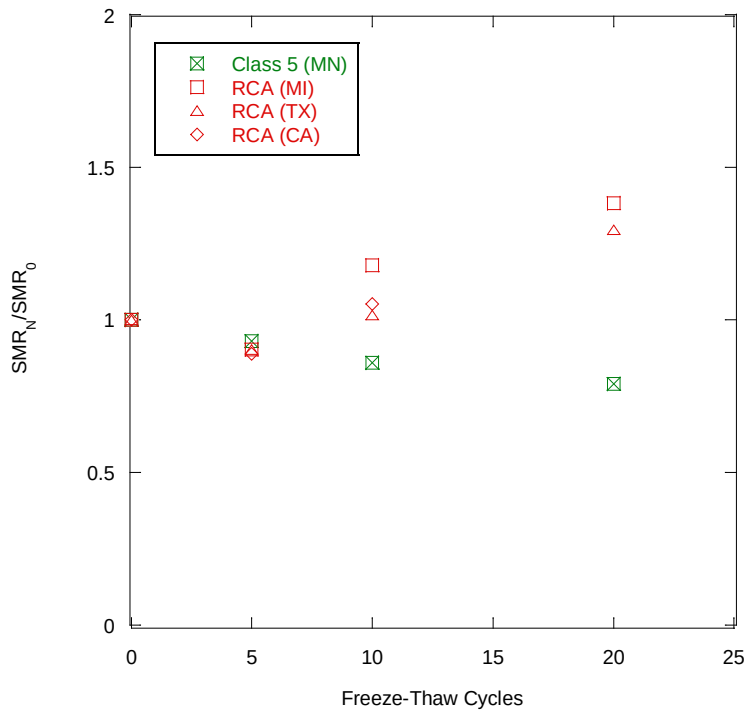

Figure 5.12 Normalized Summary Resilient Modulus (SRM) of RCA and Class 5 Aggregate after 0, 5, 10 and 20 Freeze-Thaw Cycles

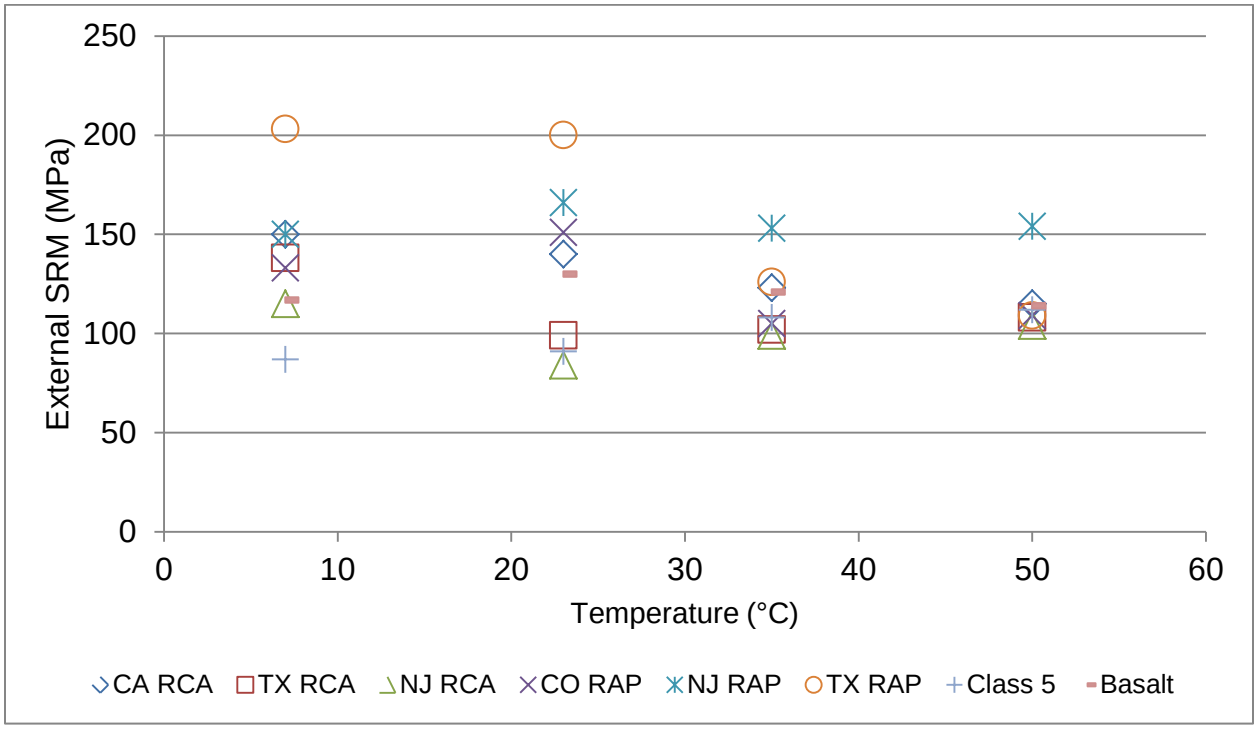

Figure 5.13 External LVDT Recorded NCHRP SRM Results at Varying Temperatures

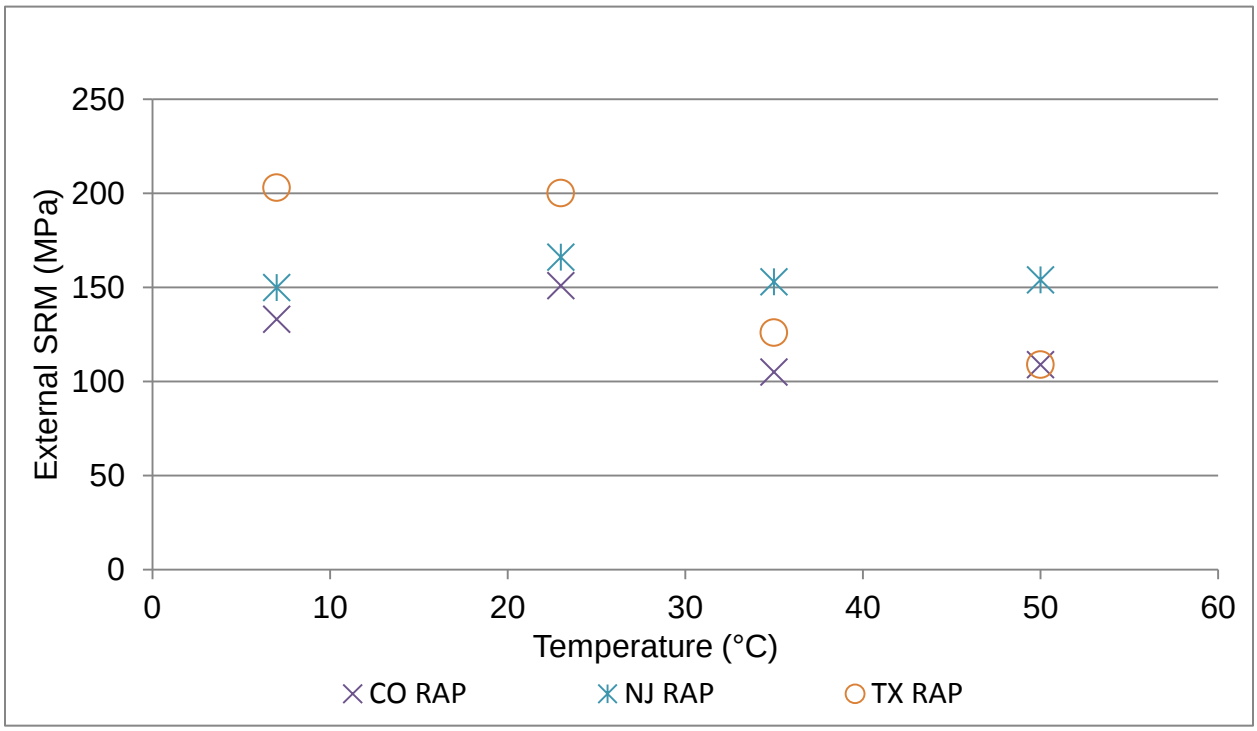

Figure 5.14 External LVDT Recorded NCHRP SRM Results of RAP at Varying Temperatures

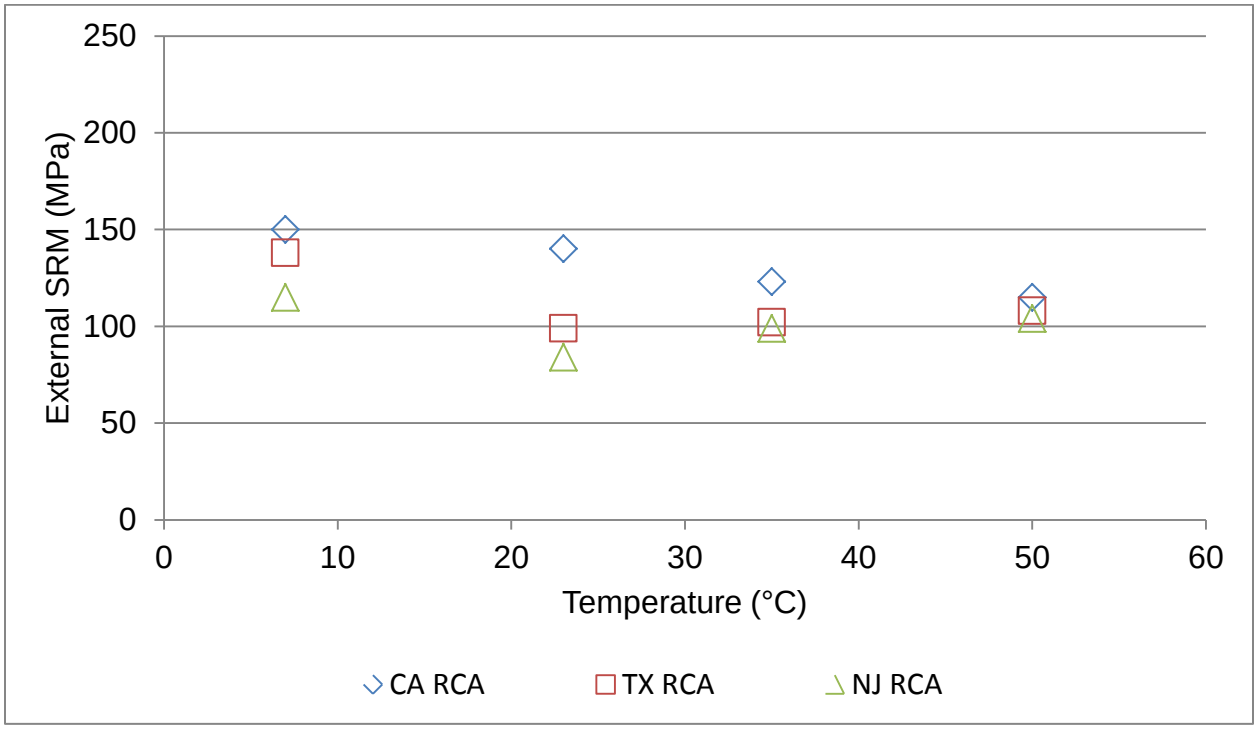

Figure 5.15 External LVDT Recorded NCHRP SRM Results of RCA at Varying Temperatures

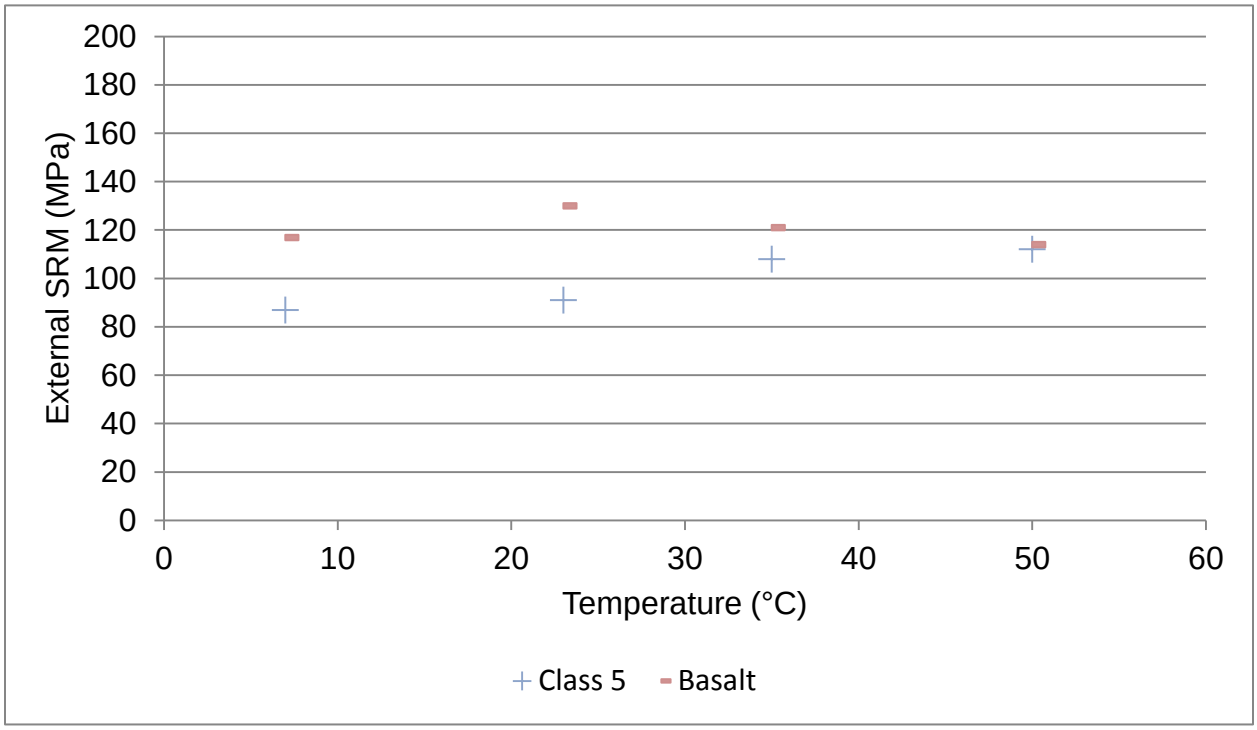

Figure 5.16 External LVDT Recorded NCHRP SRM Results of Natural Aggregate at Varying Temperatures

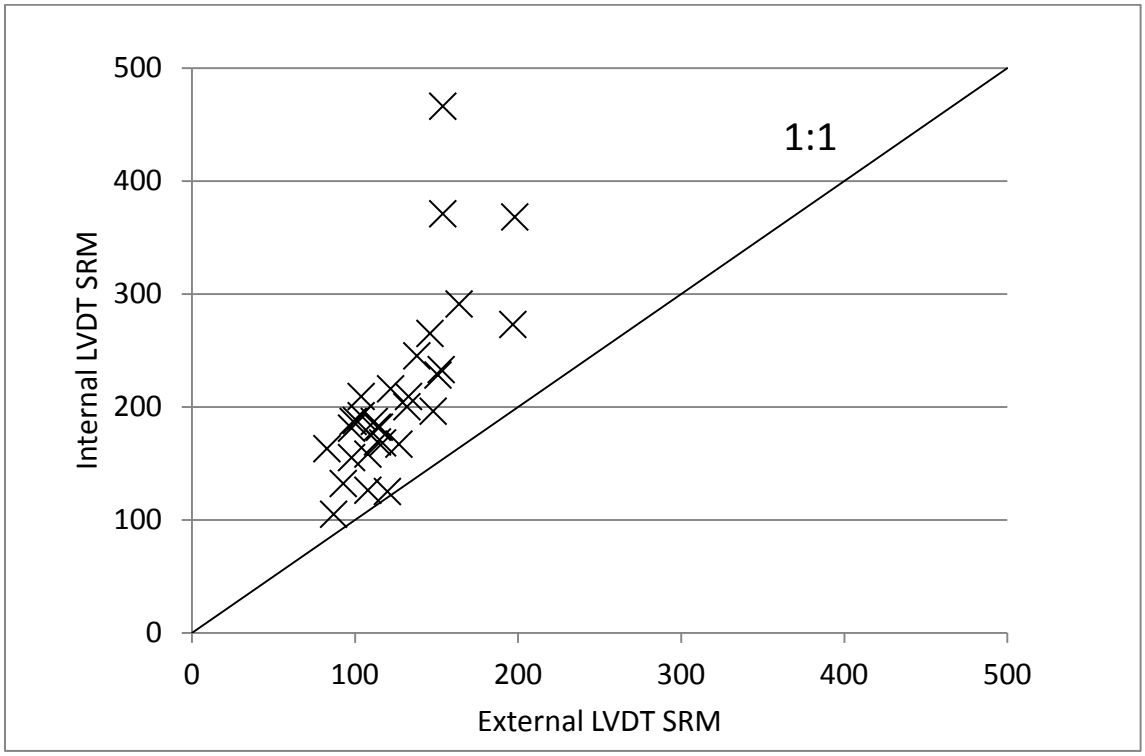

Figure 5.17 1:1 Comparison of Internal SRM and External SRM (NCHRP Model) at 23 °C

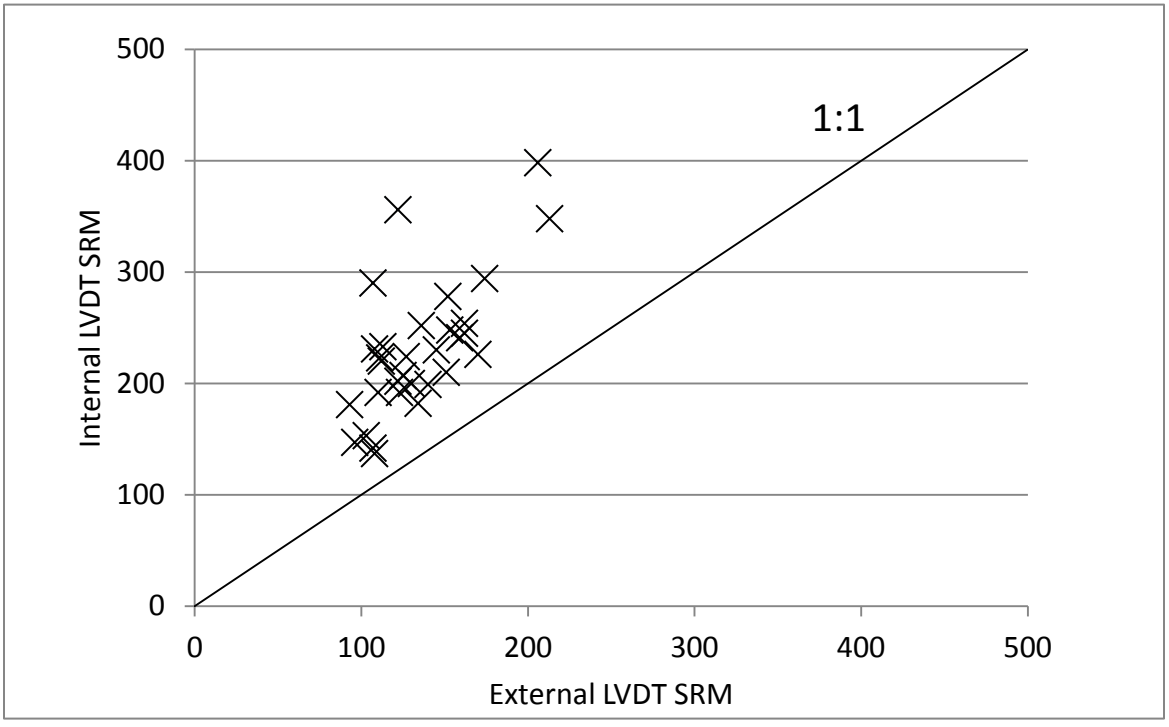

Figure 5.18 1:1 Comparison of Internal SRM and External SRM (Power Model) at 23 °C

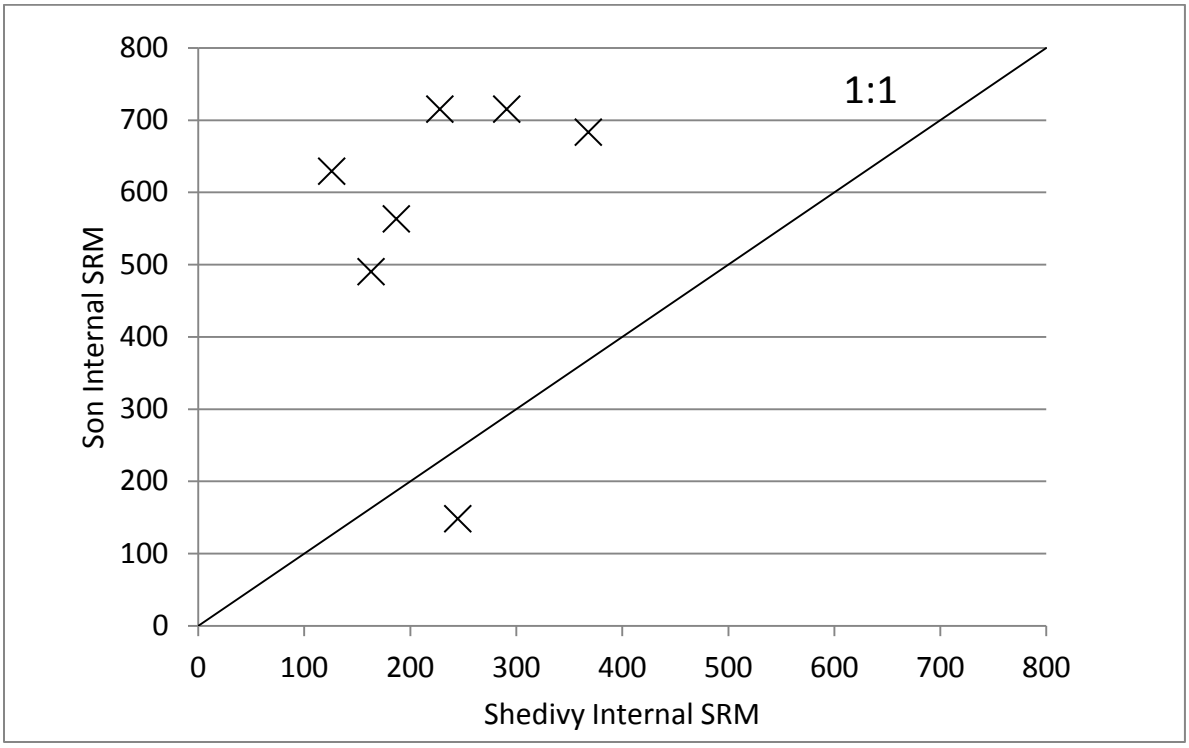

Figure 5.19 1:1 Comparison of Shedivy's Internal SRM and Son's Internal SRM

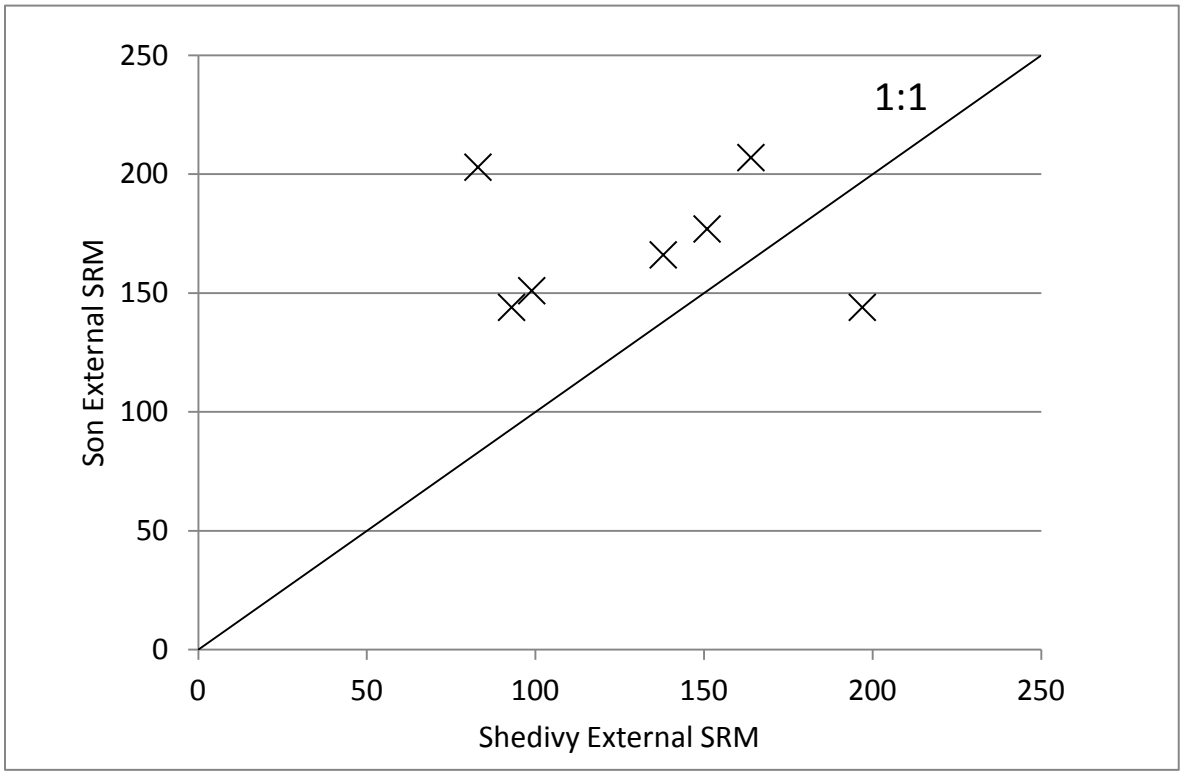

Figure 5.20 1:1 Comparison of Shedivy's External SRM and Son's External SRM

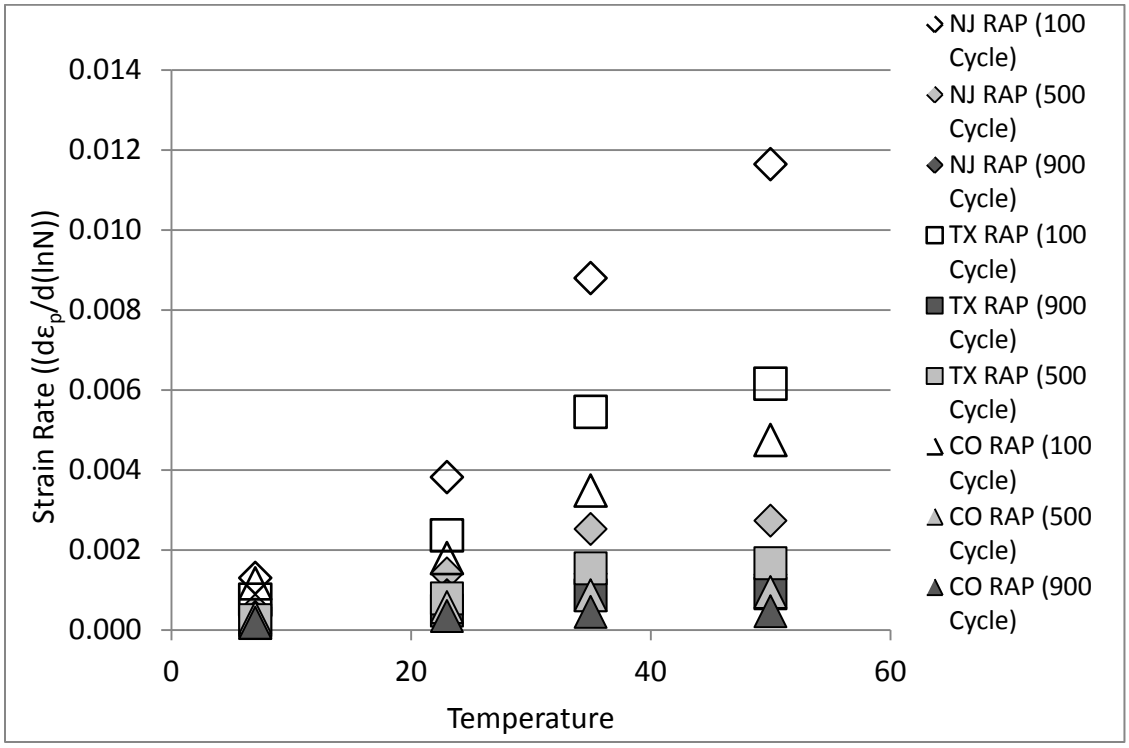

Figure 5.21 RAP Strain Rate at Varying Temperatures for 100, 500, and 900 Cycles of the 1st Sequence (Conditioning Phase)

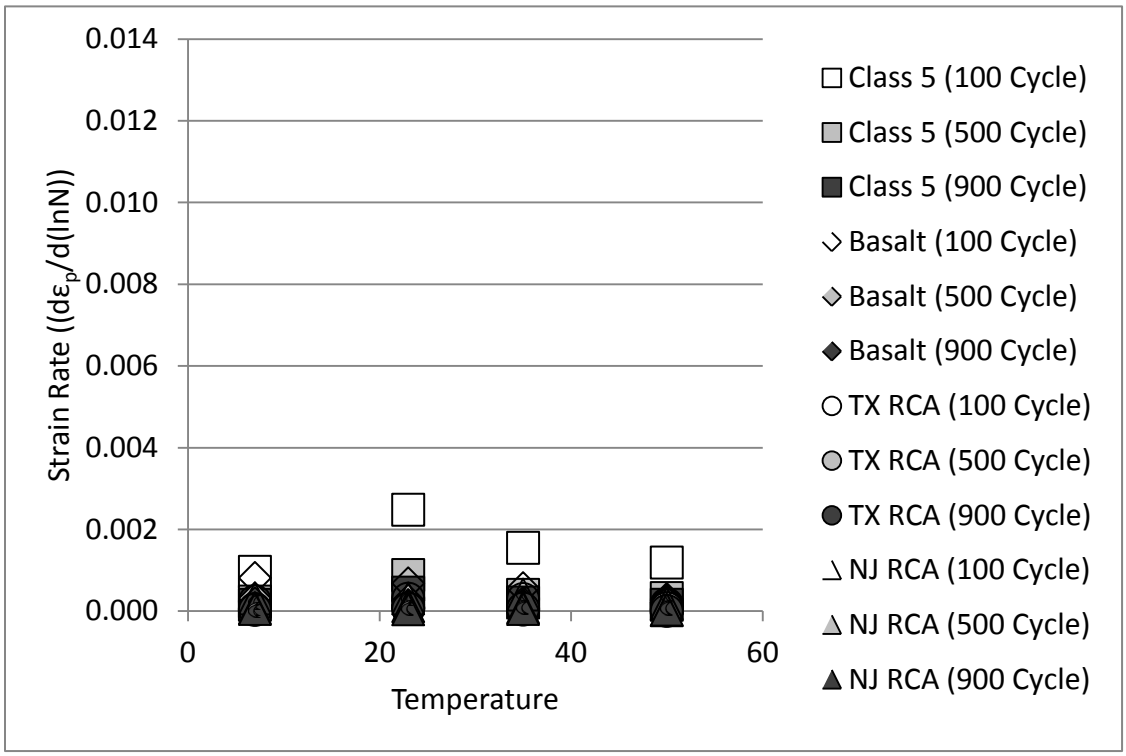

Figure 5.22 RCA and Natural Aggregate Strain Rate at Varying Temperatures for 100, 500, and 900 Cycles of the 1st Sequence (Conditioning Phase)

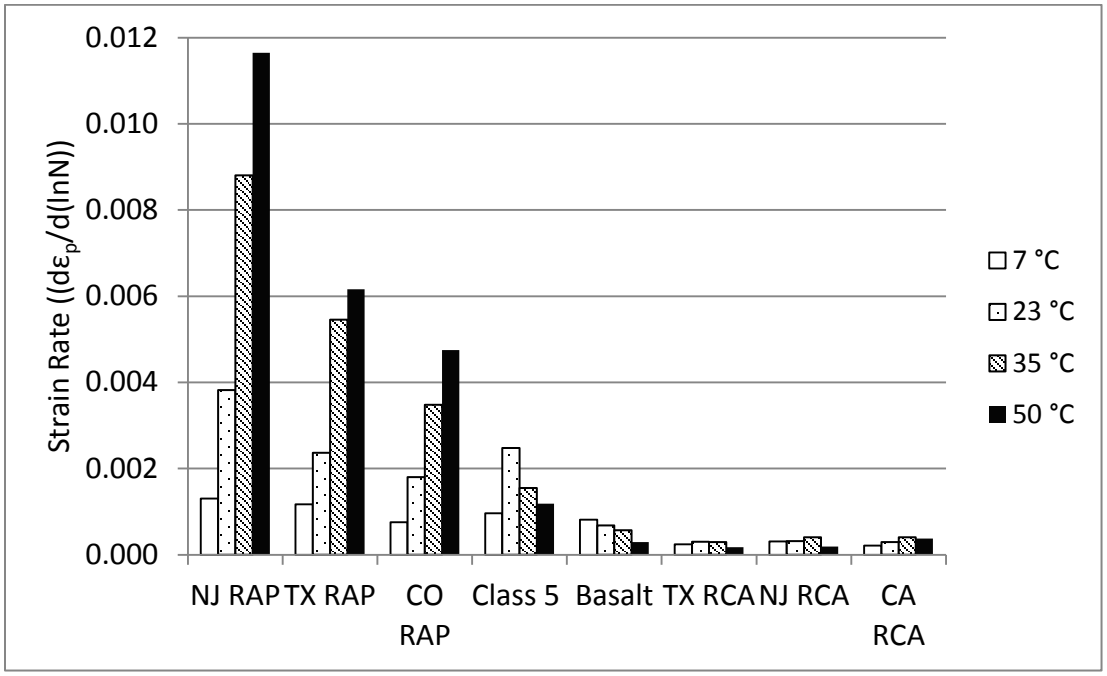

Figure 5.23 Strain Rates for Each Material at Varying Temperatures after the First 100 Cycles of the Mr Test

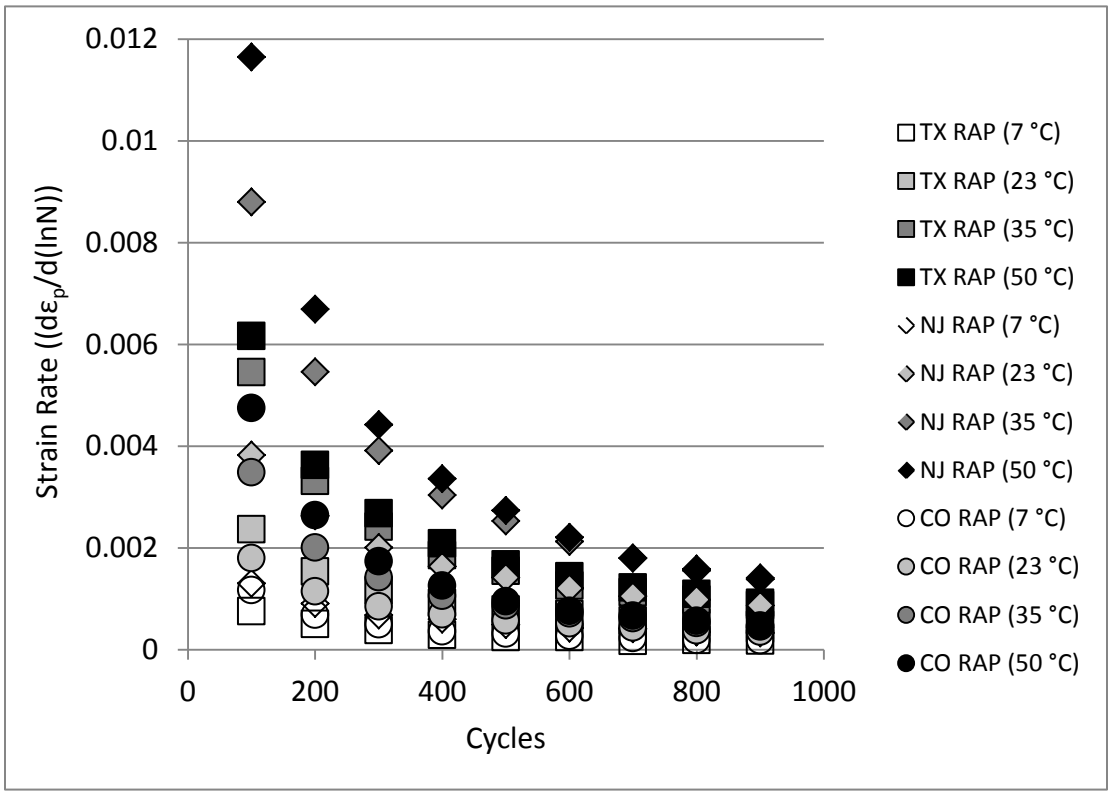

Figure 5.24 RAP Strain Rates at Varying Temperatures during the 1st Sequence (Conditioning Phase)

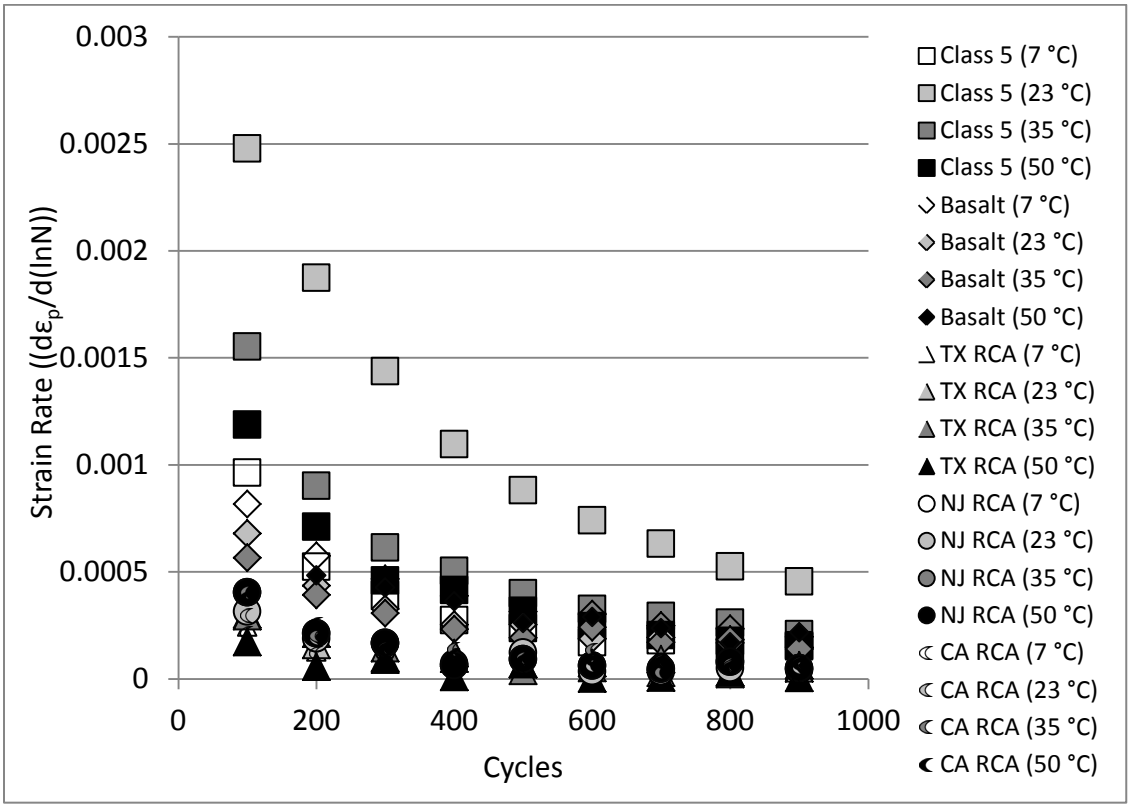

Figure 5.25 RCA and Natural Aggregate Strain Rates at Varying Temperatures during the 1st Sequence (Conditioning Phase)

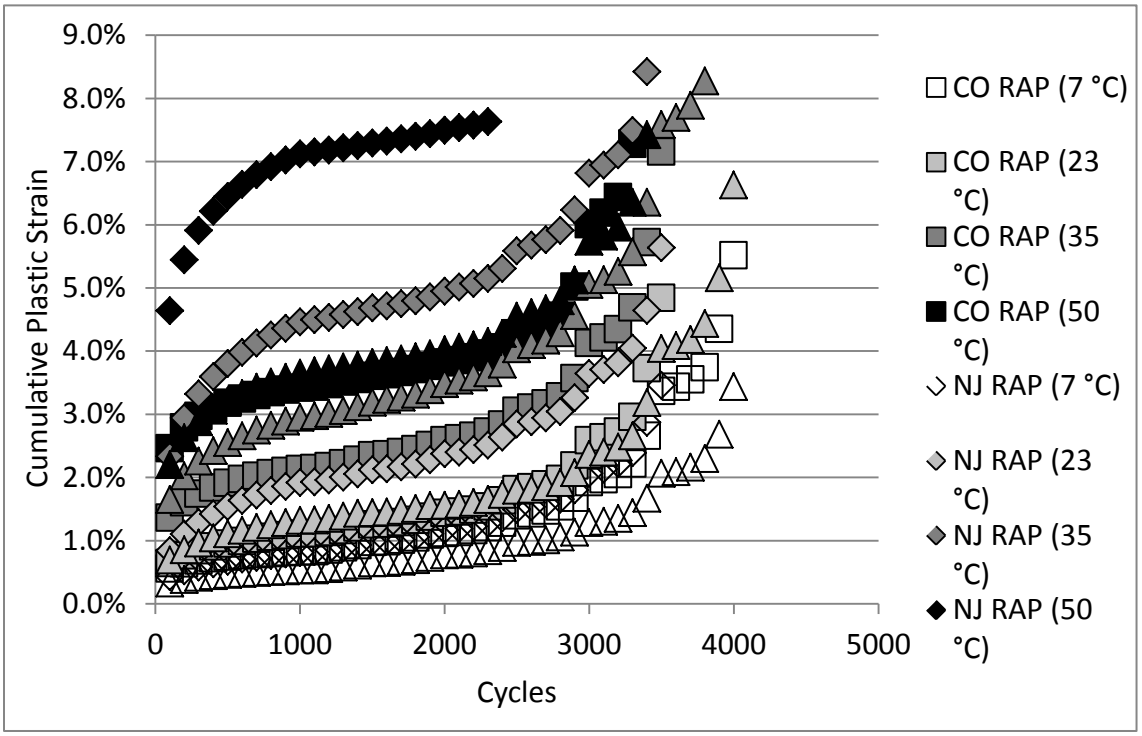

Figure 5.26 RAP Cumulative Plastic Strain throughout Mr Test at Varying Temperatures

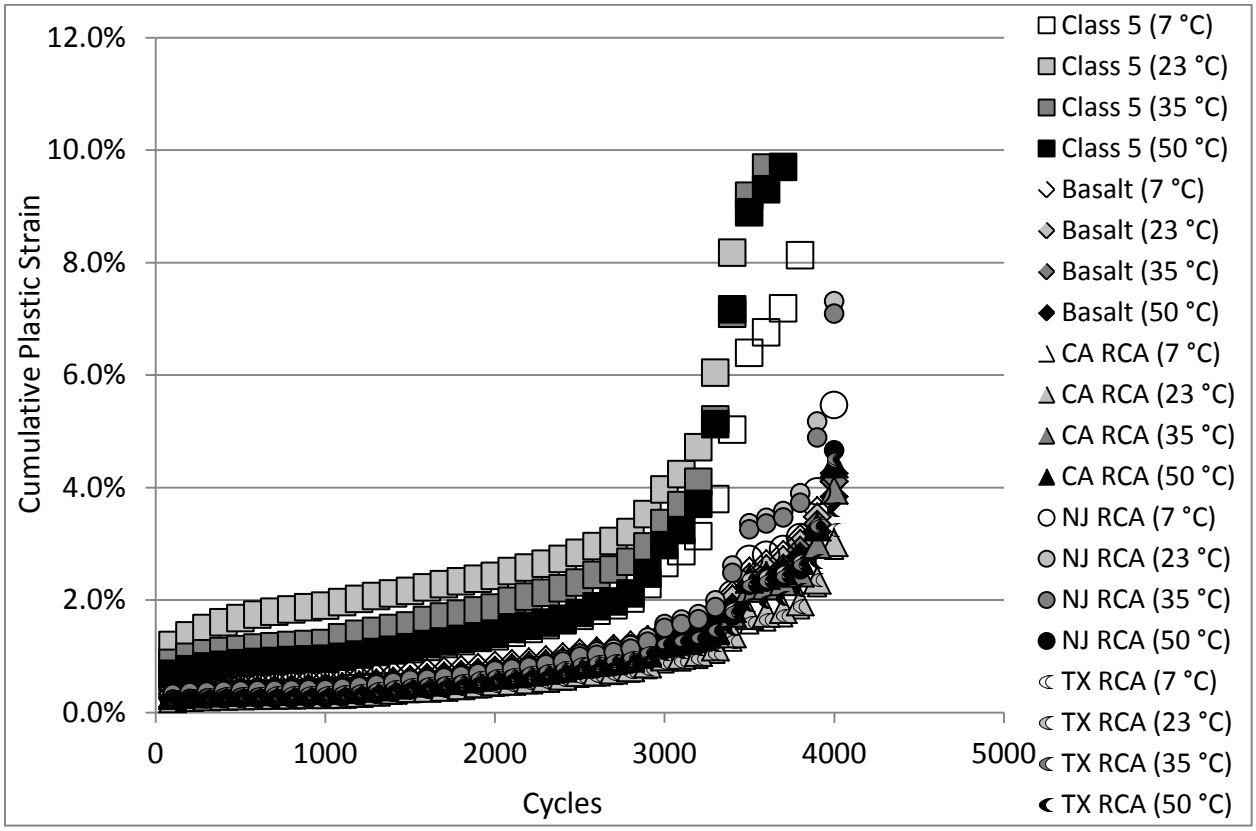

Figure 5.27 RCA and Natural Aggregate Cumulative Plastic Strain throughout Mr Test at Varying Temperatures

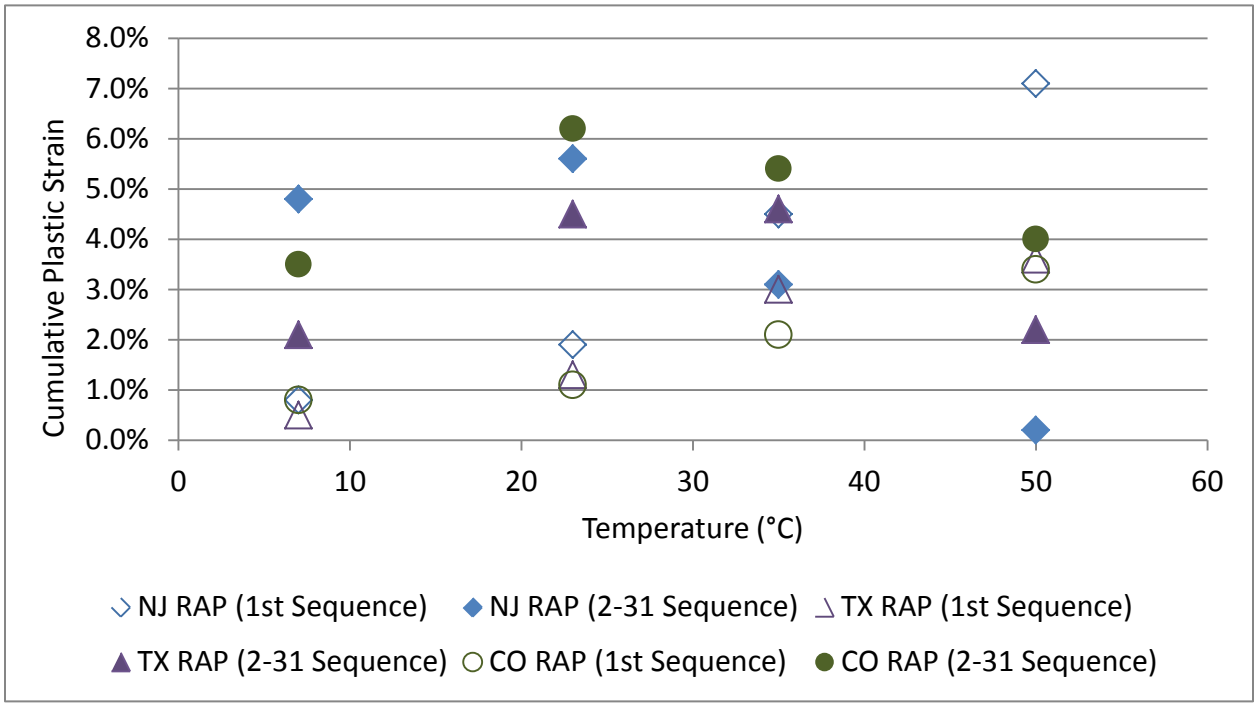

Figure 5.28 1st and 2nd-31st Sequence RAP Plastic Strain

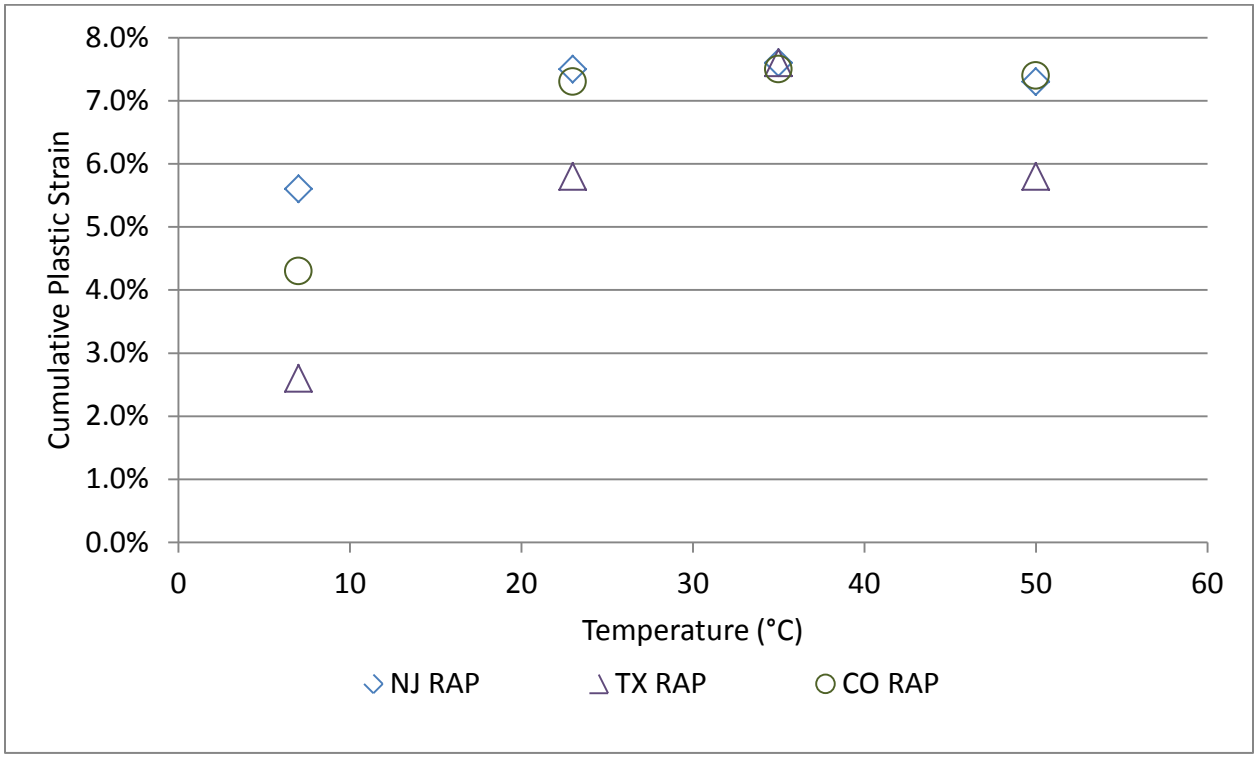

Figure 5.29 Total RAP Plastic Strain

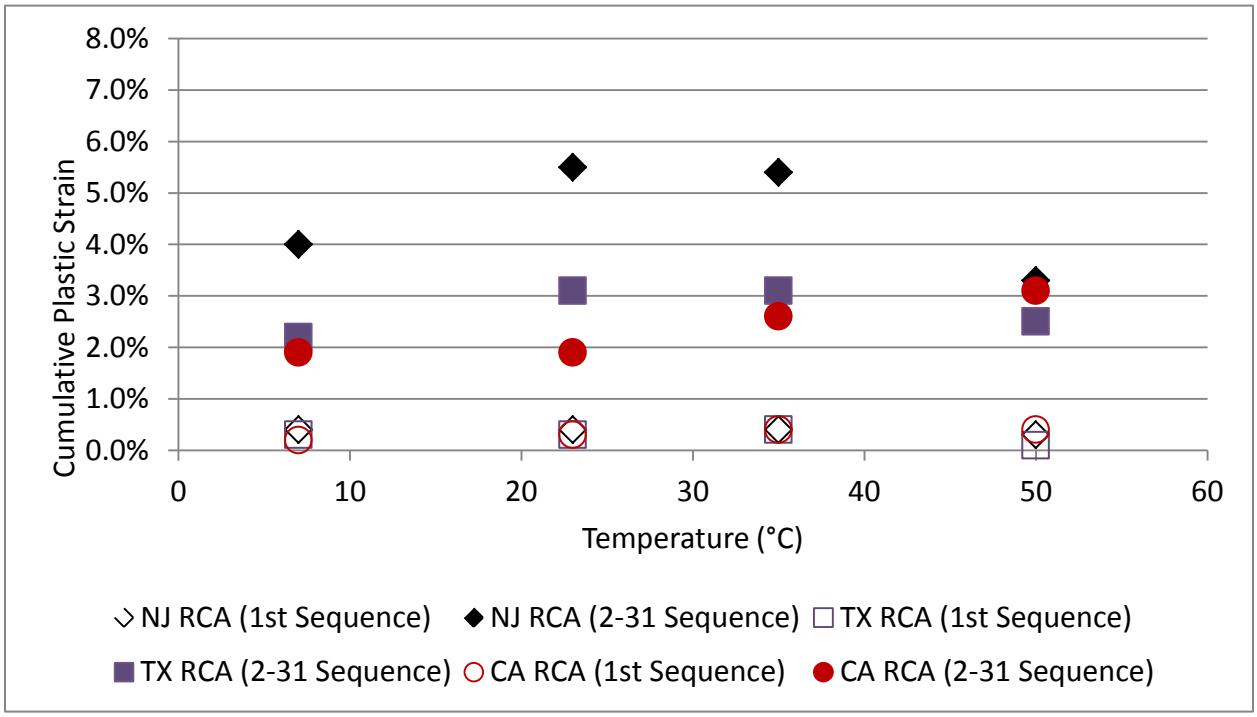

Figure 5.30 1st and 2nd-31st Sequence RCA Plastic Strain

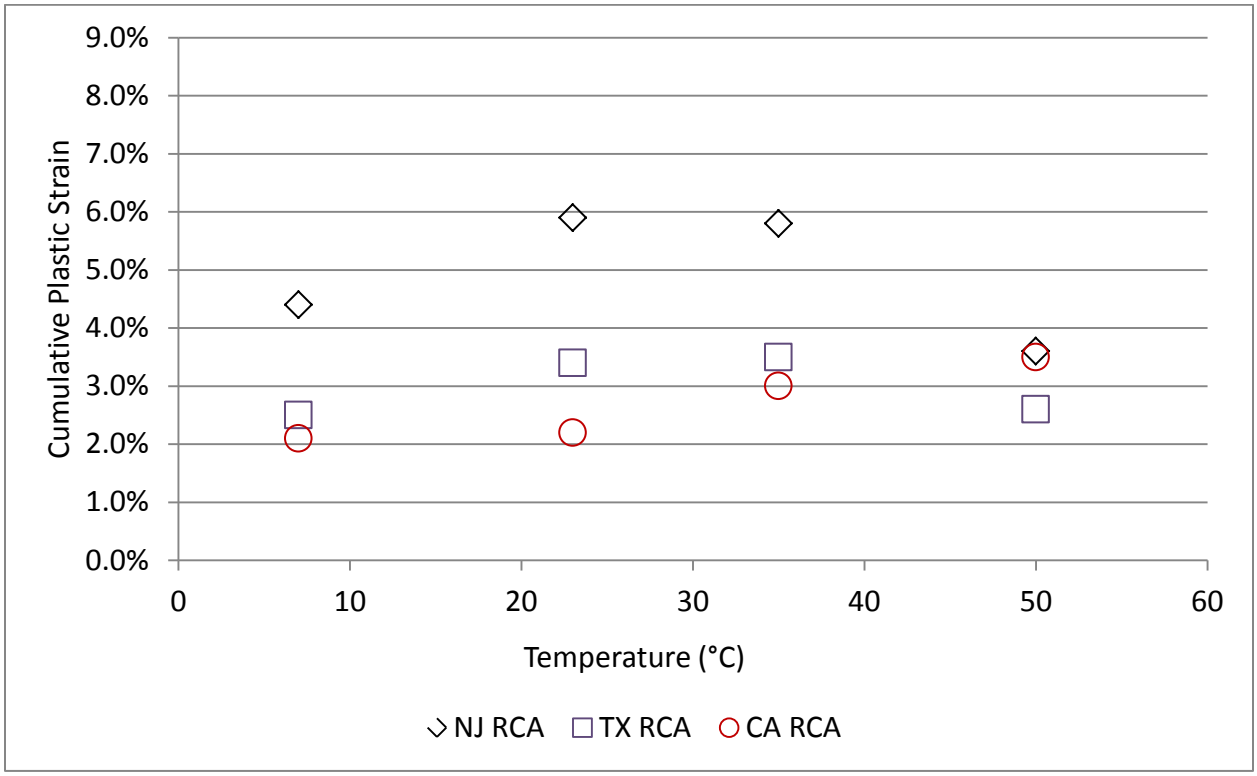

Figure 5.31 Total RCA Plastic Strain

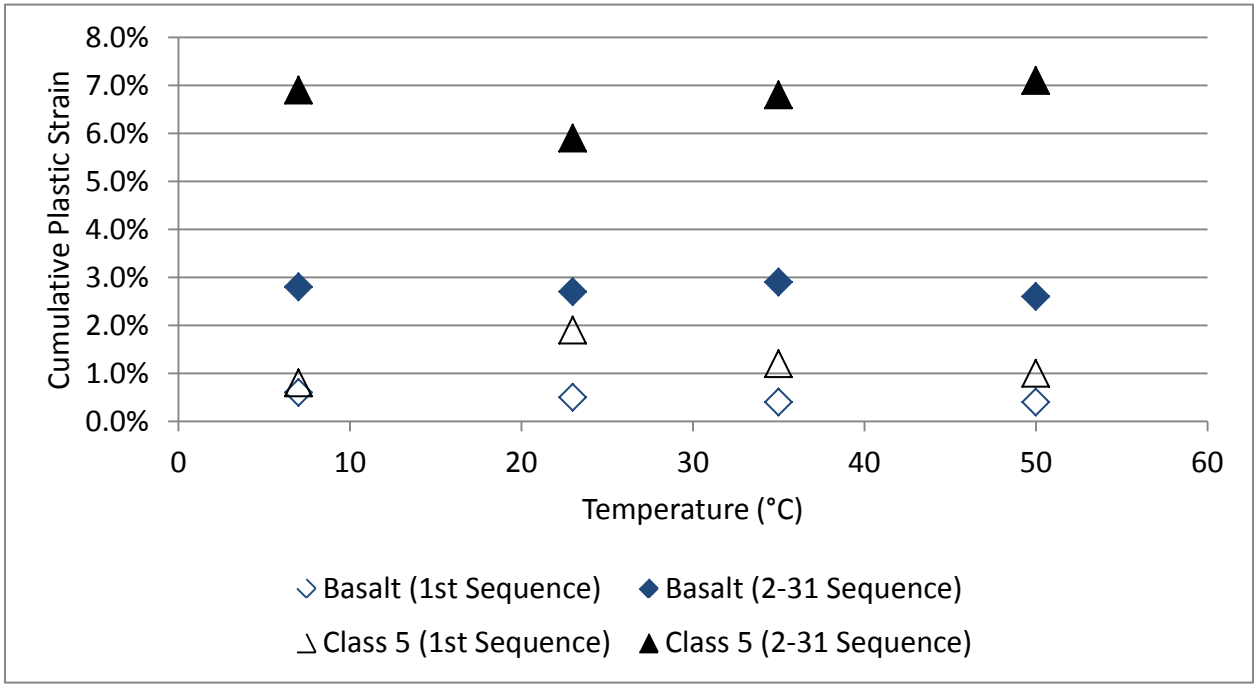

Figure 5.32 1st and 2nd-31st Natural Aggregate Plastic Strain

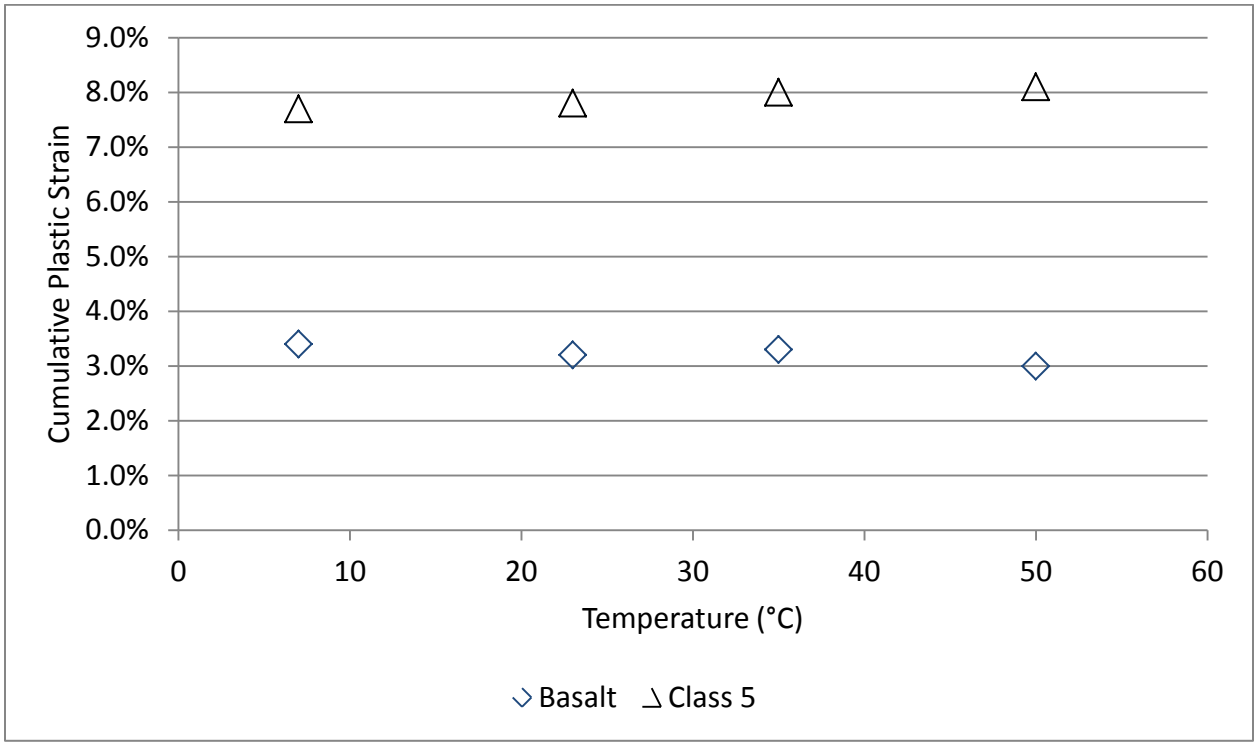

Figure 5.33 Total Natural Aggregate Plastic Strain

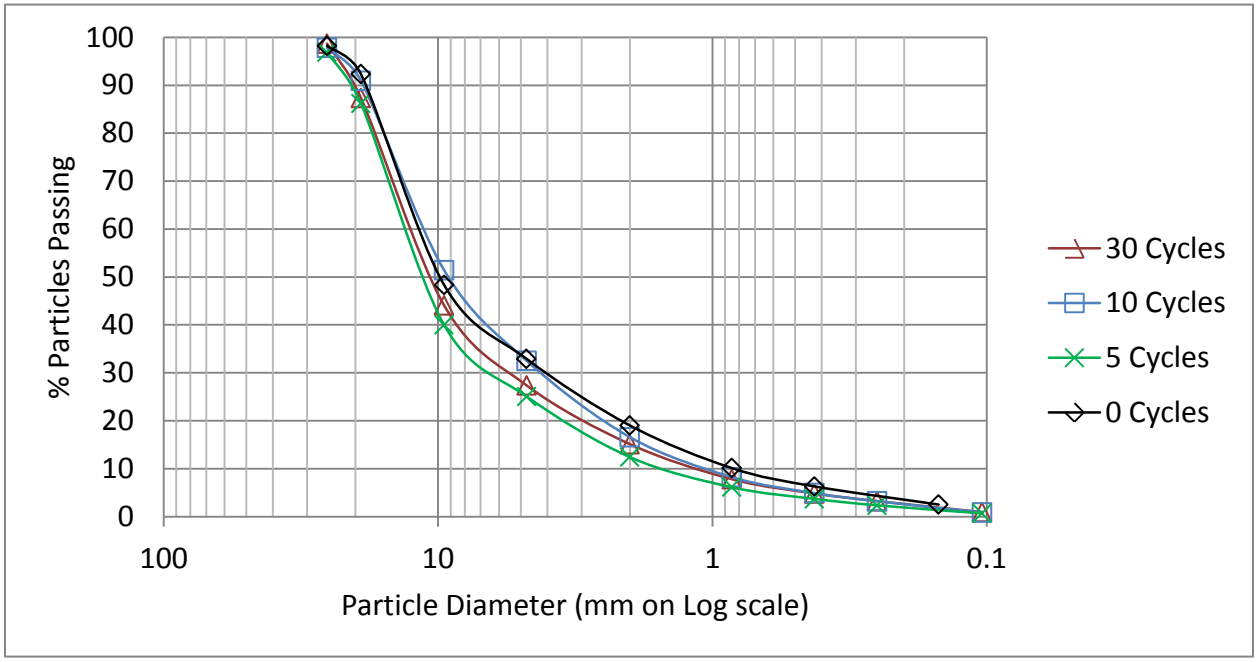

Figure 5.34 Basalt Wet/Dry Particle Size Distributions

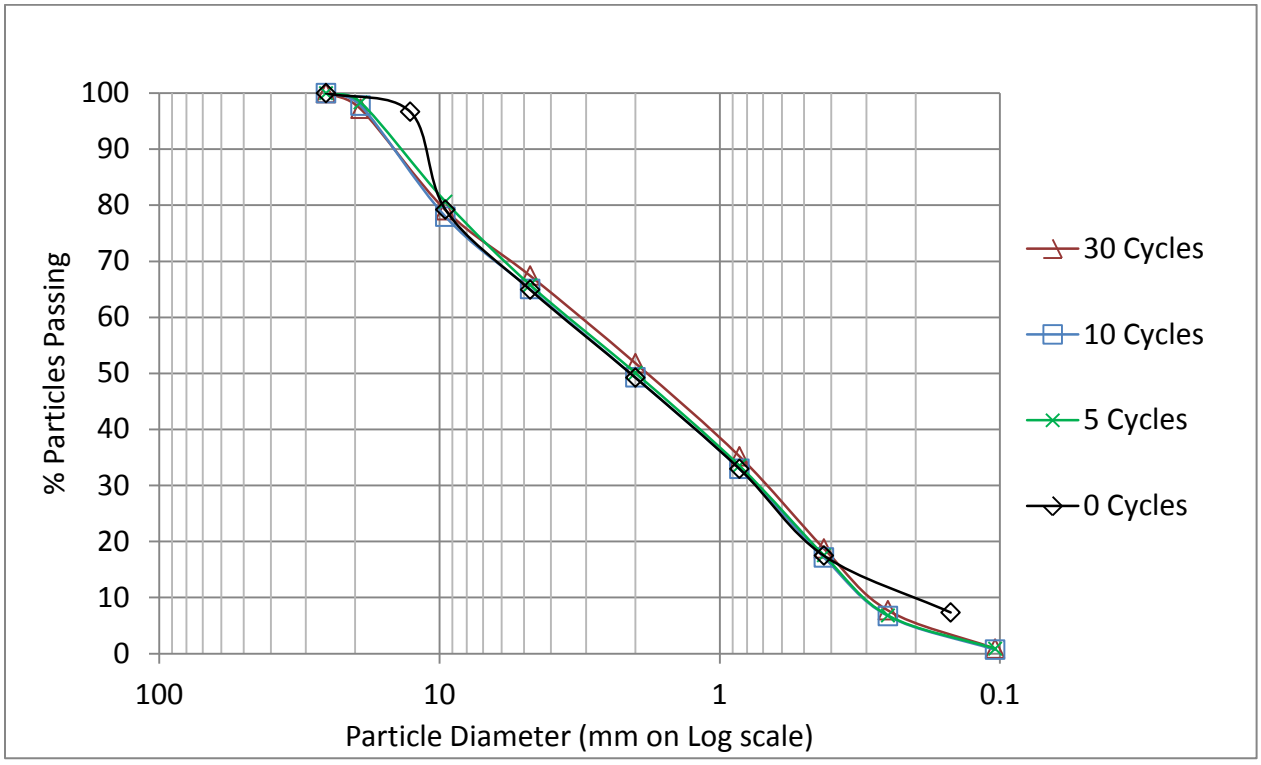

Figure 5.35 Class 5 Wet/Dry Particle Size Distributions

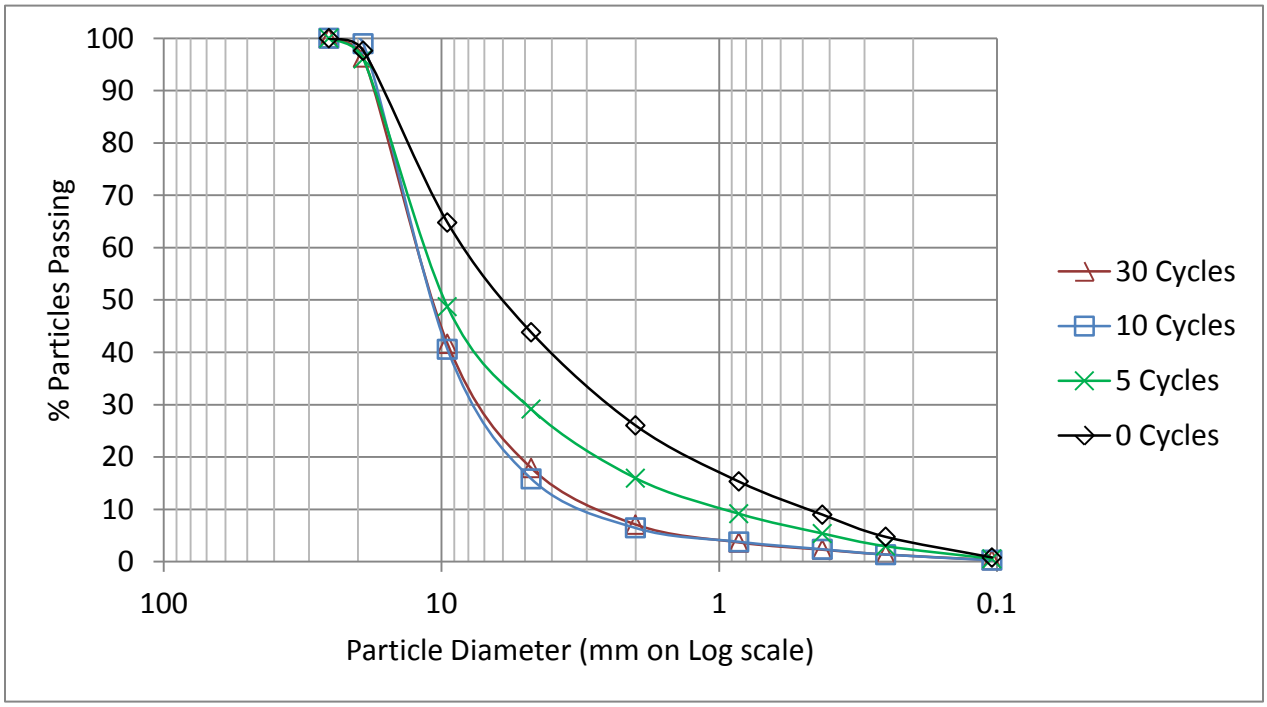

Figure 5.36 CA RCA Wet/Dry Particle Size Distribution

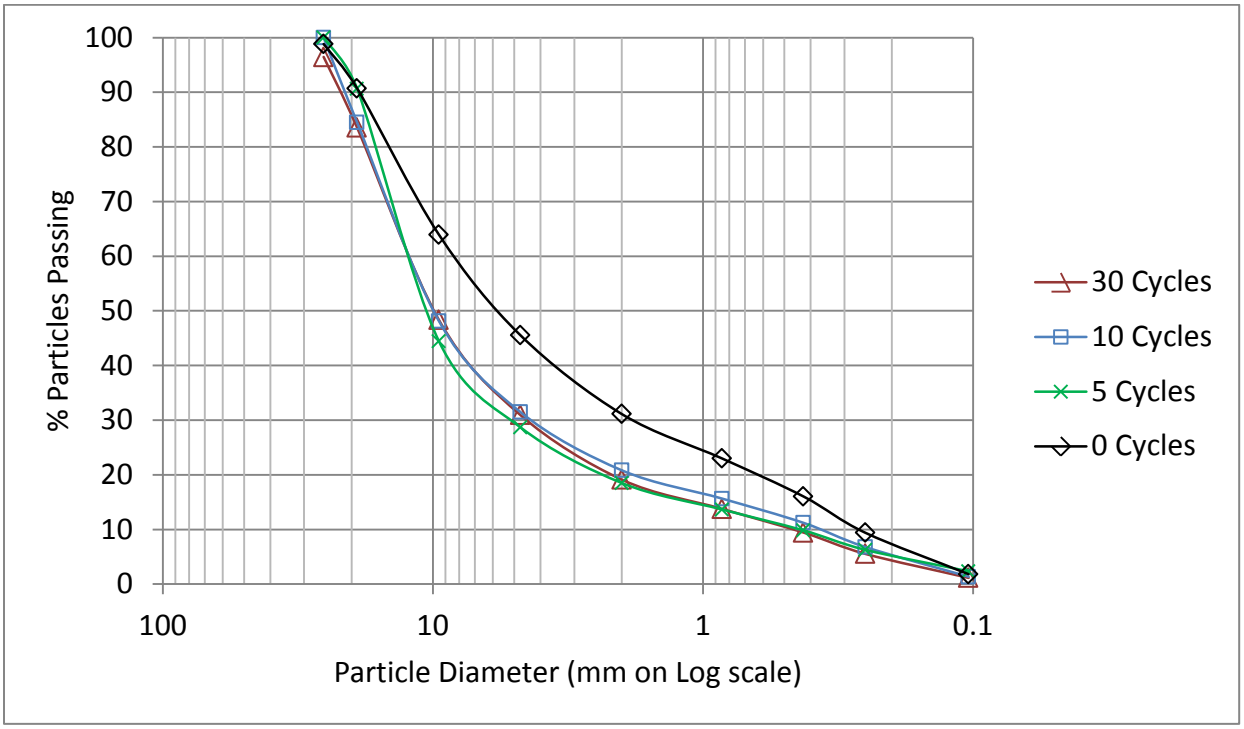

Figure 5.37 TX RCA Wet/Dry Particle Size Distributions

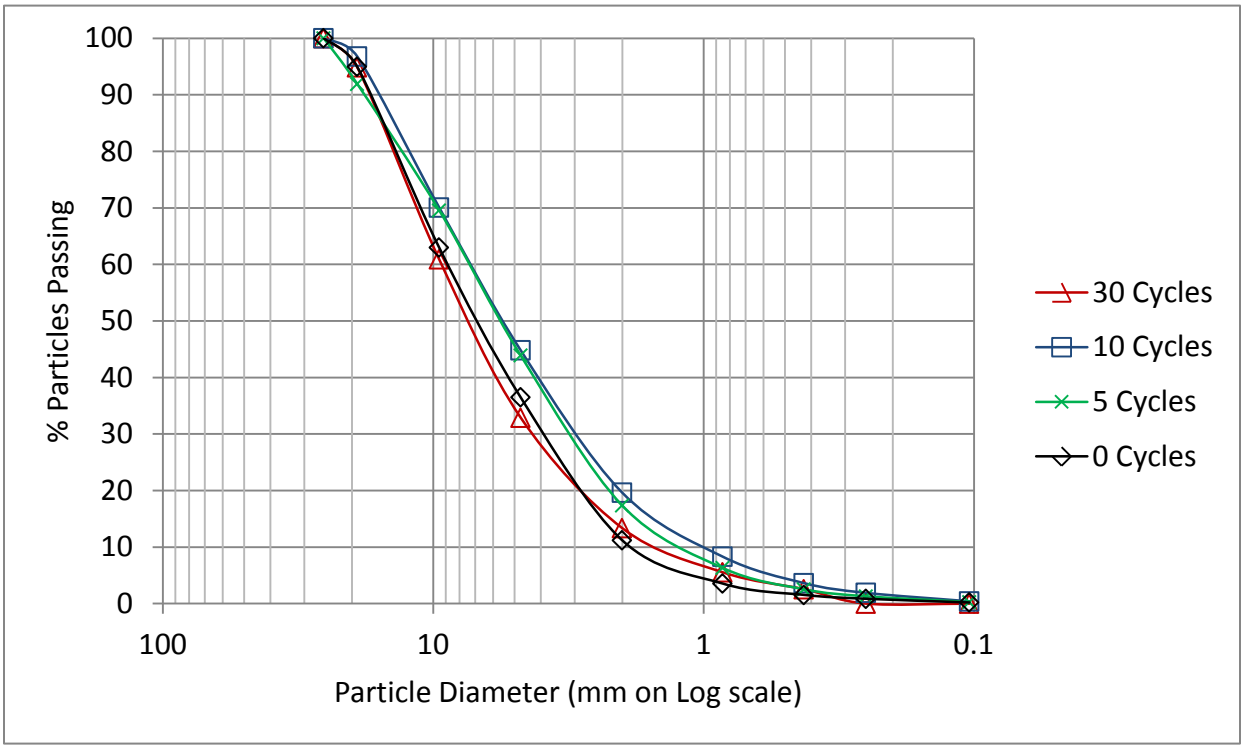

Figure 5.38 TX RAP Wet/Dry Particle Size Distributions

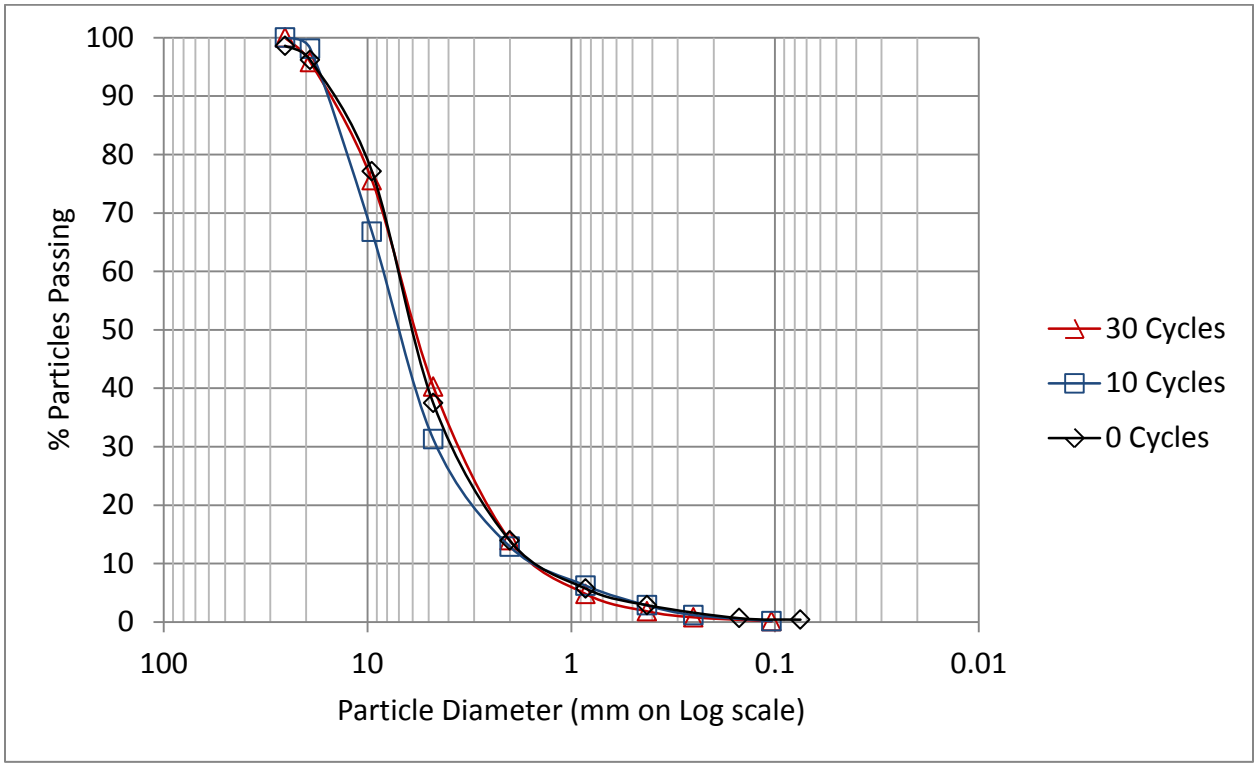

Figure 5.39 NJ RAP Wet/Dry Particle Size Distributions

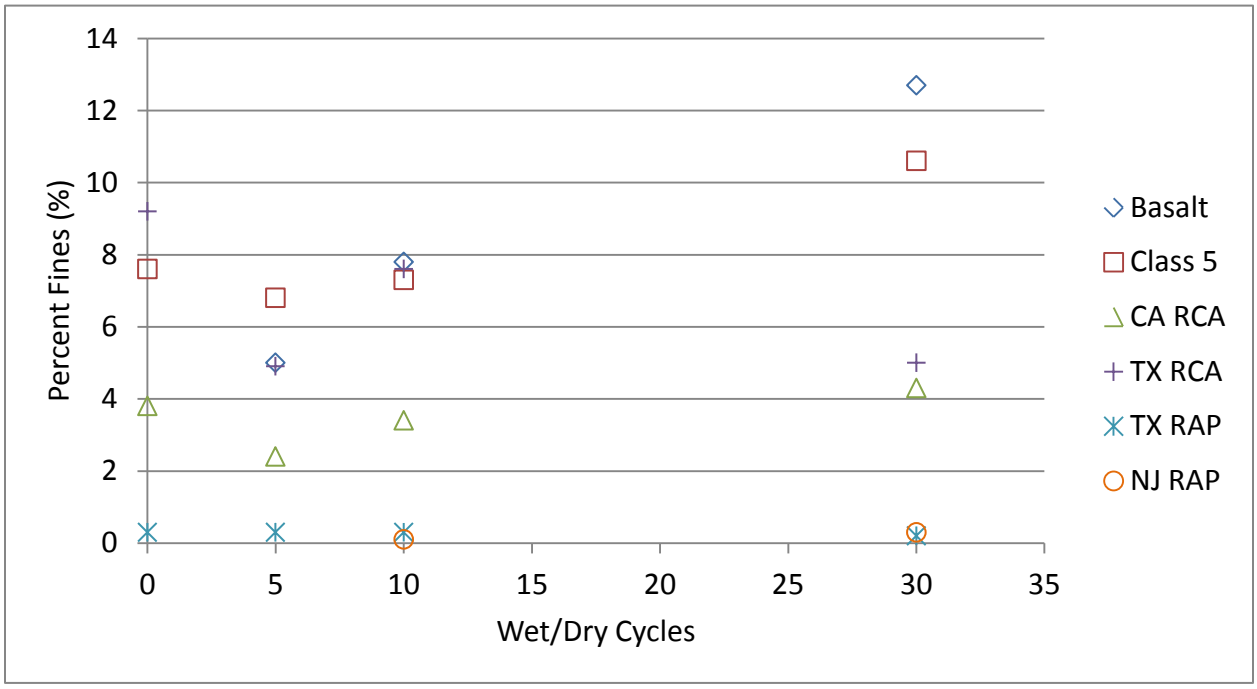

Figure 5.40 Percent Fines at Varying Wet/Dry Cycles

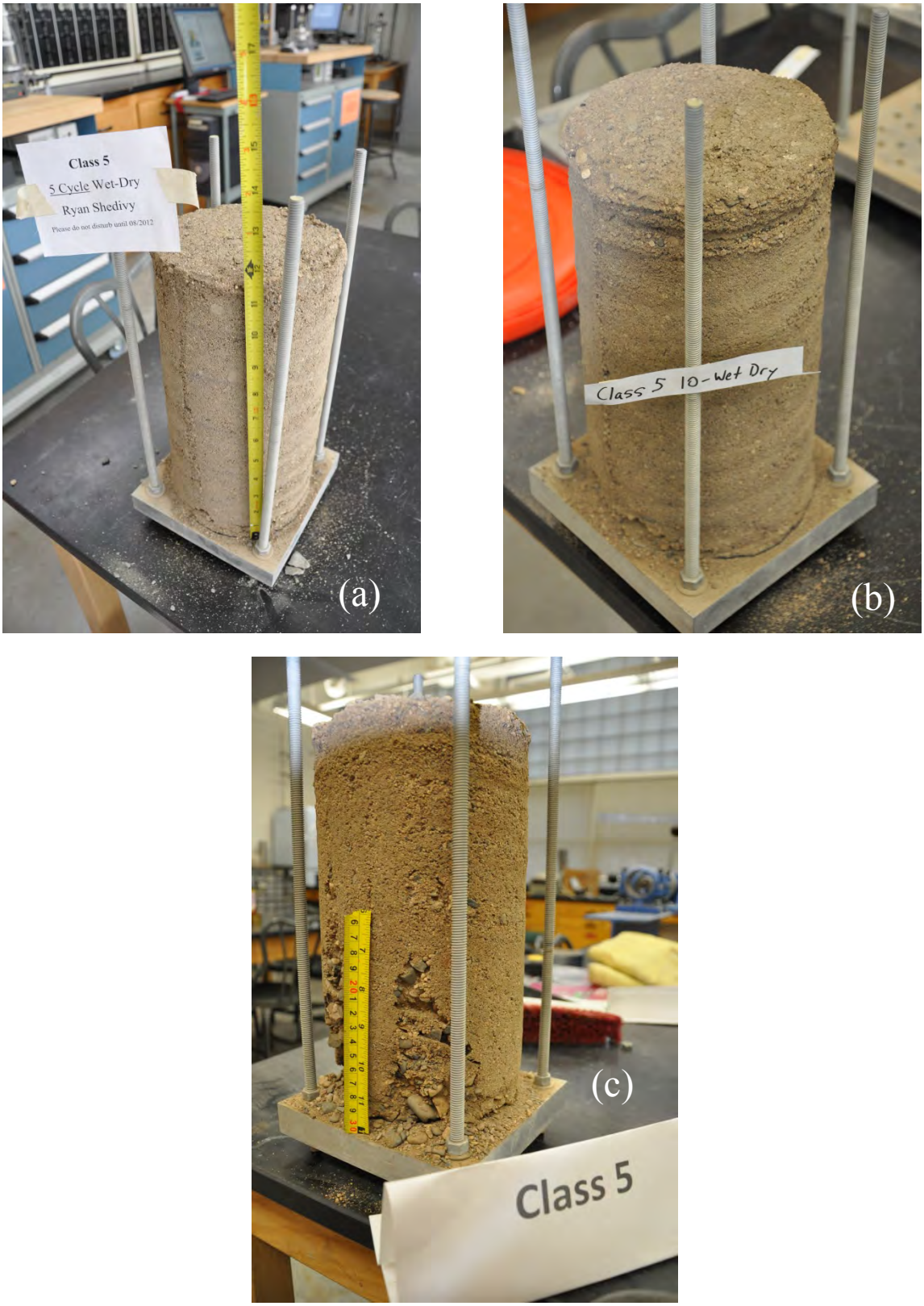

Figure 5.41 Class 5 after Wet/Dry Cycles: (a) 5 Cycles; (b) 10 Cycles; (c) 30 Cycles

Figure 5.42 African Basalt after Wet/Dry Cycles: (a) 5 Cycles; (b) 10 Cycles; (c) 30 Cycles

Figure 5.43 CA RCA after Wet/Dry Cycles: (a) 5 Cycles; (b) 10 Cycles; (c) 30 Cycles

Figure 5.44 TX RCA after Wet/Dry Cycles: (a) 5 Cycles; (b) 10 Cycles; (c) 30 Cycles

Figure 5.45 TX RAP after Wet/Dry Cycles: (a) 5 Cycles; (b) 10 Cycles; (c) 30 Cycles

Figure 5.46 NJ RAP after Wet/Dry Cycles: (a) 5 Cycles; (b) 10 Cycles; (c) 30 Cycles

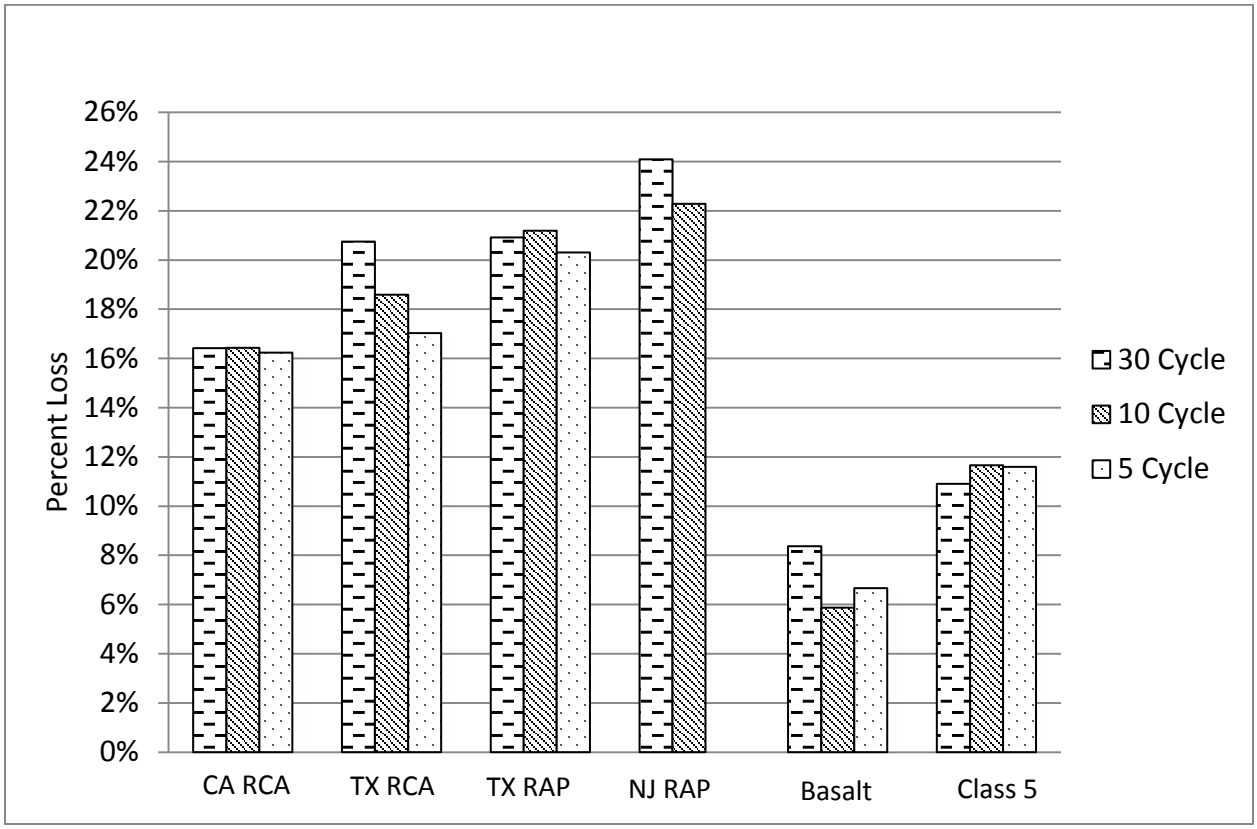

Figure 5.47 Wet/Dry Micro-Deval Results

6. Unsaturated Hydraulic Characteristics of Recycled and Natural Pavement Aggregate

6.1 Introduction

Recycled pavement materials including recycled concrete aggregate (RCA), recycled asphalt pavement (RAP), and recycled pavement material (RPM) are widely used in recent decades as a base course because of their environmental stewardship and economic benefits. Past studies indicate that RCA, RAP and RPM can provide high stiffness and durability suitable for using as a mixture or full replacement for natural coarse aggregates (Blankenagel and Guthrie 2006; Bennert et al. 2000). However, the hydraulic properties, especially for soil-water characteristic curves (SWCC) and the unsaturated hydraulic conductivity (K_ψ) of the recycled pavement aggregates have not been thoroughly investigated.

Hydraulic properties of base course are crucial parameters affecting the long-term performance and service life of pavement (Cedergren 1988). Water entering into the pavement structure can induce excess pore pressure, and consequently results in stiffness reduction for natural base and subgrade. The Mechanistic-Empirical Pavement Design Guide (MEPDG) realized effect of moisture in pavement structure, and has proposed the model to adjust resilient modulus as the function of degree of saturation. The MEPDG has also proposed the Pedotransfer function to predict SWCC of conventional aggregate based on gradation and index properties. However, RCA, RAP, and RPM are generated from different types of material tending to provide different degree of water repellency or hydrophobicity characteristics. For instance, RCA obtained from demolished concrete and natural aggregate tend to be highly hydrophilic materials while RAP derived from old asphalt pavement tends to perform as a strong hydrophobic material. RPM, originating from crushed old asphalt surface mixed with base course or subgrade materials, has a tendency to be hydrophobic. The apparent contact angle of the RCA and natural aggregate tends to be zero, while the contact angle of RAP and RPM tend to be larger than 90^o. Based on Physics principal, matric suction is the function of contact angle. As a result, the SWCC and K_ψ of RAP, RCA, RPM and conventional aggregate may perform differently although the recycled pavement aggregates have the similar grain size distribution.

The objectives of this chapter are (1) to determine unsaturated hydraulic properties including SWCC and K_ψ for compacted RCAs, RAPs, RPMs, Class 5, and lime stone used for base course; and (2) to compare two regression methods including using simultaneously SWCC and K_ψ data for regression analysis and using only SWCC data for regression (conventional method fix pore inter action term, L =0.5); and (3) to discuss the effect of the degree of water repellency and grain sized distribution on SWCC and K_ψ for recycled aggregate. The results of this study will be compared to those of the lime stone, basalt and Class 5, which are conventional aggregate used for conventional base course.

The hanging column test fitted with an air aspirator with a large-scale testing cell was used to determine SWCC, and multistep outflow method (MSO) was used to calculate the K_ψ for recycled and conventional aggregate. The degree of water repellency of water was characterized using water drop penetration time (WDPT) and measured apparent contact angle. The van

Genuchten (1980) and van Genuchten-Mualem (1980) equation were used to do a regression analysis for hydraulic parameters based on the least square method.

6.2 Background

6.2.1 *Water Characteristic Curve and Unsaturated Hydraulic Conductivity Prediction*

One of the most widely used for SWCC equation is the van Genuchten (1980) equation. The van Genuchten (1980) equation provides smooth sigmoid curves suitable for various types of soil, and requires three fitting parameters with physical meaning. The van Genuchten equation for SWCC is:

$$S_e = \frac{(\theta-\theta_r)}{(\theta_s-\theta_r)} = [1 + [\alpha\psi]^n]^{-m} \quad (6.1)$$

Where S_e is the normalized volumetric water content, θ is the volumetric water content, θ_r and θ_s are the residual and saturated volumetric water contents, ψ is soil suction, α (>0) is related to the inverse of air entry pressure, n (>1) relates to pore size distribution, and m is frequently defined as 1-1/ n.

The K_ψ can be predicted based on SWCC parameters. The Mualem-van Genuchten (VGM) equation is:

$$K_\psi = K_o S_e^l \left[1 - \left(1 - S_e^{1/m}\right)^m\right]^2 \quad (6.2)$$

Where l is the pore interaction term related to pore sized distribution and tortuosity of soil textures. Mualem (1976) found that l can be either negative or positive, and the optimal value of l is 0.5. K_o is the hydraulic conductivity at saturation retrieved from regression. If the saturated hydraulic conductivity, K_s, is not known, then K_o is assumed to be K_s and is used.

6.2.2 *Effect of Water Repellency (Hydrophobicity) on Soil Suction*

Different types of recycled and natural pavement aggregates have various water repellency characteristics. For example, RAP and RPM comprising of asphalt tend to be hydrophobic, while RCA and conventional aggregate tend to perform as hydrophilic materials. The degree of water repellency of soil can be characterized by the contact angle between a gas-liquid interface on the surface off the material. A perfectly hydrophobic soil has an effective contact angle of 180^o, while the effective contact angle of a perfectly hydrophobic material tends to be 0^o (Letely et al. 2000).

In general, soil can be classified as a repellent soil when the drop of water cannot spontaneously infiltrate the soil surface (Letey et al. 2000). The simple method commonly used to characterize the degree of water repellency of soil is to determine water drop penetration time (WDPT). The WDPT is the time that it takes for a water drop to completely infiltrate the material after the water drop is placed at the surface of soil or porous material. Another method is to measure effective contact angle. However, effective contact angle is a dynamic property depending on

energy state of water in soil. Therefore, the apparent contact angle, contact angle at zero energy state of water, is preferable to indicate the degree of water repellency of soil (Bauters et al. 2000). Jury et al. (1991) suggest using the water entry value, a pressure head when the water starts to infiltrate the pores of porous material. Bauters et al. (2000) summarized the relationship between water entry (cm), apparent contact angle, and WDPT, and gave a description for repellent soil as summarized in Table 6.1.

Based on the physics concept, the contact angle (α_o) can change the soil suction, resulting in SWCC change. The metric suction (ψ_m) at a specific pore radius (r) is the function of surface tension (σ) and the contact angle (α) with the following equation:

$$\psi_m = -\frac{\sigma}{\rho_w g R} \tag{6.3}$$

$$R = \frac{r}{cos\alpha_o} \tag{6.4}$$

Where R is the radius of the meniscus, ρ_w is the density of water, g is the gravitational acceleration, and r is the pore radius.

Degree of water repellency or hydrophobicity affects the soil suction through the contact angle which can be described by Eq (6.3) and Eq (6.4), and also can change the water flow characteristic. For hydrophilic material, contact angles tend to be positive and approximately 0^o, generating negative matric suction or soil suction. In case of saturated soil, after applying suction to soil specimens the water will drain from large pore first. In contrast, for hydrophobic materials which have contact angle greater than 90^o, soil suction will be positive; resulting in water draining easily as compared to hydrophilic materials having the same pore size. As a result, the small pores will drain first. Therefore, soil having similar gradation curves can have different SWCC if the degree of water repellency of soil is different. Figure 6.1 presents effect of contact angle on SWCC. Increasing of contact angle results in air entry pressure and residual water content decrease.

6.3 Materials

6.3.1 *Basic Properties*

Six RCAs, six RAPs, two RPMs and two conventional aggregates were collected from different states across the US under the Pooled Fund Project. The materials were named according to the origin of material source. All specimens are non-plastic, coarse grain materials, which mainly have majority of gravel and sand with low percent of fines. All specimens are broadly graded, and were prepared at 95% of maximum dry density, and compacted using modified Proctor effort based on ASTM D1557. The grain size distributions of recycled and natural aggregates were characterized based on ASTM D422 as shown in

Figure 6.2. All specimens were classified following ASTM D2487. The specific gravity (G_s), porosity (n), dry unit weigh ($\square_d$), percent of gravel, sand, and fines portion and percent of absorption size, and percent of absorption were summarized in Table 6.2.

6.3.2 *Percent of Absorption and Hydrophobicity*

The degree of water repellency of soil was characterized using WDPT and apparent contact angle (by visual). The percent of absorption was conducted according to ASTM C127-07. Degree of water repellencies of recycled and natural pavement aggregates were classified based on Bauters et al. (2000) as shown in Table 6.3. The results show that RCA and natural aggregate are classified as wettable or hydrophilic materials, while RAP and RPM are classified as slightly to severely, severely, or extremely hydrophobic materials. RCA and conventional aggregate have percent of absorption between 5 to 5.8 percent, while RAP and RPM have percent of absorption.

6.4 Methods

6.4.1 *Hanging Column Test*

Hanging column tests (ASTM D6836) incorporated with air (suction) aspirators were used to measure SWCCs. Details of experimental set up are presented in Nokkaew et al. (2012) and Breitmeyer and Benson (2011). The hanging column test is comprised of three main parts: the testing cell, an outflow measurement, and a suction supply apparatus. The large-scale cylinder specimens (305-mm inner diameter and 76-mm height) were used for the testing cell to reduce a disturbance of scale effect and replicate field condition for compacted base course. The outflow was measured using a cylinder column with an accuracy of 1.1 mL. Suctions were supplied to the specimens using hanging column by adjusting the elevation of two reservoirs to create suction, and the soil suction was measured by a manometer with an accuracy of $\pm$0.02 kPa (2 mm of water). Normally hanging column can measure suction in the range of 0.05 kPa to 80 or 90 kPa (limitation due to water cavity). However, the height of the ceiling can limit the applied suction with the hanging column. Thus, suction higher than 25 kPa was supplied to the specimens using air aspirators with the accuracy of $\pm$0.2 kPa.

6.4.2 *Multistep Outflow Method*

Unsaturated hydraulic conductivities (K_ψ) were measured using the multistep outflow method (MSO). The MSO measured K_ψ based on the unsteady method using one-dimensional flow analysis. The following are assumptions for the MSO (Benson and Gribb, 1997): (i) the material is homogeneous, (ii) gravity gradient and impendence of ceramic plate are negligible, (iii) the suction is linear with water content, and (iv) K_ψ for each suction step are constant. The K_ψ can be calculated by the following relationship:

$$K_\psi = D_\psi \frac{\Delta\theta}{\Delta\psi} \tag{6.5}$$

Where $\Delta\theta$ is the change of volumetric water content due to an incremental soil suction, $\Delta\psi$ (m). The water diffusivity, D_Ψ (m^2/s) can be determined by analytical solution proposed by Gardner (1956) as:

$$ln\left(\frac{V_\infty - V_t}{V_\infty}\right) = ln\left(\frac{8}{\pi^2}\right) - D_\Psi \frac{\pi^2 t}{4L^2} \tag{6.6}$$

Where V_t is the outflow volume (m^3) at time, t, V_∞ is the outflow volume (m^3) at ultimate or equilibrium (m^3), and L is the length of the specimens (m).

The influence of impedance for the ceramic plate was taken into account for determining the unsaturated hydraulic conductivity. In this study, the high flow ceramic plate with air entry pressure of 1 bar (100 kPa) was used for conducting MSO. Because the saturated hydraulic conductivity of the ceramic plate was $8.6x10^{-8}$ m/s., only K_s obtained from rigid wall permeameter testing and K_ψ lower than $8.6x10^{-8}$ m/s determined from MSO were used for regression for hydraulic parameters.

6.4.3 *Regression Method and Error Analysis*

The measured SWCC from the hanging column test was fitted with Eq (1) to determine SWCC fitting parameters using non-linear regression proposed by Wraith and Or (1998). The objective function $O_w(p)$ that was minimized for SWCC regression can be written by:

$$O_w(p) = \frac{1}{\bar{\theta}^2}\sum_{i=1}^{N}[\theta_i - \theta'_i]^2 \quad (6.7)$$

Where $\bar{\theta}$ is the average volumetric water content and θ_i and θ'_i are the measured and predicted volumetric water content, respectively. N is the number of SWCC data derived from the hanging column test, and p is parameter vectors (θ_r,$\theta_s\alpha, n$).

The pore interaction term, l was determined based on Eq (2) by using measured SWCC from hanging column test and K_θ from MSO. The fitting parameters, α, m, and n obtained from the first optimization Eq (7) were used to calculate l . The K_o was assumed to be K_s. The minimized objective function was:

$$O_K(p) = \frac{1}{\bar{\theta}^2}\sum_{i=1}^{N}[\theta_i - \theta'_i]^2 + \frac{1}{(\overline{logK_i})^2}\sum_{i=1}^{N_k}[logK_i - logK'_i]^2 \quad (6.8)$$

Where $\overline{logK_i}$ is the average hydraulic conductivity in logarithmic scale, K_i and K'_i are the measured and predicted hydraulic conductivity, respectively. N_k is the number of hydraulic conductivity data obtained from MSO.

The accuracy of the fit of Eq 1 and Eq 2 were quantified using root mean square error (RMSE):

$$RMSE_{\theta,K} = \sqrt{\frac{O_{w,K}(p)}{N_{\theta,k}}} \quad (6.9)$$

The value of $RMSE_K$ is dimensionless because the logarithmic hydraulic conductivities are used.

6.5 Results

6.5.1 *Soil-Water characteristic curve*

The measured SWCCs for RCAs, RAPs, RPMs, and conventional aggregate obtained from the hanging column test are presented in Figure 6.3. All specimens were prepared at saturation, and then dried out by applying soil suction to 75 kPa, which is the maximum capacity of air aspirator for this study. Although RCAs tend to have high porosity due to their characteristically large aggregates from the crushing process, RCA tends to have the best ability to retain water. The cement portion in RCA exhibits plenty of small pores in the surface, which can absorb more water in their small pore. The high percent of gravel for MI RCA and TX RCA creates distinct large and small pores in the RCA structure. The SWCCs of MI RCA and TX RCA exhibit double air entry pressure as shown in Figure 6.3. The first air entry pressure starts at very low suction (0.03 kPa for MI RCA and TX RCA). At this stage the majority of water was drained out of specimens immediately under soil suction less than 0.2 kPa within inter-granular pore. Then, water tends to be constant until the soil suction can overcome the second air entry pressure of the soil matrix (flow inter-granular pore).

Considering SWCCs, RAPs tend to provide the best ability to drain water than other recycled and natural aggregate. RAPs tend to have low air entry pressure (0.03 kPa to 2 kPa) and a steep desorption slope. At a soil suction of 75 kPa, almost all SWCCs of RAPs have reached a residual state where increasing of soil suction does not significantly affect the volumetric water content. SWCC of RPMs exhibits lower air entry pressure than 2 kPa. After reaching the air entry pressure, the water will decrease rapidly when subjected to soil suction.

NJ RPM, having lower porosity, provides higher air entry pressure than MI RPM. The residual water content can be observed for NJ RPM while it is not clear for MI RPM. The SWCCs of Class 5 and lime stone are presented in Figure 6.3. Also, natural aggregates with low porosity provide lower air entry pressure.

The van Genuchten model provides a continually smooth fit for all SWCC data except MI RCA and TX RCA. For these two materials, the conventional model cannot be fitted with the SWCCs. The two SWCCs of RCAs perform dual porosity. The van Geuchten's parameters were determined from simultaneously evaluating the SWCC and K_{ψ} data and from using SWCC data only. The air entry pressure and saturated hydraulic conductivity are listed in Table 6.4.

6.5.2 *Influence of percent of gravel and fines on air entry pressure*

The semi-logarithmic relationship between air entry pressure and percent of gravel is shown in Figure 6.4. Increasing percent of gravel tends to create large inter-granular pores in porous materials, resulting in air entry pressures decreasing. At a similar percent of fines, RAPs tend to provide lower air entry pressure. The trend line for percent of gravel and air entry pressure is presented only for RCAs and RAPs because the amount of data for RPMs and natural aggregate is not enough to generate a strong relationship. The air entry pressure (ψ_a) of RCA and RAP can be estimated with percent of gravels (G) using an exponential function as:

$$\psi_a = 68.7\exp(-0.11G) \quad \text{for} \quad \text{RCAs} \tag{6.10}$$

$\psi_a = 2.2\exp(-0.05G)$ for RAPs (6.11)

Increasing percentage of fines tends to increase air entry pressure for the studied porous materials because fine particles can fill the intergranular or large pores of the aggregate.

Figure 6.5 presents the relationship between percent of fines and air entry pressure for recycled and conventional aggregate. The exponential function represents the relationship between percent of fines (F) and air entry pressure for RCAs and RAPs and can be written by:

$\psi_a = 0.11\exp(0.28F)$ for RCAs (6.12)

$\psi_a = 0.14\exp(-0.71F)$ for RAPs (6.13)

6.5.3 *Unsaturated Hydraulic Conductivity*

The measured unsaturated hydraulic conductivities (K_ψ) as a function of soil suction calculated from the MSO for RCAs, RAPs, RPMs, and conventional materials are presented in Figure 6.6. The MVG model was used to fit SWCC and K_ψ data simultaneously and is also presented in Figure 6.6. Increasing soil suction can reduce the flow channel and can create a more tortuous flow path (Vanapali et al. 1996), resulting in a hydraulic conductivity decrease for all porous materials. Because the limitation of the impedance of water by using a ceramic plate, only hydraulic conductivities lower than 10^{-7} m/s are presented in this study.

6.5.4 *van Genuchten Parameters regression by using simultaneously SWCC and K_ψ and WCC data only*

The pore interaction term, l, for all porous materials obtained from the SWCC and K_ψ data and only from SWCC data (fixed l =0.5) are summarized in Table 6.4. The pore interaction terms are positive (>0) for RCAs, RPMs and conventional aggregates. However, for RAPs the pore interaction term can be either positive or negative. The RMSE for SWCC and K_ψ from the two regression methods are listed in Table 6.5. The RMSE of SWCC using simultaneously SWCC and K_ψ and using SWCC data only, range from $2.4\text{x}10^{-3}$ to $9.3\text{x}10^{-3}$ and $7.6\text{x}10^{-4}$ to $6.1\text{x}10^{-3}$, respectively. The RMSE of K_ψ using simultaneously SWCC and K_ψ and using SWCC data only, range from 0.2 to 0.93 and 0.55 to 7.46, respectively. The results show that the conventional regression method (using SWCC data and fixed l = 0.5) cannot provide accurate predicted K_ψ for RAP with average RMSE of 3.52 when compared to general soil which usually have RMSE around 1.0 (Schaap and Leij 2000, Schaap et al. 2005). The Box plot indicating RMSE for SWCC and K_ψ using two regression analyses are presented in Fig 6.7. The box plot indicates that using SWCC and K_ψ data collected simultaneously provide lower accuracy prediction for SWCC than those using SWCC data only, but exhibits better prediction for hydraulic conductivity.

6.5.5 *Discussion about effect of water repellent on hydraulic properties of recycled pavement aggregate*

According to the results, the degree of water repellency of soil can directly affect the soil suction through capillary phenomena, which results in SWCC change for porous material. To eliminate the effect of grain sized distribution of studied materials, CA RCA, TX RAP, and MI RPM with different degree of soil repellency and similar gradation curves as shown in Figure 6.8 were selected to investigate the effect of water repellency on SWCC and K_ψ. Figure 6.9 presents an example of a water drop on the dry CA RCA, TX RAP, and MI RPM. The apparent contact angle of RCA and Class 5 tend to be approximately 0^o while RAP and RPM have an apparent contact angle larger than 90^o.

Figure 6.10 presents the relationship between soil suction and degree of saturation of the CA RCA, TX RAP, and MI RPM. After applying soil suction of 75 kPa to the specimens, the water around 60%, 30%, and 5% are stored in the pore structure of CA RCA, MI RPM, and TX RAP, respectively. The average apparent contact angle of CA RCA, MI RPM, and TX RAP are 0^o, 83^o and 96^o, respectively. Therefore, at the similar gradation curves, hydrophobic material having high contact angle such as RAP and RPM, have better ability to drain the water than hydrophobic material such as RCA. However, TX RCA has larger particle sizes than MI RPM. As a result, at the same soil suction TX RCA is significantly lower than those of MI RPM.

Figure 6.11 presents the comparison of measured unsaturated hydraulic conductivity of CA RCA, TX RAP, and MI RPM. NJ RAP has lowest K_ψ when soil suction is larger than 1 kPa as expected, while CA RCA and MI RPM does not have K_ψ , implying that the pore size distribution is a priority factor affecting to K_ψ of porous materials.

6.6 Conclusions

Soil water characteristic curves (SWCC) and unsaturated hydraulic conductivities (K_ψ) of six RCAs, six RAPs, two RPMs, and two conventional aggregate materials using hanging column test and multistep outflow method were studied. The SWCC and K_ψ of recycled and conventional aggregates were fitted with the van Genuchten model and Mualem-van Genucthen model by using (i) SWCC and K_ψ data collected simultaneously and (ii) SWCC data only. The effect of water repellency of recycled and conventional materials on SWCC and K_ψ was discussed based on the concept of contact angle. The following are conclusions from this study:

1. Among recycled and natural pavement aggregates, RAPs tend to provide the best drainage capacity while RCAs tend to have the best ability to retain the water in their pore structures.
2. RCAs such as MI RCA and TX RCA containing a high percent of gravel larger than 55 lead to segregation of coarse grain and fine grain materials, and consequently exhibit double air entry pressure.
3. Increasing the percent of gravel tends to decrease air entry pressure while increasing percent of fines leads to an air entry pressure increase for recycled and natural pavement aggregate.

4. Using SWCC and Kψ data collected simultaneously in regression analysis tends to provide lower RMSE for Kψ prediction than using only SWCC data, but resulted in a higher RMSE for SWCC prediction than using only SWCC data.
5. Hydrophobic material such as RAPs and RPMs tend to provide better drainage capacity hydrophilic materials such as RCAs and natural aggregate materials.

6.7 Tables

Table 6.1 The Water Drop Penetration Time (WDPT) for different Degrees of Water Repellency of Soil (Bauters et al. 2000)

WDPT (s)	Apparent contact angle (^{o})	Water entry (cm)	Description
<0.5	0	-7.5	Wettable (<5sec)
40	67	-3	Slightly water repellent
2400	90	0	Severely water repellent
>3600	98	1	Extremely water repellent
>3600	122	4	Extremely water repellent

Table 6.2 Summarized Basic Properties and Percent of Gravel, Sand, and Fines, for Recycled and Natural Aggregate Pavement Materials

Material		USCS Classification	Basic Properties			Percent of		
			G_s	n	γ_d (kN/m^3)	Gravel	Sand	Fines
RCA	California (CA)	GW	2.63	0.27	18.8	50.6	47.1	2.3
	Colorado (CO)	SM	2.63	0.30	18.0	40.9	46.3	12.8
	Michigan (MI)	GP	2.72	0.26	19.8	68.5	28.3	3.2
	Minnesota (MN)	SP	2.71	0.30	18.5	31.8	64.9	3.3
	New Jersey (NJ)	SP	2.64	0.28	18.7	31.9	54.6	4.3
	Texas (TX)	SW-SM	2.60	0.27	18.7	56.4	41.6	2.0
RAP	Colorado (CO)	SP	2.39	0.16	19.6	31.7	67.7	0.6
	Minnesota (MN)	SP	2.52	0.20	19.8	26.3	71.2	2.5
	New Jersey (NJ)	GW	2.49	0.21	19.3	51.0	48.3	0.7
	Ohio (OH)	SP	2.46	0.22	18.8	32.1	66.2	1.7
	Texas (TX)	GW	2.41	0.18	19.3	41.1	44.9	1.0
	Wisconsin (WI)	SP	2.46	0.21	19.0	30.9	68.5	0.6
RPM	Michigan (MI)	GP	2.50	0.17	20.4	43.7	43.6	0.6
	New Jersey (NJ)	GP	2.50	0.20	19.5	46.5	53.1	0.4
Natural Aggregate	Class 5	SW-SM	2.72	0.26	19.1	22.9	67.6	9.49
	Lime stone	GP-GM	2.58	0.16	21.1	50.7	41.0	8.3

Table 6.3 Summarized Percent of Absorption, WDPT, Average Apparent Contact Angle, and Water Repellency Classification of Studied Materials

Materials		Percent of Absorption	WDPT(s)	Average Apparent contact angle	Description
RCA	California (CA)	5	4.8	0	Wettable
	Colorado (CO)	5.8	<0.5	0	Wettable
	New Jersey (NJ)	5.4	<0.5	0	Wettable
	Texas (TX)	5.5	0.8	0	Wettable
RAP	Colorado (CO)	3	171	69	Slight to severely water repellent
	New Jersey (NJ)	2.1	>3600	101	Extremely water repellent
	Ohio (OH)	0.6	>3600	-	Extremely water repellent
	Texas (TX)	1.3	>3600	96	Extremely water repellent
RPM	Michigan (MI)	1.7	>3600	83	Extremely water repellent
	New Jersey (NJ)	2.6	960	96	Severely water repellent
Natural Aggregate	Class 5	-	<0.5	0	Wettable
	Lime stone	2.47	<0.5	0	Wettable
	Basalt	-	<0.5	0	Wettable

Table 6.4 Unsaturated Hydraulic Conductivity Parameters, Air Entry Pressure, and Saturated Hydraulic Conductivity by Using Regression from Simultaneously SWCC and K□Data and Using SWCC Data Only

Materials	WCC+k_θ data						WCC Data						Ψ_a	K_s
	θ_r	θ_s	α (kPa^{-1})	n	m	L	θ_r	θ_s	α (kPa^{-1})	n	m	L	kPa	(m/s)
RCA-CA	0.00	0.25	1.14	1.11	0.10	0.50	0.13	0.25	0.75	1.37	0.27	0.50	0.50	$1.93x10^{-5}$
RCA-CO	0.00	0.27	0.36	1.15	0.13	5.24	0.00	0.26	0.14	1.23	0.19	0.50	3.00	$1.57x10^{-5}$
RCA-MI	NA	NA	NA	NA	NA	NA	NA	NA	NA	NA	NA	NA	0.05	$2.62x10^{-5}$
RCA-MN	0.13	0.25	0.20	2.19	0.54	0.48	0.14	0.25	0.24	2.48	0.60	0.50	1.70	$1.78x10^{-5}$
RCA-NJ	0.01	0.31	0.36	1.19	0.16	0.10	0.15	0.30	0.20	1.76	0.43	0.50	1.03	$2.38x10^{-6}$
RCA-TX	NA	NA	NA	NA	NA	NA	NA	NA	NA	NA	NA	NA	0.03	$7.56x10^{-6}$
RAP-CO	0.08	0.24	0.56	1.58	0.37	1.09	0.10	0.24	0.37	2.27	0.56	0.50	1.10	$3.82x10^{-5}$
RAP-MN	0.03	0.20	0.31	1.52	0.34	-0.20	0.00	0.20	0.27	1.54	0.35	0.5	1.03	$1.10x10^{-6}$
RAP-NJ	0.04	0.21	2.02	2.01	0.50	0.51	0.04	0.21	2.36	1.88	0.47	0.50	0.20	$3.69x10^{-4}$
RAP-OH	0.00	0.26	1.28	1.25	0.20	-0.45	0.00	0.28	2.28	1.22	0.18	0.5	0.35	$5.03x10^{-5}$
RAP-TX	0.01	0.21	1.92	1.42	0.30	0.50	0.04	0.22	2.83	1.50	0.34	0.50	0.16	$3.18x10^{-5}$
RAP-WI	0.02	0.23	2.43	1.57	0.36	-1.10	0.04	0.23	2.83	1.81	0.45	0.50	0.10	$5.19x10^{-5}$
RPM-MI	0.13	0.27	0.70	1.60	0.38	0.09	0.13	0.27	0.53	1.90	0.47	0.5	0.80	$2.31x10^{-4}$
RPM-NJ	0.04	0.19	0.28	1.94	0.48	1.25	0.05	0.19	0.26	2.05	0.51	0.5	1.90	$1.03x10^{-4}$
Class 5	0.00	0.25	0.06	1.40	0.29	0.78	0.10	0.25	0.05	2.20	0.55	0.50	8.00	$4.62x10^{-7}$
Lime Stone	0.00	0.21	0.16	1.34	0.25	7.74	0.00	0.21	0.21	0.17	1.30	0.23	1.13	$5.71x10^{-4}$

Table 6.5 RMSE for Estimated SWCC and K_Ψ for MVG Model Using Simultaneous SWCC and K_Ψ Compared to Using Only WCC Data with Fixed L =0.5

Material	Soil-water chracteristic curves		Hydraulic conductivity (unitless)	
	WCC+ k_Ψ Data	WCC Data	WCC+ k_Ψ Data	WCC Data (L=0.5)
RCA-CA	2.6E-03	1.7E-03	0.40	0.55
RCA-CO	5.3E-03	7.6E-04	0.36	1.46
RCA-MN	5.0E-03	4.4E-03	0.84	0.85
RCA-NJ	6.1E-03	4.5E-03	0.20	0.63
RAP-CO	6.8E-03	4.1E-03	0.45	7.31
RAP-MN	7.7E-03	5.4E-03	0.40	1.22
RAP-NJ	2.4E-03	4.6E-03	0.67	7.46
RAP-OH	6.0E-03	4.8E-03	0.93	0.85
RAP-TX	9.3E-03	4.3E-03	0.48	2.28
RAP-WI	8.2E-03	2.1E-03	0.18	2.01
RPM-MI	6.1E-03	6.1E-03	0.41	1.02
RPM-NJ	3.6E-03	3.5E-03	0.68	0.91
Class 5	5.2E-03	5.8E-03	0.35	0.57
Lime Stone	7.5E-03	8.3E-03	0.40	2.00

6.8 Figures

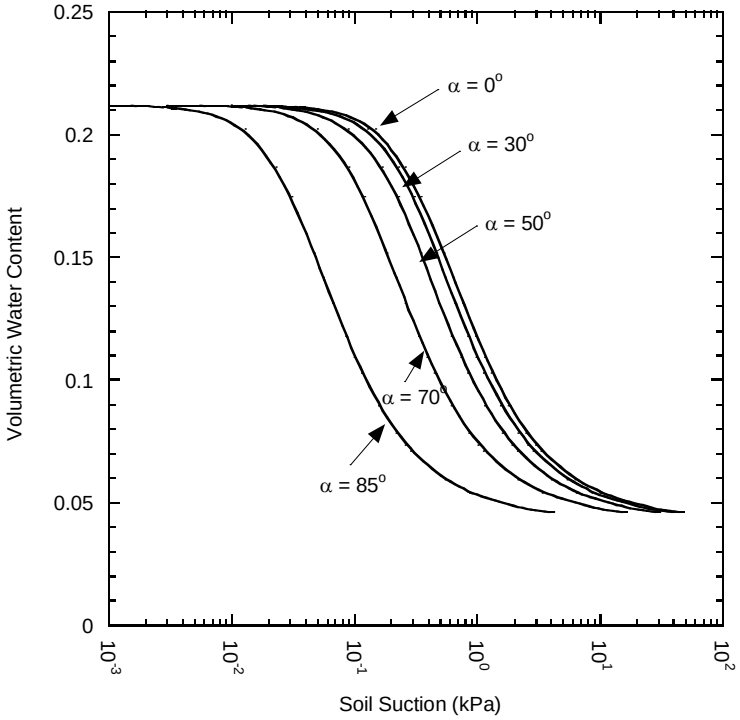

Figure 6.1 Effect of Contact Angle on Soil Water Characteristic Curves

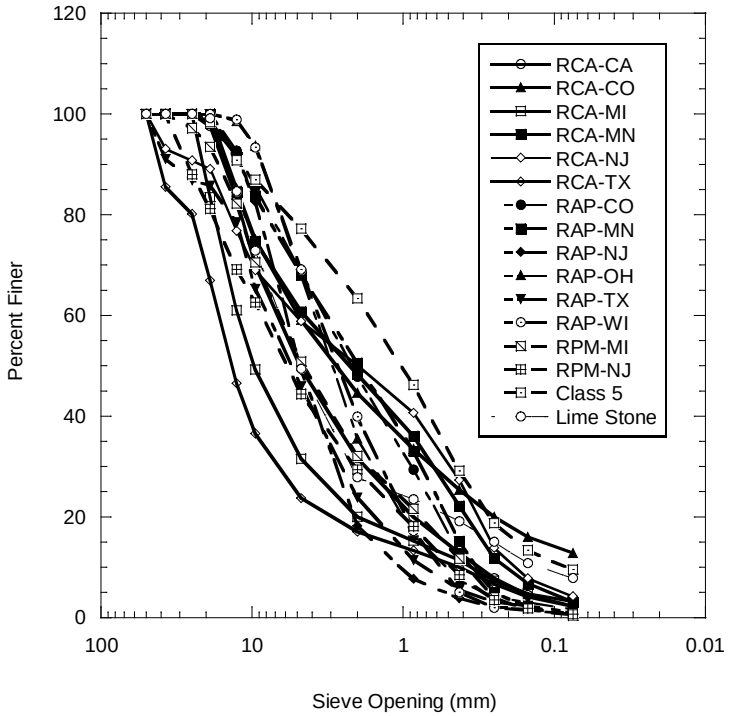

Figure 6.2 Gradation of Recycled and Natural Pavement Aggregate

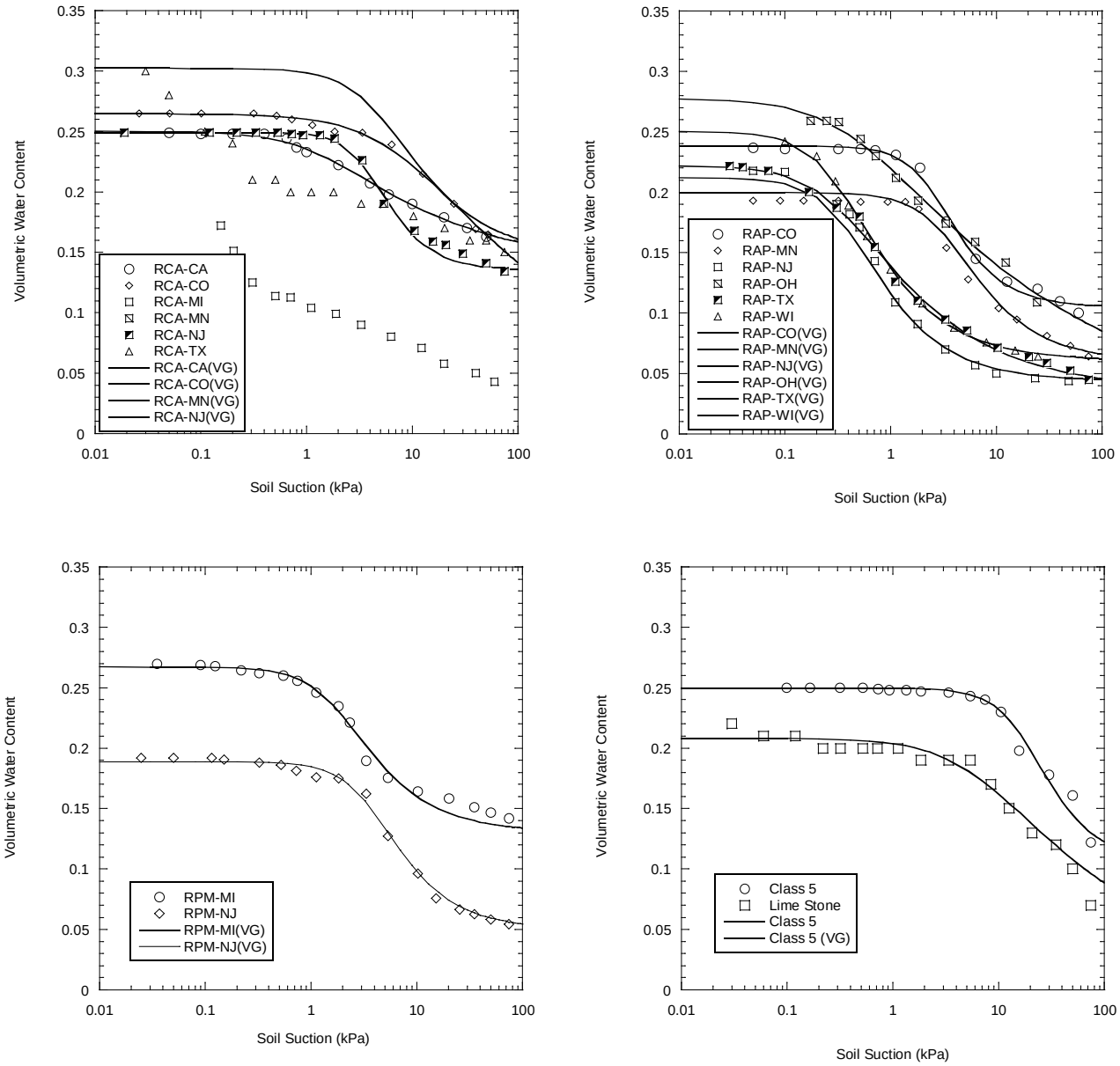

Figure 6.3 Water Characteristic Curves of RCAs, RAPs, RPM and Conventional Materials Fitted with van Genuchten (1980)'s Model 1

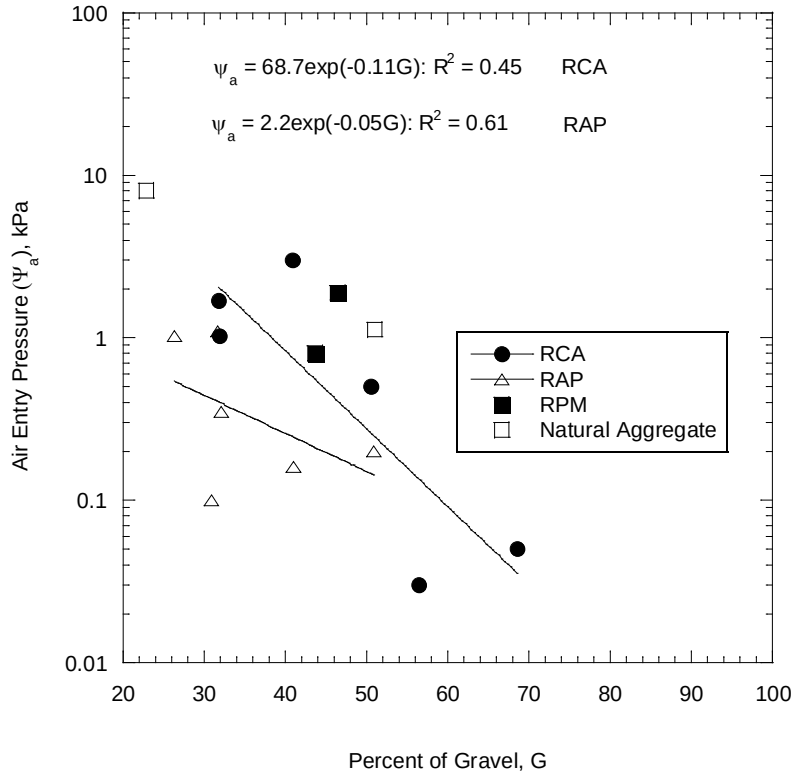

Figure 6.4 Effect of Percent of Gravel on Air Entry Pressure

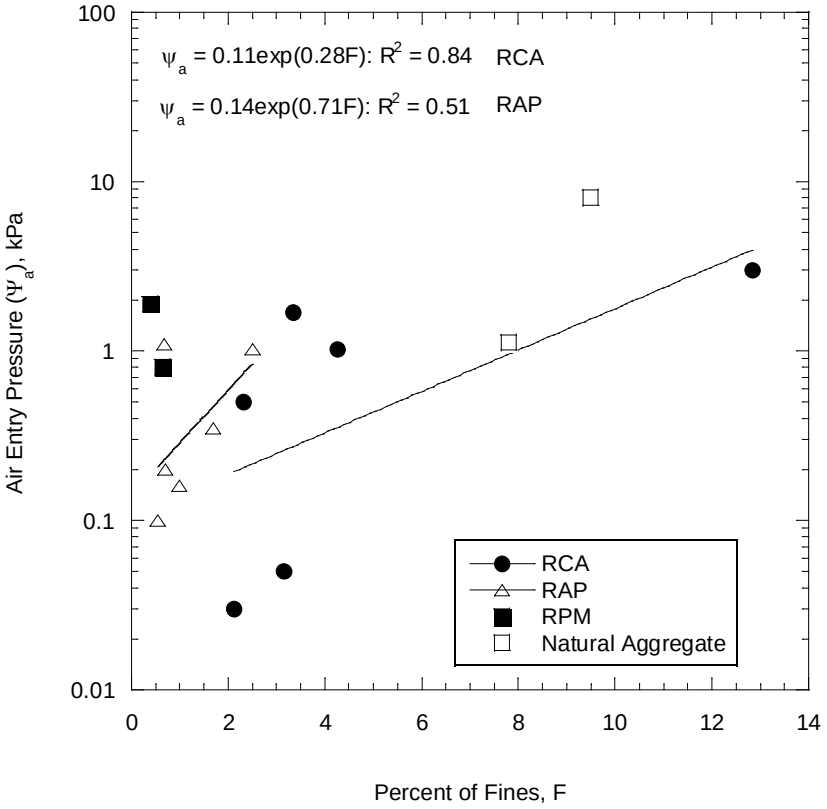

Figure 6.5 Effect of Percent Fines on Air Entry Pressure

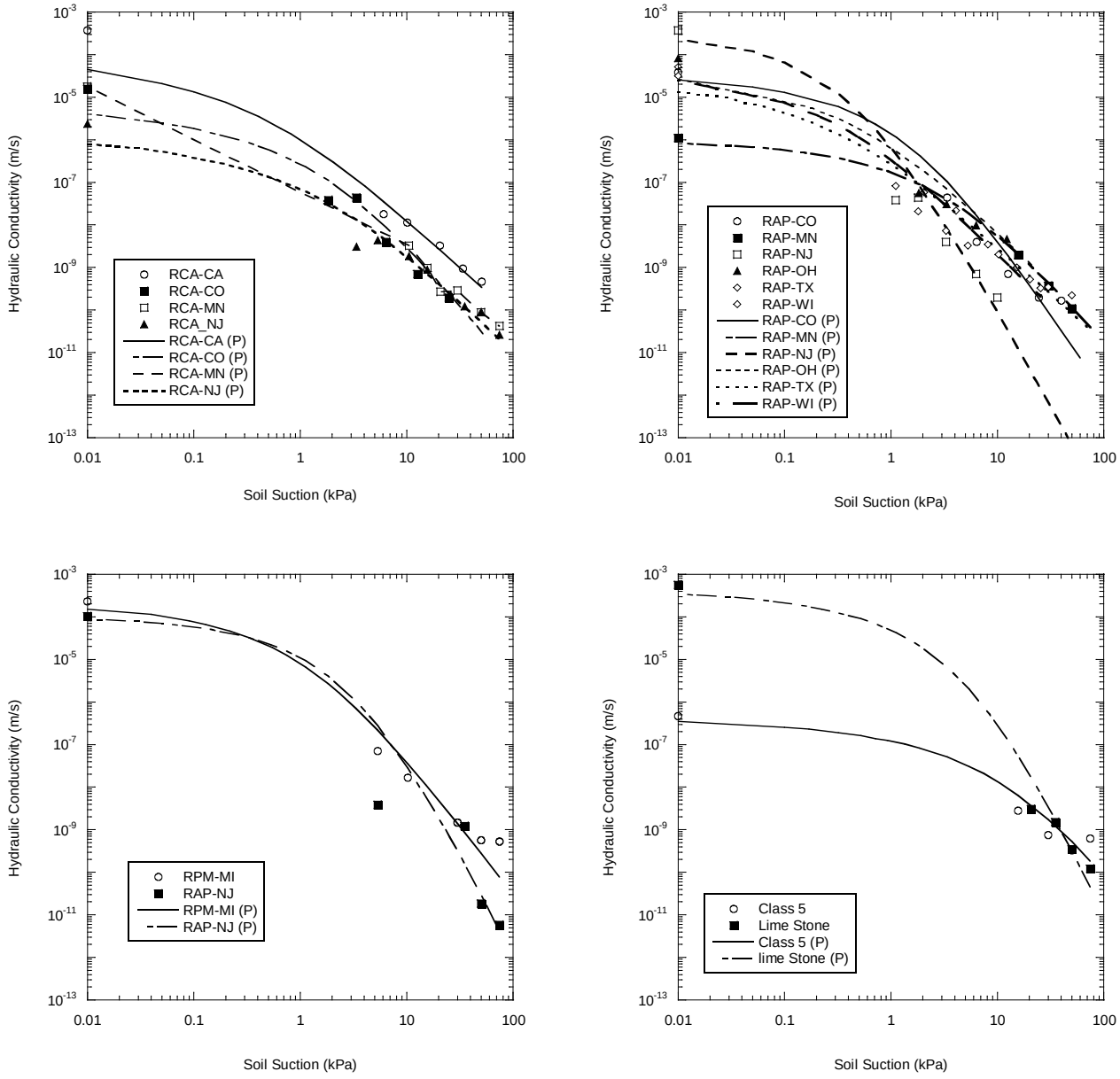

Figure 6.6 Unsaturated Hydraulic Conductivity of RCAs, RAPs, RPM and Class 5 Fitted by MVG Model

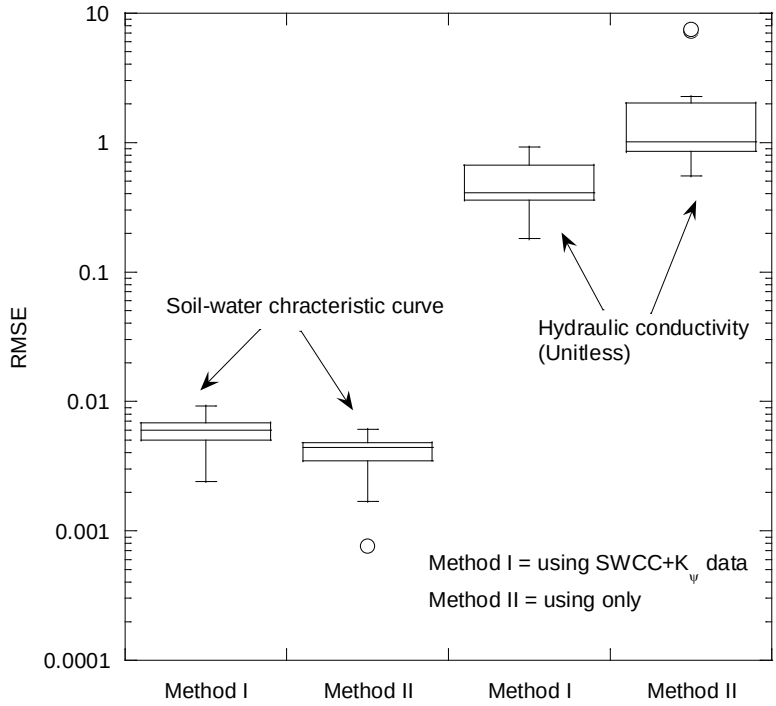

Figure 6.7 Box Plot Endicating RMSE for SWCC and K_ψ Using Simultaneously SWCC and K_ψ Data, and only SWCC Data for all Studied Porous Materials

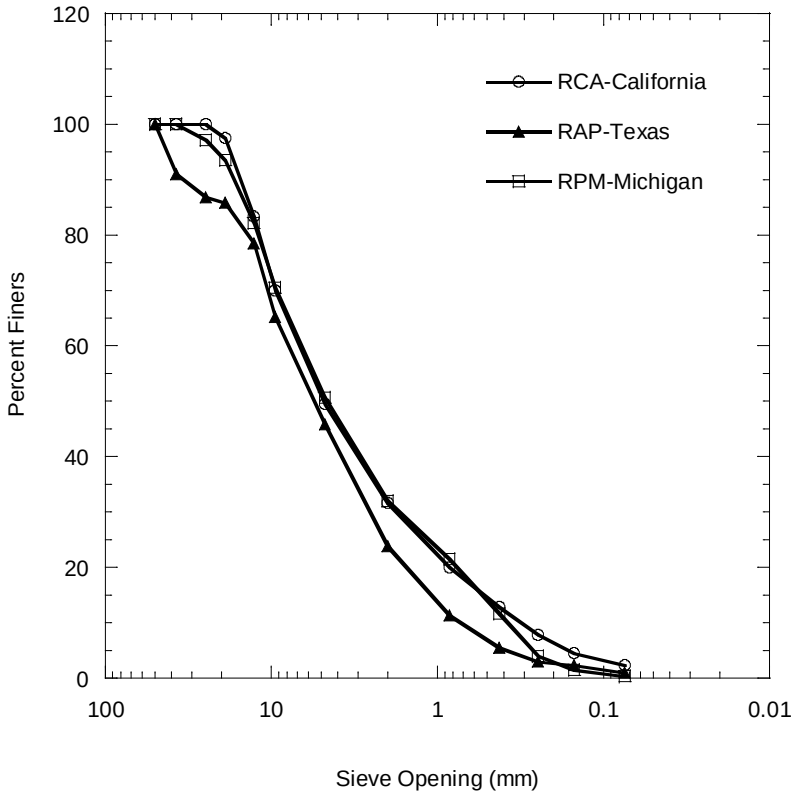

Figure 6.8 Gradation Curves for RCA-California, RAP-Texas, and RPM-Michigan

a) RCA-California (K_ψ) ~0^o) b) RAP-Texas(K_ψ) > 90^o) c) RPM-Michigan (K_ψ) > 90^o)

Figure 6.9 Form of Water Drop on Recycled Pavement Aggregates

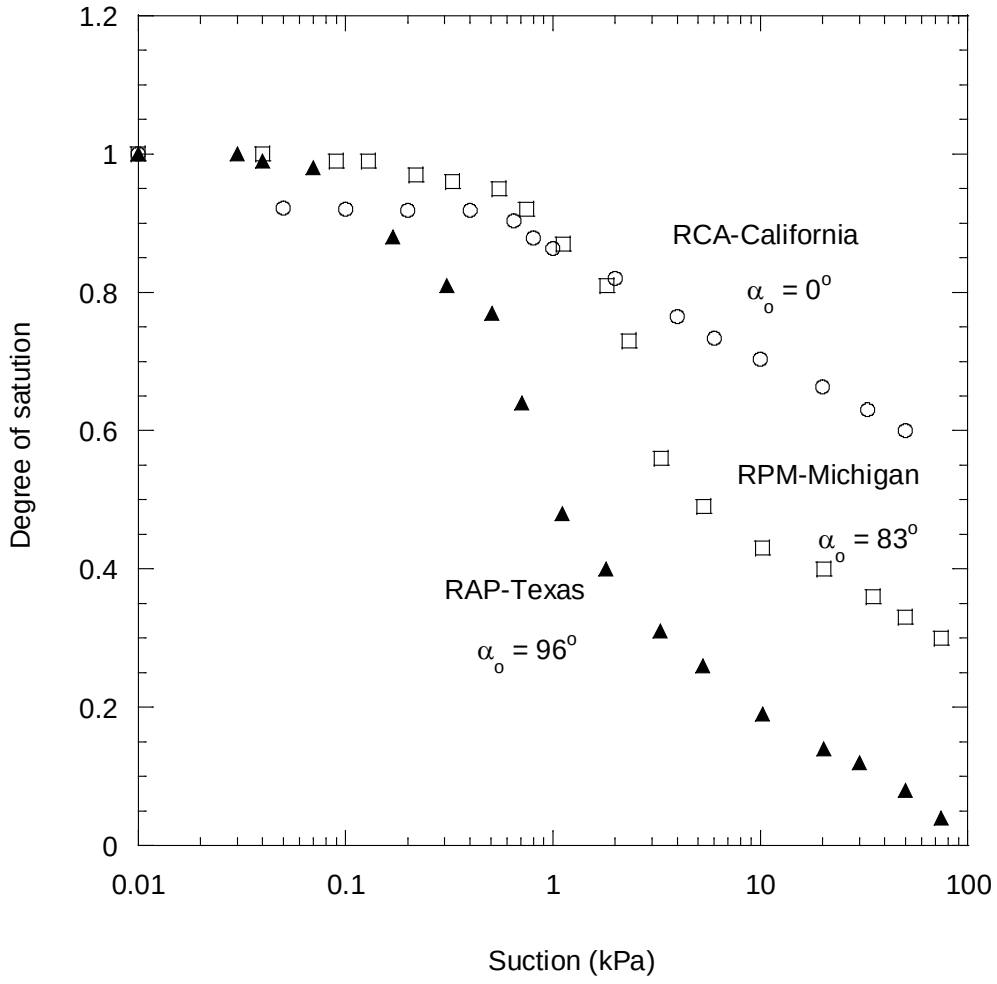

Figure 6.10 SWCCs of CA RCA, TX RAP, and MI RPM

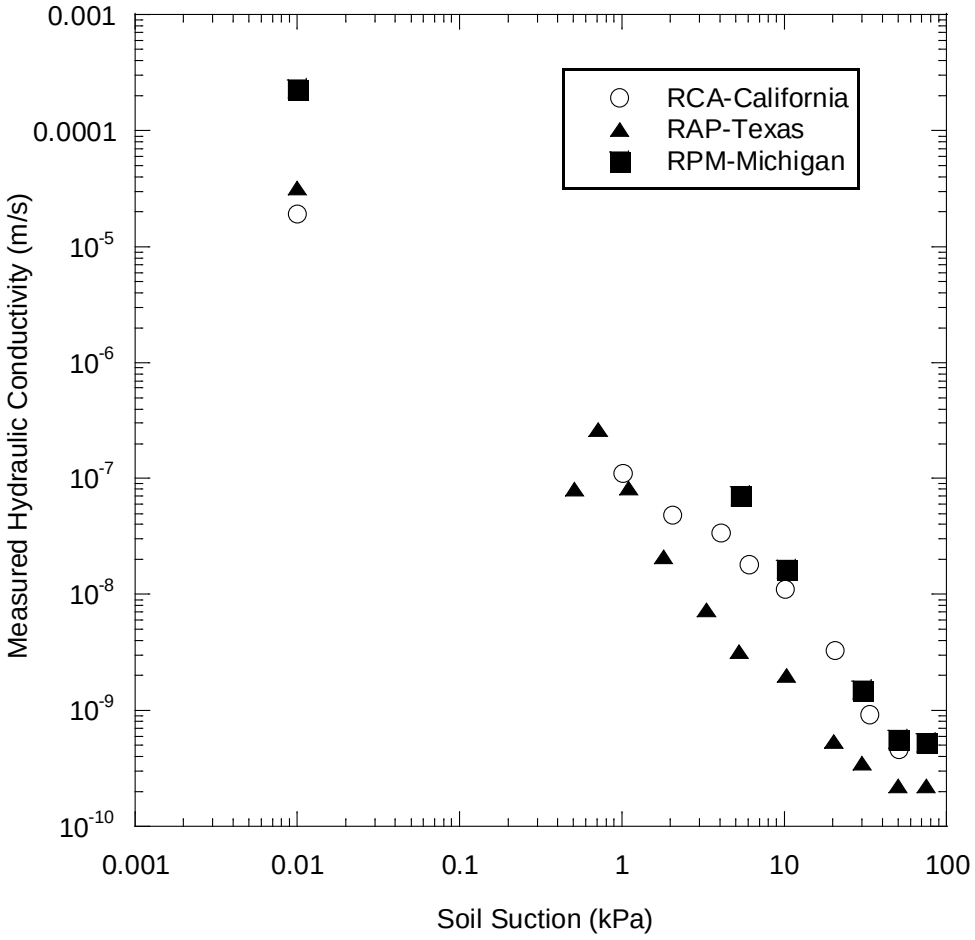

Figure 6.11 Hydraulic Conductivities of CA RCA, TX RAP, and MI RPM

7. Compaction Level and Assessment

7.1 Introduction

The most common C&D materials used as unbound base course in pavement construction are recycled concrete aggregate (RCA) and recycled asphalt pavement aggregate (RAP). RCA is the product of the demolition of concrete structures such as buildings, roads, and runways. RAP is produced by removing and reprocessing existing asphalt pavement (Kuo et al. 2002, Guthrie et al. 2007, FHWA 2008). By beneficially reusing concrete and asphalt, a waste product is converted to a resource for pavement construction (Langer 1988). An increase in the amount of RCA used to replace natural aggregates in pavement construction has economic and environmental benefits, while extending the supply of traditional construction materials (Saeed et al. 2006).

RAP and RCA compete with natural aggregates that are currently used in roadway base applications (Guthrie et al. 2007, FHWA 2008). Despite the increased acceptance of recycled base material in construction, research concerning the mechanical properties and durability of such materials is limited (Bennert et al. 2000, Nataatmadja and Tan 2001, Guthrie et al. 2007). Recycled materials should perform well under the intended use in pavement design; therefore, the mechanical properties of recycled materials need to be investigated thoroughly such that appropriate design procedures and specifications can be established.

Schaertl (2010) indicates that RCA and RAP used alone or in blends with natural aggregates can have different resilient modulus (M_r), sensitivity to stress state, and rutting performance compared to natural aggregates. The durability and toughness of recycled materials can also be different than that of natural aggregates (Weyers et al. 2005).

The objective of this chapter is to characterize the properties of RCA and RAP as unbound base or subbase material without treatment or stabilization and to assess their behavior under laboratory conditions. Variability in material properties, homogeneity of material, and the identification and control of material quality are addressed in this study.

The impacts of compaction effort on the stiffness of the unbound base layer constructed from RCA and RAP were investigated to determine how the compaction level is influential on properties and varies by composition of materials. The compaction moisture effect on the stiffness of RCA and RAP were also assessed. RAP and RCA may contain impurities that affect their mechanical properties and long-term performance, the impurity type and content affecting the stiffness of RAP and RCA were investigated.

7.2 Background

7.2.1 *Recycled Material as Unbound Base Material*

The advanced age of transportation infrastructure in the US, coupled with increasing traffic loads, has accelerated deterioration of this network of roads, necessitating considerable maintenance expenditures. On a parallel path, the road construction industry is being

encouraged, through political and societal pressures, to incorporate recycled material and by-products in pavement structures as alternatives to diminishing aggregate resources (Lekarp et al. 2000). Recycling of pavement material is a viable alternative to use of natural aggregates in road maintenance and rehabilitation activities. Conservation of resources, preservation of the environment, and retention of existing highway geometrics are some of the benefits obtained by reusing pavement material.

Pavement systems are designed to withstand, for a given lifespan, the stresses imposed by traffic and the damaging effects of environmental factors (Warner 2007). Pavement is a multi-layered structure, composed of a concrete or asphalt slab resting on a foundation system that may include base, subbase and subgrade (Poon and Chan 2005). Conventionally, natural material including crushed stone, gravel, and stabilized soil are used in road base and subbase.

Researchers have investigated the use of RCA in road base or subbase courses to provide a viable option for the reuse of this C&D waste (Poon and Chan 2005). RCA is used predominantly in pavement construction as replacement for natural aggregates and cement-treated subbase layers (Saeed et al. 2006). Molenaar and Niekerk (2002) investigated the engineering properties of RCA and suggested that good-quality road base or subbase can be built from these materials. The Federal Highway Administration (FHW) (2008) reported that, when compared to natural aggregates, RCA has lower density, higher water absorption, higher soundness mass loss, and higher content of foreign material. In most cases, the properties of RCA are within the specifications for base course or concrete aggregate.

Park (2003) investigated the characteristics and performance of dry and wet RCA as road base and subbase for concrete pavement by comparing the engineering properties of RCA with those of crushed stone aggregate. The performance characteristics were evaluated based on compactibility, shear resistance, and stability of RCA; and the mechanical properties were evaluated in the field by using a falling weight deflectometer to determine deformation. RCA had the same compactibility as crushed stone aggregate and shear resistance equal to or better than crushed stone aggregate. Park (2003) concluded that the RCA can be used as base and subbase materials in place of crushed stone aggregate for supporting a concrete pavement system.

The National Asphalt Pavement Association (NAPA) (2009) reported that asphalt pavement is the most recycled material in the US. The US highway construction industry annually produces more than 100 million tons of RAP that is recycled into new pavements (NAPA 2009). According to FHWA (2011), RAP is a valuable and high-quality material that may demonstrate good performance as a granular road base and a replacement for more expensive virgin aggregate.

Guthrie et al. (2007) conducted free-free resonant column tests on RAP and natural aggregate blends to evaluate the effects of percentage change of RAP on the stiffness of road base. Blends were prepared according to the following RAP and natural aggregate percentages: 100/0, 75/25, 50/50, 25/75, and 0/100. Stiffness was determined after compaction at OMC, after a 72 hour period of heating at 60 ^{0}C to simulate summer conditions; and after a 10 day period of capillary soaking followed by a 24-h period of submersion to simulate conditions of field saturations. At OMC, the stiffness decreased with the addition of 25% RAP, then increased with the addition of

50%, 75%, and 100% RAP. When the material was heated for 72 hour, the stiffness increased with the addition of 25% RAP and then decreased with the addition of 50%, 75% and 100% RAP. According to Guthrie et al. (2007), the decrease in stiffness is related to the softening behavior of asphalt due to heat. In the soaked condition, the stiffness of the material behaved similar to the samples in the dry condition, but with stiffness values between 40% and 90% lower.

Bennert et al. (2000) compared the mechanical properties of two types of C&D waste, RCA and RAP, with dense-graded aggregate base course, used in roadway base applications in New Jersey. The RAP and RCA were mixed at varying percentages with the dense-graded aggregate base course. Bennert et al. (2000) found that the pure RAP and RCA samples had higher stiffness than the dense-graded aggregate base course, and the stiffness of the base course increased with an increase in RAP and RCA content. The pure RCA specimens accumulated the least amount of permanent strain. Even though pure RAP was found to be stiffer than the dense-graded aggregate base course, the RAP accumulated the greatest amount of permanent strain. Bennert et al. (2000) reported that the resulting contrast between the pure RAP resilient modulus and its permanent deformation might be due to the breakdown of asphalt binder under loading.

7.2.2 *Definition of Resilient Modulus*

The design of roadway pavement relies on proper characterization of the load-deformation response of the pavement layers (Tian et al. 1998). Base and subgrade deform when subjected to repeated loads from moving vehicular traffic. The M_r defines the nonlinear elastic response of pavement geomaterials, such as unbound aggregate base and subbase, under repeated traffic loading. The resilient behavior of unbound aggregate layers is affected by the stress state experienced because of wheel loading and the physical properties of aggregate (Pan et al. 2006). The M_r is a linear-elastic modulus obtained from dynamic loading, defined as the ratio of the cyclic deviator stress to the resilient (recoverable) strain, and is defined as:

$$M_r = \left({}^{\sigma_d}/_{\varepsilon_r} \right) \tag{7.1}$$

where ε_r is the recoverable elastic strain and σ_d is the applied deviator stress.

Design of pavements and rehabilitation of layered pavement systems use M_r as an essential parameter in the design process (Heydinger et al. 2007). The M_r is a key input in NCHRP 1-37 (mechanistic-based pavement design approach), which is being evaluated for adoption by numerous state highway agencies (Pan et al. 2006). The performance of pavement is dependent on the stiffness of the pavement structure under specified traffic loads and environmental conditions. Generally, a high M_r for a base course infers a stiffer base course layer, which increases pavement life. The resilient response of granular material is important for the load-carrying ability of the pavement and the permanent strain response, which characterize the long-term performance of the pavement and rutting phenomenon (Lekarp et al. 2000).

7.2.3 *Factors affecting the Resilient Modulus of Unbound Aggregate*

The M_r of unbound granular material is dependent on loading stress states, material characteristics (e.g., material type, gradation, particle shape and angularity), dry density,

moisture condition. For unbound pavement layer design, the resilient response of aggregate is affected by these influencing factors (Lekarp et al. 2000). Although several different factors can influence the resilient behavior of a granular base course, stress state has the greatest overall effect (Lekarp et al. 2000). The M_r of untreated granular material has shown primary dependency on confining pressure and sum of principal stresses. The M_r of RAP and RCA increases significantly with an increase in confining stress and decreases somewhat with an increase in deviator stress (Bennert et al. 2000, Bejarano et al. 2003, Molenaar and Niekerk 2002, Kim et al. 2007). Kim et al. (2007) found that increasing deviator stress decreased the M_r of RAP, but had less of an effect than the confining stress.

Compaction is the process of densifying soil by the application of mechanical energy due to which the strength characteristics of the soil improves. Through compaction, soil strength can be increased, bearing capacity of pavement layers can be improved, and undesirable volume changes (e.g., caused by frost action, swelling, and shrinkage) may be controlled (Holtz 1990). Most construction specifications for unbound aggregate layers reference the maximum dry unit weight (MDU) and optimum moisture content (OMC) as determined from Proctor (standard or modified) testing. Density is used in pavement construction as a quality control measure to help to determine the compaction level of the constructed layers (Mishra et al. 2010). Generally, increasing the density of granular material results in a stiffer layer while reducing the magnitude of the resilient modulus and the permanent deformation under static and dynamic loads (Seyhan 2001).

The degree of compaction (DOC) of a soil is measured in terms of the dry unit weight and is affected by compaction effort (energy per unit volume), soil type (i.e., grain-size distribution, shape of soil grains, specific gravity of soil solids), moisture content, and dry density of soil. According to Molenaar and Niekerk (2002), DOC is the most important factor affecting the mechanical characteristics of recycled, unbound material.

Molenaar and Niekerk (2002) reported that the mechanical characteristics of an unbound base course made with recycled concrete and masonry rubble were mainly governed by the degree of compaction. Gradation had the smallest influence on the M_r of the recycled material. Bejarano et al. (2003) also concluded that increasing density increased the stiffness of RAP and RCA.

Taha et al. (1999) conducted the modified Proctor compaction and the CBR tests on RAP and virgin aggregate blends with the following percentages: 100/0, 80/20, 60/40, 40/60, 30/80, and 0/100. They found that RAP might be suitable for replacement of virgin aggregate in the pavement subbase if RAP is mixed with virgin aggregate. RAP is highly permeable and the moisture retention capacity of RAP is almost negligible due to asphalt coating and the low amount of fines (Nokkaew et al. 2011). Therefore, water may drain during compaction. All RAP/virgin aggregate mixtures, with the exception of the 100/0 and 80/20 blends, qualified for use in road base. As more RAP is added to a blend, the maximum dry unit weight tends to decrease. The maximum dry density (MDD) of pure RAP was about 83% of the maximum density of pure virgin aggregate, the addition of more virgin aggregate made compaction and handling easier, decreased the OMC, and increased the MDD. Poon and Chan (2005) also investigated the possibility of using RCA as unbound subbase, finding that the use of pure RCA increased OMC and decreased the MDD of the subbase compared to those of natural subbase.

The degree of saturation or water content affects the resilient response characteristics of most untreated granular materials (Lekarp et al. 2000). Water content is a primary factor affecting the stiffness characteristics of granular materials (Zaman and Zhu 1999). An increase in moisture content commonly leads to a decrease in M_r (Pan et al. 2006). The stiffness of typical granular specimens is nearly constant at lower saturation levels, but decreases significantly as degree of saturation rises (Hicks and Monismith 1971). Heydinger et al. (1996) studied the behavior of granular materials at high degrees of saturation and reported that M_r decreased with increasing saturation level. According to Lekarp et al. (2000) the excess pore water pressures developed during cyclical loading decreases the effective stress in the material at high degree of saturation. Consequently, the decrease in effective stress causes a subsequent decrease in both the strength and stiffness of the material. The effect of moisture content on the M_r of unbound granular materials also depends on the applied stress levels and material types (Pan et al. 2006). A study conducted by Kim et al. (2007) on RAP found that specimens tested at 65% OMC had higher M_r when compared to specimens prepared at 100% OMC at all confining pressures.

Mishra et al. (2010) evaluated aggregate properties (e.g., aggregate type, amount of fines, moisture content) that affect the strength and deformation behavior of crushed limestone and dolomite and uncrushed gravel used for road subgrade replacement and subbase. The aggregate type (i.e., crushed or uncrushed particle) that controls the angularity and the amount and plasticity of fines was the most important parameter in controlling the aggregate performance. Mishra et al. (2010) concluded that the performance of crushed aggregates used as unbound layers was better than uncrushed aggregates. Several studies about the effects of surface characteristics of unbound aggregates were also analyzed by Mishra et al. (2010). They reported that angular materials resist permanent deformation better than rounded particles because of improved particle interlock and higher angle of shear resistance between particles. An increase in the proportion of crushed particles beyond 50% increased the friction angle significantly, indicating resistance to the accumulation of permanent deformation (Mishra et al. 2010).

Heydinger et al. (2007) exolored the effects of aggregate type, gradation, and moisture condition on M_r. Three aggregate sources (crushed lime-stone, natural stone, and slag) at five gradations and three moisture conditions (dry, moist, and saturated) were used. The effect of material source was more significant on the M_r of aggregates than the effect of gradation and moisture condition. The natural stone consistently has the highest M_r, followed by limestone and then slag. Even though, there was no strong variation of the M_r of gravel aggregates (natural stone and crushed lime-stone) with respect to gradation, the M_r of open-graded limestone aggregate was higher than the dense-graded specification The moduli obtained from moist samples were lower than those from the dry samples, particularly at the lower stress levels.

7.3 Materials

The recycled materials used in this study were obtained from various states in the US and named according to state of origin. The reference base course was a gravel meeting the Class 5 specifications for base course in Minnesota per the Minnesota Department of Transportation (MnDOT). The blended material was a mix of approximately equal parts (by mass) RCA from MnDOT (50%) and Class 5 (50%). The Class 5 gravel was used as the control material in this study.

To evaluate the effects of compaction effort on stiffness of unbound recycled materials three RAPs (TX RAP, CA RAP, MN RAP), three RCA (TX RCA, MI RCA, CA RCA), one blend (50% RCA-50% Class 5 aggregate) material and Class 5 aggregate used. The materials represent coarser, medium, and finer gradations based on their grain size.

The particle size distribution (PSD) curves for the investigated materials were determined according to ASTM D 422. Samples were wet-sieved through a No. 200 (75 μm opening) sieve to separate the fine particles attached to the coarser aggregates. The PSDs for the RCA and the RAP samples are shown in Figure 7.1, along with the upper and lower bounds from the literature (Bennert et al. 2000, Bejarano et al. 2003, Blankenagel and Guthrie 2006, Gutrie et al. 2007, Saeed 2008, Kuo et al. 2002)

To evaluate the effects of compaction moisture effect on M_r, TX RAP, OH RAP, CO RCA and OH RCA were selected. These materials represent medium and finer gradations for RCAs and coarser and finer gradations for RAPs based on their grain size (D_{10}, D_{30}, D_{50} and D_{60}). The PSDs for the RCA and the RAP samples are shown in Figure 7.2, along with the upper and lower bounds from the literature (Bennert et al. 2000, Bejarano et al. 2003, Blankenagel and Guthrie 2006, Guthrie et al. 2007, Saeed 2008, Kuo et al. 2002).

A summary of the index properties and soil classifications is shown in Figure 7.1. The materials used in this study are classified as non-plastic per ASTM D 2487, the Unified Soil Classification System (USCS).Specific gravity (G_s) and absorption tests were conducted according to AASHTO T 85. Asphalt content was determined by ASTM 6307. The modified Proctor compaction test (ASTM D 1557) was performed to determine the optimum moisture content (w_{opt}) and maximum dry unit weight (γ_{dmax}).

7.4 Methods

7.4.1 *Compaction*

The modified Proctor compaction test was performed on each material in accordance with ASTM D 1557, and the OMC and maximum dry unit weight were determined. Before running the compaction test, the samples were screened through a 25 mm sieve.

7.4.2 *Resilient Modulus Test*

Resilient modulus tests were performed on compacted specimens according to NCHRP 1-28a Procedure Ia, which applies to base and subbase materials. The materials used in this study classify as Type I material in NCHRP 1-28A, which requires a 152 mm diameter and 305 mm high specimen for resilient modulus testing (NCHRP 2004). Specimens were prepared at OMC and compacted to 95% of maximum modified Proctor density. Specimens were compacted in six lifts of equal mass within 1% of the target dry unit weight and 0.5% of target moisture content to ensure uniform compaction (NCHRP 2004).

Resilient modulus tests were conducted with internal and external linear variable displacement transducers (LVDT). External LVDTs have an accuracy of ± 0.005 mm, and internal LVDTs have an accuracy of ± 0.0015 mm. Clamps for the internal LVDTs were built in accordance with

NCHRP 1-28a specifications. Internal LVDTs were placed at quarter points of the specimen to measure the deformations over the half-length of the specimen, whereas external LVDT measured deformations of the entire specimen length. An MTS Systems Model 244.12 servo-hydraulic machine was used for loading the specimens. Loading sequences, confining pressures and data acquisition were controlled from a computer running LabView 8.5 software.

The resilient modulus (M_r) for each load sequence was obtained by averaging the M_r from the last five cycles of each test sequence. The M_r data were fitted with the power function model proposed by Moosazedh and Witczak (1981)

$$M_R = k_1 \times \theta^{k_2} \tag{7.2}$$

where θ is bulk stress and k_1 and k_2 are empirical fitting parameters. The constants k_1 and k_2 are unique to a given material and are independent of one another. For a given material, k_2 obtained from replicate tests were averaged and fixed for that material (Camargo 2008). Bulk stress is another means of quantifying confining pressure and deviator stress in a single term and is defined as the sum of the three principle stresses. Bulk stress is defined as

$$\theta = \sigma_1 + \sigma_2 + \sigma_3 \tag{7.3}$$

where σ_1, σ_2, and σ_3 are the principal stresses acting on the specimen.

For base course, the summary resilient modulus (SRM) corresponds to the M_r at a bulk stress of 208 kPa, as suggested by Section 10.3.3.9 of NCHRP 1-28a. SRM is a primary pavement design variable used directly in the empirical-mechanistic pavement design. It is also used to determine the layer coefficient, which is a required input in the older AASHTO pavement design (Tian et al. 1998).

7.4.3 *Compacted Moisture Effect on Stiffness of Recycled Materials*

Three moisture contents (OMC, 2% dry of OMC, 2% wet of OMC) were selected to evaluate the as-compacted moisture content on the stiffness of RCA and RAP. Resilient modulus tests were performed on compacted specimens according to NCHRP 1-28a Procedure Ia. Specimens were prepared at OMC, OMC +2% and OMC-2% and compacted to 95% of maximum modified Proctor density. Specimens were compacted in six lifts with equal mass per layer, and different moisture content levels were achieved by controlling the amount of compacted mass per layer for each test.

7.4.4 *Compaction Effort Effect on Stiffness of Recycled Materials*

Maximum dry unit weight was controlled at three different compaction levels, 95% of MDU (modified), 90% MDU (standard) and 85% MDU (reduced) for the same OMC. Resilient modulus tests were performed on compacted specimens according to NCHRP 1-28a Procedure Ia. Different compaction levels were achieved by controlling the amount of compacted mass and the sample height during the compaction process.

7.5 Results

7.5.1 *Effect of Compaction Effort on Stiffness of Unbound Base/Subbase Layers*

Camargo (2008) reported that deformations measured with internal LVDTs more accurately described deformation of the specimens for computation of resilient modulus. External LVDT measurements are affected by bedding errors, sample end effects, and machine compliance (Bejarano et al. 2002). Therefore, the resilient modulus presented herein this chapter is based on deformations measured with internal LVDTs. Variability in determining M_r was assessed by performing duplicate tests.

The increase in fines content as a result of compaction is evaluated by conducting dry PSD tests after compacting the specimens to modified Proctor compaction at OMC. The resulting gradations (pre-compaction and post-compaction) are compared. The increase in fines was more pronounced for RCA (ranging from 2.5 to 7.8%) than RAP (ranging from 1.9 to 4.9 %) and Class 5 aggregate (4.6 %), details are in Bozyurt (2011). Degradation during compaction for RCA may be related to breaking of cementitious materials from the particles. For RAP, it was not as pronounced but the aged asphalt coating may be more prone to break away from the particles.

The SRM along with the parameters k_1 and k_2 for the resilient modulus power function model summarized in Table 7.2 for Class 5 aggregate, Blend (MN), and representative recycled materials at three different compaction levels. (Equation 7.2), are. These SRM and parameters correspond to modified, standard, and reduced Proctor efforts (95%, 90%, and 80% of MDU) at OMC.

The rate of decrease of SRM for Class 5 aggregate for standard and reduced compaction levels was 28% and 47%, respectively. TX RAP exhibited the smallest rate of decrease (22%) of SRM after reduced compaction effort compared with CA RAP (32%) and MN RAP (40%). The different rates of decrease for RAP from different sources could be related to the gradation of the RAPs before compaction. TX RAP has coarser, CA RAP medium, and MN RAP finer gradations. As seen from Figure 7.3, the highest decreased of SRM observed for the finer gradation.

For the RCA samples, the highest rate of decrease in SRM are observed in CA RCA (48%), followed by TX RCA (42%) and MI RCA (36%) after reduced compaction effort. The effects of different compaction levels on SRM of materials varied amongst recycled materials could be attributed to their differences in mechanical properties and the sources of the materials.

Leite et al. (2011) investigated the compactive effort influence on the physical characteristics of the recycled construction and demolition waste (RCDW) aggregates used in pavement applications. The effect of compaction effort on the RCDW aggregate properties was evaluated by using intermediate (50% of the modified effort) and modified Proctor energies. CBR for the modified effort was 60% higher compared to the intermediate effort and the resilient modulus as well increased with the increment of the Proctor energy. Leite et al. (2011) concluded that the use of high compaction effort could reduce the resilient displacement of the RCDW aggregate from 10% to 20 % by increasing the stiffness of the base layer.

Bejarano et al. (2003) evaluated the stiffness of RAP compared to typical base course aggregate using the resilient modulus tests by compacting samples to optimum moisture content (OMC) at 95% and 100% maximum density. Bejarano et al. (2003) found that when the compaction density increased from 95% to 100% of maximum density, the stiffness of RAP and typical base course increased.

Since the density of the materials decreased through the change of compaction effort, the decrease in stiffness is expected (Bejarano et al. 2003). A trend of decreasing SRM observed for all materials can be seen in Figure 7.4. Even though the rate of decrease is higher for RCA and RAP, the SRM of RCA and RAP remained higher as revealed in Figure 7.5. The lower compaction effort has significant influence on the stiffness of any kind of materials. However the decrease in the amount of stiffness varied upon material sources and gradations.

7.5.2 *Effect of Compaction Moisture Content on Stiffness of Unbound Base/Subbase Layers*

Recent studies show that the M_r of unbound conventional road base layers is dependent on the moisture content (Hicks and Monismith 1971, Heydinger et al. 1996, Zaman and Zhu 1999, Lekarp et al. 2000). The SRM of the CO RCA, OH RCA, and OH RAP, and TX RAP are summarized in Table 7.3, along with the parameters k_1 and k_2 form varying compaction moisture contents. These SRM and parameters correspond to OMC-2%, OMC, OMC+2% at 95 % of MDU.

Figure 7.6 represents the effect of compaction moisture content on the stiffness of recycled materials. Even though specimens are prepared at the same MDU, the SRM is higher at dry of OMC and lower at wet of OMC. A decrease in moisture content leads to increase the SRM values of RAP and RCA compacted at the same MDU. This increase in the stiffness could be attributed to the increase in matric suction with decreasing moisture content. (Tian et al. 1998)

The moisture contents of recycled materials before and after resilient modulus test at OMC-2% and wet of OMC+2% are presented in Table 7.4. As shown in Table 7.4, the water drained from the RAP samples during compaction and Mr testing, especially for the samples compacted at wet of OMC. Even though the materials were kept in sealed plastic bags after adding water for 24 hour before testing, the excess water (OMC+2%) was not absorbed by the fines in RAP and drained freely. The rate of decrease observed in SRM for OH RAP (4%) and TX RAP (11%) is less than CO RCA (21%) and OH RCA (38%) as seen from Figure 7.7. The rate of decrease in SRM for RAP is lower than RCA, since the moisture holding capabilities of RAP fractions were reduced due to asphalt coating (Attia and Abdelrahman 2010). For RAP materials, the percent material passing No. 200 sieve was less than 3%. The lack of fines in RAP could be another reason that explains why the materials did not hold the extra moisture (Alam et al. 2010).

Researches have shown that M_r typically decreases with an increase in moisture content (Pan et al. 2006). The stiffness of typical granular specimens is nearly constant at lower saturation levels, but decreases significantly as degree of saturation rises (Hicks and Monismith 1971). This decrease could be attributed to the decrease in matric suction, and increase in the lubricating effect of water with increasing moisture content. A study conducted by Kim et al. (2007) on RAP

found that specimens tested at 65% OMC had higher Mr when compared to samples prepared at 100% OMC at all confining pressures.

Attia and Abdelrahman (2010) investigated the effect of moisture content on Mr of base layer containing RAP (from rehabilitation projects in MN) and Class 5 aggregate (conventional base aggregate) at varying MC between OMC-3% and OMC+2%. The Mr test was conducted in accordance with NCHRP 1-28a test protocol, by compacting the samples with gyratory compactor. The M_r of Class 5 aggregate exhibited an increase by 150-300% at low and high confining pressures comparing for samples compacted at OMC-3% versus compacted at OMC+2%. RAP showed an increase in the Mr by 250-320% comparing samples compacted at OMC-3% versus compacted at OMC+2%.

In this study, the rate of increase in SRM for OH RAP and TX RAP was 113% and 121%, respectively; comparing samples compacted at OMC+2% and OMC-2%. The results are differed from Attia and Abdrahman (2010) due to the difference in the compaction process of materials during M_r test and the percent change in OMC.

7.6 Conclusion

This laboratory investigation dealt with the characterization of the engineering properties of the recycled materials (recycled asphalt pavement (RAP) and recycled concrete aggregate (RCA), as well as one field blended materials consisting of 50% RCA and 50% conventional base material used as unbound base/subbase layer without treatment. These recycled materials were collected from a wide geographical area, covering six states in the U.S: California, Colorado, Michigan, Minnesota, Ohio, Texas. A conventional base material meeting the gradation standard of Minnesota Department of Transportation Class 5 aggregate used as a reference material. The investigation also dealt with the determination of the influence of compaction effort and compaction moisture content on the engineering properties of unbound recycled materials, and the behavior of RAP or RCA blended to Class 5 aggregate used as unbound base/subbase layer.

The objectives of this investigation were to evaluate the impacts of compaction effort on the stiffness of the unbound base layer constructed from RCA and RAP were investigated to determine how the compaction level is influential on properties and varies by composition of materials. The compaction moisture effect on the stiffness of RCA and RAP were also assessed. RAP and RCA may contain impurities that affect their mechanical properties and long-term performance, the impurity type and content affecting the stiffness of RAP and RCA were investigated. The objectives were met by determining the resilient modulus of the recycled materials in accordance with NCHRP 1-28a protocol measuring deformations both externally and internally on the specimens.

Compaction effort has an impact on resilient modulus of recycled materials greater than observed for natural aggregate. Compaction moisture effect has an impact on resilient modulus greater for RCA than RAP. The M_r decreases with an increase in moisture content for RAP and RCA. The rate of decrease in SRM for RAP is lower than RCA, since the moisture holding capabilities of RAP fractions were reduced due to asphalt coating. This decrease could be attributed to the decrease in matric suction, and increase in the lubricating effect of water with increasing moisture content.

7.7 Tables

Table 7.1. Index properties for Recycled Materials, Blend and Class 5 aggregate

Material	States	D_{10} (mm)	D_{30} (mm)	D_{50} (mm)	D_{60} (mm)	C_u	C_c	G_s	Absorption (%)	Asphalt Content /Mortar Content (%)	Impurities (%)	Gravel (%)	Sand (%)	Fines (%)	USCS	AASHTO
Class 5 Aggregate	MN	0.1	0.4	1.0	1.7	21	1.4	2.57	_	_	0.25	22.9	67.6	9.5	GW-GM	A-1-b
Blend	MN	0.2	0.6	1.5	2.8	13	0.5	_	_	_	0.36	32.7	63.8	3.4	SP	A-1-b
RCA	MI	0.4	4.1	9.7	12.3	35	3.9	2.37	5.4	_	0.35	68.5	28.3	3.2	GP	A-1-a
	CO	0.1	0.6	2.8	4.9	66	1.1	2.28	5.8	47	0.26	40.9	46.3	12.8	SC	A-1-b
	CA	0.3	1.7	4.8	6.8	22	1.4	2.32	5.0	37	0.26	50.6	47.1	2.3	GW	A-1-a
	TX	0.4	6.5	13.3	16.3	38	6.0	2.27	5.5	45	0.86	76.3	21.6	2.1	GW	A-1-a
	OH	0.2	1.2	3.4	5.3	34	1.7	2.24	6.5	65	0.16	43.2	49.5	7.3	SW-SM	A-1-a
RAP	MN	0.3	0.7	1.6	2.3	7	0.7	2.41	1.8	7.1	0.06	26.3	71.2	2.5	SP	A-1-a
	CA	0.3	1.3	3.0	4.2	13	1.2	2.56	2.0	5.7	0.33	36.8	61.4	1.8	SW	A-1-a
	TX	0.7	2.5	5.4	7.9	11	1.1	2.34	1.3	4.7	0.05	41.0	44.9	1.0	SW	A-1-a
	OH	0.5	1.6	2.9	3.8	7	1.3	2.43	0.6	6.2	0.06	32.1	66.2	1.7	SW	A-1-a

Note: Asphalt Content found for RAP/RPM and Mortar Content found for available RCA

D_{10} = effective size, D_{30} = particle size for 30% finer, D_{50} = median particle size, D_{60} = particle size for 60% finer, C_u = coefficient of uniformity, C_c = coefficient of curvature, G_s= Specific Gravity, AC= Asphalt Content, Abs=Absorption, Note: Particle size analysis conducted following ASTM D 422, G_s determined by ASTM D 854, Absorption of coarse aggregate were determined by ASTM C127-07, USCS classification determined by ASTM D 2487, AASHTO classification determined by ASTM D 3282, asphalt content determined by ASTM D 6307

Table 7.2 Summary Resilient Modulus (SRM) and Power Model Fitting Parameters k1 and k2 (Equation 7.1) for Base Materials for Different Compaction Efforts (Modified (95%), Standard (90%) and Reduced (85%)

Material	States	Compaction Effort (%)	External			Internal			$SRMSRM_{CE*\%}/SRMSRM_{95\%}$
			k_1	k_2	SRM (MPa)	k_1	k_2	SRM (MPa)	
Class 5 Aggregate	MN	95%	66.2	0.198	191	129.2	0.146	281	1.0
		90%	29.0	0.310	152	34.7	0.328	200	0.7
		80%	10.7	0.446	116	8.6	0.536	150	0.5
Blend	MN	95%	90.71	0.174	229	116.8	0.206	350	1.0
		90%	47.30	0.281	212	95.9	0.221	311	0.9
		80%	39.4	0.285	181	61.6	0.284	280	0.8
RCA	CA	95%	119.4	0.148	262	273.6	0.131	550	1.0
		90%	61.9	0.227	208	199.4	0.151	447	0.8
		80%	33.8	0.320	187	55.8	0.305	285	0.5
	MI	95%	49.6	0.278	219	107.2	0.134	400	1.0
		90%	43.7	0.272	188	88.2	0.203	352	0.9
		80%	34.0	0.314	182	50.4	0.306	258	0.6
	TX	95%	74.6	0.233	258	236.1	0.126	464	1.0
		90%	67.2	0.223	220	62.9	0.319	345	0.7
		80%	47.1	0.275	205	46.7	0.329	271	0.6
RAP	CA	95%	122.5	0.138	256	348.8	0.057	473	1.0
		90%	94.8	0.157	219	177.8	0.152	400	0.8
		80%	35.0	0.330	203	112.9	0.197	322	0.7
	MN	95%	93.9	0.174	238	236.1	0.127	464	1.0
		90%	87.8	0.168	215	113.1	0.220	366	0.8
		80%	42.2	0.289	197	53.1	0.312	280	0.6
	TX	95%	156.6	0.142	334	358.7	0.122	686	1.0
		90%	101.8	0.194	287	261.8	0.153	592	0.9
		80%	75.5	0.245	280	226.0	0.163	540	0.8

Table 7.3 Summary Resilient Modulus (SRM) and Power Model Fitting Parameters k1 and k2 (Equation 7.1) for Recycled Materials for different Optimum Moisture Contents (OMC), (+2% OMC, OMC, -2% OMC)

Specimens	Water Content	External			Internal			SRM_{wc}/SMR_{OMC}
		k_1	k_2	SRM (MPa)	k_1	k_2	SRM (MPa)	
CO RCA	2% Dry	150.33	0.11	268	100.47	0.28	440	1.3
	OMC	98.01	0.17	247	118.30	0.20	350	1.0
	2% Wet	58.66	0.22	193	38.37	0.37	275	0.8
OH RCA	2% Dry	94.09	0.17	239	127.50	0.22	404	1.3
	OMC	48.94	0.28	222	49.20	0.34	310	1.0
	2% Wet	11.93	0.47	148	10.66	0.54	193	0.6
OH RAP	2% Dry	133.97	0.15	297	191.41	0.17	485	1.1
	OMC	83.43	0.23	287	158.62	0.19	429	1.0
	2% Wet	75.32	0.22	243	131.79	0.21	411	1.0
TX RAP	2% Dry	168.66	0.13	341	307.49	0.17	758	1.2
	OMC	156.58	0.14	334	269.07	0.16	625	1.0
	2% Wet	113.60	0.19	317	202.55	0.19	557	0.9

Table 7.4 The Change in Water Content Before and After Resilient Modulus Test for Recycled Materials

Specimens	Water Content	Before Test (%)	After Test (%)	Difference (%)
CO RCA	2% Wet	13.0	12.9	0.2
	OMC	10.9	10.9	0.1
	2% Dry	9.0	8.2	0.8
OH RCA	2% Wet	13.4	12.3	1.1
	OMC	11.8	11.5	0.3
	2% Dry	9.5	9.4	0.0
OH RAP	2% Wet	11.1	9.0	2.2
	OMC	8.9	8.8	0.0
	2% Dry	7.1	7.0	0.1
TX RAP	2% Wet	10.8	6.8	4.0
	OMC	8.3	6.1	2.2
	2% Dry	6.3	6.0	0.4

7.8 Figures

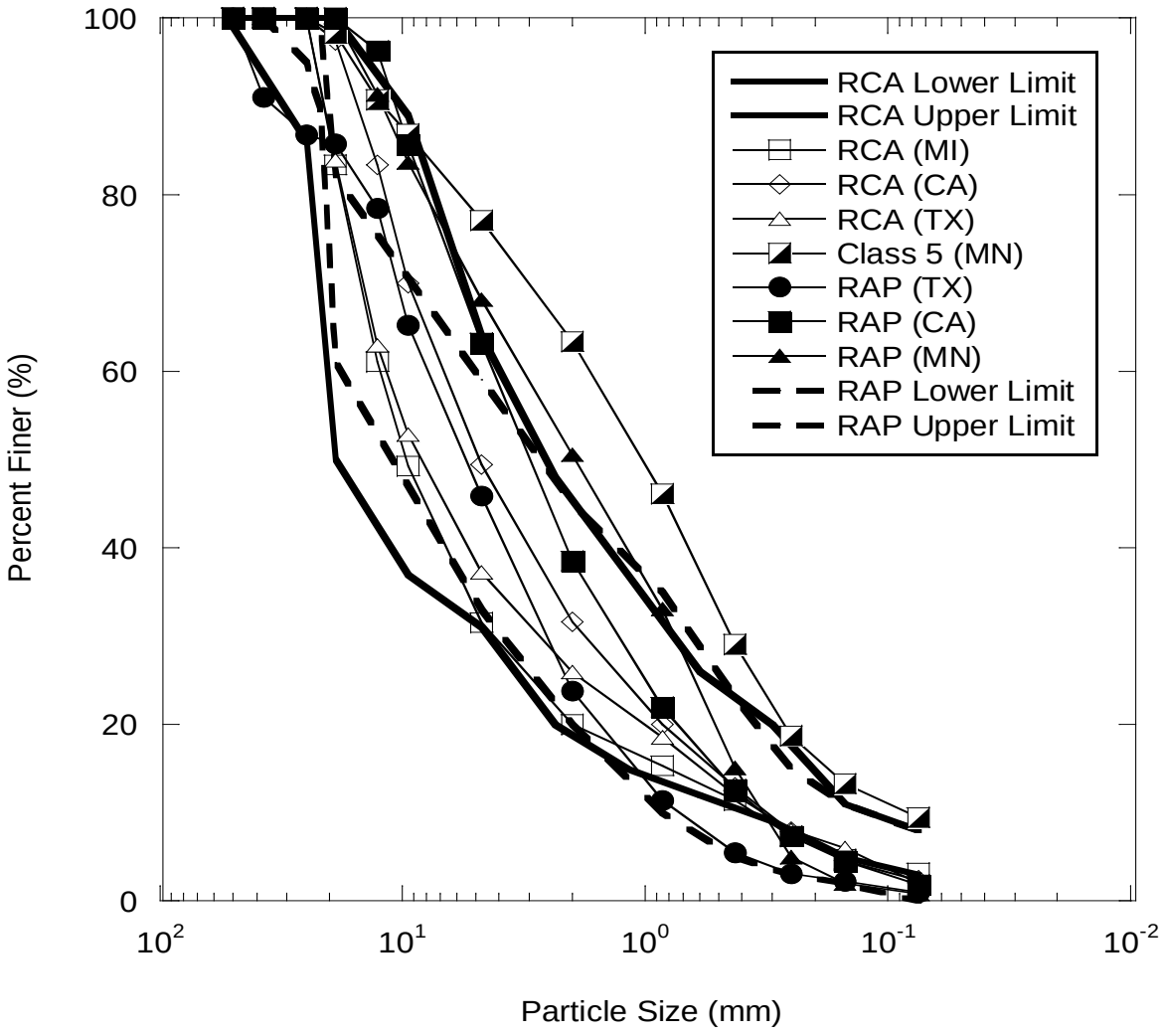

Figure 7.1 Particle Size Distribution for RCA, RAP, and Class 5 Aggregate and Lower and Upper Limits of RAP/RCA from the Literature.

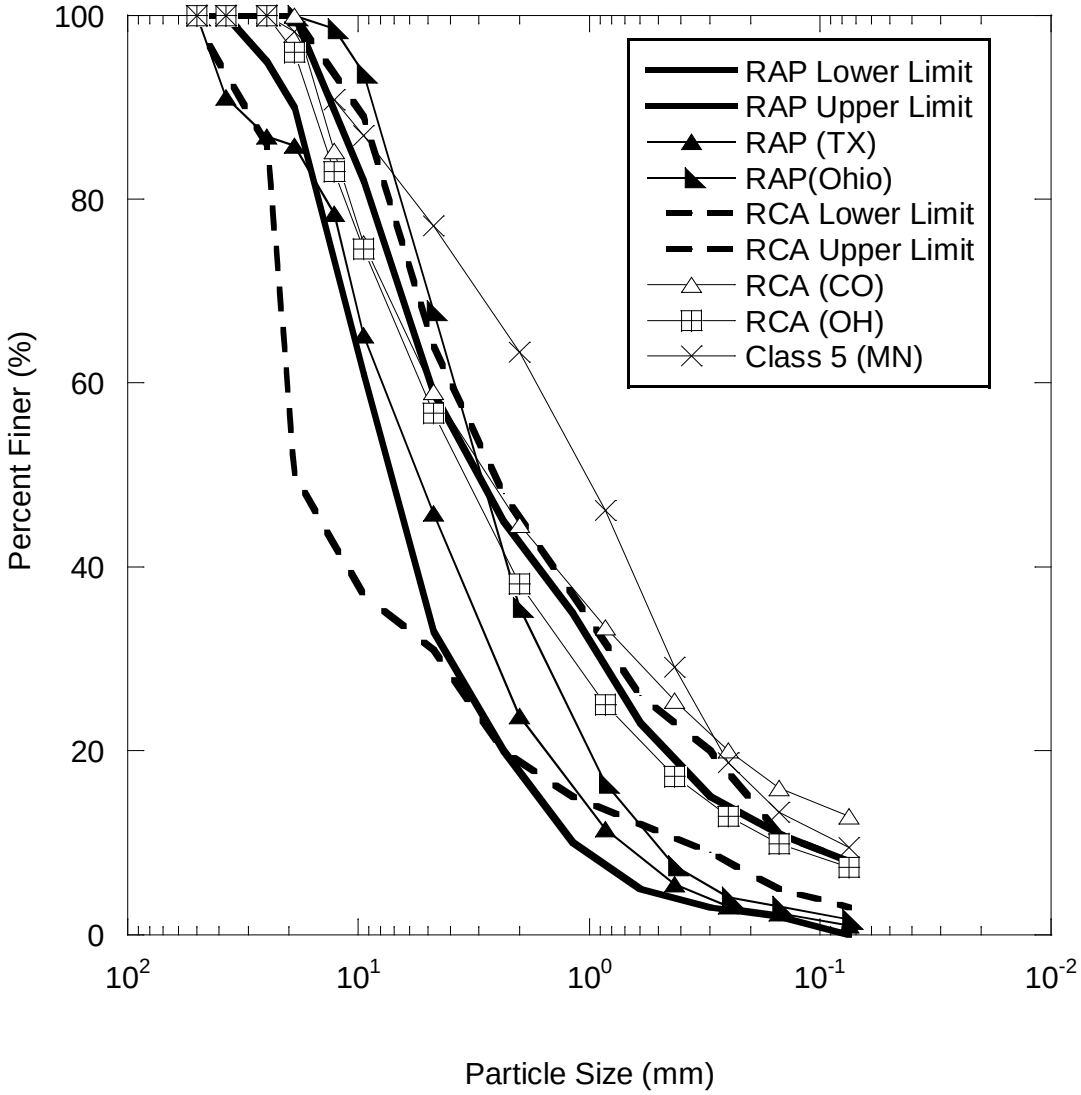

Figure 7.2 Particle Size Distributions for CO RCA, OH RCA, TX RAP, OH RAP, and Class 5, and RAPs and RCAs Reported Lower and Upper Limits from Literature

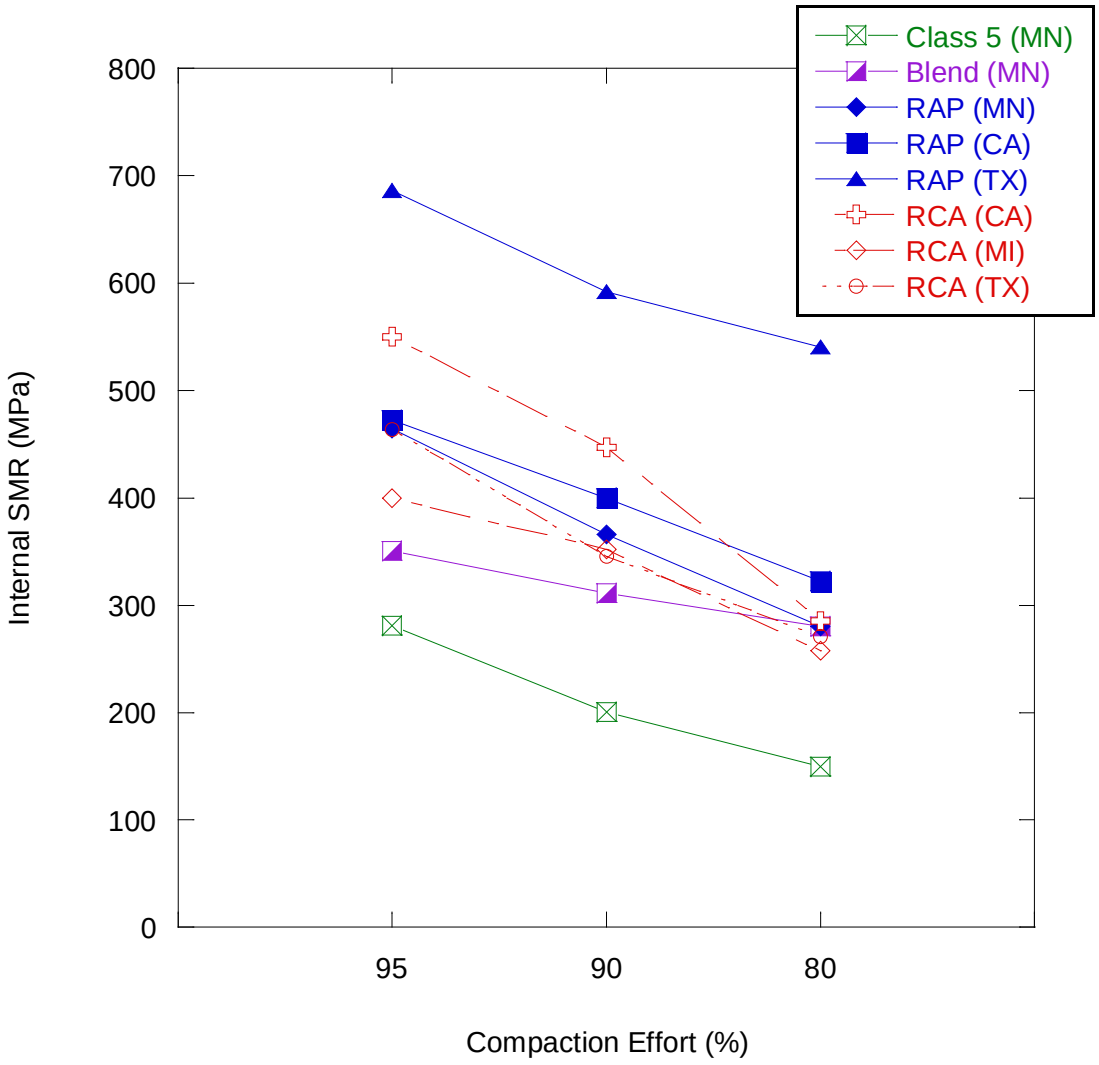

Figure 7.3 Internal Summary Resilient Modulus (SRM) for Different Compaction Efforts for RAP, RCA , Blend and Class 5 Aggregate

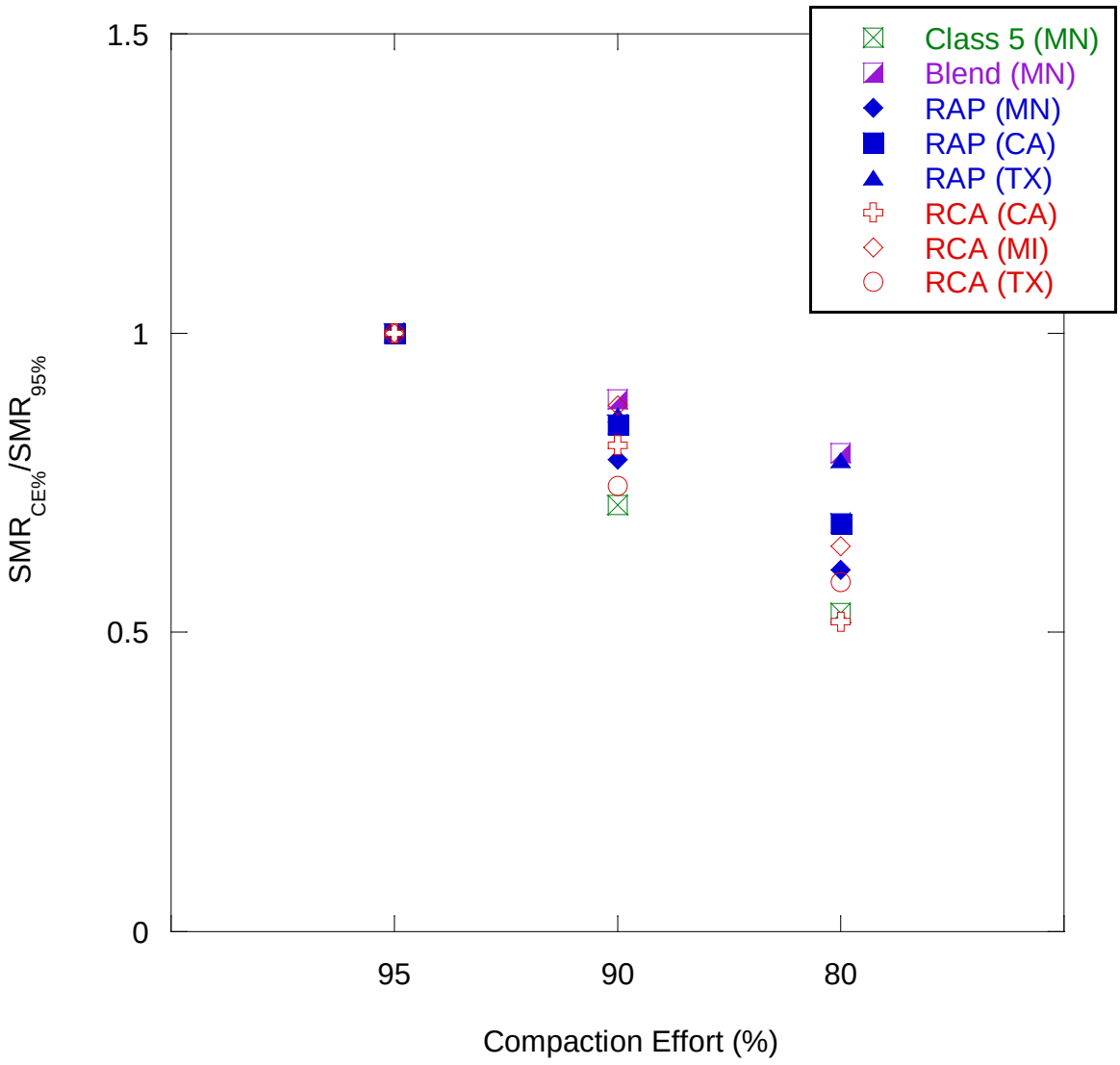

Figure 7.4 Normalized Value of Summary Resilient Modulus (SRM) for different Compaction Efforts for RAP, RCA, Blend and Class 5 Aggregate

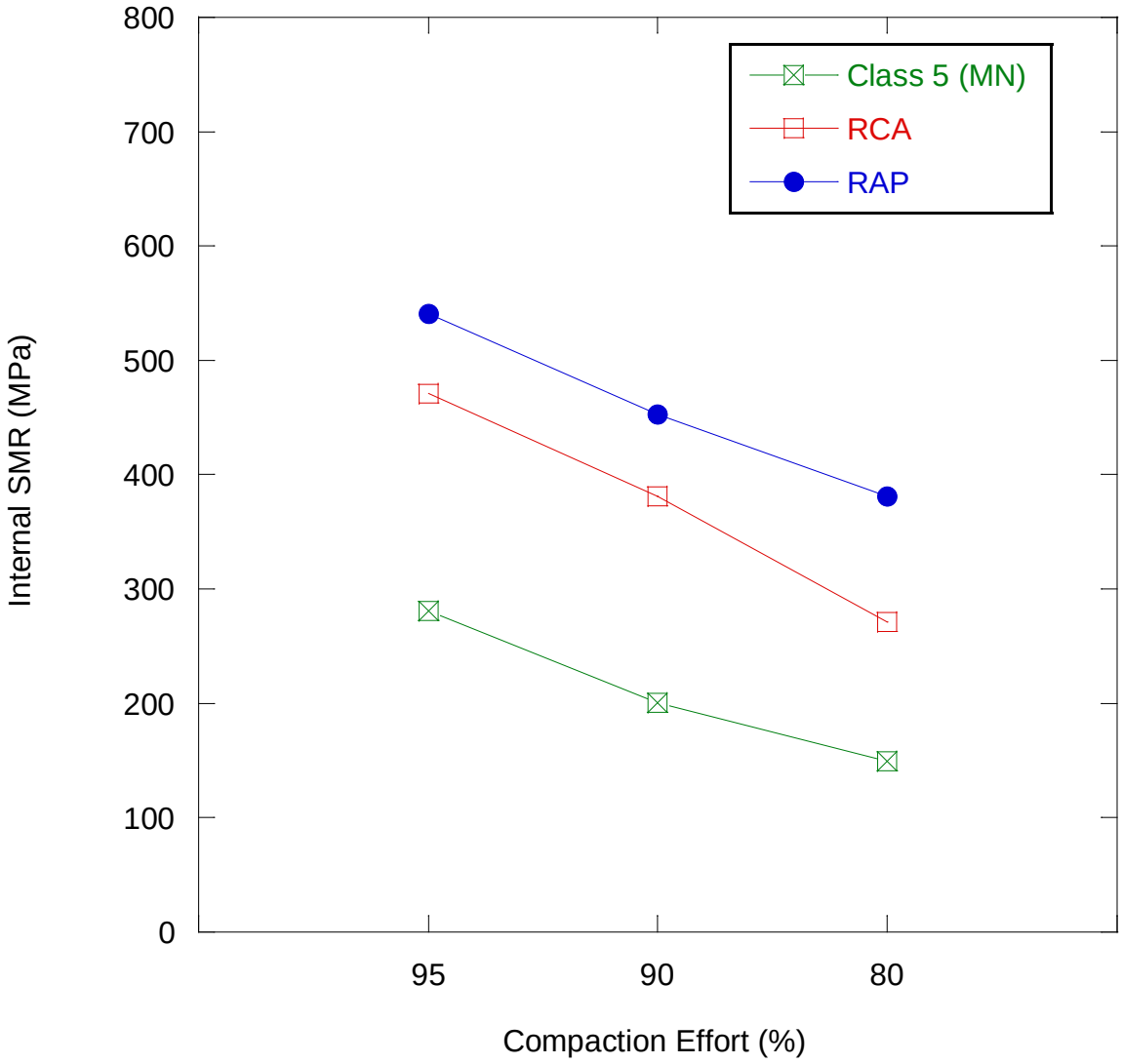

Figure 7.5 Average Internal Summary Resilient Modulus (SRM) for RCA, RAP and Class 5 Aggregate at different Compaction Efforts

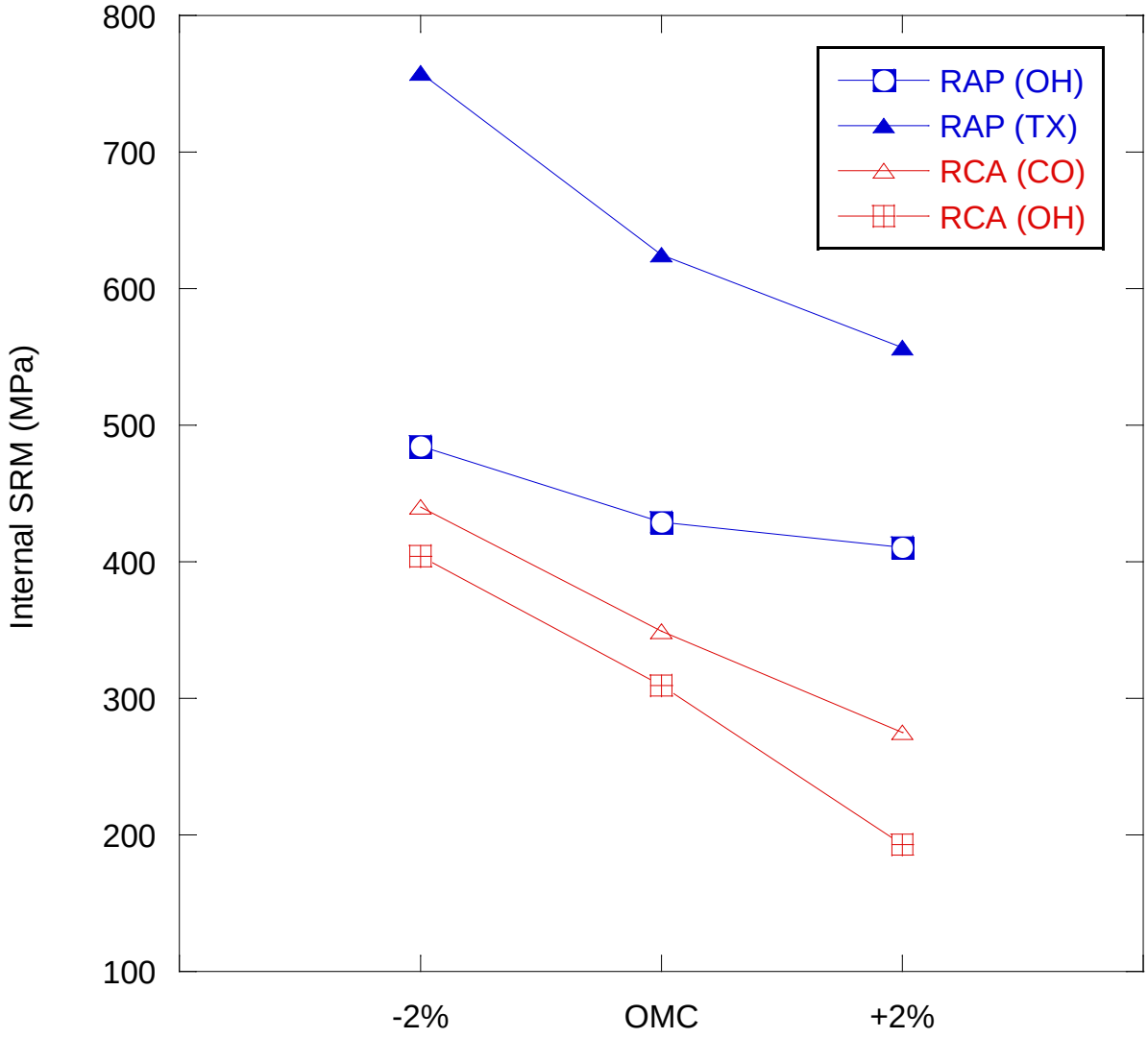

Figure 7.6 Internal Summary Resilient Modulus (SRM) for RAP and RCA at 2% Dry of Optimum Moisture Content (OMC), OMC and 2% Wet of OMC

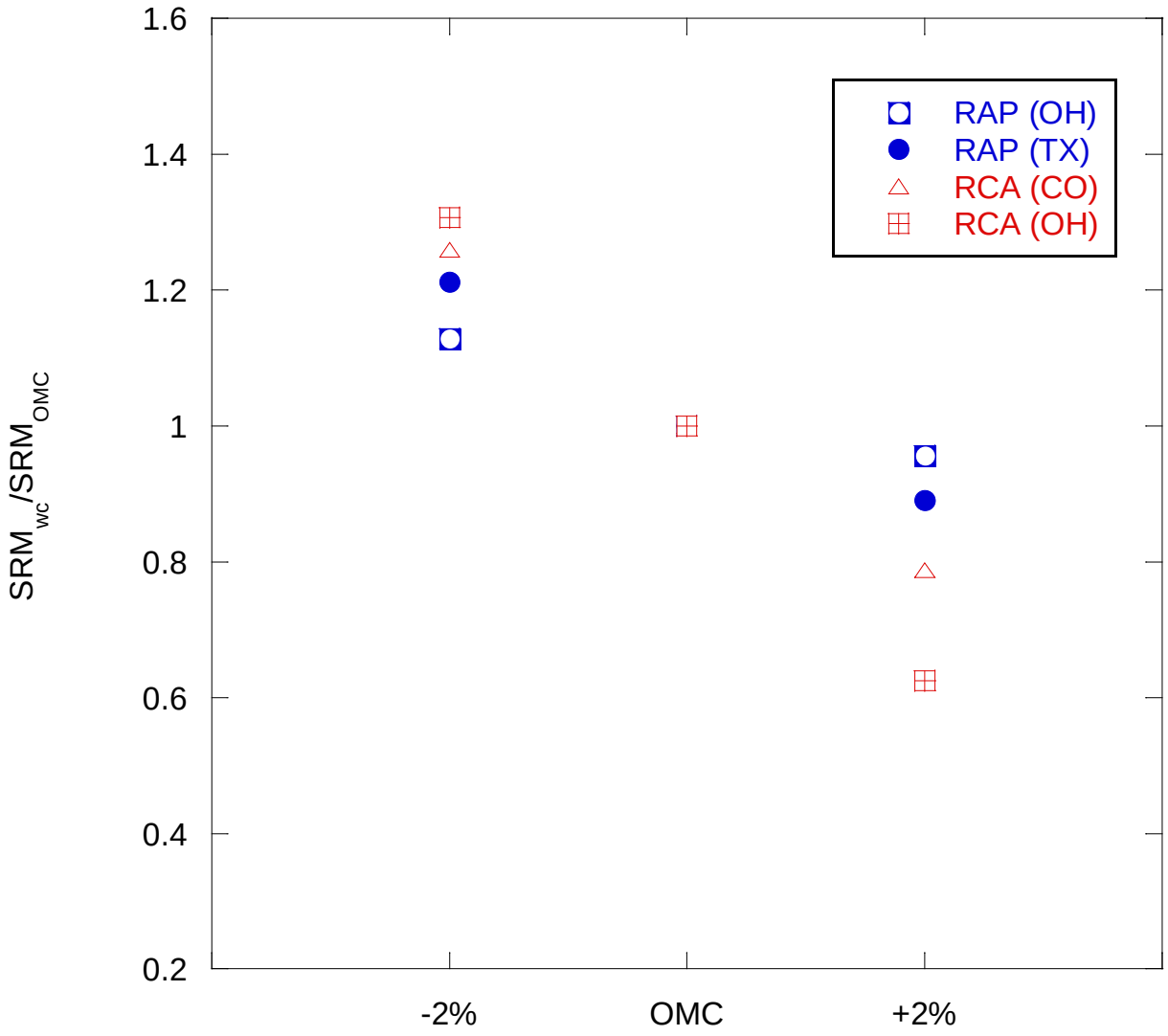

Figure 7.7 Normalized Summary Resilient Modulus for RAP and RCA at 2% Dry of Optimum Moisture Content (OMC), OMC and 2% Wet of OMC

8. Field Performance: Falling Weight Deflectometer Data Analysis

8.1 Introduction

The objectives of this study were (1) to determine the maximum deflection of each pavement section under simulated loading by the FWD and (2) to determine the resilient modulus of the pavement layers, focusing on the performance of base course layers composed of recycled asphalt pavement (RAP), recycled concrete aggregate (RCA) and a 50-50 blend of RCA with conventional base course aggregate (Class 5). RAP refers the removal and reuse of the hot mix asphalt (HMA) layer of an existing roadway, and RCA refers to the reuse of materials reclaimed from roadways as well as from other structures such as old buildings and airport runways. A conventional base course meeting the gradation standard of a Minnesota Department of Transportation Class 5 aggregate was used as a reference material in this study.

8.2 Materials and Methods

Index properties and compaction data for RAP, RCA, blended RCA/Class 5, and Class 5 are presented in Table 8.1, with particle size distribution graphs presented in Figure 8.1. Each of the four materials is classified as non-plastic, poorly graded gravel, with the RAP specimen having an asphalt content of 4.8%.

Field-scale in-situ moduli of the materials were obtained from Falling Weight Deflectometer (FWD) tests performed at the MnROAD testing facility near Albertville, Minnesota. Traffic is diverted from westbound I-94 and onto the MnROAD mainline, which is 3.5 miles long by 2 lanes wide. Four test cells were constructed for each of the four base materials tested; the pavement profiles are shown in Figure 8.2. FWD analysis is performed on different dates throughout the year, and the modulus of each base course can be determined over time.

Testing was performed using a trailer-mounted Dynatest model 8000 FWD. The FWD was controlled by an on-site computer that recorded and stored load and deflection data. A 40 kN load was applied by the FWD to a 300-mm-diameter plate in contact with the pavement surface. Surface deflections were measured by nine load transducers located at distances of 0, 0.30, 0.61, 0.91, 1.22, 1.52, and 1.83 meters from the center of the load. FWD tests at each cell were conducted at 100 feet intervals along the mainline alignment, as well as at lateral intervals corresponding to the mid-lane and outer-wheel paths of both the driving and passing lanes.

The measured deflections were used to back-calculate the elastic modulus of the pavement layers using the MODULUS program developed at the Texas Transportation Institute. MODULUS uses linear-elastic theory to back-calculate elastic moduli from FWD data. The back-calculation was based on a four-layer model consisting of asphalt concrete, base course, sub-base and subgrade layers. For the purposes of this analysis, the Class 3 aggregate and select granular material indicated in Figure 8.2 were combined as one layer. The Pavement profile and deflection data were provided by the Minnesota Department of Transportation (Mn/DOT). The asphalt surface, base course, and sub-base layers were assigned a Poisson's ratio of 0.35, and the subgrade layer was assigned a Poisson's ratio of 0.40 (Huang 2004).

8.3 Results and Discussion

8.3.1 *Maximum Deflection of Test Cells*

The average maximum elastic deflection and one standard deviation of all tests at a given time experienced by each of the four test cells is presented in Figure 8.3 as a function of time. As the air temperature warms during spring 2009, the gradual increase in deflection can be attributed to decrease in stiffness of the HMA layer and a gradual thawing of the subgrade and subbase layers. The maximum deflection occurs during summer when air temperature is highest and HMA stiffness is the lowest. The deflection gradually decreases through the fall season as the air temperature drops and the viscosity of the HMA increases. The deflection recorded during February 2010 is less than 0.1 mm for all test cells, and most likely reflects frozen conditions at the time of testing. Warming temperatures cause the deflection to once again increase during spring 2010 to levels that are comparable in magnitude to deflections experienced during the same time period in 2009. The same deflection behavior occurs in 2011 and 2012. The change in deflection decreases in 2012, possibly due to settlement of the roadway which decreases the void ratio of the material.

Overall, Class 5 experienced the greatest elastic maximum deflections, followed by blended RCA/Class 5, RAP, and RCA, respectively. Similar results were reported for small-scale and large-scale tests performed on the same materials by Schaertl (2010) and Son (2010), respectively.

8.3.2 *Resilient Modulus of All Layers*

The average resilient moduli of the HMA, base course, subbase and subgrade layers for each of the four test cells is presented in Figure 8.4 as a function of time. The error bars represent one standard deviation of the resilient modulus data for the given layer and time. MODULUS 6.0 was not able to analyze deflection data recorded during February and March due to very small deflections recorded, most likely due to frozen conditions. Therefore, Figure 8.4 does not present resilient modulus of the pavement layers between November and April (frost-penetration period) of each year. The magnitude of the resilient modulus experienced by the HMA is inversely proportional to the air temperature, gradually decreasing from spring to summer, and gradually increasing from summer to fall. The decreased viscosity allows the layer to deflect to a greater degree, resulting in a decrease in stiffness. The base, subbase, and subgrade are not as sensitive to temperature and therefore the resilient moduli of these layers remain relatively constant compared to that of the HMA.

8.3.3 *Resilient Modulus of Base Course Layers*

The resilient modulus of the base course at the midlane (M) and outer wheel paths (O) of both the driving (D) and passing lanes (P) for the four test cells is presented in Figure 8.5 as a function of time. The data points represent the average of the resilient moduli calculated along each of the measurement alignments. There are no connecting lines between November and April of each year since MODULUS 6.0 was not able to calculate the resilient modulus most likely due to

low deflections recorded during the frost-penetration period. The resilient modulus was greater at the midlane compared to the outer wheel path. The outer wheel path of both lanes encounters a greater amount of wheel loading, and as a consequence experiences a greater degree of compaction. The increased compaction contributes to a denser particle matrix which increases the overall stiffness of the material. The trend of the base course resilient modulus over time is the opposite of the trend of the HMA: the base course resilient modulus increases with a decrease in HMA modulus, and then decreases with an increase in HMA modulus. This is probably a result of changing state of stress and strain in the base layer with changing stiffness of the HMA layer.

The resilient modulus of the base course at each cell is presented in Figure 8.6 as a function of time. The resilient modulus from all FWD tests conducted at each cell (varying spatially and temporally) is presented as a box plot in Figure 8.7. Class 5 had the lowest resilient modulus of the four base course materials tested. Although there was a significant amount of overlap, RCA had the greatest resilient modulus, with blended RCA/Class 5 and RAP having resilient moduli that were comparable in magnitude. The relationship between the magnitudes of the four materials are consistent with the results of small and large-scale laboratory testing conducted by Son (2010) and Schaertl (2010).

8.4 Conclusion

1. Test cells that incorporated Class 5 as a base course experienced the greatest elastic maximum deflections, followed by blended RCA/Class 5, RAP, and RCA, respectively. An increase in air temperature increases the deflection of the pavement system. Frozen subgrade contributes to a decrease in deflection during the winter months.
2. The stiffness of the HMA layers decreases during periods of increased temperature. The stiffness of the base, subbase, and subgrade are relatively constant compared to that of the HMA.
3. The resilient modulus was greater at the midlane compared to the outer wheel path due to greater overall loading in these areas. The base course resilient modulus increases with a decrease in HMA modulus and decreases with an increase in HMA modulus. This is probably a result of changing state of stress and strain in the base layer with changing stiffness of the HMA layer.
4. RCA and Class 5 had the highest and lowest resilient moduli, respectively. Blended RCA/Class 5 and RAP had resilient moduli that were comparable in magnitude.

8.5 Tables

Table 8.1Index Properties for RAP, RCA, Blended RCA/Class 5, and Class 5

Sample	w_{opt} (%)	$\gamma_{d\,max}$ (kN/m^3)	LL (%)	PL (%)	Gravel Content (%)	Sand Content (%)	Fine Content (%)	USCS Symbol
RAP	6.7	20.8	NP	NP	31.8	67.4	0.8	SP
RCA	11.2	19.5	NP	NP	31.8	64.9	3.3	SP
Blend	8.9	20.1	NP	NP	32.7	63.9	3.4	SP
Class 5	8.0	20.7	NP	NP	28.1	64.2	7.7	SP

8.6 Figures

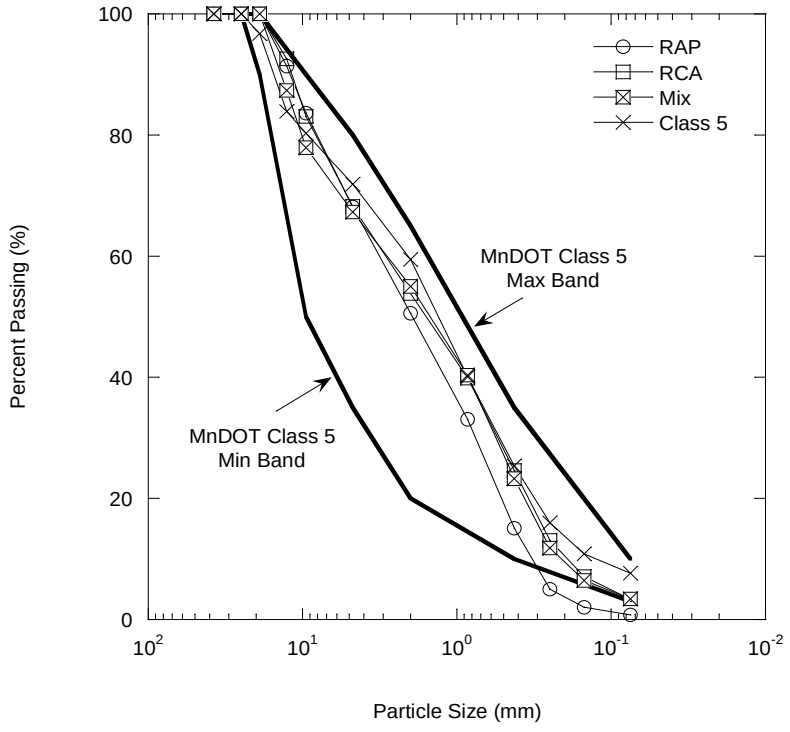

Figure 8.1 Particle Size Distributions for RAP, RCA, Blended RCA/Class 5 and Class 5 with MnDOT Specifications

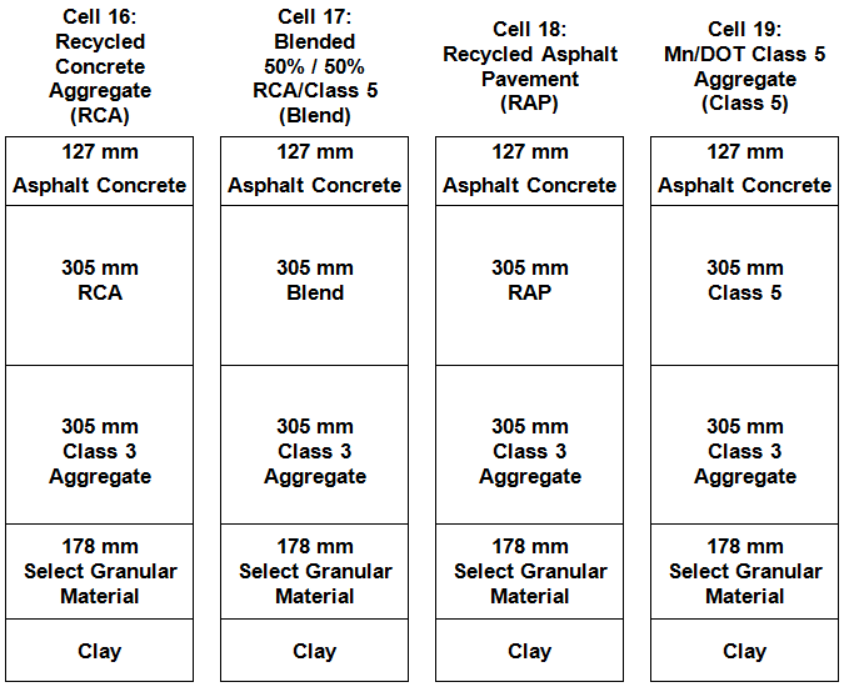

Figure 8.2 Pavement Profiles of Cells Tested Using FWD at MnROAD Testing Facility (Adapted from Johnson et al. 2009)

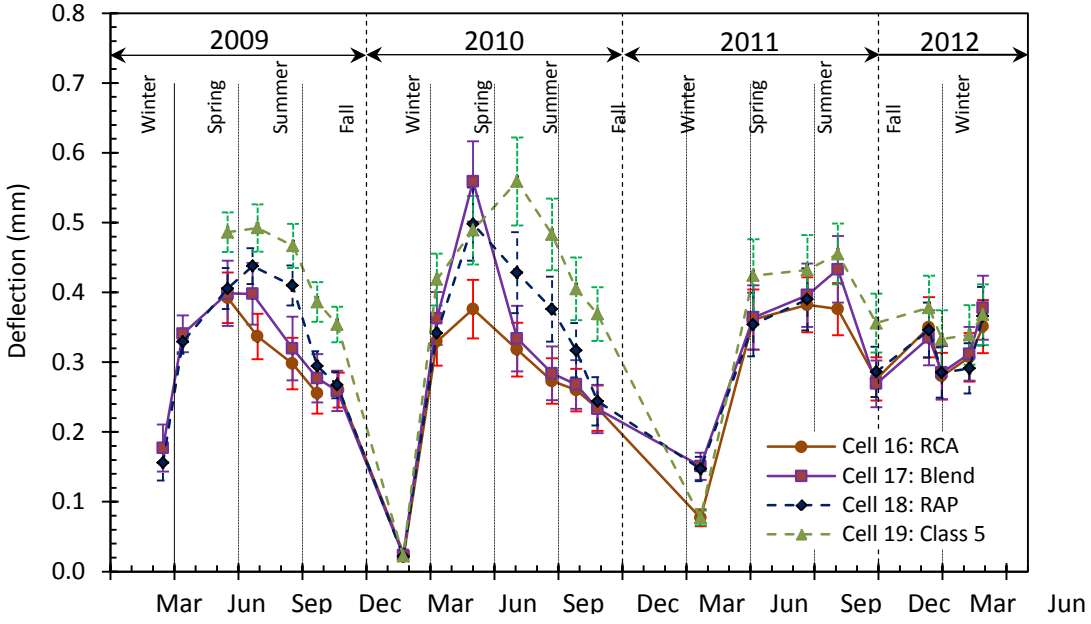

Figure 8.3 Average Center Deflection as a Function of Time for Test Cells Constructed with RAP, RCA, blended RCA/Class 5, and Class 5 Base Course (error bars represent one standard deviation)

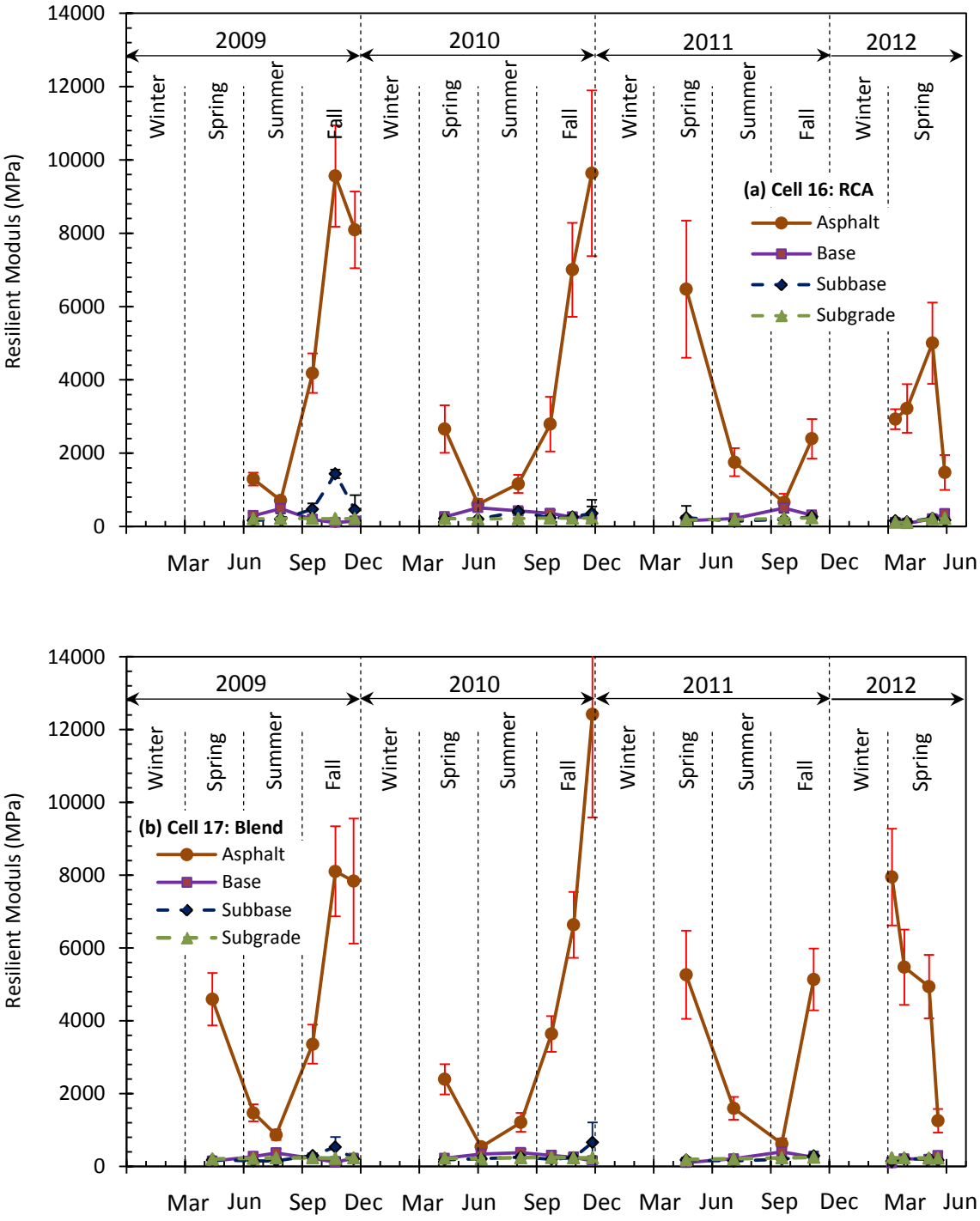
Resilient Moduls (MPa)
14000
12000
10000
8000
6000
4000
2000
0
2009
2010
2011
2012
Winter
Spring
Summer
Fall
Mar
Jun
Sep
Dec
(a) Cell 16: RCA
Asphalt
Base
Subbase
Subgrade
(b) Cell 17: Blend

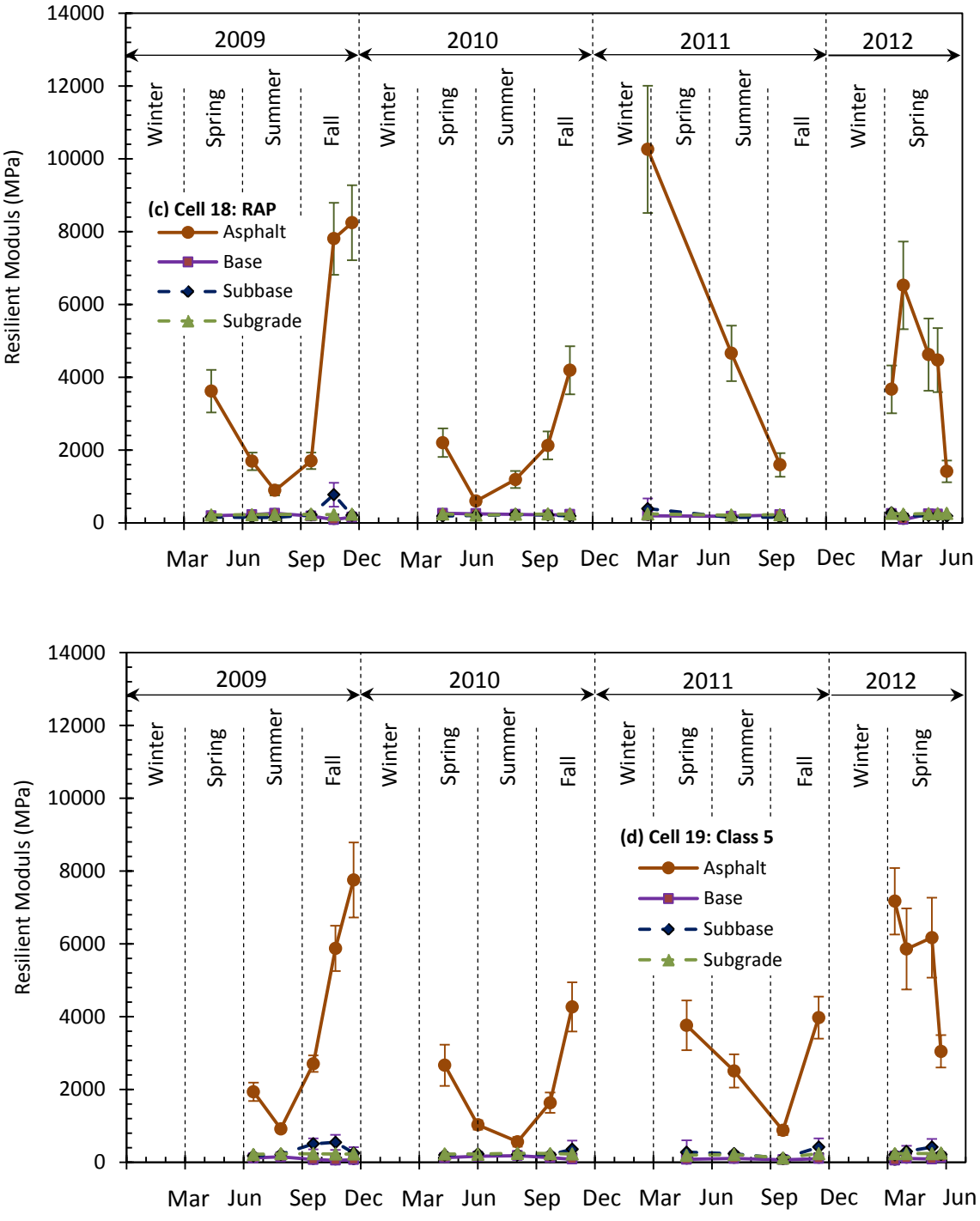

Figure 8.4 Resilient Modulus of HMA, Base Course, Subbase and Subgrade as a Function of Time for Test Cells Constructed with (a) RCA, (b) Blended RCA/Class 5, (c) RAP, and (d) Class 5 Base Course

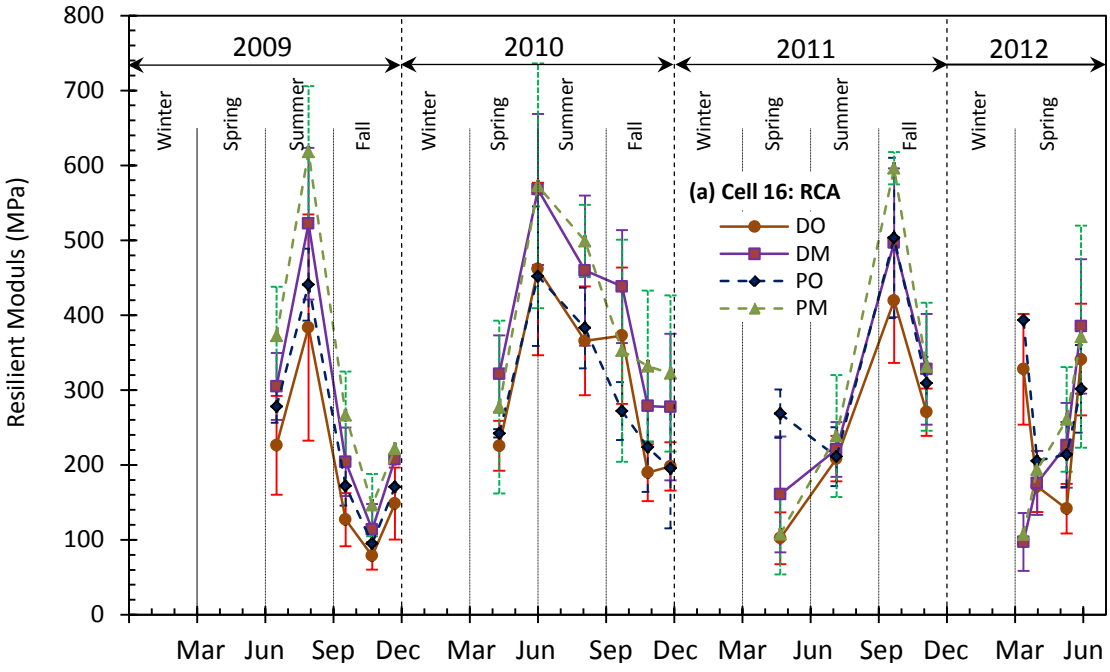
Resilient Moduls (MPa)
800
700
600
500
400
300
200
100
0
2009
2010
2011
2012
Winter
Spring
Summer
Fall
Mar
Jun
Sep
Dec
(a) Cell 16: RCA
DO
DM
PO
PM

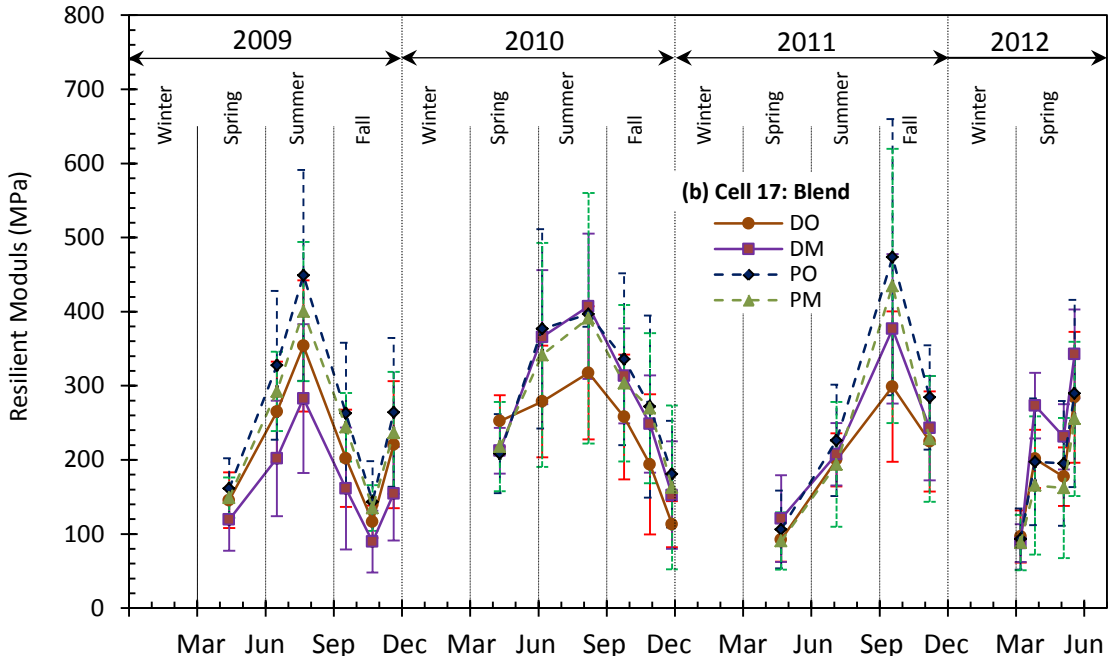
Resilient Moduls (MPa)
800
700
600
500
400
300
200
100
0
2009
2010
2011
2012
Winter
Spring
Summer
Fall
Mar
Jun
Sep
Dec
(b) Cell 17: Blend
DO
DM
PO
PM

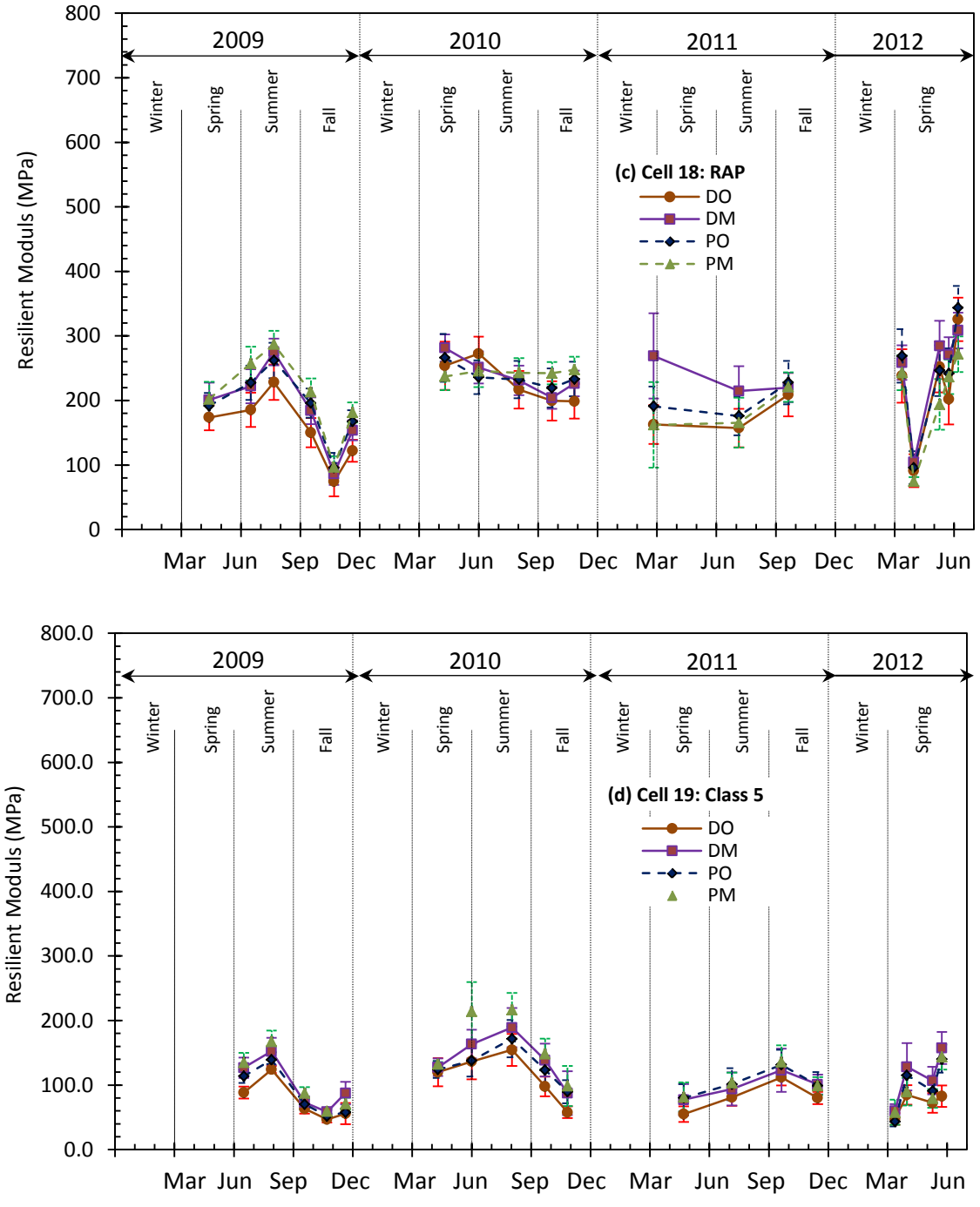

Figure 8.5 Resilient Modulus of Base Course at the Mid-Lane and Outer-Wheel Paths of the Driving and Passing Lanes as a Function of Time for Test Cells Constructed with (a) RCA, (b) blended RCA/Class 5, (c) RAP, and (d) Class 5 Base Course

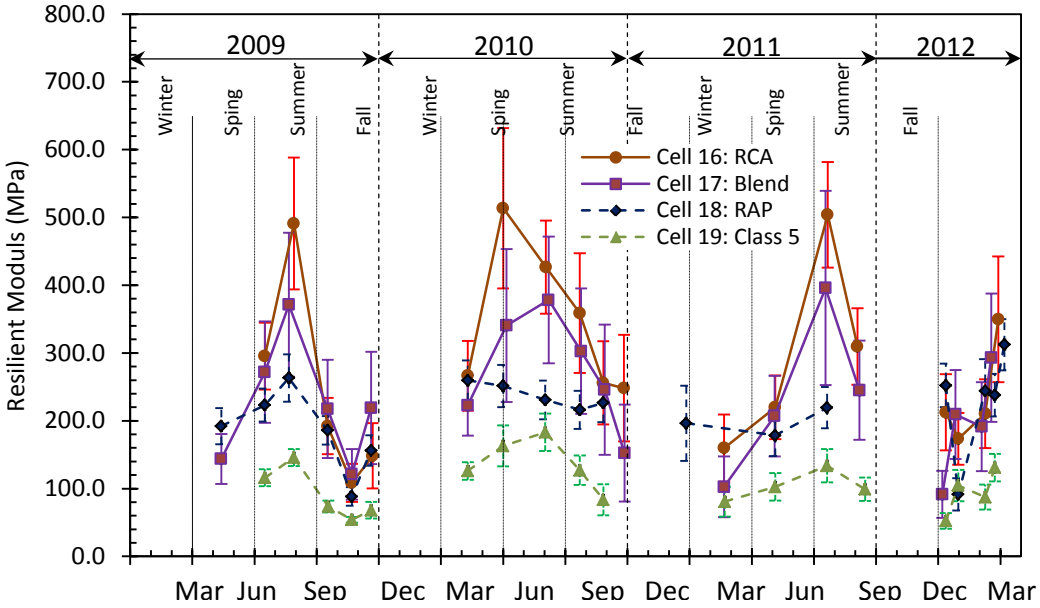

Figure 8.6 Resilient Modulus of Base Course as a Function of Time for Test Cells Constructed with RAP, RCA, blended RCA/Class 5, and Class 5 Base Course (error bars represent one standard deviation)

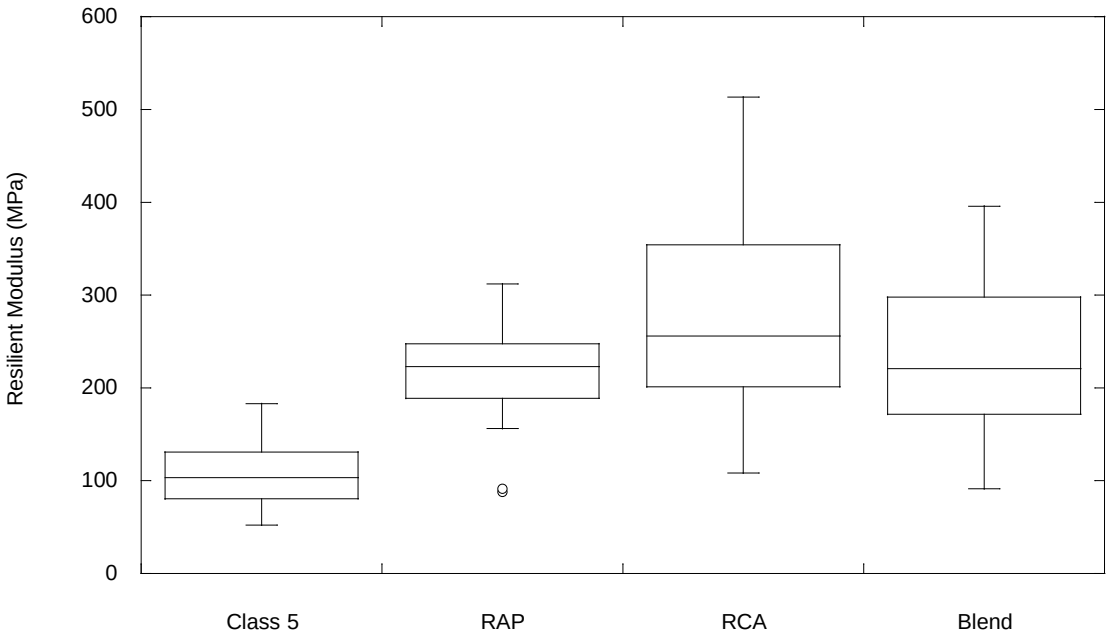

Figure 8.7 Comprehensive Resilient Modulus of all Tests for Cells Constructed with RAP, RCA, blended RCA/Class 5, and Class 5 Base Course

9. Materials Control

9.1 Introduction

RCA and RAP/RPM may contain impurities that affect their mechanical properties and long-term performance. These impurities include soft bituminous materials such as crack sealants as well as pavement markings, metallic objects, recycled clay brick (RCB), and other potentially deleterious materials. A testing program was conducted to assess how impurity type and content affect the resilient modulus and plastic strain of RAP and RCA. This program was conducted in two parts. The first part of the testing program consisted of identifying the types and amounts of impurities present in RCA and RAP/RPM. This was accomplished by carefully segregating and identifying the components of each of the samples of RCA and RAP/RPM collected. Each component impurity was weighed and described. The second part of the testing program consisted of investigating the effects of RCB on compaction characteristics and resilient modulus when mixed with RCA.

RCB is a construction material most commonly used for facades. Clay is the main component of RCB, which is a very fine soil that is highly absorbent and can be hardened into brick when fired in a kiln. The use of RCB in tandem with RCA can benefit both cost and efficiency because of the operational difficulty of separating RCB from the RCA. The effects of RCB at various contents with RCA were evaluated because of the potential for brick to be mixed with RCA to be beneficially reused and because of the lack of literature on the subject. Brick is typically sorted from RCA at demolition sites and disposed of in landfills. The AASHTO (2002) standard for using RCA as an unbound base course puts a limit on RCB percentage (5%); however, AASHTO allows higher percentages than 5% based on comparative structural testing (e.g., CBR, resilient modulus) that demonstrate that RCA with higher brick content is equivalent or better than RCA that complies with granular base specifications. Impurities other than RCB were not investigated past the first part of the testing program due to the lack of impurities present in all materials

9.2 Background

9.2.1 *Deleterious Materials (Impurities) in Recycled Materials*

Kuo et al. (2002) reported that impurities (foreign material) present in RCA are one of the biggest concerns surrounding the use of this material in construction. Kuo et al. (2002) investigated the impurities in RCA made with limestone aggregate for a base course in flexible pavement. The amount of impurities was identified by means of visual inspection. Impurities were classified into categories including wood chips and paper, plastics, steel, asphalt, and RCB. Asphalt was found to be the most predominant type of impurity in the samples. The average impurity content was 3.67% by mass for RCA and 1.99% for limestone aggregates; both of these percentages were considered as negligible.

According to AASHTO Designation M 319-02, (2002), RCA for unbound base course shall be free of all materials that fall into the category of solid waste or hazardous material. Additionally,

RCA should not contain more than 5% bituminous concrete material by mass and 5% brick by mass. No information or studies were provided for the basis of this limitation of materials other than the potential for properties of the material to be affected. The 5% limit on RCB is most likely due to the clay nature and general notion that RCB is more susceptible to degradation and weathering than other building materials (e.g., concrete, rock, etc.). AASHTO (2002) also suggests that the engineer might select stockpiling as an approach to assist in qualitatively identifying the presence of deleterious materials. Stockpiling conditions of recycled material plays an important role in qualitatively assessing the uniformity of the material. Even though AASHTO (2002) defines mean percentages of impurities, AASHTO allows engineers to make some adjustments during construction on the amount of impurities allowed. However, visual examination of the material may not be helpful in determining the detrimental amount of wood chips or brick material in recycled material. Therefore, additional research or study will be important in establishing the acceptable amount of deleterious materials for recycled materials.

The Greenbook specification for construction materials (CMB) allows 3% brick by weight in RCA (Greenbook, 2009). The deleterious content should not comprise a detrimental quantity as defined in section 200-1.1. Various deleterious materials have different specific weights (i.e., wood chips are lighter than brick, plastic is lighter than small piece of wire meshes etc.). Wire mesh, plastic, and brick would be degraded less than sticks or pieces of wood, which would than leave voids in the base layer causing possible failures in the pavement. For concrete production, the amount of deleterious material is defined with many different specifications, but for unbound recycled base material, there are few specifications defining the effect of impurities.

9.2.2 *Recycled Clay Brick Mixed with Recycled Concrete Aggregate*

The use of RCB as a natural aggregate substitute is not typically accepted in construction practices because of the lack of research pertaining to the beneficial reuse of RCB. The majority of research on RCB is on the mechanical properties of the material for use as a substitute for natural aggregate when used in concrete. Debieb and Kenai (2008) investigated using coarse, fine, and coarse/fine RCB as a substitute for natural aggregate in concrete mixes. Introducing RCB reduced bulk density and increased water absorption of the concrete when compared to natural aggregate. Densities of RCB before mixing with cement were also found to be lower (up to 17%) when compared to natural aggregate.

Yang et al. (2011) also evaluated the effects of substituting natural aggregate with RCA and RCB in concrete. Water absorption of the RCA and RCB were 4.2% and 10.2%, respectively, while that of natural aggregate was 1.4%. Particle densities for RCA and RCB were 24.71 kN/m^3 and 21.97 kN/m^3, which were lower than the natural aggregate (26.28 kN/m^3). Arulrajah et al. (2011) evaluated the potential use of RCB as an unbound subbase. They found similar values for RCB with absorption of 6.15% and density at 26.19 kN/m^3. The maximum dry density of the RCB after modified Proctor compaction was 19.82 kN/m^3 and the OMC was 10.7%. Arulrajah et al. (2011) also evaluated permanent strain and resilient modulus of 100% RCB and reported satisfactory performance as a subbase at 98% maximum dry density and 65% OMC.

Poon and Chan (2006) reported that RCB mixed with RCA decreased the maximum dry density and increased the OMC of the mixture. The assumed reasoning for the decrease in maximum dry density was due to the reduced density of the RCB and irregular shape of the manually crushed RCB. California bearing ratio also decreased as RCB content increased. Cameron et al. (2012) investigated the effects of varying RCB content on two types of RCAs, one premixed at 20% RCB by mass and the other mixed at 10%, 20%, and 30% RCB. A decrease (< 80 MPa) in resilient modulus was observed with increased RCB content from 10% to 30% at approximately 90% OMC.

Arulrajah et al. (2011) also evaluated the effects of mechanical degradation and abrasion on RCB using the LA Abrasion test. The results showed a LA Abrasion loss of 36, higher than typical natural aggregate and RCA. 35 is the typical maximum percent loss adopted by state departments of transportation, suggesting the need to mix RCB with stronger aggregates such as RCA or natural aggregate.

9.3 Materials

Sixteen recycled materials, one conventional base course, and one blended recycled/conventional material were used in the first part of this investigation, which evaluated the percentages of impurities present. Seven of the recycled materials were recycled asphalt pavement (RAP), six were recycled concrete aggregate (RCA), and two were recycled pavement material (RPM). The recycled materials used in this study were obtained from a wide geographical area, covering eight different states: California, Colorado, Michigan, Minnesota, New Jersey, Ohio, Texas and Wisconsin (Figure 9.1). The materials were named according to the origin of the materials. The reference base course was a gravel meeting the Class 5 aggregate specification for base course in Minnesota per the Minnesota Department of Transportation (MnDOT). The Class 5 aggregate used in this study contains quartz, granite and carbonates (limestone and dolomite). The ratio of quartz/granite to carbonates is 2.1. The percentage of mineral type in Class 5 aggregate is 68% for quartz/granite and 32% for carbonates. Percent quartz/granite (aggregate and concrete) and percent carbonate of gravel (aggregate and concrete) of gravel are 43% and 20%, respectively. The blend (MN) was a mix of approximately equal parts (by mass) RCA from MnDOT (50%) and Class 5 aggregate (50%). The Class 5 aggregate was used as the control in this study.

The material from MnDOT was obtained during construction of roadway cells at the MnROAD test facility in Maplewood, Minnesota for investigation of the field behavior. The RAP was milled from the surface of roadway cells that were previously constructed at the MnROAD test facility. The RCA was obtained from a stockpile maintained by the Knife River Corporation at their pit located at 7979 State Highway 25 NE in Monticello, Minnesota.

The RAP from the Ohio Department of Transportation (ODOT) came from an existing asphalt pavement, processed through a portable plant, and stored in approximately 2268 Mg stockpiles. The Ohio RCA is from a 1.2-m-high barrier wall that existed between the north- and south-bound lanes of State Route 315 in downtown Columbus, Ohio. The broken-up concrete was taken from the project to a portable processing plant, crushed, sized, and stockpiled. The material

for this project came from stockpiles of approximately 9071 Mg. The RCA samples provided were 100% RCA.

The material received from the Colorado DOT was collected from over 500 demolition sites from curb, gutter, sidewalk, highways, high-rise buildings, and housing foundations. Although the concrete came from varied sources, the aggregates for the production of the concrete originated from rock in Colorado, most from quarries in Morrison and Golden and some aggregates were sourced from the Platte River.

The material provided by the New Jersey DOT (NJ DOT) is from stockpiles for demolition projects, primarily in New Jersey. The material in the stockpiles is in flux since NJ DOT constantly adds new loads and removes content for different purposes.

The RAP from California DOT is a combination of roadway millings and waste from an HMA plant (discharge from warm up and cleaning processes). The RCA is broken concrete rubble from the demolition of structures. Stockpiling in California is usually done three times a year. These stockpiles are not added to throughout their life-cycle. If stockpiled material is still unavailable during visits from subcontractors, new material is used to create a new stockpile.

The RCA sent by the Texas DOT is from a commercial source; therefore, the individual sources of aggregate or material characteristics included in the RCA are not known. The Texas RAP is from a highway project where the contractor milled the "binder" course after approximately 1.5 years of service. The RAP from Michigan was provided by the Michigan DOT and is from highway reconstruction projects.

A summary of the grain characteristics and classifications for the seventeen materials is shown in Table 9.1. The materials used in this study are classified as non-plastic per the Unified Soil Classification System (USCS). The Class 5 aggregate is classified as well-graded gravel (GW-GM) per USCS (ASTM D 2487) and A-1-b per the AASHTO Soil Classification System (ASTM D 3282). The blended RCA/Class 5 is classified as A-1-b according to ASTM D 3282 and as poorly graded sand (SP) according to ASTM D 2487. The samples of RCA range from an SP to a well-graded gravel (GW) classification via USCS and A-1-a or b for AASHTO. The various RAPs and RPMs classify as SP, SW, or GW, whereas their AASHTO classifications are A-1-a or b. All materials are coarse-grained granular materials with fines content less than 7% except Class 5 aggregate and one RCA (CO) sample.

The particle size distribution (PSD) curves were determined according to ASTM D 422. Samples were wet-sieved through a No. 200 (75-μm opening) sieve to separate the fine particles attached to the coarser aggregates. The PSDs for the RCA and the RAP/RPM samples are shown in Figure 9.2 and Figure 9.3, respectively, along with the upper and lower bounds from the literature.

The RCB was obtained from the demolition of the University of Wisconsin Credit Union’s drive-through structure. The approximate age of the clay brick was 16 years. Brick and attached mortar were manually crushed using sledge hammers and then sieved to match the PSDs of each

four RCAs used in the tests conducted. For the brick study, the RCAs from New Jersey, Minnesota, Texas, and Ohio were used.

9.4 Methods

9.4.1 *Impurity Test*

Impurities are one of the biggest concerns surrounding the use of the recycled materials in construction (Kuo et al. 2002). To determine the amount of impurities, 15 kg from each sample defined in Section 3.1 were air dried and passed through sieves to separate the aggregates into different sizes to facilitate the removal of impurities. Impurities collected visually from each sieve were weighed and described. Impurities were classified into different categories. For RAP, the types of impurities are pavement markings, metallic objects, wood chips, plastic objects and glass materials and for RCA, metallic objects, wood chips, asphalt aggregates, aggregates with plastic fibers, plastic objects, and glass and geotextile materials.

9.4.2 *Resilient Modulus*

The design of roadway pavement relies on proper characterization of the load-deflection response of the pavement layers (Tian et al. 1998). Base and subgrade deform when subjected to repeated loads from moving vehicular traffic. Resilient modulus (M_r) defines the nonlinear elastic response of pavement geomaterials, such as unbound aggregate base and subbase, under repeated traffic loading. The resilient behavior of unbound aggregate layers is affected by the stress state experienced because of wheel loading and the physical properties of aggregate (Pan et al. 2006). The M_r is a linear-elastic modulus obtained from dynamic loading, defined as the ratio of the cyclic deviator stress to the resilient (recoverable) strain, and is defined as:

$$M_r = \left({}^{\sigma_d}/_{\varepsilon_r} \right) \tag{9.1}$$

where ε_r is the recoverable elastic strain and σ_d is the applied deviator stress.

Design of pavements and rehabilitation of layered pavement systems use M_r as an essential parameter in the design process (Heydinger et al. 2007). The M_r is a key input in NCHRP 1-37 (mechanistic-based pavement design approach), which is being evaluated for adoption by numerous state highway agencies (Pan et al. 2006). The performance of pavement is dependent on the stiffness of the pavement structure under specified traffic loads and environmental conditions. Generally, a high M_r for a base course infers a stiffer base course layer, which increases pavement life. The resilient response of granular material is important for the load-carrying ability of the pavement and the permanent strain response, which characterize the long-term performance of the pavement and rutting phenomenon (Lekarp et al. 2000).

For base course, the summary resilient modulus (SRM) corresponds to the M_r at a bulk stress of 208 kPa, and octahedral shear stress of 48.6 kPa as suggested by Section 10.3.3.9 of NCHRP 1-28a. SRM is also used to determine the layer coefficient, which is a required input in the AASHTO pavement design equation (Tian et al. 1998).

9.4.3 *Crushed Clay Brick Tests*

To evaluate the effects of RCB on the resilient modulus and compaction properties, percentages of RCB to RCA were first determined. 10%, 20%, and 30% RCB by mass were used because these percentages have the possibility of being accidentally or purposely mixed in with RCA. These percentages also matched the percentages of the study completed by Cameron et al. (2012). The RCB was sieved through 25, 19, 9.5, 4.75, 2.36, and 0.425-mm sieves and matched to the PSD of the RCA it was mixed with. Once mixed, modified Proctor compaction tests were completed on the 30% RCB mixture per ASTM D422. Compaction tests were not completed on New Jersey RCA or at 10% and 20% RCB due to lack of RCA available.

For the resilient modulus tests, RCB/RCA specimens were compacted at OMC and 95% of maximum dry unit weight of the corresponding RCA the RCB was mixed with. The mixtures were compacted to the RCA's compaction characteristics to evaluate the effects associated with RCB unnoticeably being added to the RCA. The specimens were compacted in six lifts using a modified Proctor hammer into a 152-mm-diameter, 305-mm-high mold. Cyclic load triaxial tests were then completed according to NCHRP 1-28a on the RCB/RCA mixtures at 0%, 10%, 20%, and 30% RCB to determine the resilient modulus (M_r) and plastic strain of the material. Two interior and two external linear variable differential transducers (LVDTs) were used to record the strain response of the loading on the specimens. The data was fitted using the Power fitting and NCHRP models shown as equation 9.2 and 9.3, respectively. Plastic strain was also calculated using both interior and exterior LVDT data from the triaxial test.

$$M_R = k_1 \times \theta^{k_2} \tag{9.2}$$

$$M_r = k_1 . p_a . \left(\frac{\theta - 3k_6}{p_a}\right)^{k_2} . \left(\frac{\tau_{oct}}{p_a} + k_7\right)^{k_3} \tag{9.3}$$

Where k_1, k_2, k_3, k_6, and k_7 are constants, p_a is atmospheric pressure (101.4 kPa), τ_{oct} is octahedral shear stress, and θ is bulk stress. Using the data collected, a summary resilient modulus (SRM) was determined at θ = 208 kPa and τ_{oct} = 48.6 kPa.

The Power function (Equation 9.2) is a simple model widely used for granular material. The estimated SRM per the Power function model was compared to the measured modulus. Statistical analysis indicated that results from the Power function model are significant at a 95% confidence level, and the model represents the data reasonably well for RCA (R^2 = 0.85) and for RAP (R^2 = 0.90) (Bozyurt 2011).

9.4.4 *Toughness and Abrasion*

Handling, mixing, and weathering of aggregates are common occurrences that have the potential to degrade the material before, during, and after construction. To test how tough and abrasion resistant these materials are, LA Abrasion testing was completed on MN RCA and Class 5 and then compared to RCB values from literature. Only MN RCA and Class 5 were used in this study due the large quantity of material needed for the test. LA Abrasion testing was completed

following AASHTO T 96. LA Abrasion testing was conducted at the Wisconsin Department of Transportation laboratory in Madison, WI.

9.5 Results and Discussion

9.5.1 *Impurity Test*

Deleterious materials were classified into different categories such as wood chips, glass, geotextiles, steel, and asphalt aggregate, aggregate with plastic fibers, and sea shells, and the percentage by weight of the deleterious materials present in RCA, RAP/RPM and Class 5 aggregate is summarized in Table 9.1 and plotted in Figure 9.4. Asphalt aggregates and aggregate with plastic fibers are heavier than the wood chips, sea shells and geotextile materials; therefore their percentage by weight is high.

The amount of deleterious materials present in RCA and RAP/RPM varied amongst the source of the materials (Figure 9.5). Even though, RCA had higher amount of deleterious materials compared to RAP/RPM, the source of RCA affected the occurrence of deleterious materials. These differences may be related to the production process or stockpiling conditions of RCA. Generally, asphalt aggregate, aggregate with plastic fibers, and wood chips were the most predominant type of impurities for RCA (Figure 9.6). As shown in Figure 9.7, the average impurity content was 1% for RCAs obtained from different states (CO, OH, TX, MN, CA, MI, WI, and NJ). Kuo et al. (2002) investigated the impurities in RCA made with limestone aggregate for a base course in flexible pavement. The amount of impurities was identified by means of visual inspection. Impurities were classified into different categories such as wood chips and paper, plastic, steel, asphalt, and brick. Asphalt was found to be the most predominant type of impurity in the samples. The average impurity content was 3.67% for RCA and 1.99% for limestone aggregate, which are higher than determined in this study covering a larger range of RCA covering a broader geographic distribution. This may be reflective of the improvements in recycling processes in more recent years minimizing the impurities. Kuo et al. (2002) considered their percentages to be negligible.

Geotextiles and pavement markings were the predominant type of impurities for RAP/RPM. The average impurity amount was 0.2% for all RAP/RPM samples from different states (CO, OH, TX, MN, CA, MI, WI, and NJ) (Figure 9.8). During the production of RAP/RPM, some extraneous content may be mixed into the recycled material, such as pavement markings or wood chips from the environment around the road. The stockpiling conditions of the recycled material also could create additional impurities.

9.5.2 *Compaction Characteristics of RCB/RCA Mixtures*

Compaction tests conducted on TX RCA, MN RCA, and OH RCA with 30% RCB resulted in an increase in OMC and decrease in maximum dry unit weight when compared to the 0% RCB compaction tests (Table 9.3 and Figure 9.9 to Figure 9.11). The results for the RCA mixed with 30% RCB do not reflect parabolic curves as well as the 0% RCB material. The curves do not descend for any of the 30% RCB material, but stay very constant at OMC. This was caused by

excessive drainage of water during compaction, reducing the moisture content in the middle of the compacted specimen and keeping a constant density. Regardless of the amount of water added to create a specimen above OMC, water is drained to the OMC of the material in the center of the compacted specimen. This could be viewed as a potential attribute of using RCB/RCA mixtures because the material cannot retain more than the optimum moisture content, so the hydraulic conductivity is quite high. This also could be viewed in the negative realm because of the increased OMC requiring more water to be added to achieve compaction requirements. Additional tests to determine the hydraulic conductivity of the mixture is recommended to further explain the compaction characteristics.

These compaction results are similar to the Poon and Chan (2006) results, which tested brick and RCA at 0%, 25%, and 50% brick. Similar conjectures can be made as Poon and Chan (2006) did as to the reasoning for this increase in OMC and decrease in maximum dry unit weight. Lower specific gravity of RCB compared to RCA can cause a decrease in maximum dry unit weight. The lower specific gravity in the RCB compared to the RCA is likely due to the increased air voids within the particles of RCB. This increased void space in RCB was also indicated by the RCB's 11.5% absorption, more than double the absorption of three of the four RCAs used. Higher absorption can also lead to the increase in OMC observed in compaction testing (Poon and Chan 2006).

9.5.3 *Summary Resilient Modulus of RCB/RCA Mixtures*

The SRM results fitted with the NCHRP and Power models for both the internal and external LVDTs are displayed in Table 9.4 and Figure 9.12 and Figure 9.13. Table 9.5 and Table 9.6 display the fitting parameters for the NCHRP and Power models, respectively. Table 9.7 shows the coefficients of variations in SRM for each control specimen and its replicates. Four replicate M_r tests were conducted on the basalt, Class 5, and all three RCAs. The highest coefficient of variation for the replicate control specimens was 15%, which was deemed the margin of error for all M_r tests due to instrumentation and rounding. As seen in Table 9.8, no coefficients of variation between the RCB SRM values are above 15%, which is the amount of error due to instrumentation and rounding. With none of the SRM values for the varying brick content specimens showing a coefficient of variation above the expected error, there is no apparent trend in SRM with change in RCB content up to 30% for the materials evaluated.

The result of no trend in SRM with increase RCB content up to 30% is similar to the results of the only previous study completed on resilient modulus of RCB/RCA mixtures by Cameron et al. (2012). Cameron et al. (2012) observed a marginal decrease (< 80 MPa) in resilient modulus with increased RCB content (0% to 30% RCB), which could be within the error for that specific test but no information is noted on error in the study. Cameron et al. (2012) used a different method (i.e., AUSTROADS method) that uses approximately 50,000 cycles, whereas the NCHRP method only uses about 4,000 cycles. In addition, the study completed by Cameron et al. (2012) was more focused towards evaluating resilient modulus of RCB/RCA mixtures at varying water content (60% to 100% OMC) than the SRM of RCB/RCA mixtures at OMC and found that lower (80% OMC) water contents was more favorable for stiffness of RCB/RCA blends. This finding was similar to the study by Arulrajah et al. (2011) which evaluated 25%

RCB/75% RCA mixtures and found that 65% OMC was the highest water content RCB/RCA could be mixed at to be a viable material for road subbase applications. Arulrajah et al. (2011) used the same resilient modulus testing method as Cameron et al. (2012). This testing method change between this study and Arulrajah et al. (2011) and Cameron et al. (2012); and the lack of reporting SRM in the other two studies could both contribute to the different trend results observed. Both studies found that resilient modulus and permanent strain were marginal factors with RCB/RCA mixtures compared to moisture content and density changing the design.

The difference in material between this study and the studies by Arulrajah et al. (2011) and Cameron et al. (2012) may contribute to the difference in resilient modulus observed. This study used clay brick as the material tested, whereas neither Arulrajah nor Cameron state the type of brick used. A fly ash based brick or cement based brick could tremendously alter the physical characteristics of the RCB. The RCB used in this study had higher absorption values (11.5% compared to ~6.5%) than the RCB used in both Arulrajah et al. (2011) and Cameron et al. (2012). The particle dry unit weight of the RCB in this study was also lower (19.3 kN/m^3 compared to 26.2 kN/m^3) than that of Arulrajah et al (2011) (Cameron et al. 2012 did not report a dry unit weight of RCB alone). Both of these large differences in physical characteristics of the RCB between this study and the other two studies could explain the noticeable trend change in resilient modulus with increased RCB content.

9.5.4 *Plastic Strain of RCB/RCA Mixtures*

Plastic strains were calculated as an index using the data from the M_r tests and presented in Table 9.9 and Table 9.10 for the 1st load sequence and 2nd through 31st load sequences, respectively. There were no apparent trends in plastic strain observed from the data for the first sequence (conditioning phase) or last 30 sequences. All data suggests very little change in accumulation of plastic strain in all specimens regardless of RCB content, suggesting RCB has little impact on stiffness of RCA when mixed at or below 30% RCB. Cameron et al (2012) evaluated plastic strain and found that marginal (< 0.7%) changes were observed between 0% RCB and 30% RCB/RCA mixtures. It is recommended that tests designed specifically for plastic strain be completed if further analysis is wanted on plastic strain of the specific materials used in this study. The resilient modulus test (NCHRP 1-28a) used in this study are not designed for calculating plastic strain accurately.

9.5.5 *Weathering and Abrasion Resistance of RCB/RCA Mixtures*

The results of the LA Abrasion tests conducted on MN RCA, Class 5, and RCB from literature can be seen in Table 9.11. RCB appears to be less tough and less resistant to abrasion than both Class 5 and MN RCA. This is most likely due to the clay-based nature of the RCB, which depending on the source of the clay and the original firing temperature the clay brick was created at, could have lower bond strength than concrete and natural aggregates (Amrhein 1998). The variability in manufacturing of the clay brick directly impacts the weathering and strength of the RCB and the manufacturing specifications for the brick used in this study and Arulrajah et al. (2011) and Cameron et al. (2012) are unknown. Further weathering tests (i.e. freeze-thaw, wet/dry, and Micro-Deval) are recommended to determine the impact weathering has on RCB.

9.6 Summary and Conclusions

The amount of deleterious material present in RCA and RAP/RPM varied depending on source of the material. Generally, asphalt aggregate, aggregate with plastic fibers, and wood chips were the most predominant type of impurities for RCA. The average impurity content was 1% for RCAs obtained from different states (CO, OH, TX, MN, CA, MI, WI, and NJ). Geotextiles and pavement markings were the predominant type of impurities for RAP/RPM. The average impurity amount was 2% for all RAP/RPM samples from different states (CO, OH, TX, MN, CA, MI, WI, and NJ).

The production of RCA and RAP/RPM involves the removal and reprocessing of existing asphalt pavement from roadway structures. During the removable process of asphalt pavement, some additional materials were mixing to the recycling materials, such as wood chips from the nature around the road or the pavement markings. Even though the majority of the recycled materials is recycled and used in the same year, some of them were stockpiled in order to use in long terms. The stockpiling conditions of the recycled materials also could create additional impurities.

Due to the general lack of deleterious materials found in recycled materials, possibility for beneficial reuse and lack of research on its use, brick was chosen to be investigated further using resilient modulus at 0%, 10%, 20%, and 30% by mass with RCA. Brick acquired from a demolition site was crushed and sieved to match particle size distributions of each of the four RCAs it was mixed with. The four RCAs used were NJ, OH, MN, and TX. Compaction tests were completed at 0% and 30% RCB on all RCA materials except NJ RCA because of lack of material available. When 30% RCB compaction characteristics were compared to 0% RCB, OMC increased while maximum dry unit weight decreased. This was attributed to RCB having higher absorption and lower specific gravity and dry unit weight than RCA. The compaction curves for the 30% RCB mixtures did not decrease in maximum dry unit weight above OMC because water drained out of the molds not allowing for a water content above OMC to be achieved. This lack of decrease was observed in all three RCB/RCA mixtures tested at 30% RCB.

Resilient modulus tests were completed on the four RCA samples at 0%, 10%, 20%, and 30% RCB content. Each specimen was compacted at OMC and 95% of maximum dry density of the RCA it was compacted with. No apparent trends in SRM outside of the standard 15% margin of error were observed at any RCB content for all four RCAs. This trend was not seen by previous studies, but difference in materials tested and methods used to test for resilient modulus could contribute to this difference in results. Further testing at higher RCB content is recommended to determine an exact limit to the amount of RCB that can be added to RCA or other aggregates for beneficial reuse. It is also recommended that further testing be completed to evaluate the hydraulic conductivity, effects of weathering (i.e., freeze-thaw and wet-dry), and abrasion resistance (i.e., micro-deval) of the RCB/RCA mixtures.

9.7 Tables

Table 9.1 Index properties for Recycled Materials and Class 5 aggregate

Material	States	D_{10} (mm)	D_{30} (mm)	D_{50} (mm)	D_{60} (mm)	C_u	C_c	G_s	Dry Unit Weight (kN/m^3)	Absorption (%)	Asphalt Content (%)	Impurities (%)	Gravel (%)	Sand (%)	Fines (%)	USCS	AASHTO
Class 5	MN	0.1	0.4	1.0	1.7	21	1.4	2.57	25.11	_	_	0.25	22.9	67.6	9.5	GW-GM	A-1-b
Blend	MN	0.2	0.6	1.5	2.8	13	0.5	_		_	_	0.36	32.7	63.8	3.4	SP	A-1-b
RCA	MN	0.1	0.4	1.0	1.7	21	1.4	2.39	23.34	5.0	_	0.87	31.8	64.9	3.3	SW	A-1-a
	MI	0.4	4.1	9.7	12.3	35	3.9	2.37	23.16	5.4	_	0.35	68.5	28.3	3.2	GP	A-1-a
	CO	0.1	0.6	2.8	4.9	66	1.1	2.28	22.3	5.8	_	0.26	40.9	46.3	12.8	SC	A-1-b
	CA	0.3	1.7	4.8	6.8	22	1.4	2.32	22.74	5.0	_	0.26	50.6	47.1	2.3	GW	A-1-a
	TX	0.4	6.5	13.3	16.3	38	6.0	2.27	22.22	5.5	_	0.86	76.3	21.6	2.1	GW	A-1-a
	OH	0.2	1.2	3.4	5.3	34	1.7	2.24	21.95	6.5	_	0.16	43.2	49.5	7.3	SW-SM	A-1-a
	NJ	0.2	0.5	2.0	5.1	28	0.3	2.31	22.64	5.4	_	1.67	41.2	54.6	4.3	SP	A-1-b
RAP	MN	0.3	0.7	1.6	2.3	7	0.7	2.41	23.54	1.8	7.1	0.06	26.3	71.2	2.5	SP	A-1-a
	CO	0.4	0.9	2.2	3.3	9	0.7	2.23	21.8	3.0	5.9	0.09	31.7	67.7	0.7	SP	A-1-a
	CA	0.3	1.3	3.0	4.2	13	1.2	2.56	18.31	2.0	5.7	0.33	36.8	61.4	1.8	SW	A-1-a
	TX	0.7	2.5	5.4	7.9	11	1.1	2.34	22.86	1.3	4.7	0.05	41.0	44.9	1.0	SW	A-1-a
	OH	0.5	1.6	2.9	3.8	7	1.3	2.43	23.73	0.6	6.2	0.06	32.1	66.2	1.7	SW	A-1-a
	NJ	1.0	2.8	4.9	5.9	6	1.3	2.37	23.17	2.1	5.2	0.48	50.9	48.4	0.7	GW	A-1-a
	WI	0.6	1.4	2.7	3.6	6	0.9	2.37	23.22	1.5	6.2	0.08	30.9	68.5	0.5	SP	A-1-b
RPM	NJ	0.5	2.1	5.8	8.7	18	1.0	2.35	23.42	2.6	4.3	0.04	55.7	43.6	0.6	GW	A-1-b
	MI	0.4	1.7	4.6	6.5	17	1.1	2.39	23.00	1.7	5.3	0.13	49.3	50.4	0.4	SW	A-1-b
RCB	WI	NA	NA	NA	NA	NA	NA	2.20	19.33	11.5	_	NA	NA	NA	NA	NA	NA

C_u = coefficient of uniformity, C_c = coefficient of curvature, G_s= Specific Gravity, AC= Asphalt Content, Abs=Absorption, Note: Particle size analysis conducted following ASTM D 422, G_s determined by ASTM D 854, Absorption of coarse aggregate were determined by ASTM C127-07, USCS classification determined by ASTM D 2487, AASHTO classification determined by ASTM D 3282, asphalt content determined by ASTM D 6307

Table 9.2 Quality Control of Specimen Preparation

	Brick Content of Material	ω_{opt}	$\omega_{compacted}$	Percent ω Difference	Std. Dev. (Percent ω Difference)	Mass after Compaction Goal (kg)	Mass after Compaction (kg)	Percent Mass Difference	Std. Dev. (Percent Mass Difference)	*95% Dry Unit Weight (kN/m^3)*	Dry Unit Weight of Compacted Material (kN/m^3)	Dry Unit Weight Difference	Std. Dev. (Dry Unit Weight Difference)
MN RCA	0%	11.20%	11.70%	0.50%	0.10%	11.68	11.6	0.68%	0.57%	18.53	18.32	1.15%	0.23%
	10%	11.20%	11.50%	0.30%		11.68	11.85	1.46%		18.53	18.75	1.16%	
	20%	11.20%	11.60%	0.40%		11.68	11.9	1.88%		18.53	18.81	1.50%	
	30%	11.20%	11.50%	0.30%		11.68	11.9	1.88%		18.53	18.82	1.59%	
TX RCA	0%	9.20%	9.60%	0.40%	0.10%	11.56	11.55	0.09%	0.22%	18.68	18.59	0.50%	0.26%
	10%	9.20%	9.50%	0.30%		11.56	11.5	0.52%		18.68	18.52	0.84%	
	20%	9.20%	9.00%	0.20%		11.56	11.5	0.52%		18.68	18.61	0.38%	
	30%	9.20%	9.60%	0.40%		11.56	11.5	0.52%		18.68	18.51	0.93%	
NJ RCA	0%	9.50%	9.80%	0.30%	0.06%	11.65	11.6	0.43%	0.73%	18.76	18.63	0.67%	0.50%
	10%	9.50%	9.30%	0.20%		11.65	11.45	1.72%		18.76	18.48	1.51%	
	20%	9.50%	9.70%	0.20%		11.65	11.5	1.29%		18.76	18.49	1.44%	
	30%	9.50%	9.20%	0.30%		11.65	11.4	2.15%		18.76	18.41	1.85%	
OH RCA	0%	11.80%	12.10%	0.30%	0.05%	11.66	11.55	0.94%	0.54%	18.39	18.17	1.18%	0.57%
	10%	11.80%	12.10%	0.30%		11.66	11.45	1.80%		18.39	18.02	2.04%	
	20%	11.80%	12.10%	0.30%		11.66	11.45	1.80%		18.39	18.02	2.04%	
	30%	11.80%	12.20%	0.40%		11.66	11.4	2.23%		18.39	17.92	2.55%	

Note: ω_{opt} = Optimum moisture content; $\omega_{compacted}$ = Compacted moisture content; ω Standard Deviation = Variability in percent moisture content difference ; Std. Dev. = Standard Deviation

Table 9.3 Maximum Dry Unit Weight and Optimum Moisture Content Changes with Varying Brick Content

Material	Percent Brick	Max Dry Unit Weight (KN/m^3)	ω_{opt}
TX RCA	0	19.7	9.20%
	30	18.44	11.70%
MN RCA	0	19.5	11.20%
	30	18.6	11.80%
OH RCA	0	19.8	11.80%
	30	17.52	12.40%

Table 9.4 External and Internal LVDT Summary Resilient Modulus Values at Varying Brick Content Calculated using NCHRP and Power Function Models

		SRM (MPa)			
		OH RCA	TX RCA	NJ RCA	MN RCA
0% Brick	Int NCHRP	233	173	169	132
	Int Power	254	197	200	176
	Ext NCHRP	150	129	114	108
	Ext Power	166	142	130	128
10% Brick	Int NCHRP	188	194	176	162
	Int Power	217	237	208	200
	Ext NCHRP	140	121	129	113
	Ext Power	162	139	152	132
20% Brick	Int NCHRP	173	232	168	144
	Int Power	201	277	199	171
	Ext NCHRP	110	127	122	94
	Ext Power	128	145	140	107
30% Brick	Int NCHRP	156	156	176	111
	Int Power	166	200	193	133
	Ext NCHRP	120	122	106	105
	Ext Power	142	145	120	125

Note: Bulk Stress (θ) = 208 kPa, Octahedral Stress (τ_{oct} = 48.6 kPa)

Table 9.5 NCHRP Fitting Parameters and Summary Resilient Modulus (SRM) Values

Material	Brick %	Internal						External						SRM_{int}/ SRM_{ext}
		k_1	k_2	k_3	k_6	k_7	SRM (MPA)	k_1	k_2	k_3	k_6	k_7	SRM (MPA)	
OH RCA	0	0.01	5.7	-2.73	-478.4	2.89	233	1.00	5.07	-3.75	-480.3	5.72	150	1.55
	10	142.00	2.03	-1.27	-82.3	1	188	20,029.90	1.69	-2.76	-77.3	6.01	140	1.34
	20	0.1	5.87	-4.07	-480.1	4.83	173	5,158.60	1.56	-2.17	-56.1	4.82	110	1.57
	30	0.002	5.11	-1.31	-478.1	1	156	137,928.30	1.76	-3.57	-71.2	7.19	120	1.30
TX RCA	0	34.80	2.35	-1.08	-141.3	1	173	857.60	1.94	-1.9	-145.2	4.94	129	1.34
	10	188	2	-1.28	-68.8	1	194	507.60	1.31	-0.91	-29.5	1.38	121	1.60
	20	377.80	2.14	-1.82	-99.4	2	232	3,055.70	1.39	-1.79	-49.9	3.9	127	1.83
	30	11,782,048.70	1.76	-4.67	-39.5	10.1	156	14,824.20	1.76	-2.81	-71.8	5.51	122	1.28
NJ RCA	0	0.0002	5.87	-1.46	-480.1	1	163	1,287.00	1.88	-2.03	-105.9	5.28	83	1.96
	10	0.001	6	-2.96	-479.9	3.07	176	747.10	1.67	-1.66	-63.6	2.39	129	1.36
	20	287.6	1.7	-1.16	-56.3	1.05	168	1632.70	1.42	-1.63	-47.2	3.07	122	1.38
	30	0.003	5.57	-1.49	-479.1	1	176	3,593.80	1.48	-1.93	-63	4.97	106	1.66
MN RCA	0	0.0001	5.95	-1.18	-479.7	1	132	357,340.80	1.7	-3.95	-50.1	7.04	108	1.22
	10	1,092.70	1.87	-1.97	-53.9	2.35	162	1,332.70	1.63	-1.83	-59.1	3.16	113	1.43
	20	942.8	1.57	-1.5	-37.2	2.05	144	793.70	1.33	-1.18	-36.5	2.71	94	1.53
	30	338	1.48	-0.89	-25.5	1	111	694.10	1.47	-1.36	-32	1.98	105	1.06

Table 9.6 Power Model Fitting Parameters and SRM Values

Material	Brick %	Internal			External			SRM_{int}/SRM_{ext}
		k_1	k_2	SRM (MPA)	k_1	k_2	SRM (MPA)	
OH RCA	0	20,000.00	0.48	254	16,064.50	0.44	166	1.53
	10	20,146.20	0.44	217	12,438.70	0.48	162	1.34
	20	20,000.00	0.43	201	7,601.40	0.53	128	1.57
	30	12,951.30	0.48	166	11,000.20	0.48	142	1.17
TX RCA	0	15,201.60	0.48	197	10,334.30	0.49	142	1.39
	10	17,887.80	0.48	237	7,868.20	0.54	139	1.71
	20	28,302.00	0.43	277	11,745.00	0.47	145	1.91
	30	7,208.50	0.62	200	10,279.90	0.5	145	1.38
NJ RCA	0	11,755.20	0.51	181	4,429.00	0.57	93	1.95
	10	18,648.40	0.45	208	13,870.90	0.45	152	1.37
	20	17,344.40	0.46	199	11,596.80	0.47	140	1.42
	30	16,098.30	0.47	193	7,471.40	0.52	120	1.61
MN RCA	0	14,631.30	0.47	176	7,311.30	0.54	128	1.38
	10	14,335.60	0.49	200	9,489.20	0.49	132	1.52
	20	10,533.70	0.52	171	5,048.90	0.57	107	1.60
	30	4,995.50	0.61	133	7,348.70	0.53	125	1.06

Table 9.7 Control Specimen Error Values

		Int (NCHRP)	Ext (NCHRP)
Basalt	Average	170	118.75
	Std. Dev.	12.19	5.91
	Coef. Var.	7%	5%
Class 5	Average	122	100
	Std. Dev.	11.75	11.92
	Coef. Var.	10%	12%
CA RCA	Average	209.75	130.75
	Std. Dev.	27.33	15
	Coef. Var.	13%	11%
TX RCA	Average	192.25	108.5
	Std. Dev.	12.04	16.54
	Coef. Var.	6%	15%
NJ RCA	Average	168.75	99
	Std. Dev.	14.06	12.73
	Coef. Var.	8%	13%

Table 9.8 RCA with Brick SRM Error Values

		Int (NCRP)	Ext (NCHRP)
OH RCA	Average (MPa)	187.5	130
	Std. Dev.	33.03	18.26
	Coef. Var.	18%	14%
TX RCA	Average (MPa)	188.75	124.75
	Std. Dev.	32.76	3.86
	Coef. Var.	17%	3%
NJ RCA	Average (MPa)	172.25	117.75
	Std. Dev.	4.35	9.95
	Coef. Var.	3%	8%
MN RCA	Average (MPa)	137.25	105
	Std. Dev.	21.41	8.04
	Coef. Var.	15%	8%

Table 9.9 1st Load Sequence Deformation and Plastic Strain

		1st Load Sequence Deformation and Plastic Strain			
		OH RCA	**TX RCA**	**NJ RCA**	**MN RCA**
0% Brick	Int Deformation (mm)	0.2	0.2	0.3	0.7
	Int Plastic Strain (%)	0.10%	0.10%	0.20%	0.40%
	Ext Deformation (mm)	0.7	0.9	1.2	1.7
	Ext Plastic Strain (%)	0.30%	0.30%	0.40%	0.60%
10% Brick	Int Deformation (mm)	0.1	0.2	0.2	0.4
	Int Plastic Strain (%)	0.10%	0.10%	0.10%	0.30%
	Ext Deformation (mm)	0.6	2.3	1.1	1.3
	Ext Plastic Strain (%)	0.20%	0.80%	0.40%	0.40%
20% Brick	Int Deformation (mm)	0.3	0.1	0.2	0.4
	Int Plastic Strain (%)	0.20%	0.10%	0.20%	0.30%
	Ext Deformation (mm)	1	1	0.9	1.7
	Ext Plastic Strain (%)	0.30%	0.30%	0.30%	0.60%
30% Brick	Int Deformation (mm)	0.2	0.3	0.2	0.5
	Int Plastic Strain (%)	0.10%	0.20%	0.10%	0.30%
	Ext Deformation (mm)	1	1	1.3	1.5
	Ext Plastic Strain (%)	0.30%	0.30%	0.40%	0.50%

Table 9.10 2nd-31st Load Sequence Deformation and Plastic Strain

		2nd-31st Load Sequence Deformation and Plastic Strain			
		OH RCA	**TX RCA**	**NJ RCA**	**MN RCA**
0% Brick	Int Deformation (mm)	2.1	2.9	8.8	9.3
	Int Plastic Strain (%)	1.40%	1.90%	5.80%	6.10%
	Ext Deformation (mm)	4.6	5.6	16.8	16.1
	Ext Plastic Strain (%)	1.50%	1.80%	5.50%	5.30%
10% Brick	Int Deformation (mm)	1.4	1.4	3.8	6.9
	Int Plastic Strain (%)	0.90%	0.90%	2.50%	4.50%
	Ext Deformation (mm)	3.5	4.8	7.3	13
	Ext Plastic Strain (%)	1.20%	1.60%	2.40%	4.30%
20% Brick	Int Deformation (mm)	2.4	1.6	3.1	5.6
	Int Plastic Strain (%)	1.60%	1.10%	2.00%	3.70%
	Ext Deformation (mm)	5	5	6.5	10.3
	Ext Plastic Strain (%)	1.70%	1.65%	2.10%	3.40%
30% Brick	Int Deformation (mm)	2.9	1.8	3	4.2
	Int Plastic Strain (%)	1.90%	1.20%	2.00%	2.80%
	Ext Deformation (mm)	5.4	4.1	5.9	8.3
	Ext Plastic Strain (%)	1.80%	1.40%	2.00%	2.70%

Table 9.11 LA Abrasion Results

Specimens	LA Abrasion Loss (%)
Class 5 Natural Aggregate	23
MN RCA	30
RCB (Arulrajah et al., 2011)	36

9.8 Figures

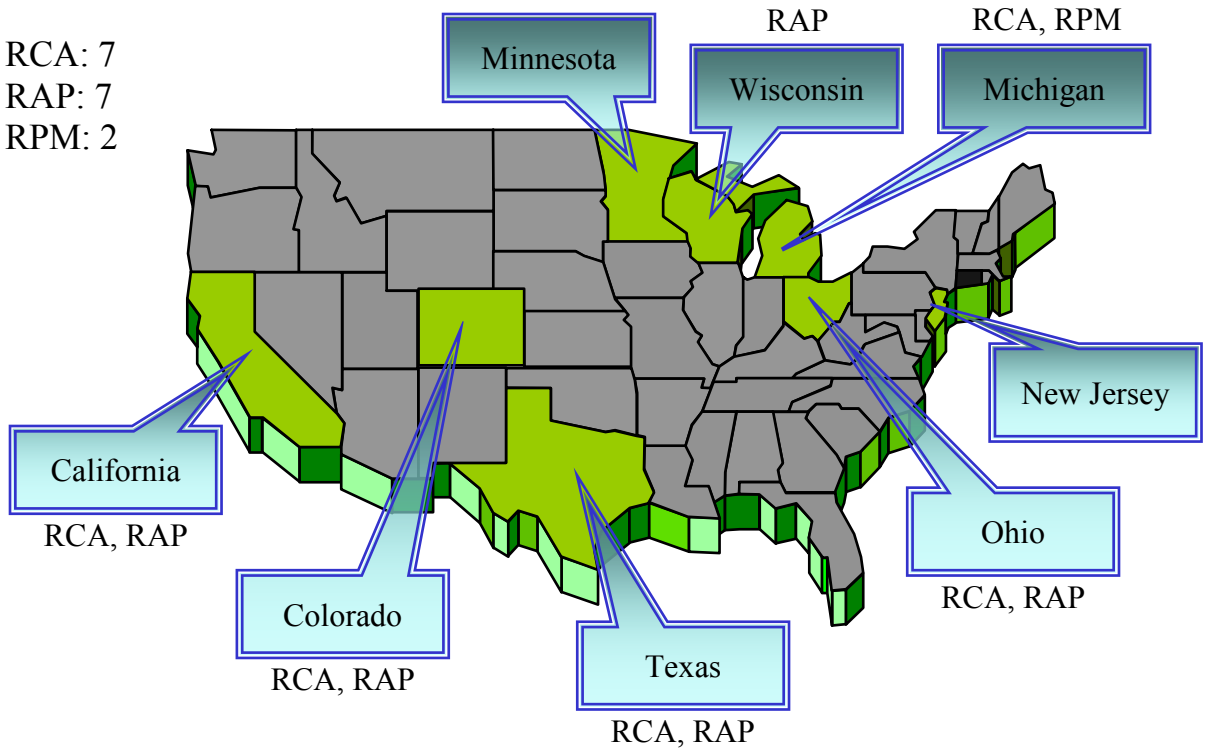

Figure 9.1 Locations of recycled material used in this study

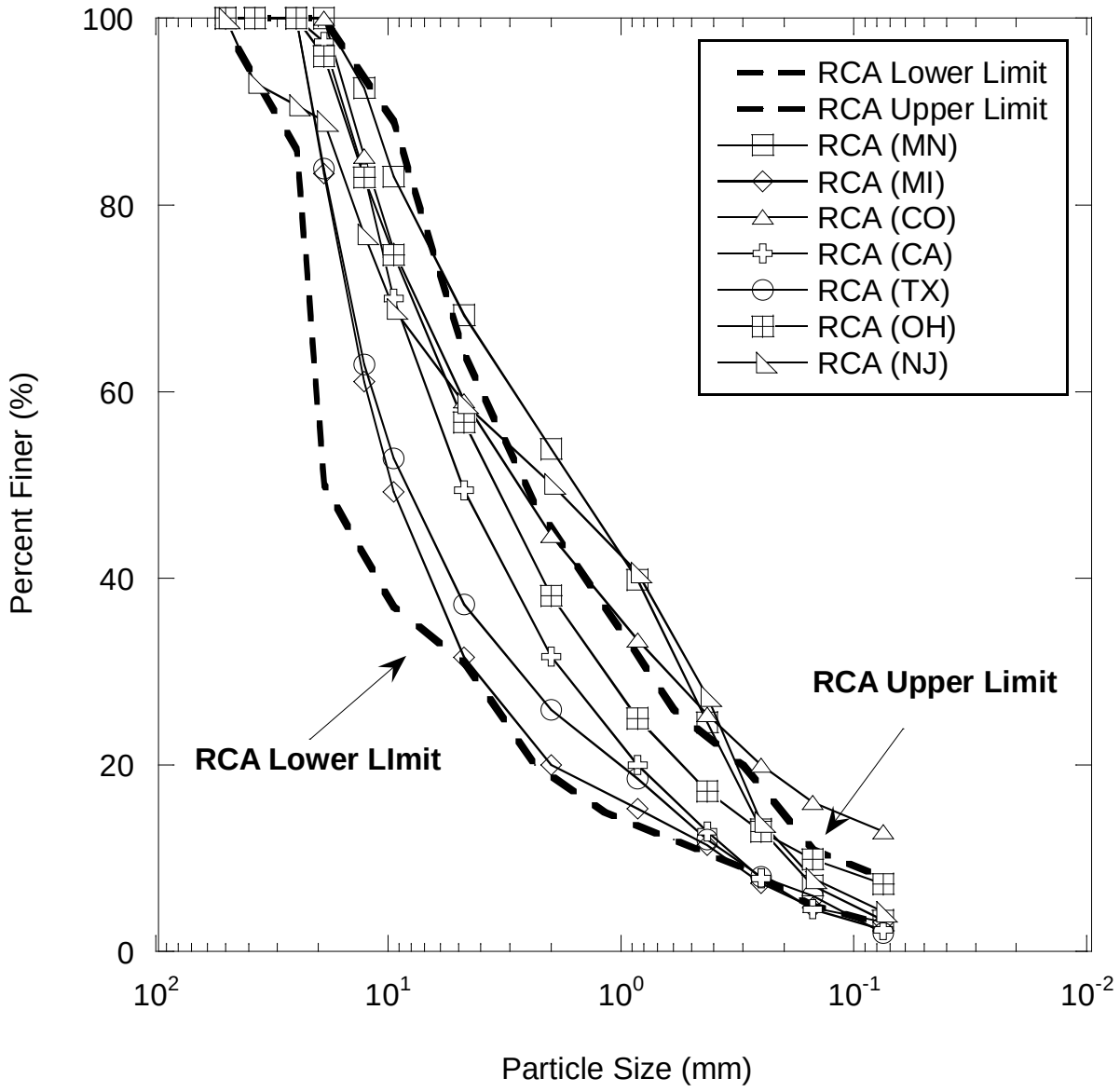

Figure 9.2 Particle Size Distribution for RCA and RCAs Reported Lower and Upper Limits from Literature

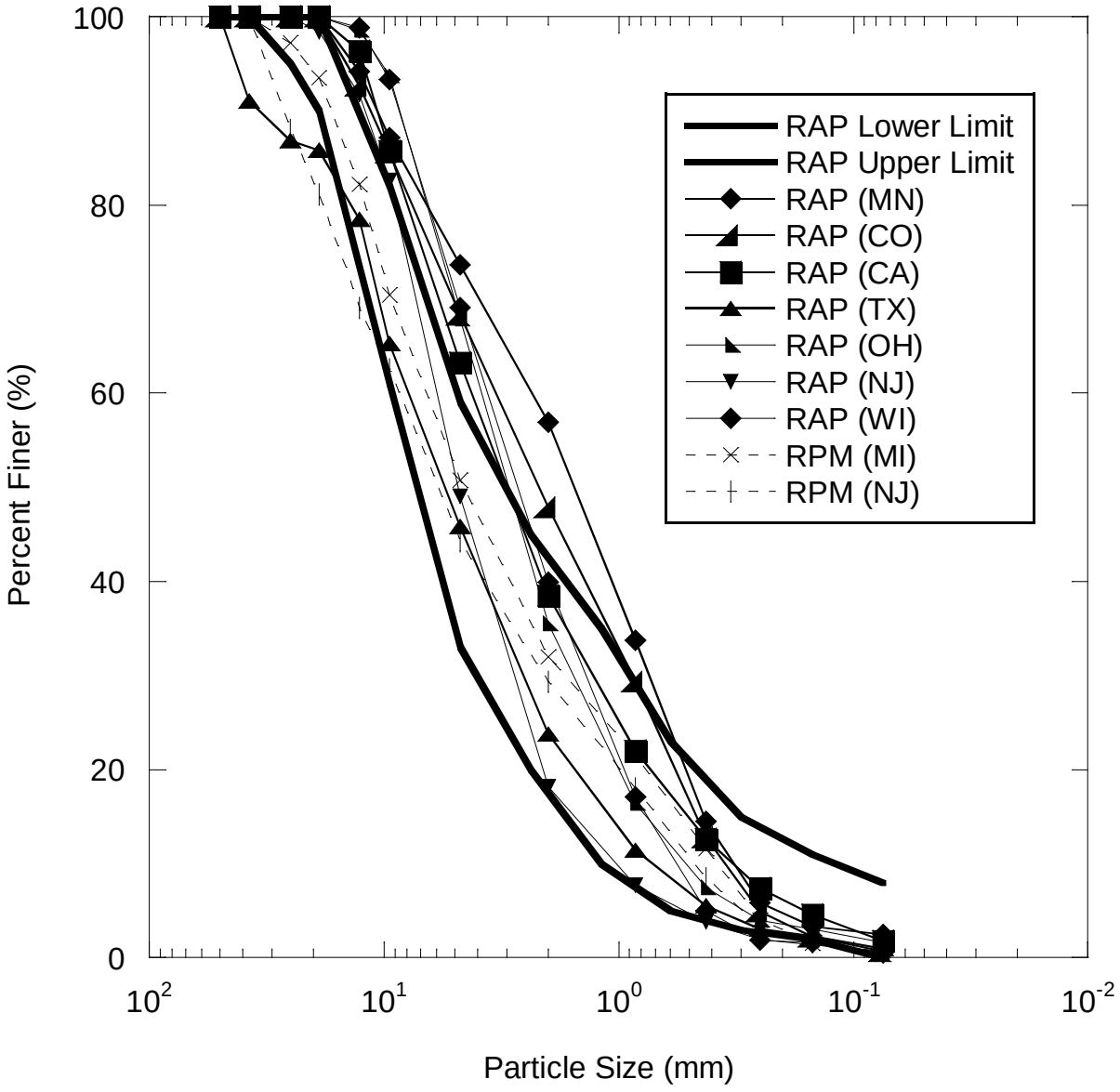

Figure 9.3 Particle Size Distribution for RAP/RPM and RAPs Reported Lower and Upper Limits from Literature

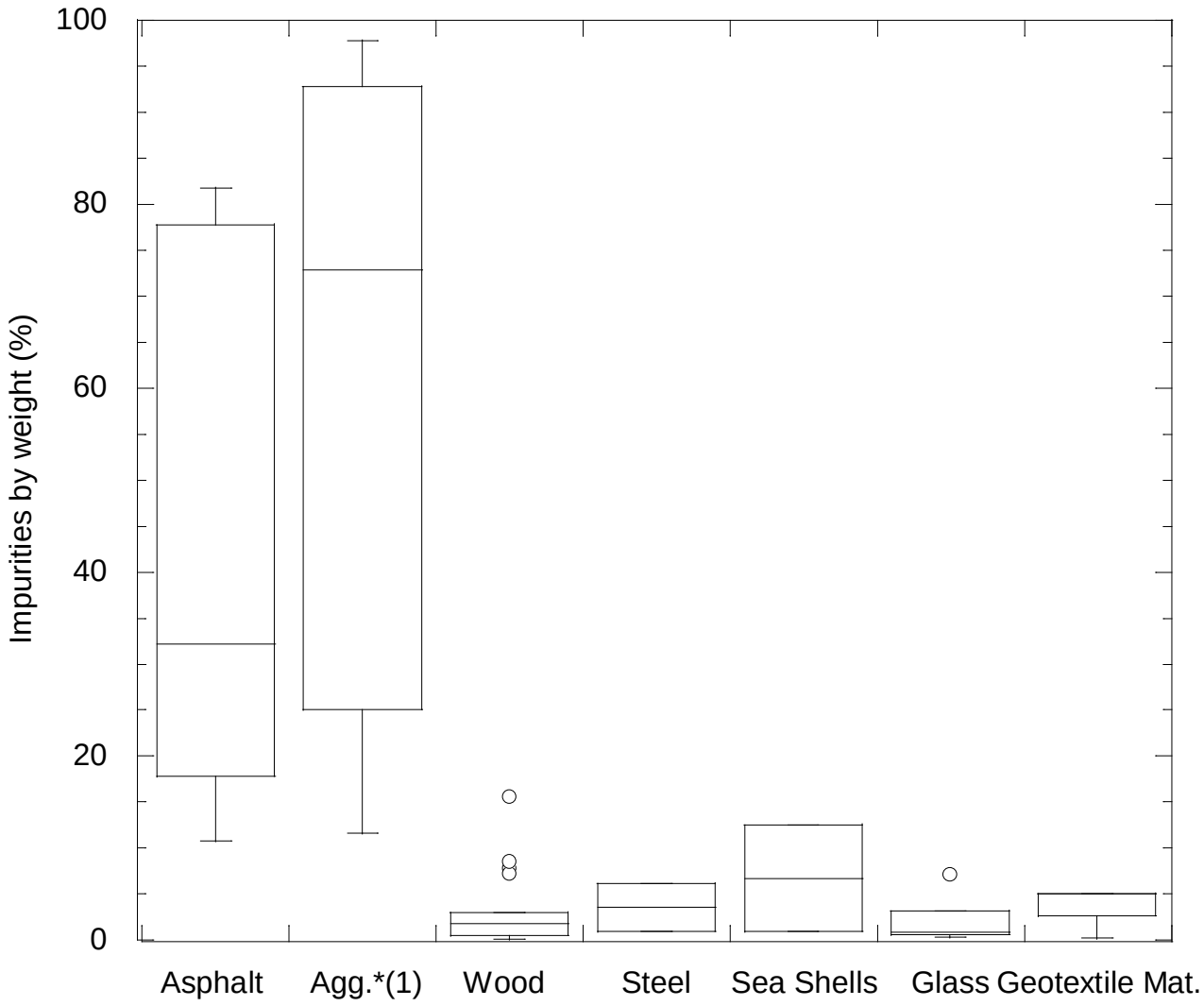

*(1): Aggregates with plastic fibers

Figure 9.4 Distribution of Impurities by Weight Percentage

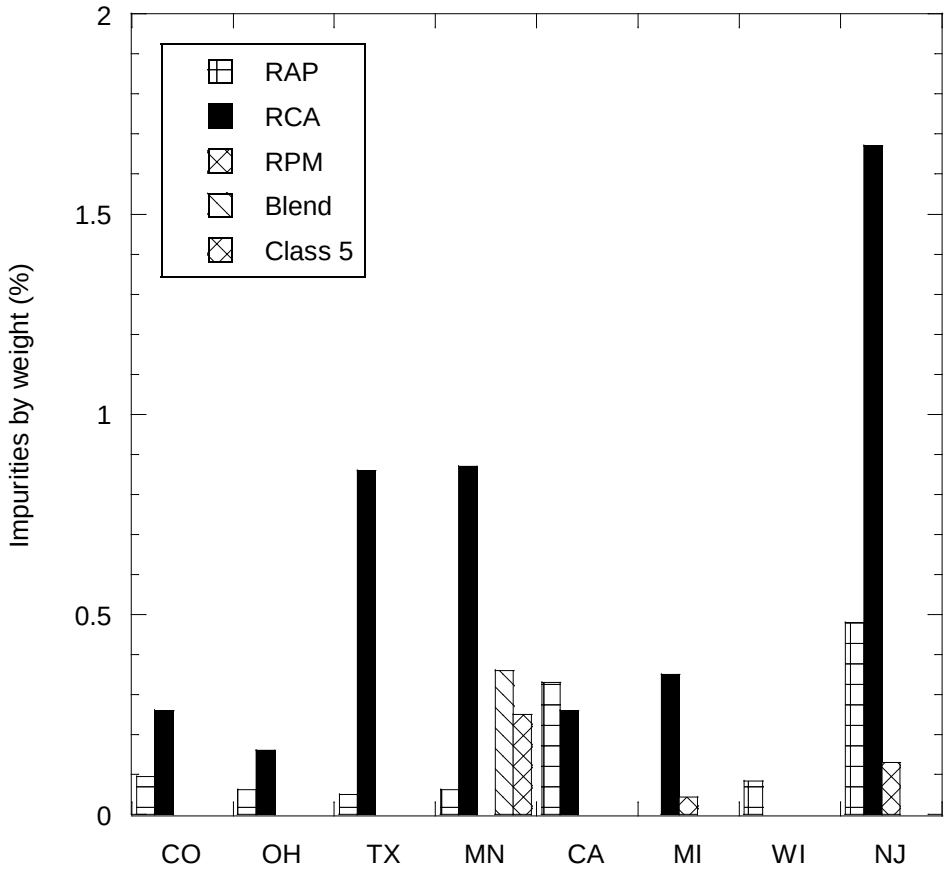

Figure 9.5 Percent Impurities Found in Recycled Materials from different States

Figure 9.6 Deleterious Material Found in RCA: Sea Shells and Steel

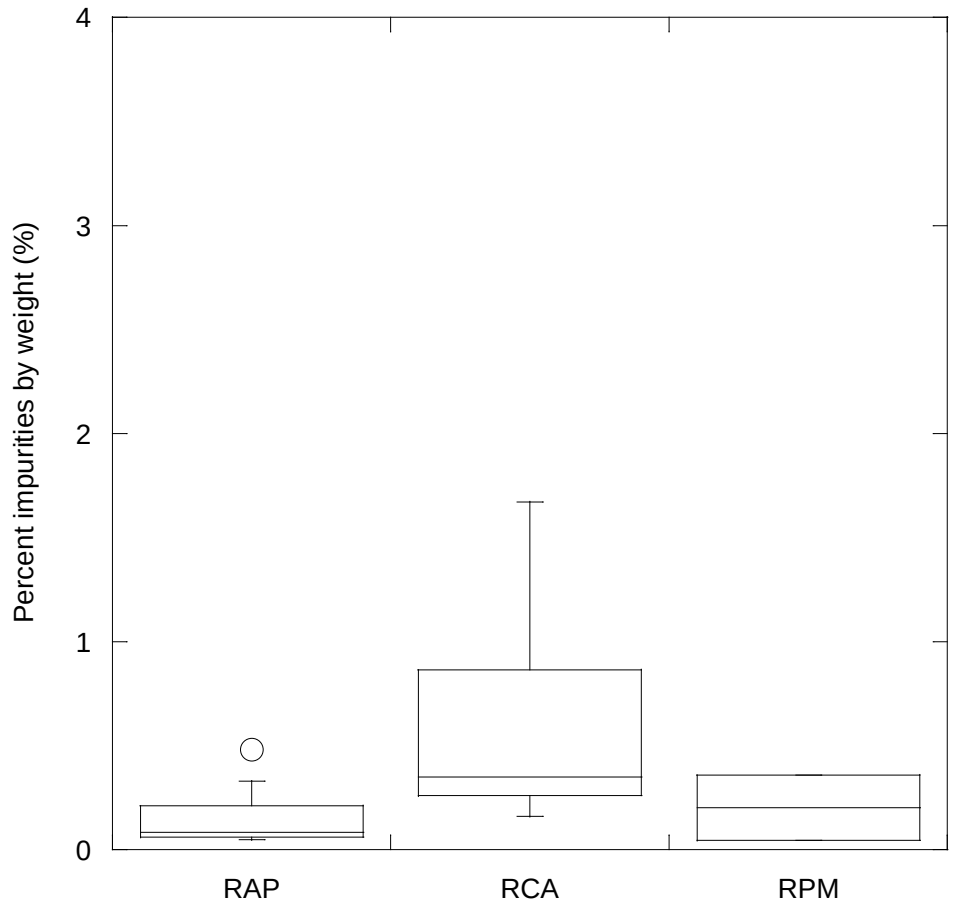

Figure 9.7 Average Percentage Impurities by Weight for Recycled Materials

Figure 9.8 Deleterious Materials Found in RAP: Pavement Markings and Wood Chips

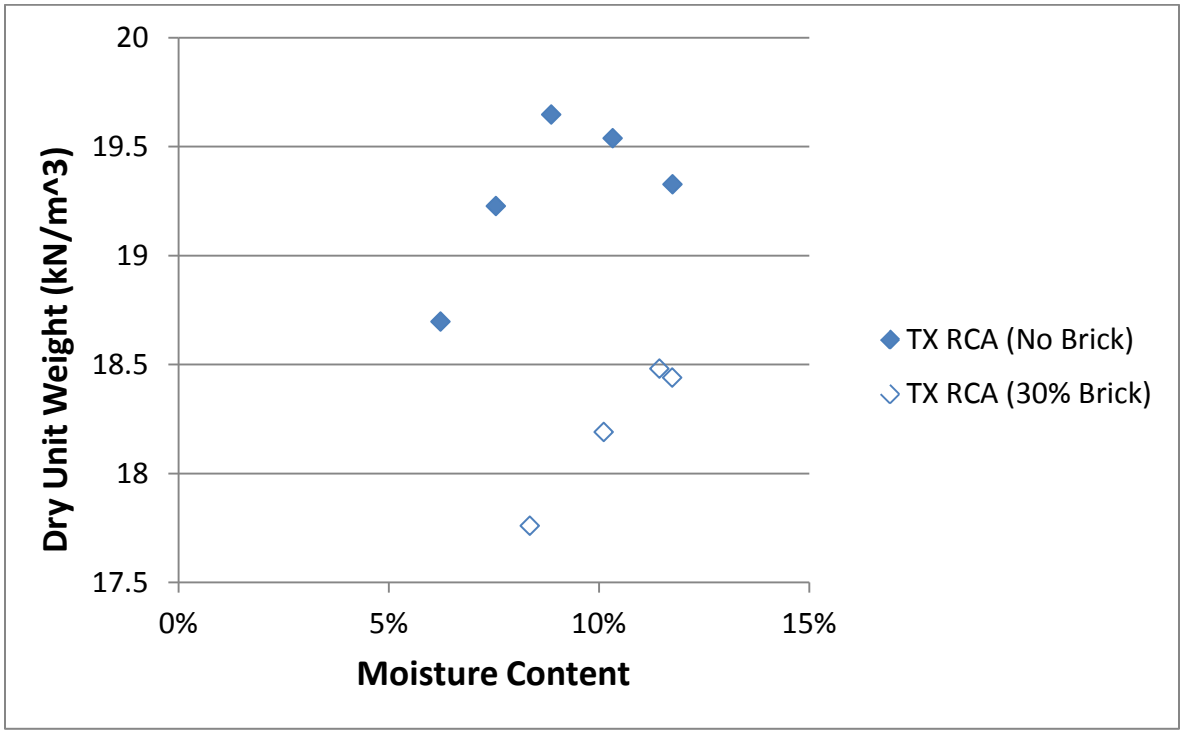

Figure 9.9 TX RCA Compaction Data at 0% Brick and 30% Brick

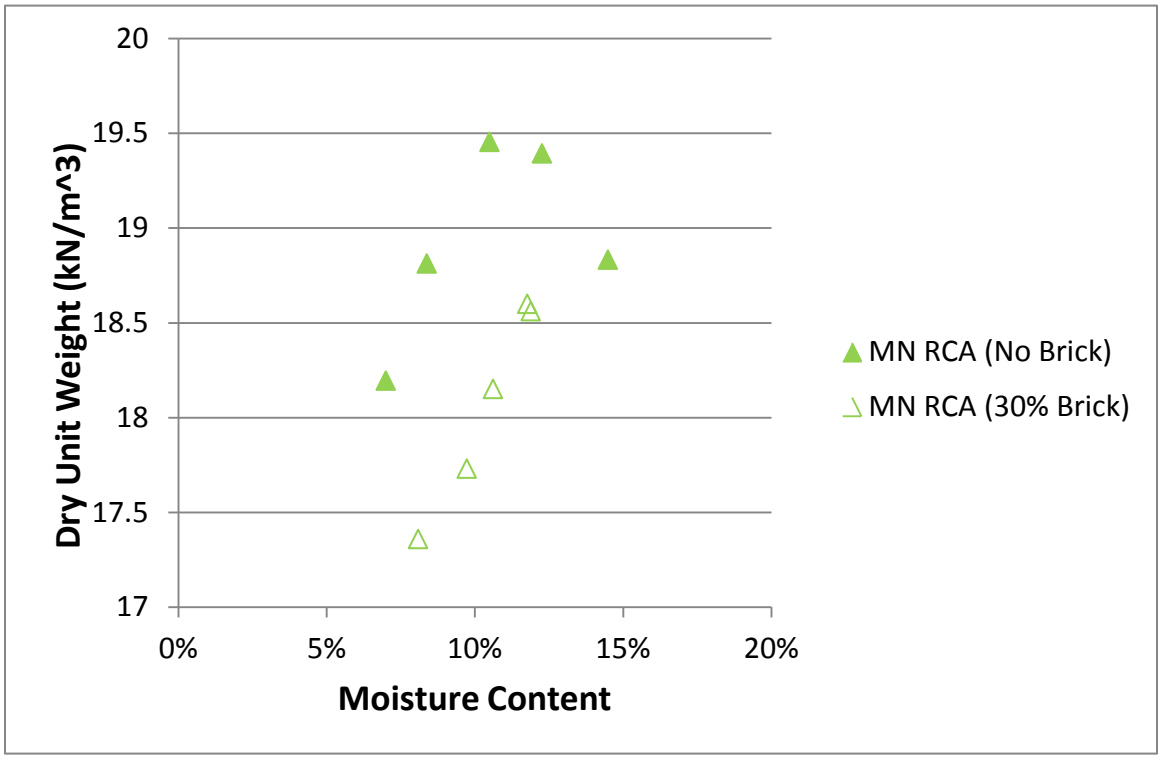

Figure 9.10 MN RCA Compaction Data at 0% Brick and 30% Brick

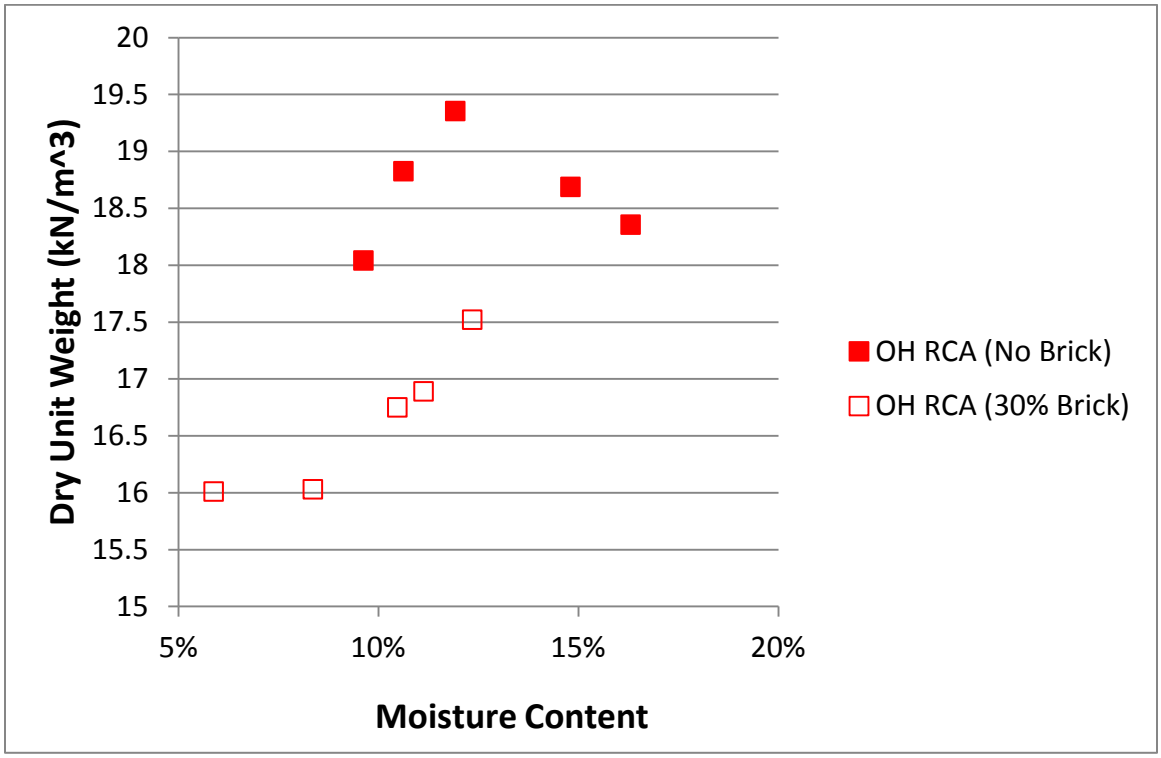

Figure 9.11 OH RCA Compaction Data at 0% Brick and 30% Brick

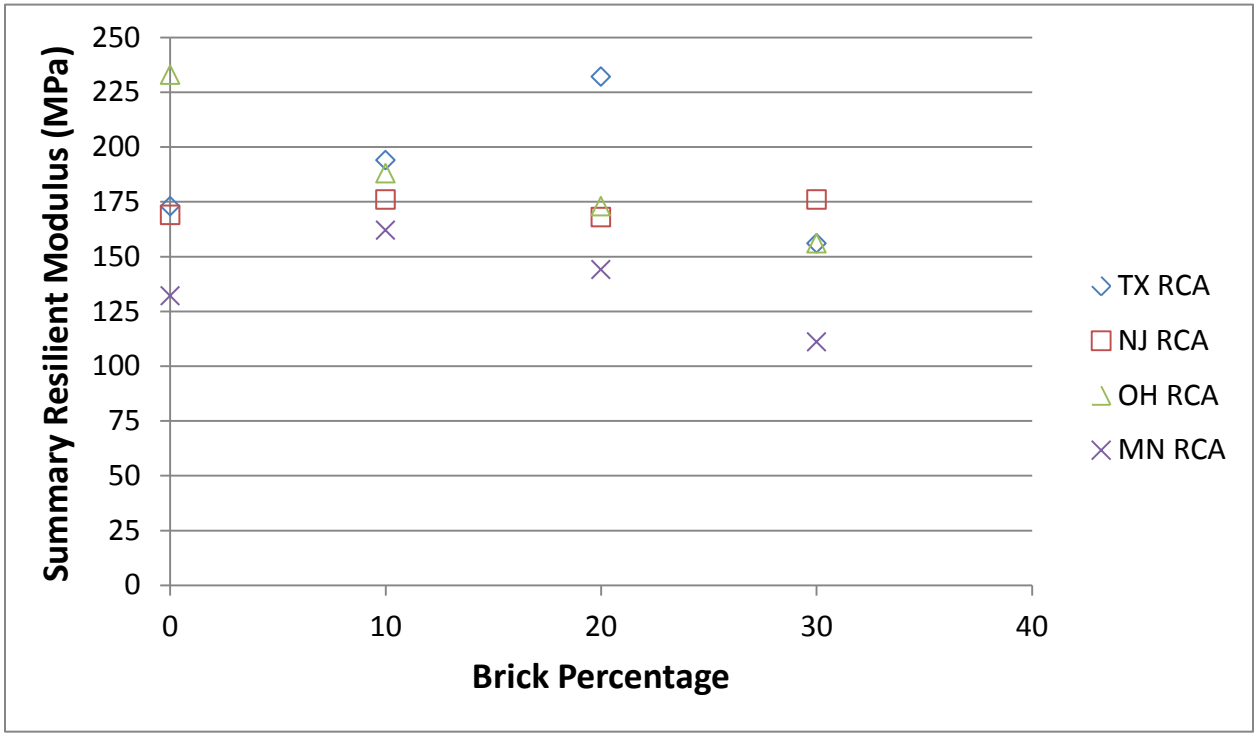

Figure 9.12 Internal LVDT Recorded SRM (NCHRP) at Varying Brick Contents

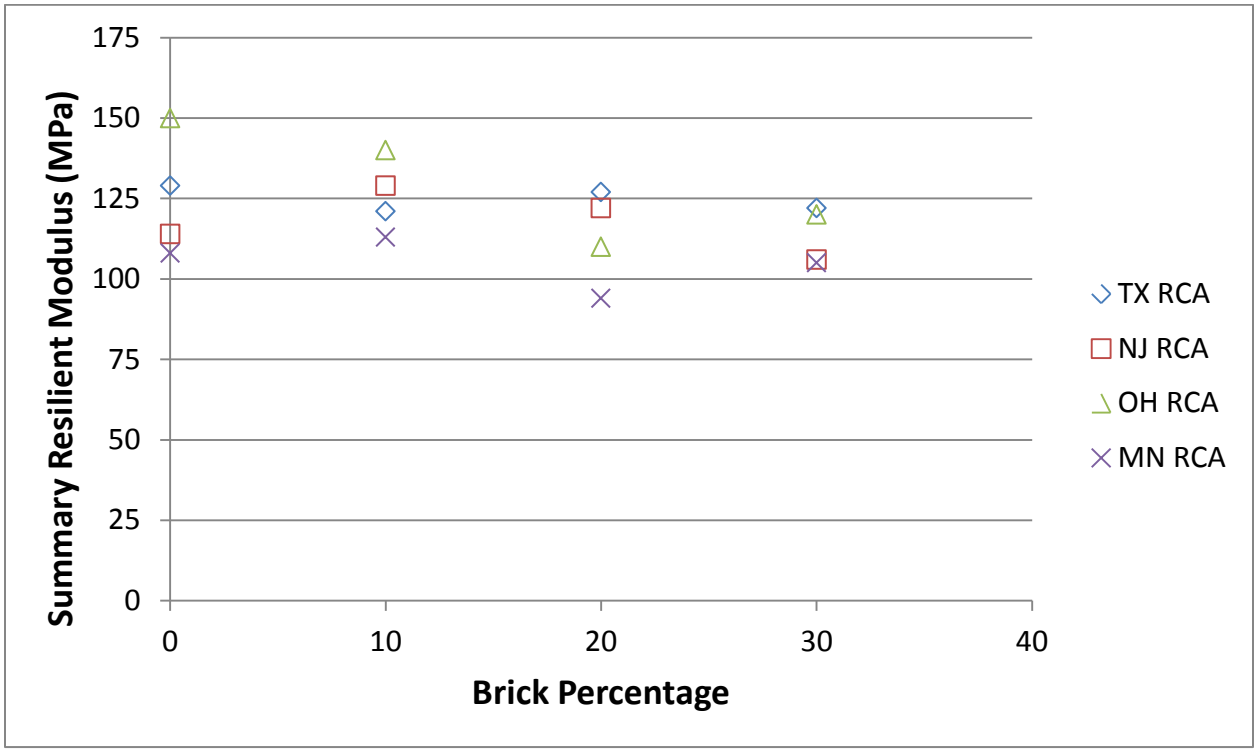

Figure 9.13 External LVDT Recorded SRM (NCHRP) at Varying Brick Content

Figure 9.14 Crushing Brick and Final Product

Figure 9.15 0%, 10%, 20%, and 30% RCB with MN RCA at OMC

Figure 9.16 10%, 20%, and 30% RCB with NJ RCA at OMC

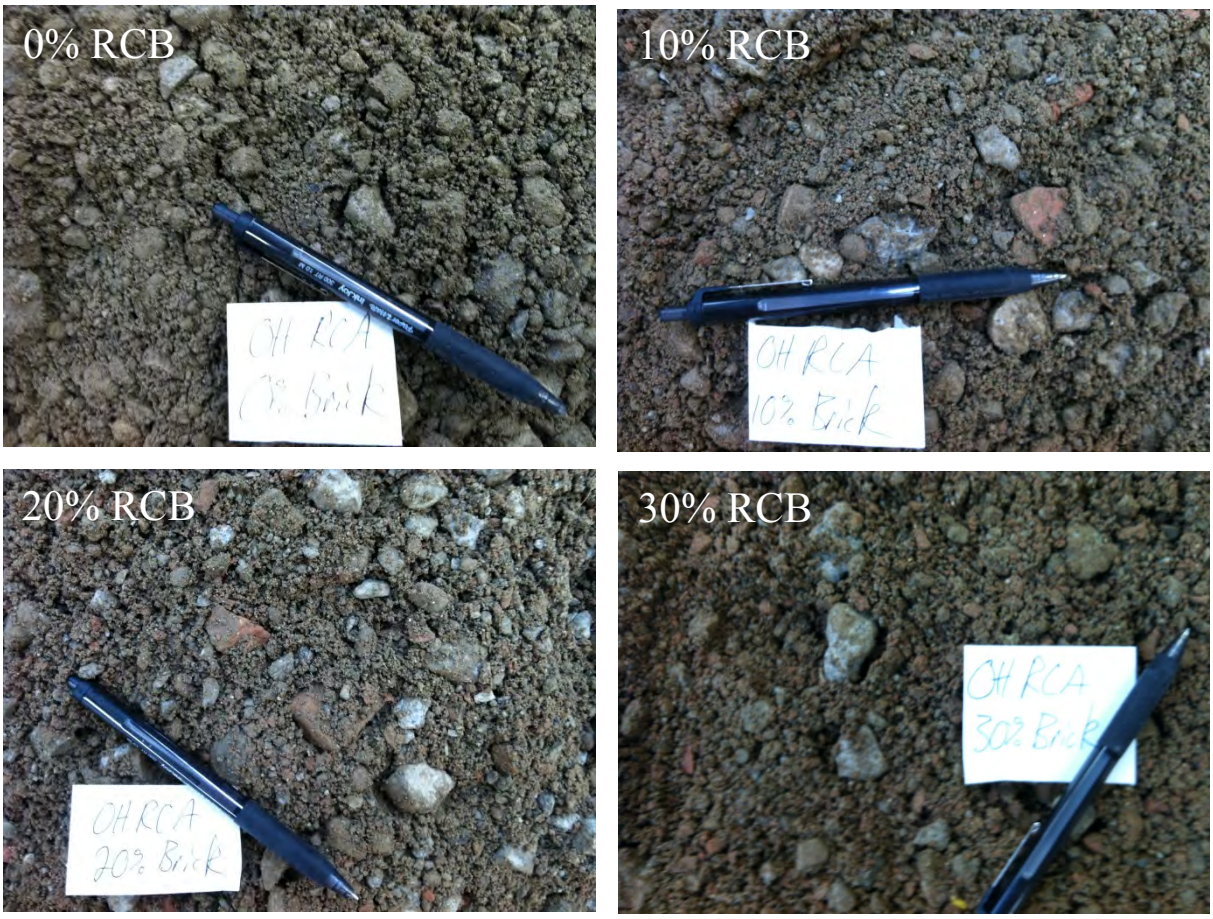

Figure 9.17 0%, 10%, 20%, and 30% RCB with OH RCA at OMC

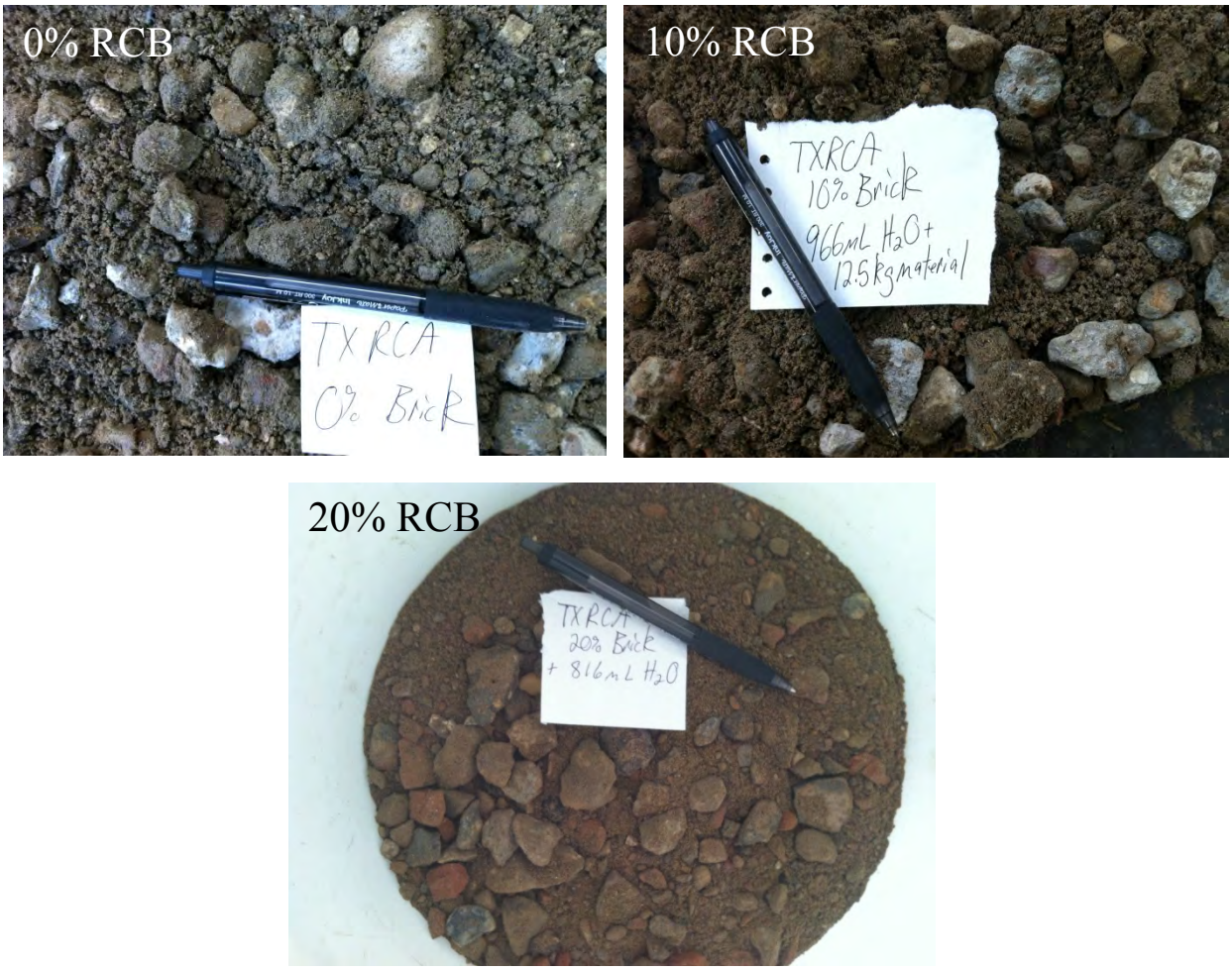

Figure 9.18 0%, 10%, and 20%, RCB with TX RCA at OMC

Figure 9.19 30% RCB with MN RCA compacted for Resilient Modulus Test

10. Leaching Characteristics of RCA and RAP

10.1 Introduction

The growth in the construction and rehabilitation of roadway systems in the United States (US) has increased the consumption of natural aggregates and energy required to process and transport these materials (Lee et al. 2010). The United States Geological Survey (USGS 2011) estimated that 508 million tons of crushed stone was consumed in the US in 2010, 82% as construction material. Natural aggregate is extensively used for public infrastructure, mostly for highway and road construction and related maintenance (Langer 1988). Road base or road surfacing materials are the major uses of natural aggregate (i.e., unbound aggregate) (USGS 2011). However, rapidly decreasing sources of natural aggregate, along with limits placed upon aggregate production by environmental regulation and land use policies, has caused the price of these materials to increase dramatically (ACPA 2009).

There is an increasing trend towards use of recycled material in construction in the US. Specifically, recycled concrete aggregate (RCA) and recycled asphalt pavement (RAP) possess excellent mechanical properties for use as base course aggregate in pavement structures and significant life-cycle benefits such as reducing greenhouse gas emissions and energy consumption in pavement construction (Lee et al. 2010, FHWA 2004). However, wide use of recycled material also requires their safe use. Since RCA usually contains cement hydration products (e.g., calcium hydroxide, calcium-silicate-hydrates), concerns have focused on the highly alkaline leachate from RCA in laboratory studies and associated high-pH leaching patterns, such as vegetation die-off, the clogging of highway drainage pipes, and heavy metal release from RCA (e.g., Cr, Pb, and As) (Sadecki 1996, Iowa DOT 1999).

In 2004, 41 states allowed for the use of RCA as unbound base course (FHWA 2004). RCA provides excellent mechanical properties (e.g., lower specific gravity, higher resilient modulus, and freeze-thaw durability) and is largely available for use as base course in pavement structures (Bozyurt 2011, ACPA 2008). However, potential environmental risks associated with highly alkaline effluent and heavy metal leaching from RCA have been reported by various state departments of transportation (Sadecki et al. 1996, Iowa DOT 1999, VDOT 2003). Heavy metals can come from concrete additives (e.g., fly ash and ordinary portland cement) and natural stone (ACPA 2008). In a field case study, As and Cr exceeded the maximum contaminant levels (MCL) in surface runoff generated by rainwater wash through a RCA stockpile (Sadecki et al. 1996). Cement phases (e.g., calcium silicate hydrate, portlandite, Afm, Aft, and ettringite) in RCA have the potential to generate highly alkaline leachate (pH 12~13) (Sadecki et al. 1996, Iowa DOT 1999, Engelsen et al. 2006). pH is a master variable affecting heavy metal leaching from RCA (Engelsen et al. 2006, Mulugeta et al. 2010).

RCA is sensitive to the exposure environment by carbonation (CO_2 uptake) and hydration (contact with water), and both process can change the chemical and mineralogical properties of RCA (Engelsen et al. 2006, Mulugeta et al. 2010, Engelsen et al. 2009, Engelsen et al. 2010). In practice, RCA can be used as backfill around infrastructure immediately after demolition and size reduction, or can be stockpiled for future use (typically up to five years). Crushed RCA has

more exposed, fresh surfaces than monolithic concrete and thus is impacted by weathering. The full extent of weathering of RCA in stockpiles is unknown, including leaching trends.

Lab-scale leaching studies of RCA have been carried out by Engelsen et al. (2009, 2010), Mulugeta et al. (2010), and Sani Sani et al. (2005), but systematic field leaching studies on RCA used as base course have not been reported in the US. In this study, laboratory column leaching tests and batch leaching tests were conducted on seven samples of RCA from a wide geographical area. Two field sites were installed and instrumented to supplement the laboratory results and for comparison between laboratory- and field-scale leaching trends. Field sites including pavement sections and lysimeters were installed beneath pavements to collect percolating leachate in Minnesota and Wisconsin to replicate field-scale conditions. Another objective of this project was investigating the differences of leaching behavior between freshly crushed RCA and stockpiled RCA.

There has been less concerns raised relative to RAP leaching characteristics. However, laboratory batch leaching tests as well as Toxicity Characteristic Leaching Procedure (TCLP) tests were performed on RAP samples as well collecting field lysimeter leaching samples at MNROAD test section.

10.2 Materials

Seven RCA samples from a wide geographical range were used in this study: California (CA), Colorado (CO), Michigan (MI), Minnesota (MN), Texas (TX), Wisconsin Fresh (WR-F), and Wisconsin Stockpiled (WR-SP) RCA. MN, WR-F and WR-SP RCA were also used as base course in the two field sites. Two sources of natural aggregate (similar in mineralogy to the aggregate used in concrete production) were used as control material in the field leaching sites: MNROAD Class 5 (Class 5) and Wisconsin aggregate (WA). The CA, CO, MI, MN, and TX RCA were provided by the corresponding State Departments of Transportation (DOT) as part of this Pooled Fund project. CA, CO, and MN RCA samples had been stockpiled for more than one year. MN RCA was from demolition of Portland cement concrete (PCC) pavement, while CO RCA came from multiple concrete demolition sources. MI RCA, which was freshly crushed, came from demolition of concrete pavement; TX RCA was a commercial product, with unknown source properties. X-ray power diffraction (XRD) results showed that CA, CO, and TX RCA mainly contained feldspar, quartz, and calcite, while MI and MN RCA also contained dolomite.

The two sources of RCA from Wisconsin have detailed source information. WR-F RCA was from the demolition of concrete pavement in Madison, WI. The material was obtained just three days after demolition and processing; thus, WR-F RCA is considered a ‘fresh’ RCA sample. WR-SP RCA was from the demolition of a concrete building in Madison, WI, and has been stockpiled in a quarry for over five years; thus, WR-SP RCA is considered a ‘weathered’ RCA sample. XRD results showed that WR-F and WR-SP RCA both contain dolomite, feldspar, quartz, and calcite. The fines (< 0.075 mm in size) bonding to the gravel surfaces showed a similar XRD pattern to the bulk sample (Figure 10.1). All samples met the USDOT required gradation as base course, with a maximum grain-size of 50 mm (the grain size distribution curves (ASTM D 422) are shown in Figure 10.2. The physical, hydraulic, and chemical properties of the aggregates are summarized in Table 10.1.

There were not enough samples of RAP; nonetheless RAP samples from a wide geographical range were used in this study: California (CA), Ohio (OH), and New Jersey (NJ), and Wisconsin (WI) RAP were used in the laboratory tests and Minnesota RAP was used in the MNROAD field experimental site. Also a typical asphalt binder (AB) was tested.

10.3 Experimental Section

10.3.1 *Field Leaching Test Sites*

Two field leaching test (FLT) sites, the 'MNROAD site' and the 'UW site', were constructed using RCA as base course with lysimeters installed. A RAP site was also constructed at MNROAD exactly the same as the RCA site. The MNROAD site was constructed on the MNROAD test facility mainline (westbound of I-94) between St. Cloud and Minneapolis, MN, in September 2008. Four experimental cells were installed and paved on the mainline: cell 16 contained 100% MN RCA, cell 17 contained 50-50 MN RCA-Class 5 mix, cell 18 contained 100% RAP, and cell 19 contained 100% Class 5 natural aggregate. A 127-mm-thick, warm-mixed asphalt was placed above the base course, which consisted of these four materials each 305-mm-thick underlain with a 305-mm-thick Class 3 aggregate and 178-mm-thick select granular material over the clay subgrade. Cell 16 was originally designed to investigate high pH effluent from RCA, and cell 17 was designed to test the neutralization of high alkaline material by mixing with natural aggregate. Cell 18 was for RAP leaching. Cell 19 was the control cell. Pan lysimeters (3 m × 3 m) were installed under each of the test materials (RCA, RCA/Class 5, RAP, and Class 5) to collect percolated leachate.

The UW site was constructed in Parking Lot 60 on the campus of the University of Wisconsin-Madison in September 2011. Three small experimental cells with a pan lysimeter (1.5 m × 1.5 m) were installed in parking lot aisles: cell 1 with WR-F RCA, cell 2 with WR-SP RCA, and cell 3 with WA. One layer of 127-mm-thick porous asphalt (porous mix asphalt, DRS Ltd., WI) was paved above each 0.3-m-thick base course section. Batch testing of the asphalt with deionized water (DI) showed insignificant heavy metal leaching and the leachate pH was 7.8 (pH_{DI} = 8.1).

A schematic view of the lysimeter and leachate collection system is shown in Figure 10.3. The 3 m × 3 m high-density polyethylene (HDPE) lysimeters were installed at the MNROAD site under the base course. In contrast, at the UW site, 1.5 m × 1.5 m lysimeters were installed with side walls up to the asphalt layer to isolate the testing cells from flux coming from adjacent base course layers. Leachate flowed through a PVC pipe and was collected in 120 L HDPE tanks.

A weather station was installed at both sites. A standard 20-cm tipping bucket rain gauge and thermocouples were installed, and data was collected with a Campbell CR-23 datalogger (all supplied by Campbell Scientific Inc.). Leachate samples were collected with a polyvinyl chloride bailer from the collection tanks. Leachate remaining after sampling was pumped out such as to record the total volume of leachate collected during each sampling period. Leachate samples from the MNROAD site were collected consistently every one or two months beginning in April 2009 through November 2010 (although some data collection continued through 2012). At the UW site, leachate samples were collected weekly beginning in September 2011.

10.3.2 *Column Leaching Tests*

Long-term column leaching tests (CLT) were conducted using CA, CO, MI, MN, and TX RCA. The specimens were compacted with modified Proctor effort (ASTM D 1557) at 90% of maximum dry unit weight (field specification) and optimum water content into a PVC column (diameter = 20 cm, height = 10 cm). All fittings in contact with RCA were non-metallic. A synthetic rainwater, as described in (Scalia and Benson 2010), was used as inflow. A continuous, upward flow was generated by a peristaltic pump at a Darcy flux of 1.6 cm/day (approximately 0.5 pore volumes of flow, PVF, per day), which was sufficient to avoid preferential flow paths, wet-dry cycles, and air bubbles in the system. Specimens were saturated 24 h before test initiation, and leachate samples were collected every three days from sealed, teflon sampling bags.

10.3.3 *pH-Dependent Batch Tests*

pH-dependent batch tests were conducted according to methods outlined in Kosson et al. (2002). One representative sample was taken from each source and homogenized by hand mixing. The representative samples were separated into two specimens: one used to represent the entire sample and the other for grain size fractioning. The fractionated samples were sieved into three grain size fractions: fine particles (<0.075 mm), sand-sized particles (<4.75 mm, >0.075 mm), and gravel-sized particles (<75 mm, >4.75 mm). All fractions were then reduced to less than a 2 mm size with a steel jaw crusher (50 mm × 152 mm opening high Mn-steel jaw crusher by Sturtevant Inc., MA, USA).

The total elemental composition of each RCA specimen was determined by acid digestion according to ASTM D 5198-09. A 1:1 nitric acid digestion of 5 g of solid sample was performed at 90 °C to 95 °C for two hours. The total carbon (TC), total inorganic carbon (TIC), and total organic carbon (TOC) were determined with a SC144 DR sulfur and carbon analyzer (LECO Inc., St. Joseph, MO, USA). The batch tests were performed with unfractionated (entire) samples and fractionated samples at a liquid to solid ratio of 10:1 by weight. Samples were agitated in an end-over-end tumbler at a speed of 30 revolutions per min (rpm) ± 2 rpm. A pH range of 2 to 13 was used for the pH-dependent leaching tests, with target pH of 13, 12, 10.5, 9, 8, 7, 5.5, 4 and 2. A pre-test titration was conducted to determine the contact time to equilibrium and the acid/base addition required for each batch. pH, electrical conductivity (EC), and oxidation-reduction potential (Eh) were determined after testing. The acid neutralization capacity (ANC) curve of each material was also derived from the pH-dependent batch test by the quantity of acid/base addition to each batch and the corresponding final pH reading of the eluate. Development of the ANC is an important step in conducting pH-dependent leaching tests on cement-based materials, since the acid buffering ability of the material will affect the leaching characteristics of the contaminants by both controlling the pH and maintaining the integrity of the solid matrix when exposed to acid (Giampaolo and Mastro 2001).

10.3.4 *Chemical Analysis*

pH, electrical conductivity (EC), and redox potential (Eh) readings were recorded immediately after sampling. Leachate samples were filtered using 0.45-μm filter paper, preserved with trace-grade nitric acid (HNO_3), and stored at 4 °C. Major elements (Ca, Fe, Al, Mg, Na, K, Si) and

trace elements (As, Ba, Cd, Cr, Co, Cu, Mo, Ni, Pb, Sb, Se, Zn) were determined by inductively coupled plasma optical emission spectrometry (ICP-OES)

10.4 Results and Discussion

10.4.1 *Weather Data and Leachate Volume from Field Sites*

Figure 10.4 shows weather data and measured leachate volumes from the MNROAD and UW testing cells. The effluent volumes matched the precipitation data well, indicating that the leachate collection system performed as intended. Precipitation was typically higher in the fall (September to November) and spring seasons (April to June). Volumes of leachate greater than 120 L indicate that leachate accumulated in the drainage pipe as well (Figure 10.4a). During colder weather (December to March), snow was removed from the surface during plowing operations and leachate collection was rare. The depth of frost penetration at the MNROAD and UW sites could reach 2.0 and 1.5 m at maximum (Floyd 1979), respectively, at maximum; thus water might have frozen in the base course itself and/or within the leachate drainage pipes. A small volume of leachate was collected from WR-F and WA during January to March (Figure 10.4b), which may have been due to the warm winter of 2012.

10.4.2 *Leaching of Alkaline Substances from RCA*

10.4.2.1 Field Leaching Tests-RCA

Leachate pH from the MNROAD and UW sites is shown in Figure 10.5a. The leachate pH of the cells containing MN RCA and MN RCA/Class 5 aggregate mix ranged from 6.5 to 8.0 for the entire monitoring period and was similar to the Class 5 cell (pH = 6.5 to 8.4). At the UW site, the WR-F RCA cell started with a high leachate pH (12.6) and remained relatively constant for the first 5 PVF, with a peak pH of 12.9 at 2.8 PVF. In contrast, the WR-SP RCA started at a lower pH (7.3) and gradually increased upward, to pH of 12.1 after 2 PVF. The natural dolomite aggregate (WA) showed a neutral leachate pH (between 5.0 and 8.5). The material pH of all three RCAs (Table 10.1) showed a potential of leaching high alkaline effluent, with pH = 11.3 for MN RCA, pH = 12.3 for WR-F RCA and 11.8 for WR-SP RCA, while WA also had a material pH of 10.0. The differences of pH in field lysimeter tests (FLT) and material pH from WA could be limited by water residence time and exposed surface, which hinders the establishment of chemical equilibrium (Engelsen et al. 2012).

10.4.2.2 Column Leaching Tests-RCA

Leachate pH from long-term, continuous-flow CLTs was strongly related to the corresponding material's pH (Table 10.1), with a decreasing order of MI, TX, CO, CA, and MN RCA (Figure 10.5b). The column tests had very consistent pH levels for all five RCA specimens, and RCA showed elevated leaching potential of alkaline substances over 100 PVF. MN RCA showed different trends of leachate pH between field leaching test and lab column leaching tests. Compared to the neutral leachate pH (6 to 8) at the MNROAD field site, pH levels for MN RCA were consistently high (11.3 to 11.6) during the first 6 PVF in column leaching tests , which presented a continuous leaching of alkaline substances.

10.4.2.3 Leaching of Major Elements at MNROAD Field Site-RCA

Ca, Si, Mg, Al, and Fe were considered major elements due to their high weight percentages in the RCA samples and also because they comprise the cement hydration phases (e.g., portlandite, calcium silicate hydrate (C-S-H, Afm, and Aft) of traditional portland cement (Engelsen et al. 2010, Giampaolo et al. 2000, Sani et al. 2005). Thus, the trends in leaching of Ca, Si, Mg, Al, and Fe are expected to portend a broader understanding of the leaching characteristics of RCA. Silica (Si) cannot be analyzed accurately by acid digestion, but has been reported at 24% to 28% by weight in solid RCA material (Engelsen et al. 2009).

Leachate from the MN RCA cell at the MNROAD site showed a high leaching concentration of Ca ($1.2 \sim 7.6 \times 10^4$ µg/L), Si ($0.2 \sim 1.1 \times 10^4$ µg/L), and Mg ($0.6 \sim 1.4 \times 10^4$ µg/L) before 6 PVF. However, CLT using MN RCA at first 6 PVF showed a slightly lower concentration of Ca ($0.6 \sim 1.7 \times 10^4$ µg/L) and Si ($0.7 \sim 0.8 \times 10^4$ µg/L); moreover, Mg (1.4 ~22.0 µg/L) from CLT was up to more than three orders of magnitude lower than that from FLT (Figure 10.6). In contrast, Al concentrations from CLT were one order of magnitude higher than the results from FLT (FLT peak 53.7 µg/L and CLT peak 833.5 µg/L), and showed a higher solubility under the more alkaline environment, which could be explained by the amphoteric nature of aluminum with pH-controlled solubility. A relatively low Fe concentration was observed from both FLT and CLT, with concentrations only slightly higher than the method detection limit (MDL) of 2.6 µg/L (FLT peak concentration = 39.1 µg/L and CLT peak concentration = 43.4 µg/L), and indicated the tendency of Fe to form precipitate under both FLT and CLT pH scenario.

10.4.2.4 Comparison between Field and Column Leaching Tests – MN RCA

The average Ca/Mg ratio in FLT leachate was 3.0, which is similar to the average Ca/Mg ratio of 1.6 and 2.2 in dolomite aggregate (WA) and Class 5 leachates. The Ca concentrations were $2.2 \sim 7.9 \times 10^4$ µg/L for Class 5 and $0.8 \sim 4.8 \times 10^4$ µg/L for WA, while Mg concentrations were $1.5 \sim 1.9 \times 10^4$ µg/L in Class 5 and $0.4 \sim 2.7 \times 10^4$ µg/L in WA. Since MN RCA was mainly comprised of dolomite stone, quartz sand, and portland cement, the leaching of Ca and Mg could be dominated by the solubility of dolomite stone ($CaMg(CO_3)_2$), and excessive Ca could come from the dissolution of calcite or other Ca-bearing minerals. The reason for the observed neutral pH effluent from MNROAD FLT after 7 months needs more investigation. The difference of leaching behavior between FLT and CLT may be explained by the interaction with air (mainly carbon dioxide) and preferential flow caused by wet-dry and freeze-thaw cycles in the field and their absence in the CLTs, which are more highly controlled than the actual field scenario (e.g., 100% saturation and controlled temperature, flow rate, and inflow). The percolation water could bring in dissolved carbon dioxide to neutralize the alkaline environment within the base course, and preferential flow could allow heavy rainfall to flow along the preferential path. During the field investigation of MNROAD site, an asphalt crack was visually observed above MN RCA cell (100% MN RCA), which could accelerate the neutralization process and allow more air and water intrusion.

10.4.2.5 Leaching of Major Elements at University of Wisconsin Field Site-RCA

Leaching of Ca, Si, and Mg from WR-F and WR-SP showed seemingly different leaching patterns (Figure 10.6 a and b). WR-F RCA released Ca in concentrations around 3×10^4 µg/L, and

kept a steady Ca leaching concentration during the first 5 PVF; however, the Ca concentration of WR-SP RCA leachate fluctuated extensively (0.8 to 4.8 $\times 10^4$ μg/L) as a function of PVF. Similar observations were found with Mg and Si. Mg concentrations in WR-F RCA leachate ranged from 1.4 (MDL) to 15.3 μg/L; however, WR-SP RCA released much higher Mg with a wide range of 23.2 to 1421.3 μg/L. Si in WR-F leachate decreased from 840.4 μg/L at the first 1.5 PVF, and kept a steady leaching concentration around 160.0 μg/L thereafter, while WR-SP RCA released much higher concentration of Si within the range of 3.5 $\times 10^3$ to 1.0 $\times 10^4$ μg/L.

10.4.2.5.1 Stockpiled RCA Versus Freshly Crushed RCA

The lower effluent pH at the first 0.5 PVF and fluctuation of elemental leaching of WR-SP RCA could be due to the high disturbance of material. Since recycled concrete is usually stockpiled after size-reduction, the larger inner surface will be exposed to the atmosphere. During a long stockpile period, degradation of cement hydration phase may occur; i.e., carbonation, hydration, and water absorption, which will consume the original alkaline cement hydration phase in uncrushed concrete (Houst and Wittmann 2002). Observations at the stockpile site of WR-SP RCA showed significant re-cementation on the surface of WR-SP stockpile. Moreover, during size reduction and long-term stockpiling, finer particles generated by the crushing process or abrasion from larger grains are gradually mixed and coated onto other particle surfaces. The similar XRD patterns between the bulk sample and fines which coated the gravel surface indicate the fines could be a blend of both natural (e.g., dolomite) and cement minerals (Figure 10.1). The lower pH start point of WR-SP RCA could be the result of higher carbonate levels on the surface layer or crushed dolomite and quartz fines coating of the aggregate. Additionally, freshly crushed RCA (WR-F and MI) generally had a lower Si leaching concentration (up to one order of magnitude) than stockpiled RCA (WR-SP, CA, MN). The solubility of Si could be controlled by different minerals; e.g., Calcium-Silicate-Hydrates (C-S-H) and Silica gel (Engelsen et al. 2009, Engelsen et al. 2012). C-S-H in cement is more stable under alkaline conditions than silica, but will transfer to silica gel through the carbonation process, which is alkaline soluble; thus, enhanced leaching of Si takes place (Engelsen et al. 2012).

10.4.3 *Leaching of Heavy Metals from RCA - Field and Column Leaching Tests*

Concentrations of heavy metals in leachate were compared with the maximum contaminant lever (MCL) required in the USEPA drinking water standard. The elemental concentration as a function of PVF from the field sites is shown in Figure 10.7. For the MN site, concentration of As, Pb, and Se from MN RCA were observed to exceed the corresponding MCL at least once, but no distinguishable leaching differences were found between MN RCA and Class 5. All three elements only exceeded the corresponding MCL once, with most measurements corresponding to the minimum detection limit (MDL), especially Se for which both MN RCA and Class 5 exceeded the MCL, with peak concentration of 110.4 μg/L and 89.3 μg/L, respectively.

At the UW field site, concentrations of As, Cr, Pb, and Se were observed to exceed the corresponding MCLs. Pb was only observed to exceed MCL twice in WR-F RCA, with peak concentration of 35.2 μg/L at 0.1 PVF, while Cr was observed to exceed MCL in WR-SP RCA only at its peak concentration of 124.4 μg/L at 0.003 PVF. From digestion results, As and Cr were mainly sourced from cement mortar when compared with WA (Table 10.1). Pb and Se had similar concentrations in two RCA samples of WA. Pb and Se could come from both mortar and

natural sediment. In the WR-F leachate, As and Cr had a slight concentration drop (223.3 to 56.5 μg/L for As and 65.8 to 7.1 μg/L for Cr) within the first 2.5 PVF, but tended towards an equilibrium state afterwards. Se kept a steady leaching concentration within the range of 118.0 to 321.9 μg/L. However, leaching of As, Cr and Se from WR-SP RCA showed different patterns: a sharp drop at 0.5 PVF followed by enhanced leaching from 0.5 to 1.2 PVF, thereafter decreasing.

As, Cr, and Se are elements forming negatively charged oxyanions under certain conditions (Cornelis et al. 2008) and have a tendency to have a higher solubility on the carbonation layer (Mulugeta et al. 2010). The decreasing trend of As, Cr, and Se through the first 0.5 PVF of WR-SP RCA could come from the dissolution of the carbonation layer coating on the aggregate, and the increasing leaching afterward could be due to other leaching processes, which are likely controlled by the solubility of As, Cr, and Se-bearing minerals (e.g., $Cr(OH)_4^-$ and CrO_4^{2-}) under different pH-Eh conditions (i.e., Redox: WR-F -50.5 to 320.4 mV, WR-SP 71.8 to 335.6 mV). The pourbaix diagram can foster a better understanding of the leaching behavior of oxyanions (Mulugeta et al. 2010). The pH-dependent leaching results of Cr (As and Se were similar) from RCA were shown in Chen et al. (2012).

Column leaching tests of five RCA samples also showed that As, Cr, Pb, and Se exceeded the corresponding USEPA MCL at least once for each material (Figure 10.8). Especially for As and Se, all five RCAs tended to release higher than MCL, and irregular leaching patterns were observed during the entire 100 PVF with fluctuations around the MCL. The peak concentration of Cr occurred before 2 PVF with 161.7 μg/L in MN RCA leachate. Pb only exceeded the MCL once from both MI RCA (peak 19.7 μg/L) and TX RCA (peak 25.7 μg/L), and all other leachate data were well below the MCL for Pb (15 μg/L).

10.4.3.1 Acid Neutralization Capacity – Acid/Base Addition and pH-RCA

Figure 10.9 shows the ANC curve of the unfractionated (entire) RCA samples and their fractionated subsets. Negative values in Figure 10.9 represent base additions. pH data from the ANC for fractionated RCA and unfractionated RCA are shown in Table 10.1. The material pH (no acid or base added) of the RCAs ranged from 11.3 to 12.1, with CA, CO, and TX RCA having similar pH, and relatively low pH from MN RCA. Similar ANC curves were observed for CO, TX, and MN RCA – rapid drop of pH followed by a plateau around pH 4.9 to 7.0. Garrabrants et al. (2004) concluded that the plateau in the ANC can be explained by dissolution of calcium carbonate (carbonation) in concrete, which is caused by a reaction between portlandite and calcium silicate hydrate with carbon dioxide from the environment. Carbonation conditions may occur during the concrete service life and in stockpile storage. In comparison, the CA RCA showed a pH plateau that was less obvious. The TIC results showed that the CA RCA had much less inorganic carbon (0.4% of mass) compared with the CO RCA (1.5% by mass), TX RCA (2.7% by mass), and MN RCA (1.2% by mass).

The gravel-sized and sand-sized particles (87.2% to 97.8% of total RCA mass fraction) presented an ANC curve similar to the unfractionated RCA. Moreover, the gravel-sized particles had higher material pH (11.5 to 12.1) than sand particles (11.1 to 11.9) and fine particles (10.9 to 11.8), and likely control the bulk (unfractionated) pH (11.3 to 12.1). Carbonation is the most probable reason for this pH difference among fractions, since all fractions are sourced from the same monolithic concrete and treated using the same procedure. Carbonation begins on the

surface of the concrete and slowly penetrates the interior of the concrete (Houst and Wittmann 2002, Garrabrants et al. 2004). After crushing, the fines have a much higher surface area than gravel-sized particles, which results in more reactive surface for carbonation, consuming more cement and leading to a lower material pH. The higher carbonation degree in the fines can also be shown by comparing the ANC curve of the fines fraction with the other fractions. The fines fraction had a higher resistance of acid attack than other fractions. In general, the acid neutralization capacity decreased as the particle size increased.

10.4.3.1.1 Leaching of Trace Elements Cu and Zn from RCA

Cu and Zn are the most concentrated trace elements in RCA samples. Figure 10.10 shows pH-dependent leaching of Cu and Zn from the unfractionated RCAs. Cu and Zn showed similar leaching trends, with maximum leached concentrations at pH ≈ 2.0 and minimum leached concentrations at alkaline or near-neutral pH (7.5–13.0). An increase in leaching concentration with decreasing pH was observed for both elements, with Cu starting at pH≈6.5 and Zn at pH≈7.5.

The concentrations of leached Cu and Zn were not directly related to the total elemental content of the RCA (Table 10.1). CO RCA tended to leach more Cu and Zn than the other RCAs within the pH range of 2.0 to 13.0, even though the total elemental composition had lower quantities of Cu and Zn available to leach compared to the other three RCAs tested. This trend in leaching behavior was also observed in waste material leaching studies performed by Van der Sloot et al. (1997) and Kosson et al. (2002).

Figure 10.11 shows the pH-dependent leaching patterns of Cu and Zn from three fractions. The grain-size specific fractions showed a similar leaching trend for all RCA sources. In the pH range of 2 to 13, fine particles showed a higher leaching concentration than coarser-sized particles, and the leaching was enhanced as particle size decreased. At a pH > 12, slightly enhanced leaching of Cu and Zn were observed from fines, while gravel-sized particles showed no obvious difference in leaching behavior. Previous studies with field road base have shown that this alkaline effluent usually occurs in the first few flushes from field road base and has been observed in previous studies (Sadecki et al. 1996, Engelsen et al. 2006). At pH typical of field-scale studies (6.5 ~ 8.0), leaching of Cu and Zn from smaller sized fractions increased, with the fine fraction having leached concentrations of Cu and Zn up to an order of magnitude higher.

10.4.3.2 Leaching of Oxyanion Cr from RCA

Chromium, which usually forms negative-charge oxyanions (e.g., CrO_4^{2-}), showed a V-shaped pH leaching pattern (Figure 10.12). The minimum release of Cr occurred between pH 5.0 and 6.5, and increasing concentrations were observed towards both pH = 2 and pH = 13. The most acidic region (pH≈2) showed higher leaching levels (3.2 mg/kg to 6.1 mg/kg) relative to the most alkaline region (pH≈12) where concentrations were between 0.9 mg/kg and 1.2 mg/kg. The leaching amount was also independent from the total elemental content. All RCAs showed similar Cr leaching levels at pH≈2 and pH≈13, while Cr contents in solid samples showed notable differences, ranging from 7.5 to 20.2 mg/kg. Figure 10.13 shows the various Cr species across the range of pH and Eh conditions (Cornelis et al.. 2008). The Eh data of the unfractionated RCAs are also plotted in Figure 10.13. At high pH (pH>11.0), CrO_4^{2-} (toxic

hexavalent chromium) is the dominant form of Cr, whereas various tri-valent chromium forms occur at pH<11.0.

A similar V-shaped leaching pattern was also observed among each grain-size fraction (Figure 10.14). There is no obvious differences in Cr leaching among the three fractions at pH 2.0 to 13.0. Finer particles showed a slightly higher leaching ability than gravel-sized and sand-sized particles at pH<2.

10.4.3.3 pH and Leaching of Heavy Metals from Laboratory Batch tests and Field Site for RAP

As mentioned earlier, there is limited concern for RAP leaching. Figure 10.15 shows the pH of RAP leachate in batch tests as well as in the field. Field pH is similar to the pH of the batch test leachate as well as the pH of Class 5 natural aggregate. Field pH is within the EPA groundwater limits, i.e., 6.5 to 8.5.

Concentration of As, Se and Sb were slightly higher than the corresponding USEPA groundwater maximum contaiminant level (MCL) (Figure 10.16, Figure 10.17 and Figure 10.18), with peak As concentration of 37.9 μg/L, peak Se concentration of 113 μg/L and peak Sb concentration of 10.6 μg/L. However, leachate from Class 5 also presented similar leaching of As, Se and Sb, with peak As concentration as 27.5 μg/L, peak Se concentration as 89.3 μg/L and peak Sb concentration as 20.3 μg/L. The peak concentration of As and Se were slightly higher and Sb slightly lower than those from Class 5. The TCLP test results indicate that the asphalt binder contributed leaching of As, Se and Sb, moreover, leaching of those elements could largly come from the asphalt binder in the surface layer (Figure 10.16, Figure 10.17, and Figure 10.18). RAP samples from various states have the same TCLP As, Se and Sb concentrations with a range from 73.5 to 82.6 μg/L for As, and 87.9 to 129.3 μg/L for Se and 6.7 to 13.8 μg/L for Sb. As and Sb appear to be in a form that is more water soluble than Se in batch leaching test results.

10.5 Conclusions and Recommendations

Seven samples of recycled concrete aggregate (RCA) from various states were tested in the laboratory. Two field sites using three RCAs as unbound base course were also investigated. Lysimeters were placed under the base course, and leachate samples were collected periodically to track the effluent pH and released metals during the base course service life. Laboratory column leaching tests and batch leaching tests on five RCA samples (one of which also used in field leaching test) were conducted to compare with the field data and characterize RCA leaching behavior. Based on the collected data, the following conclusions are drawn for RCA:

1. Highly alkaline leachate from lysimeters was observed in the University of Wisconsin field site with peak effluent pH of 12.9. Fresh RCA started with a high leachate pH (12.6) that remained constant throughout the testing period (5 pore volumes of flow, PVF), with peak pH of 12.9 at 2.8 PVF. Stockpiled RCA started at a lower pH (7.3), but gradually increased to a pH of 12.1 during the testing period (2 PVF).
2. The MNROAD site, however, showed a consistently neutral pH (6.6 to 8.0) after 7 months of sampling, and the leaching trend was different than that observed in the laboratory column leaching tests using the same RCA material. Carbonation of

percolating water and/or preferential flow due to weathering could explain the behavior. More field investigations and tests are needed to verify these hypotheses.

3. Laboratory column tests showed high alkaline leachate (pH = 10.8 to 12.5) from all RCA materials and no pH decline during the long testing period (100 PVF). Stockpiled RCA had a lower leachate pH and material pH.
4. As, Cr, Pb, and Se exceeded the maximum contaminant levels (MCLs) in the USEPA drinking water standard at some point both in the field and laboratory column leaching tests. Cr and Pb usually exceeded the MCL at first flush and sporadic exceedances occurred afterwards, while As and Se exceeded the MCLs consistently throughout the test period. As and Cr were mainly sourced from the cement mortar based on acid digestion results. The oxyanions (As, Se, and Cr) should be given more attention as they have enhanced leaching in highly alkaline environments.

Limited tests on recycled asphalt pavement (RAP) indicated pH within the EPA groundwater limits, i.e., 6.5 to 8.5. Concentration of As, Se and Sb were slightly higher than the corresponding USEPA groundwater maximum contaiminant level (MCL). The TCLP test results indicate that the asphalt binder is probably the source of As, Se and Sb.

10.6 Tables

Table 10.1Physical, Hydraulic, and Chemical Properties of RCAs

Location (State)	CA	CO	MI	MN	TX	Class V	WR (F)	WR (SP)	WA
Physical properties									
Optimum Water Content[1] (%)	10.9	11.9	8.7	11.2	9.2	8.0	10.8	9.9	-
Max Dry Unit Weight[1] (kN/m^3)	19.8	18.9	20.8	19.5	19.7	20.7	19.4	19.9	16.2
Specific Gravity[2]	2.6	2.6	2.7	2.7	2.6	2.7	2.7	2.6	2.8
Absorption[2] (%)	5.0	5.8	5.4	4.9	5.5	2.2	4.2	4.2	1.8
Void Ratio[2]	0.30	0.36	0.28	0.29	0.30	0.29	0.36	0.30	0.68
USCS	SP	SM	GP	SP	GP-GM	SW-SM	GP	SP	GP
Hydraulic Properties									
Hydraulic Conductivity[3] ($\times 10^{-5}$ m/s)	1.9	1.6	2.6	1.8	0.8	0.05	120	71	58
Carbon Content[4]									
Total Carbon (%)	1.9	1.9	4.6	1.6	3.2	2.6	6.8	7.4	11.7
Total Organic Carbon (%)	1.4	0.3	0.2	0.4	0.4	0.1	0.3	0.5	1.0
Total Inorganic Carbon (%)	0.5	1.5	4.4	1.2	2.8	2.5	6.5	6.9	10.7
Total element concentrations[5]									
Major elements									
Ca (%)	6.9	8.5	7.6	16.3	4.9	0.3	>20	>20	>20
Fe (%)	2.3	1.1	1.0	1.6	0.8	0.6	0.8	0.7	0.3
Al (%)	1.7	1.5	1.0	0.8	1.0	0.4	0.5	0.4	0.1
Mg (%)	1.0	0.3	2.0	1.1	0.3	0.2	8.5	8.7	>10
Na (%)	0.4	0.5	0.6	0.4	0.3	0.02	0.8	0.4	0.5
K (%)	0.14	0.14	0.20	0.16	0.13	0.08	0.15	0.11	0.08
Trace elements									
As (mg/kg)	2.5	6.5	2.2	2.4	2.2	0.5	10.9	11.2	6.3
Ba (mg/kg)	165.2	88.8	40.8	69.4	58.0	31.7	20.4	22.8	3.7
Cd (mg/kg)	0.2	0.2	0.1	0.1	0.1	0.7	0.6	0.4	0.3
Co (mg/kg)	4.0	1.8	1.2	2.8	1.2	2.2	2.9	2.3	0.4
Cr (mg/kg)	20.2	7.5	6.2	11.5	8.9	18.7	6.7	6.3	2.5
Cu (mg/kg)	16.5	10	9.1	13.6	6.1	8.2	13.8	10.7	2.6
Mo (mg/kg)	0.1	1.0	0.1	1.0	0.1	0.1	1.1	0.5	0.3
Ni (mg/kg)	21.0	4.7	3.0	8.1	2.7	7.2	5.1	4.6	1.3
Pb (mg/kg)	9.1	8.7	2.1	2.6	5.0	2.5	3.6	3.2	3.7
Sb (mg/kg)	0.9	0.4	0.5	0.2	0.7	0.9	2.8	2.2	1.7
Se (mg/kg)	0.8	0.9	1.0	0.9	1.3	2.6	16.7	17.4	16.3
Zn (mg/kg)	32.4	58.8	34.9	30.4	20.4	11.7	26.8	18.9	17.6
Material pH[6]									
Bulk Specimens	12.1	12.1	12.6	11.3	12.0	9.1	12.3	11.8	10.0
Gravel-sized (75-4.75 mm)	12.1	12.1	12.5	11.6	12.1	-	12.6	11.9	-
Sand-sized (4.75-0.075 mm)	11.9	11.9	12.5	11.2	11.7	-	12.4	11.5	-
Fines (< 0.075 mm)	11.9	11.8	12.1	10.9	11.1	-	12.1	10.9	-

Methods: 1. ASTM D1557; 2. AASHTO T85; 3. ASTM D5856; 4. SC144 DR sulfur and carbon analyzer (LECO Inc., St. Joseph, MO, USA); 5. USEPA 3050(B); 6. Batch tests (de-ionized water only) with liquid to solid ratio = 1:10, contact time = 72 h, in a 30 revolution per min tumbler. 7. " –" = data unavailable.

10.7 Figures

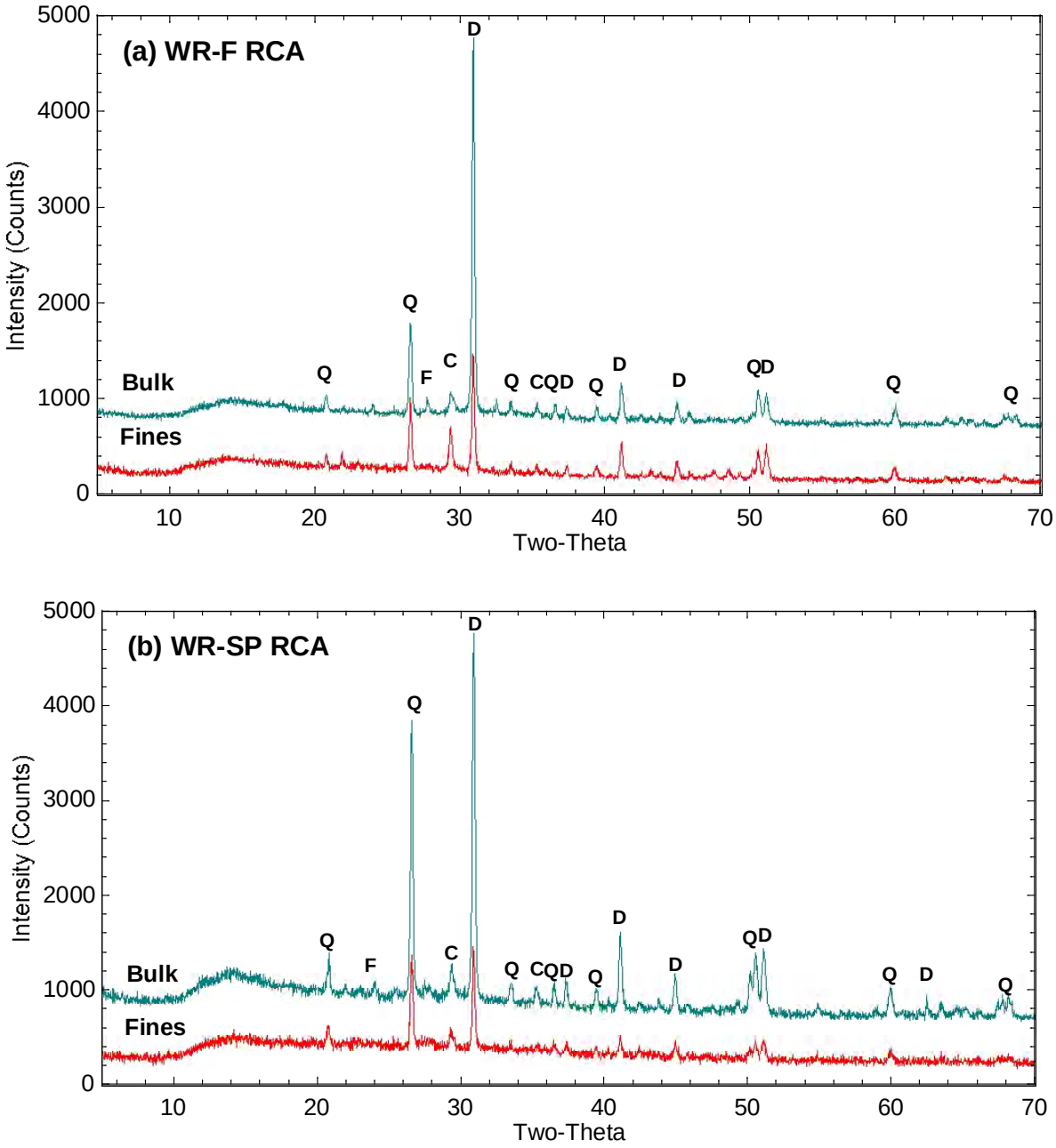

Note: (C) Calcite, (D) Dolomite, (F) Feldspar, (Q) quartz.

Figure 10.1 XRD Patterns of Bulk Sample and Fines in (a) WR-F RCA and (b) WR-SP RCA

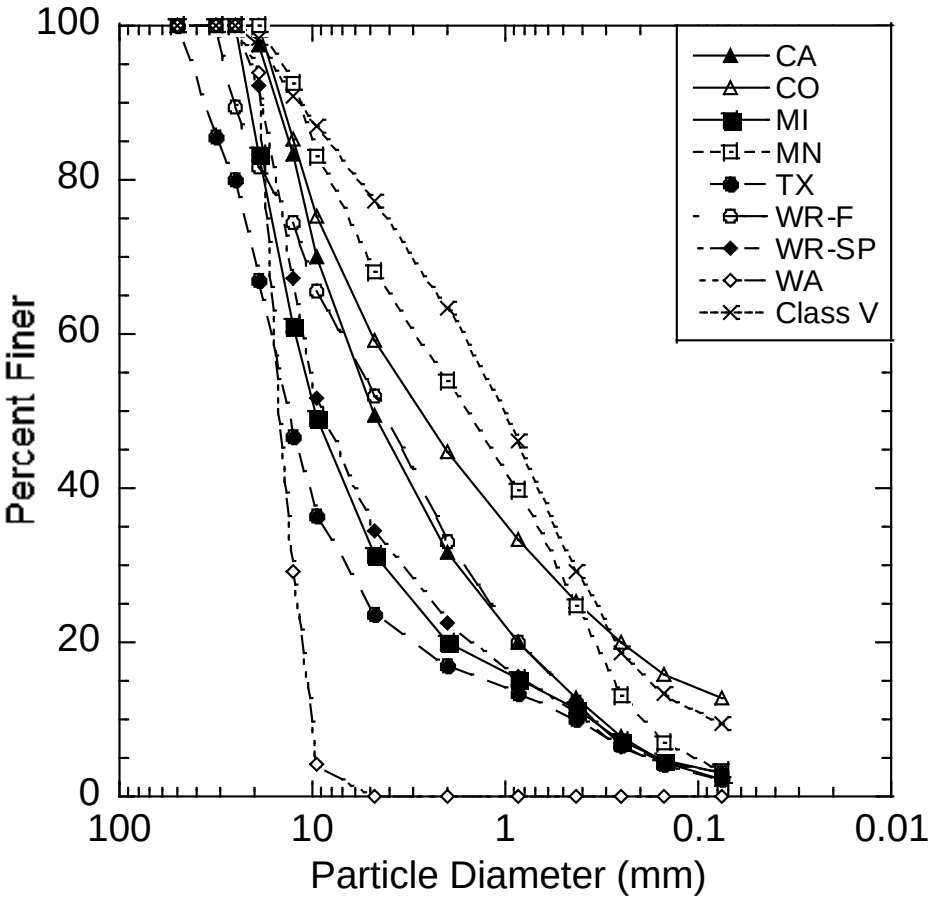

Figure 10.2 Grain Size Distribution Curves of the Studied Aggregates

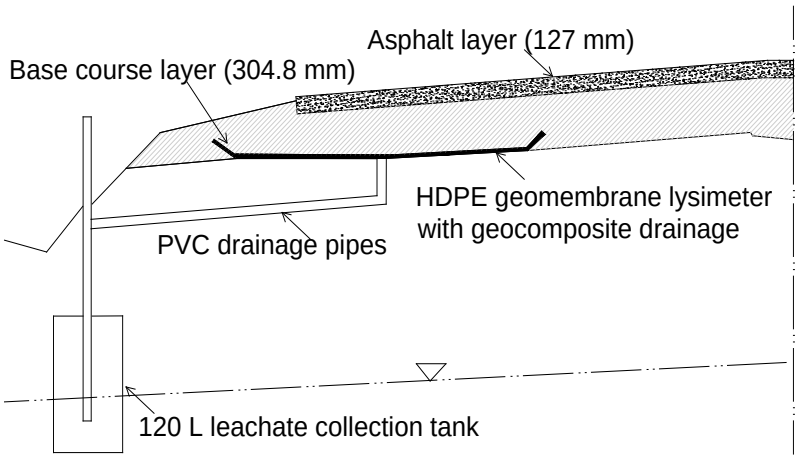

Figure 10.3 Lysimeter Design

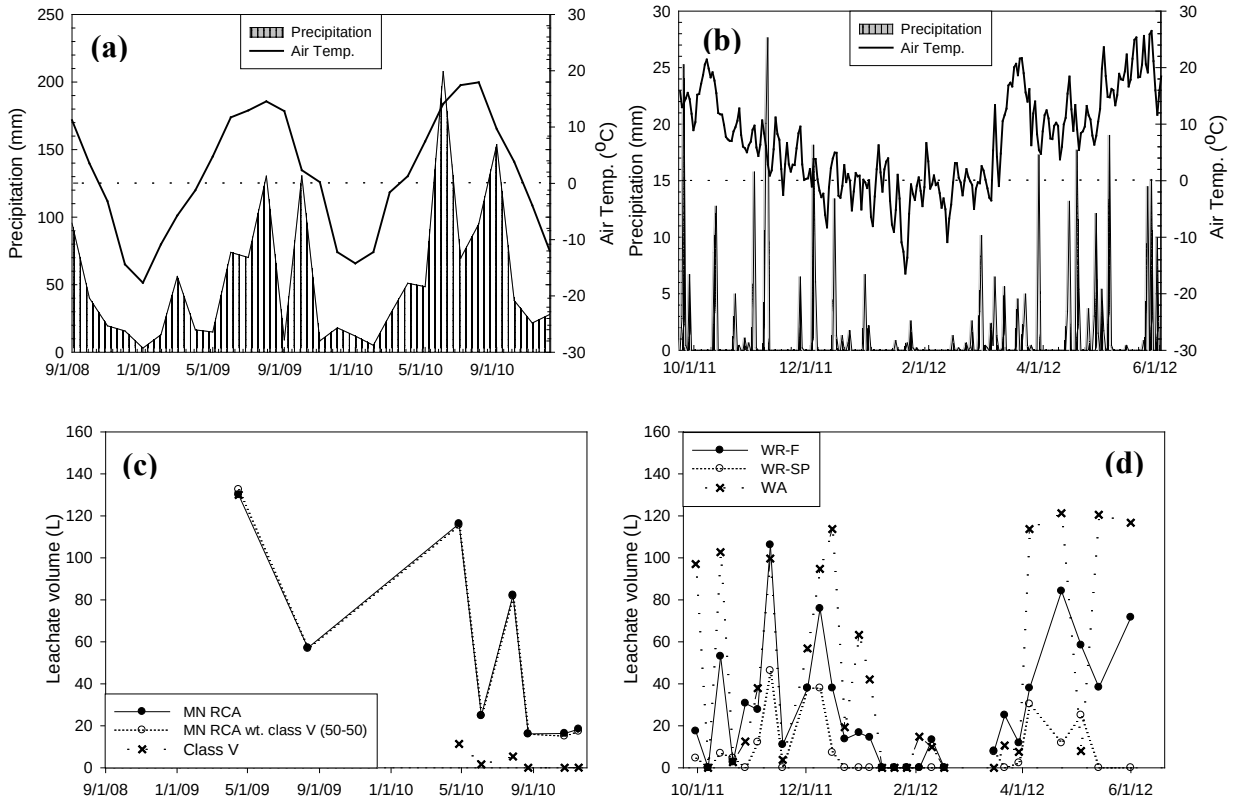

Figure 10.4 Precipitation and Air Temperature Data for the (a) MNROAD Site, (b) UW Site, (c) Leachate Volume from the MNROAD Site, and (d) Leachate Volume from the UW Site

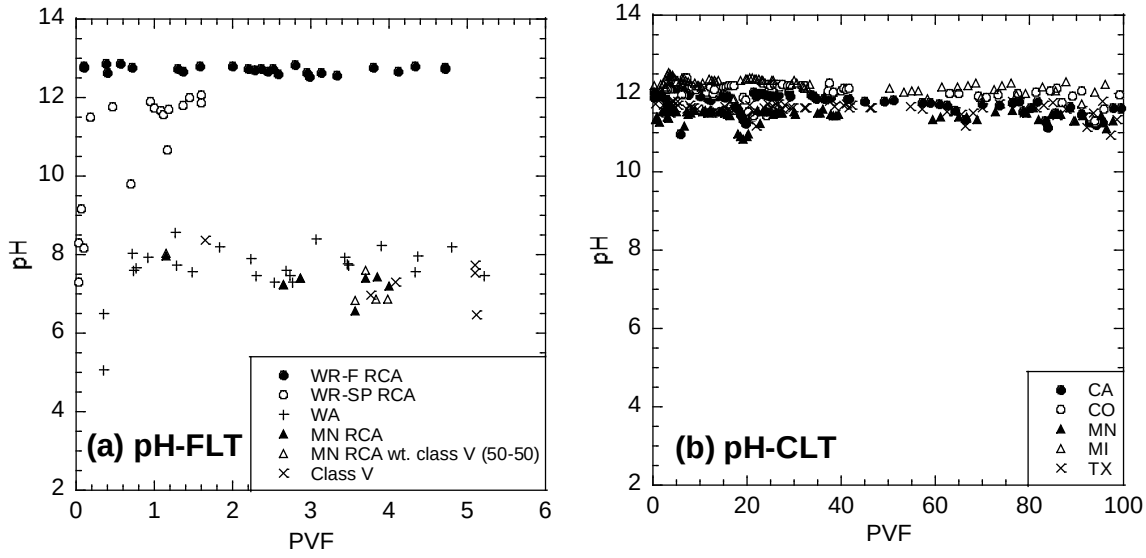

Figure 10.5 pH of Field Leachate (a) FLT (b) CLT

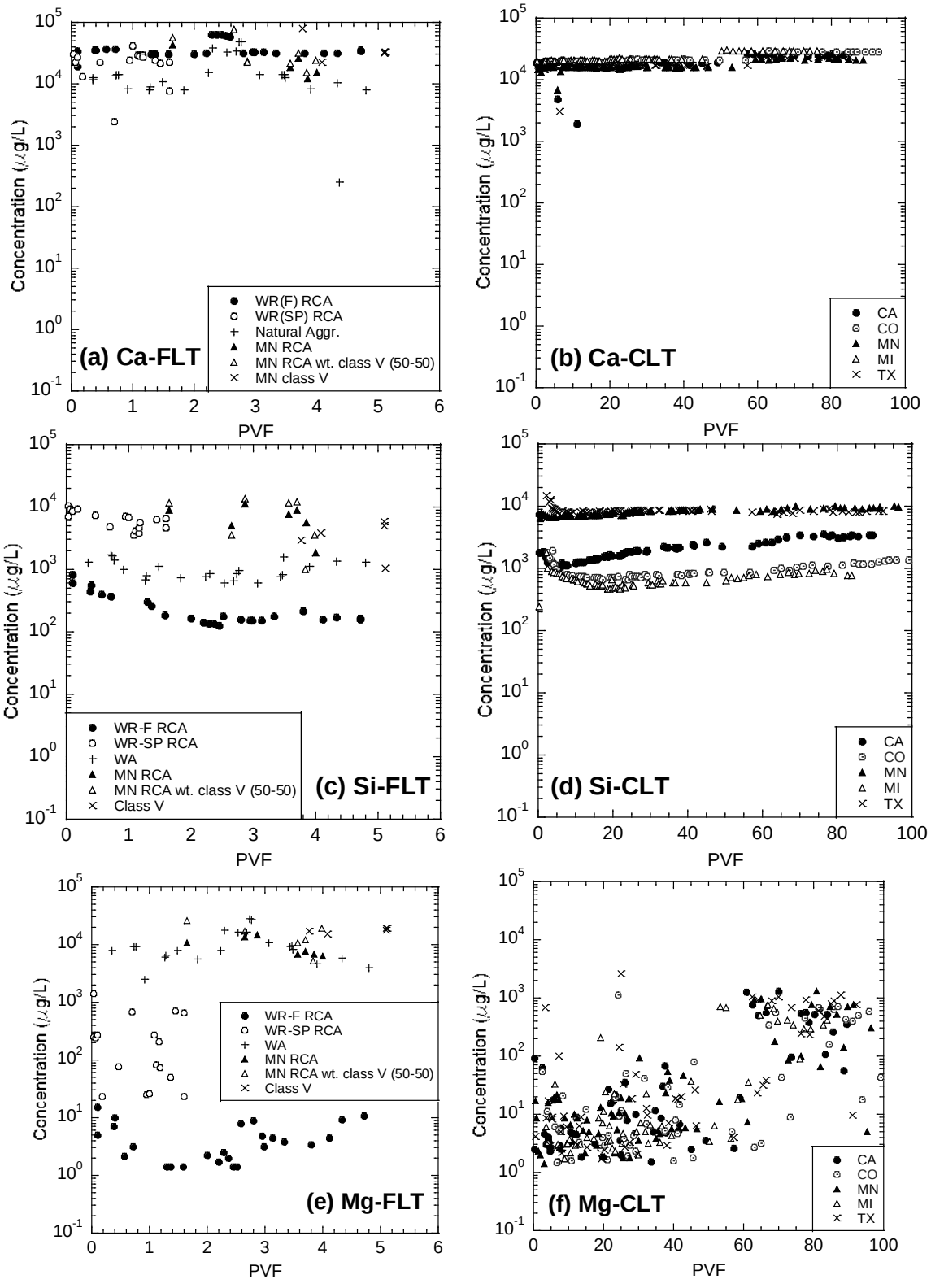

Figure 10.6 Ca, Si, and Mg Concentration in Leachate from FLT and CLT as a Function of PVF (a) Ca-FLT (b) Ca-CLT (c) Si-FLT (d) Si-CLT (e) Mg-FLT (f) Mg-CLT

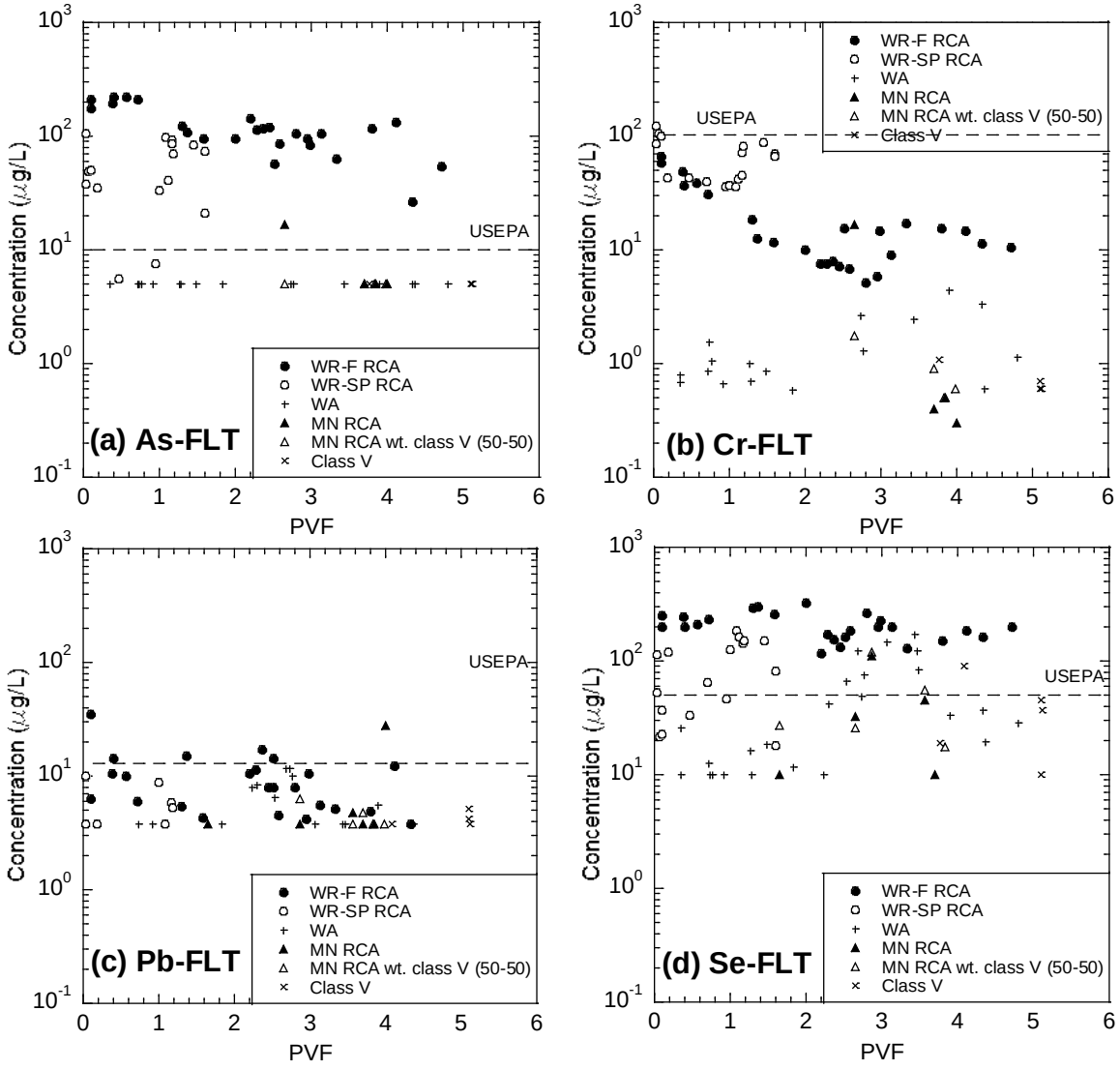

Figure 10.7 As, Cr, Pb and Se Concentrations in Leachate from FLT as a Function of PVF (a) As (b) Cr (c) Pb (d) Se

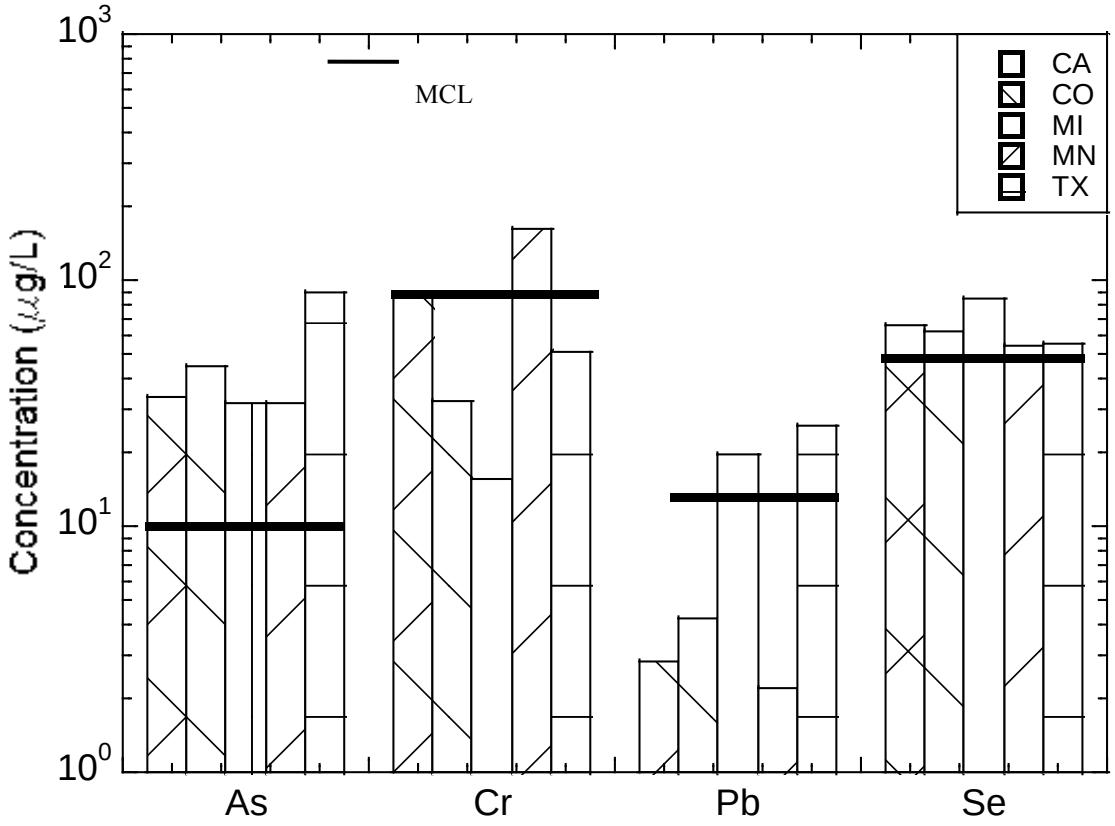

Figure 10.8 As, Cr, Pb and Se Concentrations in Leachate from CLT as a Function of PVF.

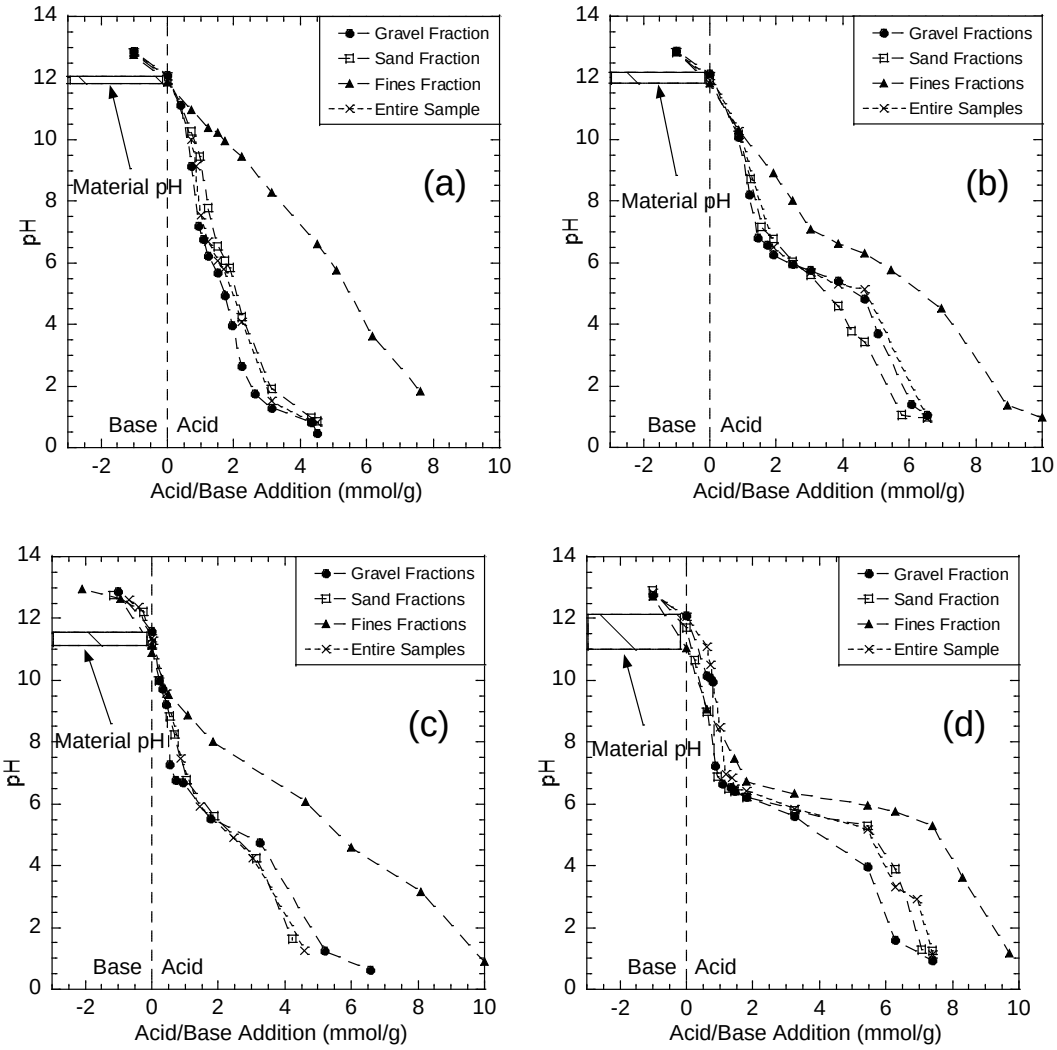

Figure 10.9 ANC Curves of (a) CA RCA (b) CO RCA (c) MN RCA (d) TX RCA.

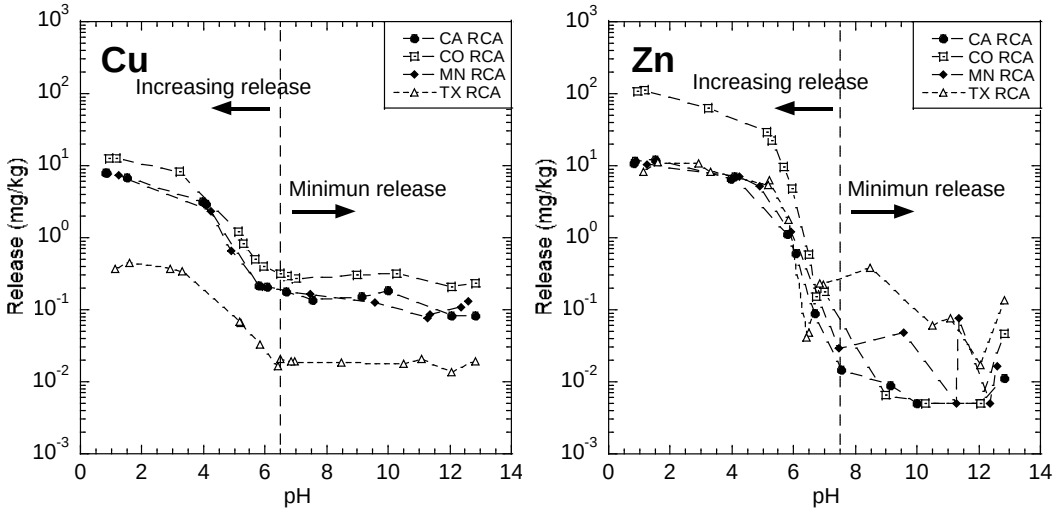

Figure 10.10 pH-Dependent Leaching of Cu and Zn from Unfractionated RCAs

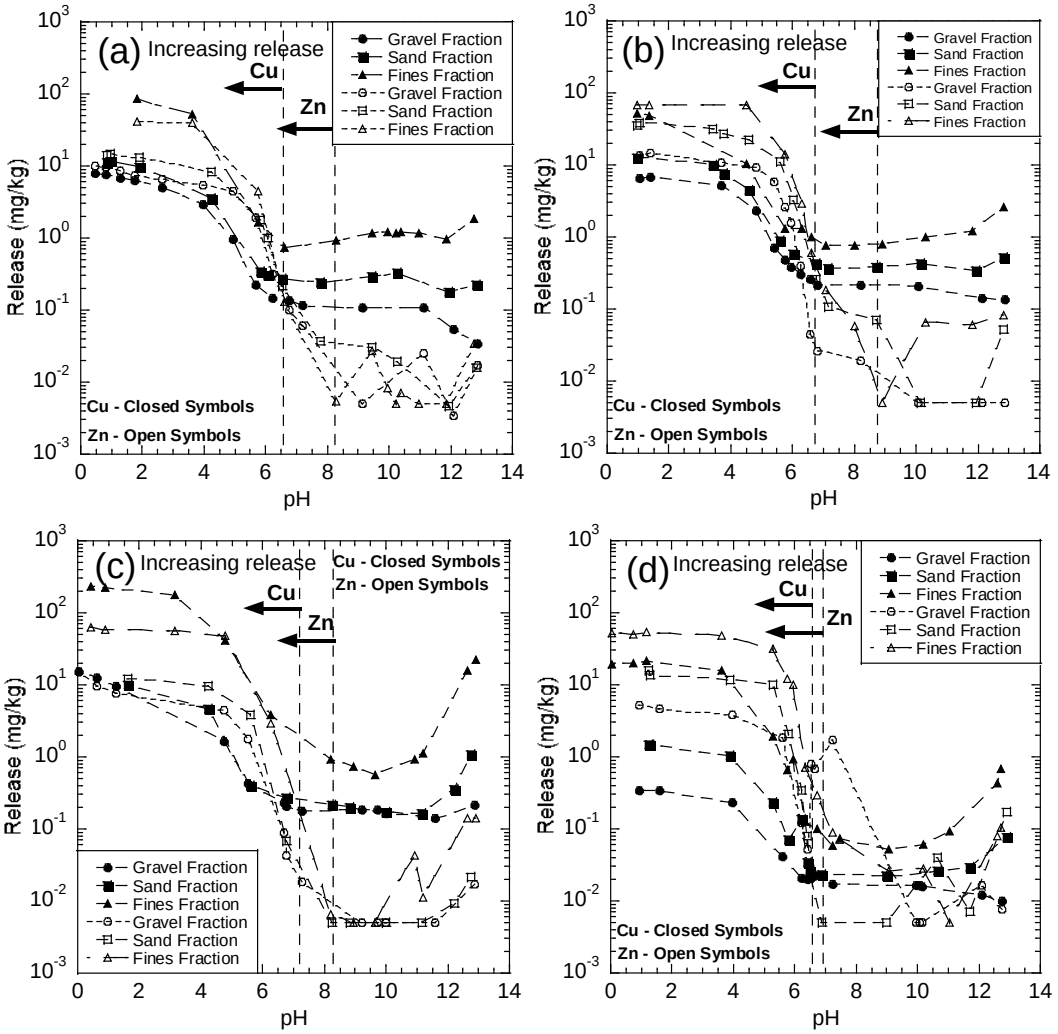

Figure 10.11 pH-Dependent Leaching of Cu (closed symbol) and Zn (open symbol) from (a) CA RCA(b) CO RCA (c) MN RCA (d) TX RCA

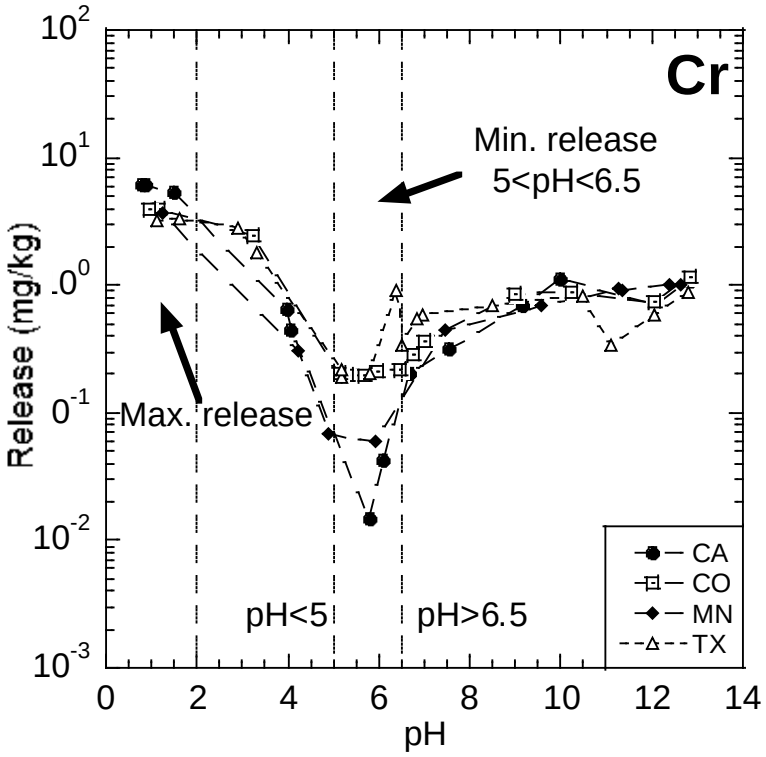

Figure 10.12 pH-Dependent Leaching of Cr from Four Unfractionated RCAs

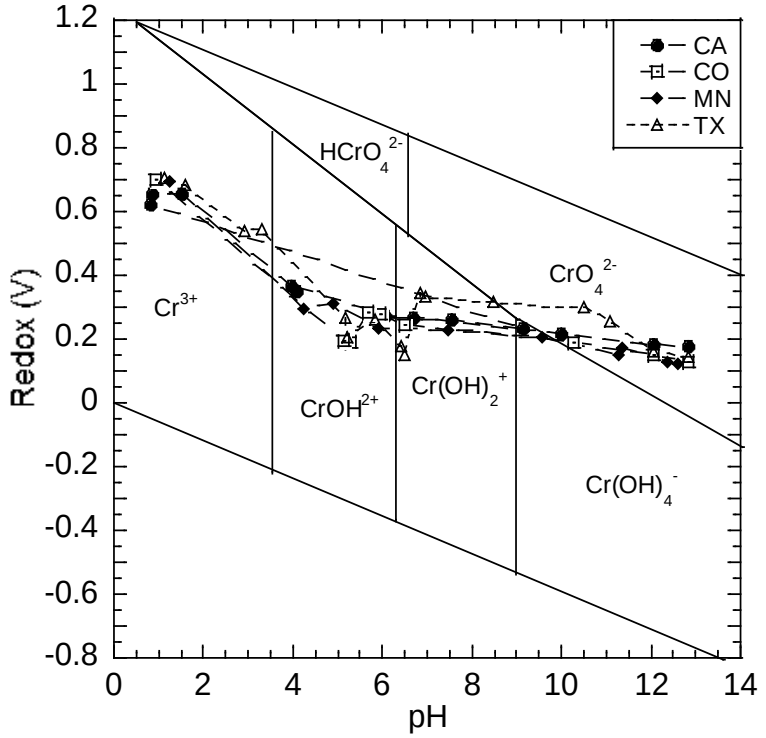

Figure 10.13 Cr Species as a Function of pH and Eh (Cornelis et al.. 2008)

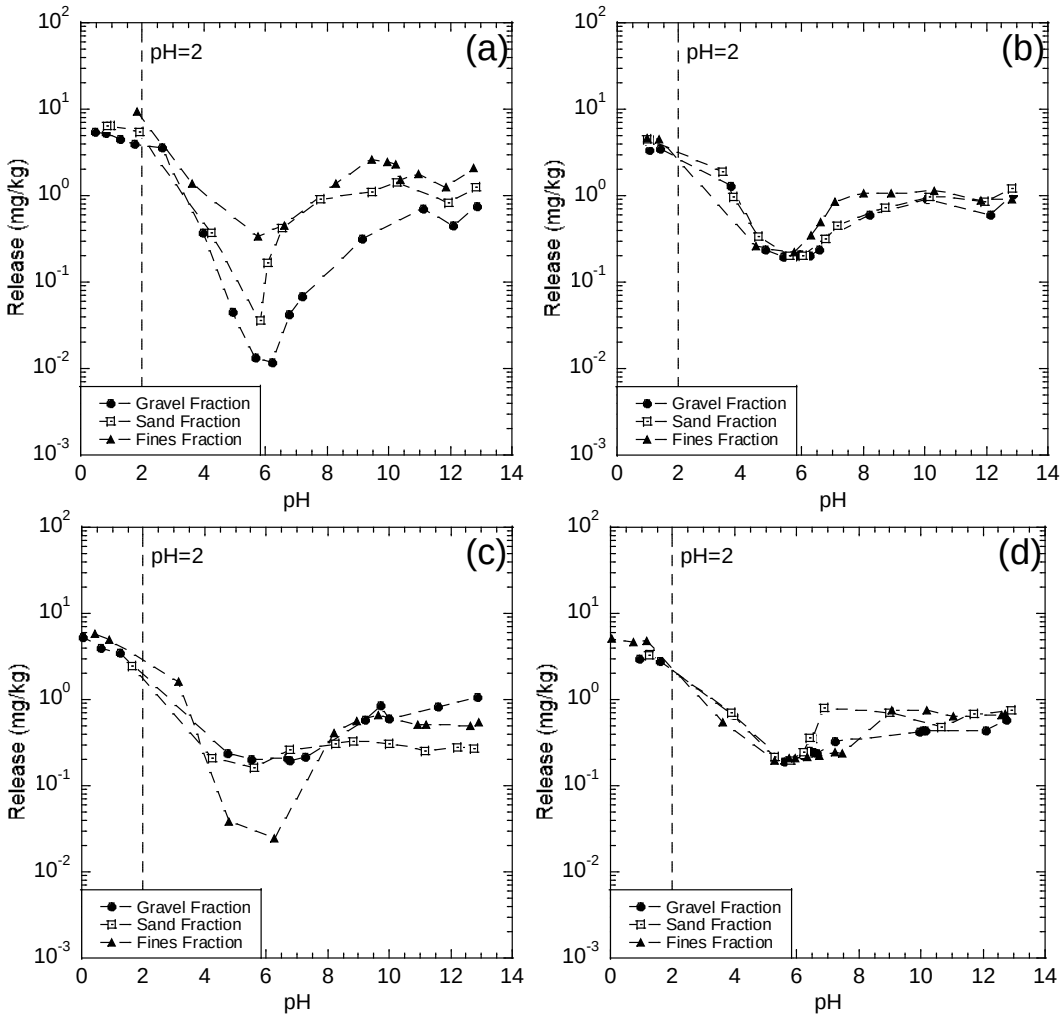

Figure 10.14 pH-Dependent Leaching of Cr from Fractionated (a) CA RCA (b) CO RCA (c) MN RCA and (d) TX RCA

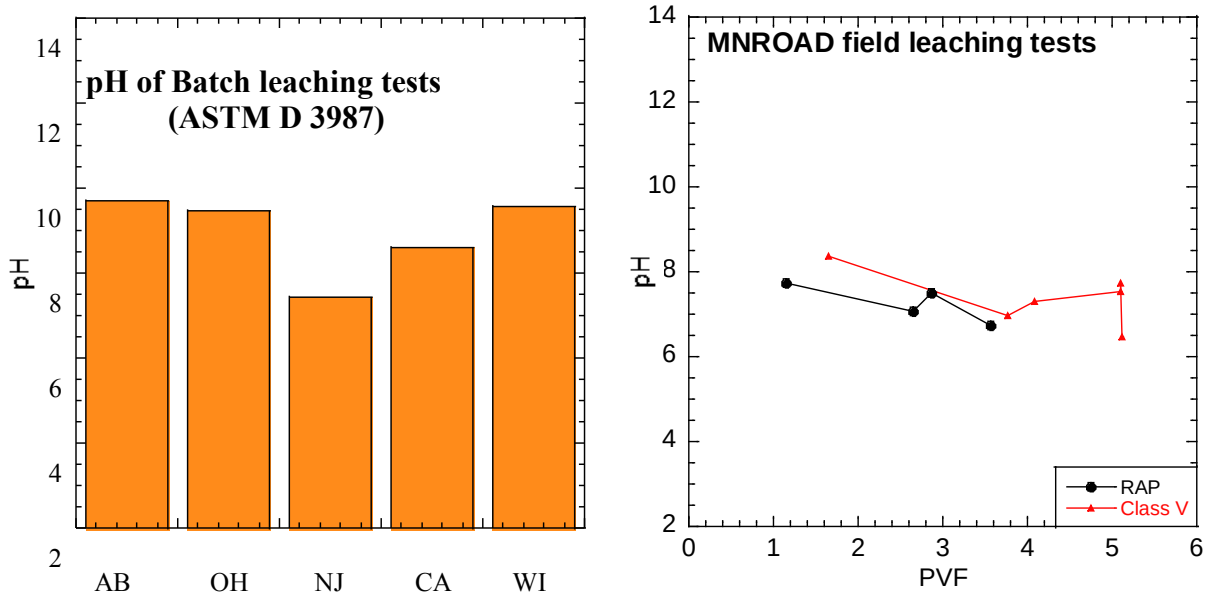

Note:

ASTM D 3987. Liquid to solid ratio = 1 : 20, de-ionized water

AB: Fresh asphalt binder(not recycled)

Figure 10.15 pH of Leachate from Field Leaching Tests and Batch Leaching Tests

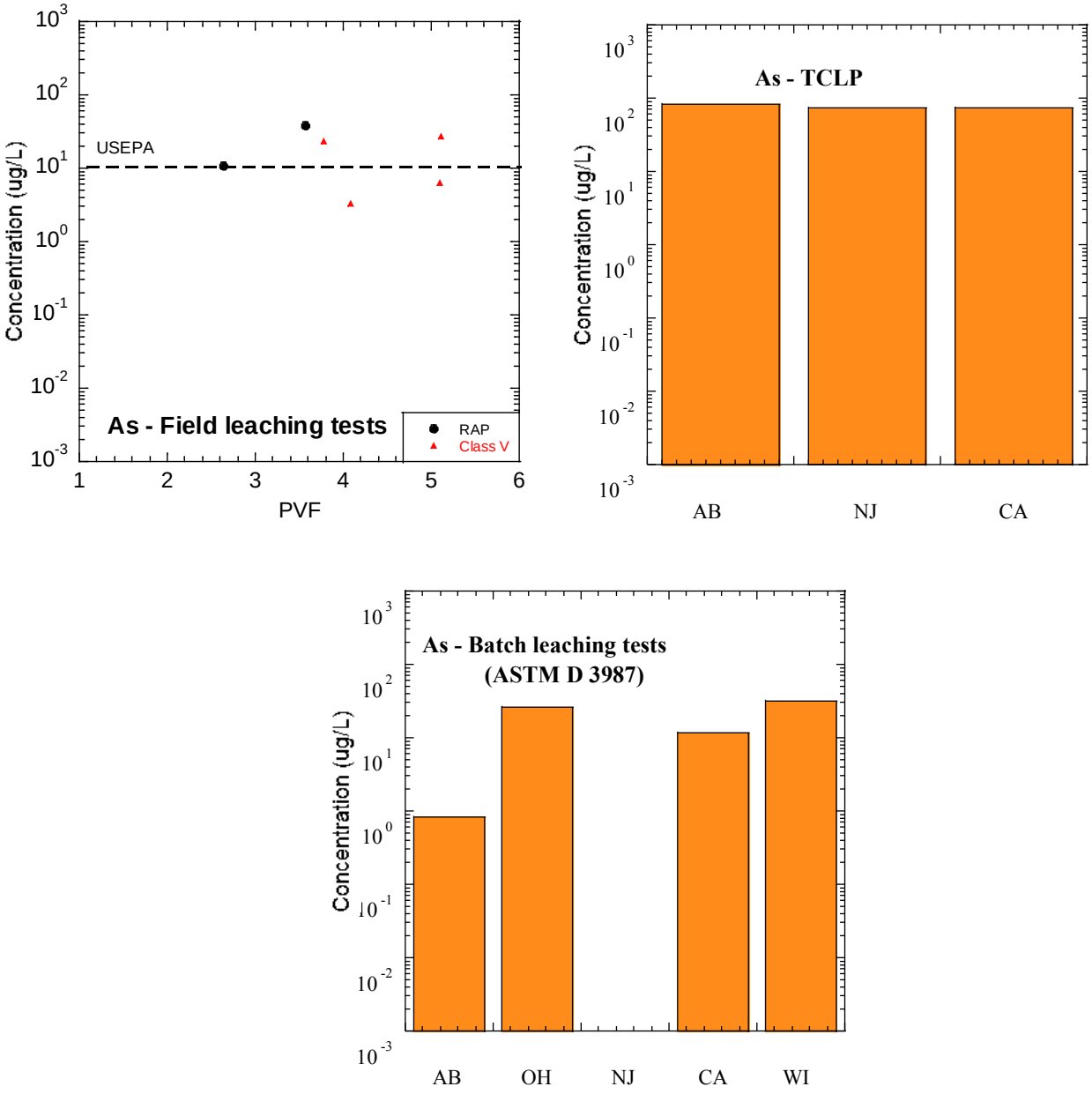

Figure 10.16 As Concentration of Leachate from Field Leaching Tests, Batch Leaching Tests and TCLP

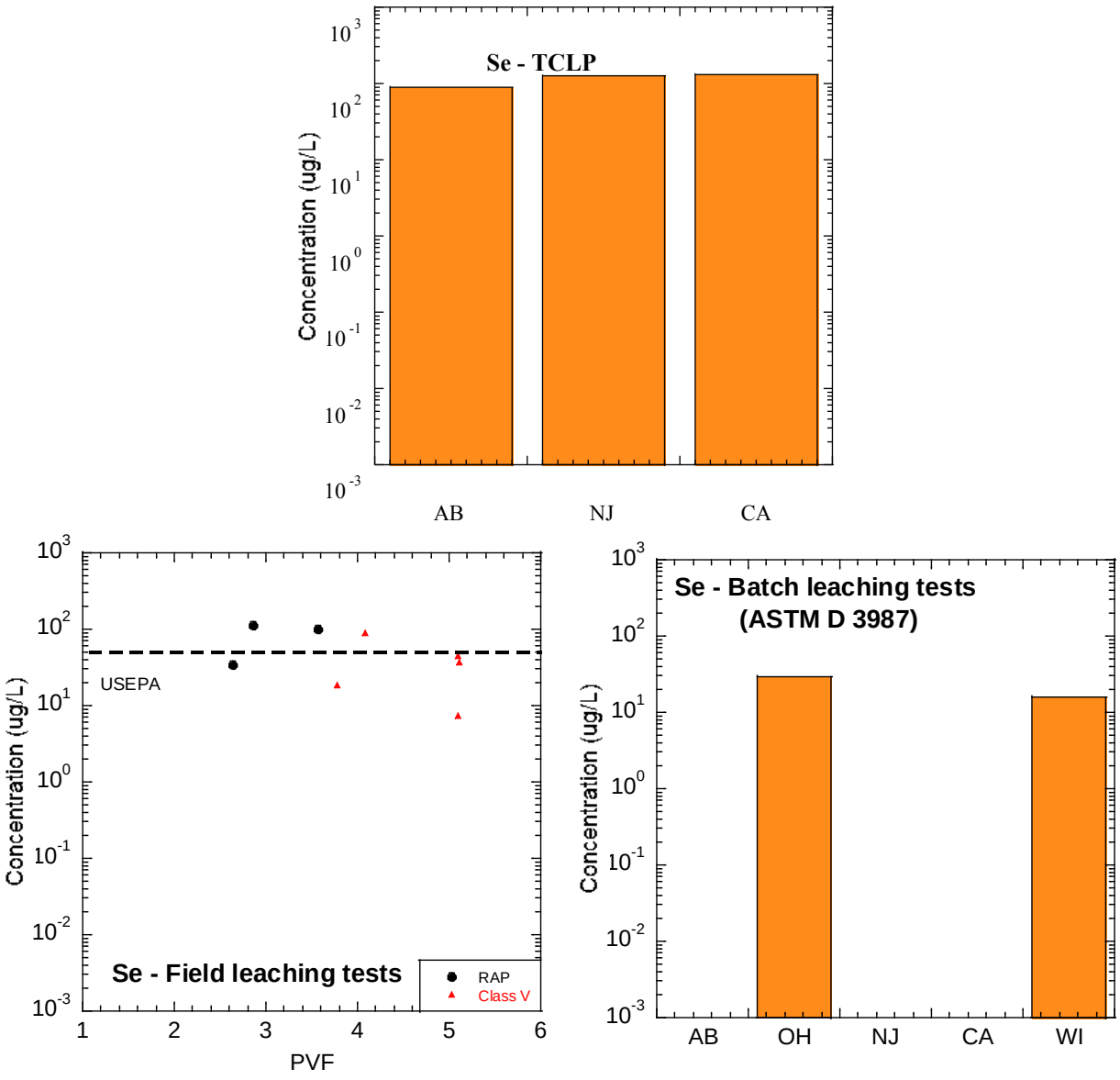

Figure 10.17 Se Concentration of Leachate from Field Leaching Tests, Batch Leaching Tests and TCLP

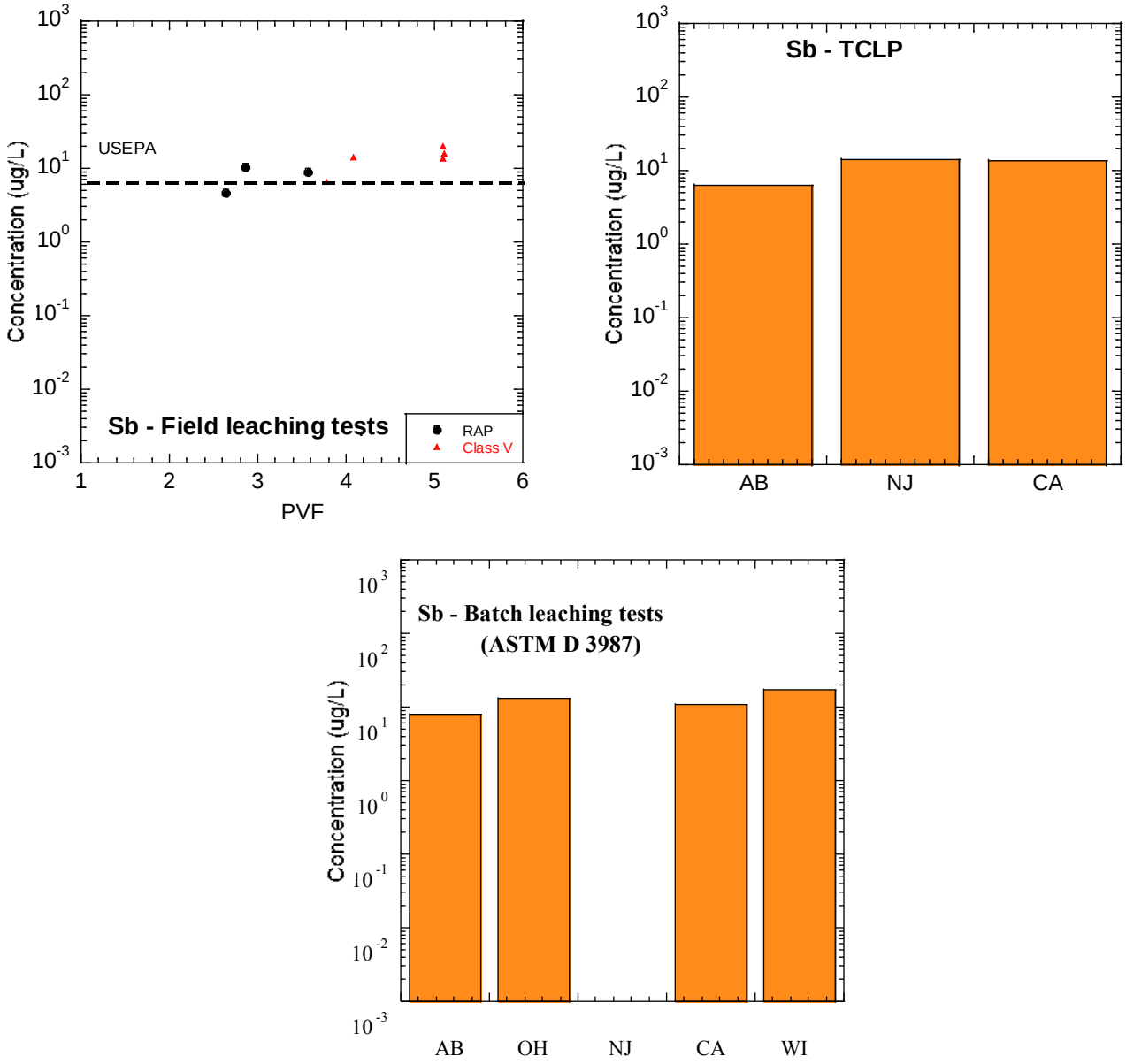

Figure 10.18 Sb Concentration of Leachate from Field Leaching Tests, Batch Leaching Tests and TCLP

11. Summary and Conclusions

This document is the final report that presents the findings of research on unbound recycled materials, specifically recycled asphalt pavement (RAP) and recycled concrete aggregate (RCA), as road base course. The **objective** of this project was to characterize the properties of crushed recycled concrete pavement (RCA) and asphalt (RAP) as unbound base without being treated or stabilized, to assess how RCA and RAP behave in the field and to determine how pavements can be designed using RCA and RAP. Issues to be considered include variability in material properties, purity of material and how to identify and control material quality. This project included laboratory studies, examination of existing field sites and evaluation of data from MnROAD test sections. Anticipated results from this project include a suite of tests and/or protocols that may be used to identify the critical characteristics of these recycled materials, as well as optimum design criteria and best construction practices needed for a durable base that meets the properties proposed for layer design. The three cells were constructed using recycled materials in the granular base layers at the MnROAD test facility. One test section include 100% RAP, another 100% RCA and the third a 50/50 blend of RCA/natural aggregate. A fourth cell was constructed as control including only natural aggregate. The material properties were monitored during construction and throughout the pavement life by others, especially the variation with changing seasons and moisture regimes in order to determine their effects on pavement performance. The cost of the instruments and installation was covered under a different program; however this project analyzed the data being generated from the test sections in conjunction with other data from the project.

Scope of Work consisted of a number of tasks as they relate to major themes of design, construction practices, maintenance, and materials. The following tasks were undertaken with a task report as the deliverable. Some of the tasks were expanded to include additional items by support of Recycled Materials Resource Center.

Task IA: Literature Review. This task was supplemented with a survey of state DOTs relevant to their use of RAP and RCA and their specifications.

Task IB: Relationship between Resilient Modulus and Composition of RCA or RAP. The recycled materials were obtained from eight different states in the United States and a suite of tests was completed to characterize them compositionally and mechanically as well as relative to their environmental suitability and durability.

Task IC: Scaling and Equivalency: Specimen Tests to Field-Scale Conditions

In this task, small-strain elastic modulus measurements, bench-scale resilient modulus measurements, back-calculated large-scale model experiment modulus, and modulus from falling weight deflectomer tests at the field sections were used to study scaling and layer equivalency.

Task ID: Climate Effects

Effects of freeze-thaw and wet-dry cycles were investigated. This task was expanded to include temperature effect on RAP stiffness and plastic deformation. Another expansion related to hydraulic properties and water retention characteristics of recycled materials.

Task IIA: Compaction Level and Assessment

Effect of degree of compaction and compaction moisture content on modulus was investigated.

Task IIB: Field Performance and Maintenance

Falling weight deflectometer data collected at the field sections were analyzed to assess the seasonal and long-term effects on modulus.

Task III: Materials Control

The nature and amount of impurities in samples from 8 different states were characterized. Effect of brick content on RCA compaction, stiffness, and durability was specifically investigated.

Task IV: Leaching Characteristics

Laboratory pH and leaching tests were carried out along with the analysis of field lysimeter leaching samples from both the field sections and an additional field site established for RCA at the University of Wisconsin-Madison.

Task V: Extended Monitoring

This task aims at extending field data collection at the field section for several years beyond the project duration.

Task VI/VII: Final Report and Dissemination

The main **conclusions** of this project include:

1. The materials, although obtained form 8 different states, had reasonably consistent properties with relatively small fines content, mortar content for the RCA samples, and the asphalt content for the RAP samples. The most distinguishing physical characteristics was the grain size with some samples coarser and others finer. Most samples had grain size distributions within the bounds for RCA and RAP given in the literature.
2. The amount of deleterious materials present in RCA and RAP varied amongst the source of the materials. The average impurity content was 1% for RCA and 0.2% for RAP, indicating that the recycling industry has developed sufficient controls.
3. The effect of brick content on the resilient modulus and compaction of RCA was investigated. No apparent trends were observed between modulus and brick content of RCA, but a decrease in plastic strain was observed with increased brick content up to 30%.

4. Maximum dry unit weight varies within a narrow range for RAP and RCA. Optimum moisture content of RAP is lower than RCA's. Empirical relations were developed to predict compaction characteristics in terms gradation characteristics.
5. Resilient modulus of the samples measured on specimens compacted at optimum moisture content and 95% modified Proctor maximum dry unit weight indicate that modulus of RAP/RPM is the highest of the recycled materials evaluated. RCA has slightly lower modulus in comparison to RAP/RPM, while Class 5 aggregate has the lowest summary resilient modulus (SRM). Both the NCHRP model with 5 coefficients and the Power model with 2 coefficients fit the data satisfactorily with the NCHRP being slightly better but more cumbersome than the Power model. Modulus is significantly correlated to grain size characteristics and moisture content. Empirical relationships were developed to predict modulus in terms gradation and moisture characteristics. Modulus of the recycled materials seems to be more sensitive to compaction than natural aggregate. Compaction moisture effect has an impact on resilient modulus greater for RCA than RAP. Blending recycled materials with natural aggregate results in intermediate modulus between the moduli of the two materials. Recycled materials had higher moduli then natural aggregate in this study.
6. Large-Scale Model Experiment (LSME), a large prototype-scale test, confirmed the findings regarding the modulus as obtained from bench-scale laboratory tests, i.e., modulus of RCA and RAP from the LSME was greater than that of Class 5. After applying corrections for stress-state and strain level, the resulting low-strain moduli for the field falling weight deflectometer, LSME, and bench-scale tests were found to be of the same magnitude within a reasonable amount of variance thus indicating the scalability of laboratory modulus to operating field modulus although the directly obtained moduli from the three have different values.
7. LSME allows determination of plastic deformations of the materials tested. The plastic deformation of RAP was much greater than that experienced by Class 5, whereas the plastic deformation of RCA was smaller than the plastic deformation experienced by the Class 5. However, the service life of a pavement constructed with RAP/RPM may be similar to the service life for a pavement with natural crushed aggregate base, even though RAP/RPM has higher rutting potential compared to crushed aggregate. This is because RAP/RPM has higher resilient modulus than crushed aggregate.
8. The mechanical properties of RAP and RCA determined under different climatic conditions indicated that both RAP and RCA had higher stiffness than Class 5 regardless of the number of freeze-thaw cycles even though they displayed some sentivity to freeze-thaw. The decrease of SRM for RAP over 20 freeze-thaw cycles ranged from 20 to 66%, which is similar to the range reported for various coarse- and fine-grained soils. For the RCAs, SRM decreased after five freeze-thaw cycles, followed by a consistent increase.
9. Micro-Deval and particle size distribution tests were conducted on RAP, RCA, and natural aggregate after 5, 10, and 30 wet/dry cycles and no apparent trend was found between particle degradation and wet/dry cycling of the material.
10. The effect of temperature on resilient modulus of on RCA and natural aggregate at 7, 23, 35, and 50 °C was not evident; however, a decrease of approximately 30% was observed in two of the three RAPs tested between the 23 and 35 °C temperatures. This suggests that the service life of a pavement constructed with RAP/RPM may be shorter than the service life for a pavement with natural crushed aggregate base in terms of rutting

because of the combined effects of decreasing stiffness and increasing plastic deformation due to temperature increase. Thus, the temperature effects need to be assessed using RAP and RPM.

11. All materials had high drainage capacities. RAP had the best drainage capacity while RCAs tended to have the best ability to retain water. It was found that increasing the gravel content decreased the air entry pressure in recycled and natural aggregates while increasing the fines content increased the air entry pressure.
12. Samples of RCA were tested in the laboratory to determine their pH and leaching characteristics. Additionally, lysimeters were placed under the RCA base course and leachate samples were collected periodically to track the effluent pH and released metals during the base course service life in the field. Although the MNROAD site showed a consistently neutral pH (6.6 to 8.0), the leaching trend was different than that observed in the laboratory column leaching tests using the same RCA material and a Madison field site. The reasons are not known for this observation. As, Cr, Pb, and Se exceeded the maximum contaminant levels (MCLs) for the USEPA drinking water standard both at the Madison field site and in the laboratory column leaching tests. However, although the MNROAD site concentrations of As, Pb, and Se for RCA were observed to exceed the corresponding MCL only once or twice and the leaching behaviors was similar to that of Class 5. For RAP, concentration of As, Se and Sb were slightly higher than the corresponding USEPA groundwater maximum contaiminant level (MCL).
13. Falling Weight Deflectometer (FWD) tests were conducted at the MnRoad facility since the construction (2009-2012). All pavement layers below the surface layer (i.e. base, subbase, and subgrade) retained a relatively constant stiffness regardless of temperature and no deterioration of modulus was evident over the last 4 years.

Overall, RAP and RCA pass all necessary standards for being a suitable base course material. They are structurally and mechanically comparable, if not superior, to many natural aggregates. Resilient moduli of RAP and RCA are higher than the natural aggregates used as a control material, hydraulic properties are similar if not superior to that of natural aggregate, and they withstand the extreme effects of climate very similarly as natural aggregate. It is noted, however, that some RAP may be sensitive to temperature change that may lead to rutting. This aspect needs to be considered in design.

References

AASHTO. (2002). Standard Specification for Reclaimed Concrete Aggregate for Unbound Soil-Aggregate Base Course. In *American Association of State Highway and Transportation Officials.*

AASHTO. (2009). "Standard Method of Test for Resistance of Coarse Aggregate to Degradation by Abrasion in the Micro-Deval Apparatus." Washington, D.C.

ACPA. (2008). "Recycling Concrete Pavements." American Concrete Pavement Association, Skokie, IL.

ACPA. (2009). "Recycling Concrete Pavements." *Bulletin B043P,* American Concrete Pavement Association. Skokie, IL.

Alam, T.B., Abdelrahman, M., and Schram, S.A. (2010). "Laboratory Characterisation of Recycled Asphalt Pavement as a Base Layer." *International Journal of Pavement Engineering* , No. 2, pp. 123-131.

ARA. (2004). "Guide for Mechanistic-Emprical Design on New and Rehabilitated Pavement Structures." Publication NCHRP Project 1-37A, NCHRP.

Arm, M. (2001). "Self-cementing Properties of Crushed Demolished Concrete in Unbound Layers: Results from Triaxial Tests and Field Tests." *Waste Management*, pp. 235-239.

Arulrajah. A., Piratheepan, J., Aatheesan, T., and Bo, M.W. (2011). "Geotechnical Properties of Recycled Crushed Brick in Pavement Applications." *Journal of Materials in Civil Engineering*, Vol. 23, No. 10, pp. 1444-1452.

ASTM. (2003). "Standard Test Methods for Wetting and Drying Compacted Soil-Cement Mixtures." West Conshohocken, PA.

ASTM. (2007). "Standard Test Method for Particle-Size Analysis of Soils." West Conshohocken, PA.

Attia, M. and Abdelrahman, M. (2010). "Modeling the Effect of Moisture on Resilient Modulus of Untreated Reclaimed Asphalt Pavement." *Transportation Research Record: Journal of the Transportation Research Board,* No.1981, pp. 30-40.

Bareither, C.A., Edil, T.B., Benson, C.H. and Mickelson, D.M. (2008). "Geological and Physical Factors Affecting the Friction Angle of Compacted Soils." *Journal of Geotechnical and Geoenvironmental Engineering,* No.10, pp. 1476-1489.

Barksdale, R. D., and Itani, S. Y. (1989). "Influence of Aggregate Shape on Base Behavior," *Transportation Research Record*, No. 1227, Transportation Research Board, Washington, D.C., pp. 173-182.

Bejarano, M.O., Harvey, J.T. and Lane, L. (2003). "In-Situ Recycling of Asphalt Concrete as Base Material in California." *Proc. 82nd Annual Meeting,* Transportation Research Board, Washigton, D.C., pp. 22.

Bennert, T., Papp Jr. W., Maher, A. and Gucunski, N. (2000). "Utilization of Construction and Demolition Debris Under Traffic-Type Loading in Base and Subbase Applications." *Transportation Research Record,* No. 1714, Washington, D.C., pp. 33-39.

Benson, C. and Gribb, M. (1997). "Measuring Unsaturated Hydraulic Conductivity in the Laboratory and Field." *Unsaturated Soil Engineering Practice*, GSP No. 68, ASCE, Houston, S. and Fredlund, C., Eds., pp. 113-168.

Benson, C.H., Edil, T.B., Ebrahimi, A., Kootstra, R.B., Li, L., and Bloom, P. (2009). "Use of Fly Ash for Reconstruction of Bituminous Roads: Large-Scale Model Experiments." Minnesota Department of Transportation, St Paul, MN.

Blankenagel, B.J. and Guthrie, W.S. (2006). "Laboratory Characterization of Recycled Concrete for Use as Pavement Base Material." *Geomaterials 2006*, No.1952, pp. 21-27.

Breitmeyer, R.J. and Benson, C.H. (2011). "Measurement of Unsaturated Hydraulic Properties of Maicipal Solid Waste." *Geo-Frontiers 2011*, ASCE, Dallas, TX, pp. 1433-1441.

Brown, S.F., and Pell, P.S. (1967). ''An Experimental Investigation of the Stresses, Strains and Deflections in a Layered Pavement Structure Subjected to Dynamic Loads." *Proc, 2nd Int. Conf. Struct. Des. of Asphalt Pavements*, pp. 487–504.

Bozyurt, O. (2011). Behavior of Recycled Asphalt Pavement and Recycled Concrete Aggregate as Unbound Road Base. MS Thesis, Department of Civil and Environmental Engineering, University of Wisconsin-Madison.

Bozyurt, O., Tinjum, J.M., Son, Y.H., Edil, T.B. and Benson, C.H. (2012). "Resilient Modulus of Recycled Asphalt Pavement and Recycled Concrete Aggregate," *GeoCongress 2012*, American Society of Civil Engineers, GSP No. 225, Oakland, CA, pp. 3901-3910.

Buaters, T.W.J., Steenhuis, T.S., DiCarlo, D.A., Nieber, J.L., Dekker, L.W., Ritsema, C.J., Parlange, J.-Y., and Haverkamp, R. (2000). "Physics of Water Repellent Soils." *Journal of Hydrology,* Vol. 231, pp. 233-243.

Burreglo, S.B., Yuan, D., Nazarian, S. (2009). "Cement Treated RAP Mixes for Roadway Base and Subbase: Evaluation of RAP Variability," *Technical Memorandum 0-6084-3*, Center for Transportation Infrastructure Systems, The University of Texas at El Paso, El Paso, TX.

Bush, A.J. and Alexander, D.R. (1985). "Pavement Evaluation Using Deflection Basin Measurements and Layered Theory." *Transportation Research Record* 1022, Transportation Research Board, National Research Council, Washington DC, pp. 16-29.

Camargo, F.F. (2008). "Strenght and Stiffness of Recycled Base Materials Blended with Fly Ash." MS Thesis, University of Wisconsin-Madison, WI

Camargo, F.F., Edil, T.B. and Benson, C.H. (2009). "Strength and Stiffness of Recycled Base Materials Blended with Fly Ash." *Transportation Research Board 88th Annual Meeting.* Washigton, D.C.

Cameron, D.A., Azam, A.H., and Rahman, M.M. (2012). "Recycled Clay Masonry and Recycled Concrete Aggregate Blends in Pavement." *GeoCongress 2012*, Oakland, CA, pp. 1532-1541.

Carpenter, A.C., Gardner, K.H., Fopiano, J., Benson, C.H., Edil, T.B. (2007). "Life Cycle Based Risk Assessment of Recycled Materials in Roadway Construction." *Waste Management*, *27*, pp. 1458-1464.

Cedergren, H.R. (1988). "Why All Important Pavement Should Be Well Drained." *Transportation Research Record*, No. 1188, Washington, D.C., pp. 56-62.

Chen, J., Bradshaw, S.L., Benson C.H., Tinjum, J.M., Edil, T.B. (2012). "pH-dependent Leaching of Trace Elements from Recycled Concrete Aggregate." *Proceeding of GeoCongress 2012*, March 25-29, Oakland, CA.

Chini, A.R., Kuo, S.-S., Armaghani, J.M. and Duxbury, J.P. (2001). "Test of Recycled Concrete Aggregatenin Accelerated Test Track." *Journal of Transportation Engineering,* No.127, Washington, D.C., pp. 486-492.

Cornelis, G., Johnson C.A., Gerven, T.V., Vandecasteele, C. (2008). "Leaching mechanisms of Oxyanionic metalloid and metal species in alkaline solid wastes: a review." *Applied Geochemistry*. 23, pp. 955–975.

Debieb, F. and Kenai, S. (2008). "The Use of Coarse and Fine Crushed Bricks as Aggregate in Concrete." *Construction and Building Materials*, Vol. 22, pp. 886-893.

Ebrahimi, A., Kootstra, B. R., Edil, T.B., and Benson, C.H. (2010). "Equivalency-Based Design and Mechanical Properties of Recycled Roadway Materials With or Without Fly Ash Stabilization", *Proc. 89th Annual Meeting*, Transportation Research Board, Washington D.C.

Ebrahimi, A. (2011). "Deformational Behavior of Fouled Railway Ballast." PhD Dissertation. Department of Civil and Environmental Engineering, University of Wisconsin-Madison.

Ebrahimi, A., Tinjum, J.M., and Edil, T.B. (2011). "Deformational Behavior of Fouled Railway Ballast." *Journal of Geotechnical and Geoenvironmental Engineering*, ASCE.

Edil, T.B. and Fratta, D. (2009). "Development of Testing Methods to Determine Interaction of Geogrid-Reinforced Granular Material for Mechanistic Pavement Analysis." *Wisconsin Highway Research Program #0092-07-05*, Wisconsin Department of Transportation, Madison, Wisconsin.

Edil, T.B. and Luh, G.F. (1978). "Dynamic Modulus and Damping Relationships for Sands." *Proc. Geotechnical Engineering Specialty Conference on Earthquake Engineering and Soil Dynamics*, American Society of Civil Engineers, Pasadena, California, Vol. I, pp. 394-409.

Engelsen, C.J., Van der Sloot, H.A., Petkovic, G., Wibetoe, G. Stoltenberg-Hansson, E., Lund, W. (2006). "Constituent release predictions for recycled aggregates at field site in Norway." *WASCON 2006*, 6th International Conference on the Environmental and Technical Implications of Construction with Alternative Materials, Beograd, Serbia and Montenegro, June 2006.

Engelsen, C.J., Van der Sloot, H.A., Petkovic, G., Wibetoe, G. Stoltenberg-Hansson, E., Lund, W. (2009). "Release of major elements from recycled concrete aggregates and geochemical modeling." *Cement and Concrete Research,* 39(5)*,* pp. 446-45.

Engelsen, C.J., Van der Sloot, H.A., Wibetoe, G., Justnes, H., Lund, W., Stoltenberg - Hansson, E. (2010). "Leaching characterization and geochemical modeling of minor and trace elements released from recycled concrete aggregates." *Cement and Concrete Res.,* 40 (12), pp. 1639-49.

Engelsen, C.J., Wibetoe, G., Van der Sloot, H.A., Lund, W., Petkovic, G. (2012). "Field site leaching from recycled concrete aggregates applied as sub-base material in road construction." *Science of the Total Environment*, 427, pp. 86-97.

FHWA. (2003). “Highway Statistics 2003 - Usage Factors for Major Highway Construction Materials and Labor.” http://www.fhwa.dot.gov/policy/ohim/hs03/htm/pt4.htm (accessed May 15, 2012).

FHWA. (2004). “Recycled Concrete Aggregate – Federal Highway Administration National Review.” Federal Highway Administration. Washington, D.C.

FHWA. (2008). “User Guideline for Byproducts and Secondary Use Materials in Pavement Construction.” *FHWA Report FHWA-RD-97-148*, FHWA, VA.

FHWA. (2011). “Reclaimed Asphalt Pavement in Asphalt Mixtures: State of the Practice.” FHWA-HRT-11-021, FHWA, VA.

Floyd, R.P. (1979). Geodetic Bench Marks, NOAA Manual NOS NGS 1, National Oceanic and Atmospheric Administration, pp. 58.

Gardner, W. (1956). “Calculation of Capillary Conductivity from Pressure Plate Outflow Data.” *Soil Sci. Amer. Proc*., Vol 20, pp. 317-320.

Garrabrants, A.C., Sanchez, F., Kosson, D.S. (2004). “Changes in constituent equilibrium leaching and pore water characteristics of a Portland cement mortar as a result of Carbonation.” *Waste Manage*. 24(1), pp. 19–36.

Giampaolo, C., Mastro, S. Lo. (2000). “Acid neutralization capacity and hydration Behavior of incineration bottom ash-Portland cement mixtures.” *Cement Concrete Research*, 32, pp. 769–775.

Gokce, A., Nagataki, S., Saeki T., and Hisada, M. (2011). “Identification of Frost-susceptible Recycled Concrete Aggregates for Durability of Concrete.” *Construction and Building Materials*, Vol. 25, pp. 2426-2431.

GREENBOOK. (2009). Construction Materials, Section 200-Rock Materials. In *Greenbook Standard Specifications for Public Works Construction*.

Griffin, R.L., Simpson, W.C., and Miles, T.K. (1959). “Influence of Composition of paving Asphalt on Viscosity, Viscosity-Temperature Susceptibility, and Durability.” *Journal of Chemical and Engineering Data*, Vol. 4, No. 4, pp. 349-354.

Guthrie, S.W., Cooley, D., and Eggett, D.L. (2007). “Effects of Reclaimed Asphalt Pavement on Mechanical Properties of Base Materials.” *Journal of the Transportation Research Board,* No.2005, Washington, D.C., pp. 44-52.

Hardin, B.O. and Drnevich, V.P. (1972). "Shear Modulus and Damping in Soils: Design Equations and Curves." *Journal of the Soil Mechanics and Foundation Division, Proceedings of the ASCE*, Vol. 98, No. SM7, pp. 667 – 692.

Harichandran, R.S., Baladi, G.Y., Yeh, M. (1989). "Development of a Computer Program for Design of Pavement Systems Consisting of Bound and Unbound Materials." Dept. of Civil and Environmental Engineering, Michigan State University, Lansing, Michigan.

Heydinger, A.G., Xie, Q.L., Randolph, B.W. and Gupta, J.D. (1996). "Analysis of Resilient Modulus od dense and Open-graded Aggregates." *Transportation Research Board*, Washington, D.C., No.1547, pp. 1-6.

Hicks, R.G. (1970). "Factors Influencing the Resilient Properties of Granular Materials." PhD Thesis, University of California, Berkeley, Berkeley, CA.

Hicks, R.G. and Monismith, C.L. (1971). "Factors Influencing the Resilient Properties of Granular Materials." *Highway Research Record*, No.345, pp. 15-31.

Hidalgo, A., Petit, S., Domingo, C., Alonso, C., Andrade, C. (2006). "Microstructural characterization of leaching effects in cement pastes due to neutralization of their alkaline nature Part I: Portland cement pastes." *Cement and Concrete Research*, 37(1), pp. 63-70.

Holtz, R. (1990). "Compaction Concepts." Chapter3. In *Guide to Earthwork Compaction. In State of the Art Report 8*, Washigton, D.C.: TRB, National Research Council, pp. 9-23.

Horvath, A. (2003). "Life-Cycle Environmental and Economic Assessment of Using Recycled Materials for Asphalt Pavements." *University of California Technical Report,* 29p.

Houst, Y.F., Wittmann, F.H. (2002). "Depth profiles of carbonates formed during natural carbonation Original Research Article." *Cement and Concrete Research*, 32 (12), pp. 1923-1930.

Huang, Y. (2004). *Pavement Analysis and Design*, 2nd Ed., Prentice-Hall, Inc., Upper Saddle River, New Jersey.

Iowa DOT (1999). "Laboratory study of the leachate from crushed portland cement base material." Final report for MLR-96-4. Iowa DOT, Ames, Iowa.

Johnson, A., Clyne, T.R., and Worel, B.J. (2009). "2008 MnROAD Phase II Construction Report." Minnesota Department of Transportation, Maplewood, Minnesota.

Jong, D.-T., Bosscher, P.J., and Benson, C.H. (1998). "Field Assessment of Changes in Pavement Moduli Caused by Freezing and Thawing." *Transportation Research Record:*

Journal of the Transportation Research Board, No.1615, Transportation Research Board of the National Accademies, Washington, D.C., pp. 41-48.

Juan, M.S., and Gutierrez, P.A. (2009). "Study on the Influence of Attached Mortar Content on the Properties of Recycled Concrete Aggregate." *Construction and Building Materials*, Vol. 23, pp.872-877.

Jury, W.A., Gardner, W.R., Gardner, W.H. (1991). Soil Physics, Wiley, New York (328pp).

Juan, M.S. and Gutierrez, P.A. (2009). "Study on the Influence of Attached Mortar Content on the Properties of Recycled Concrete Aggregate." *Construction and Building Materials*, No.23, Washington, D.C., pp. 872-877.

Kim, W., and Labuz, J.F. (2007). "Resilient Modulus and Strength of Base Course with Recycled Bituminous Material." *Minnesota Department of Transportation Report* No. MN/RC-2007-05, pp. 1-270.

Kim, W., Labuz, J.F. and Dai, S. (2007). "Resilient Modulus of Base Course Containing Recycled Asphalt Pavement." *Journal of the Transportation Research Board ,* No.2005, Washington, D.C., pp. 27-35.

Kim, D.S., and Stokoe II, K.H. (1992). "Characterization of Resilient Modulus of Compacted Subgrade Soils Using Resonant Column and Torsional Shear Tests." *Transportation Research Record*, No. 1369, Transportation Research Board, National Research Council, Washington, DC, pp. 83-91.

Kolisoja, P. (1997). "Resilient Deformation Characteristics of Granular Materials." PhD Thesis, Tampere University of Technology, Pub. No. 223, Tampere, Finland.

Kootstra, B.R., Ebrahimi, A., Edil, T.B., and Benson, C.H. (2010). "Plastic Deformation of Recycled Base Materials." *GeoFlorida'2010*, ASCE Geo Institute, submitted.

Kosson D.S., Van der Sloot, H.A., Sanchez, F.,Garrabrants, A.C. (2002). "An integrated frame work for revaluating leaching in waste management and utilization of secondary materials." Environmental Eng. Sci. 19, pp.159–204.

Kramer, S.L. (1996). *Geotechnical Earthquake Engineering*. Prentice Hall. Upper Saddle River, NJ.

Kuo, S.-S., Mahgoub, H.S., and Nazef, A. (2002). "Investigation of recycled concrete made with limestone aggregate for a base course in flexible pavement." *Transportation Research Record,* No.1787, Washington, D.C., pp. 99-108.

Langer, W.H. (1988). “Natural aggregates of the conterminous, United States:” *Geological Survey Bulletin,* No.1594, pp. 33.

Lee, S.J., Amirkhanian, S.N., Shatanawi. S., and Thodesen, C. (2008). “Influence of compaction temperature on rubberized asphalt mixes and binders.” *Can. J. Civ. Eng.*, 35, pp. 908-917.

Lee, J., Edil, T.B., Tinjum, J.M., and Benson, C.H. (2010). "Quantitative Assessment of Environmental and Economic Benefits of Using Recycled Construction Materials in Highway Construction." *J. Transportation Research Board*, 2158, pp. 138- 142.

Lee, J., Edil, T.B., Benson, C.H. and Tinjum, J.M. (2010). “Use of BE^2ST in Highways for Green Highway Construction Rating in Wisconsin.” *Proceeding of The 1st T&DI Green Streets and Highway Conference*, Denver, CO.

Leigh, N.G. and Patterson, L.M. (2004). “ConstructionDemolition Debris Recycling for Environmental Protection and Economic Development.” Southeast Regional Envrionmental Finance Center.

Leite, F.d., Motta, R.d., Vasconcelos, K.L., and Bernucci, L. (2011). “Laboratory Evaluation of Recycled Construction and Demolition Waste for Pavements.” *Construction and Building Materials*, pp. 2972-2979.

Lekarp, F., Isacsson, U. and Dawson, A. (2000). “State of the Art.II: Premanent Strain Response of Unbound Aggregates.” *Journal of Transportation Engineernig ,* No.126, Washington, D.C., pp. 76-83.

Letey, J., Carrillo, M.L.K., and Pang, X.P. (2000). “Approaches to Characterize the Degree of Water Repellency.” *Journal of Hydrology*, Vol. 231, pp. 61-65.

Li, L., Benson, C.H., Edil, T.B., Hatipoglu, B., and Tastan, O. (2007). “Evaluation of Recycled Asphalt Pavement Material Stabilized with Fly Ash.” *ASCE Geotechnical Special Publication*, CD-Rom, 10 pp.

Marasteanu, M.O., and D.A. Anderson. (1996). “Time-Temperature Dependency of Asphalt Binders: An Improved Model.” *Proc., Association of Asphalt Paving Technologists*, Vol. 65, pp. 408–448.

Matschei, T., Lothenbach, B., Glasser, F.P. (2007). “Thermodynamic properties of Portland cement hydrates in the system CaO-Al2O3-SiO2-CaSO4-CaCO3-H2O.” *Cement and Concrete Research.* 37(10), pp. 1379-1410.

Mishra, D., Tutumluer, E. and Butt, A.A. (2010). "Quantifying Effects of Particle Shape and Type and Amount of Fines on Unbound Aggregate Performance Through Controlled Gradation." *Transportation Research Record: Journal of the Transportation Research Board,* No.2167, Washington, D.C., pp. 61-71.

Molenaar, A.A .and Niekerk, A.A. (2002). "Effects of Gradation, Composition, and Degree of Compaction on the Mechanical Characteristics of Recycled Unbound Materials." *Transportation Research Record: Journal of the Transportation Research Board*, No.187, Washington, D.C., pp. 73-82.

Monismith, C.L., Seed, H.B., Mitry, F.G., and Chan, C.K. (1967). "Prediction of Pavement Deflections from Laboratory Tests." *Proc. 2nd Int. Conf.. Struct. Des. of Asphalt Pavements*, pp. 109–140.

Moosazedh, J. and Witczak, M. (1981). "Prediction of Subgrade Moduli for Soil that Exhibits Nonlinear Behavior." *Journal of Transportation Research Board*, No.810, Washington, D.C., pp. 10-17.

Morgan, J.R. (1966). "The Response of Granular Materials to Repeated Loading," *Proc. 3rd Conf.,* ARRB, pp 1178–1192.

Mulugeta, M., Engelsen, C.J., Wibetoe, G., Lund, W. (2010). "Charge-based fractionation of oxyanion-forming metals and metalloids leached from recycled concrete aggregates of different degrees of carbonation: A comparison of laboratory and field leaching tests". *Waste Management*, 31 (2), pp. 253–258.

NAPA. (2009). "*How to Increase RAP Usage and Ensure Pavement Performance."* NAPA.

Nataatmadja, A. (1992). ''Resilient Modulus of Granular Materials Under Repeated Loading." *Proc., 7th Int. Conf. on Asphalt Pavements*, Univ. of Nottingham, Nottingham, U.K., 1, pp. 172–185.

Nataatmadja, A. and Tan, Y.L. (2001). "Resilient Reponse of Recycled Concrete Road Aggregates." *Journal of Transportation Engineering,* No.127, Washington, D.C., pp. 450-453.

NCHRP. (2004). "Laboratory Determination of Resilient Modulus for Flexible Pavement Design." NCHRP Research Results Digest.

Nokkaew, K., Tinjum, J.M., Benson, C.H. and Edil, T.B. (2011). "Hydraulic Properties of Recycled Asphalt Pavement and Recycled Concrete Aggregate", *GeoCongress*, FL.

Nokkaew, K., Tinjum, J.M., and Benson, C.H. (2012). "Hydraulic Properties of Recycled Asphalt Pavement and Recycled Concrete Aggregate." *GeoCongress*, ASCE, Oakland, CA 2012, pp. 1476-1485.

Pan, T., Tutumluer, E. and Anochie-Boateng, J. (2006). "Aggregate Morphology Affecting Resilient Behavior of Unbound Granular Materials." *Trasnportation Research Record: Journal of the Transportation Research Board,* No.1952, Washington, D.C., pp. 12-20.

Park, T. (2003). "Application of Construction and Building Debris as Base and Subbase Materials in Rigid Pavement." *Journal of Transportation Engineering,* No.129, Washington, D.C., pp. 558-563.

Plaistow, L.C. (1994). "Non-Linear Behavior of Some Pavement Un-bound Aggregates," MS Thesis, Dept. of Civil Engineering, University of Nottingham, Nottingham, England.

Poon, C.S. and Chan, D. (2006). "Feasible Use of Recycled Concrete Aggregates and Crushed Clay Brick as Unbound Road Sub-Base." *Construction and Building Materials*, Vol. 20, pp. 578-585.

Poon, C.-S., Qiao, X., and Chan, D. (2006). "The Cause and Influence of Self-Cementing Properties of Fine Recycled Concrete Aggregates on the Properties of Unbound Sub-Base." *Waste Management,* No.26, pp. 1166-1172.

Pratt, E. (1993). "Current Uses and Evaluation of Recycled Materials in Highway Construction: Overview of the Northeastern States." Northeast Recycling Council.

Pucci, M.J. (2010). "Development of a Multi-Measurement Confined Free-Free Resonant Column Device and Initial Studies." MS thesis, Department of Civil, Architectural and Environmental Engineering, University of Texas, Austin.

Read, J. and Whiteoak, D. (2003). "The Shell Bitumen Handbook, Fifth Edition." *Thomas Telford Publishing*, London, UK.

Richart, F.E., Jr., Hall, J.R., and Woods, R.D. (1970). *Vibrations of Soils and Foundations*, Prentice Hall, Inc., Eaglewood Cliffs, NJ.

Roberts, F.L., Kandhal, P.S., Brown, E.R., Lee, D.Y. and Kennedy, T.W. (1996). "Hot Mix Asphalt Materials, Mixture Design, and Construction." *National Asphalt Paving Association Education Foundation*. Lanham, MD.

Robinson, G.R., Jr. and Brown, W.M. (2002). "Sociocultural Dimensions of Supply and Demand for Natural Aggregate-Examples from the Mid-Atlantic Region, United States." US Geological Survey Open-File Report 02-350.

Rosa, M. (2006). “Effect of Freeze and Thaw Cycling on Soils Stabilized using Fly Ash.” MS Thesis, University of Wisconsin-Madison, WI.

Sadecki, R.W., Busacker, G.P., Moxness, K.L., Faruq, K.C., Allen, L. G. (1996). "An Investigation of Water Quality in Runoff from Stockpiles of Salvaged Concrete and Bituminous Paving." Report MN/PR-96/3. Minnesota DOT.

Saeed, A. (2008). “Performance-Related Tests of Recycled Aggregates for Use in Unbound Pavement Layers.” Transportation Research Board of the National Academies. Washigton, D.C.

Saeed, A., Hammons, M.I., Feldman, D.R. and Poole, T. (2006). “Evaluation, Design and Construction Techniques for Airfield Concrete Pavement Used as Recycled Material for Base.” Innovative Pavement Research Dpindation Airport Concrete Pavement Technology Program, Skokie, IL.

Sani, D., Moriconi, G., Fava, G., Corinaldesi, V. (2005). “Leaching and mechanical behavior of concrete manufactured with recycled aggregates”. *Waste Management,* 25(2), pp. 177-182.

Santamarina, J.C., Klein, K.A., and Fam, M.A. (2001). *Soils and Waves*. John Wiley & Sons Ltd., West Sussex, England, 488 pp.

Scalia, J. and Benson, C.H. (2010). “Effect of Permeant Water on the Hydraulic Conductivity of Exhumed GCLs.” *Geotechnical Testing Journal*, 33(3), pp. 201-211.

Schaap, M.G. and Leij F.J. (2000). “Improved Prediction of Unsaturated Hydraulic Conductivity with the Mualem-van Genuchten Model,” *Sci Soc. Am. J.,* Vol. 64, pp. 843-851.

Schaap, M.G. and van Genuchten, M. (2005). “A Modified Mualem-van Genuchten Formulation for Improved Description of the Hydraulic Conductivity near Saturation,” *Vadose Zone J*., Vol. 5, pp. 27-34.

Schaertl, G.J. (2010). “Scaling and Equivalency of Bench-scale Tests to Field Scale Conditions.” MS Thesis, University of Wisconsin-Madison, WI.

Schuettpelz, C.C., Fratta, D., and Edil, T.B. (2010). “Mechanistic method for determining the resilient modulus of base course materials based on elastic wave measurements.” *Journal of Geotechnical and Geoenvironmental Engineering*. Vol. 136, No. 8, pp. 1086-1094.

Scullion, T. and Saarenekto, T. (1997). "Using Suction and Dielectric Measurements as Performance Indicators for Aggregate Base Materials." *Transportation Research Record*, No. 1577, pp. 37-44.

Seed, H.B., Mitry, F.G., Monismith, C.L., and Chan, C.K. (1967). ''Prediction of Flexible Pavement Deflections from Laboratory Repeated Load Tests.'' *NCHRP Rep. No. 35*, National Cooperative Highway Research Program.

Seed, H.B. and Idriss, I.M. (1970). "Soil Moduli and Damping Factors for Dynamic Response Analyses," *Report No. EERC 70-10*, University of California, Earthquake Engineering Research Center, Berkeley, CA, 1970.

Seyhan, U. (2001). "Characterization of Anisotropic Granular Layer Behavior in Flexible Pavements." Doctoral Thesis, University of Ilinois, Urbana, IL.

Son, Y.H. (2010). "Resilient Moduli of Recycled Materials." Personal Communication.

Taha, R., Ali, G., Basma, A. and Al-turk, O. (1999). "Evaluation of Reclaimed Asphalt Pavement Aggregate in Road Bases and Subbase." *Transportation Research Record: Journal of the Transportation Research Board,* No.1652, Washington, D.C., pp. 264-269.

Tanyu, B.F., Kim, W.H., Edil, T.B., and Benson, C.H. (2003). "Comparison of Laboratory Resilient Modulus with Back-Calculated Elastic Moduli from Large-Scale Model Experiments and FWD Tests on Granular Materials," *Resilient Modulus Testing for Pavement Components*, ASTM STP 1437, G. N. Durham, W. A. Marr, and W.L. De Groff, Eds., ASTM International, West Conshohocken, Pa.

Thom, N.H., and Brown, S.F. (1988). "The Effect of Grading and Density on the Mechanical Properties of a Crushed Dolomitic Limestone." *Proc. 14th ARRB Conf.*, Vol.14, Part 7, pp. 94–100.

Thom, N.H., and Brown, S.F. (1989). "The Mechanical Properties of Unbound Aggregates from Various Sources." *Unbound Aggregates in Roads*, R. H. Jones and A. R. Dawson, eds., pp. 130–142.

Tian, P., Zaman, M.M. and Laguros, J.G. (1998). "Gradation and Moisture Effects on Resilient Moduli of Aggregate Bases." *Transportation Research Record,* No.1619, Washington, D.C., pp. 75-84.

Toros, U., and Hiltunen, D.R. (2008) "Effects of Moisture and Time on Stiffness of Unbound Aggregate Base Course Materials." *Transportation Research Record: Journal of the Transportation Research Board* , No.2059, Transportation Research Board of the National Accademies, Washington, D.C., pp. 41-51.

Tutumluer, E. and Seyhan, U. (1998). "Neural Network Modeling of Anisotropic Aggregate Behvior from Repeated Load Triaxial Testa." *Transportation Research Record,* No.1615, Washington, D.C., 86-93.

USGS. (2011). "Crushed Stone Statistics and Information." http://minerals.usgs.gov/minerals/pubs/commodity/stone_crushed/myb1-2010-stonc.pdf (Accessed May 15, 2012)

Van Genuchten, M. (1980). "A Close-Form Equation for Predicting the Hydraulic Conductivity of Unsaturated Soils," *Soil. Sci. Am. J.*, 44, pp. 892-898.

Vanapali, S.K. Fredlund, D.G., Pufahl, D.E., and Clifton, A.W. (1996). "Model for the prediction of shear strength with respect to soil suction," *Can. Geotech. J.* 33, pp. 379-392.

Van der Sloot, H.A., Heasman, L., Quevauviller, P. (1997). "Harmonisation of leaching/extraction tests." Elsevier Science B.V, Amsterdam.

Van der Sloot, H.A., Van Zomeren, A., Stenger, R., Schneider, M., Spanka, G., Stoltenberg-Hansson, E., Dath, P. (2008). "Environmental CRIteria for CEMent based products, Phase I: Ordinary Portland Cements, Phase II: Blended Cement." ECN-E--08-011, the Netherlands.

Van Niekerk, A.A., Houben, L.J.M., and Molenaar, A.A.A. (1998). "Estimation of Mechanical Behavior of Unbound Road Building Materials from Physical Material Properties." *Proc., 5th Int. Conf. on the Bearing Capacity of Roads and Airfields*, R.S. Nordal and G. Rafsdal, eds., Vol.3, pp. 1221–1233.

VDOT. (2003). "Minimizing the impact pn water quality of placing grout underwater to repair bridge scour damage." Final report for VTRC 03-R16. Virginia DOT, Charlottesville, Virginia.

Warner, J.D. (2007). "The Beneficial Reuse of Asphalt Shingles in Roadway Construction." MS Thesis, University of Wisconsin-Madison, WI

Wen, H., Baugh, J., and Edil, T.B. (2007). "Use of Cementitious High Carbon Fly Ash to Stabilize Recycled Pavement Materials as a Pavement Base Material." *Proceedings of the 86th Annual Meeting*, Paper No. 07-2051, National Research Council, Washington D.C., CD-ROM.

Wen, H., Warner, J., Edil, T. and Wang, G. (2008). "Laboratory Comparison of Crushed Aggregate and Recycled Pavement Material With and Without High Carbon Fly Ash." *Geotechnical and Geological Engineering* , No.28, pp. 405-411.

Wen, H. and Edil, T.B. (2009). “Sustainable Reconstruction of Highways with In-Situ Reclamation of Materials Stabilized for Heavier Loads.” *BCR2A Conference*,. Champaign, IL, pp. 1011-1017.

Wen, H., Mengqi, W., and Uhlmeyer, J. (2011). “Evaluation of The Effects of Climatic Conditions on Modulus of Base Materials with Recycled Asphalt Pavement.” *Journal of ASTM International*, Vol. 8, No. 10, pp. 1-13.

West, R.C., Watson, D.E., Turner, P.A., and Casola, J.R. (2010). “Mixing and Compaction Temperatures of Asphalt Binders in Hot-mix Asphalt.” *National Cooperative Highway Research Program*, Report No. 648, Trans. Res. Board, Washington, DC.

Weyers, R.E., Gregory, S.W., David, W.M., S, L.D. and Cady, P.D. (2005). “Testing Methods to Determine Long Term Durability of Wisconsin Aggregate Resources.” Virginia Polytechnic Institute.

Williams, R.R., and Nazarian, S. (2007). “Correlation of Resilient and Seismic Modulus Test Results.” *Journal of Materials in Civil Engineering*, Vol 19, No.12, ASCE, pp. 1026-1032.

Wilburn, D.R., and Goonan, T.G. (1998). “Aggregates from Natural and Recycled Sources.” U.S. Geological Survey Circular 1176, 36p. http://greenwood.cr.usgs.gov/pub/ciculars/c1176/ (Accessed July 25, 2012)

WisDOT (2009). "Layer Coefficient Values for Cracked and Seated Concrete." *Transportation Synthesis Report,* Wisconsin Department of Transportation, Madison, Wisconsin.

Wu, Y., Parker, F. and Kandhal, P.S. (1998). “Aggregate Toughness/Abrasion Resistance and Durability/Soundness Tests Related to Aspahlt Concrete Performance in Pavements.” *Transportation Research Record,* No.1638, Washington, D.C., pp. 85-93.

Yang, J., Du, Q., and Bao, Y. (2011). “Concrete with Recycled Concrete Aggregate and Crushed Clay Bricks.” *Construction and Building Materials*, Vol. 25, pp. 1935-1945.

Zaman, M.M., & Zhu, J.-H.L. (1999). “Durability Effects on Resilient Moduli of Stabilized Aggregate Base.” *Transportation Research Record ,* No.1687, Washington, D.C., pp. 29-39.

Appendix A: Implementation of Abbreviated Test Pit Area

A.1 Introduction

Previous testing using the LSME incorporated the entire 3.0 m x 3.0 m test area to measure deformations and determine the resilient modulus for a given base course material under cyclical loading. However, limited amounts of base course material available for testing made it necessary to reduce the evaluated test area within the LSME to 1.0 m x 1.0 m. The remainder of the 3.0 m x 3.0 m test area was made up of recycled pavement material (RPM) to maintain the boundary stress that would otherwise be lost by a reduction in test area. The equivalency of the abbreviated LSME test area to the full LSME test area was determined by comparing the resilient modulus of RPM obtained using both test methods.

The RPM was compacted to a thickness of 0.3 m within the entire 3.0 m x 3.0 m LSME test area according to methods described in section 3.3.1. The abbreviated 1.0 m x 1.0 m test area was then excavated in the center of the LSME test area, leaving approximately 2.0 m of RPM around the LSME perimeter, as shown in Figure A.1. The exposed subgrade was loosened and recompacted prior to placement of the specimen material to establish a consistent initial density that would be repeated for all subsequent tests. The circumference of the abbreviated test area was lined with nonwoven, heat bonded geotextile to separate the RPM from the test specimen and allow confinement of the test specimen from the surrounding RPM, as shown in FigureA.2. RPM was recompacted within the abbreviated test area and the summary resilient modulus of the tested material was determined using methods described in section 3.3.4.

The resilient modulus of the RPM determined for the abbreviated test area was measured to be 538 MPa. Benson et al. (2009) reported a summary resilient modulus of 505 MPa on LSME tests for the same material using the full 3.0 m x 3.0 m test area. Using the smaller test area increased the summary resilient modulus by approximately 6%. A comparison of the summary resilient modulus determined for the two specimen sizes is presented in Figure A.3. The summary resilient moduli determined for the 0.3-m thick LSME tests on RAP, RCA, blended RCA/Class 5 and Class 5 as discussed in section 4.2 are also presented in Figure A.3. for scale. The magnitude of the RPM resilient modulus is similar for both the full and abbreviated test pit areas. Boudreau (2003) tested the repeatability of bench-scale resilient modulus tests and found that the coefficient of variance was as high as 4.5% for specimens tested at the same stress level. The mean average and the standard deviation measured between the two tests were 522 MPa and 23 MPa respectively, indicating a coefficient of variance of 4.4%. Assuming a correlation between the bench-scale and LSME tests, the two test methods are within an acceptable amount of variance.

Figure A.1. Overview of Abbreviated Test Pit Area prior to Material Placement.

Figure A.2. Placement of RPM within Abbreviated Test Pit Area

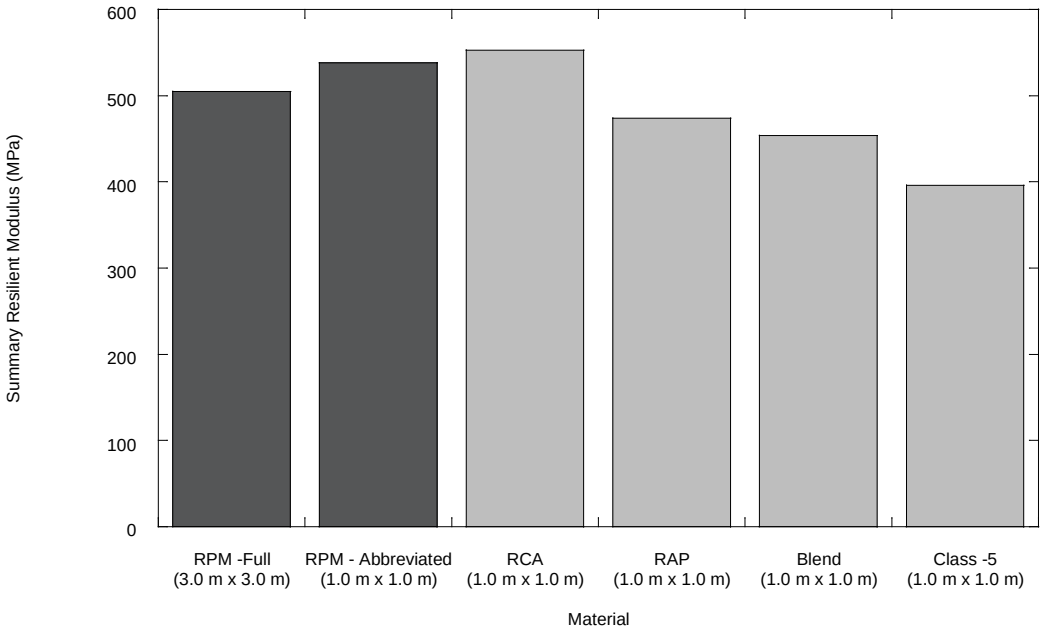

Figure A.3. Comparison of Resilient Modulus of RPM Obtained for Full and Abbreviated Test Pit Areas with RCA, RAP, Blended RCA/Class 5 and Class 5 Obtained for Abbreviated Test Pit Area.

Appendix B: Determination of Layer Coefficients

B.1 Determination of Layer Coefficients

The design of pavement structures is dependent on the determination of appropriate layer thicknesses based on the mechanical properties of the associated pavement layers. The AASHTO design procedure relates the structural capacity of a given layer to a structural number, SN_i, which is defined as the product of the layer thickness, D_i, and layer coefficient, a_i. The SN for the pavement structure as a whole is calculated according to Eqn. B.1.

$$SN = SN_1 + SN_2 m_2 + SN_3 m_3 = a_1 D_1 + a_2 D_2 m_2 + a_3 D_3 m_3 \quad \text{(B.1)}$$

The variable m_i is the drainage modification facto, which is assumed to be 1.0 for the base materials used in this study. Design layer thicknesses are chosen in such a way that the resulting SN is greater than or equal to a required SN. The required SN is typically determined based on estimated traffic, serviceability loss, and effective roadbed resilient modulus (AASHTO 1993).

The layer coefficient measures the relative ability of a unit thickness of a given material to function as structural component in a pavement (Haung 2007). The layer coefficient for untreated base course can be estimated from the resilient modulus of the layer according to the relationship proposed by Rada and Witczak (1981) and presented in Eqn. B.2.

$$a_2 = 0.249(\log M_r) - 0.977 \quad \text{(B.2)}$$

where M_r is the resilient modulus measured in psi.

The layer coefficients were calculated for the 0.2-m and 0.3-m thick layers tested in the LSME using the SRM according to Eqn. B.2 for RAP, RCA, blended RCA/Class 5 and Class 5. The relationship between layer coefficient and layer thickness for these materials is presented in Figure B.1. The SN for each of the base course materials tested in the LSME was calculated as the product of the layer thickness (in inches) and the associated layer coefficient. The SN and layer coefficients for each LSME test are presented in Table B.1.

The magnitude of the layer coefficients follow the hierarchy seen previously for SRM, with RCA and Class 5 having the highest and lowest values, respectively, and RAP and blended RCA/Class 5 having the second and third highest values, respectively. The layer coefficients of RAP, blended RCA/Class 5, and Class 5 all increased at the same rate with an increase in layer thickness. The layer coefficient of RCA increased with increased layer thickness as well, albeit at a much slower rate. The Class 5 layer coefficients of 0.16 and 0.21 determined for the LSME layer thicknesses of 0.2 m and 0.3 m, respectively, are marginally higher than typical values for granular base course of 0.10 and 0.14 (Huang 2004). RCA had layer coefficients of 0.21 and 0.24 for layer thicknesses of 0.2 m and 0.3 m, which is within typical values for rubblized concrete as reported by WisDOT (2009).

Table B. 1. Layer Coefficients and Structural Numbers for different LSME Thicknesses.

Material	Layer thickness (m)	Summary Resilient Modulus (kPa)	Layer Coefficient, a_2	Structural Number, SN
RAP	0.2	314	0.18	1.44
	0.3	474	0.23	2.76
RCA	0.2	418	0.21	1.68
	0.3	553	0.24	2.88
Blended RCA/Class 5	0.2	278	0.17	1.36
	0.3	454	0.22	2.64
Class 5	0.2	243	0.15	1.2
	0.3	396	0.21	2.52

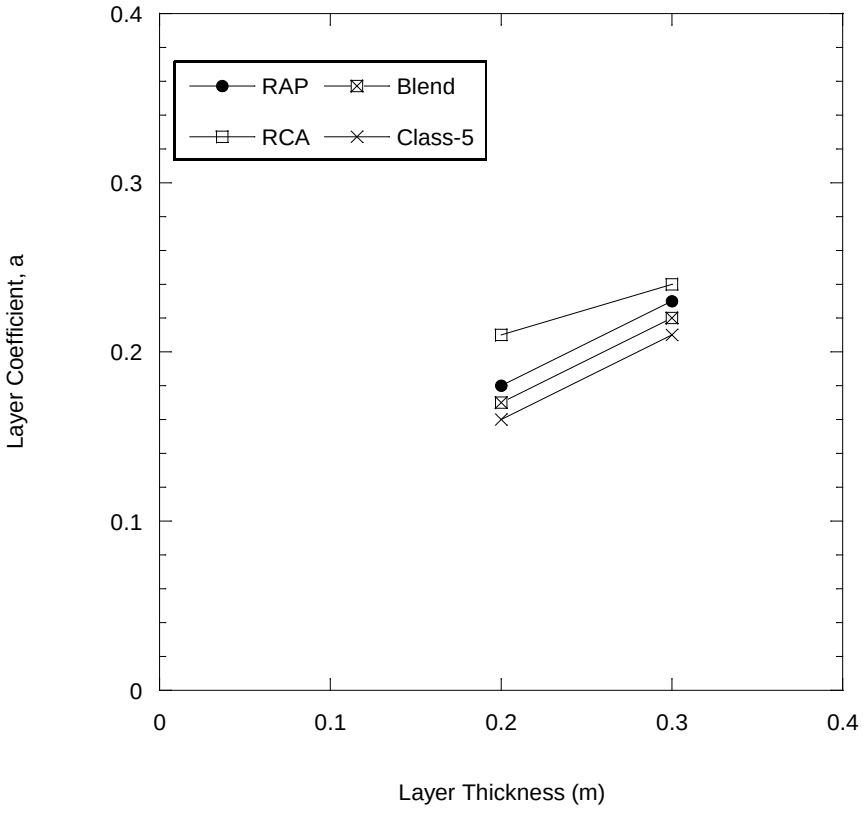

Figure B.1. Layer Coefficient versus Base Layer Thickness for RAP, RCA, Blended RCA/Class 5, and Class 5.